



Published in final edited form as:

Chem Rev. 2018 August 22; 118(16): 7409–7531. doi:10.1021/acs.chemrev.7b00678.

Intracellular Delivery by Membrane Disruption: Mechanisms, Strategies, and Concepts

Martin P. Stewart^{1,2,†}, Robert Langer^{†,1,2}, Klavs F. Jensen^{†,1}

¹Department of Chemical Engineering, Massachusetts Institute of Technology, Cambridge, USA.

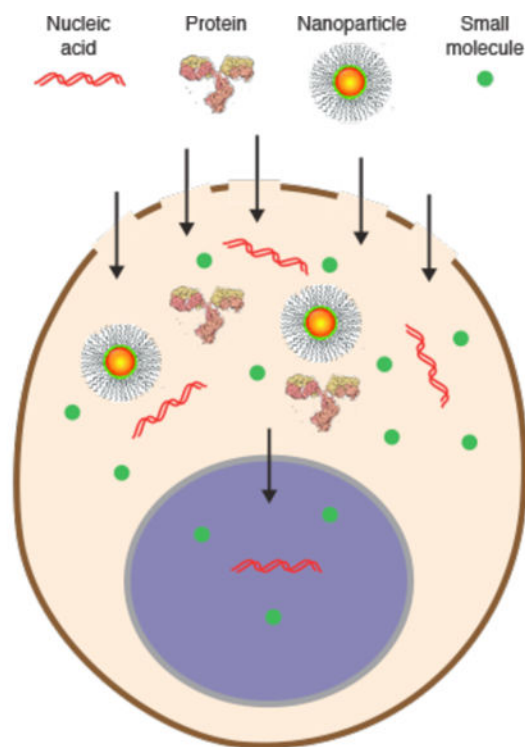
²The Koch Institute for Integrative Cancer Research, Massachusetts Institute of Technology, Cambridge, USA.

Abstract

Intracellular delivery is a key step in biological research and has enabled decades of biomedical discoveries. It is also becoming increasingly important in industrial and medical applications ranging from biomanufacture to cell-based therapies. Here, we review techniques for membrane disruption-based intracellular delivery from 1911 until the present. These methods are important because they achieve rapid, direct, and universal delivery of almost any molecule that can be dispersed in solution. We start by covering the motivations for intracellular delivery and the challenges associated with the different cargo types – nucleic acids, proteins/peptides, small molecules, synthetic nanomaterials, and large cargo. The review then presents a broad comparison of delivery strategies followed by an analysis of membrane disruption mechanisms and the biology of the cell response. We cover mechanical, electrical, thermal, optical, and chemical strategies of membrane disruption with a particular emphasis on the applications, challenges, and mechanisms of action. We hope the concepts discussed in our review inspire scientists and engineers with further ideas on how to improve intracellular delivery.

Graphical Abstract

[†]Corresponding Authors martstew@mit.edu, rlanger@mit.edu, kfjensen@mit.edu.



MEMBRANE DISRUPTION-MEDIATED INTRACELLULAR DELIVERY

1. Introduction

Cells transmit information through molecules. Just as computer chips process information using electronic signals, the currency of information exchange in cells is molecules. DNA encodes RNA and proteins. Proteins perform work, transmit signals, and act as building blocks of cellular structure. Lipids form membranes and store energy. The cell is infinitely more complex than an electronic device - we are still learning how it works. In addition to the natural molecules that comprise cells, new technologies are enabling synthetic materials to be sent into cells. Introducing such cargo is an important step in decoding cell function, guiding cell fate, and reprogramming cell behavior. Thus, intracellular delivery is central to our ability to understand biology and potential to treat disease.

This review is intended for anyone interested in intracellular delivery. For example: a biologist looking for the most appropriate method in their project, a chemist who has produced a new molecule that requires verification in live cells, an engineer searching for inspiration on feasible intracellular delivery technology, a cell physiologist seeking deeper understanding of the cell biological issues surrounding membrane disruption-based delivery, or a biomanufacturing expert examining ways to improve production yield. This review seeks to deconstruct the literature into a unique and understandable framework. More than 1500 papers are referenced but we've examined almost 4000 in the process of compiling this paper.

The scope of this review is focused on membrane disruption-based intracellular delivery, as opposed to carrier-mediated methods. There are many more reviews on carriers (also known as vectors, vehicles, nanocarriers, and delivery nanoparticles), particularly for nucleic acid delivery¹⁻⁹, including in this journal¹⁰⁻¹⁴. Comparatively fewer reviews exist on membrane disruption-based delivery, possibly due to the diverse array of approaches for creating holes in membranes. Our review is one of the few that attempt to catalogue and compare these modalities.

In this review we cover literature from 1911 until the present. However, the field of membrane disruption-mediated delivery was small until the mid 1980's, which coincided with the rise of electroporation along with other means of cell permeabilization. We have narrowed the discussion of membrane disruption-mediated delivery primarily to cells *in vitro*, as opposed to *in vivo* scenarios. The review will focus mostly on cells of animal and human origin, although we will sometimes venture beyond this scope to highlight particular examples in bacteria, single-celled organisms, and plants.

To begin the review, we will first cover the types of cargo that researchers seek to deliver and their applications. The dimension, scale, and properties of these cargos will be discussed, as these characteristics are inextricably linked to the challenges involved in their delivery. The review then conducts a wide sweeping examination of the methods of delivery, defining what is membrane disruption-mediated and what is not. Next, we explain some basic background on cell membranes, their function, and mechanisms of disruption and cell recovery. This background information sets the stage for the bulk of the review, and is designed to make it more understandable. We then cover each membrane disruption category one-by-one, highlighting the history, mechanisms, prime examples, pros and cons, and where appropriate, a perspective of opportunities and predictions. In keeping with the title, our review seeks to underscore mechanisms, strategies, and concepts.

2. Intracellular Delivery Cargo & Applications

2.1 Overview of Key Applications

For decades researchers have been developing, synthesizing, and adapting molecular and synthetic cargo for deployment to the intracellular environment. Most of these cargos are membrane impermeable despite having intracellular targets. In this section, we provide an overview of the key applications of intracellular delivery and the categories of cargo that researchers seek to deliver along with related challenges.

Intracellular Delivery is Moving Beyond Traditional Transfection—Transfection refers to intracellular delivery of nucleic acids: DNA and RNA. Most intracellular delivery experiments performed at a population scale are transfection. This is probably because genetic modulation with DNA or RNA is generally viewed as the obvious route for controlling cell function. Increasingly, however, researchers have discovered ways to manipulate cells with other forms of cargo, for example, genome-editing nucleases^{15,16}, synthetic intracellular probes¹⁷, and combinations of proteins and/or inhibitors that guide cell fate¹⁸. Thus, we believe the field is undergoing a transition from a narrower focus on transfection toward the wider concept of intracellular delivery. To illustrate this, Figure 1

depicts the diversity of cargo that can be delivered into cells and the potential outcomes. The schematic highlights the progression from input cargo to cellular output states and end-point applications. In all these cases, the prime challenge is that impermeable cargo must be introduced to the cell interior without untoward damage to the cell. The five horizontal tiers are not mutually exclusive, having significant overlap between inputs and output. This “menu” of options reflects the combinatorial potential of intracellular delivery to engineer cell function and analyze cell behavior. Next, we highlight several examples of the medical potential of intracellular delivery before reviewing the main cargo categories.

Intracellular Delivery for Cell-Based Therapies—There are several cases where cell engineering via intracellular delivery could impact the future of medicine. One is the concept of cell-based therapy, where cells that have been modified, repaired or reprogrammed are introduced into a patient to restore lost function. In cell-based therapies, the cells can be viewed as a living drug to be administered to the patient. For example, when endogenous immune cells lose their ability to eliminate cancer cells, modified T-cells can be introduced to compensate¹⁹. In the case of CAR-T cells, novel function is conferred through induced expression of specific T-cell receptors (TCRs) or chimeric antigen receptors (CARs) that guide the T-cells to bind to, and attack, cancer cells^{20,21}. Recent clinical trials against B cell malignancies validate the power of this approach²², which was approved by the FDA in 2017.

Currently, most cell-based therapies are carried out through *ex vivo* manipulation, wherein cells are extracted from the patient, manipulated *in vitro*, and then reintroduced to the body for a therapeutic effect²³. Intracellular delivery is required for the *in vitro* manipulation step. *Ex-vivo* cell-based therapies have demonstrated efficacy in treating several human diseases in clinical trials^{23,24}. Examples include hematopoietic stem cell (HSC) transplantation²⁵ and engineering of immune cells for cancer immunotherapy^{19,21,26,27}, as mentioned above. Disease-causing mutant HSCs can be genetically corrected with *ex vivo* gene therapy, whereby stable genomic modifications confer a durable therapeutic effect²³. Recent successes include viral vector-mediated gene therapy for correction of monogenic diseases such as severe combined immunodeficiency (SCID-X1), Wiskott-Aldrich syndrome (WAS), and β -thalassemia²⁴. In future, delivery of genome editing components for precise gene correction is anticipated to improve the safety and efficiency of HSC gene therapy above what is currently attained with viral vectors^{15,28,29}.

Intracellular Delivery in Stem Cell Reprogramming—In 2006 it was shown that expressing a combination of transcription factors in somatic cells reprogrammed them into induced pluripotent stem cells (iPSCs)³⁰. Early results were achieved with expression from potentially mutagenic viral vectors, an approach considered problematic for medical applications. To address this concern, iPSCs have since been produced via direct intracellular delivery of proteins³¹, mRNA^{32,33}, microRNA³⁴ and in combination with small molecules³⁵. Medical applications of iPSCs include *in vitro* expansion for drug screening of patient cells and gene therapy before re-implantation³⁶. Reprogrammed iPSCs also offer potential for cell-based regenerative medicine³⁷, for example to generate immune-

compatible organs for patient transplants³⁸, off-the-shelf T cells for cancer immunotherapy³⁹, or gene-edited endothelial cells to correct hemophilia⁴⁰.

2.2 Cargo Categories

Cargoes of interest for intracellular deployment are highly variable in size, shape, architecture and chemical properties (Figure 2). They range from small hydrophilic molecules around 1 nm, such as the cryoprotectant trehalose, to large micron-sized organelles and bacteria approaching the size of the cell itself. This scale represents more than 3 orders of magnitude. It also encompasses a diversity of origins, from typical biomolecules like proteins, DNA, and RNA, to synthetic materials such as carbon nanotubes (CNTs), quantum dots, nanoparticles, and microdevices. In the following, we categorize these cargoes for discussion of their properties, delivery challenges, and intracellular applications.

2.2.1 Nucleic Acid Transfection—The word transfection is derived from *transformation* and *infection*. It has paradoxically come to refer to non-viral (i.e. non-infectious) methods of nucleic acid delivery. The analogous term *transduction* refers to the introduction of nucleic acids by viruses or viral vectors. Transfection has mainly been conducted with plasmid DNA, mRNA, and oligonucleotides. Recently, nucleic acid-based constructs and devices are also being deployed to the intracellular space.

Brief History & Motivations: Starting from the 1960s, researchers observed that mixing nucleic acids, which are negatively charged, with cationic molecules leads to the formation of macromolecular complexes that enter cells and release the nucleic acids inside. Early examples include the polymer DEAE-dextran (1968)^{41–43} and precipitates formed with calcium phosphate (1973)⁴⁴. Lipid-based transfection came onto the scene in the 1980s, first with liposomes(1980)^{45,46} and then via ‘lipofection’ with cationic lipids(1987)⁴⁷. The most effective methods were commercialized, with the launch of the cationic lipid-based product lipofectamine in 1993, cationic polymers such as PEI from 1995⁴⁸ (marketed as “polyjet” soon after) and dendrimers like PAMAM⁴⁹ from 1993 (“superfect” reagent launched in late 90s). Cationic polymers such as polybrene⁵⁰ and poly-l-lysine^{51,52} also formed the basis of several transfection technologies. Electroporation, first used for DNA transfection in 1982⁵³, is useful for certain cell types and was commercialized from the mid-1980s by Biorad and others. Today, most transfection is performed with lipid reagents, while polymer reagents and electroporation are the next most popular options.

By 2020 the transfection market is predicted to be worth USD one billion, and market reports place the applications into three areas: 1) basic research, 2) biomanufacture, and 3) cell-based therapies (Figure 3). Transfection is central to biological research, in both academic and corporate settings and impacts fields from cell biology and genetics to immunology and drug discovery. In the context of biomanufacture, it is used for bio-production of proteins, antibodies, viral vectors, and virus-like particles for vaccines. In cell-based therapies, transfection has been a key approach in *ex vivo* gene therapy²⁴, hematopoietic stem cell engineering^{25,54}, production of induced pluripotent stem cells³², and preparation of cells for immunotherapy^{55–57}. As exemplified in figure 3, nucleic acid

transfection is currently the primary sub-category of intracellular delivery. In future, however, demand for delivery of non-nucleic acid materials (for example, antibodies, genome editing nucleases, and synthetic materials) is expected to compete with transfection in several applications⁵⁸.

DNA Vectors: A vector is a DNA molecule that acts as a vehicle for the expression or replication of DNA. Vectors include plasmids, cosmids, viral vectors, and artificial chromosomes. Plasmids are circular double-stranded DNA molecules originally discovered in bacteria⁵⁹. Cosmids are similar to plasmids but exhibit phage packaging capability⁶⁰. Viral vectors pack a limited amount of DNA within a viral envelope – a configuration that confers self-delivery through viral entry pathways⁶¹. Artificial chromosomes have larger DNA capacity than other vectors, containing up to a million base pairs, and can physically be around the micron size range. They are used in specialized situations where their larger capacity and natural chromosome-like behavior are advantageous⁶².

The most commonly used vectors are plasmids, which are usually around 5–10 kilo-basepairs. DNA engineering techniques enable the manipulation of vectors through recombination so that sequences can be cut and paste into them. Pioneering studies in the 1970s inserted foreign DNA into viral vectors⁶³ and plasmids⁶⁴ for subsequent intracellular delivery and gene expression. By decoding the genetic elements of vectors, such as expression promoters and origins of replication, it became possible to introduce and express genes from one organism into another and vice versa⁶⁵. For example, plasmids were exploited to express eukaryotic genes in bacteria^{66,67}, then foreign genes in animal cells via calcium phosphate transfection^{68,69} or microinjection^{70–72}. That plasmids must enter the nucleus to undergo expression was established by microinjection experiments that compared cytoplasmic with nuclear injection⁷².

A 5–10 kilo-basepair plasmid is >100 nanometers in diameter when uncondensed^{73,74} (Table 1). Each nucleotide carries a negative charge due to repeating phosphate groups along the polymer backbone. Cationic compounds, such as lipids and polymer reagents, condense plasmids into solid nanoparticles with dimensions down to tens of nanometers^{10,75,76}. Such compaction promotes cellular uptake by reducing the plasmid size and shielding its negative charge. The level of supercoiling also influences the durability and compaction, with plasmids bearing a smaller footprint being capable of better transfection and expression^{77,78}.

Oligonucleotides: Oligonucleotides are single- or double-stranded sequences of DNA or RNA, generally less than 30 nucleotides in length. Antisense oligonucleotides (ASOs) were first discovered in 1978, when it was shown that a single-stranded 13-mer of DNA hybridized with complementary mRNA inhibits its translation⁷⁹. Antisense inhibition occurs when RNA is either sterically blocked or flagged for enzymatic degradation. In the 1980s ASOs were established as tools for performing genetic loss of function studies in cell and developmental biology^{80–82}. In these cases ASOs were either expressed from plasmids or microinjected after *in vitro* transcription. Thereafter, several companies began developing antisense therapeutics, with the first approved medication in 1998 being fomivirsen, a 21-mer oligonucleotide that blocks the translation of cytomegalovirus mRNA^{83,84}.

The discovery of RNA interference (RNAi) by Fire and Mello in 1998⁸⁵ led to the revelation of double-stranded RNA for silencing gene expression. Subsequently, it was shown that RNAi in mammalian cells could be mediated by intracellular delivery of short 21–22 base pair duplexes, termed small interfering RNAs (siRNAs)⁸⁶. Once in the cytoplasm, siRNAs binds to protein machinery known as the RNAi-induced silencing complex (RISC), which searches out matching RNA and enzymatically degrades it. Micro RNAs (miRNAs), discovered in 1993⁸⁷, represent the endogenous mechanism of gene silencing. Small hairpins of miRNA are processed by enzymes within the cell into smaller pieces similar to siRNAs, which then silences genes through antisense or RNAi effects.

Oligonucleotides may modify cell behavior through a number of mechanisms. These include: (1) activating toll-like receptors in the endosome, (2) siRNAs, (3) miRNA mimics, (4) antagomirs, sterically blocking endogenous miRNA, (5) ASOs such as gapmers, inducing RNase H degradation or sterically blocking RNA, (6) oligonucleotides directed against nuclear regulatory RNA species such as long noncoding RNAs (lncRNAs), (7) splice switching oligonucleotides that perturb mRNA maturation, (8) anti-gene oligonucleotides that bind to genomic DNA, perturbing transcription or binding of other proteins, and (9) aptamers, which to bind, and alter the function of, proteins⁸⁸. Aptamers are distinct in that they form higher order structures with conformations exhibiting affinity to specific target molecules. With the exception of the first mechanism, oligonucleotides must enter the cytoplasm or nucleus to exert their effects.

As negatively charged polar molecules in the size range of small proteins (Figure 2), cellular permeability of oligonucleotides is poor. siRNA duplexes have approximate dimensions of 7.5 nm length by 2 nm diameter⁸⁹ (Table 1). miRNA is only slightly larger than siRNA because it is single stranded hairpin with an extraneous loop. An ASO of 16 bases is about 5 nm long by 1 nm wide. Apart from size and charge, challenges associated with oligonucleotide delivery include susceptibility to enzymatic degradation and binding to undesirable targets⁹⁰. However, the molecules can be functionalized with various chemical modifications to prevent premature degradation and cleavage^{9,91}. One approach is to neutralize the charge of the polymer backbone by replacement of natural bases with morpholinos⁹² or peptide nucleic acids (PNAs)⁹³, or addition of specific functional groups⁹⁴. Thus, delivery strategies can include combinations of chemical modification of the oligonucleotide itself, use of lipid or polymeric nanocarriers, and linking oligonucleotides to cell targeting agents such as carbohydrates, peptides or aptamers^{90,95}. In these examples, it is thought that the biological effects of oligonucleotides are mostly due to a small amount of material that escapes from endosomes and reaches key cytosolic or nuclear compartments^{96,97}. In terms of oligonucleotide delivery methods, lipid reagents have been the most prevalent^{98–100}. In cells that are recalcitrant to reagents, success been obtained with electroporation^{101–106} and pore-forming agents^{107,108}.

mRNA: Gene expression from messenger RNA (mRNA) represents an attractive alternative to DNA vectors, particularly for therapeutic applications. Pioneering studies of mRNA expression were conducted from the 1970s via microinjection^{109–111}. Following that, mRNA was transfected into mammalian cells using the cationic polymer DEAE-dextran^{112,113} and

with cationic lipid complexes^{114,115}, the latter of which became the standard¹¹⁶. Transfection via electroporation was also shown in a number of common cell lines^{117,118}.

Expression from mRNA has a number of advantages over DNA vectors^{119,120}. First, there is no risk of the genomic integration that occasionally occurs with DNA. Second, mRNA expression is based upon interaction with ribosomes located in the cytoplasm, not needing to cross the nuclear envelope as DNA does. Third, expression is dose-dependent and rapid, occurring within minutes. Fourth, subcellular control of mRNA delivery can lead to local expression when desired¹²¹. Fifth, mRNA can be less toxic and immunogenic than DNA vectors in sensitive cells, making it a preferred option for certain primary cell types. In particular, these features make mRNA a strong candidate for potential therapeutic applications¹²². Antigen presentation arising from *ex vivo* mRNA transfection has been deployed in dendritic cells and T cells as a strategy for cancer immunotherapy purposes^{57,123–126}. In this context, electroporation of mRNA has become a preferred option for therapeutic cell types that are difficult to transfect with cationic lipids, such as dendritic cells^{127–129}.

Similar to DNA, mRNA is a large negatively charged polymer that can be condensed into cationic nanoparticles to promote uptake^{116,130}. mRNA is single stranded, however, and usually forms secondary structures featuring various loops and hairpins (Figure 2). As a rule of thumb, the dimensions of mRNA are approximately 10 times larger than the protein it encodes for, putting it in the range of 20–200 nm¹³¹. Disadvantages of mRNA are that it may invoke immune responses or be unstable, but both concerns can be circumvented with appropriate chemical modifications^{9,132}.

Nucleic Acid-Based Constructs & Devices: Nucleic acids can be designed to form higher-order two- or three-dimensional shapes with extreme precision. An emerging example is that of DNA origami, a concept that rose to prominence in 2006¹³³. With this approach precise nanostructures of pre-determined size and shape can be assembled into template structures via specific folding interactions. Tian et al. recently developed octahedrons of ~60 nm with encoded sites for molecular positioning, allowing multiple nanoparticles with different functions to be integrated into a single structure¹³⁴. In another example, DNA icosahedra found use as vehicles for quantum dots¹³⁵. DNA origami, with a limited number of binding sites, has recently been used to calibrate fluorescence for determination of protein copy number inside cells¹³⁶. Oligonucleotides may also be deployed inside cells as probes. For example, molecular beacons are short (~25 base) hairpins featuring internally quenched fluorophores that alter their fluorescence upon hybridizing with a target sequence^{137,138}. Aptamers, previously mentioned as inhibitors, can also be used as conjugates, receptor-targeting moieties, intracellular biosensors, and imaging probes^{139–142}.

Hard-to-Transfect Cells: While the challenge of transfection has been adequately addressed for many cell types, particularly immortalized cell lines *in vitro*, effective transfection remains a significant hurdle for primary cells. Moreover, even when high transfection efficiencies are achieved, toxic and off-target effects may confound results. This is a well known barrier in studies of immune cells, where cell types such as T cells, B cells, natural killer cells, dendritic cells, and macrophages have proven difficult to

transfect^{103,143–155}. Primary stem cells, cells of the hematopoietic lineage, and neurons are other prominent examples^{156–159}. The ability to conduct biological studies in these important cell types is often restricted by limitations on transfection efficiency and tolerance to treatment. Thus, while there has been a huge amount of work on refining transfection approaches over the last decades, unresolved frontiers still exist.

2.2.2 Proteins & Peptides—Proteins are polymers of amino acids that form three-dimensional, tertiary, structures with specific biological functions. Proteins catalyze biochemical reactions, transmit signals, form receptors and transporters in membranes, and provide intracellular and extracellular structural support. Peptides are shorter sequences of amino acids, generally less than 40, that may or may not form defined three-dimensional structures.

Brief History of Protein Delivery: Intracellular delivery of purified proteins began in the 1960s, even before the advent of nucleic acid transfection. In proof-of-concept demonstrations, amoebae were microinjected with ferritin (450 kDa)¹⁶⁰ and mouse eggs with bovine albumin (67 kDa)¹⁶¹. In the 1970s, more advanced studies were carried out, as proteins labeled with fluorescent dyes were delivered into living cells to investigate intracellular processes and structures^{162–166}. Concomitantly, protein delivery was reported by new methods such as fusion of red cell ghosts^{167–169} and liposomes^{170,171}. After that came transient permeabilization approaches including hypotonic shock^{172,173}, osmotic lysis of pinosomes^{174,175}, Paul McNeil's scrape¹⁷⁶, bead¹⁷⁷ and syringe¹⁷⁸ loading methods, detergent exposure¹⁷⁹, electroporation^{180,181}, and treatment with the pore-forming toxin Streptolysin O (SLO)^{182,183}. Since 2000, a new generation of membrane disruption delivery techniques has been developed through the precision conferred by microfluidics and nanotechnology⁵⁸, such as cell squeezing¹⁸⁴ and nanoneedles¹⁸⁵.

In comparison to transfection, reagents for protein delivery came on stage relatively late, inspired by the rise of lipid and polymer compounds for DNA delivery in the 90s (see review¹⁸⁶). Protein delivery mediated by chemical carriers is also referred to as protein transduction, or less often by the misnomers protein transfection or profection¹⁸⁶. In general, there are four categories reported: 1) Lipid and polymer compounds analogous to transfection reagents^{187–189}, 2) Cell penetrating peptides (CPPs), also known as protein transduction domains (PTDs)^{190,191}, 3) Bacterial toxins and viral components^{192–196}, and 4) Engineered nanocarriers^{197–199}. Lipid and polymer reagents, while successful for some proteins, are not a one-size-fits-all solution. Unlike DNA and RNA, proteins are vastly different in size, charge, and structure. Thus, the reagents can only be optimized for a limited set of proteins¹⁸⁶. On the other hand, PTDs and CPPs, can be attached to most proteins but they are prone to endocytic entrapment, cell toxicity, and poor efficiency of cytosolic delivery²⁰⁰. Despite promise, the history of PTD and CPP research is rife with artifacts and controversies regarding delivery mechanisms^{191,201,202}. Protein delivery via attachment to bacterial toxins and viral components is similar in many ways to PTDs and CPPs, but with more precise, well-defined mechanisms^{193,196}. The idea is to mimic pathogenic entry process by targeting the protein of interest to a particular endocytic pathway then triggering natural mechanisms of endosome escape. However, this strategy has to be tailored to

particular cell types, is quite preparation-intensive, and not tangible for most researchers seeking to perform protein delivery. Lastly, engineered nanocarriers have seen a huge rise of interest in the last 15 years. They can be designed as higher ordered structures with multifunctional and stimuli-responsive properties. Such nanocarriers are constructed from, and functionalized with, combinations of biomolecules, lipids, polymers, and inorganic materials. They have yet to be translated into commercial products. Overall, intracellular delivery of proteins still has a long way to go. For example, a comparative study of available techniques for antibody delivery suggested electroporation remains the best option for loading effective concentrations into cells *in vitro*²⁰⁰.

Research Motivations: Straightforward intracellular delivery of proteins and peptides holds significant, yet currently unrealized, potential for many areas of science and medicine¹⁸. Delivery of proteins into living cells, such as genome-editing nucleases²⁰³, active inhibitory antibodies²⁰⁰, or stimulatory transcription factors³¹, represents a powerful toolset for manipulating and analyzing cell function¹⁸. For example, the localization and visualization of engineered antibodies within living cells, in conjunction with precise perturbation of their associated cellular processes, may allow functional analysis at a level not possible with genetic methods²⁰⁰. As well as classical antibodies (~150 kDa), a number of recombinant small antibody-based molecules such as immunoglobulin (Ig) derived Fab (~50 kD) and scFv (~25 kD), non-Ig derived monobodies (~10 kD), nanobodies (~14 kDa), and affibodies (~6.5 kD) have been developed²⁰⁴. When combined with fluorescent labels they are able to serve as precise functional probes for intracellular imaging applications²⁰⁵. There are many cases when direct protein delivery is favorable over indirect expression from nucleic acids, for example to avoid the risk of insertional mutagenesis associated with DNA transfection. However, one challenge is that the amount of protein delivered has to be sufficient to generate the desired effect, whereas plasmid DNA can be amplified by replication. Unlike nucleic acids, with their uniform properties, one-size-fits-all protein delivery has been elusive due to the inherent variance in size, structure and charge amongst proteins^{18,206}.

Expanding Protein Therapeutics Through Intracellular Delivery: Since the advent of human recombinant insulin in 1982, the number of protein therapeutics has been growing rapidly²⁰⁷. There now more than 200 approved protein therapeutics, of which around half are monoclonal antibodies. According to market reports, annual worldwide revenue from protein therapeutics is anticipated to reach USD 200 billion by 2020. Protein therapeutics can be grouped into molecular types that include antibody-based drugs, anticoagulants, blood factors, bone morphogenetic proteins, engineered protein scaffolds, enzymes, Fc fusion proteins, growth factors, hormones, interferons, interleukins, and thrombolytics^{207,208}. Notably, these therapeutics exert their action outside the cell, by modulating molecular interactions in the blood, interstitial fluids, or at the cell membrane. Part of the success of protein therapeutics is due to their intrinsic precision. In particular, proteins and peptides can generate surfaces capable of recognizing targets that their small molecule counterparts fail to¹⁸.

Around two thirds of the human proteome lies inside the cell, inaccessible to binding by impermeable molecules²⁰⁹. Such proteins are currently unavailable for therapeutic

modulation. While an extensive discussion of intracellular protein delivery *in vivo* is beyond the scope of this review, it is important to note that protein delivery also holds a key role in *ex vivo* cell-based therapies. One example is the preparation of anti-tumor vaccines for cancer immunotherapy. By loading mutant tumor proteins into dendritic cells, they can be programmed to prime cytotoxic T cells to attack and kill tumor cells exhibiting those same mutant proteins. The strategy has been verified in animal models^{210,211} and is beginning to be tested for safety and feasibility in clinical trials^{212,213}. Intracellular delivery of genome editing molecules is another area where intracellular delivery of proteins may lead to advances from basic biology to cell-based therapies.

Gene Editing Through Intracellular Delivery of Nucleases & RNPs: Gene editing allows precise, targeted changes in the genomic DNA of a cell¹⁶. Recent advances rely on enzymes known as nucleases, protein machinery that can cut or alter DNA. Key examples include zinc fingers (ZFNs), transcription activator-like effector nucleases (TALENs), meganucleases, and the clustered regularly interspaced short palindromic repeats (CRISPR)/Cas system of RNA-guided nucleases. CRISPR-based gene editing is usually performed with the bacterial nuclease Cas9, which forms a complex, or ribonucleoprotein (RNP), with a single guide RNA (sgRNA) to become targetable and active²¹⁴. The resultant Cas9 RNP is capable of cleaving DNA that is complementary to a 20-nt sequence within the sgRNA. Genome editing requires that nucleases enter the nucleus to exert their action on genomic DNA^{16,215}. In the case of CRISPR, initial studies in live cells introduced Cas9 indirectly via expression from plasmids or mRNA^{215,216}. However, subsequent experimentation with delivering the pre-formed Cas9 RNP indicates this to be a more efficient and straightforward approach^{217,218}. RNP delivery was shown to be a superior method when tested in therapeutically relevant cells types, such as iPSCs, primary T cells and HSCs^{219–221}.

Since the first reports in 2014, Cas9 RNPs have been delivered by electroporation^{218,219,221,222}, microinjection^{223,224}, lipid nanoparticle formulations²²⁵, osmotically-induced endocytosis followed by endosome disruption²²⁶, microfluidic deformation²²⁷ and CPPs²²⁸. Typically, sgRNA is about 100 base pairs of single-stranded RNA (~30 kDa, -100 charges) while native Cas9 is ~158 kDa (~10 nm diameter) with theoretical net charges of +22^{225,229,230}. Thus, the resultant RNP complex should have about -80 negative charges, be ~188 kDa, and up to 15 nm in size (Table 1). These properties may also explain the relative success of electroporation methods for RNP delivery²⁰³. They also make Cas9 RNPs amenable to complexation with cationic lipid and polymer reagents for carrier-mediated delivery^{225,231,232}. Indeed, other types of RNPs, have previously been delivered with cationic polymer reagents²³³. RNP delivery strategies are currently a topic of intense research for the purpose of therapeutic genome editing, especially for *ex vivo* cell-based therapies^{15,29}. Recently, CRISPR-based gene therapy for correction of disease-causing genes was achieved in human embryos²³⁴. Cas9-sgRNA RNPs and a 200-mer ssODN correction template were microinjected into human embryos for correction of a common 4 basepair deletion in the MYBPC3 gene known to cause hypertrophic cardiomyopathy²³⁴.

Delivery-Relevant Properties of Proteins & Peptides: Most proteins lie in the range of 5 kDa up to several hundred kDa, which corresponds to physical dimensions of 2–20 nm, ~10x smaller than the encoding mRNA. Peptides are typically below 5 kDa and less than 3 nm in size. Examples of common protein dimensions are green fluorescent protein (GFP, 28 kDa), a 2×4 nm barrel, bovine serum albumin (BSA, 67 kDa), a 12×4×4nm rod, and Cas9 (158 kDa), a globular endonuclease of ~10 nm diameter (discussed above). A typical immunoglobulin antibody (~150 kDa) measures 14×8×4 nm in size²³⁵. Proteins form tertiary structures with hydrophobic residues buried within and hydrophilic segments exposed to the outside. More so than nucleic acids, chemical modifications or packaging in carrier particles may compromise the structure and function of proteins. Delivery formulations have been achieved in some cases²³⁶, but many proteins can be considered specific cases requiring a specific solution. Moreover, proteins denature much more easily than nucleic acids (e.g. due to heat, salt concentrations or pH changes) restricting the treatments that can be used in their formulations.

Effect of Charge on Delivery: The overall charge on proteins and peptides is dependent on the amino acid composition. An excess of arginine and lysine, for example, will bias a molecule toward being positively charged. On the other hand, glutamate and aspartate carry negative charges at pH 7. The majority of proteins, such as antibodies, are mildly negatively charged under physiological conditions while peptides can be highly variable. This is an important consideration because highly positively charged molecular assemblies tend to be more proficient at entering cells. Examples include so-called supercharged proteins²³⁷, cationic cell-penetrating peptides (CPPs) such as the arginine-rich TAT peptide from HIV²³⁸, and cationic lipids and polymers commonly used as transfection agents¹⁰. Strongly cationic molecules are thought to associate robustly to the cell surface, for example via attachment to negatively charged proteoglycans, induce endocytosis, and possibly be more proficient at generating membrane defects¹⁹¹. However, strongly charged molecules may face more energetic barriers to diffuse through disruptions in the plasma membrane unless there is an electrophoretic driving force, such as typically supplied during electroporation pulses²³⁹.

Permeability of Peptides: Unlike nucleic acids and proteins, some peptides possess an intrinsic ability to permeate cells, although mostly at permeability coefficients substantially below typical small molecule drugs. One example is the 11 amino acid cyclic peptide cyclosporin A ($M_w \sim 1.2$ kDa), which is a useful inhibitor of cyclophilin in T cells. Cyclosporin A is a feasible drug for oral delivery due to the reported permeability coefficient within the range of small molecules ($2.5 \times 10^{-7} \text{ cm} \cdot \text{s}^{-1}$ across membranes²⁴⁰), low concentration required for intracellular activity (7–10 nM)²⁴¹, and relative chemical stability conferred by its cyclic conformation. Despite such success stories, many inhibitory peptides are limited in their usefulness due to inconsistent or low cell permeability or sensitivity to degradation by proteases. Researchers in the field have made efforts to decipher the rules governing peptide permeability in the hope of applying this knowledge to design better peptides^{191,242–244}. The challenge is complicated by the observation that multiple entry mechanisms appear possible. The most straightforward is a passive diffusion as a result of the molecule partitioning into the hydrophobic cores of membranes, such as is believed to be

the case for cyclosporin A²⁴⁵. Alternatively, transmembrane transporters have been proposed to shuttle short peptides across the membrane²⁴⁵. Other peptides are believed to induce endocytosis and subsequent endosomal escape. Most cell-penetrating peptides (CPPs) are thought to enter cells via endocytosis¹⁹¹, although other routes such as direct translocation across the membrane, inverted micelle formation, transient pore formation, adaptive translocation, and local electroporation-like effects have been suggested²⁰².

Some general characteristics have been established that appear to promote peptide permeability. For example, most CPPs are between 8 and 20 amino acids long and possess somewhere between 5 and 8 positively charged residues (usually arginines) in various configurations¹⁹¹. Other strategies involve the use of stapled peptides, where a synthetic brace (typically a covalent crosslink between two residues) is added to lock small peptides into an active conformation, often an alpha-helix^{246,247}. For example, Verdine and colleagues produced a synthetic, cell-permeable, stabilized alpha-helical peptide of 16 amino acids that targets a critical protein-protein interface in the NOTCH transactivation complex²⁴⁸. Ongoing research efforts are expected to decode the optimal size, conformation, charge, polarity and amphiphilicity that improve the intracellular delivery of peptides and their cargo.

2.2.3 Small Molecules

Small Molecule Drugs: Small molecule drugs are organic compounds of 900 Da or less, a molecular weight which corresponds to a physical size of 1 nanometer or less. The first small molecule drugs were natural products isolated from plants, microbes, marine invertebrates, or other lifeforms. An early example is morphine, a metabolite purified from opium extract in 1815 and dispensed by Merck as pain relieving medicine from 1827²⁴⁹. Today thousands of small molecule drugs are used as medicines. Advances in chemistry have enabled the purification of countless natural products, production of derivatives and mimics of them, or completely synthetic compounds²⁴⁹.

If the drug target is intracellular, one of three scenarios makes it feasible 1) passive diffusion across the membrane, 2) active transport through membrane proteins, or 3) intracellular delivery. Small molecules that exhibit passive membrane permeability usually align with Lipinski's classic "rule of 5"²⁵⁰. Such molecules should ideally be less than 500 Da, of intermediate lipophilicity, of limited hydrogen bonding capacity, and uncharged. These requirements have been used to narrow drug discovery efforts to candidates that are likely to be bioavailable. This is especially important for synthetic molecules. On the other hand, a number of natural products undergo active transport, and in these cases do not need to be permeable or obey Lipinski's rule of 5²⁵¹. Oxidized ascorbate, for example, is membrane impermeable due to its hydrophilic nature but readily undergoes transport into cells through GLUT1, a glucose transporter that is overexpressed in many cancer cells²⁵².

In instances where small molecules are neither permeable nor actively transported, intracellular delivery is required. One of the simplest strategies is to administer the molecule alongside a solvent such as ethanol or DMSO. Not only do these solvents improve the solubility of the small molecule, they may also increase the incidence of nanoscale membrane defects that assist the passage of small molecules across membranes²⁵³.

Alternatively, several anti-cancer drugs have been encapsulated in nanocarriers such as liposomes to improve their intracellular delivery¹. Intracellular delivery enables the deployment of drugs that are larger than 500 Da. An example is bleomycin (M_w 1.4 kDa, ~2 nm diameter), an anti-cancer drug with poor permeability due to its positive charge and hydrophilicity. Its potency can be increased more than a hundred fold by cell permeabilization through electroporation^{254,255}. This strategy has been demonstrated both *in vitro* and *in vivo*²⁵⁵.

Small Molecule Probes: Apart from drugs, another category where small molecules are useful is as intracellular probes²⁵⁶. PBFI (~0.9 kDa) is a fluorescent dye that can be employed for the measurement of intracellular potassium concentration, however, it is naturally cell impermeable^{257,258}. The native form of PBFI can be loaded into cells via intracellular delivery methods such as osmotic lysis of pinosomes, microinjection, or electroporation. Alternatively, it can be AM-esterified to shield the charge, thus making it more permeable. Once inside cells, the AM ester is hydrolyzed by intracellular enzymes and the dye returns to the natural, impermeable state²⁵⁸. This approach has become a standard practice for monitoring intracellular potassium concentrations. Other small molecule probes requiring intracellular delivery are terbium cryptate probes (~1 nm)²⁵⁹. Researchers have delivered them to the cytosol by osmotic lysis of pinosomes or transient permeabilization with pore-forming toxins^{260,261}. Upon loading, the terbium-based probe TMP-Lumi4 enables luminescence resonance energy transfer (LRET) for imaging of specific protein–protein interactions in live cells²⁶¹.

Cryoprotectants: Cryoprotectants are substances used to protect biological cells and tissues from freezing damage incurred by ice crystal formation. Penetrating cryoprotectants such as DMSO, glycerol, and ethylene glycol are small enough to enter the cytosol but limited in their cryoprotection capabilities. Impermeable sugars may be better cytoprotectants, but are highly hydrophilic and do not readily diffuse across cell membranes. Trehalose (M_w 342 Da) is a natural disaccharide synthesized by a range of organisms to withstand desiccation or freezing. Studies have shown that intracellular loading of trehalose into animal cells at concentrations up to 0.2 M may provide superior cryoprotection compared to alternative methods^{262,263}. So far delivery strategies include influx during thermal shock²⁶⁴, stimuli-responsive nanocarriers²⁶⁵, engineered pores²⁶⁶, and electroporation^{267,268}.

2.2.4 Synthetic Nanomaterials & Devices—Synthetic nanomaterials and devices represent another frontier where demand for suitable intracellular delivery solutions exceeds supply^{17,269}. Probes engineered from functional nanomaterials, including carbon nanotubes(CNTs)^{270–272}, quantum dots^{273,274}, and various fluorescent reporter probes^{17,275–278}, have potential as sensors for intracellular processes. Yet ineffective intracellular delivery, a poor understanding of their interaction with biological environments, and toxicity issues have retarded their deployment in the cellular context. Many of these materials and devices still await systematic intracellular testing due to ineffective delivery^{17,269,279}. Thus, the delivery challenges of these molecules and unconventional materials must first be addressed before their potential in research, therapeutic and

diagnostic applications can be fully realized. Below we highlight several examples of progress in the field.

CNTs have been proposed as sensors, labels and next-generation devices in biological applications^{271,280}. The smallest single-walled configurations exhibit diameters from 1.2 nm and lengths spanning from tens of nanometers up to microns²⁸¹. Chemical functionalization can be employed to increase the solubility and biocompatibility of CNTs²⁸¹, however their toxicity profiles and suitability for intracellular applications are still a matter of controversy²⁸². One example where they have been useful in probing the intracellular environment was published by Fakhri et al. in which functionalized CNTs were loaded into cells by electroporation²⁷². By tracking the near-infrared luminescence of kinesin-targeted single-walled CNTs, they observed a regime of non-equilibrium stirring dynamics driven by active cellular motors²⁷². Another recent study used microinjection to load high concentrations of single-walled CNTs of length ~150 nm into frog embryos²⁸³. The localization of CNTs and potential toxicity were tracked throughout the growth of the animal. They found CNTs tended to localize to the perinuclear region within most cells, however, there were no obvious structural defects, developmental abnormalities or toxicity to report²⁸³. These results suggest CNTs might be safe for intracellular applications.

Quantum dots are semiconductor crystal configurations in the size range <10 nm. Due to their advantageous optical properties, intracellular labeling and analysis applications have been proposed^{274,284}. Quantum dots are usually negatively charged and surface passivation with a poly-ethylene glycol (PEG) shell is a standard strategy to increase the biocompatibility of the structure, with a final diameter of 20 nm being typical for this configuration²⁷⁹. An early study compared microinjection, electroporation, and lipid transfection reagents for quantum dot delivery into cultured cells²⁷³. The investigators found that lipid reagents and electroporation failed to disperse the dots homogeneously into cells, instead leading to aggregation or endosomal entrapment. On the other hand, low-throughput microinjection was able to deliver quantum dots homogeneously to the cytoplasm. Since then a number of approaches have been tested for quantum dots delivery. They include osmotic loading of pinosomes²⁸⁵, CPPs²⁸⁶, microfluidic cell squeezing²⁸⁷, controlled laser-induced cavitation^{288,289}, detergent permeabilization²⁹⁰, and successful examples of electroporation^{291,292}. We point the reader to dedicated reviews on intracellular delivery of quantum dots for further information^{279,293,294}.

Various nanoparticle systems have also been deployed as intracellular temperature probes²⁹⁵. In one report, temperature-responsive nanodiamonds of approximately 100 nanometer were introduced into cells via nanowires²⁹⁶. The nanodiamonds were then used as local temperature gauges to perform nanometer-scale thermometry in living cells at microkelvin resolution²⁹⁶. Another study used smaller, but less accurate, particles for intracellular temperature measurements. Okabe et al. prepared a fluorescent polymeric thermometer of ~9 nm diameter, functionalized it with hydrophilic residues, and microinjected it into the cytoplasm of living cells. With a temperature measurement resolution of 0.18–0.5 K, they claimed to measure temperature differences between various organelles²⁹⁷.

2.2.5 Large Cargo—Relative to most cells, large cargo is anything from hundreds of nanometers up the range of the cell itself (usually tens of microns). Examples of large cargo that have been delivered into cells are shown in the bottom left of Figure 3, and include bacteria, mitochondria, whole chromosomes, microbeads, sperm, nuclei, and micro-electro-mechanical systems (MEMS) devices. The first demonstration of large cargo delivery occurred alongside the invention of microinjection itself in 1911²⁹⁸. Marshall Barber demonstrated that a single bacteria, once inside the cytoplasm of a plant cell, was sufficient to kill it^{298,299}.

For a century microinjection has been the dominant method for introducing large cargo into cells. Microinjection was used for the first nuclear transplant experiments that surgically dissected the nucleus from blastula cells and inserted them into living frog eggs³⁰⁰. To the amazement of the researchers, these eggs then had the potential to grow and produce a new animal. Building on this breakthrough, John Gurdon and colleagues showed that nuclei transplanted from fully differentiated somatic cells were capable of generating a new animal^{301,302}. Gurdon later shared the Nobel prize for “the discovery that mature cells can be reprogrammed to become pluripotent”. Microinjection was also required for the nuclear transplant that led to the first mammalian cloning, as exemplified by the birth of Dolly the sheep in 1997³⁰³. In an unconventional form of gene therapy, transplant of pronuclei from human eggs with pathological mitochondria to donor eggs with functional mitochondria has been shown to correct diseases of mitochondrial inheritance³⁰⁴.

Other examples emphasizing the importance of microinjection in biotechnology include *in vitro* fertilization (IVF) and chromosome or mitochondrial transplantation. IVF occurs through the artificial delivery of sperm into eggs cells. The IVF concept was first demonstrated through microinjection of sperm into sea urchin eggs³⁰⁵. Decades of optimization extended IVT to culminate in IVF in the first human pregnancies in the early 90s³⁰⁶. Chromosome transplantation techniques have also been described with microinjection apparatus³⁰⁷. Indeed, artificial chromosomes have been engineered and transferred into cells by microinjection for transgenic studies or proof-of-concept gene therapy^{308,309}. In another example of large cargo delivery, transplant of mitochondria (~1–2 μm) via microinjection has been demonstrated in several different cell types and model systems^{310–312}.

While microinjection has traditionally dominated large cargo delivery, it is not the only option. Indeed, several rival methods have arisen mainly out of the need for greater throughput. For example, Chiou et al. pioneered an approach using laser-triggered cavitation bubbles to deliver ~2 μm bacteria into cultured cells at both single cell³¹³ and high throughput scales³¹⁴. The same approach was extended to delivery of functional mitochondria for studies of mitochondrial dysfunction in metabolic diseases³¹⁵. Another method of mitochondrial transfer is cell fusion, where the mitochondria are supplied from donor cells^{316,317}. In studies involving gene therapy with human artificial chromosome they are also transferred by cell fusion, in a process termed microcell-mediated chromosome transfer (MMCT)^{62,318–321}. Engineered CHO donor cells carry the human chromosome and are triggered to fuse with the acceptor cell, thus transferring the genetic material³¹⁸.

Apart from delivery of organelles and subcellular components, insertion of large synthetic materials and devices is another area of recent interest. As a case in point, micron-scale particles, spheres, and beads are loaded into cells for intracellular microrheology studies that analyze the internal mechanics and dynamics of cells. So far they have been delivered by microinjection^{322,323} or ballistic propulsion^{324–327}. A recent study microinjected PEGylated tracer beads of up to 0.5 μm into cells to show that motor-driven cytoplasmic mixing substantially enhances intracellular movement of both small and large components³²⁸. In other instances, MEMS can measure intracellular properties, such as cytoplasmic pressure³²⁹. One group deployed a MEMS-based intracellular hydrostatic pressure sensor, about 6 microns in size, that was claimed to be delivered into HeLa cells via lipofection³²⁹. The same researchers also microinjected silicon MEMS barcodes up to 10 μm in length into mouse embryos for tracking and labeling purposes³³⁰.

3. Approaches for Intracellular Delivery

As outlined in the previous section, a diverse range of cargos has been introduced to the intracellular space through a wide range of delivery approaches. Here, we categorize these approaches according to the mechanism at the plasma membrane (Figure 4), rather than traditional classifications of biological, physical, and chemical techniques^{331–335}. As the cell is agnostic to our distinction between scientific disciplines, we believe this categorization better reflects mechanistic exploration⁹⁶. Broadly, methods may involve either 1) disruption of the cell membrane to facilitate entry of cargo, or 2) packaging with carriers, which then undergo uptake into endosomal trafficking routes or fuse with the host cell membrane. Although chemical or structural modifications can be used to increase the passive permeability of some small molecules or short peptides, most cargo of interest require an active delivery method.

3.1 Carrier-Mediated

Most of the early developments in carrier-mediated delivery were directed towards nucleic acid transfection, particularly for DNA plasmids. As mentioned in the transfection section (see 2.2.1), cationic lipids and polymers can condense plasmids and other nucleic acids into solid nanoparticles with dimensions down to tens of nanometers^{10,75,76}. This makes the task of delivering these molecules significantly more manageable. The positive charge of these particles facilitates their interactions with the cell surface, which is negatively charged due to the typical -35 to -80 mV membrane potential of cells. The positive charge may also promote binding to certain receptors¹⁰. Upon binding, subsequent internalization via endocytosis is thought to be most efficient for particles in the size range $50 - 100$ nm³³⁶. Nanoparticle complexes additionally confer protection of DNA from degradation in the cytoplasm³³⁷. One possible disadvantage of complexation may be delayed unpacking, making it inaccessible for expression³³⁸ or excessive toxicity³³⁹. In the last two decades researchers have expanded the scope of transfection strategies to include carriers designed from lipids, polymers, inorganic nanomaterials, carbon nanotubes, protein-based nano-assemblies and functionalizations with various peptides, ligands, and chemical modifications^{6,7,9,10,337}.

The other major type of carriers for nucleic acid delivery are viral vectors, which exploit the viral infection pathway to enter cells but avoid the subsequent expression of viral genes that leads to replication and pathogenicity⁶¹. This is done by deleting coding regions of the viral genome and replacing them with the DNA to be delivered, which either integrates into host chromosomal DNA or exists as an episomal vector. At present, viral vectors are the most clinically advanced nucleic acid delivery agents owing to their high efficiency and specificity. They were first employed from the 1970s - constructed from SV40³⁴⁰ or retroviruses^{341,342}. New generations of viral vector platforms have been produced based on components from lentivirus, retrovirus, adenovirus or adeno-associated virus, and other viruses³⁴³⁻³⁴⁵. While highly efficient for DNA delivery, key weaknesses of viral vectors are: 1) labor-intensive and expensive protocols; 2) safety issues, 3) liable to cause immune/inflammatory responses; 4) integration into the genome with recombinant vectors; risk of insertional genotoxicity, 5) limited packaging capacity (Adeno and AAV typically restricted to carry 5 to 7.5 kb)^{159,346}. These issues continue to motivate the development of non-viral carriers^{9,10,347}.

Beyond nucleic acid transfection, researchers initially explored protein delivery through the use of red cell ghosts¹⁶⁷⁻¹⁶⁹ and liposomes^{170,171}. Newer generations of nanocarriers are now being designed to address intracellular delivery of proteins on a broader scale^{6,199,206,348}, although these developments are more at a nascent stage. Intracellular delivery of genome editing complexes is a particular application that is driving the evolution of next-generation nanocarriers^{231,232}.

Mechanistic investigations indicate that most carriers enter cells via endocytosis before escaping into the cytoplasm^{336,349-351} (Figure 5). Cargo not able to escape endosomes are trafficked through lysosomes for degradation or recycled back out to the cell surface³⁵²⁻³⁵⁴. Maximal efficiencies of around 1% endosomal escape have been reported for the most advanced nonviral carrier strategies, including lipid nanoparticles^{353,355} and cell-penetrating peptides¹⁹¹. Moreover, the exact mechanisms of endosome escape remain unclear and are a matter of ongoing research^{352-354,356}. Alternatively, some carriers are able to fuse with the plasma membrane. These systems were first inspired by viruses that deploy specialized surface proteins to induce fusion with target membranes^{169,357}.

Fusogenic carriers are bound by a phospholipid bilayer that hosts the fusion machinery. Examples include cell ghosts, dead cells that have had their cytoplasm replaced with cargo^{169,357}, and virosomes, loaded vesicles reconstituted to display functional viral proteins³⁵⁸. More recently, cell-derived vesicles known as exosomes have been discovered to fuse with target cell membranes for the exchange of RNA and proteins between immune cells³⁵⁹. Although the exact fusion mechanisms are yet to be described, it is anticipated that exosome-inspired systems may represent a new generation of vehicles for efficient and biocompatible intracellular delivery³⁶⁰.

3.2 Membrane Disruption-Mediated

Unlike carriers that may be restricted in the feasibility of cargo-carrier combinations, membrane disruption-based strategies are near-universal, being able to rapidly deliver almost any cargo that can be dispersed in solution (Figures 4 & 5). The challenge for membrane

disruption-based approaches is 1) to open up the right kind of holes in the plasma membrane to achieve substantial delivery of the cargo, and 2) to avoid undesirable cell perturbation or death associated with membrane damage. The main two ways this is accomplished are through direction penetration or permeabilization.

3.2.1 Direct Penetration—Strategies involving direct penetration use a conduit or vehicle to break through the membrane, thereby creating a passage for the cargo. Prevalent examples are microinjection, ballistic particles, and nanoneedles, as shown in Figure 4. Microinjection is the first intracellular delivery method to be invented and a classic case of a direct penetration strategy^{299,361}. The cell membrane is disrupted with a pipette, which is then used to pump fluid containing the molecule of interest inside the cell. Nanoneedles operate on a similar principle except that they are scalable in large arrays and typically consist of finer, more intricately fabricated structures^{185,362,363}. Ballistic particles are coated with the material to be delivered and fired at high velocity into the cell³⁶⁴. They are categorized as membrane disruption in this review (rather than carriers) due to the critical role of active force in puncturing the cell membrane to achieve access. In all direct penetration strategies the damage sustained by the plasma membrane or other cellular structures must subsequently be repaired.

3.2.2 Permeabilization—In contrast to direct penetration, permeabilization strategies make the cell transiently permeable to cargo present in the extracellular solution. The membrane is considered permeable when membrane disruptions are of sufficient size and lifetime to permit passage of the cargos of interest. Thus, the threshold level of permeabilization needed depends on the properties of the cargo. Terms that have been used to describe membrane disruptions include pores, defects, inhomogeneities, lesions, holes, and perforations.

As seen in Figure 4, many different permeabilization strategies have been attempted. They range from mechanical and laser-based to electrical and chemical^{331,365–367}. The key events associated with permeabilized-based intracellular delivery are shown in Figure 6. First, the cargo of interest is dispersed into solution at a concentration conducive to influx. Second, the cells are exposed to the membrane disruption event. Physical methods of permeabilization generally have better control of the intensity, duration, and placement of the membrane disruption effect^{331,366}. Biochemical methods, such as exposure to pore-forming toxins, are more scalable but can be harder to control since it is not a discrete event³⁶⁵. Upon membrane disruption cargo begins to diffuse into the cell according to its concentration gradient while some cytoplasmic contents are lost. In some cases, additional effects, such as electrophoretic force, can also be harnessed to augment influx of the cargo. Third, within several seconds of membrane disruption, the target cell responds with membrane active repair processes. Healing of the plasma membrane can take anything from a few seconds up to several minutes to complete. Once membrane integrity is restored, the cell may engage metabolic and transport processes to restore cytoplasmic composition and bring itself back to full health^{368,369}. Most permeabilization strategies apply specific conditions, such as temperature and buffer composition, to first promote permeabilization and delivery, and then facilitate cell recovery. The membrane disruption must not be too

severe or prolonged, otherwise the cells will be unable to repair and recover. Effective permeabilization strategies must therefore find a balance, optimizing both the membrane damage and cell treatment conditions.

The remainder of this review will focus on membrane disruption-based approaches. This exploration will mostly be centered around animal and mammalian cells *in vitro* and *ex vivo*. In the next section we will discuss background concepts helpful in understanding how and why membrane disruption can be a successful approach. Following that, we will offer a detailed appraisal of the various delivery methods. Each section will cover content areas that include history, mechanisms, feasibility, performance, toxicity, applications, technical advances, and envisaged future opportunities.

4 Membrane Disruption-Mediated Delivery: Background Concepts

In this section we will discuss cell and membrane properties, mechanisms of membrane disruption, and cell response to membrane disruption. These background concepts lay a foundation to explore the common issues that arise in membrane disruption-based intracellular delivery. The following sections then examine all the direction penetration (section 5) and permeabilization (section 6) methods.

4.1 Cell Structure & Properties

Plasma Membrane Function—The primary barrier to intracellular delivery is the plasma membrane, which defines the essential boundary between inside and outside of a cell. The plasma membrane enables cells to control their composition and properties. It is composed of a ~5 nm thick phospholipid bilayer with polar heads facing the aqueous environment and fatty acyl chains pointing inward to form a hydrophobic core. This hydrophobic core is the main limiting barrier to the passage of macromolecules and polar molecules. The permeability of a given molecule across such a lipid membrane depends on the properties of the membrane (e.g. composition, heterogeneity, thickness), the properties of the molecule itself (e.g. charge, size, polarity), and environmental factors (e.g. temperature)^{245,370}.

The plasma membrane allows compartmentalization of electrolyte concentrations between the cell interior and external solutions (Figure 7A). For example, relatively high intracellular potassium (140 mM) and low sodium (5–15 mM) are generated by the action of the Na⁺/K⁺ ATPase, a plasma membrane-embedded transport protein. Intracellular chloride, calcium, and magnesium are all lower than their corresponding extracellular concentrations. The maintenance of these electrolyte gradients is key for the typical negative membrane potential (–35 to –80 mV) of most animal cells and a host of other essential functions. The cell also has a higher concentration of metabolites such as ATP (typically ~2–5 mM), amino acids and other biomolecules. The difference between intracellular and extracellular composition is an important consideration in membrane disruption-based intracellular delivery, as strategies that factor this into account can lead to more efficiency treatments and better cell health. Minimizing the depletion of intracellular contents, for example, can improve treatment outcomes (see section 4.3).

Plasma Membrane Composition & Properties—The plasma membrane has characteristic properties distinct from other types of lipid membranes (Figure 7B). It is much more complex and dynamic than pure lipid bilayers, containing hundreds of different lipid species and up to 50% membrane proteins by weight. Proteins associated with the plasma membrane include various transporters, receptors, and enzymes, and may span the membrane via transmembrane domains or be anchored to one side via lipophilic appendages. The spatial organization of plasma membranes features both lateral heterogeneity (lipid domains) and uneven distribution between inner and outer leaflets (lipid asymmetry)³⁷¹. Cells use up to 5% of their genes for synthesis of a diverse array of lipids, reflecting the importance of the functions arising from this diversity³⁷².

The different types of lipids are distributed in a highly regulated and distinct manner across the various membranes of the cell, giving them unique properties³⁷¹ (Figure 7B). In eukaryotes there are three main categories of membrane lipids: glycerophospholipids, sphingolipids, and sterols. Glycerophospholipids are the major structural lipids of membranes, of which common species are phosphatidylcholine (PtdCho), phosphatidylethanolamine (PtdEtn), phosphatidylserine (PtdSer), and phosphatidylinositol (PtdIns). Their hydrophobic tail is a diacylglycerol (DAG), which contains saturated or *cis*-unsaturated fatty acyl chains of varying lengths. Unsaturated tails don't pack as tightly, increasing the lateral space between lipids and promoting lateral fluidity in the membrane. PtdCho is the most common lipid, accounting for >50% of the phospholipids in most eukaryotic membranes³⁷¹. PtdSer and PtdIns exhibit negatively charged head groups and localize to the inner (cytoplasmic) leaflet. The major sphingolipids in mammalian cells are sphingomyelin (SM) and sugar-decorated glycosphingolipids (GSLs). The sphingolipids feature a ceramide as their hydrophobic backbone, having saturated (or *trans*-unsaturated) tails so they tend to form a taller, narrower cylinder shape than their glycerophospholipid counterparts.

Sterols are highly abundant in the plasma membrane, contributing greatly to barrier function and lateral organization^{373,374}. In mammals, the predominant species of sterol is cholesterol, which represents up to 40% of the lipid molecules in the plasma membrane³⁷⁴. This is in contrast to other internal membranes, such as the endoplasmic reticulum (ER), where the corresponding number is only ~5%. Cholesterol tends to straighten out hydrophobic chains and fill in structural defects in membranes. Thus it serves to stiffen and thicken the plasma membrane, improving its durability. Cholesterol is also essential to the formation of lipid rafts, which are characterized by the assemblage potential of sterol-sphingolipid interactions and particular proteins that have affinity for the raft phase (i.e. raft proteins)³⁷⁴. These lateral raft domains are thought to serve as platforms for key structural, signaling and membrane trafficking phenomena, such as the nucleation of caveolae pits in the plasma membrane³⁷⁵. In contrast to the plasma membrane, internal membranes such as the ER, feature less cholesterol, more unsaturated lipids, and less diversity of lipid species³⁷¹. These membranes are thinner, sparser, and less durable, being more adapted for biogenesis rather than the comparatively robust and stable barrier function of the plasma membrane³⁷¹.

The unique characteristics of the plasma membrane are a key factor in certain membrane disruption strategies. For example, certain pore-forming toxins, such as cholesterol-

dependent cytolysins (CDCs)³⁷⁶, and detergents, such as saponins³⁷⁷, are specific for high cholesterol-containing membranes. This makes it possible to disrupt plasma membranes in a relatively specific manner without damaging internal membranes³⁶⁷.

Intrinsic Membrane Permeability—Although the plasma membrane comprises a highly regulated barrier to control the intracellular composition, it is naturally permeable to certain substances. Phospholipid bilayers are permeable to gas molecules such as O₂, CO₂, N₂ (permeability coefficients 10¹ – 10⁻² cm·s⁻¹), solvents such as H₂O, ethanol, and dimethylsulfoxide (DMSO) (permeability coefficients 10⁻³ – 10⁻⁴ cm·s⁻¹), and to some extent other small uncharged polar molecules like urea and glycerol (permeability coefficients 10⁻⁶ – 10⁻⁷ cm·s⁻¹)^{245,378}. Most cell-penetrant small molecule drugs and peptides have permeability coefficients approaching a maximum of about 10⁻⁶ cm·s⁻¹²⁴⁵. Despite their small size, the cations Na⁺ and K⁺ are relatively impermeable with coefficients of 10⁻¹⁴ – 10⁻¹⁵ cm·s⁻¹.

In live cells it is often a challenge to decipher whether permeability arises due to passive properties of the plasma membrane, the presence of membrane transporters and solute carriers, or fluctuations in transient bilayer defects (such as can be promoted by ethanol and DMSO)^{245,379}. In many instances the apparent permeability of a molecule is actually regulated by the cell. For example, membrane proteins called aquaporins increase the flux of water and glycerol³⁸⁰, the expression of which can vary significantly across a cell population or between cell types. The cell actively opens and closes sodium channels to dynamically alter the Na⁺ permeability during action potentials. Furthermore, many small molecule drugs have also been postulated to enter cells via metabolite transporters whose structures they often mimic³⁸¹. In other cases, peptide transporters, such as PepT1 and OATP, have been reported to pump small peptides and peptide-based drugs into cells²⁴⁵. Regardless of the mechanisms, few candidate drug molecules exhibit passive permeability or are amenable to active uptake by the cell. Chemical modifications or conjugations can be conferred to increase the permeability in some cases, but this is not feasible for most macromolecular cargo, especially for those larger than one nanometer in size.

Structure & Properties of the Cell Surface—The durability of the plasma membrane may be reinforced by intra- or extra-cellular scaffolds. Some lipids (e.g. glycosphingolipids) and proteins (glycoproteins) have extracellular carbohydrate domains. When sufficiently dense, these carbohydrate moieties can form a thick outward coating known as the glycocalyx, which is prominent in animal epithelial/endothelial cells and some types of bacteria³⁸². On the interior side, the plasma membrane may be reinforced by the underlying actin cytoskeleton, which can form a cortical structure hundreds of nanometers thick³⁸³(Figure 7C). Other cytoskeletal elements such as microtubules, intermediate filaments, septins, and spectrins can also assemble into supporting structures that affect membrane properties. Because the actin cortex is often more mechanically robust than the plasma membrane, in many cases it is thought to control cell shape and apparent surface area³⁸³. Indeed, the plasma membrane features a plethora of small folds, wrinkles, and reservoirs in the form of outward-protruding actin-filled filopodia/microvilli and actin-void blebs or inward-bending endocytic pits, such as caveolae. The excess of plasma membrane

surface area is thought to be in the range 2–10 fold the apparent cell surface area³⁸³. These excess reservoirs allow the cell to accommodate rapid shape and volume changes without tearing the membrane^{384,385}, a key property to ensure durability of the cell in mechanically challenging environments.

In cases where the plasma membrane is significantly reinforced by other components, it may become more difficult to mechanically disrupt. This is an important factor to consider particularly for mechanical membrane disruption techniques. For example, the cell surface has been reported to exhibit an impressive ability to conform to nanoneedles and other penetrating objects, making intracellular delivery less efficient than anticipated^{386,387}.

As living cell membranes are much more complicated, dynamic, and heterogeneous than artificial lipid bilayers, insights from simplified model systems and simulations must be taken with a grain of salt³⁷⁹. The full complexity of the properties and behavior of the cell surface must be accounted for when thinking about intracellular delivery approaches and the cell response. Furthermore, plasma membrane variability across cell types is a frontier that must be addressed in order to better understand how to target certain cell types.

4.2 Defect Formation in Lipid Membranes

Membrane disruption-based delivery approaches rely on various methods to nucleate and expand defects in the plasma membrane. Mechanistically, the most well studied examples are electroporation and mechanical tension, probably due to their relative simplicity and ease of modeling and simulating. There are also a host of molecules that can bind to and disrupt membranes by chemical means. Here we provide a theoretical overview of the various mechanisms underlying membrane disruption. Further details on the individual disruption methods are discussed later on in their respective sections.

Mechanical & Electrical—Theories seeking to explain the energetics and formation of membrane disruptions by mechanical tension and electrical potential have arrived at very similar models^{388–390}. At near-physiological temperatures, there is a finite probability of thermally-driven defect formation. Such defects take the form of a so-called hydrophobic pore, where a small gap opens up between hydrophobic tails (Figure 8). Hydrophobic pores are thought to be at a local free energy maximum when the radius is around 0.5 nm. From there, further lateral growth permits the rearrangement of hydrophobic tails into a hemispherical conformation at the edge of the pore. Once polar head groups face the aqueous solution, the pore becomes hydrophilic, thereby permitting the passage of water and becoming conductive to electrical charge. Hydrophilic pores are thought to occupy a local energy minimum and thus exhibit notable stability at a minimum radius of around 0.8 nm.

Over time the most likely scenario is that thermal fluctuations lead to closure of a hydrophilic pore. This happens through a reversal over the energy barrier represented by the hydrophobic pore, thus returning to a defect-free lipid bilayer. On the other hand, there is the low probability of crossing the much larger energy barrier towards destruction of the whole membrane bilayer via infinite expansion of the pore. Increased input of mechanical tension or electrical potential into the system tilts the energy landscape towards this possibility. Opposing pore expansion is line tension, an inward force produced around the rim of a

hydrophilic pore. Under certain conditions, line tension has been observed to drive closure of micron-scale holes in giant vesicles and is directly related to the composition of the membrane, being boosted by the incorporation of cholesterol, for example³⁹¹. The line tension may also be influenced by supporting structures, such as the actin cortex, which the cell can regulate to influence membrane resealing³⁹².

Thus, electroporation and mechanical disruption can be viewed in the following way. For a given cell, the combined effects of temperature, expansive electrical or mechanical forces, and line tension within the pores conspire to yield a population of hydrophilic defects of various sizes that can be modeled by a probability density function³⁸⁹. In real world numbers, biomembranes can generally handle up to 3% mechanical area strain³⁹³ or 200 mV electrical potential³⁸⁸ before persistent loss of integrity occurs.

Chemical—Apart from physical insults, a host of chemical agents and effects can lead to membrane perforation (Figure 9). Chemical disruption of lipid barriers can occur through modification of constituent lipids, for example by oxidation, insertion of pore-forming proteins and peptides, and exposure to agents acting as detergents and surfactants. Because the modeling of these phenomena is more complicated, energy landscapes have not been described for most of these scenarios³⁹⁴. Instead, simulations are increasingly being exploited to capture, model, and visualize molecular critical events^{379,395}.

Membrane disruption can proceed via localized chemical reactions, especially peroxidation³⁹⁶ (Figure 9A). Simulations and experiments suggest that oxidized lipids exhibit distorted hydrophobic tails that decrease the lateral ordering of lipids and cause an increased area per lipid head. This in turn triggers bilayer thinning and variations in the lateral diffusion coefficients, which is associated with a decrease in the bending rigidity and increase in membrane deformation and permeability^{397–399}. If the effects are sufficiently extreme and localized, it can lead to formation of membrane pores, as seen in simulations^{379,399}.

Another biochemical trigger for membrane disruption involves the exposure of bilayers to pore-forming agents, predominantly in the form of amphiphilic peptides or proteins (Figure 10B). Subunits associate with the membrane before assembling into a pore complex with variable size ranges, some being as large as several tens of nanometers^{400,401}. Membrane disruption can also occur via detergents or surfactants (Figure 10C). These amphiphilic molecules integrate into the membrane and distort or buckle the bilayer, inducing conformational stresses that relax via pore formation and loss of integrity^{402,403}. Detergents and surfactants thereby solubilize membranes in a concentration-dependent manner^{402,403}.

4.3 Cell Response to Membrane Disruption

The previous subsections covered cell and membrane properties as well as the basic mechanisms how membranes can be disrupted. Here we will examine how cells respond to membrane disruption (summarized in Figure 10). The first response is an urgent call to action to repair the breached membrane. If this is not accomplished rapidly, the cell will die. The second major response from the cell is after membrane repair, where it seeks to rebalance the homeostasis of its intracellular contents. This response takes place over

minutes to hours and will determine whether the cell returns to its previous state, lives with permanent alterations, or dies through a form of programmed cell death. This section provides an overview of these events and the strategies and concepts associated with their manipulation in order to optimize membrane disruption-based intracellular delivery.

Plasma Membrane Repair—Plasma membrane resealing was thought to be a passive process until the mid 90s when Steinhardt and colleagues discovered that rapid exocytosis drives plasma membrane repair⁴⁰⁴. In a mechanism analogous to neurotransmitter release, exocytosis was found to be triggered by calcium influx⁴⁰⁴. The concentration difference between inside (~1 mM) and outside (~100 nM) is ~4 orders of magnitude, and serves as an acute alarm signal to detect and repair plasma membrane breaches⁴⁰⁵.

Since Steinhardt's discovery, a number of different mechanisms and pathways have been implicated in membrane repair. The topic has been discussed in detail in recent reviews^{368,406–414}. Overall, up to six repair variations have been proposed⁴⁰⁸. As illustrated in figure 11, the mechanisms include contraction, exocytosis, patching, internalization, externalization, and plugging⁴⁰⁸. Multiple membrane repair processes may cooperate together to achieve resealing at timescales of anywhere from a few seconds to several minutes⁴⁰⁸. The type of membrane repair is thought to depend on factors such as environmental conditions (e.g. temperature, extracellular ions), size of the hole, and cell type.

Studies have shown that, while large holes (>0.2 μm) cause more immediate trauma in cells, they tend to be detected and repaired more quickly^{369,405,415}. Rapid exocytosis, plugging, and patching are typical mechanisms that cells deploy to repair large holes⁴⁰⁵. For smaller disruptions, internalization through endocytosis or externalization through shedding serves to extract lesions into disposable vesicles^{415–417}. Very small holes, particularly from electroporation or lingering pore-forming toxins, can persist for longer durations and drain the cell of resources^{369,415,418,419}. Thus, strategies to plug small disruptions post-treatment should be of benefit to membrane permeabilization-based methods. In this regard, the polymers poloxamer-188 and PEG have shown potential as cell recovery agents^{178,420–425}. Vitamin E and other lipid antioxidants represent further options for restoring membrane integrity after delivery^{426,427,428}.

Cell Swelling—Although rarely mentioned in the membrane disruption literature, cells tend to swell when their membranes are disrupted in physiological buffers. From Figure 7A one can see that Na^+ and Cl^- will flow into a compromised cell while only K^+ ions will exit. The net influx of osmolytes and osmotically obliged water causes cell swelling through a colloid osmotic effect, a process that goes hand-in-hand with depolarization of the cell membrane potential. Cell swelling has been observed with electroporation^{429–438}, microinjection⁴³⁹, laser optoporation^{440–446}, and exposure to cavitation⁴⁴⁷ or fluid shear⁴⁴⁸. In these reports swelling usually reaches a maximum within 1–2 minutes of membrane disruption before plasma membrane repair and regulatory volume mechanisms synergize to bring cells back to normal volume.

Interestingly, cells can survive up to 50% volume increase and still recover^{429,430,435,437,445,449}. Above that, the risk of instant death from bursting becomes imminent⁴⁵⁰. It is known that swelling activates specific stress signaling events⁴⁵¹ and is a classic hallmark associated with necrotic cell death^{452,453}. Inhibition of cell swelling has been explored as a strategy to improve cell function during and after membrane disruption-based intracellular delivery⁴⁵⁰. Related to this notion, cell shrinkage has been observed in electroporation conditions where the induced membrane disruptions are small and the buffer is composed of osmolytes that are too big to flow into the cells (for example, an isotonic large molecular weight PEG buffer)^{435,454}. Unlike physiological media, such a buffer is devoid of electrolytes that can flow into the cell, thus K⁺ and Cl⁻ ions exit the cytoplasm along with water⁴³⁵. Such results give further insight into changes in cell volume upon membrane disruption along with the role of buffer composition.

The State of the Resealed Cell—When the plasma membrane is compromised to allow cargo influx, there is uncontrolled exchange of molecules between the inside and outside of the cell. In standard physiological buffer (see Figure 7A), disrupted cells will sustain elevated Na⁺, Cl⁻, and Ca²⁺, and reduced levels of K⁺, ATP, metabolites, amino acids, proteins, and other intracellular contents (Figure 10). Even after plasma membrane integrity is fully restored, cells may still undergo necrosis, a type of cell death caused by irreversible disturbance of cellular homeostatic mechanisms³⁶⁹. In particular, dramatically reduced levels of ATP and potassium can trigger necrotic cell death due to deregulation of mitochondrial activity³⁶⁹. Necrotic cell death is almost indistinguishable from an initial failure to reseal, also being characterized by swelling and loss of membrane integrity⁴⁵².

Once the cell reseals its plasma membrane, homeostatic processes will kick in to restore intracellular contents. The most critical molecules are thought to be ATP, potassium, and calcium³⁶⁹. ATP is a particularly crucial metabolite as it is the primary energy source for the cell. Studies have shown it can take from two^{455,456} to five⁴⁵⁷ hours to recuperate ATP levels after electroporation⁴⁵⁶ or treatment with pore-forming toxins^{455,457}. Potassium has been observed to drop from ~140 mM to ~20 mM when cells are exposed to transient membrane damage⁴⁵⁸ and recovery can take from minutes to hours³⁶⁹. Influx of calcium can be viewed as a double-edged sword, although it assists the cell in detecting and repairing damage, excessive amounts can be toxic and lead to cell death^{417,459–461}. High intracellular calcium serves as an activator of certain proteases, such as calpains, enzymes that promote apoptosis and degradation of cytoplasmic components³⁶⁹.

Membrane disruption and recovery is often paralleled by cytoskeletal disruption and recovery. In particular, microtubule depolymerization has been observed upon electroporation^{462–465}, mechanical wounding^{466,467}, and pore-forming toxins⁴⁶⁸. Microtubule depolymerization manifests locally around the wound sites due to calcium influx^{466,467}. This is evidenced by the observation that electroporation does not alter microtubule structure in media devoid of calcium⁴⁶³. In standard calcium conditions recovery of microtubule integrity has been reported to take minutes up to an hour^{463,464,467}. In some cases, membrane disruption has also appears to cause depolymerization of F-actin and intermediate filaments^{464,469}.

Stress Response After Membrane Disruption—A number of secondary consequences occur as a result of the perturbations associated with membrane disruption^{369,455}. For example, a decrease in cytosolic potassium can lead cells into a quiescent state characterized by autophagy (recycling of cellular building blocks), formation of lipid droplets to conserve energy, and arrest in global translation⁴⁵⁵. Time taken to restore intracellular potassium homeostasis correlates with duration of these effects⁴⁵⁵. Furthermore, a drop in potassium is thought to be responsible for activation of MAP kinase stress response and proteolytic signaling cascades including the inflammasome, which in turn trigger downstream effectors including caspase proteins and the unfolded protein response^{369,470–473}. In all systems tested so far pore-forming toxins activate the three main MAP kinase stress response pathways: p38, JNK, and ERK^{369,474–477}. Cell permeabilization in media containing high potassium prevents MAP kinase activation, indicating that potassium depletion is the key trigger^{478,479}. MAP kinase and its downstream effectors promote cell survival and their inhibition appears to worsen cell death after membrane disruption^{478,479}.

Many of the characteristic responses elicited from pore forming toxins are also shared with electroporation and mechanical wounding, further reinforcing that membrane disruption is the key event³⁶⁹. In the early days of the field, McNeil and colleagues witnessed that expression of c-fos and NF- κ B, two transcriptional activators, are strongly and selectively increased in cells that suffered and resealed a mechanically-induced membrane disruption⁴⁸⁰. Detectable NF- κ B and innate inflammatory responses were also measured in endothelial cells subject to membrane attacks with pore-forming toxins⁴⁸¹. Furthermore, mechanical micropuncture was found to activate MAP kinases, CREB1, and protein kinase C (PKC) to promote cell survival^{482–484}. Interestingly, engagement of PKC is thought to prime cells to cope with future membrane wounding events⁴⁸², and has similarly been observed upon SLO exposure⁴⁷² and electroporation⁴⁸⁵. Recently, electroporation was also demonstrated to activate MAP kinase pathways⁴⁸⁶ and trigger transcriptional changes to support MAP kinase activity, membrane repair, and recovery from oxidative stress⁴⁸⁷. Finally, reports have emerged that electroporation triggers autophagy in response to nanosecond pulsed electric fields⁴⁸⁸.

A key implication in all of these findings is that activation of stress response pathways prioritizes cell survival and threat surveillance at the expense of proliferation and synthesis. If stress levels reach a critical threshold cells trigger a shutdown response via apoptosis or other forms of regulated cell death⁴⁵². In certain cell types delayed cell death has been a significant problem after electroporation, for example, even when the initial membrane repair is successful^{450,489}. In some cases, cell outcomes may be improved by adding inhibitors of apoptosis⁴⁹⁰. As more inhibitors of specific cell death processes become available, they may find use in such applications.

Manipulating Cell Response to Optimize Outcomes—The concept of optimizing intracellular delivery by manipulating cell response has received sporadic attention over the past decades. As mentioned above, some positive results have been reported from supplementation with membrane healing polymers^{178,420–425} and antioxidants^{421,426,427,428}. Most of the work to date, however, has focused on engineering the permeabilization buffer.

The electroporation field, in particular, has extensively explored this aspect in an effort to optimize cargo delivery and cell health outcomes.

An analysis of 300 membrane disruption-based delivery papers compiled in this review reveals four main types of buffers: 1) Na-rich “physiological” buffers such as PBS; 2) Cell media, which is essentially physiological buffer plus nutrients; 3) K-rich “intracellular” buffers; and 4) buffered sugar solutions. In our analysis, cell media (37%) and Na-rich buffers (34%) are the most popular, ahead of buffered sugar solutions (17%) and K-rich buffers (9%)(Table 2). Deconstructing these trends by modes of membrane disruption reveals further insights. For example, buffered sugar solutions have historically been used by the electroporation community to avoid electrolytic effects associated with higher conductivity salt-based buffers^{491,492}. Their origins can be traced back to the mid-80s and early 90s^{462,491,493–496}. In contrast, physical non-electroporation-based methods, such as mechanical wounding and optoporation, have mostly opted for cell media (58%) or Na-rich buffers (32%). Biochemical methods, of which detergents and pore-forming toxins are the main options, have been the most likely to experiment with K-rich “intracellular” buffers (22%) but most often used their Na-rich counterparts (43%). Biochemical permeabilization methods, which have less control over the timing of membrane disruption, seem more concerned with maintaining intracellular homeostasis through implementation of K-rich buffers^{497,498}.

K-rich buffers have been in use since the pioneering days of membrane permeabilization, with detergents⁴⁹⁹, electroporation⁵⁰⁰, and mechanical scraping⁵⁰¹ being early examples. The argument in favor of these buffers is simple – by mimicking the intracellular composition as closely as possible, homeostasis and cell health should theoretically be maintained^{367,500,502}. One study compared K-rich buffers to Na-rich ones, concluding that K-rich are superior for gene expression and cell recovery after delivery by mechanical membrane disruption⁵⁰³. A different investigation found that electroporation in buffers designed to match intracellular contents (with appropriate levels of ATP, GTP, amino acids, K⁺, Mg²⁺, and Ca²⁺) accelerated recovery of protein synthesis to within 5 minutes compared to from >1 hour for standard PBS⁵⁰⁴. Another group observed electroporation in intracellular mimicking buffer featuring high K⁺, Mg²⁺, ATP and glutathione promoted cell survival compared to cell media or PBS^{505,506}. Furthermore, a cold-storage solution for organ transplants, containing high K⁺ and Mg²⁺ and antioxidants, was reported to markedly improve survival of electroporated cells⁵⁰⁷. Although most of the commercial electroporation buffers today are based on high sodium⁵⁰⁸, nucleofection offers a K-rich variant with high magnesium, ATP and glucose, which appears to be useful in treating primary human cells²²¹. Whether K-rich intracellular mimicking buffers are underutilized in membrane disruption-mediated delivery remains to be established.

Commercial electroporation systems such as nucleofection appear to have put significant effort into optimizing proprietary buffers, mostly arriving at formulations featuring high Na⁺, 10–20 mM Mg²⁺, strong pH buffering, and extra organic osmolytes⁵⁰⁸. Several academic groups have lifted the lid on these formulations and screened their effectiveness in an attempt to lower costs^{509–511}. Indeed, several studies testing nucleofection buffers found only marginal benefits over PBS⁵¹² or cell media⁵¹³, suggesting that the high cost of these

proprietary buffers may not be justified. On the other hand, Biorad electroporation guides suggest more basic options such as cell media, strongly buffered Na-rich saline, or buffered sugar solutions^{514,515}. Neon electroporation buffers seem to be based on PBS bolstered by extra pH buffering, sugar, and magnesium^{516,517}. Interestingly, many of the electroporation-based pre-clinical or clinical studies simply use OPTIMEM (a popular cell media) in place of commercial electroporation buffers^{56,518}.

Taken together, consistent benefits seem to be obtained by supplementing buffers with Mg^{2+} , ATP, glucose, antioxidants, and by lowering or avoiding Ca^{2+} . Additionally, strong pH buffering probably helps to negate potential detrimental effects of electrolytic reactions in the case of electroporation. Magnesium is slightly antagonistic to calcium, possibly helping to blunt some of the damaging aspects of calcium influx⁴⁰⁴. It is also a co-factor to hundreds of enzymes, including those involved in energy metabolism and stabilization of mitochondrial membranes^{519,520}. ATP supplementation might be beneficial not only in preventing its loss from the cytoplasm³⁶⁷, but also in engaging extracellular receptors to activate 'purinergic' signaling, which is thought to prime cells against the danger of membrane disruption^{417,521}. As an example of its potential benefits, electroporation buffers supplemented with ATP help to achieve faster gene expression after plasmid delivery⁵²². Glucose is added to some buffer formulations^{221,509} and would tend to prevent cell energy depletion due to cytoplasmic leakage. Anti-oxidants have been reported to promote membrane repair and overall cell health by neutralizing ROS⁴²⁶⁻⁴²⁸. ROS may damage proteins, lipids, and nucleic acids, the latter of which can lead to mutations in DNA. Most of the optimized buffers also tend to contain little or no Ca^{2+} . Although it is the prime trigger for membrane repair, precise studies have shown that only ~5 – 20 μM is required⁵²³⁻⁵²⁵. High Ca^{2+} comes into play when cells are returned back to cell media for final recovery.

Other potential supplements for augmenting cell health could be addition of Zinc⁵²⁶ and recombinant proteins that participate in repair – such as MG53⁵²⁶⁻⁵²⁹, annexins⁵³⁰, and ASMase⁵³¹. Conducting cell membrane disruption and/or recovery in the presence of certain inhibitors may also be beneficial in guiding cell fate, however, has received little attention to date. Recombinant proteins and inhibitors might be worth using in clinical scenarios, such as an important *ex vivo* cell-based therapy.

Temperature is a core consideration for any *in vitro* cell treatment procedure, and deliberate membrane disruption is no exception. Despite this, there is no consensus in the literature on which temperatures are best for membrane disruption-based intracellular delivery. An analysis of 300 membrane disruption-based delivery papers compiled in this review reveals three categories of temperature that have been used: 1) 4 °C; 2) room temperature (usually in the range 18–25 °C); and 3) ~37 °C (Table 3). The rationale for treating cells at 4 °C is that it can facilitate a preservative effect. Most stress responses and programmed cell death pathways are inhibited at 4 °C, so unless the cell is killed by the treatment itself, the long-term cell survival may be improved. One detergent-based protocol credited low temperature and intracellular buffer as the two main factors increasing cell survival⁴⁹⁷. Biochemical protocols employed 4 °C 38% of the time compared with 11% for electroporation and 12% for physical non-electroporation. Low temperatures probably slow down membrane repair, but it also makes cells more resistant to disruption, particularly electroporation^{532,533}.

Furthermore, many pore-forming toxins do not assemble at 4 °C, so a switch to warmer conditions can be used as a trigger to control the timing of permeabilization⁵³⁴.

The rationale for treating cells at room temperature is simply convenience, as it does not require any additional temperature control equipment. Membrane repair in mammalian cells seem to proceed quite normally at 25 °C, as evidenced by studies of annexin-mediated resealing^{460,524,535,536}. Electroporation protocols, in particular, favor room temperature (67% of papers analyzed). Because Joule heating associated with electroporation can spike the temperature of a solution by up to 20 °C⁵³⁷, using a baseline of 37 °C may be harmful to cells undergoing electroporation. On the other hand, the rationale for treating cells at 37 °C is maintenance of physiological function. Most non-electroporation protocols choose to employ such physiological conditions, with biochemical procedures using 37 °C 43% of the time and physical non-electroporation 34% (Table 3). Membrane repair and stress response are expected to be at their most efficient at 37 °C.

Semi-Intact Cells—Although most applications of intracellular delivery by membrane permeabilization aim for a transient permeabilization from which the cell recovers, there are situations where a persistent ongoing permeabilization is opted for. Such systems have been referred as semi-intact cells⁵³⁸, semipermeable cells⁵³⁹ or perforated cells⁵⁴⁰. They involve irreparable disruption of cell membranes by mechanical^{538–540} or biochemical means^{541–548}. Strategies such as low temperature and low calcium concentrations may be employed to deliberately prevent membrane resealing⁵³⁸. Efflux of cytoplasmic constituents follows, but the extracellular media is manipulated to “reconstitute” the cytoplasmic composition replete with desired inhibitors, activators, antibodies, metabolites, ATP-regenerating systems, and other macromolecules of interest^{544,545,549}. Semi-intact systems have therefore been useful for functionally reconstituting intracellular processes while being able to manipulate the buffer. Apart from high potassium, such buffers usually contain high magnesium, low calcium, ATP at mM concentrations, strong buffering, and reducing agents or anti-oxidants. The major concern in using these methods is that it has been difficult to assess to what extent the semi-intact cells are a valid model for intact cells³⁶⁵. The concept of semi-intact cells illustrates the lengths biologists have pursued to address intracellular delivery and manipulation challenges. Despite their limitations, these reconstituted systems have been key in discovering fundamental mechanisms of secretory pathways and principles underlying trafficking of proteins, lipids, and nucleic acids between intracellular organelles, for example decoding the rules that govern nuclear import^{550,551}. Semi-intact cells remain popular for certain types of studies, such as probing mitochondrial function in muscle cells⁵⁵².

5 Intracellular Delivery by Direct Penetration

Direct penetration mechanisms are utilized in the techniques of microinjection, particle bombardment, and nanoneedles. In each of these cases penetrating elements provide direct access to the intracellular space. Microinjection is the classic embodiment of the direct penetration mechanism and was the first intracellular delivery technique to be deployed in the early 1900s. Particle bombardment and nanoneedles were introduced in the late 1980s

and early 2000s respectively. In this section we discuss the key details of each of these methods.

5.1 Microinjection

In 1911 Marshall Barber reported the invention of microinjection²⁹⁸. By pulling glass capillaries over a flame Barber generated pipettes with sharp micron-sized ends suitable for injection into living cells. Combined with micromanipulators and pressure control systems, dual pipettes were demonstrated with holding, dissecting, extraction, and injection capabilities. The apparatus was used to extract nuclei from living amoebae, inject various fluids into cells, and deliver single bacteria into plant cells²⁹⁹. Barber rightly predicted that *“The introduction of foods, poisons, stains, and fixatives is made possible and cells may be probed or dissected under high powers, methods which may be of use in the study of the structure, chemistry, and physiology of cells. Finally, materials may be withdrawn from one cell and injected into another, and it is possible that investigations on fertilization and heredity may be extended by this technic”*. After inventing microinjection, Barber trained others in its use before leaving the field²⁹⁹. In 1915 Kite used it to inject dyes into the cytoplasm of living animal and plant cells to investigate their permeability⁵⁵³. Chambers then introduced an improved version of the instrument in the early 1920s, which became the standard going forward⁵⁵⁴.

As microinjection spread to other researchers, it was initially adopted by plant, developmental, and micro-biologists, for example to determine cytoplasmic pH, introduce viruses into cells, or perform nuclear transplants⁵⁵⁵⁻⁵⁵⁸. Moreover, it became the basis for patch clamp and a host of similar pipette-mediated cell manipulation and analysis techniques^{299,559}. As covered in section 2.2.5, microinjection has long been the dominant method for large cargo delivery. It was used for the first nuclear transplants in 1952³⁰⁰, cloning frogs in 1958³⁰¹, cloning mammals in 1997³⁰³, mitochondrial transplants in 1974³¹⁰, chromosome transplant protocols in 1973³⁰⁷, intracellular delivery of sperm into egg cells in 1962³⁰⁵, and the first human pregnancies achieved by IVF in 1992³⁰⁶. More recent examples of large cargo delivery include micron-sized beads for intracellular microrheology analysis^{322,323,328} and silicon MEMS barcodes up to 10 μm in size³³⁰.

Although microinjection was employed for large cargo delivery from the beginning, it took more than half a century for it find routine use for intracellular delivery of proteins, DNA, and other such biomolecules in animal cells. Purified proteins began to be injected into animal cells in the 1960s. The protein ferritin was introduced into amoebae to follow its intracellular distribution¹⁶⁰. Then mouse oocytes injected with bovine gamma globulin were shown as capable of developing into defect-free animals¹⁶¹. In 1972, the calcium sensitive protein aequorin was injected into the squid giant synapse to determine intracellular calcium⁵⁶⁰. Other studies in the 1970s used fluorescently labeled proteins and dextrans to study nuclear permeability^{162,163} and autophagy¹⁶⁴. Microinjection of peptides also emerged around that time⁵⁶¹. Fluorescently labeled actin¹⁶⁵ and alpha-actinin¹⁶⁶ were injected into cells to visualize and elucidate their role in the cytoskeleton. A classic example where intracellular delivery of a protein led to discovery of its function is the case of vinculin⁵⁶². Microinjection of the uncharacterized protein labeled with fluorescent dyes was

used to identify its role as a mediator of cytoskeletal adhesion assemblies by observing localization dynamics in living fibroblasts⁵⁶².

Along with protein delivery, researchers began experimenting with microinjection of DNA and RNA. The first mRNA expression studies were carried out by microinjection from 1973 onward^{109–111,563}. Viral DNA was injected into cells to investigate its ability to transform cells⁵⁶⁴. Recombinantly engineered plasmids were expressed in cells post-injection in 1977⁷⁰. Several years later, Capecchi demonstrated that nuclear injection of plasmid DNA encoding thymidine kinase was successfully expressed in 50–100% of cells. Yet the same construct injected into the cytoplasm led to 0% expression in hundreds of cases⁷². Thus, microinjection studies were used to prove that plasmids must be delivered to the nucleus to undergo expression. In 1980, transgenic mice were successfully produced by microinjection of recombinant plasmid DNA into the nucleus of fertilized oocytes⁵⁶⁵. Following the elucidation of antisense oligonucleotides in the 1980s, antisense RNA was injected into cells to inhibit protein expression in studies of developmental biology^{81,566}. The Nobel Prize winning experiments that elucidated RNAi were performed by microinjection of double stranded RNA into *C. Elegans* cells in 1998⁸⁵.

As illustrated in the above examples, microinjection is a versatile delivery platform, being able to deliver almost any cargo to most cell types. In its current form, microinjection is commonly performed with commercial systems fitted with glass micropipettes of diameter 0.3 to 1.0 μm (Figure 12A). It is important to note that microinjection does suffer some degree of cell type-dependence. Small cells, such as blood cells with diameters less than 10 μm , can be difficult to microinject due to their small volume and poor tolerance for needle penetration⁵⁶⁷. For non-adherent or suspension cells an additional holding pipette is used to keep cells in place (Figure 12B), but this adds to the complexity and time-consuming nature of the procedure. Researchers and clinicians most often use microinjection for experiments or procedures involving single cells or small batches of cells where high fidelity of intracellular delivery is ensured. For example, due to its accuracy and control, microinjection has been a routine technique to achieve human pregnancies by *in vitro* fertilization.

Advances in Technical Precision of Microinjection—Significant advantages of microinjection include precise control of dose volume and injection location. In one innovation, organelle targeting was demonstrated with an ultra-fine tip and femtoliter to attoliter control provided by a galinstan expansion syringe⁵⁶⁸. Using a tip diameter of ~ 100 nm, researchers were able to inject single chloroplasts in plant cells without dissipation of intracellular turgor pressure or untoward impact on other cellular structures (Figure 12C). Exploiting a different mechanism of volume control, an electrochemical attosyringe with aperture size of 100 – 400 nm achieved picoliter to attoliter volume control of injections⁵⁶⁹. Such fine electrochemical control of fluid motion allowed the accurate dispensation of precise volumes from the fabricated ‘nanopipette’⁵⁶⁹. Another group employed carbon nanotubes as the pipette. The device, termed a nanotube endoscope, was demonstrated to deliver fluorescent molecules to subcellular localizations at a resolution down to 100 nm⁵⁷⁰. Recently microinjectors that take advantage of electrophoretic delivery were claimed to enable higher cell viability post-injection⁵⁷¹. It was based on a 100 nm diameter

nanoinjector that drives materials into cells via electrophoretic force rather than bulk pumping of fluid⁵⁷¹.

Some interesting adaptations of the microinjection concept have been produced by modifying atomic force microscope (AFM) systems to allow injection or extraction⁵⁷². One technology, called FluidFM, was first demonstrated by the use of hollow cantilevers with fluid control capabilities for force-controlled injection of soluble materials into cells (Figure 12D)⁵⁷³. AFM force feedback was reported to enable unprecedented control of contact force thereby facilitating the determination of required penetration forces⁵⁷². Recently, the FluidFM system has been used for non-destructive sampling from cells for time-resolved analysis of molecular composition⁵⁷⁴ and metabolite profiles⁵⁷⁵. It also features the precision to deliver or extract from the nucleus^{574,576}. In a similar approach to FluidFM, another group used a scanning probe system to detect cell surfaces and provide voltage pulses to deliver fluorescent dyes into individual cells⁵⁷⁷.

Attempts Toward Higher Throughput Microinjection—The primary limitation of standard microinjection is the serial, low-throughput, and tedious nature of the process. Even an experienced operator is limited to approximately one successful injection per minute. An early attempt at automated microinjection was published in 1988, with a reported throughput of 1500 cells per hour when performed on adherent cells^{578,579}. For unknown reasons, this innovation was not widely adopted. Other attempts at high-throughput microinjection include a vacuum-enabled embryo holding array, which allows injections based on robotic motion control and image recognition by computer vision processing⁵⁸⁰. The reported throughput of 15 cells per minute was demonstrated to yield a high survival rate (98%) for large non-adherent cells such as embryos and oocytes. In a semi-automatic approach, a microrobotic system achieved up to 25 injections per minute on adherent endothelial cells⁵⁸¹. In this embodiment a human operator selects injection destinations through mouse clicking on a computer screen and the system executes with a survival rate of >95% and a success rate of >80%⁵⁸¹.

Microfluidic systems have been explored to address microinjection throughput challenges. Adamo and colleagues reported a microfluidic version of microinjection that works by suction of cells onto a 0.5 μm diameter hollow-tip glass needle embedded in a PDMS device (Figure 12E)⁵⁸². Several picoliters of liquid could be injected into the cell in ~ 0.5 seconds followed by flow reversal to dislodge the cell, which could be then routed through an exit channel⁵⁸². However, problems with cell clogging and fouling from biological debris prevented the device from achieving consistent operation. A follow-up concept sought to address this problem with high-pressure fluid jet injection but synchronization of jet firing with cell passage at the injection nozzle presented a significant unsolved challenge⁵⁸³.

Microinjection Summary—Microinjection was the first intracellular delivery method to be invented. It is a method of choice to deliver almost any cargo, whether large or small, to single cells or small groups of cells (<100). Despite technical advances, however, the intrinsic low-throughput of microinjection remains a serious limitation for the great majority of applications. An effective platform for high-throughput microinjection would be groundbreaking, but remains elusive.

5.2 Penetrating Projectiles (Biolistics)

Biolistic intracellular delivery employs high-velocity microprojectiles to deliver nucleic acids and other substances into intact cells and tissues. The particles are accelerated to adequate velocity by release of pressurized inert gas or high-voltage electronic discharge⁵⁸⁴. Particles then collide with the cells, busting through the plasma membrane and releasing cargo molecules from their surface (Figure 13A). Biolistic intracellular delivery has been referred to as the biolistic process, ballistic particle delivery, microprojectile bombardment, and in certain embodiments, the ‘gene gun’.

Biolistic delivery came onto the scene in 1987, where it was first invented for the purpose of DNA transfection in plants³⁶⁴. In the late 1980s and early 1990s it was adapted for transfection of diverse microorganisms (yeast, fungi, algae, bacteria), many of which are difficult to transfect with other methods^{584,585}. It was also attempted for transfection of an assortment of animal cells and tissues. Given the limited penetration distance of particle bombardment into tissue, it was initially tested with cell cultures *in vitro* and skin or exposed tissue sections *in vivo*^{584,586–588}. For cell cultures *in vitro*, particles are sprayed down on a monolayer of adherent cells or a thin dispersion of suspension cells. As a rule of thumb, particle sizes should be around one tenth the size of the cell⁵⁸⁵. Heavy metal particles are durable, dense, and do an excellent job of maintaining the momentum needed for breaching the plasma membrane⁵⁸⁵. Particles used in biolistic systems tend to be tungsten (occasionally toxic), gold or silver (less toxic) and in the size range 0.5 to 2 μm ⁵⁸⁹.

Cell Type Applicability—Several early efforts in biolistic intracellular delivery sought to test applicability to hard-to-transfect mammalian cells, particularly immune cells, blood cells, and neurons. It was shown that both adherent and suspension cell cultures can be transfected with plasmid-coated metal particles. Transfection efficiencies in T cells were reported to be maximum 2%⁵⁹⁰, 6%⁵⁹¹ and 3%⁵⁹² respectively. Particle bombardment could also be used to transfect HSCs *ex vivo*, but the efficiency was either not directly reported⁵⁹³ or achieved a maximum of 6% alongside 75% viability⁵⁹⁴. Both adherent and suspension tumor cells could be transfected with the plasmid-coated ~1–2 μm gold particles shot from a helium driven gene gun⁵⁹⁵. But this study reported only the yield of expressed protein and not percentage cells transfected⁵⁹⁵. A comparison across many cell types observed from 2% to 40% transfection efficiency depending on cell line⁵⁹⁶. Upper limits of 30–40% were obtained for common adherent cell lines such as prostate cancer cell lines⁵⁹⁷ or HEK cells⁵⁹⁸. Due to the random spray of particles over a cell sample, it is unlikely that particles will penetrate the nucleus of every cell to deliver their DNA cargo for subsequent expression. For large cells that ‘catch’ many particles, such as myotubes, 20–70% transfection can be obtained⁵⁹⁹.

Some reports claim biolistic delivery is a highly efficient DNA transfection method in mammalian cells⁶⁰⁰. However, it is only efficient in its use of DNA, not necessarily in the percentage of cells treated. It has been estimated that about 200 plasmids are delivered per gold particle⁶⁰¹. Hence, the amount of DNA required to produce a given yield of protein is very efficient⁶⁰². In comparison, electroporation and lipid reagents are highly wasteful of DNA (most is lost in solution) but produce a large proportion of cells that are successfully

transfected. Empirical optimizations aimed at improving the performance of biolistic delivery in animal cells identified parameters such as size of the particles, the target distance, extent of vacuum, and the size of the cell culture plate^{585,600}. Tuning of such parameters, however, has yielded limited success. Thus, after an initial excitement surrounding biolistic transfection, electroporation and viral vectors have risen to prominence as the preferred methods in hard-to-transfect cells such as HSCs and immune cells.

One area where the biolistic process gained notable traction is delivery to neurons and organotypic brain slices^{598,603–608}. Neurons are regarded as very difficult to transfect with conventional methods. Early studies of plasmid delivery into neural cell cultures have achieved transfection efficiencies of <2%⁶⁰⁹, 2–8%, depending on the type of neurons⁶⁰⁶, and up to 10%⁶⁰⁵. Although most of the protocols hover below 10%^{605–609}, maximums of 20–30% were reported with a highly optimized protocol⁵⁹⁸. As the alternatives are generally poor, such performance has proven sufficient to carry out several interesting studies in neuronal cultures⁵⁹⁸. Particle bombardment has been particularly useful in organotypic brain slices, where alternative methods such as electroporation lack access to cells⁶⁰⁸.

After three decades of experimentation, the main cells and tissues that have proven amenable to biolistic delivery are: 1) plants, especially for generating transgenic crops³⁶⁴, 2) neurons and organotypic brain slices^{598,603–608}; 3) microorganisms that are difficult to transfect with other methods⁵⁸⁵, 4) inoculation of skin or muscle for applications such as vaccination^{586,610–612}. Efficient DNA immunizations against influenza have been achieved by using a gene gun to deliver DNA-coated gold beads to the epidermis in mice and chicken⁶¹³. Projectile bombardment is suitable for these applications because the immunization is thought to be effective even when only a small fraction of cells are transfected. For intracellular delivery to skin cells, there is a notable trade-off between power, size and number of bombarding particles, and cell viability⁶¹⁴.

Cargo Applicability—In terms of cargo, the biolistic process has been used mainly for plasmid transfection. However, it has also proven particularly advantageous for delivery of larger DNA vectors such as cosmids and artificial chromosomes^{601,609,615}. In the early 2000s researchers successfully experimented with attaching dyes and indicators to the projectiles^{616–619}, mostly for delivery to neural cell types and brain slices. Following that, mRNA and siRNA were shown to be feasible for transfection into a variety of cells and organisms^{620–624}. Biolistic methods have also been deployed for delivery of large beads to the cytoplasm for analysis of intracellular mechanical properties. In these cases cytoplasmic microrheology was assessed by monitoring fluctuations in polymer beads within the cytoplasm^{324–327}. In a recent example, ~1 μm melamine particles coated with PEG were shot into HeLa cells to study glassy dynamics in the cytosol⁶²⁵. More recently, protein delivery has been demonstrated with particle bombardment, first in plants^{626,627}, then in mammalian scenarios⁶²⁸. Furthermore, protein delivery protocols have been adapted for biolistic Cas9 RNP delivery⁶²⁹. RNPs were dried onto gold particles and fired into immature wheat embryos to produce gene-edited crops⁶²⁹.

Biolistic Systems & Variations—Biorad is the main supplier of commercial biolistic delivery platforms. The gene gun is a hand-held device with a ‘point and fire’ mode of

operation. The more advanced biolistic systems employ a vacuum chamber for higher momentum and evenness of microparticle dispersion. The vacuum systems are typically used for *in vitro* applications where the sample is more amenable to manipulation. A major weakness of biolistic delivery is the damage that high velocity particles can cause to cells. This is one of the reasons why it is popular for plants, which have stiff cell walls that can tolerate harsh mechanical impacts⁵⁸⁵. Damage from gene guns has been identified as a key limiting factor in treatment of cell cultures *in vitro*, as well as skin and muscle tissues⁶³⁰. In general, damage is intensified as the projectile diameter increases relative to the cell size. Nanoparticles of ~40 nm have been tested with the biolistic method and found to provide better cell survival, especially with small cells⁶³¹. ~80 nm silver nanoparticles were also evaluated and found to exhibit less damage to cells⁶³². In both cases delivery efficiency of cargo was not reported to be adversely compromised by using nanoparticles instead of micro-sized beads, and the higher surface area to volume ratio of nanoparticles could be a potential advantage. Overall, implementation of biolistic particle bombardment approaches to mammalian systems at the cellular level requires a number of empirically determined parameters to be optimized. These include size of particles, distribution, density, impact speed and loading technique³⁶⁶.

In a nano-inspired adaptation of the projectile delivery approach, Cai et al. used DNA-carrying nickel-embedded nanotubes propelled by magnetic fields to “spear” cells⁶³³. Nanotubes in solution were attracted to a magnet placed underneath the substrate, thus creating the driving force for penetration of cells placed on the substrate (Figure 13B). With this method they demonstrated efficient GFP expression in primary mouse B cells and neurons with minimal cell death⁶³³. Thus, particularly for *in vitro* and *ex vivo* applications, smaller projectiles that minimize damage to cellular structure may present an opportunity for projectile-mediated intracellular delivery.

5.3 Nanowires & Nanostraws

Nanowires, also referred to as nanoneedles, nanosyringes, nanofibers and high aspect ratio nanostructures, are thin elongated structures typically with diameters of hundreds of nanometers or less and lengths on the micrometer scale. For intracellular delivery at high-throughput, nanowires are fabricated into vertically aligned arrays that can interface with thousands of cells. Nanostraws are hollow versions of nanowires, which can deliver fluid from an external reservoir directly to the intracellular space.

Intracellular delivery by penetrating nanowires was first demonstrated by McKnight and colleagues in the early 2000s^{363,634}. They produced conical spikes of 6–10 μm in length, tip diameters of 20–50 nm and base diameters of ~1 μm . These carbon/nitrogen-based structures were grown via plasma-enhanced chemical vapor deposition off nickel-spotted silicon wafers³⁶³. The first cargo to be delivered with them was DNA plasmids, which were physically absorbed or covalently tethered to the tips of the conical nanowires. CHO cells were then forced against the array by centrifugation at 600 g followed by sandwiching against an opposing substrate. This provided an active force for penetration, which proved to be necessary for efficient transfection in this system (Figure 14A). The nanowires were able to achieve nuclear penetration as evidenced by rapid GFP expression. Interestingly, GFP

plasmids that were physically absorbed to the nanowires were passed on to cell progeny while covalently tethered plasmids were not, suggesting that the former dissociate in the cell interior while the latter are able to mediate expression even though they remained attached to the nanostructures. In follow-up studies the same researchers extended the application of their nanowire platform to include spatially indexed substrates for long-term cell tracking⁶³⁴ and simultaneous delivery of multiple different plasmids⁶³⁵.

Expanding the Repertoire of Deliverable Cargo—As mentioned above, the first demonstrations of intracellular delivery with nanowire arrays were conducted with DNA transfection^{363,634–636}. Since then delivery of siRNA^{185,637–639}, proteins^{185,638,640,641}, molecular beacons⁶⁴², quantum dots⁶⁴³, DNA nanocages⁶⁴⁴, and impermeable drugs¹⁸⁵ have also been shown. One of the first such examples was achieved by Park et al., who produced nanosyringes of 50 nm outer diameter and 120 nm height⁶⁴³. The cup-like hollow nanostructures were pre-filled with DNA or ~3 nm quantum dots, which were then released into cells upon penetration⁶⁴³. This was one of the first examples where passive settling of cells onto penetrating nanostructures appeared sufficient for efficient delivery (Figure 14B). In 2010 Shalek et al. showcased the multifaceted potential of nanowires by demonstrating successful intracellular delivery of a wide range of materials to various cell types. Functional siRNA, plasmid DNA, peptides, proteins, and membrane impermeable drugs were non-covalently and non-specifically bound to the surface of silicon nanowire arrays and cells were allowed to settle on top, thus taking advantage of passive penetration. These materials were successfully introduced into a range of immortalized cell lines and primary cell types, including hard-to-transfect mammalian neurons¹⁸⁵. Patterning of target molecules on the nanostructure arrays is a further advantage of this approach, as it can enable spatially encoded delivery of cargo materials¹⁸⁵. Shalek's nanowire platform was then adapted for hard-to-transfect primary immune cells^{637,645}. By screening nanowire density and height against different cell types and sizes, optimal parameters were supposedly established for each cell type. Efficient delivery of molecules to primary B cells, dendritic cells, macrophages, natural killer cells, and T cells was reported without the adverse immune responses that confound common transfection reagents⁶³⁷.

Kim et al. also used a nanowire strategy to deliver molecular beacons for the quantitative detection of mRNA⁶⁴². In their strategy, ZnO nanowires were incorporated into a PDMS device and pneumatic pumping provided the force to push cells down onto nanowires. Another group reported the delivery of peptide-functionalized DNA nanocages by passive incubation of cells on 1 μm long 150 nm diameter cargo-coated nanowire arrays⁶⁴⁴. Other modes of nanowire delivery have been shown to be capable of intracellular loading of proteins such as Cre recombinase⁶⁴⁰ and antibodies against cytoskeletal proteins⁶⁴¹. Apart from large cargo, nanowire arrays have proven capable of delivering most categories of macromolecules. Thus, nanowires represent a relatively universal delivery platform capable of introducing a wide range of cargo molecules into the cytosol of various cell types.

Nanowire Penetration Mechanisms—Despite the reports of successful delivery of multiple cargo types, it is not fully understood how nanowires breach the plasma membrane. Indeed, the mechanisms and efficiency of nanowire penetration have been a matter of debate

for almost a decade. For example, several groups claim that active force is not required if the density, length, and diameter of nanowire arrays is optimized for a particular cell type^{185,636,637,646}. On the other hand, other reports indicate that a majority of nanowires fail to penetrate cells that passively settle on top^{647–649}. For example, nanowires ranging from 2 to 11 μm in length and 100 nm diameter were found to be excluded from the cytoplasm as observed by confocal imaging⁶⁴⁹. TEM images also revealed that both the plasma membrane and nuclear envelope resist nanowire penetration, and overall DNA transfection efficiency was low in the absence of active forces⁶⁴⁷. Using ~ 100 nm diameter hollow nanostraws to conduct a time-resolved GFP quenching assay, researchers from the Melosh lab determined that only $7 \pm 3\%$ of features were penetrant, even in adherent cells³⁸⁷. Studies of the mechanism suggest that puncture does not occur upon initial cell contact, but requires active cell spreading and coincident build up of traction forces from focal adhesions^{387,636,650}. Once penetrant, however, a given nanowire continues to provide sustained intracellular access as long as the cell remains adherent.

On balance, the majority of the literature indicates that provision of active forces is necessary or at least helpful for penetration and subsequent cargo delivery. In several studies with hard-to-transfect immune cells, it was found that intracellular delivery of plasmid DNA, siRNA, and proteins was only possible with the addition of g-forces to push cells against vertically aligned nanowires^{638,643}. Notably, this was the case even when the same nanowire architecture was previously successful with standard cell lines^{638,643}. This raises the possibility that some cell types, particularly those that naturally exist in a non-adherent state, may require active forces to achieve nanowire-mediated intracellular delivery.

Several strategies have been used to provide active forces for nanowire penetration. As mentioned above, one technique is to generate g-forces from centrifuging cells onto nanowire arrays^{363,634,638}. Another method is to sandwich the cells between nanowires and an opposing surface. For example, DNA delivery into hard-to-transfect algae was augmented by using an engineered PDMS microvalve to press cells against an array of ZnO nanowires⁶⁵¹. Other strategies have been inspired by cell printing, whereby jetting velocity upon ejection from the printing nozzle is directly proportional to penetration force and can be tuned to balance efficiency of cell impalement versus cell bursting⁶⁵². Movement of nanoneedles by a piezoelectrically actuated stage has also been tested⁶⁴⁰. In this case an inverted array of nanoneedles was oscillated with an amplitude of 10 μm against an immobile monolayer of cells to improve plasmid transfection⁶⁴⁰.

What are the forces involved in nanowire penetration? Researchers have attempted to address this question with a number of different methods and calculations. Using a model that estimates traction forces associated with long term cell adhesion, calculations of 1.5 to 6 nN were obtained for cells cultured on ~ 100 nm diameter nanowires⁶⁵³. In another case, active centrifugation of a grid of diamond nanowires was used to poke holes in cells for diffusive delivery of cargo from the extracellular solution⁶⁵⁴. They estimated a force of ~ 2 nN was needed to breach the membrane with ~ 400 nm diameter nanowires. Other groups have used AFM to more directly quantify the forces of penetration for different diameter objects. For example, it was observed that 30–40 nm wide multi-walled CNTs had a penetration force of 100–200 pN and require an indentation depth of only 100–200 nm⁶⁵⁵.

Obataya et al. found that silicon AFM tips sculpted into thin nanowires of 200–800 nm diameter exhibited penetration forces in the range of 0.65 to 1.9 nN when tested on cultured human epidermal cells^{656,657}. Nanowires of 200 nm were found to breach the plasma membrane after ~1–2 μm indentation, and be much more efficient at both plasma membrane and nuclear envelope penetration compared to pyramidal tips^{656,657}. As evidence of penetration, a 200 nm diameter nanowire inserted into the nuclei of HEK cells successfully induced expression of attached plasmid DNA⁶⁵⁸. Another study with larger AFM probe tips estimated that the forces required to penetrate supported lipid membranes range from 5 nN for a sharp (<300 nm diameter) nanoneedle probe to 20 nN for a standard pyramidal tip⁶⁵⁹. However, the supported lipid membranes may be more difficult to break through than the plasma membrane, depending on approach speed and temperature. One group used antibodies attached to nanowires to detect membrane penetration and found that lowering temperature to 4 °C appeared to improve nanowire penetration by reducing membrane adaptability⁶⁴¹. Together, mechanistic studies indicate that biological membranes under physiological conditions are able to passively adjust to nanowire conformations, and therefore small tip area, low temperature, high forces or critical velocity may help to facilitate effective disruption of the lipid bilayer.

Nanowire Effects on Cells—It has been established that long-term culture of cells on nanowires is not damaging, however, there are concerns over unexpected changes in the behavior of cells cultured on nanowires⁶⁶⁰. Early studies indicated that nanowires significantly perturbed the growth rate and cell cycle progression of cells⁶³⁴. Nanowire arrays have also been reported to interfere with cell division in fibroblasts and lead to a higher frequency of multinuclear cells, an effect that was more pronounced with longer nanowires⁶⁶¹. Moreover, when nanowire density increases, it may inhibit stable cell adhesion and trigger cells into a more motile and less proliferative state⁶⁶². On the other hand, Bonde et al. obtained results suggesting that the growth rate of HEK cells may be stimulated by arrays of nanoneedles⁶⁶³. Although nanowire induced-perturbations appear trivial in most reports, details of their effects on cell physiology should remain open for further investigation.

Nanostraw Arrays for Injection & Extraction—Nanostraws, which are essentially hollow nanowires, can be used for injection of cargo-laden fluid from an external reservoir (Figure 14C). In one of the first examples of nanostraw delivery, researchers from the Melosh lab fabricated beds of aluminum nanostraws on polycarbonate track-etched substrates followed by seeding of HeLa cells and CHO cells. By controlling the composition and pressure of the fluidic reservoir underneath the nanostraws, temporal control over delivery of dyes and quenching agents was achieved, thus providing direct fluidic access to the cell interior⁶⁶⁴. In a different study, hollow nanostraws were fabricated from silicon oxide. Only nanostraws that pumped a mixture of membrane-perturbing saponin and cargo were able to introduce fluorescently labeled dextran, indicating that nanostraws acted to localize the membrane permeabilizing effects of saponin and to function as conduits for delivery into cells⁶⁶⁵. In an analogous fashion, nanostraws have been reported to localize the membrane-perturbing effects of electric fields⁶⁶⁶. Low voltage pulses acted as a gating mechanism to enable access to the cytosol for delivery of membrane impermeable dyes and

plasmid DNA⁶⁶⁶. A key benefit of hollow nanostraws (as opposed to solid nanowires) is the temporal control over delivery, volume, and dosage concentration.

In further studies of nanostraw technology, intracellular administration of calcium with complex signal patterns, such as oscillations over time⁶⁶⁷ and delivery of cell impermeable small molecule probes⁶⁶⁸ has been achieved. Nanostraws were also adapted for cytoplasmic extraction, being capable of continuous time-resolved sampling from the intracellular space for up to five days⁶⁶⁹. In another example, ~6 μm long conical nanostraws were employed for delivery of ~10 nm quantum dot to microalgal organisms⁶⁷⁰. Moreover, Golshadi et al. showed that an array of short, dense, nanotubes of 200 nm outer diameter, 140 nm inner diameter and 180 nm protrusion height were capable of intracellular dye delivery and efficient plasmid transfection in HEK cells⁶⁷¹. Because of the dense clustering of these structures, fully adherent cells could cover almost 1000 nanotubes⁶⁷¹.

Mechanisms of Cargo Delivery by Penetrating Elements—The mechanisms by which nano- and micro-scale penetrating elements deliver molecules into cells are threefold: injection, dissociation, and permeabilization (Table 4). Microinjection, mostly featuring tip diameters of ~0.3–1 μm , is the classic example of delivery by injection (*see* section 5.1). Advanced versions of microinjection have also been introduced with ~100 nm diameter tips (nanoinjection^{568–571}) and AFM control (FluidFM⁵⁷³). Nanostraws can be considered a highly parallelized adaptation of the microinjection mechanism with capability for much higher throughput^{387,664–666}. However, some degree of control over the penetration and injection process is sacrificed.

To date, most of the nanowire systems deliver cargo by dissociation. These include the original nanowire arrays introduced by McKnight et al.^{363,634} and Shalek et al.^{185,637} for simultaneous treatment of thousands of cells as discussed above. Single cell versions of nanowire delivery have also been explored. One system attached multi-walled CNTs of 10–20 nm diameter and up to 1.5 μm length to AFM tips to deliver quantum dots to selected single cells⁶⁷². Dissociation was achieved by the action of intracellular enzymes that cleave the linker holding the cargo to the penetrating CNT⁶⁷². AFM-controlled nanoneedles sculpted by focused ion beams have been shown to provide nuclear penetration and mediate gene expression^{656–658,673}. Another method used a ~500 nm diameter gold nanowire to penetrate mouse embryos and release plasmids inside. The plasmids are released through dissociation triggered by an electric pulse. Because the technique is thought to be less violent, embryo survival was reported to be significantly higher than traditional microinjection⁶⁷⁷.

Finally, nanowire delivery can also be mediated by permeabilization whereby the mechanism involves diffusive influx of cargo from the extracellular solution. In this case the penetrating element is withdrawn from the cell and the influx occurs before completion of plasma membrane repair. Both single cell⁶⁷⁸ and parallelized⁶⁵⁴ versions of this approach have been published. They will be further discussed in section 6 below, which deals with delivery by permeabilization.

Summary—In the reported nanowire and nanostraw delivery modalities demonstrated thus far, the cargo material is delivered by (1) dissociation from the penetrating structure upon cytosolic entry, (2) direct injection through hollow nanostraws, and (3) permeabilization of the plasma membrane (Table 4). In most cases active forces improve penetration and resultant delivery efficiency. So far, high aspect ratio nanowires for intracellular delivery have been successfully fabricated out of carbon, diamond, silicon, silicon oxide, zinc oxide, gold, and various other inorganic semiconductors, metals, and metal oxides^{660,684–686}. Polymer coatings have been suggested to improve delivery performance and cell health, for example, in the case of siRNA delivery⁶³⁹ and DNA transfection⁶⁸⁷. The physiological effect of exposing nanowire materials to the intracellular space will be essential knowledge if nanowires are to proceed toward biomedical applications. Furthermore, open questions remain regarding the membrane conformation adopted around nanowires and the subsequent degree of penetration. Understanding the effect of nanowire dimensions and density, the requirement of active forces, surface functionalization and chemistry, as well as the influence of culture conditions, cell properties, and cell type will be key information for the future implementation of nanowires and nanostraws.

6 Intracellular Delivery by Permeabilization

As specified in section 3, permeabilization methods work by transiently permeabilizing the cell for cargo in the extracellular solution. Here we will discuss methods for intracellular delivery that rely on mechanical, electrical, optical, thermal, and chemical means of permeabilizing the plasma membrane. A major advantage of permeabilization-based delivery is that it is near-universal, being able to deliver almost any material that can be dispersed in solution. Because most cells can recover from micron-sized membrane disruptions⁴⁰⁵, delivery of large cargo is also feasible.

6.1 Mechanical Membrane Disruption

Mechanical methods of membrane permeabilization have been performed by (1) solid contact of foreign objects with cells, such as is the case for direct penetration mediated delivery discussed in the previous section. Membranes have also been permeabilized without solid contact, such as with (2) fluid shear forces and (3) hydrostatic pressure changes. These three mechanisms of membrane permeabilization are categorized and discussed separately below.

6.1.1 Mechanical: Solid Contact

Scrape & Bead Loading: Among the earliest reported mechanical permeabilization methods were those published by Paul McNeil and colleagues in the 1980s, which include scraping loading¹⁷⁶ and glass bead loading¹⁷⁷. In cell scraping, a rubber spatula is passed over a cell-laden substrate to dislodge adherent cells and bring them into solution, hence the technique is only applicable to adherent cells (Figure 15A). Moreover, the amount of damage to each cell is stochastic, with some cells being instantly killed while others remain unaffected. In cells that receive optimal amounts of damage, cargo molecules dispersed in solution diffuse through transient membrane disruptions to achieve delivery. Glass bead loading involves shaking the adherent cells with medium containing glass beads and the

cargo to be delivered (Figure 15B). The impact of collisions between beads and cells imparts sufficient strain to generate disruptions in the plasma membrane. Again, the magnitude of plasma membrane damage that each cell sustains is highly variable, and may lead to inconsistent delivery and cell survival. The generation of cellular and biological debris may be another problematic aspect of cell scraping and bead loading. Moreover, delivery of expensive reagents that need to be concentrated into small volumes can be difficult to achieve with these protocols. On the other hand, potential benefits are the low-cost and accessible nature of these protocols, as they can be performed with common lab equipment. In applications where high cell viability is not a priority, scraping and bead loading may represent convenient options. A later adaptation of bead loading termed ‘immunoporation’ used beads functionalized with antibodies to bind to cells and permeabilize them by ripping off bits of their membranes^{688–694}.

Bead and scrape loading techniques have been used to deliver a variety of cargoes into cells. Bead loading has been used to deliver dye-conjugated dUTP for fluorescent visualization of chromosome formation⁶⁹⁵, antibody loading into macrophages^{696,697} and fibroblasts⁶⁹⁸, intracellular delivery of proteins^{699–701}, peptides⁷⁰², fab fragments^{703,704}, peptide nucleic acid probes⁷⁰⁵, SNAP-reactive dyes⁷⁰⁶, CNTs⁷⁰⁷, and quantum dots up to 15 nm in several cell lines⁷⁰⁸. Scrape loading has achieved intracellular delivery of proteins^{176,501,709–715}, antibodies^{716–718}, peptides^{719,720}, morpholinos⁷²¹, high molecular weight dextrans^{176,722}, lipopolysaccharides⁷²³, dyes^{724,725}, pH-sensitive probes⁷²⁶, and transfection of plasmids⁵⁰³.

A variant of the scrape loading technique is scratch loading⁷²⁷. Also introduced by Paul McNeil, it involves dragging a needle or other kind of sharp object across a layer of adherent cultured cells. The cells that brush the edge of the needle undergo membrane damage but remain adherent to the substrate. Intracellular delivery of dextrans⁷²⁷, dyes⁷²⁸, fluorescently-labeled nucleotides⁷²⁹, and quantum dots⁷⁰⁸ has been achieved in cells adjacent to the scratch zone. Although the method is lower throughput than scrape loading, one advantage of scratch loading is that cells remain adherent for immediate analysis.

Sudden Cell Shape Changes & Protease Treatments: Sudden contraction of cells from an adherent, elongated shape to a rounded shape has the potential to generate membrane disruptions. Grinnell and colleagues found that the sudden contraction involved in the fibroblast-driven collapse of collagen matrices is able to induce permeabilization and uptake of dextrans up to 150 kDa in size^{730,731}. In this approach, fibroblast-colonized collagen matrices that are stabilized by substrate attachment are peeled away from their support. The isometric contractile forces generated by the fibroblasts then trigger compaction of the collagen matrix into a dense body one tenth of its original size⁷³¹. This process induces plasma membrane disruptions in the contracting fibroblasts. Membrane permeabilization is thought to be due to the tearing of focal adhesion sites associated with rapid cell shape change and compression of the collagen matrix^{534,730}. The lesions are resealed in a Ca²⁺-dependent fashion, with the fibroblasts reported to be impermeable to uptake several seconds after return to standard physiological media^{534,730}. Fibroblasts that detach from their substrates to round up in mitosis also exhibit permeability to dextrans up to 150 kDa, peptides, proteins, or oligonucleotides⁷³². This observation is in congruence with other

studies that have observed plasma membrane damage and dye uptake during mitotic cell rounding^{733,734}.

In what could be a related phenomena, permeabilization has been observed when attached fibroblasts are treated with strong doses of the proteases trypsin, pronase, or collagenase^{735,736}. Cytoplasmic delivery of the proteins insulin (6 kDa), lysozyme (14 kDa), BSA (76 kDa), and thyroglobulin (660 kDa) were achieved with this simple treatment. Although the mechanisms were not investigated, cells presumably become permeable as they detach from the substrate⁷³⁰. Indeed, membrane ripping has previously been observed when certain cell types move across or detach from surfaces⁷³⁰. However, intracellular delivery of proteins by protease permeabilization has been reported for both adherent⁷³⁷ and non-adherent cell types⁷³⁸. If protease-mediated permeabilization is not due to membrane ripping during detachment, it could be that cells are permeabilized through the action of the proteases themselves. Trypsin can trigger signaling events that culminate in vigorous contractile activity at the cell surface and loss of coherence between the cortex and plasma membrane⁷³⁹. Such events could potentially induce transient plasma membrane disruptions. Thus, further studies may be needed to identify the mechanisms of membrane disruption by rapid cell shape changes and the action of proteases, and whether these phenomena can be made more widely useful.

Projectile Permeabilization: Sautter et al. pioneered a variation of the biolistic approach that retains free DNA in solution⁷⁴⁰. It is distinct from the projectile bombardment methods covered in section 5.2 in that the particles are used to permeabilize the cells rather than carry cargo. Projectiles are accelerated towards target cells in a Bernoulli air stream as a fine mist of droplets. The projectile particles create membrane disruptions that allow influx of plasmid DNA dispersed within the droplets. This stream of droplets can be targeted toward 150 μm areas of cells or tissue for localized targeting with dynamic adjustment of particle density and velocity.

Filtroporation: In 1999 a constriction-based method for generating disruptions in the plasma membrane was reported⁷⁴¹. The technique, termed “filtroporation”, works by forcing cell suspensions through uniformly-sized micropores in commercially available track-etched polycarbonate filters (Figure 15C). In the reported study, a polycarbonate filter of approximately 12 μm thick with pore sizes ranging from 5–18 μm was used. Plasmid DNA and dextran-conjugates up to 500 kDa were successfully delivered to CHO cells of nominal diameter $\sim 13 \pm 2 \mu\text{m}$. The cell suspensions were driven through the polycarbonate filter by a pressure regulator supplying constant pressures of 0 to 175 kPa. Delivery efficiency and cell damage were both increased as a function of driving pressure. Severity of the treatment also increased as the micropore diameter was decreased when all other parameters were held constant. By tuning parameters, optimal conditions of 8 μm pore size and driving pressure of 35 kPa were identified in $\sim 13 \mu\text{m}$ CHO cells. Thus, the cells experienced 40% constriction of their diameter as they passed through the polycarbonate filter. These conditions permitted uptake of a luciferase reporter plasmid, which resulted in transfection of the cells with a reported transfection efficiency above 50% after 2 days in culture. Despite these results,

further work on filtration is absent from the literature as the technique does not appear to have gained traction.

Microfluidic Cell Squeezing: Microfluidic and lab-on-chip methods of plasma membrane perturbation offer the opportunity for precise control of the membrane disruption process⁵⁸. In 2013 Sharei and colleagues reported on the development of a microfluidic platform for intracellular delivery by rapid cell deformation (or squeezing) through channel constrictions (Figure 15D). This innovative method has demonstrated delivery of diverse macromolecular materials into a wide range of cell types^{184,287,742}. The delivery mechanism is via diffusion of macromolecular cargo through membrane disruptions generated by rapid deformations of cell shape (Figure 16A(i)). The device is comprised of parallel constrictions generated by deep reactive ion etching in silicon wafers, followed by bonding to pyrex glass and drilling holes for inlet and outlets (Figure 16A(ii)). Gas pressures of 10–100 kPa are then used to drive cell suspensions through constrictions of 4 to 8 μm in width, 10 to 50 μm length, and 20 μm channel depth. The ability to engineer angle of entry and repeated constrictions is also possible. In the first published study, the bona fide cytoplasmic delivery of unaggregated quantum dots was demonstrated in HeLa cells²⁸⁷. Then a wider range of cell types was screened to showcase efficacy with blood derived immune cells (T cells, B cells, and macrophages), primary dendritic cells, embryonic stem cells, and primary fibroblasts, as well as a panel of immortalized cell lines¹⁸⁴. Efficient cytosolic delivery of siRNA, carbon nanotubes, quantum dots, antibodies, transcription factors and dextran-conjugated dyes was observed in many of these cell types.

A major strength of cell squeezing is the simplicity of the approach – no moving parts or external power are required, simply a pressure source and controller to modulate flow rate. Weaknesses include cell type and size dependence for a particular device geometry, and the potentially narrow range of flow rates required to achieve optimal balance between delivery and viability. However, a variety of chip geometries have been developed to address a broad range of cell types. Furthermore, experiments with buffer composition (e.g. Ca^{2+} concentration) indicate that it can successfully be tuned to optimize membrane recovery kinetics and cell survival⁷⁴³. In line with what is known from the cell biology of membrane repair, it was observed that buffers with calcium promoted rapid (~30s) closure of membrane wounds while no calcium conditions allowed the membrane to remain open for several minutes⁷⁴³. By modulating treatment parameters as well as temperature, a further demonstration of immune cell engineering with siRNA, antibodies and proteins was shown in T cell, B cells, dendritic cells, and monocytes/macrophages at throughputs of millions of cells per second^{744,745}. These results suggest cell squeezing might be a promising path towards engineering cell function for immune cell therapy at high-throughput.

The cell squeezing platform has been used for protein delivery to primary mammalian plasmacytoid dendritic cells with a device consisting of 10 μm and 4 μm wide constrictions repeated 5 times in series⁷⁴⁶. Zoldan and colleagues employed microfluidic cell squeezing to perform high throughput delivery of fluorescently labeled tRNAs into multiple myeloma cells with a transfection efficiency of ~45%⁷⁴⁷. Delivery of fluorescently labeled tRNAs enabled monitoring protein synthesis inside the cells in real time⁷⁴⁷. Because of the sensitivity of cells to constriction size, it was tested whether the squeeze platform could

exploit size differences of cells to facilitate selective intracellular delivery⁷⁴⁸. As a proof of concept, Saung et al. showed that the system is able to selectively deliver molecules to pancreatic cancer cells within a heterogeneous mixture containing T-cells⁷⁴⁸. One future application of this concept would be to selectively tag CTCs or other abnormal large cells in the blood⁷⁴⁸.

Electric Field-Enhanced Microfluidic Cell Squeezing: Like most other mechanical membrane disruption techniques, DNA transfection efficiencies upon cell squeezing are generally quite low in many cell types. Ding and co-workers explored the idea of adding a downstream electric field to investigate whether it could improve DNA transfection results (Figure 16B)⁷⁴⁹. The strategy, termed ‘disruption and field enhancement’ (DFE), was compared with standard cell squeezing, microfluidic flow-based electroporation, commercial electroporation (Neon – Thermo Fisher), microinjection directly to the nucleus, and lipofection⁷⁴⁹. In HeLa cells, DFE was able to achieve similar transfection efficiencies as lipofection and commercial electroporation. Surprisingly, plasmid expression approached its maximum within 1–2 hours of treatment, which was also the case with microinjection. This contrasts with the delayed onset on expression after lipofection and standard electroporation, which can take 24 hours or longer due to requirement of endocytosis and other intracellular trafficking processes to deliver DNA to the nucleus⁷⁴⁹. Fixation and imaging of cells directly after treatment indicated that DFE, like microinjection, could deliver plasmids directly into nucleus for immediate expression. To determine whether DFE was permeabilizing the nuclear envelope to permit DNA uptake, a HeLa cell line expressing the protein CHMP4B–GFP was imaged with confocal microscopy. CHMP4B is a component of the ESCRT-III complex, recently discovered to be involved in repair of both plasma membrane and nuclear envelope disruptions^{415,751–753}. While squeezing and standard electroporation only permeabilized the plasma membrane, DFE was found to also generate disruptions in the nuclear envelope. After treatment, nuclear envelope repair appeared to be completed within ~15 minutes, in agreement with previous studies^{751,752}. It was speculated that by first disrupting the plasma membrane, subsequent exposure to the electric field was able to electroporate the nucleus. Indeed, specific types of electroporation have previously been found to selectively permeabilize intracellular compartments (reviewed in⁵³⁷). DFE thus represents a useful strategy for high-throughput nuclear delivery and rapid expression of DNA⁷⁴⁹. Further work should clarify the exact mechanisms of cargo influx upon complex mechanical/electrical hybrid treatments such as DFE.

Variations on Microfluidic Cell Squeezing Architecture: In 2015 the Qin lab introduced microfluidic intracellular delivery devices featuring various types of PDMS-based micro-constrictions⁷⁵⁴. Until this point, most results had been obtained in microfabricated silicon devices¹⁸⁴. By using repeated arrays of constrictions fabricated from PDMS, Qin and co-workers reported delivery of single-stranded DNA, siRNA, and plasmids into HEK cells and several other cell lines⁷⁵⁴. Moreover, they demonstrated genome editing in MCF7 and HeLa cells via delivery plasmids that express Cas9 and gRNA, although transfection efficiencies were not directly reported⁷⁵⁴. In a subsequent study, the group modified their device architecture to perform siRNA delivery to cancer cells with a repeated pattern of 5 μm constrictions in a reverse wishbone configuration⁷⁵⁰(Figure 16C). Experiments and

simulations both indicate that sharper constrictions conferred by the reverse wishbone intensified the local stress on the plasma membrane to increase the magnitude of membrane disruption⁷⁵⁰. Another of their publications featured sharp star-shaped constrictions to facilitate delivery of dextrans, siRNA, and Cas9 RNPs to the intracellular space of hard-to-transfect suspension cell lines and T cells²²⁷. By delivering RNPs targeting GFP, they were able to achieve CRISPR-mediated GFP knockout in several standard cell lines. Also demonstrated was low-efficiency CRISPR-mediated knock-in editing of the PD-1 gene in primary T cells, an application that could be relevant for cell based therapies²²⁷.

So far, the results on cell squeezing indicate that the rapid deformation of cells in suspension is able to create holes in the plasma membrane in a relatively well-controlled and reproducible manner. In an extension of this concept, it is possible to asymmetrically deform cells by flowing them past an abrasive object positioned on one side of a microfluidic channel. Such a strategy would presumably disrupt the plasma membrane in a more localized manner, preferentially permeabilizing one side of the cell. To explore this idea, the Qin lab introduced a device with sharp silicon nanoblades protruding from one side of PDMS microfluidic channels⁷⁵⁵. The protruding edge of the silicon nanoblade was essentially formed a spike of ~200 nm radius, creating a gap of ~2 μm for cell passage. By optimizing the flow rate and number of nanoblade constrictions, they achieved ~70% delivery efficiency of 70 kDa dextran with ~80% cell viability in hard-to-transfect HSCs⁷⁵⁵. Compared to electroporation, the delivery efficiency was the same, however, survival and ability of HSCs to remain pluripotent were claimed to be superior with the nanoblade device. Cas9 RNPs were successfully delivered into HSCs, but the actual gene editing efficiencies as a percentage of total cells treated were not reported⁷⁵⁵.

Potential Off-Target Effects of Cell Squeezing: Cell squeezing strategies often rely on significant cell deformations – sometimes up to 70% of the cell diameter. An unresolved issue is to whether off-target damage may be inflicted upon intracellular structures, such as the cytoskeleton, nucleus, and even genomic DNA. For example, it has been observed that cells migrating through tight constrictions undergo transient nuclear ruptures and DNA damage⁷⁵¹. As the stiffest object in the cell, the nucleus is widely regarded as the determining factor governing passage of cells through micro-sized constrictions^{756,757}. It has also been observed that apoptotic and cell stress response can significantly impact cell survival after passage of cells through constrictions⁷⁵⁸. Lamins, which mechanically reinforce the nuclear envelope, play a protective role in physically buffering the nucleus from mechanical stress and their depletion was shown to make cells more vulnerable to death after passage⁷⁵⁸. Moreover, DNA damage has previously been observed with imposed cyclic mechanical stresses in certain cell types⁷⁵⁹. Experiments from Ding and colleagues that visualized nuclear disruptions with CHMP4B-GFP indicated that squeezing HeLa cells (nucleus diameter ~8–12 μm) through 7 μm constrictions did not disrupt the nuclear envelope⁷⁴⁹. Because disruption of the nuclear envelope can be associated with DNA damage, it indicates genomic DNA may be safe even when cell are squeezed by more than 50% of their initial diameter. Moreover, measurements of DNA damage with a high throughput COMET assay⁷⁶⁰ failed to indicate significant DNA damage in HeLa cells forced through 6 μm constrictions (unpublished observations). However, further

investigations with different types cells (particularly those of clinical relevance), with a variety of constriction architectures, may be required to fully address the question of off-target DNA damage.

Nanowires for Transient Permeabilization: Arrays of sharp nanowires have been used to permeabilize cells by transiently piercing their plasma membranes. In those cases nanowires are thrust into the cells followed by withdrawal to promote diffusive influx from the surrounding media (Figure 15E). This mode of plasma membrane penetration is similar to the nanowires/nanostraws described in section 5.3, except that the delivery mechanism is via diffusion through a permeabilized plasma membrane rather than dissociation from the nanoneedles themselves. In one notable example, a grid of diamond nanowires was centrifuged onto cultured cells at controlled forces using standard lab centrifuges⁶⁵⁴. Thin diamond nanowires were fabricated by first depositing a nanodiamond film on silicon wafers followed by microwave plasma chemical vapor deposition to grow a uniform field of needles. In the versions used for experiments, dimensions were optimized to ~300 nm diameter, ~4.5 μm height with straight sidewalls at a density of ~6 nanowires per $10 \times 10 \mu\text{m}^2$. It was found that nanowires of diameter >800 nm caused excessive damage to cells but those < 400 nm produced a suitable balance between delivery efficiency and cell damage. For this geometry, it was calculated that centrifugation at 300 r.p.m. yields ~2 nN penetration force per nanowire, which was claimed to be an ideal penetration force for monolayers of cells grown in culture. Upon withdrawal of nanowires from cells, influx of IgG antibodies, ~20 nm quantum dots, and ~200 nm polystyrene nanoparticles into the cytoplasm of primary neurons was demonstrated. Furthermore, by packaging DNA with lipid-based lipofectamine complexes, plasmid transfection in neurons was boosted from around 1–5% (lipofectamine alone) to almost 50% with additional nanowire permeabilization. If nanowire permeabilization were used with naked DNA alone, transfection efficiency was <1%, suggesting that: 1) centrifuged the nanowires did not consistently permeabilize the nucleus, and 2) that lipid complexes may facilitate nuclear targeting and protect the DNA from premature degradation. Thus, direct cytosolic delivery of DNA-lipid complexes may boost efficiency of transfection in otherwise difficult-to-transfect cells such as neurons.

Several other groups have also used arrays of nanowires to permeabilize cells for delivery. In one case arrays of silicon lances were pressed against cell monolayers with a compliant suspension system instead of centrifugation⁶⁸³. The silicon lances were larger than typical nanowires, with lengths of 8 μm , diameters around 0.5 to 1.0 μm , and sharpened tips. Although this setup yielded diffusion-based intracellular delivery of propidium iodide, delivery of larger molecules of biological interest was not tested⁶⁸³. Matsumoto produced nanowire arrays of 25 μm length and 200 nm diameter⁷⁶¹. They were attached to a piezoelectric actuator stage and lowered onto cell monolayers then vertically oscillated at a frequency of 5 kHz at an amplitude of ~0.5 μm for up to 2 minutes⁷⁶¹. Continuous delivery of molecules from solution appeared to be augmented by the agitation associated with nanowire oscillation. Up to 50% of cells retained detectable levels of 70 kDa dextran after treatment. Efficiency of plasmid transfection, however, was only ~7%, which was less than the 18% achieved when plasmids are directly attached to nanowires⁶⁴⁰. Interestingly, the

abovementioned examples of nanowire permeabilization are essentially scaled-up versions of single cell permeabilization previously performed with sharpened AFM tips. In 2006 a method introduced by Hara et al. demonstrated stab and withdraw permeabilization by using AFM tips that had been sharpened by focused ion beam technology⁶⁷⁸. Expression of plasmid DNA from the culture media was achieved with serial penetrations of sharpened tips into HeLa cell nuclei using a computer controlled device called the “CellBee”⁶⁷⁸.

Section Summary: Classic methods of mechanical contact-mediated permeabilization such as scrape and bead loading provide low-cost, accessible and crude solutions for delivery of certain cargoes, especially proteins, small molecules, and oligonucleotides. However, delivery efficiency and cell survival may not be sufficient for certain applications, particularly in sensitive cell types. Recent progress in solid contacted-mediated mechanical membrane disruption takes advantage of the increased precision afforded by MEMS, microfluidics, lab-on-chip, and nanotechnology capabilities to more finely control the level of cell injury^{58,331,762}. Prominent examples include microfluidic constrictions for squeezing of cells in suspension^{184,749} and nanowires to transiently permeabilize adherent cell monolayers for high throughput intracellular delivery⁶⁵⁴.

6.1.2 Mechanical: Fluid Shear—Lipid bilayers can be disrupted by fluid shear forces in a number of ways. If water molecules flow parallel to a membrane surface at a sufficiently rapid velocity, it can tilt the lipid heads in the direction of the shear and lead to buckling instabilities that eventuate in bilayer rupture⁷⁶³. Alternatively, a jet of water molecules propelled perpendicularly into a membrane can pierce it in an analogous way to a mechanical object⁷⁶⁴. Unlike membrane disruption via solid contact (discussed above), fluid shear forces are less invasive. On the flipside, fluid shear forces in aqueous environments tend to be significantly more difficult to control. In this section we discuss the strategies and methods that have been used to perform membrane disruption-based intracellular delivery by harnessing fluid shear forces. First, we will explore shear forces generated by flow of fluid relative to microscale channels and objects. Second, acoustic sonoporation, which is thought to depend mainly on the forces associated with cavitation bubbles will be discussed. Third, we will cover laser-induced cavitation as a strategy for generating highly localized and intense zones of fluid shear.

Syringe Loading—One of the simplest approaches for generating zones of high fluid shear force is to drive a liquid through tight constrictions. In 1992 Paul McNeil and colleagues introduced an intracellular delivery method called syringe loading, where cell suspensions mixed with high concentrations of a cargo to be loaded are repeatedly aspirated and expelled through fine-gauge syringe needles to transiently permeabilize cells (Figure 17A)¹⁷⁸. A typical protocol consists of eight passes of cell suspension through a 1 ml syringe affixed with a 30 G needle, which has an inner diameter of 160 μm ¹⁷⁸. In the initial publication, delivery of cargo sizes up to 150 kDa were obtained in several mammalian cell lines¹⁷⁸. Furthermore, the addition of pluronic F-68 (also known as poloxamer 188) was found to increase the tolerance of cells to membrane permeabilizing shear forces, thereby enabling the cells to undergo harsher treatments and improve cell survival. In the cell types tested, syringe loading in the presence of pluronic F-68 appeared more efficient than both

bead and scrape loading¹⁷⁸. Low-volume versions of the protocol were also developed, using a 25 μ l Hamilton syringe with 25 G fixed needle (inner diameter 260 μ m) for 80 passes. A 5 μ l version of the protocol was described with a 10 μ l micropipette tip (inner diameter not reported) involving 60 passes.

In subsequent reports, syringe loading has demonstrated utility in a variety of delivery applications, mostly to conduct studies in basic biology. In one example, it has been used to perform DNA transfection⁷⁶⁵. Using a selection strategy, stable integration of plasmid DNA into the genome of host CHO and mouse Ltk(-) cells was estimated in approximately one of every 50,000 cells treated, which was considered a success given the low cost of the technique⁷⁶⁵. Ghosh and colleagues that syringe loading could deliver neutrally charged antisense phosphorodiamidate morpholinos into cells for the purpose of gene silencing⁷⁶⁶. Moreover, the same delivery strategy has been used for loading of small molecular weight nucleotides, GTP and GDP (~0.5 kDa), and their analogues to explore G-protein biology in immune cells and endothelial cells^{767,768}. In another application, fluorescent labeling of the neuronal cytosol was achieved when trypsinized ganglia were syringe loaded with 10 kDa dextrans⁷⁶⁹.

The most common application of syringe loading, however, has been delivery of proteins and antibodies to the intracellular space. GST-FAK fusion proteins were loaded into fibroblasts by passing them through a 30 gauge syringe needle 30 times⁷⁷⁰. HEp-2 cells were loaded with monoclonal antibodies by 20 cycles through a 27 gauge needle⁷⁷¹. A modified version of the protocol was employed by Sydor et al. to deliver fluorescently-labeled antibodies into trypsinized neurons by using ~100 cycles of aspiration-expulsion through pipette tips⁷⁷². For delivery of monoclonal antibodies to fibroblasts, a mixture of cells and antibodies was cycled 20 times through a 30 gauge needle⁷⁷³. Kasier et al. syringe loaded a fluorescently labeled version of the protein profilin into amoebas and human cells to study its binding to intracellular actin⁷⁷⁴. In other studies of the actin cytoskeleton, FITC-conjugated anti-fascin immunoglobulins were delivered into ~95% of fibroblasts or myoblasts by 4 passages through a 1 ml syringe fitted with a 25 gauge needle⁷⁷⁵. Researchers from the Schwartz lab loaded endothelial cells with alexa-labeled versions of the p21 binding domain of PAK1 to investigate mechanobiology of the Rac1 pathway^{776,777}. Several studies have also employed syringe loading to study the effect of bacterial and viral proteins inside cells. For example, fibroblasts were syringe-loaded with HIV proteins to examine their impact on intracellular and nuclear architecture⁷⁷⁸. In another case, CHO cells were drawn up and expelled slowly (~0.2 ml·s⁻¹) through a 30 gauge syringe needle 6 times for intracellular delivery of the bacterial toxin ExoU⁷⁷⁹. Moreover, Xu et al delivered the *Legionella pneumophila* protein SidK into macrophages by 100 cycles of pipetting through a 200 μ l pipette tip⁷⁸⁰. In studies of herpes simplex virus replication, herpesvirus and nucleoporin antibodies were introduced into vero cells by 50 passages through a 27 gauge needle⁷⁸¹.

Microfluidic Control of Shear Forces: Syringe loading presumably works by creating regions of significant shear force around the entrance and exit of the syringe needle (Figure 17A). Because the fluid flow is controlled manually, however, it may require extensive empirical testing and skill to reproducibly obtain optimal cell treatment⁷⁸². Improved

precision and reproducibility could potentially be achieved by using microfluidic devices to generate controlled zones of fluid shear. Along these lines, Prausnitz and colleagues fabricated a simple flow-through microfluidic device with parallel constrictions⁷⁸³ (Figure 17B). Lasers were used to bore out 50 – 300 μm conical microchannels from 100 to 250 μm thick mylar sheets and syringe pumps were employed to flow cell suspensions through the channels at controlled flow rates, thereby subjecting cells to well-defined shear forces. The resultant loading of fluorescently labeled dextrans and proteins into DU145 prostate cancer cells, as well as the viability, however, turned out to be less favorable than syringe loading. Further attempts towards plasma membrane permeabilization through microfluidic control of shear forces have not been reported and therefore present an opportunity for future investigations.

Other Examples of Cell Permeabilization Through Shear Forces: Driving fluid through narrow constrictions is not the only way to generate fluid shear forces for cell permeabilization. Indeed, researchers have used cone-plate viscometers to generate hydrodynamic shear forces above cell monolayers, obtaining uptake of fluorescent molecules in neuronal and endothelial cultures (Figure 17C)^{784,785}. In 1997, LaPlaca and colleagues confirmed permeabilization of neurons by observing an increase in intracellular Ca^{2+} , release of enzymes to the extracellular solution, and cell swelling⁷⁸⁴. Later, Blackman and colleagues used a modified cone-plate setup to expose endothelial cell monolayers to fluid shear forces⁷⁸⁵. When forces were too high, cells peeled away from the substrate. After empirical optimization, however, conditions were identified where all cells remained attached to the substrate yet 16% of cells retained 4 kDa⁷⁸⁵. The Blackman cone-plate viscometer was then used to permeabilize cultured neurons, investigate their physiological response, and test strategies to improve neuron survival⁷⁸⁶. Relative permeabilization efficiency was analyzed by influx of small molecular weight fluorescent dyes⁷⁸⁶.

Intense pulses of fluid shear can be directed at cells by firing jets of pressurized inert gas toward them^{787,788}. Similar to the case of cone-plate viscometers, it was found that excessive shear forces can rip cells from the underlying substrate, but if modulated just below this range, were capable of permeabilizing cell membranes while leaving adherent cells in place. With the appropriate optimizations, intracellular delivery of dextrans, plasmids and other cargo has been demonstrated in common adherent cell lines^{787,788}.

Sonoporation: Sonoporation is the disruption of cell membranes by acoustic pressure waves, mostly in the ultrasound frequency range (20 kHz to GHz). Its deployment for intracellular delivery purposes first arose in the mid 1980s through the use of ultrasound to permeabilize cultured cells^{503,789–791}. Permeabilization was achieved by placing cell suspensions in a plastic tube and applying 3 half-second pulses of the ultrasonic transducer directly to the tube. With this rudimentary approach, Fechheimer et al. demonstrated intracellular loading of dextrans and proteins into Amoebae^{503,789,791}. Moreover, ultrasound-mediated permeabilization was compared head-to-head with scrape loading⁵⁰³. However, the latter was found to yield superior delivery of dextran-conjugated dyes and DNA plasmids to HeLa cells, hepatic tissue cultures, and mammalian fibroblasts⁵⁰³.

About a decade later, sonoporation began to be taken seriously as a method for DNA transfection^{792–794}. Several factors converged to motivate this trend⁷⁹⁵. First, high intensity focused ultrasound was gaining prominence as a non-invasive method for therapeutic treatment of targeted cells and tissues *in vivo*^{796,797}. Examples include local tissue ablation, local drug delivery stimulated by ultrasound, and, gene therapy by targeted nucleic acid transfection⁷⁹⁸. Second, the mechanisms of ultrasonic effects were being increasingly clarified, with cavitation bubbles implicated as the prime instigators of membrane disruption effects⁷⁹⁹. These mechanistic insights enabled a more rational approach toward sonoporation that greatly boosted its efficiency. Particularly key was the deployment of gas body ultrasound contrast agents to act as cavitation nuclei. This modification was found to drastically improve transfection efficiency compared to ultrasound alone^{793,800,801}. For example, commercially available microbubbles were mixed with cultured immortalized human chondrocytes and exposed to 1.0 MHz ultrasound transmitted through the bottom of a six well culture plate. The addition of microbubble cavitation nuclei, along with other empirical optimizations, enhanced DNA transfection nearly 20-fold over previous reports and indicated that ultrasound could be a feasible DNA transfection technique⁸⁰¹.

Mechanisms of Sonoporation: As the field currently stands, hundreds of studies have been published on the subject of understanding and improving sonoporation. Although non-invasive *in vivo* applications may be the final goal, many of these efforts have exploited *in vitro* experiments for in-depth mechanistic investigations and proof-of-principle studies. Recent reviews have covered the sonoporation field in detail^{802–807}. The mechanisms underlying sonoporation are diverse and may involve: 1) microstreaming caused by stable cavitation, whereby a cavitation bubble oscillates in synchrony with the acoustic field (Figure 17E), 2) jetting forces from inertial cavitation, which is triggered by the collapse of a cavitation bubble (Figure 17D), 3) a shrinking cavitation bubble pulling against the plasma membrane⁸⁰⁸, 4) an expanding cavitation bubble pushing against the plasma membrane⁸⁰⁸, 5) bubble translation, whereby acoustic radiation forces push a bubble through the plasma membrane, 6) nucleation of a cavitation bubble between bilayer leaflets, rupturing the membrane upon expansion, 7) non-bubble acoustic effects, such as acoustic streaming due to pressure differences of the acoustic field^{803,805,809}. The literature consensus indicates that the first two mechanisms are the most prevalent. Below we discuss how these cavitation phenomena generate membrane disruptions.

Cavitation bubbles form and/or expand when the low pressure part of the acoustic wave passes through a liquid medium. Conversely, the high pressure peak of the wave corresponds with compression and/or implosion of cavitation bubbles^{803,805,809,810}. The bubbles may be created by the pressure waves themselves or provided by the supplementation of stabilized microbubbles in the form of commercially available contrast agents. A bubble that expands and contracts in synchrony with the acoustic field (stable cavitation) generates local oscillatory shear forces due to microstreaming^{811,812}. The microstreaming forces are sufficiently potent to permeabilize nearby cells. On the other hand, a bubble that implodes (inertial cavitation) can trigger extreme phenomena including electromagnetic radiation (sonoluminescence), severe temperature spikes up to thousands of degrees, sonochemical reactions such as production of free radicals, and intense microjetting. Although any of those

phenomena can perturb lipid bilayers, the permeabilizing effects of bubble collapse have primarily been ascribed to the potent fluid shear forces generated by microjetting^{803,805,809}. As a cavitation bubble implodes, surrounding water molecules rush in to fill the void. If there is a surface nearby (such as a lipid membrane) less water molecules are available to flow from that region. This biases the flow towards that surface and results in the microjet being oriented in that direction. Thus, imploding cavitation bubbles can result in the selective puncture of an adjacent cell (Figure 17D). High pressure ultrasound is more likely trigger inertial cavitation while lower pressure procedures bias the system toward stable cavitation⁸⁰⁵.

Cargo Delivered by Sonoporation: Because of the variation in magnitude and mode of fluid shear phenomena that can produce sonoporation, it is perhaps not surprising that the resultant holes have been reported to range from nanometers up to several micron^{803,805,809,813–815}. Under conditions where large holes are generated, sonoporation can be expected to enable delivery of small and large cargos alike. Because of the motivation for gene therapy, significant efforts have gone into optimizing sonoporation for DNA transfection over the last two decades^{792,793,795,801,816–822}. Transfection of other nucleic acids, such as antisense oligonucleotides⁸²³, siRNA^{824,825}, and mRNA⁸²⁶ have received less attention, but also been demonstrated. To study mechanisms, much work in the field has exploited delivery of fluorescently labeled dextrans of varying molecular weight (~1–30 nm hydrodynamic radius)^{503,789,790,812–814,827–836} and small molecular weight dyes (<1 nm)^{764,808,813,814,820,828,835,837–845}. Also demonstrated has been intracellular delivery of small molecule drugs^{835,846–850}, polymer nanoparticles of 25–75 nm⁸³¹, viral particles⁸⁵¹, proteins⁸²⁸, antibodies⁸⁵², and peptides⁸⁵³. In some cases delivery has been ascribed to endocytosis and not influx after permeabilization⁸³². This could be applicable to larger cargo such as plasmid DNA, where delayed expression kinetics akin to electroporation have been observed⁸⁰⁹.

The majority of reports on sonoporation-mediated delivery have focused on technology development and not its use to carry out basic research. In the early days of sonoporation in the late 80s and early 90s, however, there were some examples of biologists using it to carry out basic science research^{789,791,837,851,852}. Although at least one commercial sonoporation system has been available for more than a decade (Sonidel SP100), its use for intracellular delivery appears confined within the ultrasound community^{854,855}. The most significant challenge for sonoporation *in vitro* remains the random and uncontrolled nature of cavitation events leading to excessive cell damage and death⁸⁰⁷. A 2012 review of 26 published studies conducted over more than a decade concluded that conventional *in vitro* sonoporation with nucleation agents almost never yielded above 50% for both delivery efficiency and cell viability⁸⁰⁷. Poor viabilities are perhaps due to cavitation-related side effects such as high local temperatures and generation of reactive oxygen species⁸⁵⁶. Thus bulk sonoporation may be inherently limited as a delivery approach *in vitro*. *In vivo* applications have been more promising⁷⁹⁸, especially in skin where optimal parameters have been identified and barriers to delivery of therapeutic cargo are more on the tissue, rather than cellular, level⁸⁰².

Shock Wave-Mediated Permeabilization: Shock waves differ from acoustical waves in that they are higher pressure and propagate at supersonic speed⁸⁵⁷. They are best known as the by-products of explosions. Various devices and strategies have been employed for producing shock waves to permeabilize cell membranes. They include shock wave lithotripters^{858–861}, shock tubes^{862–864}, underwater spark discharge⁸⁶⁵, and laser-induced shock waves^{863,864,866–872}. These systems mostly administer pulses one at a time instead of the continuous waves characteristic of acoustic ultrasound. Lithotripters generate potent high pressure pulses that are used to break down tissue obstructions such as kidney stones. Up to 4000 individual pulses may be repeated in a typical kidney stone removal operation. In 1994, Gambihler and colleagues placed polypropylene vials containing a mixture of suspended mouse L1210 lymphocytic leukemia cells and fluorescent dextrans under the focal point of lithotripter shock waves⁸⁶⁰. After treatment, the uptake and retention of dextran molecules was detected by flow cytometry. Although the authors admitted electroporation was more consistent and efficient, lithotripter treatment showed a significant uptake of 2000 kDa dextran (~50 nm) with reasonable cell survival.

Kodama et al. employed shock tubes to generate intense shock waves in cell suspensions and obtain intracellular delivery of labeled dextrans^{862–864}. Shock tubes generate a mechanical pulse when a thin diaphragm between a high pressure and low pressure chamber ruptures. The pulse then propagates through a second diaphragm and is focused into the cell solution via a reduction nozzle, thereby achieving membrane permeabilization⁸⁶³.

A number of studies have employed laser-induced shock waves for membrane permeabilization^{863,868–872}. Laser-induced stress waves can be generated by one of the following mechanisms: optical breakdown, ablation, or rapid heating of an absorbing medium⁸⁷⁰. In one configuration, laser irradiation of an absorbing polymer film produces shock waves that emanate into a solution containing cells and cargo^{869,871,872}. Depending on experimental conditions, the mechanism of cell membrane disruption may or may not rely on cavitation. In one set of examples, the rise time of the stress wave and its duration was linked to membrane permeabilization, probably due to shear forces involved with the wavefront itself^{863,868–870,872}. Conversely, in other studies cavitation was implicated as the critical determinant of shock wave-induced membrane damage^{858,866,873}.

Laser-Induced Cavitation Bubbles: So far we have covered membrane disruption arising from acoustic pressure wave and, shock waves, as well as cavitation phenomena triggered by these these stimuli. Cavitation can also be triggered and/or controlled in a more direct manner by the action of lasers incident upon an absorbent agent in an aqueous environment^{874,875}. The absorbent agent may be the membrane itself, a photoabsorbent molecule added to the solution, a particle suspended in solution, or a material interfacing with the solution (Figure 18). When the plasma membrane absorbs laser energy and becomes disrupted (Figure 18A), this is known as optoporation and is covered in section 6.4. If the absorbing agent is in direct contact with the plasma membrane, the membrane will likely be perforated by a complex combination of secondary effects including extreme heat, chemical breakdown, and phenomena related to growth and collapse of cavitation bubbles (Figure 18B). If the absorbing agent is distant from the plasma membrane, membrane disruption is much simpler and cleaner: it most likely occurs by fluid shear (Figure 18C), as

thermal effects and near-field plasma do not propagate very far in an aqueous environment. In any of the above three scenarios the membrane may be disrupted by laser-induced cavitation. Upon absorption, the energy supplied by the laser is transduced into heat and/or chemical effects that lead to vaporization of surrounding liquid to create a cavitation bubbles^{874,875}. The bubbles disrupt cell membranes in the same way as sonoporation, either by microjetting after collapse (Figure 17D) or through microstreaming from bubble oscillation (Figure 17E). Most reports of laser-induced cavitation suggest bubble collapse, but there are a few cases where laser pulsing regimes can be tuned to sustain bubble oscillations⁸⁷⁶.

In a series of studies by Ohl and colleagues, microfluidic confinement was used to investigate the role of proximity to laser-induced cavitation bubbles⁸⁷⁷. The photo-absorbent molecule phenol red was added to solution to allow generation of cavitation bubbles from the laser focal region. Their results showed that the probability of cell permeabilization by cavitation bubble collapse could be modeled as a function of the distance of cells from the bubble and maximum cavitation bubble radius⁸⁷⁷. In a follow up study, they took advantage of arrayed microfluidic cell traps to immobilize myeloma cells and systematically analyze the conditions for controlled permeabilization at single cell level⁴⁴⁷. Again, phenol red used as an absorbing agents to facilitate the production of laser-induced cavitation bubbles that expand to ~100 μm diameter and collapse within tens of microseconds⁴⁴⁷. High frame rate imaging clearly visualized the expansion and shrinkage of cavitation bubbles in a non-symmetric manner due to the presence of a nearby structure. During bubble collapse, a fast microjet was directed toward the cell to generate a single large pore with diameters ranging from 0.2 to several μm . The diffusive uptake of trypan blue dye into the cell then took place over several seconds. If the standoff distance between cell and bubble were greater than 30 μm , no membrane disruption occurred. One concern is whether the cavitation bubbles perturb cells through temperature spikes. To address this issue, Ohl and colleagues used performed another study with fluorescence-based thermometry to measure local temperature gradients around laser-induced bubbles⁸⁷⁸. Under similar conditions as their previous experiments, it was found that the temperature rises are moderate ($< 12.8\text{ }^\circ\text{C}$), localized ($< 15\text{ }\mu\text{m}$) and short lived ($< 1.3\text{ ms}$). Thus, by developing a cavitation regime that damages cell membranes purely through mechanical forces, laser-induced cavitation may be amenable to implementation on a wider scale. It was suggested that arraying cells in microfluidic traps would allow for potential scale-up with pre-determined laser protocols to control the size and position of adjacent cavitation bubbles.

Laser-Induced Cavitation via Absorbent Particles: To transduce laser energy into cavitation, some approaches employ a deliberate seed particle to absorb the laser energy. One of the first papers to do this was published by Pitsillides et al⁸⁷⁹. They labeled lymphocytes with antibody functionalized metal microspheres and irradiated them with a 565 nm at a fluence of $0.35\text{ J}\cdot\text{cm}^{-2}$ and pulse duration of 20 ns⁸⁷⁹. Rapid emergence of microbubbles was observed around the seed particles and cell membranes were subsequently disrupted. By adjusting particle numbers, size, and laser energy delivered to the metal microspheres it was possible to tune the treatment either toward killing cancer cells for potential therapeutic purposes or transiently increasing the permeability of the plasma

membrane for intracellular delivery⁸⁷⁹. Another group used femtosecond laser irradiation of gold nanoparticles to produce plasmonic nanobubbles and permeabilize primary human cells for ex vivo intracellular delivery^{880,881}. Selective delivery of plasmids and dextrans was demonstrated in primary human cancer cells, T cells, and hematopoietic stem cells with reportedly good cell viability^{880,881}.

In 2010 Prausnitz and colleagues launched an intracellular delivery strategy involving laser irradiation of dispersed carbon black nanoparticle⁸⁸². Adherent cells were exposed to the cargo molecule to be delivered and sprinkled with ~200 nm aggregates of carbon black followed by irradiation with femtosecond lasers⁸⁸². Rather than thermal effects, they propose that the mechanism of membrane disruption was primarily due to a carbon-steam reaction at the particle surface, which subsequently propagates cavitation-related acoustic forces^{882,883}. Delivery of dyes, proteins, siRNA and plasmid DNA was achieved with acceptable cell viabilities in several cancer cell lines^{882,884}. Control experiments demonstrated that neither the carbon particles nor laser exposure alone were able to enable molecular uptake⁸⁸². This intracellular delivery concept was then extended beyond adherent cells to homogenous suspensions of carbon black nanoparticles and cells, which may be more amenable to treatment at higher throughputs⁸⁸⁵.

In one strategy from Braeckmans and co-workers, gold nanoparticles were employed as absorbing agents and laser excitation parameters were screened to test for and manipulate the balance between pure heating and bubble nucleation⁸⁸⁶. By tuning the laser energy, they identified conditions where it was possible to produce vapor nanobubbles around ~70 nm gold nanoparticles without transfer of heat to the surrounding environment. Comparing these two strategies revealed that vapor nanobubbles enabled superior delivery and siRNA transfection with less cytotoxicity⁸⁸⁶. Building on this approach, the same group delivered quantum dots into cells at high-throughput with efficiencies and viabilities above 80%²⁸⁹. Furthermore, in primary human T cells the vapor nanobubble approach was reported to yield greater siRNA transfection efficiency and cell survival when compared with nucleofection⁸⁸⁷. In congruence with these results, other groups have presented experimental and theoretical work that demonstrates nanobubble formation from the generation of a nanoscale plasma around the particle due to the enhanced near-field rather than from the heating of the particle^{888,889}.

Laser-Induced Cavitation at an Interface: Absorbing materials can be placed at a solid-liquid interface to convert laser energy into membrane-perturbing cavitation bubbles or shock waves. In recent studies, Ohta and colleagues fabricated a channel of defined height, with cells cultured on one side apposing an optically absorbing composite layer of 1 μm amorphous silicon on top of 200 nm indium tin oxide⁸⁹⁰. Instead of generating an exploding bubble, they oscillated a bubble using a 980 nm laser with 90 μs pulses over a duration of 10–15 seconds. Up to 3 oscillations of 8–10 μm without collapse were able to induce microstreaming shear forces to trigger plasma membrane permeabilization in apposing cells. Interestingly, the bubble had to be pressed tightly against the cell to induce membrane disruption. For 70 kDa fluorescently labeled dextran, they achieved up to 80% delivery at >95% viability. The pore-size was estimated to be about 30 nm based on exclusion of 500 kDa dextran and the closure dynamics indicated plasma membrane healing within ~20

seconds. In a follow-up study, the same authors lowered the channel height to 10 μm and generated stronger shear forces over 0.4 s with 60–100 μs pulses applied at a frequency of 50 Hz⁸⁷⁶. By generating larger pores with a more powerful shear forces, delivery efficiency of 500 kDa dextran improved to 70% and expression of 5.7 kb DNA plasmid was recorded at 86%.

Permeabilization of adherent cells can be achieved with by culturing them on patterned thermoplasmonic substrates followed by laser irradiation^{469,891,892}. In a strategy introduced by Mazur and colleagues, a thermoplasmonic substrate patterned with microscale gold-coated pyramids was fabricated by photolithography and template-stripping. A nanosecond pulsed laser is then scanned across the substrate to generate intense heating at the apex of each pyramid, thereby generating bubbles through plasmonic effects⁸⁹³. A large beam spot can be scanned across the substrate to permeabilize millions of cells over the course of minutes⁸⁹². Growth and collapse of the bubbles presumably disrupts cell membranes by mechanical shear forces, although plasmonic chemical effects or heat cannot be ruled out. Delivery of molecules up to 2000 kDa dextrans have been obtained with high cell viabilities⁸⁹² through holes estimated to be in the range of 20 nm⁴⁶⁹.

In a different approach, the Chiou lab developed a “photothermal nanoblade” capable of addressing single cells³¹³. A metallic nanostructure was placed at the tip of a micropipette as a seed structure to harvest short laser pulse energy and convert it into highly localized explosive vapor bubbles. Upon placement of the device next to cells, laser irradiation triggered cavitation events that yielded controlled pore sizes of up to several microns on the apical surface of adherent cells. Delivery of large cargo such as $\sim 2 \mu\text{m}$ bacteria, mRNA, plasmid DNA, polystyrene beads, and quantum dots was achieved^{288,313}. Furthermore, in an intriguing biological application, the photothermal nanoblade was used for mitochondrial transplants between cells³¹⁵. By delivering functional mitochondria to cells with normally dysfunction mitochondria, it was possible to identify mechanisms involved in restoration of metabolism³¹⁵. Consistent with what is known about membrane repair in healthy cells, electrical impedance measurement showed that it takes 1–2 minutes to recovery membrane integrity after treatment with the photothermal nanoblade⁸⁹⁴.

A high throughput version of the photothermal nanoblade concept was unveiled in 2015³¹⁴. Substrates arrayed with pores lined by metallic absorbers were irradiated to generate exploding cavitation bubbles underneath the basal side of adherent cells (Figure 17F). Membrane perturbation was synchronized with active pumping of cargo through the pores to successfully introduce living bacteria into the cytoplasm of several cell types. Showcasing the potential of the approach, it was discovered that the *igIC* gene from the bacterial species *F. novicida* is required for intracellular multiplication after cytosolic delivery. Such a high-throughput strategy to deliver micron-sized cargo clearly has broad utility with adherent cells, showcasing the power of well-controlled fluid shear forces to induce permeabilization of large batches of cells.

6.1.3 Mechanical: Pressure Changes—Osmotic and hydrostatic pressure gradients can be imposed across cell membranes leading to their rupture. The geometry of these gradients can vary, for example between a suspended cell and the extracellular solution,

across a select part of the plasma membrane (such as the apical membranes of an adherent cell monolayer), or between an intracellular vesicle (e.g. endosome) and the surrounding cytosol. Although difficult to control in time and space, transient pressure gradients achieved by osmotic or hydrostatic means represent a low-cost and simple avenue for intracellular delivery of macromolecular cargo. These methods have not been heavily pursued to date, however, perhaps due to a poor understanding of their effects and hesitance of researchers to excessively perturb cells⁸⁹⁵.

Osmotic Shock and Plasma Membrane Disruption: One of the simplest perturbations that a cell can experience is an osmotic shock, whereby a hydrostatic pressure is generated across the cell membrane due to differences in osmotic potential. Most mammalian cells normally exist in an aqueous environment of ~300 mOsm and significant deviations from this condition will induce the flow of water molecules into (hypotonic swelling) or out of (hypertonic shrinkage) the cell. When cells are placed into low osmolarity solution water rushes into the cell through the plasma membrane and aquaporin channels to solvate impermeable intracellular electrolytes and osmolytes. The subsequent swelling of cell volume leads to the unfolding of loose membrane, followed by well-described lipid bilayer rupture if area strain exceeds 2–3% (Figure 19A). Cells have been reported to possess membrane reservoirs of 2–10x their apparent surface area depending on the cell type and state³⁸⁴. Caveolae, endocytic pits, membrane folds, filopodia and microvilli are all examples of membrane reservoirs that can unfold to buffer membrane strain and accommodate cell surface area increase^{383,385}. It is thought that these reservoirs should be exhausted globally or locally before membrane stretch can result in rupture.

Hypotonic Loading of Red Blood Cell Ghosts: If the magnitude and duration of osmotic shock is optimal, partially burst cells can recover membrane integrity in the form of hollowed out “ghosts”. Although dead, ghosts can reseal and regain a limited set of functions. The concept was first established in red blood cells (RBCs) throughout the 1960s^{896–898}. Although RBCs possess little surface reservoirs compared to most nucleated cells, their capacity to reseal after a brief hypotonic shock is well proven^{899,900}. Indeed, RBC ghosts were able to enclose molecular cargo and even retain some basic biological functions despite being hollowed out of cytoplasmic components^{900,901}. In one early study, by adding ferritin at various times after the onset of hemolysis, it was determined that most cells were permeable for 15–25 seconds after hypotonic shock⁹⁰². Furthermore, the size and shape of membrane disruptions, as seen in fixed cells by SEM imaging, resembled long, narrow tears up to 1 μm long⁹⁰³. Later studies, however, indicated smaller holes around tens of nanometer or less⁹⁰⁴. Further adaptation of the technique optimized the hypotonic lysis procedures to results in high efficiency loading of proteins and enzymes into RBC ghosts^{901,905,906}. Perhaps due to their ease of hypotonic loading and autologous biocompatibility, RBC ghosts have been proposed as drug carriers for decades^{907–910}. Furthermore, fusion of loaded RBC ghosts into recipient cells was a popular method of intracellular delivery in the 70s and 80s^{167,901,911,912} before falling out of favor with the rise of electroporation and other alternatives⁵⁰².

Hypotonic Shock for Intracellular Delivery: Unlike RBCs that can passively reseal, most cell types mobilize active repair processes to recover from membrane disruption³⁹². It wasn't until the early 1980s that osmotic delivery methods would be translated beyond RBCs into other cell types. In 1982, Borle and Snowdowne devised a simple procedure to deliver the calcium-sensitive protein aequorin (21 kDa) into monkey kidney cells^{172,173}. Washed cell pellets were suspended and immersed in a ~10 mOsm hypotonic solution consisting of 3 mM MgATP, 3 mM HEPES buffer, and a given concentration of aequorin for 2 minutes at 4 °C. This was followed by sufficient addition of buffered KCl to restore isotonicity. Cells were then incubated in standard cell media for 1 hour at 37 °C to promote restoration of homeostasis before experiments. Optical readouts of aequorin activity indicated that it had been loaded successfully into fully functional cells, and it was used to measure accurate intracellular calcium concentrations of ~50 nM.

Citing Borle and Snowden's method as an inspiration, the hypo-osmotic approach for cytoplasmic delivery of aequorin was re-examined in greater detail by Klabusay et al⁹¹³. They were motivated by the need to accurately measure intracellular calcium dynamics in follicular lymphoma B cells, an application where the aequorin protein offers higher signal-to-noise ratio, better dynamic range, and more reliable calcium readouts than commonly used small fura dyes. In their method, cell suspensions of 30 μ l were added to 200 μ l of pH buffered hypo-osmotic solution (~2 mOsm) and 0.1 mg·mL⁻¹ aequorin before gentle mixing. After a pre-determined duration of hypotonic exposure, addition of 230 μ l hyperosmotic solution was used to bring the suspension back to isotonic conditions and membrane recovery. To test the cell response to hypo-osmotic exposure, the time between addition of hypo-osmotic and return to isotonic conditions was varied from 10 seconds to 10 minutes. They found that treatment times of 10–30 seconds were ineffective in loading aequorin (21 kDa) or GFP (28 kDa). Upon two minutes exposure, long term cell viability up to 18 hours was more than 50% with sufficient delivery to determine intracellular calcium concentrations, which turned out to be ~0.9 μ M in follicular lymphoma cells. 10 minutes exposure led to robust delivery but a gradual loss of viability in almost all cells after 10 hours, probably due to delayed cell death responses (see section 4.3). One major advantage of Klabusay's protocol is its applicability to treat difficult-to-transfect suspension cells and that it appears agnostic to cell size and type of material to be delivered.

In 1999 Koberna and co-workers unveiled a method based on a 'hypotonic shift' to achieve intracellular delivery of modified nucleotides, nucleosides, dyes, and peptides into a wide range of cell types⁹¹⁴. The hypotonic buffer consists of 10 mM HEPES for pH buffering and 30 mM KCl (~70 mOsm). Cells were exposed to the hypotonic buffer for 5 mins before a return to isotonic media for recovery. After treatment, metabolic production of DNA, RNA, and protein was inhibited and took ~4 hours to return to normal levels. No loss of viability or apoptosis was observed. The hypotonic shift method was reported to be highly effective for smaller molecules ~1 kDa but efficiency decreased for cargo of increasing molecular weight. For example, it was unable to deliver large proteins such as labeled antibodies. Koberna et al.'s hypotonic shift approach has been particularly popular for intracellular delivery of labeled nucleotides^{915–923}. It has also been adapted for the successful loading of the peptide actinomycin D⁹²⁴, dye-conjugated dextrans⁹²⁵, and 5 nm gold particles⁹²⁶.

Intracellular delivery has also been accomplished with milder hypotonic shocks in the range of ~150 mOsm. Mills et al. used hypotonic swelling for intracellular loading of antibodies into rat submandibular acini cells⁹²⁷. This application is notable in that cells are not individually isolated in suspension - acini are small clusters of cells organized in a quasi-circular arrangement to form a hollow duct in the center. In the procedure, acini were exposed to a mild hypotonic solution (~150 mOsm) containing 5 mM ATP and the antibody of interest for 1 minute following a switch back to isotonic conditions. The loaded antibody was found capable of inhibiting its target CTFR protein, verifying that delivery had indeed occurred. The procedure has also been used to deliver the calcium chelator BAPTA⁹²⁸ and enzymes⁹²⁹ into acini cells.

In studies that require intracellular delivery of lanthanum-based contrast agents, milder hypotonic shocks (~90–160 mOm) have been used to load normally impermeable tracers, such as the Gadolinium ion, into adherent or suspension cells⁹³⁰. In this case, a 30 minute ~160 mOsm hypotonic exposure at 37 °C was used for cytoplasmic delivery of lanthanide complexes and dyes in various macrophage and cancer cell lines⁹³⁰. A comparison with electroporation and osmotic lysis of pinosomes concluded that hypotonic shock was the most advantageous method for delivery of these small (<1 nm) molecules⁹³⁰. Other report appear to verify this strategy, as Gadolinium complexes have been delivered into HeLa cells with the same strategy⁹³¹. In other cases, a more severe shock of ~90–110 mOsm for 60 minutes at 37 °C produced loading of Lanthanide complexes into HeLa cells^{932,933}. In RBCs, iron oxide nanoparticles of up to 60 nm were loaded into RBCs with hypotonic shocks of 90–110 mOsm⁹³². Other reports in RBCs employed a 30 minute ~160 mOsm hypotonic shock at 4 °C to load RBCs with the gadolinium-based complexes without loss of RBC functionality^{934–936}.

In a strategy that synergizes hypotonic shock with the membrane perturbing effects of detergents, Medepalli and co-workers demonstrated quantum dot loading into adherent H9C2 cells by exposure to a mild hypotonic buffer (150–200 mOsm) combined with low concentrations of the detergent saponin²⁹⁰. Presumably saponin reduces the threshold for induction of plasma membrane defects under hypotonic stretch, thereby synergizing the permeabilization effects of both approaches. After delivery, quantum dots of hydrodynamic diameter 20–25 nm were observed to be evenly dispersed in the cytoplasm of treated cells.

Osmotic Gradients Acting on Part of the Plasma Membrane: When cells form a tight monolayer across a porous substrate, they form an impermeable barrier between two bodies of liquid media. An osmotic shock in one of those solution creates an osmotic gradient across the cells. Taking advantage of this principle, Widdicombe et al. cultured epithelial or endothelial cells into confluent polarized monolayers on substrates with 0.45 μm pore size⁹³⁷. The apical media was then exchanged with water containing macromolecules to be loaded while retaining the basal media as physiological saline (Figure 19B). This resulted in a ~300 mOsm osmotic gradient across the cells. Disruption of the apical cell membrane was evidenced by uptake of 67 kDa fluorescent albumin and 2000 kDa dextrans, but was reversible within ~5 mins when apical water was replaced with normal cell culture media. By adding fluorescently labeled molecules at different times after hypotonic shock, it was found that the majority of uptake occurred within the first 4 minutes. This technique was

reported to be temperature insensitive, working equally well at 4 or 37 °C, thereby indicating that endocytic activity had a minimal role and suggesting plasma membrane disruption as the prime mechanism. After the procedure, cell layers were able to recover full trans-epithelial resistance within several hours.

In a complementary study by Widdicombe's co-workers, Tawa et al. demonstrated successful transfection of airway barrier cells in rat lungs by exposure to apical water containing DNA⁹³⁸. A follow-up report argued that the hypotonic transfection of DNA to airway barrier cells could be due to active uptake by membrane trafficking, which is known to stimulate exocytosis and endocytosis associated with regulatory volume mechanisms⁹³⁹. However, this model would not fit with the original observation of rapid delivery by Widdicombe et al. In an analogous situation, hypotonic aerosols have been observed to facilitate intracellular delivery of PEI-complexed DNA by a membrane permeabilization mechanism in mouse airway epithelium⁹⁴⁰. Thus, a hypo-osmotic delivery principle might be feasible when applied to exposed cell monolayers *in vivo*, particularly in the lungs.

Hydrostatic Pressure and Hydrodynamic Delivery: Membrane disruption due to a sudden increase in hydrostatic pressure is believed to be the mechanism of so-called 'hydrodynamic delivery', where a rapid injection of fluid into the cardiovascular system causes transient disruption in the plasma membrane of cells in certain tissues. A prime example is tail vein injection, where robust transfection of hepatocytes and sometimes other cardiovascular tissues has been observed in rodents^{941,942}. In a mouse model, transfection is achieved by fast injection (~5 seconds) of almost 2 mL of saline solution containing DNA to a 20 g animal. The introduced solution is close to 10% of the body weight thus representing a rapid expansion of blood volume, which cannot be immediately pumped through the vena cava of the heart. This causes sudden distension and hydrostatic pressure build-up in the surrounding tissues. A weak point is typically retrograde flow into the liver, where it has been observed that fenestrations in hepatic tissue expand to generate disruptions in cell membranes, thereby allowing influx of cargo molecules from the blood directly into the cytosol of hepatocytes, followed by membrane recovery in these cells⁹⁴³. High delivery efficiencies have been achieved using hydrodynamic tail vein injection, with up to 40% transfection of liver hepatocytes from a single injection⁹⁴². Rapid intracellular delivery of other macromolecules such as labeled dyes, proteins, oligonucleotides, siRNA, bacterial artificial chromosomes, and linear or circular DNA fragments as large as 175 kb have also been delivered to rodent hepatocytes by this method, lending similar credence to a membrane permeabilization mechanism without reliance on endocytosis⁹⁴³⁻⁹⁵⁰. More recently, hydrodynamic tail vein injections have found use in CRISPR-based genome editing in mouse liver, albeit at lower efficiencies⁹⁵¹⁻⁹⁵⁴. The major limitation of hydrodynamic injection is that it is only available in rodents.

Apart from injection into veins, delivery of nucleic acid cargo has been observed by direct injection of solutions into skeletal muscle, heart, thyroid, skin, and liver⁹⁵⁵. Mechanistic studies indicate that this also occurs by membrane permeabilization, but have been unable to fully rule out the role of endocytosis⁹⁵⁵⁻⁹⁵⁸. The degree to which membrane permeabilization or active uptake processes underlie delivery is probably dependent upon the properties of the solution and manner in which the injection is carried out^{955,957}.

In 1999 Mann et al. introduced a method for hydrostatic pressure-mediated transfection in human vein segments and rat myocardium *ex vivo*⁹⁵⁹. ~1–2 cm segments of veins were cannulated, encased in a plastic sleeve to prevent distension, and infused with pressurized solutions of up to ~100 kPa above baseline pressure⁹⁵⁹. 10 minutes of this treatment was able to yield intracellular delivery of fluorescently-labeled antisense oligonucleotides into ~90% of endothelial cells lining the vein segment⁹⁵⁹. Moreover, *ex vivo* treatment of rat hearts pressurized inside and out at up to ~200 kPa showed ~50% transfection in myocardial cells⁹⁵⁹. Although the exact delivery mechanisms were not stated, imaging of cells after treatment suggested it was non-endocytic⁹⁵⁹. Variants of this technique have been used to perform intracellular delivery of siRNA⁹⁶⁰, antisense oligonucleotides^{959,961–965}, plasmid DNA^{961,966,967} and ~100 nm polystyrene microspheres⁹⁶⁸.

Disruption of Endosomes By Osmotic Forces: In 1982 Okada and Rechsteiner described an intracellular delivery technique, termed osmotic lysis of pinosomes. It works by harnessing osmotic forces to rupture endosomes pre-loaded with cargo of interest, thereby obtaining cytosolic delivery (Figure 19C)¹⁷⁴. In the first step, endocytic uptake is promoted by a ~10 minute incubation of cells in a ~800 mOsm hypertonic buffer containing 0.5 M sucrose, 10% polyethylene glycol (PEG)-1000 and molecules to be delivered. Exchange to a hypotonic solution (~180 mOsm) consisting of diluted media for ~2 minutes then generates a rush of water into the cell. During this hypotonic shock phase endosomes laden with cargo and osmolytes expand and rupture, thus releasing their contents. The pendulum swing from hypertonic to hypotonic conditions may also disrupt the plasma membrane, however cells are able to release osmolytes to counteract swelling⁴⁵¹. Endosomes, on the other hand, have no volume regulation and therefore swell uncontrollably until bursting^{969,970}. This means the hypotonic shock impacts endosomes significantly more than the plasma membrane. Okada and Rechsteiner reported that the osmotic lysis of pinosomes method was capable of introducing antibodies, various proteins, and 70 kDa labeled dextrans into the cytosol of L292, 3T3 fibroblasts, and HeLa cells¹⁷⁴.

Following in the example of the original paper, osmotic lysis of pinosomes has been particularly used for intracellular delivery of proteins^{174,175,970–984}, antibodies^{976,985–989}, dextrans^{174,989–991}, and peptides^{992–994}. In a landmark paper in 1988, osmotic lysis of pinosomes was used to prove that cytosolic loading of proteins could mediate their presentation as antigens through the major histone compatibility I pathway to invoke a specific immune response¹⁷⁵. In other reports, osmotic lysis of pinosomes has found success in intracellular delivery of cell lysates⁹⁹⁵, hyaluronan^{996,997}, trehalose⁹⁹⁸, Lanthanide imaging probes^{260,261}, various small molecule dyes^{989,999}, uridine triphosphate-glucuronic acid¹⁰⁰⁰, antisense oligonucleotides¹⁰⁰¹, antisense morpholinos⁷⁶⁶, virus particles¹⁰⁰², and nanomaterials such as quantum dot-labeled motor proteins for biophysical studies^{285,1003,1004}.

With the advent of RNAi-mediated gene silencing in the early 2000s, researchers tested the ability to perform transfection via osmotic lysis of pinosomes. By using up to 1.6 μ M siRNA in solution, gene silencing of >50% was reproducibly achieved in common cell lines such as HEK and HeLa¹⁰⁰⁵. In a subsequent study by a different group, improved RNAi transfection was demonstrated in hard-to-transfect immune cell lines¹⁰⁰⁶. Their modified procedure was

more extreme, involving hypertonic sucrose solutions of up to 2 M and siRNA concentrations of 10 μM ¹⁰⁰⁶. Immune cell lines including mouse macrophage RAW264.7 and J774.1 as well as the T lymphocyte cell line DO11.10 were all shown to be transfectable with this approach. Other benefits were minimal cytotoxicity and immunomodulatory responses compared to synthetic cationic lipid reagents lipofectamine and oligofectamine, or the polymer reagent jetPEI. In a microfluidic adaption of the approach, a device was deployed for rapidly cycling suspended cells through the various solutions to induce osmotic lysis of pinosomes, thus avoiding the need for centrifugation to exchange solutions⁹⁹¹. Results were reported to be superior to the conventional protocol for loading fluorescent dextrans into Jurkat cells⁹⁹¹.

The osmotic lysis of pinosomes method has several caveats: 1) cell stress, 2) delivery capacity is limited by extent of endocytosis, and 3) absence of reports on larger cargo such as plasmid DNA and mRNA. First, the hypertonic media imposes significant stress on cells and has been observed to actually inhibit endocytosis in some cell types¹⁰⁰⁷. Second, the extent of endocytosis during the hypertonic exposure window is a limiting factor that affects the final concentration of cargo delivered¹⁰⁰⁷. Multiple rounds of the procedure may be conducted to boost delivery efficiency but are time-consuming and must be balanced with considerations of cell stress⁹⁹⁰. Several publications indicate that cell function and health may be compromised as a function of duration and intensity of the osmotic challenges^{174,895}. The third consideration is that certain combinations of cell types and cargo molecules appear to be unfeasible to the procedure. This can be due to degradation of cargo in the acidic environment of endosomes or an unmet need for destabilizing agents to assist with endosome rupture, a role that PEG was later suggested to play¹⁰⁰⁷.

Interestingly, an *in vivo* application of the osmotic lysis of pinosomes concept was accomplished in rat arteries. Without surgical removal, isolated, pressurized mesenteric arteries of the rat were cycled through hypertonic and hypotonic solutions. Endothelial cells were found to take up dyes, dextrans, peptides, and labeled antibodies into the cytoplasm without comprising the structure and function of the surrounding tissues of their functionality⁹⁸⁹. The technique used to identify a critical role for connexin 40 in EDHF-mediated dilation of rat mesenteric arteries.

Induced Transduction by Osmocytosis: Motivated by limitations of the osmotic lysis of pinosomes method in primary cell types, D' Astolfo et al. introduced an adaptation, termed iTOP, which stands for induced transduction by osmocytosis and propanebetaine²²⁶. Instead of relying on hypotonic solution for endosome disruption, propanebetaine appears sufficient to trigger cargo leakage specifically from macropinosomes. The method relies on NaCl-related hypertonicity of extracellular medium to induce macropinocytosis followed by spontaneous endosomal leakage. A high extracellular concentration of Na^+ ions was shown to stimulate NHE1-mediated macropinocytosis. Unlike osmotic lysis of pinosomes, however, no discrete trigger is required for endosomal rupture. Instead, intracellular macropinosome leakage was a stochastic event promoted by the presence of propanebetaine or other compounds with similar physicochemical properties. The osmotic pressure created by hypertonic endosomes may also contribute to destabilize endosomes. Using iTOP, Cas9-sgRNA complexes were delivered into KBM7 cells and H1 human embryonic stem cells to

produce CRISPR-mediated gene deletions. Various other proteins were also delivered, thus demonstrating efficient delivery of several cargo materials into a variety of primary cell types.

6.2 Electrical Membrane Disruption (Electroporation)

In the 1980s, electroporation, which involves the transient permeabilization of cell membranes with electric pulses, rose to prominence as a powerful approach for intracellular delivery, applicable to a wide range of cell types, from animal cells to plants and lower organisms. Prior to its introduction, the stage had been set by more than a decade of research exploring the effect of voltage pulses on artificial lipid bilayers, vesicles¹⁰⁰⁸ and red blood cells¹⁰⁰⁹. In nucleated mammalian cells, Eberhard Neumann and colleagues published a report in 1982 which demonstrated that electroporation led to the efficient transfection of plasmid DNA in mouse lymphoma cells⁵³. Electroporation, while initially emphasized for DNA transfection, has subsequently shown utility for delivery of a huge variety of cargo: from small molecule drugs, dyes, and tracers, to larger proteins/antibodies and multiple forms of DNA and RNA^{239,1010–1012}. In this section we first cover the mechanisms of electroporation before exploring the challenges, technical advances and applications.

6.2.1 Mechanisms of Membrane Disruption & Cargo Entry

Mechanisms of Membrane Pore Formation: Mechanistically, electroporation is the formation of pores in a membrane by the application of a potential difference across that membrane. When the potential difference reaches a critical magnitude of voltage, the probability of electroporation taking place drastically increases. According to theory, the increase in electric field energy within the membrane and ever-present thermal fluctuations combine to create and expand a heterogeneous population of pores^{239,388,1013}. Although there is no fixed voltage threshold that triggers electroporation, the critical parameter of electroporation is the trans-membrane potential. This is because the maintenance of trans-membrane electrical potential incurs a probability of generating a membrane defect for a given field strength, time, and temperature. Membrane defects originate as so-called hydrophobic pores of radius <0.5 nm, which form due to random thermal fluctuations of the individual lipid molecules that make up the membrane (Figure 20A). Fueled by the external electrical energy provided, these defects may then traverse their energy landscape to become hydrophilic pores, which are typically lined by at least 8 – 10 phospholipid head groups and defined by their ability to permit free passage of water molecules (Figure 20B). Hydrophilic pores ($r >0.5$ nm) can be stable because the energy barrier also exists in the reverse direction. Current theory posits that small pores are not very good conductors; hence the continued application of an electric field is not only critical for their formation, but also their enlargement^{388,1013}. Pore formation and expansion are energetically favorable because it relaxes the charge buildup that would otherwise become entropically unfavorable. As the pores become better conductors, however, the electrical expanding pressure decreases, resulting in stagnation of their growth. This explains two phenomena characteristic of electroporation: 1) longer pulses (tens of ms) are required to grow larger pores, and 2) electroporation is not very good at producing large (e.g. >50 nm) pores^{537,1014}.

Electroporation phenomena is thought to be primarily related to changes in electrical conductance, but chemical, thermal, and electromechanical membrane deformation effects may also contribute^{419,1015}. The application of mechanical tension has been observed to lower the electric voltage threshold required for membrane disruption^{1016,1017}. This is because mechanical forces contribute to bias the energy landscape toward defect formation (see Figure 8). In keeping with this notion, lower temperatures have been observed to increase the voltage required for electroporation⁵³³. Furthermore, mathematical descriptions and models have been developed to assess, for example, the effect of applied voltage on the distribution of pore radii³⁸⁹ (Figure 20C). More recently, simulations have also assisted in illuminating the molecular events associated with electroporation, although (due to limitations in computational power) they currently only cover very short time scales on the order of microseconds or less^{1018,1019}.

Electroporation in Cell Suspensions: In suspensions of isolated cells electroporation is observed with applied trans-membrane potentials in the range of 0.2 – 1.5 volts. Pulse times are typically on the order of microseconds to almost a second. The membrane charges like a capacitor with a characteristic charging time proportional to the surface area of the enclosed membranous body⁵³⁷. For conventional cuvette-style parallel plate setups, a cell suspension in conducting buffer is placed between two electrodes connected to a generator of high electric field (Figure 21). This type of setup produces a linear electric field across the cell suspension. Upon application of voltage, the various regions of the plasma membrane take different times to reach their characteristic trans-membrane threshold potentials. This results in growth of a heterogeneous distribution of pores over the cell surface, both in terms of number and size. Moreover, because of the negative resting potential of cells (–35 to 80 mV for most cell types – see Figure 7A), permeabilization occurs first at the hyperpolarized side of the cell facing the positive electrode¹⁰¹⁰. This creates an inherent anisotropy in the area and degree of permeabilization between the two poles¹⁰²⁰. The hyperpolarized side of the cell is supposed to carry smaller but more numerous pores. The depolarized half, which faces the negative electrode, has fewer pores due to fewer nucleation events. The pores on the depolarized side may, however, be larger in diameter as the prolonged electrical field exposure is focused on expanding a less numerous population of defects¹⁰²¹. In general, it is thought that coverage area of permeabilization is controlled by pulse strength while the pore growth size is more strongly correlated with the pulse duration¹⁰¹⁰. Once pores are formed and begin conducting, the local electroporation effect diminishes somewhat as charge is free to flow through these defects. Therefore the amount of energy channeled into the growth of pores declines through the lifetime of a particular pulse⁴¹⁹.

Upon electroporation, the response within cell populations and between cell types is somewhat heterogeneous, reflecting differences in cell size, orientation, surface area, and physiological state, as well as variances in membrane composition and the presence of local inhomogeneities in the electric field itself. The microenvironment of the cell surface is characterized by the distribution of nearby or adhered macromolecules, membrane proteins, lipid phases and lateral domains, extracellular protrusions, membrane reservoirs, and underlying cytoskeletal linkages (see Figure 7B, C). It is currently not well understood how these complexities influence the generation of defect nucleation and growth under an electric

field¹⁰¹¹. A recent study to visualize the behavior of membrane defects in artificial planar bilayers found that electropores form preferentially in the liquid disordered phase¹⁰²². This preference is also likely to be true in live cells, but lack of experimental methods to measure such phenomena has made it challenging to validate¹⁰²². Another mystery is the lifetimes of electropores in live cells. Once hydrophilic pores of >1 nm open up in the plasma membrane, they are thought to either spontaneously close or require active cellular processes for the bilayer to heal. For active repair processes, many researchers observe timescales of seconds to minutes^{1010,1023}. The electroporation literature, however, suggests rapid shrinkage of pores after cessation of the electric field¹⁰²⁴. A memory effect, where changes in the membrane porosity remain on a longer time scale of hours has also been suggested¹⁰²³. For further reading on the theory and mechanisms of electroporation as pertaining to live cells, we recommend other more comprehensive reviews on the topic^{239,388,502,537,1010,1011,1013,1023–1026}.

Targeting Cellular Structures Across the Pulse Strength-Duration Space: The parameter space for electroporation is vast. As discussed, mechanistic investigations reveal there is no fixed threshold electroporation voltage because formation of electropores depends on a combination of voltage strength, pulse duration, number of pulses, pulse waveform, temperature, buffer conductivity, and cell properties^{1010,1011}. This large variable space presents a challenge in optimizing electroporation. All other variables being held constant, most approaches focus on tuning the “pulse strength-duration space”⁵³⁷. Manipulating this parameter space can exert a measure of spatiotemporal control over which cellular membranes are permeabilized (Figure 22). In general, high voltage ultrashort pulses have been purported to perturb internal and organelle membranes while longer and milder pulses emphasize the permeabilization of the plasma membrane and bias the effect more toward larger cell types⁵³⁷.

The charging time for the plasma membrane is about 1 μs and pulses of less duration are thought not to efficiently porate the plasma membrane³⁸⁸. On the other hand, ultrashort pulses in the nanosecond range may rupture subcellular structures and organelles while leaving the plasma membrane essentially untouched if they are of sufficient magnitude^{419,537}. A pioneering study by Schoenbach et al. in 2001 demonstrated short nanosecond pulses at $>10 \text{ kV}\cdot\text{cm}^{-1}$ field strengths selectively target intracellular organelles¹⁰²⁷. Specifically, human eosinophils were exposed to a field strength of $53 \text{ kV}\cdot\text{cm}^{-1}$ applied in a train of 5 pulses of 60 nanoseconds each. In response the cells formed intracellular granules without extensive plasma membrane permeabilization. Follow up studies by the same group indicated these nanosecond pulses induced apoptosis, as signified by exposure of annexin-V at the cell surface and the absence of ethidium homodimer fluorescence¹⁰²⁸. Further hallmarks of apoptosis were observed with fluorescent probes that report on caspase activation and the release of mitochondria-associated protein cytochrome c into the cytoplasm. Apoptosis probably occurs due to a release of cytotoxic factors from permeabilized mitochondria and breakdown of intracellular calcium stores. From these results it was concluded that apoptosis triggered by nanosecond pulsed electroporation can occur in the absence of disruption to the plasma membrane. This is of widespread interest for two reasons: 1) the targeted induction of apoptosis by ultrashort electrical pulses could

avoid an immune response from lysing or necrotic cells. Thus it has been suggested as a potential therapeutic strategy to kill malignant cells *in vivo*¹⁰²⁹. 2) For intracellular delivery applications it is an effect that should be avoided to maintain cell survival. Unwanted disruption of intracellular organelles could explain observations of delayed cell death that sometimes occur after electroporation.

Conventional electroporation systems almost exclusively target the plasma membrane. Short pulses in the microsecond to millisecond range result in numerous, but smaller sized pores distributed evenly over the poles of the plasma membrane and sometimes nucleus⁵³⁷. The longer pulse space >0.1 ms is limited to lower voltages; otherwise Joule heating becomes a problem for treated cells, a factor also dependent on conductivity of the medium. Because voltages must be lower in this regime, the dependence on size of the membrane-bound body biases poration towards larger objects at their poles, therefore favoring plasma membrane disruption of larger cells (>tens of micron diameter)⁵³⁷. At these longer durations the membranes of larger cells such as skeletal muscle and nerve cells are much more responsive to electroporation. Taken together, data compiled from multiple reports suggest that manipulation of the pulse strength-duration parameter space is able to mediate a significant measure of control over the subcellular localization and distribution of membrane disruptions generated in cells (Figure 22).

Cargo-Dependent Influx Mechanisms: Electroporation has been used to deliver a diverse range of molecules and cargo to the intracellular space. This includes dyes^{180,706,1030–1033}, radiotracers^{1034,1035}, sugars^{268,430,1036,1037}, metabolites^{1034,1038}, poorly permeable drugs^{254,255,1039,1040}, ions^{1041,1042}, molecular beacons^{1043,1044}, proteins^{180,504,1045–1051}, antibodies^{181,200,495,1052–1056}, Cas9 protein or RNP complexes^{218,219,221,222,1057}, antisense oligonucleotides¹⁰⁵⁸, siRNA^{104,1059–1063}, mRNA^{124,127,128,1064,1065}, plasmid DNA^{53,1066,1067}, quantum dots^{273,291,292,1068}, and gold nanoparticles¹⁰⁶⁹. The mechanisms of uptake of these cargos vary as a function of their size, charge, and conformational flexibility (Figure 23).

Cargo-Dependent Influx Mechanisms: Small Molecules: Small neutral molecules enter cells via diffusion throughout the duration of a pore's lifetime²³⁹ (Figure 23B). If the molecules are charged, such as propidium iodide (PI, ~660 Da), which carries two positive charges, there is an added electrophoretic component that can augment delivery during the pulse (Figure 23C). In this case, delivery will be augmented at the side of the cell facing the positive electrode, as PI will be attracted towards the negative electrode and into the cell^{1021,1070}. Due to its small size and high diffusion coefficient, PI will also enter the opposite side of the cell, but to a lesser extent. Because the lifetime of the electropores is much longer than the pulse duration, diffusion has been observed as the dominant mechanism of entry with only a minor contribution from electrophoresis^{1071,1072}. Electropores have been reported to remain open to small molecule diffusion for several minutes after pulsing^{1038,1071}.

For very small pores sizes (~1 nm) diffusion alone may be insufficient for influx of charged molecules. This is because of Born's energy barrier, which describes the energetic cost of moving an ion or small charged molecule through a hole in a dielectric membrane^{239,1073}.

The charged entity interacts with the pore wall, increasing the energy required for translocation. For pore sizes close to the molecule size, the energy barrier for crossing the membrane strongly correlates with the charge number on the molecule. For example, Venslauskas et al. compared delivery of bleomycin (radius: ~1.2 nm, charge: +1) to tetrasulfonato-porphyrin (TSPP, radius: ~1.0 nm, charge: -4) under pulsing conditions designed to generate only small pores¹⁰⁷⁴. Their experiments revealed that the electric field strength required to deliver the more highly charged molecule, TSPP, was several times greater than for bleomycin. Other groups claim to have identified ultrashort pulse electroporation conditions (~60 ns) where plasma membrane pores are so small that they do not allow transmission of PI, although they are conductive for smaller ions¹⁰⁷⁵. In such a scenario an electric field pulse can help overcome Born's energy barrier and promote influx.

Cargo-Dependent Influx Mechanisms: Proteins & Other Macromolecules: Diffusion is the most likely mechanism underlying electroporation-mediated intracellular delivery of larger macromolecules (~10 – 1000 kDa), such as proteins, antibodies and dextrans¹⁰¹⁰. Most proteins and dextrans tend to be weakly charged or neutral, thus the electrophoretic contribution is thought to be minimal. Early experiments with proteins claimed efficient loading (>80% of cells), sometimes up to micromolar cytoplasmic concentrations, in a variety of mammalian cell lines at high survival rates (>80%)^{181,1046,1076}. Dye-conjugated dextrans of known molecular weights (from 3 – 2000 kDa) have also been electroporated into cells to analyze delivery efficiency and decipher the rules governing uptake^{492,1033,1045,1077–1079}. In comparison to small molecules, which can diffuse into cells for minutes, proteins and larger molecules (>10 kDa) exhibit a narrow window of opportunity to enter cells, constituting just a few seconds¹⁰⁴⁹. It is known that electroporation produces mostly small pores with a subset of larger pores that grow as a function of the pulse duration³⁸⁸. When the electric field is turned off the large pores shrink almost instantly, while the small pores may linger in the plasma membrane for minutes²³⁹. Thus, the entry of larger cargo coincides with the pulse timing and is more efficient for longer pulse durations⁴⁹². The smaller pores that prevail for minutes are unable to facilitate diffusive influx of proteins¹⁰⁸⁰.

Although less well-accepted, some researchers have proposed alternative delivery mechanisms. For example, the electric field might augment macromolecule delivery through electrophoretic or electro-osmotic effects^{1077,1081,1082}. The models based on electrophoresis, however, have not addressed how they would be relevant to uncharged molecules. The electro-osmotic explanation, on the other hand, proposes that the application of an electric field causes a convective flow of electrolytes and osmotically obliged solution that sweeps the cargo molecules along with it. Although discussed in some papers, the few studies that have sought to investigate electro-osmotic contributions to molecular delivery in live cells are inconclusive^{1077,1081}, with most of the electroporation literature favoring explanations that emphasize diffusion or electrophoresis^{239,1010,1011,1032,1083}.

Another idea is that electroporation-stimulated endocytosis via macropinocytosis may contribute to protein uptake in the minutes following electric field exposure¹⁰⁸⁴. Strong electroporation treatments have sometimes been reported to cause proteins and dextrans to become aggregated or trapped at the plasma membrane^{1046,1076}. Such membrane-bound

proteins can be removed with the protease trypsin while dextrans could not, demonstrating that proteins were stuck to the cell surface and not inside the cell¹⁰⁷⁶. If electroporation causes cargo to aggregate at the cell surface, this would make it amenable for uptake by endocytosis¹⁰⁸⁴. The degree to which this occurs for different cargo molecules, however, has not been well investigated.

Cargo-Dependent Influx Mechanisms: Plasmid DNA: In contrast to small molecules, proteins and dextrans, the mechanisms of nucleic acid delivery via electroporation are regarded to be almost entirely dependent upon electrophoretic forces provided during the pulse^{239,1010,1085}. In particular, the case of DNA plasmids has been extensively studied due to a broad interest in exogenous gene expression over the past decades^{1086,1087}. After pioneering efforts demonstrating DNA transfection in mouse cells in the early 80s^{53,1088}, it wasn't until a decade later that researchers realized that plasmids weren't immediately crossing the cell membrane, but rather aggregating at the cell surface as a result of electrophoretic forces (Figure 23E)^{491,1067,1089}. A correlation between longer pulse durations, more prominent aggregates, and higher transfection efficiency also lent support to this view^{429,1089}. Moreover, it was observed that pre-adsorption of DNA to the cell surface dramatically increased transfection efficiency and contributed to pore formation and stabilization, most likely by spearing of plasmid molecules into the membrane^{1089,1090}.

In 2002 Golzio et al. advanced our understanding of electroporation-mediated plasmid transfection with single-cell imaging experiments that visualized the interaction of DNA at the cell surface during electroporation¹⁰⁹¹. It was found that DNA aggregated exclusively on the side of the cell facing the negative electrode (cathode) and formed localized clumps of 0.1 – 0.5 μm in size. At the cell surface, it is believed that the highly negatively charged DNA plasmids are threaded through small pores where they become stuck in the negative electrode-facing region of the plasma membrane^{1021,1089,1090}. These aggregates are then internalized via endocytosis over tens of minutes. Some of the plasmids eventually arrive at the nucleus over a timecourse of ~2 hours or longer¹⁰⁸⁶. Collectively, these results led to the emergence of an endocytic model of plasmid electrotransfer that has largely gained acceptance (Figure 24).

As membrane remodeling via endocytosis is a core pathway used by cells to repair their membranes^{408,416}, endocytic uptake could be an active cellular response to the perturbation caused by DNA entanglement in the membrane, as first predicted by Tsong¹⁰²⁴. Subsequent studies have shown that, in CHO cells for example, ~50% of DNA is internalized by caveolin/raft-mediated endocytosis, ~25% by clathrin-mediated endocytosis, and ~25% by macropinocytosis¹⁰⁹². Within 2 hours, more than half of the DNA ends up in lysosomes, as revealed by co-localization with the lysosomal marker LAMP1¹⁰⁹². Furthermore, single-particle tracking experiments of fluorescently labeled plasmids indicate that cytoskeletal processes, involving both actin and microtubule networks, are involved in trafficking of DNA-associated endosomes toward the cell nucleus¹⁰⁹³.

How plasmids enter the nucleus is poorly understood, as DNA plasmids are invariably many times larger than the ~40 kDa cutoff for passive influx through nuclear pores. DNA transfection is known to be greater in proliferating cells that undergo transient nuclear

envelope breakdown through mitosis, which allows plasmids to be entrapped inside the freshly reformed post-mitotic nucleus¹⁰⁹⁴. The revelation that nuclear membrane disruptions are not an uncommon event in the life of a cell, and thus generate a stochastic pathway of exchange between cytosol and nucleus, could also provide clues^{751,752}. Alternatively, internalization motifs, such as nuclear targeting sequences, have been reported to promote import of plasmids into cell nuclei with varying success rates¹⁰⁹⁵.

Overall, there are a protracted series of steps required for electroporation-mediated transfection and many of them require membrane trafficking and other active cellular processes. Only a small fraction of electroporated DNA vectors will arrive in the nucleus for successful expression¹⁰⁸⁶. Despite this, electroporation is one of the few membrane disruption-based methods that can achieve high rates of DNA expression in millions of cells at acceptable throughputs. Several other methods are able to introduce DNA to the cytosol, but it is often unable to migrate through the tight cytoplasmic meshwork and is therefore degraded before reaching the nucleus, as has been shown for plasmids after microinjection⁷². Thus, although taking several hours, electroporation's paradigm of plasmid aggregation and endocytosis may somehow serve to protect and concentrate DNA for the journey to the cell nucleus.

Cargo-Dependent Influx Mechanisms: siRNA & Other

Oligonucleotides: Electroporation-mediated delivery of oligonucleotides and siRNA is similar to the case of DNA in that it also relies on electrophoretic forces²³⁹. An important distinction, however, direct delivery into the cytoplasm without relying on endocytosis (Figure 23D). This is by virtue of its smaller dimensions (2×7.5 nm⁸⁹) compared to DNA plasmids (~100 – 200 nm)⁷⁶. Imaging of fluorescently labeled siRNA has shown that it enters during application of the electric field at the side of the cell facing the cathode and disperses throughout the cytosol within tens of seconds¹⁰⁹⁶. siRNA influx was reported not to occur after cessation of applied voltage, indicating that electrophoretic forces are probably required for delivery¹⁰⁹⁶. This is might only true, however, for small pores of <10 nm where the Born energy barrier would need to be surmounted by electrophoretic driving forces²³⁹. Such a scenario is analogous to that proposed for small charged molecules (Figure 23C). It is likely that large pores (>10 nm) can facilitate entry of siRNA via free diffusion, since siRNA knockdown has been observed with membrane disruption-based methods that lack electrophoretic forces, including with pore-forming toxins¹⁰⁷, microfluidic cell squeezing^{184,744}, and laser-nucleated cavitation bubbles⁸⁸⁶. Therefore siRNA delivery can probably be mediated by a combination of electrophoretic or diffusive mechanisms depending on the size and lifetime of the pores.

Cargo-Dependent Influx Mechanisms: Summary: Taken together, the literature indicates electroporation-mediated delivery is influenced by the pore diameter ($d_{\text{disruption}}$) and the cargo dimensions (d_{molecule}), as well as the charge and conformational flexibility of the cargo molecule (Figure 25). For $d_{\text{molecule}} \ll d_{\text{disruption}}$ both neutral and charged molecules should diffuse across their concentration gradient whenever the pore is large enough. Although the majority of delivery is via diffusion, electrophoretic or electro-osmotic phenomena may assist translocation during the pulse. For $d_{\text{molecule}} \approx d_{\text{disruption}}$ charge will

play a critical role. Neutral molecules may diffuse through pores while their charged counterparts will face the Born's energy barrier, only being able to translocate while driven by sufficient electrophoretic forces. For the case of $d_{\text{molecule}} \gg d_{\text{disruption}}$ only molecules that are both conformationally flexible and significantly charged will have a chance of penetrating. As exemplified by the case of DNA plasmids, parts of the molecule may be threaded into pores and therefore become embedded in the membrane. This makes the molecule available to be taken up via endocytosis, a result that may or may not be desirable for a given application.

Tailoring Pulse Parameters for Optimal Delivery: In the most elementary electroporation scenario, one wants to open up pores of sufficient size and duration to allow the desired influx of cargo molecules via diffusion. In more complicated cases, however, involving charged molecules close to or larger than the pore size (Figure 25), the efficiency of delivery depends critically on magnitude and duration of electrophoretic forces^{429,491,492,1067,1089}. Regarding plasmid delivery, for example, longer pulse durations are often found to heavily improve transfection efficiency. Longer pulses, however, can bring the problem of Joule heating and excessive cell damage¹⁰⁹⁷. One strategy to mitigate Joule heating is the use of low conductivity buffers that have lower electrolyte concentrations than standard physiological buffers or media. The osmolarity of the buffer will have an effect as well, because it can alter the size of the cell, tension on the plasma membrane, conformation of membrane reservoirs, and the interaction between cargo molecules and the cell surface¹⁰¹¹. Temperature will also affect the properties of the membrane and energy barriers of electroporation, as well as the active cell response and membrane repair dynamics¹⁰¹¹.

Electroporation can be viewed as a balancing act between a large number of parameters and conditions. There is significant debate surrounding the optimal electroporation protocols for intracellular delivery and this is further complicated by variations between cell types^{1098,1099}. Another issue is the lack of understanding associated with post-electroporation cell death, where loss of viability is sometimes delayed by hours or even days^{450,489}. This is an especially striking problem regarding electroporation in primary or sensitive cell types¹¹⁰⁰. When wanting to optimize the delivery of a particular cargo molecule into a specific cell type, the starting point is usually screen three core parameters: (1) field strength (voltage), (2) pulse duration, and (3) number of pulses.

Based on a large number of electroporation studies, several types of pulsation strategies have been devised. In a review by Gehl¹⁰¹⁰, three categories of approaches for DNA transfection were described, all of which have achieved some measure of success: (1) Exclusively short, high-amplitude pulses^{53,1067,1101}; for example, a series of six pulses of 100 μs at field strengths of $1.4 \text{ kV}\cdot\text{cm}^{-1}$ ¹¹⁰². (2) Exclusively long, low-amplitude pulses^{429,492,1066,1089}; for example, eight pulses of 20 ms at field strengths of $0.2 \text{ kV}\cdot\text{cm}^{-1}$ ¹¹⁰³. (3) A short, high-amplitude pulse followed by a long, low-amplitude pulse¹¹⁰⁴; for example a first pulse of 10 μs at $6 \text{ kV}\cdot\text{cm}^{-1}$ followed up with a second pulse of 10 ms at $0.2 \text{ kV}\cdot\text{cm}^{-1}$ as pioneered by Sukharev et al.⁴⁹¹. The rationale behind this dual pulse strategy is that the first pulse is thought to nucleate many pores over a large segment of the cell surface, while the second pulse should simultaneously grow the pores and electrophoretically propel charged

molecules into the cell. Indeed, several studies have confirmed that the duration of the second low voltage pulse correlates with DNA transfection efficiency^{491,492,1089}.

Dual Pulse Strategies: The dual pulse strategy has captivated considerable attention from the field and inspired a number of further investigations^{1078,1079,1101,1105,1106}. Figure 26 shows examples of pulse parameter sequences that constitute a typical dual pulse strategy. The first example consists of two consecutive DC square wave pulses (Figure 26A)¹⁰⁷⁸ while the second uses an AC signal for the first pulse followed by a delay then a second DC pulse (Figure 26B)¹⁰⁷⁹. The AC pulse is designed to increase the consistency of permeabilization at each pole of the cell and reduce side effects at the electrodes. These reports are a few among many to suggest that dual pulse strategies optimize delivery while preserving cell viability, not only for DNA transfection but also for other molecules like proteins and high molecular weight dextrans^{1078,1079}.

Nucleofection Mechanisms: Nucleofection, one of the most popular electroporation systems of all time, was introduced in the early 2000s and rapidly gained traction as an effective intracellular delivery method. It is based upon a classical cuvette configuration with parallel plate electrodes, but the novelty comes from the systematic selection of optimal pulsing parameters and cell-type specific buffers^{508,1107,1108}. Although the exact pulsing parameters are proprietary, patents indicate that it is based around a dual pulse approach¹¹⁰⁹. The first pulse is administered at field strengths of 2–10 kV·cm⁻¹ for durations ranging from 10–100 μs. The second pulse lasts 1–100 ms at a lower, yet unspecified, field strength. Dozens of different pulsing protocols are programmed into the nucleofector control unit, presumably based on variations on this theme. The user then finds optimal electroporation conditions by screening the programs against delivery and viability outcomes for different cell types. To facilitate best results, cell type-specific buffers are also recommended. Bucking the trend of literature touting the superiority of low conductivity buffers featuring organic osmolytes¹⁰⁹⁹ or high K⁺ cytoplasm-mimicking buffers⁵⁰⁶, patents on nucleofection buffers report near-physiological concentrations of extracellular (high) Na⁺ and (low) K⁺ augmented by >10 mM Mg²⁺ and robust pH buffering⁵⁰⁸. The high conductivity of the nucleofection buffers (ionic strength >200 mM) is thought not to cause Joule heating problems due to the emphasis on small volumes and shorter pulse durations^{508,1108}. Users have reported adapting nucleofection for use with phosphate buffered saline without a decline in performance^{510,512}. A number of publications share protocols for homemade nucleofection buffer formulations to increase transparency of the protocols and lower costs^{509,510}.

A notable appeal of the nucleofector system has been the assertion that it delivers plasmid DNA rapidly and directly to the nucleus^{1107,1110}. This speculation, however, is controversial and difficult to find direct support for it in the literature. An alternative explanation is that endocytic trafficking instead directs DNA to the nucleus, as has been observed for other types of electroporation¹⁰⁸⁶. A number of factors lend credence to the endocytic explanation. First, the cytoplasm is a highly crowded and viscous environment laced with cytoskeletal filaments and organelles. The mobility of microinjected plasmid DNA is extremely small or even negligible in the cytoplasm or cell nucleus^{1111–1113}. To be

electrophoretically propelled through the cytoplasm into the nucleus, a combination of significant plasmid compaction and large electrophoretic forces would be required, although this has not been directly proven¹⁰⁸⁶. Second, the reported timing of gene expression is in the range of 6 hours after treatment^{1107,1110}, which is actually longer than achieved with standard electroporation that relies on endocytosis¹⁰⁸⁶. In contrast, microinjection of DNA directly into the nucleus can mediate gene expression within 30 minutes. Some authors have speculated whether nucleofection permeabilizes the nucleus with its first high-voltage pulse, thus assisting in nuclear delivery^{331,537,1108}. This hypothesis has not been rigorously tested in experiments to date.

Regardless of the exact mechanisms, nucleofection has shown significant success rates for DNA transfection and expression in traditionally difficult-to-transfect cell types¹⁰⁶². This has been demonstrated in various types of stem cells, primary cells, and post-mitotic cells, for example, primary human melanocytes, smooth muscle cells, chondrocytes, and mesenchymal stem cells^{1107,1114,1115}, human monocyte-derived dendritic cells^{1116,1117}, monocytic cell lines¹¹¹⁰, primary leukemia cells and cell lines^{1118,1119}, primary natural killer cells and cell lines^{1120,1121}, primary lymphocytes^{1122,1123}, embryonic and adult stem cells^{1124,1125}, and mammalian neurons^{1108,1126}. These papers and others contributed to the emergence of nucleofection as a leading method for transfection of recalcitrant cell types.

Overall, there are many examples of pulsing strategies that have been successfully employed to electroporate molecules into the cell^{239,1010,1011,1086}. Nucleofection is but one example of a dual pulse strategy that has been systematically honed for application with a wide range of cell types, including difficult-to-transfect cells. A deeper understanding of the mechanisms of electroporation phenomena on cells and cargo molecules could yield even further advancements in both delivery performance and cell health.

6.2.2 Electroporation Challenges & Technical Advancements—As with most membrane disruption-based intracellular delivery strategies, a major challenge with electroporation is cell mortality post-treatment. Death may occur immediately due to irreversible electroporation, lysis, or excessive thermal damage⁴⁵⁰. Or it may take the form of a delayed necrosis, possibly due to failure of membrane repair, or prolonged apoptotic responses, taking place hours or days after treatment⁴⁸⁹. As an example of this problem, early reports on nucleofection of human monocyte-derived dendritic cells yielded unprecedented plasmid transfection results, with up to 60% gene expression. However, long-term functional assays indicated that cells were hampered by gradual loss of proliferative potential and poor viability¹¹¹⁶. In this section, we discuss the problems with electroporation and the efforts that have gone into reducing its toxic burden on cells.

The Problem of Joule Heating: When an electric current passes through an aqueous solution, it triggers temperature increase (Joule heating) concurrent with various chemical reactions at the solution-electrode interface (electrolysis). Electrolysis itself produces changes in the temperature, pH, and the chemical composition of the adjacent solution. The degree of Joule heating is influenced by the conductivity of the buffer, electrode architecture, electric field parameters, and capacity of the system for dissipation. For cuvette style setups, temperature spikes of more than 30 K above ambient conditions have been measured in

physiological saline at millisecond pulse durations¹⁰⁹⁷. Such observations have led some researchers in the field to assert that Joule heating is a significant problem⁵³⁷. For example, an $8 \text{ kV}\cdot\text{cm}^{-1}$ pulse of $100 \mu\text{s}$ has been calculated to lead to a temperature increase from $23 \text{ }^\circ\text{C}$ to $42 \text{ }^\circ\text{C}$ in PBS solution⁵³⁷. Lipid membranes and proteins are destabilized by temperatures above $42 \text{ }^\circ\text{C}$ ¹¹²⁷. Therefore Joule heating is not just an issue for the plasma membrane, but also for intracellular membranes and proteins throughout the cell. To reduce the negative effects of Joule heating, electroporation procedures can be performed at room temperature ($20\text{--}25 \text{ }^\circ\text{C}$) or on ice ($0\text{--}4 \text{ }^\circ\text{C}$). Lower temperatures, however, makes cells more resistant to pore formation^{532,533}, thereby reducing delivery efficiency. Another approach to combat Joule heating is to use low-conductivity buffers, which feature lower concentrations of electrolytes and instead maintain osmolarity by inclusion of organic osmolytes or sugars like sucrose and mannitol⁴⁹². Low-conductivity buffers reduce Joule heating while enabling the long pulses that are preferred for some protocols, such as for DNA transfection.

The Problem of Metal Contamination: A number of publications have assessed the detrimental effects of metal ions released into solution by electrolysis^{532,1128–1131}. For large surface area electrodes, such as cuvette style electroporation chambers, the most commonly used materials are aluminum, copper, and stainless steel. Analysis of stainless steel and aluminum electrodes found that, after a train of pulses similar to a standard electroporation protocol, both were found in solution at up to milliMolar concentrations^{532,1129,1131,1132}. Aluminium ions and aluminum hydroxides can wreak havoc on cellular processes, such as inositol phosphate activity^{532,1128}. Moreover, Stapulionis et al. found that released copper, iron, and aluminium ions can interact with nucleic acids and cause their precipitation out of solution¹¹²⁹. Other studies have found $\text{Fe}^{2+}/\text{Fe}^{3+}$ to be toxic to *in vitro* cell cultures at milliMolar concentrations¹¹³¹. $\text{Fe}^{2+}/\text{Fe}^{3+}$ released from the anode behave as a Lewis acid and hydrolyze the water molecules in the solution. This effect can reduce pH and potentially alter the medium conductivity¹¹³². Metal ions released from the electrodes can also contribute to local distortion of the electric field, further compounding these issues¹¹³³.

The Problem of pH Changes: As touched upon previously, pH changes that take place at the electrodes can have a substantial impact on cell health. The changes in pH values in solution have been measured to exceed 1–2 pH units under conditions similar to those used in standard electroporation¹¹³⁴. As with Joule heating, shift in pH depends on the medium conductivity. pH of a solution in which sucrose was substituted for NaCl, was reported to be about 5 times less than phosphate buffered saline. The electrode material also contributes, with aluminium cathodes yielding a two-fold greater pH in comparison with platinum, copper or stainless steel cathodes. This led to the recommendation of stainless steel electrodes instead of aluminium¹¹³⁴. Several studies have successfully visualized the changes in pH at electrodes with pH sensitive dyes^{532,1135,1136}. Acidic fronts form at the anode while the cathode becomes basic. A study by Li et al. used microchip-based electroporation to determine that hydroxyl ions at the cathode are more deadly than protons at the anode¹¹³⁶. They observed that strong pH buffering can, to some extent, neutralize the problem, thereby bringing cell viability up above 90% in comparisons with 60% for inadequately buffered and 40% for unbuffered solutions¹¹³⁶. The idea of switching the

polarity of electrodes between pulses has also suggested to prevent cumulative pH biases at the electrodes¹¹³⁴.

The Problem of Non-Uniformity in the Electric Field: Non-uniformity of the electric field can cause some cells to be treated too harshly while others are insufficiently permeabilized. Indeed, significant heterogeneity in electroporation arises due to a lack of consistency of the electric field^{1011,1097}. One effect of excessive electrolysis is degradation of the electrode performance. For example, a study with stainless steel electrodes in parallel plate geometry showed significant pitting of the anode¹¹³⁷. The increase in the roughness of the electrode was proposed to contribute heterogeneity and loss of consistency of the field applied across the cell suspension. Subsequent studies also showed that the pulsing frequency and presence of chloride amplified the corrosion of iron electrodes¹¹³⁸. Furthermore, in a dense suspension of electroporated cells, neighboring cells will affect the geometry of the electric field due to mutual electrical shading^{1098,1139}. When cells represent 1% of the volume fraction they behave as single cells, while for volume fractions greater than 10% or for clusters of cells, the suspension density will distort the conferred transmembrane potential^{1041,1140}.

Counteracting Electrolysis: Together, the abovementioned studies show that electrolytic effects and corrosion are a critical consideration for electroporation. This is especially important for cells and biological material bound for medical applications, such as cell-based therapies. Tactics that may be used to counteract corrosion/contamination include lowering solution conductivity, changing the pulsing schemes, buffering more strongly against pH changes, and reducing the surface area of electrodes adjacent to cells. Another strategy is to switch the polarity of electrodes between successive pulses, which has been shown to minimize cumulative electrolysis and decrease the contamination of metal ions in solution by an order of magnitude¹¹³¹. The idea of using more inert gold or platinum, or replacing metal electrodes with plastic, graphite, or liquid ones has also been explored.

Cell Damage from the Electric Field: Aside from cell damage due to electrolysis related-effects (e.g. Joule heating, contamination via corrosion of electrodes, and pH changes), the electric field itself may harm cell components more directly. For example, the application of strong electric fields has been suggested to trigger lipid peroxidation^{1141–1143}, generation of reactive oxygen species^{1144,1145}, protein denaturation, and DNA damage^{1146,1147} amongst other responses. Under electroporation conditions compatible with cell survival, it was shown that electroporation can trigger an “oxidative jump” where the level of reactive oxygen species (ROS) rises sharply¹¹⁴⁴. The measured generation of ROS was to some extent dependent on extracellular calcium and magnesium, but could be prevented by addition of anti-oxidants. In subsequent studies, lipid peroxidation, as evidenced by the presence of lipid hydroperoxides, was observed in the membranes of both plant and animal cells following electroporation^{1142,1143}. Further investigations using the chemiluminescent probe lucigenin found that CHO cells subject to millisecond pulses undergo a threshold level of oxidation of their plasma membrane lipids, but that this effect only partially correlates with cell survival¹¹⁴⁵. Interestingly, lipid peroxidation of unsaturated phosphatidyl choline species has also been observed during electroformation of giant unilamellar vesicles¹¹⁴⁸.

Membranes characterized by a high degree of peroxidized lipids tend to be weaker and more susceptible to disruption, including by electroporation¹¹⁴⁹. Indeed, lipid peroxidation is well known to influence membrane behavior, including domain formation and mechanical properties, which could have implications for cell recovery post-electroporation.

The reactive oxygen species produced by electroporation will not only target lipids, but can also degrade proteins and nucleic acids. DNA damage in proportion to the applied voltage and duration has been reported in HL60 cells, although no specific mechanisms were pinpointed¹¹⁴⁷. It could be that DNA damage is due to influx of oxidative agents from the extracellular environment. Regarding proteins, Chen and colleagues have suggested non-thermal electroconformational damage to ion channels following exposure to strong electric fields^{1150–1153}. More general models describing electroconformational damage of membrane proteins and other cellular components have subsequently been described^{1154,1155}. In particular, it is proposed that charged amino acids in membrane proteins or voltage-sensing segments in voltage-dependent transporters are vulnerable to sharp changes in electrical potential. These effects are thought to be more pronounced for shorter pulses of higher amplitude¹¹⁵⁶. Indeed, other studies showed that high voltage nanosecond pulses are likely to perturb the function of voltage-gated channel proteins¹¹⁵⁷, and possibly other proteins in general¹¹⁵⁸.

Although not typically used for intracellular delivery, nanosecond pulsed electric fields are of interest for understanding how electric fields can affect cells on different timescales and in various compartments. One study examined generation of ROS in response to nanosecond pulsed electric fields ($30 \text{ kV}\cdot\text{cm}^{-1}$ at 100 ns)¹¹⁵⁹. They found that ROS was inhibited by both calcium chelators, and the antioxidant trolox, in agreement with earlier observations that the presence of divalent ions appears to participate in ROS generation¹¹⁴⁴. Other reports have shown that H_2O_2 is among the damaging species generated by nanosecond pulsed electric fields¹¹⁶⁰. Although undesirable for intracellular delivery, non-thermal electrical destruction of proteins, cells and tissue have been proposed for a host of other medical and industrial applications¹¹⁶¹.

Molecular dynamics simulations have shown that the presence of hydrophilic pores can augment the process of lipid flip-flop, whereby lipids translocate from one leaflet of a bilayer to the other³⁷⁹. Partial abolition of the naturally uneven bilayer distribution of lipids has been observed in RBCs as a consequence of electric fields¹¹⁶². Vernier and others found that nanosecond electric pulses can facilitate phosphatidylserine (PS) exposure to the outer leaflet within seconds^{1163–1165}, indicating a biophysical mode of action rather than cell signaling. Rols and colleagues performed a follow-up study with millisecond permeabilizing pulses to examine membrane disorganization and phospholipid scrambling¹¹⁶⁶. Under the chosen conditions, PS exposure could not be detected. The threshold conditions that trigger PS exposure thus remain to be precisely determined, however, it appears that PS scrambling may only be relevant under regimes of very high field strength. Scrambling of the membrane asymmetry has implications for the long-term survival of cells, particularly *in vivo* where immune recognition mechanisms tend to destroy cells exhibiting wayward externalization of lipids.

Cargo Damage from the Electric Field: Apart from damage to the cell, administration of the field strengths commonly used for electroporation may also cause problems with the cargo molecules. Degradation and damage of electrically sensitive cargo has been suggested by some reports. For example, the Bhatia group reported aggregation of quantum dots upon electroporation, indicating it is not a suitable technique for intracellular delivery of quantum dots²⁷³. Electric pulse-induced precipitation of nucleic acids and other biological macromolecules has also been observed under certain conditions^{1129,1167}, although it is unclear why other groups haven't seen such problems. These studies noted that nucleic acids aggregated into a non-functional state under the conditions of their experiment. If they can be identified, it seems likely that the conditions leading to precipitation must simply be avoided. Nevertheless, it is worth noting that not all molecular cargo can be assumed to be compatible with strong electric fields.

Technical Innovations: Bulk, Micro- & Nano-Electroporation: The pioneering generation of electroporation delivery experiments was performed with a cuvette-style geometry¹⁰⁸⁸. Subsequently, the first commercial electroporator, the BioRad Gene Pulser, was launched with this configuration in the mid 80s. Since then, the cuvette geometry has become the standard platform for electroporation, being simple, robust, and reasonably well understood (Figure 27A(i)). The nucleofector is no exception, and as discussed previously, its novelty arises not from a deviation from this geometry, but rather from the systematic use of pulsing protocols and cell-type specific buffers. Despite its widespread adoption, the cuvette style is not without problems. For one, the large surface area of the metal electrodes presents issues concerning electrolysis as discussed above, such as Joule heating, corrosion, pH deviations, and inconsistent field profile. Second, cuvette-style electroporation is difficult to perform with low volumes (<20 μ l). As the intracellular delivery of a molecule via permeabilization is directly related to extracellular concentration, it is often advantageous to concentrate the cells into a minimal volume in the range of 10 μ l or less. This maximizes the concentration, which is especially useful for expensive or precious reagents. Below we discuss the innovations that have been produced in the electroporation field, including difference setups for bulk, micro- and nano-electroporation

Capillary Electroporation: One of the first commercial setups to challenge the dominance of the cuvette geometry came in the form of capillary electroporation (Figure 27A(ii)). This design was introduced by a company called NanoEntek in Korea and subsequently commercialized by Invitrogen/Thermo Fisher as the Neon electroporation system⁵¹⁶. In capillary electroporation cells and buffer solution are pipetted into a narrow capillary (0.56 mm wide and 30 mm long) featuring a wire gold electrode with minimal surface area at the top. The other electrode, also made of gold, is located within a conductive electrolyte bath underneath the capillary. Because of the small surface area and distance from the cells, bubbles, Joule heating, and pH waves are more effectively separated from the cells. The small size of the electrodes also means that gold plating becomes economical. Chemical stability of the electrodes is superior to those made from less inert metals like iron, aluminium, or copper. The authors compared pH deviations in the capillary system to those of conventional cuvette style chambers and it appeared to confer substantial advantages in protecting cells from the toxic electrolytic processes that can occur at electrodes. Together

these features are purported to increase the viability of cells treated in the capillary electroporation setup⁵¹⁶.

On the other hand, one disadvantage of the Neon system is the reduced flexibility in determining pulse parameters. In the commercially available units the pulse duration is limited in the range 1–100 ms and voltage from 500–2000 V. Given the distance of the conductive path between the electrodes, this means the field strength does not exceed 1 kV·cm⁻¹. The user may increase the number of pulses but there is no option to program pulses of different, voltage, or frequency. Thus, the dual pulse strategies that have become so popular with the Nucleofector system are not possible with the Neon platform. High cost of capillary tips, electrodes, and buffers is another factor that users dislike⁵¹⁷. In response to this, some researchers have published protocols advising users on how to recycle the components and employ a homemade buffer, consisting of PBS supplemented with 250 mM sucrose and 1 mM MgCl₂⁵¹⁷.

Microfluidic Electroporation: Motivated by the shortcomings of conventional electroporation equipment, a number of researchers and engineers have explored alternative solutions. Electroporation combined with microfabricated, microfluidic, and nanotechnology concepts has received a great deal of attention in the last decade as evidenced by a spate of reviews on the topic^{1168–1173}. Compared to bulk electroporation systems, it has been argued that micro- and nano-electroporation can provide the following advantages^{1171,1172}: 1) lower voltages due to smaller scale, thus obviating the need for high powered pulse generators, 2) ability to concentrate, trap, and position cells and molecules for higher efficiency delivery, 3) real time monitoring of device performance at single cell level, and 4) scalable solutions from single cells up to large populations.

One of the first microfluidic electroporation systems was constructed by Huang and Rubinsky in the late 90s¹¹⁷⁴. It was essentially a small hole of 2 – 10 μm diameter that a single cell could be sucked onto. The application of an electric pulse from below was used to permeabilize the basal side of the trapped cell and study the mechanisms of electroporation at single cell level. Although only demonstrated as a proof of concept, such developments spurred the field on to further efforts. Several years later the first microfluidic flow electroporation devices appeared on the scene. Huang and Rubinsky were again pioneers in this department, demonstrating loading of small molecule dyes and transfection with GFP encoding plasmids, albeit at low throughput¹¹⁷⁵. In the following, we will highlight a few select examples of flow-based microfluidic electroporation.

Droplet-based microfluidics enables the use of microscale compartments to expose cells to a particular chemical environment within picoliter reaction volumes¹¹⁷⁶. Zhang et al. encapsulated cells in aqueous droplets before flowing them over a pair of electrodes subjected to a constant DC voltage¹¹⁷⁷. Due to the non-conductivity of the oil phase, cells only experience a transient electric pulse when the conductive droplets pass the electrodes (Figure 27B(i)). The cell is then permeabilized to the molecular cargo loaded within the droplet. In this case a DNA plasmid encoding for GFP was successfully delivered into CHO cells¹¹⁷⁷. The pulse parameters were related to the flow speed, size of the droplet, distance between the electrode pair, and the positioning of the cell inside the droplet. Owing to the

rise in droplet-based microfluidics for high-throughput single cell analysis, techniques that can perform intracellular delivery on cells within droplets are expected to be important.

In a second example of flow-based microfluidic electroporation, electric pulse parameters are again determined by the device geometry and flow speed under constant DC voltage. But in this case electroporation occurs at narrow constrictions within the main flow channel⁴⁴⁹. The geometry of the device channels controls the field amplification so that cells undergo an electric pulse as they passage through a constriction (Figure 27B(ii)). Pulse duration experienced by the cell is determined by flow speed, while amplitude is given by width ratio of constriction to normal channel diameter. The number of constrictions in series will effectively determine the number of pulses. In subsequent efforts, Geng et al., scaled up this concept to process $20 \text{ mL} \cdot \text{min}^{-1}$ of cells in continuous flow mode with a minimalist setup featuring low-cost components, a syringe pump, and a bench top DC power supply without the need for a pulse generator¹¹⁷⁸. For plasmid transfection in CHO cells a transfection efficiency of up to 75% was achieved.

In a different microfluidic electroporation strategy, hydrodynamic flow focusing was exploited to create parallel laminar flow streams of different conductance (Figure 27B(iii)). Using a three-inlet approach, the top and bottom sheath flows were composed of highly conductive 3M KCl solutions, which acted as liquid electrodes, while cells in standard aqueous solution were flowed through the center of the configuration¹¹⁷⁹. By applying a DC voltage of only 1.5 V, electric field intensities of more than $1 \text{ kV} \cdot \text{cm}^{-1}$ could be generated across the central zone to electroporate the passing cells. The device showed up to 70% delivery efficiency of fluorescein dyes into yeast cells¹¹⁷⁹. Moreover, distancing the metal electrodes from cells using hydrodynamic focusing had the advantage of isolating cells from electrolysis issues such as heating, bubble generation, pH changes, and production of toxic ions¹¹⁷⁹. Thus, the use of non-metal liquid electrodes in hydrodynamic flow mode may overcome problems associated with cuvette-style electroporation.

In a fourth example of microfluidic ingenuity, a spiral-shaped microfluidic channel was implemented to generate flow vortices¹¹⁸⁰. As cells traverse through the curved channels, vortices caused by Dean flows facilitate their rotation in reference to the electric field (Figure 27B(iv)). This has the effect of permeabilizing the entire cell surface, rather than just the polar extremes. By increasing the cell surface area that can be electropermeabilized high delivery efficiency was achieved with both dyes and DNA plasmids¹¹⁸⁰. Other vortex-based microfluidic systems have been implemented to achieve a similar effect^{1181,1182} and have been demonstrated to deliver dyes, miRNA, siRNA, proteins, and plasmids¹¹⁸³.

Nanochannel Electroporation: Inspired by early work on electroporation through micron-sized apertures¹¹⁷⁴, Boukany et al. introduced the concept of nanochannel electroporation¹¹⁸⁴. By scaling the aperture size down to $\sim 90 \text{ nm}$, the membrane disruption effect of electroporation could be concentrated onto a very small spot on the cell surface (Figure 27C(i)). A significant claim of this strategy is dose control, i.e. the finding that the amount of delivered material directly correlated with the voltage pulse duration. Nanochannel electroporation also seemed to introduce agents faster and deeper into the cytoplasm, an effect that was attributed to enhanced and concentrated electrophoretic forces.

In support of this, finite element simulations found that fringe fields extended into the cell and could possibly be used to propel molecular cargo through the permeabilized section of the cell periphery and deep into the cytoplasm. Comparing their device to conventional electroporation and other forms of microfluidic electroporation, they proposed that their delivery mechanism is mostly based on electrophoretic forces as opposed to diffusion and/or endocytosis. Nanochannel electroporation was able to deliver dyes, oligonucleotides, siRNA, plasmids and quantum dots into recipient cells. Moreover, only nanochannel electroporation could deliver quantum dots into Jurkat cells, while conventional or microfluidic electroporation could not. However, being a single cell technique that required placement of suspended cells against the nanochannel with optical tweezers, low throughput was a main drawback of this method.

In 2016 the same group published a scaled-up version of the concept able to process up to 40,000 cells on a single chip over a 1 cm² area¹¹⁸⁵. In this version, termed “3D nanochannel electroporation”, the aperture dimensions were expanded to 300–650 nm. Positive dielectrophoresis was employed to simultaneously position thousands of cells across the array and press them against the nanochannels. This was necessary because a tight seal between the cell membrane and the nanochannel is critical to ensure consistent electroporation performance across the device. Molecules to be loaded are filled into a reservoir below the substrate and loaded into cells concurrently with application of the electric field. The system was used for transfecting plasmid DNA into batches of natural killer cells, which are otherwise difficult to transfect. A predecessor to the idea was published in 2006 by Kurosawa using an insulating substrate with an array of 2 μm holes in it¹¹⁸⁶. Just like in 3D nanochannel electroporation, the field was concentrated at the holes and molecules to be delivered were supplied from underneath. This design is essentially a scaled up version of the original microfluidic electroporation system published by Huang in 1999¹¹⁷⁴. The Luke Lee lab also published a series of papers where cells were sucked into microchannels made of PDMS. In effect, this design was not too dissimilar from a parallel array of micropipettes^{1187–1189}. An electric field was introduced to focus the electroporation effects to a region of the cell sucked into the microchannels, thereby locally permeabilizing them^{1187–1189}. The concept was later combined with electrophoresis for increasing the efficiency of delivery, where the delivery of molecules could be optically monitored in real time¹¹⁹⁰. Again, a similar concept to take advantage of using channels as trapping arrays was used to transfect plasmid DNA into stem cells¹¹⁹¹. Collectively, these innovations show the power of localizing electric fields to the subcellular scale. If the problem of scale up to high throughput can be solved at an acceptable cost, this approach can be expected to benefit the intracellular delivery toolkit.

Nanostraw Electroporation: Another form of nanoscale electroporation takes the form of so called nanostraws (Figure 27C(ii)). The key difference is that the nanoscale aperture protrudes into the target cell as a hollow nanoneedle. Although cell membranes appear to be resistant to penetration by such nanoneedle under passive conditions, the addition of an electric field permeabilizes the cell membrane at the tip of the nanostraw⁶⁶⁶. One benefit of this approach is that active forces, such as optical tweezers or positive dielectrophoresis, are probably not required to establish optimal contact between cells and the nanostraw. Rather, a

consistent period of settling might be required to facilitate uniform contact between cells and the substrate⁶⁵³. Furthermore, with sufficient adhesion to the nanostraw array, substantial pumping forces can presumably be used to flow molecules into cell cytoplasm without cell detachment. In light of poor results with aluminium electrodes in bulk conditions, however, the choice of aluminium nanostraws as the fabrication material may need to be revised in future versions of this device.

Nanofountain Probe Electroporation: A scanning probe-based approach for localized electroporation, termed nanofountain probe electroporation, has been introduced by Espinosa and colleagues^{1192,1193}. It is essentially an atomic force microscope cantilever engineering with a hollow channel for fluid flow. Target cells are cultured on a grounded coverslip and positive or negative voltages are applied to the conductive cantilever, thereby focusing the electric field at the site of contact between the cantilever and cell (Figure 27C(iii)). By coordinating the movement of the tip and the flow of fluid, introduction of dextrans and proteins into cells can be achieved¹¹⁹². In follow-up applications of this system, it has successfully been employed to deliver molecular beacons to the cytoplasm for detection of mRNA transcription¹¹⁹³.

Summary of Micro- and Nano-electroporation: Innovations in micro and nano electroporation have showcased a number of interesting proof-of-concept prototypes. Diverse architectures have been developed, including the use of micro- or nanochannels smaller than the cell, channels larger than the cell, chambers, compartments, and droplets, and hydrodynamic effects such as sheath focusing and vortices^{1169,1171}. Some of these reports claim improved delivery efficiency and viability over conventional bulk electroporation. They have also provided elegant solutions to problems that have long troubled traditional electroporation, such as electrolytic reactions at the electrodes, gas bubble formation, pH deviations, Joule heating, inconsistent cell treatment, inability to scale down reagent volumes, and excessive power consumption and equipment requirements. Yet the technical advancements of miniaturized approaches have not translated to widespread adoption, most likely due to high cost, impractical throughput, lack of focus on clinical or industrially relevant problems, or lack of user-friendly designs¹¹⁷². Thus, it remains to be seen what the next generation electroporation systems will look like, and whether they will challenge the dominance of existing methods. Apart from technical upgrades, several recent reviews propose that further theoretical studies on mechanisms of cell membrane permeabilization and cargo uptake are needed to obtain further progress in the field^{239,1086,1170}.

6.2.3 In Vitro & Ex Vivo Applications of Electroporation—Of the membrane disruption-based approaches, electroporation is currently the most mature in regard to industrial applications and clinical translation. Electroporation-based technologies have been deployed *in vivo* and as well as *in vitro*. The *in vivo* applications include electrochemotherapy, non-thermal tissue ablation, DNA vaccines, and transdermal drug delivery. These have already been discussed in other reviews^{1010,1012,1194–1198}. In biotechnology electroporation has also been used for extraction of biomolecules, sterilization/pasteurization of solutions, and transformation of microorganism¹¹⁹⁹. In

keeping with the focus of this review, we will focus our discussion on the *in vitro* and *ex vivo* applications relevant to intracellular delivery in human and animal cells. In this context electroporation has been employed mainly for nucleic acid transfection, of which there are three main market areas: 1) biomedical research, 2) biomanufacture of biologics (proteins, antibodies, and viral vectors/particles), and 3) therapeutics (cell-based therapies, gene therapy, and cell manipulation for regenerative medicine)(see Figure 3). Furthermore, intracellular delivery of non-nucleic acid cargo is beginning to enjoy increased attention, especially with the rise of genome editing and new forms of cell-based therapies. Below we highlight a selection of key applications.

Intracellular Delivery of Impermeable Drugs: Permeabilization via electroporation has been proposed for pharmacological applications to identify the cytoplasmic activity of otherwise impermeable drugs and small molecules¹²⁰⁰(Figure 28A). In the 1980s a study by Melvik et al. showed that electroporation of cell lines significantly enhanced the efficacy of cis-dichlorodiammineplatinum(II)(cisplatin) up to 3-fold greater than controls¹⁰³⁹. Using radiolabeled tracers, they found electroporation rendered cells permeable to small molecules for up to 10 minutes. Subsequently, electroporation has been used to screen for cytotoxicity of drugs that are otherwise susceptible to be pumped out of cells by the activity of cellular efflux pumps^{254,1040}. Bleomycin (~1.4 kDa) represents a particularly striking example of a drug where activity is drastically increased with electroporation-mediated intracellular delivery^{254,1040}. Thus, electroporation can be leveraged to test for the cytoplasmic activity of otherwise impermeable small molecules, peptides, and biochemical agents.

Biomanufacture Through Transfection: Biomanufacture refers to the production of biomaterials or biomolecules by the harnessing of biological systems. Transfection of common cells lines can be used for production of proteins, antibodies, and viral vectors, or viral particles^{1201–1206} (Figure 28B). These are often produced in mammalian cell lines such as CHO, HEK-293T, HeLa, A549 cells or insect cell lines, depending, for example, on the need for species-specific post-translational modifications. Significant efforts have gone into engineering these systems for maximum yield and economies of scale. Both stable genetically modified cell lines and transient transfection are key strategies for biomanufacture. Although lipid and polymer reagents are most commonly used for transfection in biomanufacture, electroporation is currently the leading option on the membrane disruption-mediated side.

Large Volume Flow Electroporation: In 2002 the use of large volume flow electroporation for clinical and industrial bioprocessing was reported in the scientific literature by the company Maxcyte¹²⁰⁷. Initial reports claimed that common suspension and adherent cells lines could be loaded with 500 kDa dextran at >90% efficiency and >90% viability while gene transfection rates could reach up to 75%. The latest versions of this technology are capable of tunable scale, from tens of thousands of cells up to 200 billion cells into liters of solution. The run time for a batch of 200 billion cells is approximately 30 minutes in a single run. Moreover, the system is sterile and compliant with current good manufacturing processes (cGMPs) for biological clean room facilities. In further demonstrations of its

utility in manufacturing scenarios, the flow electroporation platform was used to batch transfect HEK293T cells for large-scale production of lentiviral vectors¹²⁰⁸.

Recently, Zhao et al. published a different strategy for large volume flow electroporation with a device that integrates a large-sized flow tube and a miniaturized needle electrode array with uniform spacing¹²⁰⁹. The microfluidic design of the needle electrode array had the benefit of lowering the required voltage. This system demonstrated processing rates of 20 million cells per minute and was suggested to be suitable for *in vitro* and *ex vivo* batch processing applications. Another group published a similar concept constructed from custom-made microfluidics components as a solution for batch flow electroporation of mRNA into tens of millions of dendritic cells¹²¹⁰.

Delivery of Genome-Editing Proteins and RNPs: Recent advances in genome editing via programmable nuclease have spurred an interest in intracellular delivery of these proteins, particularly Cas9 RNPs. In the last few years RNP delivery has been successfully accomplished with electroporation^{218,219,221,222}, microinjection^{223,224}, lipid nanoparticle formulations²²⁵, osmotically-induced endocytosis followed by endosome disruption²²⁶, microfluidic cell deformation²²⁷ and CPPs²²⁸. Electroporation, however, is reported to be more efficient with a number of primary, blood, and immune cell types *in vitro*. RNP delivery via electroporation has been demonstrated in an array of cell types, ranging from common cell lines to blood and immune cells of clinical relevance, with both conventional cuvette style (Nucleofection)^{25,156,218,221,222} and small volume capillary electroporation (Neon)^{40,219,220,1211} platforms.

The mechanisms of RNP entry via electroporation have not been heavily studied yet. Given what we already know about the influx behavior of nucleic acids and proteins (Figures 23–25), it is worth considering the possibilities. As discussed in section 2.2.2, RNP complex should have about –80 negative charges, be ~188 kDa, and up to 15 nm in size (Table 1). The mechanisms of EP could thus be similar to siRNA, namely direct translocation of a highly negatively charged molecule into the cytoplasm at the side of the cell facing the negative electrode during the pulse (Figure 23D). Once in the cytoplasm a nuclear localization sequence (NLS) on the Cas9 would then promote its shuttling inside the nucleus. Another possibility is that RNPs are endocytosed after being entangled in the destabilized plasma membrane, such as is the case for plasmid DNA (Figure 23E, 24). Indeed, embedding of proteins into the plasma membrane post-electroporation has been observed in several cases^{1046,1076}. The ground-breaking potential of genome editing will no doubt stimulate the field toward studying mechanisms of protein and RNP delivery to the nucleus. For example, the optimal nuclear concentrations of Cas9 RNP needed for efficient genome editing are still unknown. In future, it will also be interesting to see how other membrane disruption-based delivery approaches (which do not supply electrophoretic forces) fare in their efficiencies of RNP delivery.

Hard-to-Transfect Cells: A number of sensitive primary cell types do not easily tolerate foreign nucleic acids or the toxic side-effects of common transfection reagents. For example, dendritic cells, T lymphocytes (T cells), B lymphocytes (B cells), natural killer (NK) cells, leukemia cells, hematopoietic stem cells (HSCs), macrophages, and neurons have all been

reported to be recalcitrant to polymer-or lipid-based transfection^{102,127,128,151,155,159,1123,1212,1213}. Lentiviral transduction and electroporation have emerged as the two leading alternatives. However, procedures with viral vectors are sometimes unfavorable because they can: (1) be labor-intensive, inconsistent, and expensive, (2) present safety hazards, (3) cause untoward immune or inflammatory responses *in vivo*, and (4) carry a risk of insertional genotoxicity via genomic integration. Electroporation, on the other hand, is rapid and simple, but its core weakness is poor viability or loss of cell functionality, as has been reported for nucleofection of dendritic cells or T cells^{148,1116,1212}.

Nucleofection, in particular, has sought to build a reputation on effectiveness with hard-to-transfect cells^{158,1062}. Nucleofection has demonstrated significant success with DNA and RNA transfection in various types of stem cells, primary cells, and post-mitotic cells. Published examples include primary human melanocytes, smooth muscles cells, chondrocytes, and mesenchymal stem cells^{1107,1114,1115}, dendritic cells^{1116,1117}, monocytic cell lines¹¹¹⁰, primary leukemia cells and cell lines^{102,1118,1119}, primary natural killer cells and their derivative cell lines^{1120,1121}, primary lymphocytes^{1122,1123,1214}, embryonic and adult stem cells^{1124,1125}, and mammalian neurons^{1108,1126}.

Other electroporation platforms have also achieved a measure of success in hard-to-transfect cells. Minimalist setups featuring standard 2 or 4 mm cuvettes, commercial pulse generators (such as the BioRad Gene Pulser or BTX units), and an electroporation buffer consisting of OPTIMEM media (or equivalent) have attained favorable results with macrophages^{103,144}, T lymphocytes^{56,124,509,1215–1219}, dendritic cells^{55,127–129,1064,1220,1221}, and B cells^{1222,1223}. Some of these groups have even used such setups to perform small scale clinical trials⁵¹⁸. In other cases, the Maxcyte system for large-scale clinical-grade flow electroporation has demonstrated effectiveness with leukemia cells¹²²⁴, natural killer cells^{1225,1226}, dendritic cells^{211–213}, T cells⁵⁶, and CD34(+) hematopoietic cells⁵⁴. The Neon capillary electroporation system has successfully delivered molecules into iPSCs^{40,220}, T cells²¹⁹ and HSCs¹²¹¹. Together these studies suggest that no one electroporation system has a monopoly on effectiveness with sensitive or difficult to treat cell types.

T Cells & Other Immune Cells: Immune cells are a key category of cells for biomedical investigations and therapeutic applications. In T cells it has been asserted that RNA delivery to cytoplasm is not difficult, but DNA plasmid transfection, which requires nuclear penetration, remains a significant hurdle^{148,1227}. This is an example where primary cells may exhibit an innate toxic reaction against delivered material. T cells, in particular, appear to display little tolerance to plasmid transfection regardless of delivery technique^{148,221}. Electroporation is counted among the techniques that perform well in delivering siRNA and mRNA into T cells, however, the margin of error leading to loss of viability can be narrow¹⁴⁸, and changes in the activation state, signaling pathways, and transcriptional responses of cells must be taken into account^{1228,1229}.

Many of the published electroporation protocols underscore the narrow window of appropriate parameters, emphasizing that there exists a fine line between effectiveness and cell death^{144,1119}. The challenge now for electroporation appears to be the long-term survival, potency and functionality of treated cells, not so much the initial delivery. Indeed,

post-treatment loss of viability, proliferative potential or potency has been reported for immune cells and other primary cell types^{148,1116,1212}. Moreover, electroporated immune cells have sometimes been observed to exhibit an unfavorable response or poor engraftment when infused back to the *in vivo* setting¹⁴⁸. On the other hand, several studies have shown electroporated cells to recover well and exhibit decent potency in clinical contexts^{56,518,1230,1231}.

Ex Vivo Intracellular Delivery for Cell-Based Therapies: Scientists have long envisaged the power of *ex vivo* cell manipulation for cell-based therapies, especially in regard to gene therapy, immunotherapy and regenerative medicine^{23,24,26,36}. The concept is to remove cells or tissues from the patient, engineer their function, and re-implant them to confer a therapeutic effect. Many of the relevant cell types, however, fall into the category of “hard to transfect” cells as outlined above. In the following we will highlight several areas where electroporation has been attempted for *ex vivo* cell-based therapies.

Protein Loading for Antigen Display in Cancer Immunotherapy: Loading of exogenous proteins into the cytoplasm of antigen-presenting cells leads to their processing and display through the MHC-I pathway^{175,1232} (Figure 28C). This primes cytotoxic T cells against any cells carrying these antigens, such as cancerous cells that produce mutant proteins (Figure 28C). Thus intracellular delivery of tumor proteins into antigen presenting cells, especially dendritic cells, has been proposed as a strategy for cancer immunotherapy¹²³³. Kim et al. used electroporation to load dendritic cells with exogenous antigens *ex vivo* before implanting them back into the body to elicit a robust anti-tumour response in mouse models²¹⁰. The Maxcyte clinical electroporation system was also used to achieve similar results by loading tumor cell lysate into dendritic cells²¹¹. In recent years this concept has been put to the test in human clinical trials. In 2013 a Japanese group confirmed the safety and feasibility of administering dendritic cell vaccines generated by cytosolic loading of autologous tumor lysates via the Maxcyte system²¹². This strategy was reported to produce a significant anti-tumor effect compared to passive incubation (pulsing) of dendritic cells with tumor lysate²¹³.

mRNA Transfection for Antigen Display in Cancer Immunotherapy: For induction of the MHC-I antigen presentation pathway, mRNA transfection is in many cases preferred to protein loading¹²³⁴ (Figure 28C). Van Tendeloo et al. published a paper in 2001 showcasing the efficacy of such an mRNA-based strategy in dendritic cells¹²⁷. Using a simple cuvette style electroporation setup with OPTIMEM buffer, they were able to achieve >80% expression with >80% viability compared with much poorer results from plasmid DNA in earlier studies¹²³⁵. Their analysis of options for mRNA transfection to dendritic cells suggested that electroporation was far superior to lipofection and other methods¹²³⁶. Based on these studies, the idea of electroporation-mediated mRNA transfection for *ex vivo* immunotherapy and gene therapy gained significant momentum¹²³⁷. Using similar electroporation methods as those described by Van Tendeloo et al.¹²²¹, several groups have pressed ahead with small-scale clinical trials to treat human patients suffering from melanoma and other cancers^{518,1238}. Results gathered to date indicate positive long-term survival rates and safety of the treatments.

Electroporated B Cells for Antigen Display in Cancer Immunotherapy: Apart from dendritic cells, several other types of professional antigen-presenting cells have been tested for their ability to prime T cells against a tumor antigen. Coughlin et al. employed nucleofection to demonstrate that B cells from pediatric patients can be efficient antigen presenting cells upon loading with tumor mRNA¹²¹⁴. As a proof of concept, mRNA-transfected B cells were used to successfully prime a T cell response against neuroblastoma cells¹²¹⁴. According to another study, electroporation of multiple RNAs into activated B cells with a standard cuvette style system elicited *in vitro* antigen-specific cytotoxic T cell responses with similar efficiencies as those of mature dendritic cells¹²²³. Thus, *ex vivo* activated B cells may represent an alternative source of antigen presenting cells in cancer immunotherapy, especially in pediatric cases where dendritic cells are not as readily available.

Electroporation to Produce CAR-T Cells for Cancer Immunotherapy: A more direct way of inducing an immune response against cancer is to express a T cell receptor (TCR) or chimeric antigen receptor (CAR) directly into cytotoxic immune cells, such as T cells or natural killer (NK) cells^{27,1231,1239,1240} (Figure 28D). A CAR is a genetically engineered immunoreceptor that endows modified cells with a novel specificity to kill any cell that carries molecules to which the CAR binds. The goal is to target the killing action of TCR- or CAR-modified immune cells against cancer cells carrying complementary surface markers. Electroporation of T cells has been used to deliver mRNA for TCRs or CARs, chemokine receptors, or cytokines^{56,124,1241,1242}. Similar to the case of dendritic cells, switching from plasmid DNA to mRNA was reported to allow >90% gene expression with >80% viability in T cells post-electroporation, even while using a basic cuvette-style electroporation protocol in OPTIMEM buffer¹²⁴. Using such methods, it was shown that multiple injections of mRNA-electroporated CAR-T cells mediated shrinkage of large vascularized flank mesothelioma tumors of human origin in a genetic mouse model⁵⁶. CAR expression and anti-tumor activity of mRNA-electroporated T cells was detected up to a week after electroporation. This is important because mRNA electroporation for transient expression of CARs in T cells is seen as a far safer alternative to permanent integration of CAR genes into the genome^{1239,1243}. T cells electroporated with mRNA encoding for a CAR against CD19 showed cancer killing capacity in immunodeficient mice bearing xenografted leukemia¹²⁶. Even a single injection of CD19 mRNA CAR-T cells yielded a significant prolongation in survival in this model. Because mRNA electroporation is a cost-effective and efficient path to engineer T cells for pilot studies, this approach has been pursued for high-throughput and iterative testing of novel constructs and targets in small scale clinical trials in humans^{27,1231,1239}.

Electroporation to Produce Cytotoxic NK Cells for Cancer Immunotherapy: Although most work with CARs has been carried out with T cells, NK cells represent an alternative option¹²⁴⁰. Among the first attempts to investigate this possibility were a series of experiments in 2005 by Imai et al. that used retroviral transduction to guide the activity of NK cells expressing CD19 CARs against patient leukemia cells in *in vitro* assays¹²⁴⁴. Next, electroporation of CAR mRNA into NK cells was attempted. Members of the Maxcyte team used their clinical-scale large-volume electroporation platform to transfect mRNA encoding

a CD19 CAR into natural killer cells¹²²⁵. The engineered cells demonstrated cytotoxic killing of acute lymphoblastic leukemia and B-lineage chronic lymphocytic leukemia cells for up to 3 days after electroporation¹²²⁵. Shimasaki et al. then employed the maxcyte system to scale up mRNA transfection to large batches of expanded natural killer cells with numbers reaching up to 250 million cells per run¹²²⁶. Under these conditions CD19 CAR expression reached >80% after 24 hours and mediated significant anti-tumor cytotoxicity in a mouse xenograft model of B cell leukemia.

Electroporation for Ex Vivo Gene Therapy of Blood & Immune Cells: *Ex vivo* cell-based therapies have long been pursued as an avenue for treatment of blood cells to address hematological diseases²⁴. But only recently have gene therapy clinical trials in T cells and HSCs shown significant progress. These trials used lentiviral transduction, however, which can carry a risk of genotoxicity due to random genomic integration^{22,1245–1247}. To address this problem, new approaches that deliver genome editing molecules directly into cells have attracted interest for ongoing studies¹²⁴⁸. As discussed in previous sections of this review, electroporation is among the techniques that can deliver genome-editing molecules in the form of mRNA, sgRNA, proteins, and RNPs into clinically relevant cell types at reasonable efficiencies and viabilities.

Here are two examples where electroporation of one component is combined with non-integrating viral transduction of another. First, integrase-defective lentiviral expression of donor DNA combined with nucleofection of zinc finger mRNA was used for HDR-mediated correction of monogenic mutations in the *IL2RG* gene of patient HSCs²⁵. This strategy has the potential to provide a one-time cure for the immune disorder X-linked severe combined immunodeficiency (SCID-X1) as gene-edited HSCs give rise to functional lymphoid progenitors that exhibit a selective growth advantage over disease mutants. Second, a recent study by DeRavin et al. used targeted integration of a corrected gene into CD34(+) HSCs as a treatment strategy for X-linked chronic granulomatous disease⁵⁴. Similar to the previous example, they used electroporation (in this case, the MaxCyte platform) to transfect zinc finger mRNA into cells while donor DNA for gene correction was supplied by adeno-associated viral (AAV) 6 vectors. By targeted integration of a corrected gene into the AAVS1 safe harbor locus of the genome, it was argued that genotoxicity associated with random integration can be avoided. In mice transplanted with corrected HSC progenitors, 4–11% of human cells in the bone marrow expressed the therapeutically corrected gp91phox protein.

Electroporation for Gene-Editing of Blood & Immune Cells: Other proof of concept studies for therapeutic genome editing in HSCs and T cells have been carried out with Nucleofection²²¹, Neon electroporation^{219,1211}, or standard BTX cuvette-based electroporation¹²¹⁹. In these cases, delivery of Cas9 RNPs^{219,221}, or mRNA encoding Cas9, ZFNs, TALENS, or megaTAL nucleases was demonstrated^{221,1211,1219}. In comparison, plasmid DNA encoding for these components usually led to comparatively lower efficiencies or poorer tolerance in these cell types²²¹. Also of note, electroporation-mediated co-delivery of RNPs and a single-stranded oligonucleotide DNA template (HDR template) with 90

nucleotide homology arms mediated up to 20% knock-in in primary human T cells²¹⁹, obviating the need to express DNA template from plasmids or viral vectors.

Electroporation for Genome Editing of Stem Cells: iPSCs, HSCs and embryonic stem cells hold potential for regenerative medicine as a source of autologous cells and tissues for patients. By introducing genome-editing molecules by intracellular delivery, stem cells can be prepared for gene therapy (Figure 28E). Using nucleofection, Kim et al. were among the first to determine the advantages of RNP delivery versus plasmid transfection by observing higher site-specific editing rates with reduced off-target mutations in stem cells²¹⁸. They reported that RNP delivery is less stressful to human embryonic stem cells, producing at least twofold more colonies than plasmid transfection strategies²¹⁸. In keeping with this notion, recent CRISPR protocols for implementation in human stem cells and primary cells indicate a preference for Nucleofection of Cas9-sgRNA RNPs over plasmids¹⁵⁶. Furthermore, Neon capillary-based electroporation was used to introduce CRISPR-Cas9 nucleases via plasmids and/or RNPs to correct disease-causing mutations in patient-derived iPSCs⁴⁰. This strategy mediated functional correction of large factor VIII gene chromosomal inversions in patient cells, a mutation that underlies hemophilia A. Endothelial cells derived from these iPSCs were competent in rescuing factor VIII deficiency in an otherwise lethal mouse phenotype of hemophilia. Thus, direct intracellular delivery of genome editing molecules takes us closer to the long-standing goal of exploiting patient-derived autologously sourced iPSCs for therapeutic genome editing before re-implantation³⁶.

Electroporation Summary: Electroporation can deliver a vast range of molecular cargo to a wide variety of cell types with precise temporal control. With conventional electroporation the pulse parameters (field strength, pulse duration, pulse number, frequency) are flexible, therefore the same piece of hardware can be programmed to address a large number of scenarios. Parameters can be manipulated to focus the membrane-perturbing effects on different regions of the cell, such as certain parts of the plasma membrane or membranes of intracellular organelles (Figure 22). Additionally, the dual mechanisms of pore formation and electrophoretic propulsion of cargo may be beneficial for delivery of charged cargos, such as plasmid DNA or mRNA (Figure 23).

However, electroporation has a number of challenges, especially cell death. Indeed, the window for effective treatment can be quite narrow for electroporation, especially in primary cells. Detrimental effects of electroporation can be attributed to electrochemical phenomena at the electrodes including Joule heating, pH waves, bubble formation, corrosion, and contamination of the solution. Other potential issues include electric field-based perturbation of native proteins, scrambling of lipid membranes, generation of ROS, and damage of cargo molecules. Technical innovations featuring different electrode designs or microfluidic and nanochannel designs have been developed to overcome some of these issues (Figure 27), but they have not as yet superseded the basic cuvette-style electroporation, which remains the most widely used platform for common use. Fundamentally, it is not well understood how cell structure, cytoskeleton, membrane proteins, domain phases, and membrane reservoirs influence electroporation in live cells, making it difficult to decipher critical molecular

events. Additionally, the intrinsic pore-formation mechanisms bias electroporation toward the formation of numerous small pores, somewhat limiting the delivery of large cargoes.

The challenges of current electroporation techniques notwithstanding, for many applications the benefits outweigh the weaknesses. Consequently, it has become the most widely used membrane disruption-based intracellular delivery approach. Electroporation has shown promise for treatment of a wide variety of patient derived cells and stem cells, with even the most basic electroporation platforms finding use among *in vitro* and *ex vivo* medical and industrial applications, from biomanufacture and clinical trials of cancer immunotherapy to *ex vivo* cell-based gene therapy and regenerative medicine.

6.3 Thermal Membrane Disruption

Membrane formation, dynamics, and properties are temperature-dependent. At sufficiently high temperatures, lipid bilayers will dissociate due to kinetic energy of the constituent molecules being greater than the hydrophobic forces holding phospholipid tails together. The thermodynamic considerations of lipid bilayer behavior dictate that temperature is key in determining the energy required for a given membrane disruption event. The key role of temperature has been emphasized in the electroporation literature, for example, where theory posits that electric potential differences across membranes can tilt the energy landscape of stochastic thermally-driven defect formation³⁸⁸. The implications of temperature must be fully considered in any membrane disruption event. This applies both to the physical properties of lipid membranes and the active response of the cell.

Membrane permeability is known to increase during thermal phase transitions^{262,1249,1250}. Both magnitude and rate of temperature changes influence the molecular rearrangements in membrane domains that are linked to the stochastic formation of defects¹²⁵¹. Close to phase transitions, ion channel-like events are predicted, even in the complete absence of proteins¹²⁵⁰. The occurrence of purely lipid ion channels depends on temperature, hydrostatic pressure, lateral pressure, voltage, pH, and ion concentrations. Such pore formation is expected to be especially probable adjacent to domain interfaces and protein clusters.

Strategies for permeabilizing cells by thermal means include: 1) cycling cells through a cooling-heating cycle, which may or may not involve freezing; 2) heating cells to supraphysiological temperatures, and 3) transient intense heating of a small part of the cell. The literature includes examples of each of these approaches, which will be discussed here in this section. Overall though, thermal methods of membrane perturbation have not been widely employed with animal cells, despite being universal and obvious. This can probably be attributed to challenges in spatiotemporal control of temperature exposure and concerns related to off-target damage. In future there exists an opportunity to address these challenges with emerging lab on chip, microfluidic, optical, and nanotechnological systems⁵⁸.

Thermal Shock of Competent Bacteria—In bacteria, thermal shock has been used for decades to transfect “competent” bacteria with DNA plasmids. The method was described in early papers from the 1980s where agents such as divalent cations (typically in the form of CaCl₂) and dimethyl sulfoxide (DMSO) were added to make *E. Coli* amenable or

“competent” to DNA transfection. Subsequently, the bacteria undergo transient incubation at 0 °C, a brief pulse to 37–42 °C, and subsequent return to normal growth conditions where the genes of interest are expressed^{1252,1253}. Multiple cycles are sometimes conducted to boost efficiency. Mechanistic studies suggest that phase transitions of membrane lipids cause damage to the outer membrane, and are necessary for DNA entry^{1254,1255}. Some data indicates that cold shock may not need to go down to 0 °C, as the rate and magnitude of temperature changes would be more critical than specific temperature extremes¹²⁵⁴. However, more recent reports claim that a brief freeze in liquid nitrogen for 20 seconds was found to increase the efficiency of freeze-thaw transfection, even obviating the need for standard pre-treatment steps normally employed to make bacteria competent¹²⁵⁶. Interestingly, microwave irradiation of frozen bacteria/DNA samples was also found to mediate DNA transfection¹²⁵⁶. Finally, microfluidic reactors have been employed for temperature shock transfection of bacteria¹²⁵⁷. The advantages include fewer materials, smaller sample volume, and increased precision compared to conventional bulk procedures¹²⁵⁷.

Freeze-Thaw & Other Temperature Cycling Strategies—Apart from bacteria, rapid freeze-thaw procedures have also been demonstrated to facilitate exchange between intracellular and extracellular solutions when conducted with animal cell membranes (Figure 29A). In 1989 this was shown with synaptosomes, which are vesicular sacs reconstituted from synaptic terminal membranes by mild homogenization of nervous tissue¹²⁵⁸. In the reported procedure rat brain synaptosomes were frozen and thawed in the presence of 5% DMSO¹²⁵⁸. Impermeant proteins, inhibitors and metabolites were successfully introduced to study neural signaling processes¹²⁵⁸. An updated ‘cryoloading’ procedure was reported by Nath et al. where molecules of at least 150 kDa were successfully delivered into chick synaptosomes¹²⁵⁹. After recovery ~80% of the synaptosomes were properly functional and capable of recycling synaptic vesicles¹²⁵⁹.

Intracellular delivery by cooling-heating cycles has rarely been attempted in animal cells, probably due to the delicate and complex nature of cell recovery and growth from the frozen state. In one of the few cases where it was tested, trehalose (~0.34 kDa) was loaded into suspensions of adult islet cells by cooling them through their membrane phase transition²⁶². Under conditions where cells were cooled at a rate of 1 °C per minute, permeability to trehalose was greatest around the region 0–5 °C²⁶². Loaded trehalose exhibited cryoprotectant properties, and was able to significantly increase cell survival and insulin production of islet cells. Building on this approach Puhlev et al compared intracellular delivery via cooling in suspension and adherent fibroblasts. In their procedure cells were exposed to 50 mM trehalose for 5 minutes on ice, followed by 10 minutes at 37 °C⁹⁹⁸. As with the previous paper, maximal delivery was estimated to occur below 5 °C, and was more efficient in suspended cells versus their adherent counterparts. A similar strategy was also tested by the Mehmet Toner lab²⁶⁴. Temperature cycling from 0 to 39 °C was able to load trehalose, a small molecular weight cryoprotectant, into a target cell population of suspended rat hepatocytes without compromising cell viability²⁶⁴. Using an extracellular concentration of 0.4 M in diluted culture medium, 1 hour of temperature oscillations conducted every 10 minutes produced an average cytoplasmic concentration of 0.13 M (~3% of extracellular

concentration) as detected by high-performance liquid chromatography (HPLC)²⁶⁴. Extended periods of incubation at 39 °C increased loading efficiency but came with the caveat of harming cell survival.

Supraphysiological Heating—As temperature moves above 37 °C, the probability of membrane defects arising increases. In experiments on mammalian cells, Bischof et al. exposed fibroblasts and muscle cells to temperatures ranging from 37 to 70 °C and monitored membrane integrity in real time. Permeability was assessed by tracking the leakage of calcein (0.62 kDa) with timelapse fluorescence microscopy. Slow leakage, which starts above 40 °C, was found to be a function of both temperature and time. Cells held at 45 °C were completely depleted of calcein within 25 minutes. This corroborates well with other data indicating cells must work harder to maintain their relatively high potassium concentrations during treatments at 43 °C¹²⁶⁰. In Bischof et al.'s experiment, leakage takes slightly less than 10 minutes at 50 °C. Above 55 °C, almost 50% of calcein leaks out of the cell within a minute and efflux is fully complete by 2 minutes. To explain the increase in permeability, contributions from both protein denaturation and increased kinetic diffusion of lipid molecules were suggested. Other studies in red blood cells indicate that thermally-induced membrane disruption occurs at about 60 °C and protein denaturation temperature depends on the specific protein^{1261,1262}. Interestingly, addition of membrane-healing poloxomers is able to rescue viability of thermally challenged cells, indicating that breakdown of membrane integrity is a key aspect of immediate cell toxicity upon heating¹²⁶³. For intracellular delivery purposes, supraphysiological temperatures have rarely been employed (Figure 29B), probably due to concerns of non-specific cell damage and toxicity as exemplified by the trehalose experiments discussed above²⁶⁴. Baseline temperature is a critical parameter for any delivery protocol, however, and there have been a few rare reports of supraphysiological regimes. For example, 43 °C was found employed in one study to make cell membranes more susceptible to fluid shear from laser-induced stress waves¹²⁶⁴.

Thermal Inkjet Printers—Thermal inkjet printers that disperse small volumes of fluid have been successfully deployed for mammalian cell gene transfection and intracellular delivery^{1265,1266}. By replacing standard ink with media and cells, these printers not only perform intracellular delivery but can additionally pattern cells over a substrate. In thermal inkjet printers, a metal plate is heated at one side of the nozzle, which creates small air bubbles that collapse to provide pressure pulses to eject tiny drops of fluid. Over several microseconds the plate temperature may transiently rise to 300 °C. It is not known whether membrane permeabilization is obtained by fluid shear forces or transient thermal disruption at the nozzle. In the studies performed so far Xu et al. achieved transfection efficiencies of 10% with GFP plasmids in porcine aortic endothelial cells at 90% cell viability¹²⁶⁵ while Cue and Boland obtained above 30% transfection efficiency in CHO cells with similar viabilities¹²⁶⁶. Further mechanistic insights may improve the efficiency of the approach. A potential bonus of thermal inkjet printing is the ability to array cells into specific geometries and perform intracellular delivery in a single step, thereby facilitating the possibility of *in vitro* tissue engineering¹²⁶⁷. The results with thermal inkjet printers point to an opportunity

for future studies with microfluidic systems, where it should be possible to gain spatiotemporal control over temperature exposure through microfluidics (Figure 29C).

Laser-Particle Interactions—As discussed in the sections on fluid shear, laser irradiance of an absorbent object in an aqueous environment can produce a variety of effects including cavitation, plasma production, chemical reactions, and heat^{1268–1270}. Although it is sometimes difficult to be sure of the mechanisms, we report here on studies that claim to disrupt membranes by laser-mediated temperature changes. In most of cases nanoparticles are used as nucleation sites for intense local heating (Figure 29D). Umebayashi et al. showed that laser irradiation of unbound latex particles dispersed in solution leads to the uptake of impermeant dye molecules¹²⁷¹. The mechanism was proposed to be through thermal perturbation at the particle-membrane interface, pore formation, and subsequent diffusive influx of extracellular molecules¹²⁷¹. A similar thermal delivery concept was shown by Yao et al. with selectively bound antibody-conjugated gold nanoparticles, featuring a strong correlation between nanoparticle size and heating intensity¹²⁷². Follow up studies investigated the effects of laser pulsing parameters (pulse duration, irradiant exposure, and irradiation mode) and found conditions where more than 50% of the treated suspension cells could take up a labeled 150-kDa IgG antibody¹²⁷³. In other studies, cancer cells were targeted by folate-conjugated gold nanorods. Under femto-second laser irradiation the nanorods were shown to thermally compromise the membranes as evidenced by flux of dye molecules across the plasma membrane¹²⁷⁴. Gu et al. reported using low power continuous wave near-infrared (NIR) lasers to thermally excite inert crystalline magnetic carbon nanoparticles for delivery of impermeable dyes and plasmids¹²⁷⁵. Gold nanoparticles have also been packed into a dense surface layer where tens of second of infrared laser irradiation heats the underside of cells to trigger permeabilization and delivery of dyes, dextrans and plasmids¹²⁷⁶.

Lasers-Membrane Interactions—In the absence of absorbing structures, lasers alone can be harnessed for local heating of cell membranes within the focal region (Figure 29E). The mechanisms of laser interaction with lipid membranes are complex, usually being underpinned by mixture of thermal, chemical and mechanical components^{1268–1270}. Hence, only under a narrow range of conditions are lasers thought to produce purely thermal membrane disruption. One example was published by Palumbo et al. where 0.25 seconds exposure to a 488 nm continuous wave argon laser of spot size 5–8 μm was focused onto the surface¹²⁷⁷. Their report indicated that the poration mechanism was via heating, however other effects cannot be ruled out. More information on laser optoporation is presented the next section of this review.

6.4 Optical Membrane Disruption (Optoporation)

A wide variety of laser procedures have been implemented to selectively perform nanosurgery on cells and their components¹²⁷⁸. Targets include individual chromosomes, organelles, mitochondria, cytoskeletal structures, and lipid membranes. Optoporation is the permeabilization of lipid membranes by high intensity light. In some studies it has also been referred to by terms such as photoporation, optoinjection, laserfection, and optical transfection^{446,1279,1280}. The aim of optoporation is to permeabilize the plasma membrane to

cargo while leaving other cellular structures intact, thus preserving the health of the cell to the maximum extent possible. In this review, we define optoporation as membrane disruption arising from direct interaction of laser focal region with the plasma membrane, and not absorption of laser energy by an intermediate structure such as nanoparticle or metal surface. Those strategies permeabilize membranes by secondary effects such as fluid shear and chemical breakdown, and are covered in the respective sections dealing with those phenomena.

Optoporation – Pioneering Studies—DNA transfection by laser optoporation was first reported in 1984¹²⁸¹. Nanosecond pulses of an Nd:YAG UV laser (wavelength 355 nm) at an energy of 1 mJ with spot size of ~0.5 μm were focused on the surface of adherent NRK cells. A single pulse of 5–10 ns was sufficient to open up a hole several micron wide and promote the influx of DNA plasmids from an extracellular concentration of 10 $\mu\text{g}\cdot\text{ml}^{-1}$ before closure of the wound. When manually targeting the laser pulse above the nucleus, 10% transfection efficiency was achieved while random scanning of the laser over the substrate resulted in only 0.6% chance of success¹²⁸². Laser transfection with a similar laser type but different cell types was repeated several years later, this time establishing that a small percentage of target cells stably integrated the plasmid into their genome¹²⁸³. Addition of dyes to change absorption properties of the media is another variable that was examined, with the presence of standard cell culture media additive phenol red shown to decrease the laser power needed for optoporation¹²⁷⁷. A 488 nm continuous wave argon laser with nominal power of 2 W and spot size of 5–8 μm was focused onto the surface of NIH 3T3 fibroblasts with exposure time of 0.25 seconds to puncture the plasma membrane¹²⁷⁷. After conducting the procedure in the presence of 10 $\mu\text{g}\cdot\text{ml}^{-1}$ plasmid DNA, repair of a single large hole in the membrane took 1–2 minutes, followed by detectable gene expression after 2 hours¹²⁷⁷. Plasma membrane disruption mechanisms were reported to be thermal and laser exposures of greater than 0.5 seconds were found to permanently damage cells¹²⁷⁷.

The next major breakthrough in optoporation occurred in 2002, with the implementation of femtosecond-pulsed lasers¹²⁸⁴. Tirlapur and König used a high-intensity, near-infrared (wavelength 800 nm), femtosecond-pulsed laser beam from a 80 MHz titanium–sapphire laser, with a mean power of 50–100 mW. The laser was tightly focused to a sub-femtolitre focal volume just above the cell membrane. Under 16 ms exposure time, CHO and Ptk2 cells were transfected with GFP using only 0.4 $\mu\text{g}\cdot\text{ml}^{-1}$ DNA plasmid in solution. Unprecedented high transfection efficiency and viability were reported, with both coming in at close to 100%. A prime limitation of the procedure, however, was the need to manually refocus on each cell, yielding a throughput of only a few cells per minute. Since this landmark report 1) femtosecond lasers gained prominence as the most effective pulsing strategy for optoporation, and 2) the number of optoporation publications has increased dramatically. In terms of cargo delivery, the field has placed particular focus on delivery of small molecule dyes for mechanistic studies and DNA transfection to demonstrate applications. Indeed, laser optoporation have achieved successful delivery of plasmid DNA^{441,443,444,1277,1279–1305}, mRNA^{121,1300}, siRNA^{1280,1290,1299}, antisense morpholinos¹³⁰⁰, peptides^{446,1306}, proteins^{1280,1290}, dextrans^{1280,1290,1296,1300,1307,1308}, dyes^{121,440–444,446,1280,1287,1288,1290,1292,1293,1295,1301,1304,1308–1313}, sucrose⁴⁴⁵, molecular

beacons¹³¹⁴, Ions^{1280,1290,1315}, semiconductor nanocrystals^{1280,1290}, gold nanoparticles¹³¹⁶, quantum dots¹³¹⁷, and ~1 μm polystyrene beads¹³¹⁸. Moreover, many of these studies have sought to compare the mechanisms of various laser treatment regimes in order to optimize delivery efficiency and minimize off-target damage.

Mechanisms of Optoporation—The mechanisms of laser-mediated disruption are complex, involving combinations of mechanical, thermal, and chemical effects. Possibilities include burning/evaporation, thermoelastic mechanical stress, generation of low-density free-electron plasma and reactive oxygen species (ROS), and effects beyond the focal region, such as shock wave emission and growth/collapse of cavitation bubbles, which themselves produce fluid shear stress, extreme heat, and sonochemical phenomena^{1268–1270,1278} (Figure 30). The relative dominance of these phenomena depends on factors such as wavelength, frequency, whether the source is continuous wave or pulsed, laser power, exposure time, spot size, and absorbance properties of focal region. For example, membrane wounding from continuous wave irradiation are thought to arise primarily from local heating, which intensifies as a function of exposure time. Nanosecond pulsed lasers have been suggested to produce a combination of heating, bubble formation, and thermoelastic or di-electric mechanical stresses to damage the membrane. Femtosecond laser mechanisms appear tunable based on irradiance strength, pulse duration, and frequency. Mechanisms range from almost purely chemical degradation to combinations of thermal and mechanical. In cases where laser energy is transduced into fluid shear that travels far beyond the focal region, such as cavitation or shock waves, the mechanisms of membrane damage are not strictly optoporation and these scenarios are covered elsewhere in the section on fluid shear (6.1.2). Alternatively, if transmission of thermal energy from an absorbing object in immediate contact is the mechanism of membrane disruption, these accounts are covered in the thermal section (6.3).

Femtosecond Optoporation—Most recent work favors the use of a laser regime characterized by wavelengths >700 nm administered at high frequencies (\sim MHz range) and femtosecond pulse timings with a cumulative exposure of milliseconds or less¹²⁶⁸. For example, a typical protocol might involve 5 ms of exposure to a cycle of 100 fs pulses with gaps of 10 ns (\sim 100 MHz frequency) for cooldown. When operating at wavelengths >700 nm the mechanisms are related to multi-photon effects inherently concentrated within the focal region, thus offering increased precision and high spatial resolution¹²⁶⁸. NIR and IR wavelengths also have the advantage of being less toxic to cells, as UV and blue light in particular are notorious for causing damage to DNA and other cellular structures. By using extremely short femtosecond pulses, absorbing material in focal region does not have sufficient time to transmit heat to adjacent regions. This enables extremely high-powered lasers to be deployed while avoiding excessive heating of cells. In such a scenario the resultant membrane disruption mechanisms have been reported to be due to chemical effects, such as breakdown of the lipid membrane by low-energy plasma^{1268–1270,1278} (Figure 30C). In other cases femtosecond pulsing generates a well-controlled cavitation bubble originating within the focal region, the presence of which can destroy the membrane (Figure 30B). In many of these studies, distinctions between exact mechanisms are difficult to determine, and could be multifactorial.

A number of elegant studies have been performed with femtosecond pulsed lasers. For example, in optical setups that combine laser tweezing and optoporation, optical tweezers may be used to guide a microbead (~1 μm) or nanoparticle through a hole formed by the laser, thus delivering large cargo^{1316,1318}. In studies with frog embryos quantum dots were delivered by NIR femtosecond lasers. Neither the quantum dots nor optoporation retarded the ability of these embryos to grow into tadpoles. In another case, cargo was introduced into distinct regions of adherent primary rat neurons to assess localization-dependent biological functions¹²¹. mRNA-mediated expression of the transcription factor Elk-1 was found to produce different responses whether delivered to the soma or axon of the neurons¹²¹. This optoporation protocol involved an 840 nm titanium-sapphire laser delivering 100 fs pulses at a repetition rate of 80 MHz for 1 – 5 ms at a power of 30 mW¹²¹. Other studies have quantitatively measured the loading efficiency of femtosecond optoporation, and found that targeted cells can incorporate up to 40% of the concentration of extracellular molecules before resealing⁴⁴³. Furthermore, sub-20 femtosecond pulses at MHz frequencies with sub-millisecond exposure times have been demonstrated for the effective transfection of human primary pancreatic and salivary gland stem cells¹²⁹⁵.

Towards High Throughput & More User-Friendly Optoporation—A major rate-limiting step for optoporation is the reliance on precise positioning of the laser focal spot and alignment with target membranes^{1269,1284}. A misfocus of as little as 3 μm results in greater than 50 percent reduction in membrane disruption efficiency¹²⁹¹. One strategy is the implementation of a “bessel beam”, where the focal region is stretched into a rod of light over 100 μm in length and a few microns wide¹²⁹¹. Bessel beam setups have been combined with microfluidics for hydrodynamic flow focusing to reach throughputs of tens of cells per second¹³¹². However, cell viability and delivery efficiency were substantially less than standard femtosecond optoporation¹³¹². Whether or not bessel beams cause off-target damage to non-membranous cellular structures is unknown¹²⁶⁸.

Other attempts to increase throughput of optoporation include a user-friendly “point and click” touchscreen software-based approach¹³⁰². The authors claimed throughputs of up to 100 cells per minute in adherent neurons¹³⁰². An extension of this strategy relies on automated image analysis of cell morphology, centering of target regions to the laser focus, and execution of a femtosecond laser illumination protocol¹³⁰⁴. With this system, software-controlled meandering of the sample stage allows adherent cells in a typical cell culture dish to be automatically targeted at a rate around 10,000 cells per hour¹³⁰⁴. If optoporation is to be adopted by users outside of specialized labs, further efforts will need to address the challenge of how to precisely focus the laser spot onto thousands of cells for rapid treatment. Other issues that need to be addressed are portability, instrument complexity, and high cost.

6.5 Biochemical Membrane Disruption

A range of chemical effects and biochemical agents can be used to disrupt cell membranes. These include synthetic detergents, surface-active agents (surfactants), organic solvents, and oxidizing agents to naturally secreted proteins and metabolites from a diversity of organisms. For example, organic solvents have been used for decades as penetration enhancers for transdermal delivery by fluidizing, destabilizing, or extracting components

from lipid bilayers¹³¹⁹. Since the dawn of life, living organisms have evolved a range of potent molecules to attack and disrupt the membrane integrity of competing lifeforms. Pore-forming proteins (PFPs), which are produced by humans, animals, plants, fungi, protists, and bacteria for self-defense, are one such example³⁶⁹. Many plants synthesize and secrete metabolites like saponins to serve as an innate immune barrier to disrupt the membranes of invading microbes or other threatening organisms¹³²⁰. The natural compounds tend to be relatively specific, relying on unique characteristics of the target membrane for their action, such as composition of membrane lipids and presence of external receptors. Several artificially produced detergents and solvents also exhibit a useful ability to disrupt plasma membranes in a relatively controlled manner. Furthermore, emerging concepts from nanotechnology, such as near-field ionizing plasmas, present opportunities to confine chemical destabilization phenomena to small membrane patches for short durations. This section will cover the artificial and natural biochemical permeabilization strategies that have demonstrated or theoretical potential for intracellular delivery applications.

6.5.1 Organic Solvents & Penetration Enhancers

DMSO: Organic solvents are low-molecular weight compounds that can perturb bilayer structures by burying their hydrophobic residues into the membrane. A classic example of a membrane-active organic solvent is dimethyl sulfoxide (DMSO), often used as a penetration enhancer to increase the permeability of drugs and other small molecules^{253,1321}. DMSO is amphiphilic, containing one hydrophilic sulfoxide group and two hydrophobic methyl groups. It is known to promote permeation of both hydrophilic²⁵³ and hydrophobic¹³²¹ species across membranes. DMSO's penetration enhancing effect can be attributed to two mechanisms. First, its ability to increase the solubility of amphiphilic small molecules, and second, because of increased incidence of membrane defects that allow passage of these molecules. Experiments with phospholipid vesicles have found leakage of carboxyfluorescein (~376 Da) at concentrations of DMSO >10%¹³²². For a given DMSO concentration, leakage also increases as a function of temperature¹³²².

Simulations have been used to investigate the molecular mechanisms of membrane disruption by DMSO. Gurtovenko et al. showed that at low concentrations, DMSO causes membrane thinning and increases fluidity of the membrane's hydrophobic core¹³²³. DMSO molecules are seen to penetrate into the bilayer, both expanding the distance between the lipids and reducing the thickness of the bilayer (Figure 31A). Consequently, the lipid-water interface becomes more prone to structural defects, especially due to thermal fluctuations. At higher DMSO concentrations water molecules enter the membrane interior via DMSO-mediated structural defects. As the number of penetrating water molecules increases, a significant re-orientation of lipid headgroups toward the membrane interior is required to minimize the free-energy of the system, resulting in the formation of hydrophilic channels spanning the membrane bilayer³⁷⁹. The emergence of hydrophilic channels occurs spontaneously between 10–20% molar concentration¹³²³. The addition of sterols (i.e. cholesterol) can provide stabilization to the membrane and thus increase the DMSO concentration required for pore formation¹³²⁴.

Ethanol & Other Alcohols: In contrast to DMSO, ethanol's hydrophobicity is rather limited as a short-chain alcohol. Rather than embed deep, ethanol molecules tend to remain at the water-lipid interface forming hydrogen bonds with hydrophilic lipid headgroups^{1326,1327}. Ethanol has a disordering effect on lipid hydrocarbon tails, increasing fluidity of the membrane and reducing rigidity. Simulations confirm that compromising the water-lipid interface induces ingress of water pockets into the membrane as inverse micelles, rather than pores that span the whole membrane (Figure 31B). The bilayer structure is partly destroyed due to lipid desorption¹³²⁵. Both experimental and simulation studies have shown that the bilayer structure cannot be maintained beyond an ethanol concentration around 12% molar or 30% v/v concentration. Correspondingly stronger results can be expected with longer chain alcohols, such as propanol, butanol, pentanol, as the concentration required for defect formation is inversely proportional to hydrocarbon chain length¹³²⁸. As an example, significant membrane defects have been reported in membranes exposed to only 1% butanol¹³²⁹. One case where ethanol is used for intracellular delivery purposes was reported by O'Dea et al. Ethanol sprayed with an atomizer was used to reversibly permeabilize cells for intracellular delivery of proteins, mRNA, and plasmids¹³³⁰.

Organic Solvents & Penetration Enhancers Summary: Although widely used for permeabilizing fixed cells¹³³¹ and increasing the permeability of small molecules²⁵³, organic solvents and other low molecular weight penetration enhancers have generally not been used as the sole membrane disruption agents to deliver cargo molecules. This is probably due to their non-specific nature and lack of spatiotemporal control over the membrane disruption process. They may be useful as non-specific and relatively inert adjuvants to optimize other membrane permeabilization strategies such as electroporation¹³³².

6.5.2 Detergents—Detergents are water-soluble surfactants capable of solubilizing phospholipids found in biological membranes. Solubilization refers to the dissolution of the bilayer structure by sequestration into detergent-lipid micelles^{402,403}. For the purposes of intracellular delivery, complete solubilization of membranes is lethal and undesirable, thus detergents must be used at intermediate concentrations for limited durations to yield optimal levels of permeabilization. Although the mechanisms of detergent solubilization of biological membranes have been discussed for decades^{402,1333–1335}, the milder intermediate regime of non-lethal permeabilization is less well understood. As well as intracellular delivery applications, motivations to investigate this regime include insight into the action of membrane-perturbing secondary metabolites and characterizing new candidates for antimicrobials.

Membrane Disruption by Detergents That Flip Flop: Owing to their amphiphilic properties, detergent molecules integrate into lipid membranes. Most detergents are cone-shaped, in that the head group of the detergent is disproportionately larger than the hydrophobic chains. They generally work by inserting into lipid bilayers and distorting their structure. Several mechanisms have been suggested for detergent-mediated permeabilization of lipid bilayers depending on the type of detergent⁴⁰². Those capable of flip-flopping to the

inner leaflet will distribute throughout both leaflets of the bilayer (Figure 32). Because of the cone-shaped nature of detergents, the structure of the monolayer wants to assume a degree of convex intrinsic curvature. However, this is impossible if the monolayer is part of a bilayer, because it competes with the opposite spontaneous curvature of the other leaflet as both are coupled with each other. Instead, the monolayers are 'bent straight' by an elastic deformation giving rise to a monolayer curvature strain. The major structural consequence of this curvature strain is a disordering of the hydrophobic chains. In turn, the membrane becomes thinner and more flexible. Monolayer curvature strain can be partially relaxed by the sequestering of surfactants into highly curved rims covering the hydrophobic edges of toroidal pores or leaks⁴⁰². Over time, thermal fluctuations will give rise to such events. Thus, reduction of the line tension by detergents may massively increase the lifetimes of induced pores or even stabilize them indefinitely. Above a critical surfactant concentration, leaks appear spontaneously so that permeabilization becomes effectively persistent⁴⁰².

Membrane Disruption by Detergents That Do Not Flip Flop: Detergents that embed into the membrane but cannot flip flop expand the bilayer asymmetrically (Figure 33)^{402,403}. If the bilayer is unable to bend to assume its spontaneous bilayer curvature, it develops a bilayer curvature strain by compressing the molecules in the overpopulated leaflet and/or expanding those in the underpopulated leaflet. Bilayer curvature eventually leads to mechanical failure of the membrane because the outer monolayer forms mixed micellar structures that bud off from the membrane. Shedding of these micelles into the aqueous solution results in emergence of defects and subsequent permeabilization⁴⁰³. These disruptions can have several effects. First, relaxation of the curvature strain allows the membrane leaflets to anneal, and second, they permit the passage of detergent molecules inside the cell to access the inner leaflet, thereby promoting further infiltration of the membrane by mechanisms akin to detergents that flip flop (Figure 32).

Membrane Disruption by Detergents That Do Not Embed: A third possibility is that collision of detergent micelles with the cell membranes recruits lipids units into the micelles, thereby generating defects in the membrane (Figure 34)^{421,1336}. There is little theory to support this third possibility, however it should be mentioned as a possibility. In to first achieve micelles, the detergent will need to be at concentrations above the critical micelle concentration (CMC). This will only be a realistic scenario in the case of detergents that don't embed so readily. Thus, integration of individual detergent molecules into the target membrane may not be necessary to cause defect generation and subsequent permeabilization.

Relationship Between Strain and Emergence of Defects: Most of the detergents used to permeabilize biological membranes integrate into membranes⁴⁰². In these scenarios a common factor is that curvature-driven distortion and disordering of membranes leads to perturbation of the bilayer structure and subsequent permeabilization. As discussed, the key property of a micelle-forming amphiphile inserting into a lipid bilayer is its preference for a locally curved interface that is in conflict with the (on average) planar topology of a bilayer. Indeed, strongly curvature-active detergents are known to be far more effective in membrane permeabilization⁴⁰². When local concentrations of detergents are high enough (perhaps due

to random fluctuations), defects may emerge in the form of spontaneous pores or shedding of micelles due to local mechanical distortions.

A comprehensive study from Nazari et al. compared the membrane perturbing effects of a number of different detergents and surfactants on lipid vesicles, categorizing them into homogeneously and heterogeneously perturbing surfactants¹³³⁷. In the homogeneous category were typical synthetic detergents, such as C₁₂EO₈, octyl glucoside, sodium dodecyl sulfate (SDS), and lauryl maltoside, which destroy the membrane through homogeneous disordering when a critical curvature stress is reached. In contrast, the heterogeneous category the fungicidal lipopeptides surfactin, fengycin, and iturin, as well as digitonin, CHAPS, and lysophosphatidylcholine perturb membranes without substantial overall disordering. Rather they disrupt membranes locally in surfactant-rich defect structures. Nazari et al. proposed that such heterogeneous perturbation mechanisms may account for the superior activity, selectivity, and mutual synergism of antimicrobial biosurfactants, such as lipopeptides and saponins, to efficiently permeabilize target cell membranes in discrete loci at minimal concentrations¹³³⁷.

Detergent Permeabilization of Live Cells: A further consideration influencing detergent-mediated membrane permeabilization is the composition of the target membrane of living cells. The permeabilizing activity of certain antimicrobial peptides and surfactants is strongly modulated by cholesterol, proteins and other raft components⁴⁰². Due to the heterogeneous and dynamic nature of living cell membranes, it has been a challenge to predict how detergents will permeabilize cells. One study by Vaidyanathan et al. used patch clamp to analyze permeabilization behavior of detergents as a function of concentration¹³³⁸. They observed that anionic SDS, cationic cetyltrimethylammonium bromide (CTAB), and cationic, fluorescent octadecyl rhodamine B (ORB) increased the membrane permeability of cells substantially within a second of exposure. It was reported that SDS 0.2 mM and CTAB and ORB 1 mM induced cell membrane permeability without causing acute or permanent toxicity. Thus, careful titration of the detergent concentrations enabled the identification of conditions from which cells could recover from.

In another study of detergent permeabilization in live cells, Koley and Bard used electrochemical microscopy to monitor the permeability of HeLa cells to the hydrophilic molecule ferrocyanide in the presence of increasing concentrations of the nonionic detergent triton X-100¹³³⁹. No effect on permeability was seen at triton X-100 concentrations of 0.15 mM for up to 1 hour. At 0.17 mM initial permeabilization was observed followed by recovery of cell viability. From 0.19 mM, which approaches the CMC, rapid irreversible permeabilization and cell death resulted. Thus the effective concentration window of triton-X-100 on live cells is narrow under the tested set of experimental conditions. The above results underscore the importance of conducting systematic permeabilization studies in live cells.

Saponins: Saponins are steroid and triterpenoid glycosides produced by plants and certain marine organisms as secondary metabolites in response to environmental stimuli^{1320,1340}. By perturbing the membranes of competing life forms, saponins constitute a form of innate immune system to poison microbes, parasites, insects, and herbivores^{1320,1341}. The detergent

phenomena of saponins originates from their amphiphilic properties, featuring a lipophilic sapogenin part (usually a triterpene or steroid group) and a hydrophilic glycoside moiety. A wide range of applications for saponins relating to their membrane perturbing activity have been proposed. They include augmenting the penetration of drugs and cytotoxic agents to cancer cells, vaccine adjuvants, or deployment as microbials and pest control agents^{1342–1344}.

For applications with mammalian cells, studies usually employ generic saponins or pure digitonin. Generic saponins are commercially available cocktails typified by a sapogenin content >10% while digitonin is a prototype member of the saponin family isolated from the foxglove plant *Digitalis purpurea*. Other less-studied saponins that have been reported to disrupt membranes include α -tomatine, Glycyrrhizin, α -Chaconine, and α -Hederin¹³³⁶. Saponins in general, and digitonin specifically, have been used with live cells for two main applications: 1) persistent permeabilization to produce “semi-intact cells” for real-time manipulation of cytoplasmic components, and 2) to transiently disrupt the plasma membrane for intracellular delivery. Early work emphasized the first of these two applications.

Characteristics & Mechanisms of Saponin-Induced Membrane Disruption: Saponins were characterized as membrane-perturbing agents in the scientific literature of the 1960s and 1970s^{903,1345}. Electron micrographs captured their membrane disrupting capabilities in reconstituted membranes, indicating arrays of holes around 8 nm¹³⁴⁵. Serial section electron microscopy of fixed hemolysing erythrocytes revealed lesions of 4 – 5 nm after saponin treatment⁹⁰³. Most cell permeabilization studies have employed saponins in the concentration range 10 – 1000 $\mu\text{g}\cdot\text{ml}^{-1}$, which represents ~8 – 800 μM . In this range, disruption sizes range from a few nanometers to a micron have been reported. Differences are probably related to variations in cell type, concentration, duration of exposure and other experimental conditions^{367,1346,1347}. The inconsistency of these reports may also stem from the variety of analysis techniques. For example, artifacts can occur during fixation of membranes for AFM and SEM imaging. Thus, our knowledge on saponin-based permeabilization and characteristics of holes formed may require revision with more current methods and stricter environmental conditions.

Most saponins preferentially interact with cholesterol- and hydroxysterol-rich membranes, a property that makes them relatively specific for the plasma membranes of animal cells. In this case the efficiency of their membrane perturbing effects are directly correlated with sterol content. Indeed, cholesterol-rich bilayers are thought to be about 20- to 100-fold more sensitive to saponins³⁷⁷. Hence, saponins can be exploited to target the plasma membrane while leaving those of cholesterol-poor organelles, such as the ER and mitochondria, largely unaffected^{367,543,1348}. Calcium stores within intracellular organelles are generally not eroded by the saponin concentrations that permeabilize plasma membranes⁵⁴¹.

How do saponins interact with cholesterol to disrupt membranes? Frenkel et al. conducted investigations into the mechanism using quantitative physical techniques in model membranes. Their measurements indicate that digitonin extracts cholesterol out of the bilayer core to form a surface complex, which then induces curvature and disordering of the

membrane¹³⁴⁹. The magnitude of these effects was directly proportional to the amount of cholesterol in the bilayer (Figure 35). Beyond digitonin, work has been done to explore a wider range of individual saponins for membrane permeabilization. In a recent study, a set of oleanane saponins (Glycyrrhizic acid, *Gypsophila*, *Saponaria* and *Quillaja* saponins) and digitonin were tested in live cells. These saponins showed variable permeabilizing effects on cellular membranes from 6 μM , as measured by an impedance-based plate reader in ECV-304 human urinary bladder carcinoma cells¹³⁵⁰. The results indicated that the molecular charge may be a relevant consideration in explaining the action of oleanane saponins. Further studies on α -hederin indicate that the critical micelle concentration (CMC) plays a key role in its mechanism. At concentrations lower than the CMC, α -hederin monomers bind to cholesterol and induce vesiculation and lateral phase separation^{1351,1352}. These effects are analogous to the action of detergents that do not flip flop, as depicted in figure 33. At concentrations higher than the CMC, α -hederin aggregates promote pore formation and the loss of membrane material by analogy to the scenario illustrated in figure 34. Thus, the self-aggregating properties and co-operative action of saponins may also be important for their effects. Most studies agree that the permeabilizing activity of saponins rely on the presence of cholesterol, from which it forms complexes to distort the membrane into non bilayer structures. As an exception to this rule, some bidesmosidic saponins, such as avicin D¹³⁵³, appear capable of porating cell membranes through detergent properties independent of cholesterol binding¹³³⁶.

Saponin-Mediated Permeabilization for Studies in Semi-Intact Cells: Detergent-permeabilized semi-intact cells have led to advances in several areas of biology, including decoding the rules governing nuclear import of proteins and DNA^{550,551}, studying mammalian protein synthesis and secretion machinery^{548,549}, and the analysis of functional mitochondria in muscle fibers, tissues, and cells *in situ*⁵⁵². The emergence of saponins for the production of semi-intact cells began around the early 1980s. In 1982 Wakasugi et al. used saponin or digitonin in the range 20 – 100 $\mu\text{g}\cdot\text{ml}^{-1}$ (~16 – 80 μM) to permeabilize acini from rat pancreases and probe the effect of ATP on intracellular calcium dynamics¹³⁵⁴. In another year later, the plasma membranes of isolated guinea pig hepatocytes were made permeable with 75 $\mu\text{g}\cdot\text{ml}^{-1}$ (~60 μM) saponin to study the ATP-dependent uptake of calcium into the endoplasmic reticulum⁵⁴¹. Upon saponin treatment cells were suspended in a medium resembling cytosol with an ATP-regenerating system consisting of ATP, creatine phosphate, and creatine phosphokinase. Dunn and Holz used 20 μM digitonin to permeabilize chromaffin cells, and this protocol became a popular system to study intracellular processes in this cell type^{542,1355}. Human platelets were also treated with saponins for the loading of the secondary messenger inositol 1,4,5-trisphosphate into the cytoplasm and studying of the metabolic signaling response¹³⁵⁶. Several groups reported that with optimal conditions, 50% or more of the cytoplasmic enzyme lactate dehydrogenase (~140 kDa) is able to remain inside cells for extended periods, indicating the possibility of maintaining a feasible balance between plasma membrane permeabilization and cell function in these experiments^{542,543,1357}. In most of these papers the plasma membrane resealing dynamics were not discussed. Thus, it is difficult to ascertain whether or not the cells were persistently permeabilized or whether they recovered due to plasma membrane repair.

Saponin-Mediated Permeabilization for Intracellular Delivery: An optimized protocol for peptide delivery into cardiac myocytes employed a 10 minute incubation at 4 °C with 50 $\mu\text{g}\cdot\text{ml}^{-1}$ (~40 μM) saponin⁴⁹⁷. Along with saponin, the permeabilization buffer was designed to mimic aspects of the intracellular environment by including high potassium, extracellular ATP to maintain energy stocks, and ascorbic acid as an antioxidant⁴⁹⁷. Cells were then returned to recovery conditions and the effect of inhibitory peptides was tested under optimal culture conditions. The authors reported efficient loading of peptides without loss of long-term viability. In another method, Miyamoto et al. used 7.5 $\mu\text{g}\cdot\text{ml}^{-1}$ (~6 μM) digitonin to induce reversible permeabilization of the plasma membrane in bovine, mouse, and porcine somatic cells¹³⁵⁸. By optimizing the procedure, high efficiency (~80%) loading of 70 kDa dextrans was achieved in bovine cumulus cells. Furthermore, this concept was used to introduce cytoplasmic extractions from *Xenopus laevis* eggs into several mammalian cell types for successful induction of nuclear reprogramming and activation of pluripotent genes¹³⁵⁸.

More recently, saponins have been exploited for the delivery of quantum dots and nanoparticles. Lukyanenko published a protocol for the delivery of nanoparticles up to 20 nm with a transient 30–60 second exposures to 0.01% saponin (10 $\mu\text{g}\cdot\text{ml}^{-1}$ or ~8 μM) in high potassium low calcium permeabilization buffer¹³⁵⁹. Depolymerization of cytoplasmic actin with cytochalasin D was reported to boost the efficiency nanoparticle penetration deep within the cell, as actin meshwork that underlies the plasma membrane may be considered another barrier to delivery¹³⁵⁹. Medepalli and co-workers demonstrated quantum dot loading into adherent H9C2 with a combination of 50 $\mu\text{g}\cdot\text{ml}^{-1}$ (~40 μM) saponin and 180 mOsm hypotonic media for 5 minutes at 4 °C²⁹⁰. Whether hypoosmotic shock produces a membrane tension to synergize with the membrane perturbing effect of saponin, or generate inward fluid flux to encourage delivery, remains to be determined²⁹⁰.

For intracellular analysis with antibodies, Jacob et al. developed a saponin-based permeabilization protocol to load immune cells with monoclonal antibodies for the detection of cytoplasmic antigens by flow cytometry¹³⁶⁰. They incubated primary lymphocytes and lymphoma cell lines at 4 °C in HBSS buffer with antibodies in a buffer containing 2% FBS and 0.1 – 0.3% (10 – 30 $\mu\text{g}\cdot\text{ml}^{-1}$ or ~8 – 24 μM) saponin for 30 minutes. As judged by flow cytometry analysis, monoclonal antibody delivery was achieved while cell integrity and morphology remained intact¹³⁶⁰. Interestingly, this protocol did not rely on fixation with paraformaldehyde, a step that was only incorporated in later adaptations, presumably to better prevent leakage of cytokines from the cell or avoid having to deal with apoptotic cells^{1361–1363}. An earlier method featuring lysophosphatidylcholine as permeabilization agent was similarly independent of fixation¹⁷⁹.

Detergent-Like Lipids & Other Surfactants for Intracellular Delivery: Surfactants include synthetic detergents, physiological compounds such as bile salts, lysolipids and certain amphiphilic peptides and amphiphiles. A widely used example is the naturally occurring lipid lysophosphatidylcholine (also known as lysolecithin). Miller et al. employed lysophosphatidylcholine exposures to permeabilize CHO cells and maintain them as semi-intact cells capable of DNA synthesis for several hours⁴⁹⁹. The protocol was used to explore soluble factors that inhibit or stimulate DNA synthesis. A follow up paper outlined

generalized protocols for delivery of cargo molecules to a wide range of monolayer and suspension cells¹³⁶⁴. In it, lysophosphatidylcholine concentrations from 30 – 250 $\mu\text{g}\cdot\text{ml}^{-1}$ (60 – 500 μM) were chosen depending on the balance between delivery, viability, and leakage of the representative endogenous protein lactate dehydrogenase. Balinska employed lysophosphatidylcholine to introduce the exogenous nucleoside dTTP into the DNA of hepatoma cells via permeabilization-mediated intracellular delivery¹³⁶⁵. Because there was only a slight loss (20–25%) of lactate dehydrogenase, they concluded permeabilization of cells does not persistently disrupt membrane integrity and resealing could be achieved by exchanging back to standard media¹³⁶⁵. Nomura and colleagues used lysophosphatidylcholine permeabilization for the delivery of larger proteins: diphtheria toxin (A fragment), horseradish peroxidase and antibodies against SV40 T-antigens¹³⁶⁶. These macromolecules were successfully introduced into living mouse erythroleukemia cells, baby hamster kidney, and mouse fibroblast cells. Furthermore, lysophosphatidylcholine has been used to permeabilize primary human lymphocytes and monocytes for detection of intracellular antigens by flow cytometry¹⁷⁹. 50 $\mu\text{g}\cdot\text{ml}^{-1}$ (100 μM) of lysophosphatidylcholine was incubated at 4 °C for 5 min before recovery with antibodies inside, thus avoiding the need for fixation.

Similar compounds have been investigated for their detergent-like mechanisms. For example, simulations have been performed on plant-derived resorcinols¹³⁶⁷ and dioctanoyl-phosphatidylcholine, a cone-shaped counterpart of the native lipid DPPC¹³⁶⁸. Studies with dioctanoyl-phosphatidylcholine reveal a curvature stress that can be relieved upon pore formation¹³⁶⁸. Such mechanisms may also be applicable to lysophosphatidylcholine, which is also a cone-shaped lipid. In the case of resorcinols, micelles are observed to bind to the membrane. If micelles remain compact, they displace phospholipids head groups into the bilayer center, thereby disrupting the structure of the leaflet and causing the lipids to surround the micelle¹³⁶⁷. However, if resorcinols are already embedded within the bi-layer their presence leads to stabilization instead, just like cholesterol. Thus, simulations are a promising tool to gain insight into the mechanisms and molecular events that underlie membrane disruption mechanisms that could be useful for intracellular delivery.

Microfluidic & Nanotechnological Control of Detergent Exposure: For detergents and surfactants applied in bulk solution, a key weakness is that the nature of the membrane injury lacks precise spatiotemporal control. Molecules are added indiscriminately to solution, and it is difficult to get rid of them once then job is done. Thus, it is difficult to balance the required level of membrane permeabilization against excessive toxicity (Figure 36A). Recently, Kilinc et al. used microfluidics to demonstrate controlled flux of localized saponin to perform precise axotomy (cut off an axon) on neurons cultured on chips¹³⁶⁹. In a variation on this theme, the detergent sodium dodecyl sulfate (SDS) was employed in laminar flow mode in a microfluidic device to damage specific sections of neurites and investigate the recovery process¹³⁷⁰. Saponin has also been combined with nanostraws to localize membrane disruption to the nanostraw openings⁶⁶⁵. These examples showcase the potential of microfluidic systems to localize and control damage conferred by detergents to subcellular regions (Figure 36B). It remains to be seen whether such a strategy could be

feasible for intracellular delivery at high throughput, although inventors will probably test this in the coming years.

Membrane-perturbing nanoparticles are another concept worth considering (Figure 36C). Multifunctional nanocarriers that switch to a membrane disrupting state are already being developed for endosomal escape purposes⁶. Similarly, conjugation with membrane-active peptides¹⁹¹ or pore-forming toxins¹⁹⁴ can be harnessed to produce nanoscale cargo with more potent cell penetration properties. If membrane-perturbing nanoparticles can be made switchable by light or other environmental stimuli, they may confer the level of control required for reversible permeabilization at discrete locations on the cell surface.

Detergent Summary: The abovementioned studies suggest saponins, detergents, and other membrane permeabilizing surfactants can be used to introduce a wide range of cargo molecules into various cell types. The emergence of membrane defects depends on variables such as exposure time, temperature, diffusion, random fluctuations, mixing effects, and spontaneous interactions. This is in contrast to physical methods where a well-defined stimulus triggers a clean disruption event. Electroporation, in particular, has often been reported to achieve superior results in the hands of researchers when compared with detergents¹⁰⁵². The use of physically controllable or light-switchable surfactant systems may aid in developing more precise membrane perturbation strategies. Furthermore, it is worth considering that a wide range of organisms produce secondary metabolites with membrane-disrupting properties. As an increasing abundance of these natural detergents and lipopeptides are characterized, new possibilities for ideal membrane permeabilization agents may become available. For example, anabaenolysin lipopeptide toxins have recently been proposed as a potent alternative to digitonin for the selective disruption of cholesterol-containing biological membranes¹³⁷¹. Finally, using microfluidics and nanotechnology for local and transient exposure of cells to surfactants is another frontier where spatiotemporal control of membrane disruption may increase the effectiveness of intracellular delivery.

6.5.3 Membrane-Active Peptides—Various membrane-active peptides are known to disrupt lipid bilayer membranes^{394,401}. Anti-microbial peptides (AMPs), which are usually both amphiphilic and cationic, can induce pore-formation at critical concentrations^{1372,1373}. Under certain circumstances, cell-penetrating peptides (CPPs) and pathogenic amyloid peptides can also permeabilize lipid bilayers, although the mechanisms are less well-defined³⁹⁴. Most membrane-active peptides are thought to be intrinsically disordered in solution but adopt more defined structures upon contact with biological membranes, giving rise to their membrane-disrupting properties³⁹⁴.

Anti-Microbial Peptides: The best-characterized membrane-active peptides are the AMPs. To date, more than 5,000 of them have been catalogued^{1374,1375}, with frog skin alone representing a source of more than 300 variants¹³⁷⁶. Only a small selection of AMPs have been studied for their molecular mechanisms of action. A common feature is their ability to adopt a conformation with hydrophobic segments distinct from hydrophilic/cationic segments¹³⁷². For a given AMP, the ability to disrupt membranes also depends on the lipid composition of the target membrane. In contrast to the plasma membrane of animal cells, bacterial membranes feature many negatively charged lipid headgroups on their outer

leaflets. This allows a combination of electrostatic and hydrophobic interactions to drive adsorption of cationic AMPs to the surface of bacteria with high affinity¹³⁷². Once at the interface, hydrophobic segments integrate into the membrane to disrupt it, with several different models proposed for how they generate pores^{401,1373,1377}. Due to the higher affinity for bacteria membranes, AMPs can lyse microbes at μM concentrations while having less effect on animal cell membranes. This enables them to kill microorganisms without being significantly toxic to mammalian cells. Moreover, in an opposite manner to saponins, cholesterol in the plasma membrane of animal cells serves to suppress the activity of AMPs due to its stabilizing effect. At high enough concentrations, however, AMPs will also disrupt plasma membranes of mammalian cells, and this is the regime of interest for potential intracellular delivery applications.

Mechanisms of Membrane Disruption by AMPs: The main models used to describe AMP-mediated pore formation mechanisms share a common aspect, namely two distinct peptide–lipid states: an inactive surface-bound state and a pore-like insertion state^{1372,1378}. One of the best studied AMPs is melittin, a peptide extracted from bee venom¹³⁷⁹. It is a 26 amino acid chain containing +6 positive charges in total. Amino-terminal residues 1–20 are mostly hydrophobic while carboxyl-terminal residues 21–26 are hydrophilic due to a string of positive charges. Pores produced by melittin exposure have been estimated at 2.5 – 3 nm in palmitoylcholine (POPC) vesicles¹³⁸⁰. Experiments with GUVs held by micropipettes revealed that melittin first increases the membrane surface area due to adsorption/integration before rearranging to induce stable pores without vesicle rupture¹³⁸¹. Later studies showed that melittin partitions to both sides of the bilayer, probably via transient defects, before finally reaching a concentration where stable pore formation occurs. The critical concentration lies in the μM range, and corresponds to a peptide to lipid ratio of about 1:100¹³⁸².

Another heavily studied AMP is magainin 2. Tamba et al. showed that pore-formation is triggered when magainin 2 reaches a critical concentration at the membrane interface¹³⁸³. Their studies predicted that the initial disruption size could be as large as tens of nanometers before shrinking to a more stable pore of several nanometers¹³⁸⁴. The pores are thought to be “chaotic”, lined by a mixture of peptides and lipids acting in cooperation, rather than a well-defined peptide lined channel¹³⁸⁵. In keeping with the notion of a two-state model, the human LL37 peptide has been observed to first adsorb parallel to the surface as an α -helix before inserting and rotating normal to the membrane to form pores with an estimated diameter of 2.3 – 3.3 nm¹³⁸⁶. AMPs can to some extent exhibit detergent-like effects (membrane thinning, bilayer stresses, toroidal pore formation, micellization)¹³⁸⁷, but unlike detergents they tend not to dissolve the membrane structure, rather induce smaller pores for the passage of molecules¹³⁸². One report, however, suggests that AMPs can form larger holes in some membranes¹³⁸⁸. Atomic force microscopy imaging of supported lipid bilayers was used to visualize a population of pores that could grow as a function of AMP concentration¹³⁸⁸.

In many cases the exact structure of AMP-mediated pores is unknown. Multiple models have been proposed such as toroidal, disordered toroidal, and barrel stave. The depictions of these pore models are shown in Figure 37¹³⁸⁹. Molecular dynamics simulations have been

invaluable in elucidating possible molecular events³⁷⁹. They indicate that synergistic aggregation of several peptides together cooperatively results in defect formation³⁷⁹. AMP aggregation leads to a high local density of positive charges. This dense concentration of positive charges at the membrane interface can result in a highly localized electric field, which could destabilize the bilayer by an electroporation-like effect^{1390–1392}. Interestingly, simulations indicate that the emerging defects appear to exhibit a significantly disordered shape, rather than a classic toroidal pore¹³⁸⁹. Studies of magainin MG-H2 peptide reveal that its binding creates a local tension in the exposed leaflet, which creates a compressive stress that is relieved upon pore formation¹³⁹³. Simulations of melittin¹³⁸⁹ and cateslytin¹³⁹⁴ support a similar interpretation. Overall, the prerequisites for AMP-mediated pore formation appear to be a high concentration of peptides in solution and aggregation. The simulations that been used to visualize pore formation favor a model whereby membrane defects occur as disordered non-uniform pores¹³⁸⁹.

Cell-Penetrating Peptides & Amyloid Peptides: In contrast to the case of AMPs, cell-penetrating peptides (CPPs) and amyloid peptides do not adhere to the principle of well-defined hydrophilic/cationic and hydrophobic segments. Though most CPPs tend to be cationic, they may also be uncharged and hydrophilic. Well-studied CPPs include penetratin, HIV-1 TAT peptide, and poly-arginines of 8 or 9 units. For these peptides molecular dynamics simulations have observed only very transient pores¹³⁹⁵. Other simulations reveal deformations and bending phenomena without actual pore formation, although this is controversial and it has been argued that some simulations of CPP behavior could be artifactual³⁷⁹. When attached to bulky cargo molecules, CPPs are believed to enter cells via endocytosis rather than direct translocation through the membrane, arguing that pore-formation in the plasma membrane might have very little role in actual delivery¹⁹¹. Thus the mechanisms could be different when CPPs are lone molecules versus when they are conjugated to a cargo molecule.

To explain the observations gathered from various studies, Miranker and colleagues propose a common mechanistic landscape for membrane-active peptides³⁹⁴. The initial formation of a pore is catalyzed by peptide-induced membrane tension that lowers the activation energy of spontaneous poration to a regime more accessible by thermal fluctuations (Figure 38)^{394,1396}. In other words, membrane-active peptides distort the structure of lipid bilayers to a point where pore formation becomes the most energetically favorable option at a given temperature. The structure and lifetime of such pores in live cells remain to be determined.

Summary on Membrane-Active Peptides: The disparate results and models derived from studies of membrane-active peptides can probably be attributed to the variations in methods, experimental conditions and model membrane systems, as well as the gap between theory and experiments^{394,401,1377,1399}. Some groups have sought to unify these disparate findings by looking for synergistic mechanisms between detergents and membrane-active peptides, or between different groups of membrane-active peptides^{394,1387}. Indeed, reviews of the literature increasingly look to examine common principles underlying the action of AMPs, CPPs, and amyloid peptides^{394,401,1400}. Further studies will be required to uncover their mechanisms of action in live mammalian cell membranes and whether they can be of use for

intracellular delivery¹⁴⁰¹. It remains to be seen, for example, whether peptides can create pores large enough for siRNA or protein translocation without excessive cell toxicity. Provided treatment with membrane-active peptides can be made sufficiently reversible and tolerable, their relative specificity for different types of membranes suggests they could represent a workable strategy to permeabilize plasma membranes for intracellular delivery¹⁴⁰².

6.5.4 Pore-Forming Proteins & Toxins—Organisms from all kingdoms have evolved pore-forming proteins (PFPs) that can permeabilize the membranes of competing lifeforms³⁶⁹. PFPs are produced by prokaryotes, eukaryotic parasites, fungi, marine organisms, and plants either as a defense mechanism or to access nutrients, especially under conditions of high competition or stress. Vertebrates also produce PFPs, such as the complement membrane attack complex (MAC) to kill bacteria, and the perforins expressed by immune killer cells to destroy malignant or infected cells. The best-characterized and largest class of PFPs, however, is that of the bacterial pore-forming toxins (PFTs).

PFTs are generally secreted as soluble monomers that can assemble into oligomers, undergo conformational changes, and insert into the membrane as an assembled pore complex (Figure 39)^{369,400}. Depending on the PFT, pore assembly may take place before reaching the target cell surface or via lateral diffusion and binding of monomers once embedded within the plasma membrane. For many PFTs, the stoichiometry of the assembled pore is around 7 subunits, such as is the case for *S. Aureus* α -hemolysin or the aerolysin family that form 1 – 3 nm pores to permit the passage of ions and ATP^{369,400}.

Alternatively, cholesterol-dependent cytolysins (CDCs) form multimeric assemblies of >30 units and generate large pores in the range of 20 – 50 nm (Figure 40A)⁴⁰⁰. Atomic force microscopy images of prototype CDC perfringolysin O (PFO) embedded into cholesterol-containing supported lipid bilayers reveal the formation of ring-like pores with ~25 nm diameter (Figure 40B)^{1403,1404}. Many PFTs rely on the presence of specific surface receptors to bind and insert. CDCs, for example, exploit the presence of cholesterol or other lipid raft components, making them quite specific for the plasma membrane of animal cells³⁷⁶. This cholesterol-specific action makes CDCs reminiscent of saponins in their selectivity. Owing to this specificity and their large pore size, CDCs are the PFTs that have primarily been used for intracellular delivery of larger cargo (>1 nm) and will be the focus the subsequent discussion in this section.

Streptolysin O for Intracellular Delivery: The most widely used PFT for permeabilization-mediated intracellular delivery is the prototype CDC Streptolysin O (SLO) secreted by the bacteria *Streptococcus pyogenes*. SLO has been used since the 70s for selective permeabilization of the plasma membrane to study intracellular processes in semi-intact cell models^{1405,1406}. In the 90s SLO began to be used widely for intracellular delivery purposes¹⁴⁰⁷. Barry et al. demonstrated that antisense phosphodiester oligodeoxynucleotides (ODN) could be introduced into cells during a brief permeabilization step with SLO¹⁴⁰⁷. Cells were able to recover full function and showed maximum ODN-induced down regulation of gene expression at 18 hours before recovery to normal expression at 48 hours¹⁴⁰⁷. A subsequent study compared SLO-mediated delivery versus electroporation for

delivery of a restriction enzyme, concluding that electroporation was more cytotoxic and SLO better at permeabilizing both CHO and human fibroblast cells¹⁴⁰⁸. In their hands SLO provided a more uniform permeabilization across the cell population, possibly because electroporation is to some extent cell size-dependent. In another comparative study, SLO treatment, electroporation, and lipid-carriers were tested for delivery of antisense oligonucleotides that neutralize BCR-ABL mRNA to reduce protein expression¹⁰⁵⁸. Contrasting the earlier report, greater variation in ODN uptake was seen for SLO permeabilized cells when compared with electroporated cells in the chronic myeloid leukemia model cell line KYO-1. The authors suggested that SLO exposure led to relatively under-permeabilized and over-permeabilized populations. Compared to SLO and electroporation, lipid delivery vehicles were found to be ineffective for KYO-1 cells. A separate study in primary rat ventricular myocytes used SLO to successfully deliver FITC-dextran up to 148 kDa and bovine albumin serum (67 kDa), followed by full neutralization of toxin permeabilization and cell recovery¹⁴⁰⁹.

In 2001 Bhakdi and co-workers published a report that significantly advanced our understanding of SLO-mediated delivery⁴⁵⁷. First, pre-titrated concentrations of high-quality SLO were exposed to cells to determine precise concentrations for permeabilization in a variety of mammalian cell lines. Second, they deliberately employed calcium to trigger plasma membrane repair. With this approach, effective delivery of proteins and dextrans was achieved in 60–80% of cells with >50% long-term viability. Third, they explored the size limits of cargo influx to estimate pore size. SLO permeabilization was able to deliver 150 kDa dextrans but failed to mediate the passage of 250 kDa dextrans (diameter ~23 nm)⁸²⁹. This suggested that SLO pores exhibit a cutoff size in the range 20 nm. This is in reasonably good agreement with AFM images of another CDC family member perfringolysin O, which showed pore diameters of ~25 nm¹⁴⁰³. A fourth observation was that, even with rapid Ca²⁺-induced recovery of plasma membrane integrity, calmodulin activity, intact microtubules, and cytoplasmic ATP only returned to normal levels after ~4 hrs. Under various conditions screened, their method permitted proteins to be delivered to approximately 50% of the total cell population under near-full retention of viability, a performance level that has since been confirmed by others¹⁴¹⁰.

In subsequent studies it has been shown that delivery performance can be better for siRNA-mediated gene knockdown, where the molecule to be introduced is significantly smaller (~13 kDa). Transfection with an optimized SLO permeabilization method showed > 80% RNAi-mediated knockdown in difficult to transfect myeloma cell lines (JIM-3, H929, RPMI8226 and U266 cell lines) with minimal effect on cell viability (< 10% death) and cell cycle¹⁰⁷. However, as noted by Bhakdi and colleagues⁴⁵⁷, several caveats exist for the use of SLO. Primary among them is that the quality of SLO preparations is important, because contaminations with proteases or DNAses may create deleterious artifacts. Due to variations in batch quality, the appropriate SLO concentration window usually needs to be pre-calibrated by titration experiments prior to cell treatment. Moreover, an oxygen-stable C530A substitution mutant obviates the need for a reducing agent to maintain SLO activity in the permeabilization buffer⁴⁵⁷. Thus protein engineering efforts have contributed towards improved versions of pore-forming proteins for cell permeabilization. Despite the caveats, SLO permeabilization represents a relatively cheap, simple and effective method to

introduce molecular cargo up to ~20 nm into living cells. SLO has been used to perform cytoplasmic delivery of siRNA^{107,108,1411}, antisense oligonucleotides^{1058,1407,1412–1421}, proteins^{182,196,457,1408,1409,1422–1424}, peptides^{1410,1425,1426}, cytoplasmic extracts^{468,498,1427–1442}, dextrans¹⁴⁰⁹, PNA probes^{1443–1445}, molecular beacons^{1043,1446–1452}, photosensitizers¹⁴⁵³, phosphatidic acid¹⁴⁵⁴, Rb⁺ ions¹⁸², ATP¹⁸², various RNA probe^{1455–1457}, lanthanum probes^{261,1458} and gold nanoparticles¹⁴⁵⁹. Beyond SLO, permeabilization-based delivery attempts with other CDC family members, such as Perfringolysin O and Listeriolysin O, have occasionally been reported in the literature^{1460,1461}.

Pore-Forming Proteins as Endosome Disruptors: There are a number of naturally occurring scenarios where organisms use pore-forming proteins to deliver cargo into target cells. So-called AB toxins can mediate this effect³⁶⁹. The B component permeabilizes membranes, often triggered by the acidic environment of endosomes, while the A subunit exerts separate enzymatic activity when unleashed into the cytoplasm³⁶⁹. In other words A is the cargo and B is the membrane disruptor. Under this principle, the vertebrate immune system has evolved perforins for the purpose of permeabilization to deliver toxic granzymes¹⁴⁶².

One model for how AB toxins operate was presented in an elegant study from Lieberman and colleagues. They observed that sublytic perforin permeabilization at the plasma membrane (featuring small 1 – 2 nm pores) induces endocytosis in response to calcium influx, thereby promoting endocytic uptake of the perforin plus cytotoxic granzymes¹⁴⁶³. Perforins then lodge in the membrane of endosomes, inhibit maturation, and subsequently trigger rupture to release endosome contents and cytotoxic granzymes, which then induce the death of target cells¹⁴⁶³. In an analogous scenario, adenovirus employs the viral membrane lytic protein-VI to first generate small pores that trigger plasma membrane repair processes¹⁴⁶⁴. This is followed by its endocytosis into leaky compartments from which it and potentially other viral components can subsequently escape¹⁴⁶⁴.

Recently, the natural AB-toxin mechanism has been repurposed for intracellular delivery through protein engineering efforts. Yang et al. showed that a neutralized version of perfringolysin (PFO) can be targeted to the EGF receptor of cancer cells and preferentially activated in endosomes to deliver toxic gelonin into the cytoplasm¹⁹⁴. To do this, they designed a bi-specific antibody, where one terminal binds PFO while the other targets the EGF receptor for endocytosis. Once in endosomes, the acidic environment triggers PFO to disrupt the endosomal membrane. In another example of this strategy, Pentelute and colleagues showed that the protective antigen component of anthrax toxin generates a pore that can mediate egress of polypeptides, impermeable small molecule drugs, and antibody mimics from endosomes to the cytosol¹⁴⁶⁵. The power of these bio-inspired approaches is in their specificity against different types of membranes and endosomal compartments¹⁹³. Such studies indicate the utility of pore-forming toxins and their components not just for plasma membrane permeabilization, but also controlled disruption of cargo-laden endosomes.

6.5.5 Chemical Destabilization—Chemical destabilization of lipid molecules can occur due to oxidative damage from a variety of sources. Membrane disruptive lipid

peroxidation events are thought to be a normal part of cell physiology. In a recent study, for example, endogenous production of reactive oxygen species (ROS) by the NOX2 enzyme mediates disruption of endosomal membranes to trigger leakage of antigens into the cytosol of dendritic cells for subsequent immune activation¹⁴⁶⁶. ROS and other free radicals cause peroxidation of lipid tails, leading to similar effects as those seen for surfactants, including distortion, buckling, curvature strain, and peeling off of micelles from lipid bilayers^{421,1467,1468}. Common species of peroxidized lipids have been proposed to exist in two main classes: 1) phosphatidylcholines with a hydroperoxide side chain, and 2) phosphatidylcholines with oxidized and truncated chains terminated by an aldehyde or carboxylic group (Figure 41)¹⁴⁶⁷. Lipid tails become more polar due to the presence of hydroperoxides, aldehyde or carboxyl groups. Consequently they bend toward the water phase and hydrogen bond with water and the lipid headgroups. The result is an increase in area per lipid headgroup, which leads to membrane thinning, decrease in lateral ordering, and membrane area expansion³⁹⁷.

Using GUVs as a model system, Riske et al. artificially converted the native lipid phosphatidylcholine to an oxidized version with hydroperoxides groups at the 9 or 10 chain position (Figure 41C). This was accomplished by using an amphiphile photosensitizer that generates singlet oxidation under irradiation with visible light. They found a substantial increase in GUVs membrane surface area without membrane disruption or evidence of poration³⁹⁷. They hypothesized that more intense treatment would eventually lead to the breakdown of membrane integrity, just like with detergents. Compared to the oxidized lipids investigated by Risk et al., oxidized lipids with truncated chains featuring aldehydes or carboxyl termini are much more potent perturbants of membrane organization^{1467,1468}. In latter scenarios, simulations and experiments both observe pore formation and micellation as a function of concentration, as well as an increased susceptibility to bilayer rupture^{398,399}.

Confinement of Oxidative Damage: How is it possible to confine lipid oxidation to subcellular regions? Under certain regimes, lasers exert a chemical oxidation effect on membranes through generation of an ionizing plasma, as opposed to thermal or mechanical effects. For example, femtosecond lasers can produce these effects under specific intensities, pulse durations, and frequencies^{1268,1278} (see optoporation section and figure 30D). Furthermore, near field ionizing plasma surrounding laser-irradiated gold nanoparticles has been proposed as a primary mechanism of membrane breakdown in a recent study¹⁴⁶⁹. Theoretical simulations and experiments both suggested generation of a low density plasma with multiphoton ionization of the surrounding liquid, which in turn perforates the cell membrane by oxidative effects. This strategy was reported to transfect siRNA into cells with > 90% efficiency and viability¹⁴⁶⁹. Other delivery strategies that rely on fast pulse laser irradiation of metal nanoparticles or microscale features may work through a similar mechanism of ionizing plasma-induced damage^{289,886,888,889,892,893}, and have been used to load cells with cargoes such as dyes, dextrans, siRNA, and quantum dots. The diffusive range of singlet oxidant species in an aqueous environment has been estimated at about 100 nm³⁹⁷. Thus, local confinement strategies may be feasible for transient and precise membrane perforation without damage to the rest of the cell.

7 Gated Channels & Valves

So far we have discussed membrane disruption approaches whereby cells recover through active plasma membrane repair (see section 4.3). In some cases, however, it may be possible to deliver cargo into cells by actuating opening and closing of ‘windows’ in the cell membrane. Such a strategy could be executed by external manipulation of transmembrane proteins (e.g. channels and transporters), insertion of engineered molecular valves, or deployment of synthetic nanodevices.

Endogenous Channels (ATP-activated)

Since the 1980s several reports have demonstrated the influx of small molecules through the manipulation of particular endogenous membrane transporters and channels. Impermeable dyes have been observed to enter a number of cell types in the presence of high concentrations (mM) of extracellular ATP¹⁴⁷⁰. ATP-gated channels permitting delivery are present in certain immortalized cell lines and primary immune cells¹⁴⁷¹. Steinberg et al. showed that only cargo of molecular weight less than 900 Dalton were able to enter cells in the presence of ATP¹⁴⁷². It was found that ATP permeabilizes the plasma membrane of mouse macrophages to 6-carboxyfluorescein (376 Da), lucifer yellow (457 Da), and fura-2 (831 Da) but not to trypan blue (961 Da), evans blue (961 Da), or larger dye conjugates. These studies led to the idea that purinergic (i.e. ATP-mediated) activation of membrane channels can enable passage of cations and other small molecules. Toner and colleagues later used ATP-activated channels to load cells with trehalose¹⁴⁷³, a 342 Da disaccharide with widespread applications in cryopreservation.

Endogenous Channels (Swelling-activated)

Osmotic swelling is another stimulus that can trigger the opening of mechanosensitive channels for influx of certain molecules. For example, osmotic swelling of Jurkat cells at 100 mOsm but not 200 mOsm was found to trigger opening of channels for the delivery of monomeric sugars and sugar alcohols, but not larger molecules¹⁴⁷⁴. It was found that extensive hypotonic swelling rendered the cell membrane permeable to PEG300–400, but not to PEG600–1500. By reference to the hydrodynamic radii of these PEG molecules, the size-selectivity of membrane permeation yielded an estimate of ~0.74 nm for the cut-off radius of the swelling-activated channel¹⁴⁷⁵. Further work identified SLC5A3 as an osmotically sensitive myo-inositol transporter that opens at imposed extracellular osmolarities of less than 200 mOsm¹⁴⁷⁶. Thus, this set of endogenous channels may be manipulated by osmotic stimuli to transport small molecules into cells.

Engineered Channels/Valves

One of the first efforts towards engineering a switchable channel for intracellular delivery was reported by Toner and colleagues. Using a strategy that takes advantage of site-directed mutagenesis of *S. Aureus* α -toxin, they developed a self-assembling, proteinaceous, 2 nm pore equipped with a Zn²⁺-actuated switch¹⁴⁷⁷. Toxin monomers added to solution integrate into the plasma membranes of target cells and assemble to form an oligomeric pore complex. By adjusting the concentration of extracellular Zn²⁺, reversible permeabilization of the plasma membrane to small molecules (1 kDa or less) was achieved¹⁴⁷⁷. In a follow-up

study, the switchable pore was used to load trehalose at up to 0.5 M concentration into fibroblasts²⁶⁶. These reports were an intriguing demonstration of the idea that protein engineering could be leveraged to generate membranes with inbuilt permeability switches triggered by chemical, enzymatic, and physical stimuli^{1478,1479}.

Optogenetic Control of Cell Permeability

The emergence of optogenetics heralded the concept of engineered light-activated transporters for manipulating cell permeability^{1480,1481}. Kocer and colleagues modified the mechanosensitive channel of large conductance (MscL) from *E. Coli* into a light-addressable nanovalve sensitive to 366 nm UV irradiation¹⁴⁸⁰. They verified the system by controlling the flux of calcein across proteoliposome membranes for both one-way and reversible nanovalves. In a parallel approach, Boyden et al., exploited the naturally occurring algal protein channelrhodopsin-2 as a rapidly gated light-sensitive cation channel in neurons¹⁴⁸¹. Lentiviral transduction was used to express these channels in neurons, whereby photostimulation with blue light enabled cation influx and subsequent spatiotemporal actuation of neuron action potential firing, which was a long sought goal in the field. Although limited to cations, this optogenetic proof of concept can conceivably be extended to a wider range of synthetic and bio-inspired nanovalves.

Stimuli-Sensitive Channels for Larger Cargo Delivery

Doerner et al. showed that the mechanosensitive MscL channel can be functionally expressed in mammalian cells to afford controlled uptake of membrane-impermeable molecules¹⁴⁸². The pore diameter of >2.5 nanometers allows passage of large organic ions and small proteins up to 6.5 kDa. Furthermore, gating of the channel was found to be responsive to changes in membrane tension, both in native bacteria and mammalian cell membranes. To engineer more convenient gating, charges were engineered within the pore of MscL to induce spontaneous channel closure. The addition of charged methanethiosulphonate agents such as MTSET at 1 mM was found to switch the channel between open and closed conformations. As a demonstration of utility, this system was exploited to load the bi-cyclic peptide phalloidin (789 Da) into CHO cells to label actin filaments.

Nanodevice Gating

More radical concepts for engineering switchable permeability have been demonstrated with synthetic nanodevices. Langecker et al. created an artificial membrane channel based on DNA origami nanostructures that anchor to the lipid membrane by cholesterol side chains (Figure 42A)¹⁴⁸³. The shape of the DNA-based channel was inspired by the bacterial channel protein α -hemolysin with some differences in physical properties such as charge, hydrophobicity, and size. Although not implemented in cells, future applications in cell membranes could include their deployment as antimicrobial agents, controlled interference of cellular homeostasis, or as delivery conduits¹⁴⁸³.

Carbon nanotubes (CNTs) represent another form of nanotechnology with engineering potential at the scale of the cell membrane. Geng et al. exploited the nature of their narrow hydrophobic inner pores that mimic structural motifs typical of biological channels¹⁴⁸⁴.

They developed a method to insert CNTs into lipid bilayers and live cell membranes to form conducting channels capable of transporting water, protons, small ions and DNA under physiological conditions (Figure 42B). It was found that the local channel and membrane charges control the conductance and ion selectivity of the CNT pores, thus suggesting potential starting points for engineering gating function.

Recently one group devised molecular motors that can burrow through lipid membranes upon excitation with light¹⁴⁸⁵. Upon physical adsorption of the molecular motors onto lipid bilayers and subsequent activation by ultraviolet light, holes were drilled in the cell membranes. They demonstrated intracellular delivery of the motors themselves, small molecule dyes such as PI, and accelerated cell death as a result of apoptosis or necrosis¹⁴⁸⁵. Experimental results indicated an explanation based on the transduction of light energy into nanomechanical action rather than chemical or thermal effects¹⁴⁸⁵.

8 Summary & Outlook

Summary

Motivations for better intracellular delivery range from basic research to the potential of therapeutic applications including cell-based therapies, gene therapy and regenerative medicine. Cargo of interest vary from small molecules that can naturally permeate the lipid bilayer to highly charged molecules and large complexes, genetic constructs, or organelles approaching the size of the cell itself. For the majority of these cargo, the plasma membrane is the primary barrier to intracellular delivery. Cells exhibit a distinct set of properties that can be exploited to overcome this barrier. For example, delivery methods can take advantage of the negative membrane potential, cholesterol-rich nature of the plasma membrane, or presence of specific extracellular receptors.

A broad assortment of approaches has been designed to deliver cargo into cells. They can be categorized as either carrier-mediated or membrane disruption-mediated strategies. Cells generally respond to the presence of carriers by processing them through endocytosis and other membrane trafficking pathways. On the other hand, they react to membrane disruption by deploying membrane repair processes to heal the plasma membrane and restore cell homeostasis. Due to their perturbing nature, most delivery strategies are a tradeoff between effective delivery and tolerable cell damage. Membrane disruption-mediated delivery strategies have the advantage of rapid and near-universal delivery of almost any cargo that can be dispersed in solution. The latest understanding of membrane repair pathways indicates that membrane disruption is a common event in the life of cells, and they are well equipped to deal with it. More challenging is the selection of appropriate membrane disruption modalities and their precise implementation to large batches of cells at high throughput. This is an engineering challenge that involves elements of both technological innovation and mechanistic understanding of the cell itself. Theories have been developed to explain defect formation in lipid bilayers and the phenomena that can be leveraged to achieve controlled disruption of cell membranes. In parallel, empirical studies have identified key modalities, such as electroporation and mechanical deformation, which can be deployed to achieve a relatively reproducible control over plasma membrane disruption.

Tables 5 and 6 summarize the membrane disruption approaches that have been discussed in this review. Table 5 lists each method with what is known about disruption mechanisms, size and distribution of resultant holes, treatment throughput, and whether it is applicable to adherent or suspension cells. If there is one theme that sticks out from this analysis, it is that we still lack clear mechanistic understanding on how many membrane disruption-mediated intracellular delivery methods work. Indeed, many methods may suffer from a lack of mechanistic insight to hone and optimize the salient parameters. Sonoporation is an example of a delivery strategy that has been challenging to optimize because of such complexity. In other cases the membrane disruption method may work well but a lack of knowledge on appropriate environmental conditions leads to underperformance. For example, we have a limited understanding of how cell membranes behave and recover at different temperatures and osmolarity. Other methods have clearly defined mechanisms but face intrinsic limitations because of the nature of the membrane disruption effect. For example, conventional electroporation and pore-forming toxins tend to generate membrane disruptions less than 50 nm, and are therefore limited in their ability to deliver large cargo.

Throughput and applicability to suspension or adherent cells are further considerations. In microinjection, for example, almost any cargo can be delivered to any cell type but only one cell at a time. The challenges involved in scale-up to high throughput are yet to be surmounted. Other methods, such as scrape loading, are low cost and high throughput but may lack consistency and precision across a cell populations. In a further example, large cargo delivery can be accomplished with laser-controlled cavitation bubbles, but the systems require complex equipment and may only be applicable to adherent cells. Such a scenario rules out delivery to most immune and blood cells that naturally exist in suspension.

Electroporation is currently the most dominant high-throughput method in the field. As covered in section 6.2.3, it has been demonstrated in applications ranging from testing of impermeable drugs and biomanufacture to engineering cells for cancer immunotherapy and stem cell-based gene therapy (Figure 28). However, electroporation is not without its limitations. Post-treatment cell death and inability to deliver large cargo are two such examples. Overall, no single method has a monopoly on all applications and further work is required to identify the optimal delivery strategies for a given application.

Table 6 compares the membrane disruption approaches versus the cargoes they have been reported to deliver. It is important to note that many combinations have simply not been attempted. Moreover, many papers use a technique to deliver a particular cargo because they modify the protocol from an earlier publication. Certain techniques seem to have an arbitrary emphasis on a particular cargo. For example, electroporation publications have tended to focus heavily on plasmid transfection while neglecting other cargoes. Filling out the table by screening all possible combinations would be extremely informative for the field. Comparisons of cost and cell type applicability would also add value to such an analysis and help to guide experimentalists toward optimal solutions. In future, we expect to see more publications move beyond trivial delivery of small molecules dyes (<1 kDa) and showcase delivery of a smorgasbord of diverse cargo, especially proteins, nanomaterials, and larger cargo.

Outlook

Several membrane disruption-based methods are widespread use in academic, industrial, and medical laboratories across the world, such as electroporation and microinjection. Yet the majority of modalities are either in nascent development or are yet to be pursued to their full potential. By identifying where the field can reduce costs and complexity, the potential exists to lower the barrier of entry to interdisciplinary scientists and researchers in resource-poor settings. This would no doubt strengthen global discovery. Overall, we believe that better and more streamlined intracellular delivery is more likely to arise out of a deeper understanding of current approaches and their capabilities.

The field has a number of frontiers where opportunities are ripe. One is the huge repository of unexplored membrane perturbing compounds in the form of natural and synthetic detergents, surfactants, pore-forming toxins, membrane-active peptides, and other secondary metabolites. Another is the rise of new microfluidic and nanotechnological tools that provide an unprecedented level of control to the membrane disruption process. This may be via high-throughput systems for mechanical deformation, such as microfluidic cell squeezing, or advanced fabrication of nanostructures, including nanowires and nanostraws. Combining the strengths of multiple modalities may be a prudent approach toward better technologies. For example, electroporation is biased toward producing small pores but provides a convenient electrophoretic force for the delivery of charged molecules. Methods that combine large disruption sizes with electrophoretic drive could potentially harness the benefits of both techniques. Future strategies could also be based on synthetic valves and nanodevices that embed within the membrane and enable remote control of permeability via external triggers. Light-gated methods that confer switchable control of membrane disruption are only beginning to be explored. In the coming years cost and convenience will be another important factor, as many of the current methods are either expensive or overly reliant on cumbersome equipment.

As our insight into membrane repair processes and cell recovery deepen, it may be possible to provide stimuli that switch membrane repair on and off, or to modulate stress responses that otherwise lead to untoward cell fate changes or death. How can we understand the energy landscape of defect formation to generate ideal membrane disruptions? What kinds of disruptions are optimal for delivery in specific cell-cargo combinations? How does the composition of external buffer determine which pathways are activated in response to permeabilization? The answers to these, and similar, questions will be more attainable with the establishment of better approaches to investigate plasma membrane homeostasis and the cellular response (Figure 10). Thus, along with technical advances in membrane disruption, our toolbox for studying cells must also improve.

For *ex vivo* cell-based therapies in particular, quality control procedures may be required to ensure the safety and efficacy of engineered cells. Methods for assessing DNA damage, fate changes, and cell functionality will possibly be required to avoid re-introduction of malignant or undesirable cells in cGMP settings. More accurate assays to evaluate cell function are expected to inform the appropriate use of membrane disruption-based delivery methods going forward. Combined with further technological innovations in the way we

disrupt membranes, we expect future progress in the field to catalyze breakthroughs in delivery applications ranging from fundamental research to *ex vivo* cell-based therapies.

ACKNOWLEDGEMENTS

This work was supported by the US National Institute of Health (R01GM101420-01A1). M.P.S. was supported by the Swiss NSF through the advanced postdoc mobility fellowship P300P3_151179. M.P.S. acknowledges support from a Keith Murdoch Fellowship via the American Australian Association, a Life Sciences Research Foundation Fellowship sponsored by Good Ventures, and a Broad*nex10* Catalytic Steps funding gift from the Broad Institute. We are grateful for discussion and feedback from Xiaoyun Y. Ding, James C. Weaver, Eric Van Leen, and Ronan W. O'Connell.

Biographies

Robert Langer is one of 13 Institute Professors at MIT (an Institute Professor is the highest honor awarded to a faculty member). His h-index of 242 is the highest of any engineer in history. He has over 1,300 issued and pending patents which have been licensed or sublicensed to over 350 companies. He served as Chairman of the FDA's SCIENCE BOARD (highest advisory board) from 1999–2002. Langer is one of a very few individuals elected to the National Academy of Medicine, the National Academy of Engineering, the National Academy of Sciences and the National Academy of Inventors. He is one of four living individuals to receive both the US National Medal of Science and the US National Medal of Technology and Innovation. In 2015, Dr. Langer received the Queen Elizabeth Prize for Engineering. He has also received the Draper Prize (considered the engineering Nobel Prize), Albany Medical Center Prize, Wolf Prize for Chemistry, Millennium Technology Prize, Priestley Medal (highest award of the American Chemical Society), Gairdner Prize, Kyoto Prize, Breakthrough Prize and the Lemelson-MIT prize, for being "one of history's most prolific inventors in medicine." He holds 31 honorary doctorates including honorary degrees from Harvard and Yale.

Klavs F. Jensen studied chemical engineering at the Technical University of Denmark and completed his PhD in chemical engineering at the University of Wisconsin-Madison. He started his independent career at the University of Minnesota in 1980 and moved to MIT in 1989 as professor in chemical engineering and materials science and engineering. In 2007 he became Warren K. Lewis Professor and head of MIT's department of chemical engineering until 2015. His research interests revolve around miniaturized systems for chemistry and biological discovery and manipulation. Professor Jensen is a member of the US National Academies of Engineering and Sciences, as well as the American Academy of Arts and Science.

Martin P. Stewart was born in Sydney, Australia in 1983. He received a B.Sc (Hons) from the University of Technology, Sydney in 2007. Martin then obtained his PhD from TU Dresden, Germany in 2012 working under the supervision of Professors Daniel Müller and Tony Hyman. His PhD research focused on the mechanisms of cell shape in mitosis. After a postdoctoral stint at ETH Zürich, Switzerland with Professor Daniel Müller, he joined the labs of Professors Klavs Jensen and Robert Langer at MIT, U.S.A. in 2014. Martin's current research interests are in cell manipulation and analysis, specifically in the areas of intracellular delivery and cell biophysics. He has been a recipient of postdoctoral fellowships

from the Swiss National Science Foundation and the Life Sciences Research Foundation. He has also been awarded grants from the American Australian Association and the Broad Institute.

References

- (1). Peer D; Karp JM; Hong S; Farokhzad OC; Margalit R; Langer R Nanocarriers as an emerging platform for cancer therapy. *Nature nanotechnology* 2007, 2 (12), 751.
- (2). Ganta S; Devalapally H; Shahiwala A; Amiji M A review of stimuli-responsive nanocarriers for drug and gene delivery. *Journal of Controlled Release* 2008, 126 (3), 187. [PubMed: 18261822]
- (3). Mura S; Nicolas J; Couvreur P Stimuli-responsive nanocarriers for drug delivery. *Nat Mater* 2013, 12 (11), 991. [PubMed: 24150417]
- (4). Prokop A; Davidson JM Nanovehicular intracellular delivery systems. *J Pharm Sci-U.S.* 2008, 97 (9), 3518.
- (5). Blanco E; Shen H; Ferrari M Principles of nanoparticle design for overcoming biological barriers to drug delivery. *Nat Biotechnol* 2015, 33 (9), 941. [PubMed: 26348965]
- (6). Torchilin VP Multifunctional, stimuli-sensitive nanoparticulate systems for drug delivery. *Nat Rev Drug Discov* 2014, 13 (12), 813. [PubMed: 25287120]
- (7). Yoo JW; Irvine DJ; Discher DE; Mitragotri S Bio-inspired, bioengineered and biomimetic drug delivery carriers. *Nat Rev Drug Discov* 2011, 10 (7), 521. [PubMed: 21720407]
- (8). Riley MK; Vermerris W Recent Advances in Nanomaterials for Gene Delivery-A Review. *Nanomaterials (Basel)* 2017, 7 (5).
- (9). Yin H; Kanasty RL; Eltoukhy AA; Vegas AJ; Dorkin JR; Anderson DG Non-viral vectors for gene-based therapy. *Nat Rev Genet* 2014, 15 (8), 541. [PubMed: 25022906]
- (10). Mintzer MA; Simanek EE Nonviral Vectors for Gene Delivery. *Chem Rev* 2009, 109 (2), 259. [PubMed: 19053809]
- (11). Yang JP; Zhang Q; Chang H; Cheng YY Surface-Engineered Dendrimers in Gene Delivery. *Chem Rev* 2015, 115 (11), 5274. [PubMed: 25944558]
- (12). Li YL; Maciel D; Rodrigues J; Shi XY; Tomas H Biodegradable Polymer Nanogels for Drug/ Nucleic Acid Delivery. *Chem Rev* 2015, 115 (16), 8564. [PubMed: 26259712]
- (13). Pattni BS; Chupin VV; Torchilin VP New Developments in Liposomal Drug Delivery. *Chem Rev* 2015, 115 (19), 10938. [PubMed: 26010257]
- (14). Lachelt U; Wagner E Nucleic Acid Therapeutics Using Polyplexes: A Journey of 50 Years (and Beyond). *Chem Rev* 2015, 115 (19), 11043. [PubMed: 25872804]
- (15). Cox DB; Platt RJ; Zhang F Therapeutic genome editing: prospects and challenges. *Nat Med* 2015, 21 (2), 121. [PubMed: 25654603]
- (16). Doudna JA; Charpentier E The new frontier of genome engineering with CRISPR-Cas9. *Science* 2014, 346 (6213), 1258096. [PubMed: 25430774]
- (17). Liu J; Wen J; Zhang Z; Liu H; Sun Y Voyage inside the cell: Microsystems and nanoengineering for intracellular measurement and manipulation. *Microsystems & Nanoengineering* 2015, 1, 15020.
- (18). Bruce VJ; McNaughton BR Inside Job: Methods for Delivering Proteins to the Interior of Mammalian Cells. *Cell Chem Biol* 2017.
- (19). Restifo NP; Dudley ME; Rosenberg SA Adoptive immunotherapy for cancer: harnessing the T cell response. *Nat Rev Immunol* 2012, 12 (4), 269. [PubMed: 22437939]
- (20). Gross G; Waks T; Eshhar Z Expression of Immunoglobulin-T-Cell Receptor Chimeric Molecules as Functional Receptors with Antibody-Type Specificity. *P Natl Acad Sci USA* 1989, 86 (24), 10024.
- (21). Fesnak AD; June CH; Levine BL Engineered T cells: the promise and challenges of cancer immunotherapy. *Nat Rev Cancer* 2016, 16 (9), 566. [PubMed: 27550819]

- (22). Maude SL; Frey N; Shaw PA; Aplenc R; Barrett DM; Bunin NJ; Chew A; Gonzalez VE; Zheng Z; Lacey SF et al. Chimeric antigen receptor T cells for sustained remissions in leukemia. *The New England journal of medicine* 2014, 371 (16), 1507. [PubMed: 25317870]
- (23). Naldini L Ex vivo gene transfer and correction for cell-based therapies. *Nat Rev Genet* 2011, 12 (5), 301. [PubMed: 21445084]
- (24). Naldini L Gene therapy returns to centre stage. *Nature* 2015, 526 (7573), 351. [PubMed: 26469046]
- (25). Genovese P; Schirotti G; Escobar G; Di Tomaso T; Firrito C; Calabria A; Moi D; Mazzieri R; Bonini C; Holmes MC et al. Targeted genome editing in human repopulating haematopoietic stem cells. *Nature* 2014, 510 (7504), 235. [PubMed: 24870228]
- (26). Rosenberg SA; Restifo NP Adoptive cell transfer as personalized immunotherapy for human cancer. *Science* 2015, 348 (6230), 62. [PubMed: 25838374]
- (27). June CH; Riddell SR; Schumacher TN Adoptive cellular therapy: A race to the finish line. *Sci Transl Med* 2015, 7 (280).
- (28). Dever DP; Bak RO; Reinisch A; Camarena J; Washington G; Nicolas CE; Pavel-Dinu M; Saxena N; Wilkens AB; Mantri S et al. CRISPR/Cas9 beta-globin gene targeting in human haematopoietic stem cells. *Nature* 2016, 539 (7629), 384. [PubMed: 27820943]
- (29). Maeder ML; Gersbach CA Genome-editing Technologies for Gene and Cell Therapy. *Mol Ther* 2016, 24 (3), 430. [PubMed: 26755333]
- (30). Takahashi K; Yamanaka S Induction of pluripotent stem cells from mouse embryonic and adult fibroblast cultures by defined factors. *Cell* 2006, 126 (4), 663. [PubMed: 16904174]
- (31). Kim D; Kim CH; Moon JI; Chung YG; Chang MY; Han BS; Ko S; Yang E; Cha KY; Lanza R et al. Generation of Human Induced Pluripotent Stem Cells by Direct Delivery of Reprogramming Proteins. *Cell Stem Cell* 2009, 4 (6), 472. [PubMed: 19481515]
- (32). Warren L; Manos PD; Ahfeldt T; Loh YH; Li H; Lau F; Ebina W; Mandal PK; Smith ZD; Meissner A et al. Highly Efficient Reprogramming to Pluripotency and Directed Differentiation of Human Cells with Synthetic Modified mRNA. *Cell Stem Cell* 2010, 7 (5), 618. [PubMed: 20888316]
- (33). Rohani L; Fabian C; Holland H; Naaldijk Y; Dressel R; Loffler-Wirth H; Binder H; Arnold A; Stolzing A Generation of human induced pluripotent stem cells using non-synthetic mRNA. *Stem Cell Res* 2016, 16 (3), 662. [PubMed: 27064648]
- (34). Anokye-Danso F; Trivedi CM; Jühr D; Gupta M; Cui Z; Tian Y; Zhang YZ; Yang WL; Gruber PJ; Epstein JA et al. Highly Efficient miRNA-Mediated Reprogramming of Mouse and Human Somatic Cells to Pluripotency. *Cell Stem Cell* 2011, 8 (4), 376. [PubMed: 21474102]
- (35). Shi Y; Despons C; Do JT; Hahm HS; Scholer HR; Ding S Induction of Pluripotent Stem Cells from Mouse Embryonic Fibroblasts by Oct4 and Klf4 with Small-Molecule Compounds. *Cell Stem Cell* 2008, 3 (5), 568. [PubMed: 18983970]
- (36). Robinton DA; Daley GQ The promise of induced pluripotent stem cells in research and therapy. *Nature* 2012, 481 (7381), 295. [PubMed: 22258608]
- (37). Tabar V; Studer L Pluripotent stem cells in regenerative medicine: challenges and recent progress. *Nat Rev Genet* 2014, 15 (2), 82. [PubMed: 24434846]
- (38). Takebe T; Sekine K; Enomura M; Koike H; Kimura M; Ogaeri T; Zhang RR; Ueno Y; Zheng YW; Koike N et al. Vascularized and functional human liver from an iPSC-derived organ bud transplant. *Nature* 2013, 499 (7459), 481. [PubMed: 23823721]
- (39). Themeli M; Riviere I; Sadelain M New Cell Sources for T Cell Engineering and Adoptive Immunotherapy. *Cell Stem Cell* 2015, 16 (4), 357. [PubMed: 25842976]
- (40). Park CY; Kim DH; Son JS; Sung JJ; Lee J; Bae S; Kim JH; Kim DW; Kim JS Functional Correction of Large Factor VIII Gene Chromosomal Inversions in Hemophilia A Patient-Derived iPSCs Using CRISPR-Cas9. *Cell Stem Cell* 2015, 17 (2), 213. [PubMed: 26212079]
- (41). Warden D; Thorne HV The infectivity of polyoma virus DNA for mouse embryo cells in the presence of diethylaminoethyl-dextran. *J Gen Virol* 1968, 3 (3), 371. [PubMed: 4304101]
- (42). McCutchan JH; Pagano JS Enhancement of Infectivity of Simian Virus 40 Deoxyribonucleic Acid with Diethylaminoethyl-Dextran. *J Natl Cancer I* 1968, 41 (2), 351.

- (43). Pagano JS; Vaheri A Enhancement of infectivity of poliovirus RNA with diethylaminoethyl-dextran (DEAE-D). *Arch Gesamte Virusforsch* 1965, 17 (3), 456. [PubMed: 4286824]
- (44). Graham FL; van der Eb AJ A new technique for the assay of infectivity of human adenovirus 5 DNA. *Virology* 1973, 52 (2), 456. [PubMed: 4705382]
- (45). Fraley R; Subramani S; Berg P; Papahadjopoulos D Introduction of Liposome-Encapsulated Sv40 DNA into Cells. *J Biol Chem* 1980, 255 (21), 431.
- (46). Wong TK; Nicolau C; Hofschneider PH Appearance of Beta-Lactamase Activity in Animal-Cells Upon Liposome-Mediated Gene-Transfer. *Gene* 1980, 10 (2), 87. [PubMed: 6248423]
- (47). Felgner PL; Gadek TR; Holm M; Roman R; Chan HW; Wenz M; Northrop JP; Ringold GM; Danielsen M Lipofection - a Highly Efficient, Lipid-Mediated DNA-Transfection Procedure. *P Natl Acad Sci USA* 1987, 84 (21), 7413.
- (48). Boussif O; Lezoualch F; Zanta MA; Mergny MD; Scherman D; Demeneix B; Behr JP A Versatile Vector for Gene and Oligonucleotide Transfer into Cells in Culture and in-Vivo - Polyethylenimine. *P Natl Acad Sci USA* 1995, 92 (16), 7297.
- (49). Haensler J; Szoka FC Polyamidoamine Cascade Polymers Mediate Efficient Transfection of Cells in Culture. *Bioconjugate Chem* 1993, 4 (5), 372.
- (50). Kawai S; Nishizawa M New Procedure for DNA Transfection with Polycation and Dimethylsulfoxide. *Mol Cell Biol* 1984, 4 (6), 1172. [PubMed: 6330534]
- (51). Wu GY; Wu CH Receptor-mediated gene delivery and expression in vivo. *J Biol Chem* 1988, 263 (29), 14621. [PubMed: 3049582]
- (52). Wu GY; Wu CH Receptor-mediated in vitro gene transformation by a soluble DNA carrier system. *J Biol Chem* 1987, 262 (10), 4429. [PubMed: 3558345]
- (53). Neumann E; Schaeferidder M; Wang Y; Hofschneider PH Gene-Transfer into Mouse Lyoma Cells by Electroporation in High Electric-Fields. *Embo J* 1982, 1 (7), 841. [PubMed: 6329708]
- (54). De Ravin SS; Reik A; Liu PQ; Li L; Wu X; Su L; Raley C; Theobald N; Choi U; Song A Het al. Targeted gene addition in human CD34(+) hematopoietic cells for correction of X-linked chronic granulomatous disease. *Nat Biotechnol* 2016, 34 (4), 424. [PubMed: 26950749]
- (55). Schuurhuis DH; Verdijk P; Schreibelt G; Aarntzen EHJG; Scharenborg N; de Boer A; van de Rakt MWMM; Kerkhoff M; Gerritsen MJP; Eijkeler Fet al. In situ Expression of Tumor Antigens by Messenger RNA-Electroporated Dendritic Cells in Lymph Nodes of Melanoma Patients. *Cancer Res* 2009, 69 (7), 2927. [PubMed: 19318559]
- (56). Zhao YB; Moon E; Carpenito C; Paulos CM; Liu XJ; Brennan AL; Chew A; Carroll RG; Scholler J; Levine B Let al. Multiple Injections of Electroporated Autologous T Cells Expressing a Chimeric Antigen Receptor Mediate Regression of Human Disseminated Tumor. *Cancer Res* 2010, 70 (22), 9053. [PubMed: 20926399]
- (57). Benteyn D; Heirman C; Bonehill A; Thielemans K; Breckpot K mRNA-based dendritic cell vaccines. *Expert Rev Vaccines* 2015, 14 (2), 161. [PubMed: 25196947]
- (58). Stewart MP; Sharei A; Ding XY; Sahay G; Langer R; Jensen KF In vitro and ex vivo strategies for intracellular delivery. *Nature* 2016, 538 (7624), 183. [PubMed: 27734871]
- (59). Lederberg J Cell Genetics and Hereditary Symbiosis. *Physiol Rev* 1952, 32 (4), 403. [PubMed: 13003535]
- (60). Collins J; Hohn B Cosmids - Type of Plasmid Gene-Cloning Vector That Is Packageable Invitro in Bacteriophage Lambda-Heads. *P Natl Acad Sci USA* 1978, 75 (9), 4242.
- (61). Thomas CE; Ehrhardt A; Kay MA Progress and problems with the use of viral vectors for gene therapy. *Nat Rev Genet* 2003, 4 (5), 346. [PubMed: 12728277]
- (62). Kouprina N; Tomilin AN; Masumoto H; Earnshaw WC; Larionov V Human artificial chromosome-based gene delivery vectors for biomedicine and biotechnology. *Expert Opin Drug Deliv* 2014, 11 (4), 517. [PubMed: 24479793]
- (63). Jackson DA; Berg P; Symons RH Biochemical Method for Inserting New Genetic Information into DNA of Simian Virus 40 - Circular Sv40 DNA Molecules Containing Lambda Phage Genes and Galactose Operon of Escherichia-Coli. *P Natl Acad Sci USA* 1972, 69 (10), 2904.
- (64). Cohen SN; Chang AC; Boyer HW; Helling RB Construction of biologically functional bacterial plasmids in vitro. *Proc Natl Acad Sci U S A* 1973, 70 (11), 3240. [PubMed: 4594039]

- (65). Cohen SN DNA cloning: a personal view after 40 years. *Proc Natl Acad Sci U S A* 2013, 110 (39), 15521. [PubMed: 24043817]
- (66). Wensink PC; Finnegan DJ; Donelson JE; Hogness DS A system for mapping DNA sequences in the chromosomes of *Drosophila melanogaster*. *Cell* 1974, 3 (4), 315. [PubMed: 4216403]
- (67). Chang AC; Nunberg JH; Kaufman RJ; Erlich HA; Schimke RT; Cohen SN Phenotypic expression in *D. coli* of a DNA sequence coding for mouse dihydrofolate reductase. *Nature* 1978, 275 (5681), 617. [PubMed: 360074]
- (68). Wigler M; Sweet R; Sim GK; Wold B; Pellicer A; Lacy E; Maniatis T; Silverstein S; Axel R Transformation of mammalian cells with genes from procaryotes and eucaryotes. *Cell* 1979, 16 (4), 777. [PubMed: 222468]
- (69). Wigler M; Pellicer A; Silverstein S; Axel R; Urlaub G; Chasin L DNA-Mediated Transfer of the Adenine Phosphoribosyltransferase Locus into Mammalian-Cells. *P Natl Acad Sci USA* 1979, 76 (3), 1373.
- (70). Mertz JE; Gurdon JB Purified Dnas Are Transcribed after Microinjection into *Xenopus* Oocytes. *P Natl Acad Sci USA* 1977, 74 (4), 1502.
- (71). Anderson WF; Killos L; Sandershaigh L; Kretschmer PJ; Diacumakos EG Replication and Expression of Thymidine Kinase and Human Globin Genes Micro-Injected into Mouse Fibroblasts. *P Natl Acad Sci-Biol* 1980, 77 (9), 5399.
- (72). Capecchi MR High efficiency transformation by direct microinjection of DNA into cultured mammalian cells. *Cell* 1980, 22 (2 Pt 2), 479. [PubMed: 6256082]
- (73). Cohen SN; Miller CA Multiple Molecular Species of Circular R-Factor DNA Isolated from *Escherichia-Coli*. *Nature* 1969, 224 (5226), 1273. [PubMed: 4902321]
- (74). Tsoi M; Do TT; Tang V; Aguilera JA; Perry CC; Milligan JR Characterization of condensed plasmid DNA models for studying the direct effect of ionizing radiation. *Biophys Chem* 2010, 147 (3), 104. [PubMed: 20096988]
- (75). Tang MX; Szoka FC The influence of polymer structure on the interactions of cationic polymers with DNA and morphology of the resulting complexes. *Gene Ther* 1997, 4 (8), 823. [PubMed: 9338011]
- (76). Vijayanathan V; Thomas T; Shirahata A; Thomas TJ DNA condensation by polyamines: A laser light scattering study of structural effects. *Biochemistry* 2001, 40 (45), 13644. [PubMed: 11695913]
- (77). Catanese DJ; Fogg JM; Schrock DE; Gilbert BE; Zechiedrich L Supercoiled Minivector DNA resists shear forces associated with gene therapy delivery. *Gene Ther* 2012, 19 (1), 94. [PubMed: 21633394]
- (78). Hornstein BD; Roman D; Arevalo-Soliz LM; Engevik MA; Zechiedrich L Effects of Circular DNA Length on Transfection Efficiency by Electroporation into HeLa Cells. *Plos One* 2016, 11 (12).
- (79). Stephenson ML; Zamecnik PC Inhibition of Rous-Sarcoma Viral-Rna Translation by a Specific Oligodeoxyribonucleotide. *P Natl Acad Sci USA* 1978, 75 (1), 285.
- (80). Izant JG; Weintraub H Inhibition of Thymidine Kinase Gene-Expression by Anti-Sense Rna - a Molecular Approach to Genetic-Analysis. *Cell* 1984, 36 (4), 1007. [PubMed: 6323013]
- (81). Rosenberg UB; Preiss A; Seifert E; Jackle H; Knipple DC Production of Phenocopies by Kruppel Antisense Rna Injection into *Drosophila* Embryos. *Nature* 1985, 313 (6004), 703. [PubMed: 2579337]
- (82). Knecht DA; Loomis WF Antisense Rna Inactivation of Myosin Heavy-Chain Gene-Expression in *Dictyostelium-Discoideum*. *Science* 1987, 236 (4805), 1081. [PubMed: 3576221]
- (83). Marwick C First "Antisense" drug will treat CMV retinitis. *Jama-J Am Med Assoc* 1998, 280 (10), 871.
- (84). de Smet MD; Meenken CJ; van den Horn GJ Fomivirsen - a phosphorothioate oligonucleotide for the treatment of CMV retinitis. *Ocul Immunol Inflamm* 1999, 7 (3-4), 189. [PubMed: 10611727]
- (85). Fire A; Xu SQ; Montgomery MK; Kostas SA; Driver SE; Mello CC Potent and specific genetic interference by double-stranded RNA in *Caenorhabditis elegans*. *Nature* 1998, 391 (6669), 806. [PubMed: 9486653]

- (86). Elbashir SM; Harborth J; Lendeckel W; Yalcin A; Weber K; Tuschl T Duplexes of 21-nucleotide RNAs mediate RNA interference in cultured mammalian cells. *Nature* 2001, 411 (6836), 494. [PubMed: 11373684]
- (87). Lee RC; Feinbaum RL; Ambros V The C-Elegans Heterochronic Gene Lin-4 Encodes Small RNAs with Antisense Complementarity to Lin-14. *Cell* 1993, 75 (5), 843. [PubMed: 8252621]
- (88). Lundin KE; Gissberg O; Smith CIE Oligonucleotide Therapies: The Past and the Present. *Hum Gene Ther* 2015, 26 (8), 475. [PubMed: 26160334]
- (89). Schroeder A; Levins CG; Cortez C; Langer R; Anderson DG Lipid-based nanotherapeutics for siRNA delivery. *J Intern Med* 2010, 267 (1), 9. [PubMed: 20059641]
- (90). Juliano RL The delivery of therapeutic oligonucleotides. *Nucleic Acids Res* 2016, 44 (14), 6518. [PubMed: 27084936]
- (91). Crooke ST; Wang S; Vickers TA; Shen W; Liang WH Cellular uptake and trafficking of antisense oligonucleotides. *Nat Biotechnol* 2017, 35 (3), 230. [PubMed: 28244996]
- (92). Summerton J; Weller D Morpholino antisense oligomers: Design, preparation, and properties. *Antisense Nucleic A* 1997, 7 (3), 187.
- (93). Nielsen PE; Egholm M; Berg RH; Buchardt O Sequence-Selective Recognition of DNA by Strand Displacement with a Thymine-Substituted Polyamide. *Science* 1991, 254 (5037), 1497. [PubMed: 1962210]
- (94). Meade BR; Gogoi K; Hamil AS; Palm-Apergi C; Berg A; Hagopian JC; Springer AD; Eguchi A; Kacsinta AD; Dowdy CF et al. Efficient delivery of RNAi prodrugs containing reversible charge-neutralizing phosphotriester backbone modifications. *Nat Biotechnol* 2014, 32 (12), 1256. [PubMed: 25402614]
- (95). Dowdy SF Overcoming cellular barriers for RNA therapeutics. *Nat Biotechnol* 2017, 35 (3), 222. [PubMed: 28244992]
- (96). Stewart MP; Lorenz A; Dahlman J; Sahay G Challenges in carrier-mediated intracellular delivery: moving beyond endosomal barriers. *Wires Nanomed Nanobi* 2016, 8 (3), 465.
- (97). Yang B; Ming X; Cao C; Laing B; Yuan A; Porter MA; Hull-Ryde EA; Maddry J; Suto M; Janzen WP et al. High-throughput screening identifies small molecules that enhance the pharmacological effects of oligonucleotides. *Nucleic Acids Res* 2015, 43 (4), 1987. [PubMed: 25662226]
- (98). Kanasty R; Dorkin JR; Vegas A; Anderson D Delivery materials for siRNA therapeutics. *Nat Mater* 2013, 12 (11), 967. [PubMed: 24150415]
- (99). Liu YM; Kuan CT; Mi J; Zhang XW; Clary BM; Bigner DD; Sullenger BA Aptamers selected against the unglycosylated EGFRvIII ectodomain and delivered intracellularly reduce membrane-bound EGFRvIII and induce apoptosis. *Biological chemistry* 2009, 390 (2), 137. [PubMed: 19040357]
- (100). Leung AKK; Tam YYC; Cullis PR Lipid Nanoparticles for Short Interfering RNA Delivery. *Nonviral Vectors for Gene Therapy Lipid- and Polymer-Based Gene Transfer* 2014, 88, 71.
- (101). McManus MT; Haines BB; Dillon CP; Whitehurst CE; van Parijs L; Chen JZ; Sharp PA Small interfering RNA-mediated gene silencing in T lymphocytes. *J Immunol* 2002, 169 (10), 5754. [PubMed: 12421955]
- (102). Merkerova M; Klamova H; Brdicka R; Bruchova H Targeting of gene expression by siRNA in CML primary cells. *Mol Biol Rep* 2007, 34 (1), 27. [PubMed: 17094012]
- (103). Wiese M; Castiglione K; Hensel M; Schleicher U; Bogdan C; Jantsch J Small interfering RNA (siRNA) delivery into murine bone marrow-derived macrophages by electroporation. *J Immunol Methods* 2010, 353 (1–2), 102. [PubMed: 20006615]
- (104). Chabot S; Teissie J; Golzio M Targeted electro-delivery of oligonucleotides for RNA interference: siRNA and anti-miR. *Adv Drug Deliver Rev* 2015, 81, 161.
- (105). Garcia-Sanchez A; Marques-Garcia F Gene Silencing Delivery Methods: Lipid-Mediated and Electroporation Transfection Protocols. *Methods Mol Biol* 2016, 1434, 139. [PubMed: 27300536]
- (106). Tasfaout H; Buono S; Guo S; Kretz C; Messaddeq N; Booten S; Greenlee S; Monia BP; Cowling BS; Laporte J Antisense oligonucleotide-mediated Dnm2 knockdown prevents and reverts myotubular myopathy in mice. *Nat Commun* 2017, 8, 15661. [PubMed: 28589938]

- (107). Brito JLR; Davies FE; Gonzalez D; Morgan GJ Streptolysin-O reversible permeabilisation is an effective method to transfect siRNAs into myeloma cells. *J Immunol Methods* 2008, 333 (1–2), 147. [PubMed: 18299137]
- (108). Zhou P; Ma X; Iyer L; Chaulagain C; Comenzo RL One siRNA pool targeting the lambda constant region stops lambda light-chain production and causes terminal endoplasmic reticulum stress. *Blood* 2014, 123 (22), 3440. [PubMed: 24723680]
- (109). Brachet J; Huez G; Hubert E Microinjection of Rabbit Hemoglobin Messenger-Rna into Amphibian Oocytes and Embryos. *P Natl Acad Sci USA* 1973, 70 (2), 543.
- (110). Woodland HR; Gurdon JB; Lingrel JB The translation of mammalian globin mRNA injected into fertilized eggs of *Xenopus laevis*. II. The distribution of globin synthesis in different tissues. *Dev Biol* 1974, 39 (1), 134. [PubMed: 4857973]
- (111). Gurdon JB; Woodland HR; Lingrel JB The translation of mammalian globin mRNA injected into fertilized eggs of *Xenopus laevis* I. Message stability in development. *Dev Biol* 1974, 39 (1), 125. [PubMed: 4471721]
- (112). Mizutani S; Colonno RJ In vitro synthesis of an infectious RNA from cDNA clones of human rhinovirus type 14. *J Virol* 1985, 56 (2), 628. [PubMed: 2997483]
- (113). Vanderwerf S; Bradley J; Wimmer E; Studier FW; Dunn JJ Synthesis of Infectious Poliovirus Rna by Purified T7 Rna-Polymerase. *P Natl Acad Sci USA* 1986, 83 (8), 2330.
- (114). Malone RW; Felgner PL; Verma IM Cationic liposome-mediated RNA transfection. *Proc Natl Acad Sci U S A* 1989, 86 (16), 6077. [PubMed: 2762315]
- (115). Lai CJ; Zhao B; Hori H; Bray M Infectious Rna Transcribed from Stably Cloned Full-Length Cdna of Dengue Type-4 Virus. *P Natl Acad Sci USA* 1991, 88 (12), 5139.
- (116). Islam MA; Reesor EK; Xu Y; Zope HR; Zetter BR; Shi J Biomaterials for mRNA delivery. *Biomater Sci* 2015, 3 (12), 1519. [PubMed: 26280625]
- (117). Gallie DR The cap and poly(A) tail function synergistically to regulate mRNA translational efficiency. *Genes Dev* 1991, 5 (11), 2108. [PubMed: 1682219]
- (118). Yokoe H; Meyer T Spatial dynamics of GFP-tagged proteins investigated by local fluorescence enhancement. *Nat Biotechnol* 1996, 14 (10), 1252. [PubMed: 9631088]
- (119). Tavernier G; Andries O; Demeester J; Sanders NN; De Smedt SC; Rejman J mRNA as gene therapeutic: How to control protein expression. *Journal of Controlled Release* 2011, 150 (3), 238. [PubMed: 20970469]
- (120). Yamamoto A; Kormann M; Rosenecker J; Rudolph C Current prospects for mRNA gene delivery. *European journal of pharmaceutics and biopharmaceutics : official journal of Arbeitsgemeinschaft fur Pharmazeutische Verfahrenstechnik e.V* 2009, 71 (3), 484. [PubMed: 18948192]
- (121). Barrett LE; Sul JY; Takano H; Van Bockstaele EJ; Haydon PG; Eberwine JH Region-directed phototransfection reveals the functional significance of a dendritically synthesized transcription factor. *Nat Methods* 2006, 3 (6), 455. [PubMed: 16721379]
- (122). Sahin U; Kariko K; Tureci O mRNA-based therapeutics - developing a new class of drugs. *Nat Rev Drug Discov* 2014, 13 (10), 759. [PubMed: 25233993]
- (123). Gilboa E; Vieweg J Cancer immunotherapy with mRNA-transfected dendritic cells. *Immunol Rev* 2004, 199 (1), 251. [PubMed: 15233739]
- (124). Zhao YB; Zheng ZL; Cohen CJ; Gattinoni L; Palmer DC; Restifo NP; Rosenberg SA; Morgan RA High-efficiency transfection of primary human and mouse T lymphocytes using RNA electroporation. *Mol Ther* 2006, 13 (1), 151. [PubMed: 16140584]
- (125). Kranz LM; Diken M; Haas H; Kreiter S; Loquai C; Reuter KC; Meng M; Fritz D; Vascotto F; Hefesha H et al. Systemic RNA delivery to dendritic cells exploits antiviral defence for cancer immunotherapy. *Nature* 2016, 534 (7607), 396. [PubMed: 27281205]
- (126). Barrett DM; Zhao YB; Liu XJ; Jiang SG; Carpenito C; Kalos M; Carroll RG; June CH; Grupp SA Treatment of Advanced Leukemia in Mice with mRNA Engineered T Cells. *Hum Gene Ther* 2011, 22 (12), 1575. [PubMed: 21838572]
- (127). Van Tendeloo VFI; Ponsaerts P; Lardon F; Nijs G; Lenjou M; Van Broeckhoven C; Van Bockstaele DR; Berneman ZN Highly efficient gene delivery by mRNA electroporation in human hematopoietic cells: superiority to lipofection and passive pulsing of mRNA and to

- electroporation of plasmid cDNA for tumor antigen loading of dendritic cells. *Blood* 2001, 98 (1), 49. [PubMed: 11418462]
- (128). Van Meirvenne S; Straetman L; Heirman C; Dullaers M; De Greef C; Van Tendeloo V; Thielemans K Efficient genetic modification of murine dendritic cells by electroporation with mRNA. *Cancer Gene Ther* 2002, 9 (9), 787. [PubMed: 12189529]
- (129). Benteyn D; Van Nuffel AMT; Wilgenhof S; Bonehill A Single-Step Antigen Loading and Maturation of Dendritic Cells Through mRNA Electroporation of a Tumor-Associated Antigen and a TriMix of Costimulatory Molecules. *Cancer Vaccines: Methods and Protocols* 2014, 1139, 3.
- (130). Kauffman KJ; Webber MJ; Anderson DG Materials for Non-viral intracellular delivery of messenger RNA therapeutics. *Journal of controlled release : official journal of the Controlled Release Society* 2015.
- (131). Gopal A; Zhou ZH; Knobler CM; Gelbart WM Visualizing large RNA molecules in solution. *Rna* 2012, 18 (2), 284. [PubMed: 22190747]
- (132). Kormann MSD; Hasenpusch G; Aneja MK; Nica G; Flemmer AW; Herber-Jonat S; Huppmann M; Mays LE; Illenyi M; Schams Aet al. Expression of therapeutic proteins after delivery of chemically modified mRNA in mice. *Nat Biotechnol* 2011, 29 (2), 154. [PubMed: 21217696]
- (133). Rothemund PWK Folding DNA to create nanoscale shapes and patterns. *Nature* 2006, 440 (7082), 297. [PubMed: 16541064]
- (134). Tian Y; Wang T; Liu WY; Xin HL; Li HL; Ke YG; Shih WM; Gang O Prescribed nanoparticle cluster architectures and low-dimensional arrays built using octahedral DNA origami frames. *Nature nanotechnology* 2015, 10 (7), 637.
- (135). Bhatia D; Arumugam S; Nasilowski M; Joshi H; Wunder C; Chambon V; Prakash V; Grazon C; Nadal B; Maiti PKet al. Quantum dot-loaded monofunctionalized DNA icosahedra for single-particle tracking of endocytic pathways. *Nature nanotechnology* 2016, 11 (12), 1112.
- (136). Zancchi FC; Manzo C; Alvarez AS; Derr ND; Garcia-Parajo MF; Lakadamyali M A DNA origami platform for quantifying protein copy number in super-resolution. *Nat Methods* 2017, 14 (8), 789. [PubMed: 28650478]
- (137). Tyagi S; Kramer FR Molecular beacons: Probes that fluoresce upon hybridization. *Nat Biotechnol* 1996, 14 (3), 303. [PubMed: 9630890]
- (138). Tan W; Wang K; Drake TJ Molecular beacons. *Curr Opin Chem Biol* 2004, 8 (5), 547. [PubMed: 15450499]
- (139). Hamaguchi N; Ellington A; Stanton M Aptamer beacons for the direct detection of proteins. *Anal Biochem* 2001, 294 (2), 126. [PubMed: 11444807]
- (140). Lee JF; Stovall GM; Ellington AD Aptamer therapeutics advance. *Current Opinion in Chemical Biology* 2006, 10 (3), 282. [PubMed: 16621675]
- (141). Song SP; Wang LH; Li J; Zhao JL; Fan CH Aptamer-based biosensors. *Trac-Trend Anal Chem* 2008, 27 (2), 108.
- (142). Iliuk AB; Hu LH; Tao WA Aptamer in Bioanalytical Applications. *Anal Chem* 2011, 83 (12), 4440. [PubMed: 21524128]
- (143). Siegart I; Schatz V; Prechtel AT; Steinkasserer A; Bogdan C; Jantsch J Electroporation of siRNA into Mouse Bone Marrow-Derived Macrophages and Dendritic Cells. *Electroporation Protocols: Preclinical and Clinical Gene Medicine, 2nd Edition* 2014, 1121, 111.
- (144). Jensen K; Anderson JA; Glass EJ Comparison of small interfering RNA (siRNA) delivery into bovine monocyte-derived macrophages by transfection and electroporation (vol 1,). *Vet Immunol Immunop* 2014, 158 (3–4), 224.
- (145). He W; Bennett MJ; Luistro L; Carvajal D; Nevins T; Smith M; Tyagi G; Cai J; Wei X; Lin TAet al. Discovery of siRNA Lipid Nanoparticles to Transfect Suspension Leukemia Cells and Provide In Vivo Delivery Capability. *Mol Ther* 2014, 22 (2), 359. [PubMed: 24002693]
- (146). Gul-Uludag H; Valencia-Serna J; Kucharski C; Marquez-Curtis LA; Jiang XY; Larratt L; Janowska-Wieczorek A; Uludag H Polymeric nanoparticle-mediated silencing of CD44 receptor in CD34(+) acute myeloid leukemia cells. *Leukemia Res* 2014, 38 (11), 1299. [PubMed: 25262448]

- (147). Peer D A daunting task: manipulating leukocyte function with RNAi. *Immunol Rev* 2013, 253 (1), 185. [PubMed: 23550647]
- (148). Freeley M; Long A Advances in siRNA delivery to T-cells: potential clinical applications for inflammatory disease, cancer and infection. *Biochem J* 2013, 455, 133. [PubMed: 24070422]
- (149). Novobrantseva TI; Borodovsky A; Wong J; Klebanov B; Zafari M; Yucius K; Querbes W; Ge P; Ruda VM; Milstein S et al. Systemic RNAi-mediated Gene Silencing in Nonhuman Primate and Rodent Myeloid Cells. *Mol Ther Nucleic Acids* 2012, 1, e4. [PubMed: 23344621]
- (150). Humbert JM; Halary F Viral and Non-Viral Methods to Genetically Modify Dendritic Cells. *Curr Gene Ther* 2012, 12 (2), 127. [PubMed: 22424555]
- (151). Zhang X; Edwards JP; Mosser DM The expression of exogenous genes in macrophages: obstacles and opportunities. *Methods Mol Biol* 2009, 531, 123. [PubMed: 19347315]
- (152). Li GB; Lu GX Gene Delivery Efficiency in Bone Marrow-derived Dendritic Cells: Comparison of Four Methods and Optimization for Lentivirus Transduction. *Molecular biotechnology* 2009, 43 (3), 250. [PubMed: 19598009]
- (153). Lee JS; Reiner NE Stable lentiviral vector-mediated gene silencing in human monocytic cell lines. *Methods Mol Biol* 2009, 531, 287. [PubMed: 19347324]
- (154). Ceppi M; Schmidt E; Pierre P Genetic modification of murine dendritic cells by RNA transfection. *Methods Mol Biol* 2009, 531, 145. [PubMed: 19347316]
- (155). Met O; Eriksen J; Svane IM Studies on mRNA electroporation of immature and mature dendritic cells: Effects on their immunogenic potential. *Molecular biotechnology* 2008, 40 (2), 151. [PubMed: 18543130]
- (156). Liu J; Gaj T; Yang Y; Wang N; Shui S; Kim S; Kanchiswamy CN; Kim JS; Barbas CF 3rd. Efficient delivery of nuclease proteins for genome editing in human stem cells and primary cells. *Nature protocols* 2015, 10 (11), 1842. [PubMed: 26492140]
- (157). Mandal Pankaj K.; Ferreira LMR; Collins R; Meissner Torsten B.; Boutwell Christian L.; Friesen M; Vrbanac V; Garrison Brian S.; Stortchevoi A; Bryder Det al. Efficient Ablation of Genes in Human Hematopoietic Stem and Effector Cells using CRISPR/Cas9. *Cell Stem Cell* 2014, 15 (5), 643. [PubMed: 25517468]
- (158). Gresch O; Altrogge L Transfection of Difficult-to-Transfect Primary Mammalian Cells. *Protein Expression in Mammalian Cells: Methods and Protocols* 2012, 801, 65.
- (159). Karra D; Dahm R Transfection Techniques for Neuronal Cells. *Journal of Neuroscience* 2010, 30 (18), 6171. [PubMed: 20445041]
- (160). Feldherr CM The intracellular distribution of ferritin following microinjection. *J Cell Biol* 1962, 12, 159. [PubMed: 13892125]
- (161). Lin TP Microinjection of Mouse Eggs. *Science* 1966, 151 (3708), 333. [PubMed: 4159338]
- (162). Paine PL; Feldherr CM Nucleocytoplasmic Exchange of Macromolecules. *Exp Cell Res* 1972, 74 (1), 81. [PubMed: 4342186]
- (163). Paine PL Nucleocytoplasmic Movement of Fluorescent Tracers Microinjected into Living Salivary-Gland Cells. *J Cell Biol* 1975, 66 (3), 652. [PubMed: 1158974]
- (164). Stacey DW; Allfrey VG Evidence for the autophagy of microinjected proteins in HeLA cells. *J Cell Biol* 1977, 75 (3), 807. [PubMed: 925081]
- (165). Kreis TE; Winterhalter KH; Birchmeier W In vivo distribution and turnover of fluorescently labeled actin microinjected into human fibroblasts. *Proc Natl Acad Sci U S A* 1979, 76 (8), 3814. [PubMed: 291042]
- (166). Feramisco JR Microinjection of fluorescently labeled alpha-actinin into living fibroblasts. *Proc Natl Acad Sci U S A* 1979, 76 (8), 3967. [PubMed: 291056]
- (167). Schlegel RA; Rechsteiner MC Microinjection of Thymidine Kinase and Bovine Serum-Albumin into Mammalian-Cells by Fusion with Red Blood-Cells. *Cell* 1975, 5 (4), 371. [PubMed: 168973]
- (168). Loyter A; Zakai N; Kulka RG Ultramicroinjection of Macromolecules or Small Particles into Animal-Cells - New Technique Based on Virus-Induced Cell-Fusion. *J Cell Biol* 1975, 66 (2), 292. [PubMed: 167032]

- (169). Furusawa M; Nishimur T; Yamaizum M; Okada Y. Injection of Foreign Substances into Single Cells by Cell-Fusion. *Nature* 1974, 249 (5456), 449. [PubMed: 4365359]
- (170). Poste G; Papahadjopoulos D Lipid Vesicles as Carriers for Introducing Materials into Cultured-Cells - Influence of Vesicle Lipid-Composition on Mechanism(S) of Vesicle Incorporation into Cells. *P Natl Acad Sci USA* 1976, 73 (5), 1603.
- (171). Gregoriadis G; Buckland RA Enzyme-containing liposomes alleviate a model for storage disease. *Nature* 1973, 244 (5412), 170. [PubMed: 4583499]
- (172). Borle AB; Snowdowne KW Measurement of Intracellular Free Calcium in Monkey Kidney-Cells with Aequorin. *Science* 1982, 217 (4556), 252. [PubMed: 6806904]
- (173). Snowdowne KW; Borle AB Measurement of Cytosolic Free Calcium in Mammalian-Cells with Aequorin. *American Journal of Physiology* 1984, 247 (5), C396. [PubMed: 6093570]
- (174). Okada CY; Rechsteiner M Introduction of Macromolecules into Cultured Mammalian-Cells by Osmotic Lysis of Pinocytic Vesicles. *Cell* 1982, 29 (1), 33. [PubMed: 6179631]
- (175). Moore MW; Carbone FR; Bevan MJ Introduction of Soluble-Protein into the Class-I Pathway of Antigen Processing and Presentation. *Cell* 1988, 54 (6), 777. [PubMed: 3261634]
- (176). Mcneil PL; Murphy RF; Lanni F; Taylor DL A Method for Incorporating Macromolecules into Adherent Cells. *J Cell Biol* 1984, 98 (4), 1556. [PubMed: 6201494]
- (177). Mcneil PL; Warder E Glass-Beads Load Macromolecules into Living Cells. *J Cell Sci* 1987, 88, 669. [PubMed: 2459146]
- (178). Clarke MSF; Mcneil PL Syringe Loading Introduces Macromolecules into Living Mammalian-Cell Cytosol. *J Cell Sci* 1992, 102, 533. [PubMed: 1506433]
- (179). Schroff RW; Bucana CD; Klein RA; Farrell MM; Morgan AC Detection of Intracytoplasmic Antigens by Flow-Cytometry. *J Immunol Methods* 1984, 70 (2), 167. [PubMed: 6373938]
- (180). Mir LM; Banoun H; Paoletti C Introduction of Definite Amounts of Nonpermeant Molecules into Living Cells after Electroporation - Direct Access to the Cytosol. *Exp Cell Res* 1988, 175 (1), 15. [PubMed: 3345798]
- (181). Chakrabarti R; Wylie DE; Schuster SM Transfer of Monoclonal-Antibodies into Mammalian-Cells by Electroporation. *J Biol Chem* 1989, 264 (26), 15494. [PubMed: 2768274]
- (182). Ahnert-Hilger G; Bader MF; Bhakdi S; Gratzl M Introduction of macromolecules into bovine adrenal medullary chromaffin cells and rat pheochromocytoma cells (PC12) by permeabilization with streptolysin O: inhibitory effect of tetanus toxin on catecholamine secretion. *J Neurochem* 1989, 52 (6), 1751. [PubMed: 2723634]
- (183). Bryant PE Induction of Chromosomal Damage by Restriction Endonuclease in Cho Cells Porated with Streptolysin-O. *Mutat Res* 1992, 268 (1), 27. [PubMed: 1378183]
- (184). Sharei A; Zoldan J; Adamo A; Sim WY; Cho N; Jackson E; Mao S; Schneider S; Han MJ; Lytton-Jean A et al. A vector-free microfluidic platform for intracellular delivery. *P Natl Acad Sci USA* 2013, 110 (6), 2082.
- (185). Shalek AK; Robinson JT; Karp ES; Lee JS; Ahn DR; Yoon MH; Sutton A; Jorgolli M; Gertner RS; Gujral T et al. Vertical silicon nanowires as a universal platform for delivering biomolecules into living cells. *P Natl Acad Sci USA* 2010, 107 (5), 1870.
- (186). Marschall ALJ; Frenzel A; Schirrmann T; Schungel M; Dubel S Targeting antibodies to the cytoplasm. *Mabs-Austin* 2011, 3 (1), 3.
- (187). Tinsley JH; Hawker J; Yuan Y Efficient protein transfection of cultured coronary venular endothelial cells. *Am J Physiol-Heart C* 1998, 275 (5), H1873.
- (188). Zelphati O; Wang Y; Kitada S; Reed JC; Felgner PL; Corbeil J Intracellular delivery of proteins with a new lipid-mediated delivery system. *J Biol Chem* 2001, 276 (37), 35103. [PubMed: 11447231]
- (189). Weill CO; Biri S; Adib A; Erbacher P A practical approach for intracellular protein delivery. *Cytotechnology* 2008, 56 (1), 41. [PubMed: 19002840]
- (190). Erazo-Oliveras A; Najjar K; Dayani L; Wang T-Y; Johnson GA; Pellois J-P Protein delivery into live cells by incubation with an endosomolytic agent. *Nat Meth* 2014, advance online publication.
- (191). Lonn P; Dowdy SF Cationic PTD/PPP-mediated macromolecular delivery: charging into the cell. *Expert Opin Drug Deliv* 2015, 1.

- (192). Liao XL; Rabideau AE; Pentelute BL Delivery of Antibody Mimics into Mammalian Cells via Anthrax Toxin Protective Antigen. *Chembiochem* 2014, 15 (16), 2458. [PubMed: 25250705]
- (193). Guillard S; Minter RR; Jackson RH Engineering therapeutic proteins for cell entry: the natural approach. *Trends Biotechnol* 2015.
- (194). Yang NJ; Liu DV; Sklaviadis D; Gui DY; Vander Heiden MG; Wittrup KD Antibody-mediated neutralization of perfringolysin o for intracellular protein delivery. *Mol Pharm* 2015, 12 (6), 1992. [PubMed: 25881713]
- (195). Ryou JH; Sohn YK; Hwang DE; Park WY; Kim N; Heo WD; Kim MY; Kim HS Engineering of bacterial exotoxins for highly efficient and receptor-specific intracellular delivery of diverse cargos. *Biotechnol Bioeng* 2016.
- (196). Beilhartz GL; Sugiman-Marangos SN; Melnyk RA Repurposing bacterial toxins for intracellular delivery of therapeutic proteins. *Biochem Pharmacol* 2017.
- (197). Gu Z; Biswas A; Zhao MX; Tang Y Tailoring nanocarriers for intracellular protein delivery. *Chemical Society reviews* 2011, 40 (7), 3638. [PubMed: 21566806]
- (198). Lu Y; Sun WJ; Gu Z Stimuli-responsive nanomaterials for therapeutic protein delivery. *Journal of Controlled Release* 2014, 194, 1. [PubMed: 25151983]
- (199). Ray M; Lee YW; Scaletti F; Yu R; Rotello VM Intracellular delivery of proteins by nanocarriers. *Nanomedicine (Lond)* 2017.
- (200). Marschall ALJ; Zhang CC; Frenzel A; Schirrmann T; Hust M; Perez F; Dubel S Delivery of antibodies to the cytosol Debunking the myths. *Mabs-Austin* 2014, 6 (4), 943.
- (201). Choi YS; David AE Cell Penetrating Peptides and the Mechanisms for Intracellular Entry. *Curr Pharm Biotechnol* 2014.
- (202). Bechara C; Sagan S Cell-penetrating peptides: 20 years later, where do we stand? *Febs Letters* 2013, 587 (12), 1693. [PubMed: 23669356]
- (203). DeWitt MA; Corn JE; Carroll D Genome editing via delivery of Cas9 ribonucleoprotein. *Methods* 2017.
- (204). Helma J; Cardoso MC; Muyltermans S; Leonhardt H Nanobodies and recombinant binders in cell biology. *J Cell Biol* 2015, 209 (5), 633. [PubMed: 26056137]
- (205). Rothbauer U; Zolghadr K; Tillib S; Nowak D; Schermelleh L; Gahl A; Backmann N; Conrath K; Muyltermans S; Cardoso MC et al. Targeting and tracing antigens in live cells with fluorescent nanobodies. *Nat Methods* 2006, 3 (11), 887. [PubMed: 17060912]
- (206). Fu AL; Tang R; Hardie J; Farkas ME; Rotello VM Promises and Pitfalls of Intracellular Delivery of Proteins. *Bioconjugate Chem* 2014, 25 (9), 1602.
- (207). Leader B; Baca QJ; Golan DE Protein therapeutics: A summary and pharmacological classification. *Nat Rev Drug Discov* 2008, 7 (1), 21. [PubMed: 18097458]
- (208). Dimitrov DS Therapeutic proteins. *Methods Mol Biol* 2012, 899, 1. [PubMed: 22735943]
- (209). Uhlen M; Fagerberg L; Hallstrom BM; Lindskog C; Oksvold P; Mardinoglu A; Sivertsson A; Kampf C; Sjostedt E; Asplund A et al. Tissue-based map of the human proteome. *Science* 2015, 347 (6220).
- (210). Kim KW; Kim SH; Jang JH; Lee EY; Park SW; Um JH; Lee YJ; Lee CH; Yoon S; Seo SY et al. Dendritic cells loaded with exogenous antigen by electroporation can enhance MHC class I-mediated antitumor immunity. *Cancer Immunol Immunother* 2004, 53 (4), 315. [PubMed: 14685778]
- (211). Weiss JM; Allen C; Shivakumar R; Feller S; Li LH; Liu LN Efficient responses in a murine renal tumor model by electroloading dendritic cells with whole-tumor lysate. *J Immunother* 2005, 28 (6), 542. [PubMed: 16224271]
- (212). Kamigaki T; Kaneko T; Naitoh K; Takahara M; Kondo T; Ibe H; Matsuda E; Maekawa R; Goto S Immunotherapy of Autologous Tumor Lysate-loaded Dendritic Cell Vaccines by a Closed-flow Electroporation System for Solid Tumors. *Anticancer Res* 2013, 33 (7), 2971. [PubMed: 23780988]
- (213). Wolfrum LA; Takahara M; Viley AM; Shivakumar R; Nieda M; Maekawa R; Liu LN; Peshwa MV Clinical scale electroloading of mature dendritic cells with melanoma whole tumor cell lysate is superior to conventional lysate co-incubation in triggering robust in vitro expansion of functional antigen-specific CTL. *Int Immunopharmacol* 2013, 15 (3), 488. [PubMed: 23474736]

- (214). Jinek M; Chylinski K; Fonfara I; Hauer M; Doudna JA; Charpentier E A Programmable Dual-RNA-Guided DNA Endonuclease in Adaptive Bacterial Immunity. *Science* 2012, 337 (6096), 816. [PubMed: 22745249]
- (215). Ran FA; Hsu PD; Wright J; Agarwala V; Scott DA; Zhang F Genome engineering using the CRISPR-Cas9 system. *Nature protocols* 2013, 8 (11), 2281. [PubMed: 24157548]
- (216). Shao YJ; Guan YT; Wang LR; Qiu ZW; Liu MZ; Chen YT; Wu LJ; Li YM; Ma XY; Liu MY et al. CRISPR/Cas-mediated genome editing in the rat via direct injection of one-cell embryos. *Nature protocols* 2014, 9 (10), 2493. [PubMed: 25255092]
- (217). Sung YH; Kim JM; Kim HT; Lee J; Jeon J; Jin Y; Choi JH; Ban YH; Ha SJ; Kim CH et al. Highly efficient gene knockout in mice and zebrafish with RNA-guided endonucleases. *Genome research* 2014, 24 (1), 125. [PubMed: 24253447]
- (218). Kim S; Kim D; Cho SW; Kim J; Kim JS Highly efficient RNA-guided genome editing in human cells via delivery of purified Cas9 ribonucleoproteins. *Genome research* 2014, 24 (6), 1012. [PubMed: 24696461]
- (219). Schumann K; Lin S; Boyer E; Simeonov DR; Subramaniam M; Gate RE; Haliburton GE; Yee CJ; Bluestone JA; Doudna JA et al. Generation of knock-in primary human T cells using Cas9 ribonucleoproteins. *P Natl Acad Sci USA* 2015, 112 (33), 10437.
- (220). Liang XQ; Potter J; Kumar S; Zou YF; Quintanilla R; Sridharan M; Carte J; Chen W; Roark N; Ranganathan S et al. Rapid and highly efficient mammalian cell engineering via Cas9 protein transfection. *J Biotechnol* 2015, 208, 44. [PubMed: 26003884]
- (221). Hendel A; Bak RO; Clark JT; Kennedy AB; Ryan DE; Roy S; Steinfeld I; Lunstad BD; Kaiser RJ; Wilkens AB et al. Chemically modified guide RNAs enhance CRISPR-Cas genome editing in human primary cells. *Nat Biotechnol* 2015, 33 (9), 985. [PubMed: 26121415]
- (222). Lin S; Staahl B; Alla RK; Doudna JA Enhanced homology-directed human genome engineering by controlled timing of CRISPR/Cas9 delivery. *Elife* 2014, 3.
- (223). Moreno-Mateos MA; Vejnár CE; Beaudoin JD; Fernandez JP; Mis EK; Khokha MK; Giraldez AJ CRISPRscan: designing highly efficient sgRNAs for CRISPR-Cas9 targeting in vivo. *Nat Methods* 2015, 12 (10), 982. [PubMed: 26322839]
- (224). Jacobi AM; Rettig GR; Turk R; Collingwood MA; Zeiner SA; Quadros RM; Harms DW; Bonthuis PJ; Gregg C; Ohtsuka M et al. Simplified CRISPR tools for efficient genome editing and streamlined protocols for their delivery into mammalian cells and mouse zygotes. *Methods* 2017, 121, 16. [PubMed: 28351759]
- (225). Zuris JA; Thompson DB; Shu Y; Guilinger JP; Bessen JL; Hu JH; Maeder ML; Joung JK; Chen ZY; Liu DR Cationic lipid-mediated delivery of proteins enables efficient protein-based genome editing in vitro and in vivo. *Nat Biotechnol* 2015, 33 (1), 73. [PubMed: 25357182]
- (226). D'Astolfo DS; Pagliero RJ; Pras A; Karthaus WR; Clevers H; Prasad V; Lebbink RJ; Rehmann H; Geijsen N Efficient Intracellular Delivery of Native Proteins. *Cell* 2015, 161 (3), 674. [PubMed: 25910214]
- (227). Han X; Liu Z; Ma Y; Zhang K; Qin L Cas9 Ribonucleoprotein Delivery via Microfluidic Cell-Deformation Chip for Human T-Cell Genome Editing and Immunotherapy. *Advanced Biosystems* 2017, 1 (1–2), 1600007.
- (228). Ramakrishna S; Dad AK; Beloor J; Gopalappa R; Lee SK; Kim H Gene disruption by cell-penetrating peptide-mediated delivery of Cas9 protein and guide RNA. *Genome research* 2014, 24 (6), 1020. [PubMed: 24696462]
- (229). Nishimasu H; Ran FA; Hsu PD; Konermann S; Shehata SI; Dohmae N; Ishitani R; Zhang F; Nureki O Crystal Structure of Cas9 in Complex with Guide RNA and Target DNA. *Cell* 2014, 156 (5), 935. [PubMed: 24529477]
- (230). Jinek M; Jiang FG; Taylor DW; Sternberg SH; Kaya E; Ma EB; Anders C; Hauer M; Zhou KH; Lin S et al. Structures of Cas9 Endonucleases Reveal RNA-Mediated Conformational Activation. *Science* 2014, 343 (6176), 1215.
- (231). Yin H; Kauffman KJ; Anderson DG Delivery technologies for genome editing. *Nat Rev Drug Discov* 2017.

- (232). Wang H-X; Li M; Lee CM; Chakraborty S; Kim H-W; Bao G; Leong KW CRISPR/Cas9-Based Genome Editing for Disease Modeling and Therapy: Challenges and Opportunities for Nonviral Delivery. *Chem Rev* 2017.
- (233). Bruns AM; Leser GP; Lamb RA; Horvath CM The Innate Immune Sensor LGP2 Activates Antiviral Signaling by Regulating MDA5-RNA Interaction and Filament Assembly. *Molecular Cell* 2014, 55 (5), 771. [PubMed: 25127512]
- (234). Ma H; Marti-Gutierrez N; Park SW; Wu J; Lee Y; Suzuki K; Koski A; Ji D; Hayama T; Ahmed Ret al. Correction of a pathogenic gene mutation in human embryos. *Nature* 2017, 548 (7668), 413. [PubMed: 28783728]
- (235). Sarma VR; Silverto Ew; Davies DR; Terry WD 3-Dimensional Structure at 6 Å Resolution of a Human Gamma G1 Immunoglobulin Molecule. *J Biol Chem* 1971, 246 (11), 3753. [PubMed: 5578919]
- (236). Yin T; Bader AR; Hou TK; Maron BA; Kao DD; Qian R; Kohane DS; Handy DE; Loscalzo J; Zhang YY SDF-1 alpha in Glycan Nanoparticles Exhibits Full Activity and Reduces Pulmonary Hypertension in Rats. *Biomacromolecules* 2013, 14 (11), 4009. [PubMed: 24059347]
- (237). McNaughton BR; Cronican JJ; Thompson DB; Liu DR Mammalian cell penetration, siRNA transfection, and DNA transfection by supercharged proteins. *Proc Natl Acad Sci U S A* 2009, 106 (15), 6111. [PubMed: 19307578]
- (238). Vives E; Brodin P; Lebleu B A truncated HIV-1 Tat protein basic domain rapidly translocates through the plasma membrane and accumulates in the cell nucleus. *J Biol Chem* 1997, 272 (25), 16010. [PubMed: 9188504]
- (239). Venslauskas MS; Satkauskas S Mechanisms of transfer of bioactive molecules through the cell membrane by electroporation. *European Biophysics Journal with Biophysics Letters* 2015, 44 (5), 277. [PubMed: 25939984]
- (240). Rezaei T; Bock JE; Zhou MV; Kalyanaraman C; Lokey RS; Jacobson MP Conformational flexibility, internal hydrogen bonding, and passive membrane permeability: Successful in silico prediction of the relative permeabilities of cyclic peptides. *J Am Chem Soc* 2006, 128 (43), 14073. [PubMed: 17061890]
- (241). Bockus AT; McEwen CM; Lokey RS Form and Function in Cyclic Peptide Natural Products: A Pharmacokinetic Perspective. *Curr Top Med Chem* 2013, 13 (7), 821. [PubMed: 23578026]
- (242). Passioura T; Katoh T; Goto Y; Suga H Selection-Based Discovery of Druglike Macrocyclic Peptides. *Annu Rev Biochem* 2014, 83, 727. [PubMed: 24580641]
- (243). Hewitt WM; Leung SS; Pye CR; Ponkey AR; Bednarek M; Jacobson MP; Lokey RS Cell-permeable cyclic peptides from synthetic libraries inspired by natural products. *J Am Chem Soc* 2015, 137 (2), 715. [PubMed: 25517352]
- (244). Chu Q; Moellering RE; Hilinski GJ; Kim YW; Grossmann TN; Yeh JTH; Verdine GL Towards understanding cell penetration by stapled peptides. *Medchemcomm* 2015, 6 (1), 111.
- (245). Yang NJ; Hinner MJ Getting across the cell membrane: an overview for small molecules, peptides, and proteins. *Methods Mol Biol* 2015, 1266, 29. [PubMed: 25560066]
- (246). Schafmeister CE; Po J; Verdine GL An all-hydrocarbon cross-linking system for enhancing the helicity and metabolic stability of peptides. *J Am Chem Soc* 2000, 122 (24), 5891.
- (247). Verdine GL; Hilinski GJ Stapled Peptides for Intracellular Drug Targets. *Methods in Enzymology: Protein Engineering for Therapeutics, Vol 203, Pt B* 2012, 503, 3.
- (248). Moellering RE; Cornejo M; Davis TN; Del Bianco C; Aster JC; Blacklow SC; Kung AL; Gilliland DG; Verdine GL; Bradner JE Direct inhibition of the NOTCH transcription factor complex. *Nature* 2009, 462 (7270), 182. [PubMed: 19907488]
- (249). Drews J Drug discovery: A historical perspective. *Science* 2000, 287 (5460), 1960. [PubMed: 10720314]
- (250). Lipinski CA; Lombardo F; Dominy BW; Feeney PJ Experimental and computational approaches to estimate solubility and permeability in drug discovery and development settings. *Adv Drug Deliver Rev* 1997, 23 (1–3), 3.
- (251). Keller TH; Pichota A; Yin Z A practical view of ‘druggability’. *Current Opinion in Chemical Biology* 2006, 10 (4), 357. [PubMed: 16814592]

- (252). Yun J; Mullarky E; Lu CY; Bosch KN; Kavalier A; Rivera K; Roper J; Chio IIC; Giannopoulou EG; Rago C et al. Vitamin C selectively kills KRAS and BRAF mutant colorectal cancer cells by targeting GAPDH. *Science* 2015, 350 (6266), 1391. [PubMed: 26541605]
- (253). Williams AC; Barry BW Penetration enhancers. *Adv Drug Deliver Rev* 2004, 56 (5), 603.
- (254). Orłowski S; Belehradec J Jr.; Paoletti C; Mir LM Transient electroporation of cells in culture. Increase of the cytotoxicity of anticancer drugs. *Biochem Pharmacol* 1988, 37 (24), 4727. [PubMed: 2462423]
- (255). Gothelf A; Mir LM; Gehl J Electrochemotherapy: results of cancer treatment using enhanced delivery of bleomycin by electroporation. *Cancer Treat Rev* 2003, 29 (5), 371. [PubMed: 12972356]
- (256). Li XH; Gao XH; Shi W; Ma HM Design Strategies for Water-Soluble Small Molecular Chromogenic and Fluorogenic Probes. *Chem Rev* 2014, 114 (1), 590. [PubMed: 24024656]
- (257). Minta A; Tsien RY Fluorescent Indicators for Cytosolic Sodium. *J Biol Chem* 1989, 264 (32), 19449. [PubMed: 2808435]
- (258). Kasner SE; Ganz MB Regulation of Intracellular Potassium in Mesangial Cells - a Fluorescence Analysis Using the Dye, PBFI. *American Journal of Physiology* 1992, 262 (3), F462. [PubMed: 1558163]
- (259). Heffern MC; Matosziuk LM; Meade TJ Lanthanide Probes for Bioresponsive Imaging. *Chem Rev* 2014, 114 (8), 4496. [PubMed: 24328202]
- (260). Gahlaut N; Miller LW Time-Resolved Microscopy for Imaging Lanthanide Luminescence in Living Cells. *Cytom Part A* 2010, 77A (12), 1113.
- (261). Rajapakse HE; Gahlaut N; Mohandessi S; Yu D; Turner JR; Miller LW Time-resolved luminescence resonance energy transfer imaging of protein-protein interactions in living cells. *P Natl Acad Sci USA* 2010, 107 (31), 13582.
- (262). Beattie GM; Crowe JH; Lopez AD; Cirulli V; Ricordi C; Hayek A Trehalose: A cryoprotectant that enhances recovery and preserves function of human pancreatic islets after long-term storage. *Diabetes* 1997, 46 (3), 519. [PubMed: 9032112]
- (263). Eroglu A; Russo MJ; Bieganski R; Fowler A; Cheley S; Bayley H; Toner M Intracellular trehalose improves the survival of cryopreserved mammalian cells. *Nat Biotechnol* 2000, 18 (2), 163. [PubMed: 10657121]
- (264). He XM; Amin AA; Fowler A; Toner M Thermally induced introduction of trehalose into primary rat hepatocytes. *Cell Preserv Technol* 2006, 4 (3), 178.
- (265). Zhang WJ; Rong JH; Wang Q; He XM The encapsulation and intracellular delivery of trehalose using a thermally responsive nanocapsule. *Nanotechnology* 2009, 20 (27).
- (266). Acker JP; Lu XM; Young V; Cheley S; Bayley H; Fowler A; Toner M Measurement of trehalose loading of mammalian cells porated with a metal-actuated switchable pore. *Biotechnol Bioeng* 2003, 82 (5), 525. [PubMed: 12652476]
- (267). Dovgan B; Barlic A; Knezevic M; Miklavcic D Cryopreservation of Human Adipose-Derived Stem Cells in Combination with Trehalose and Reversible Electroporation. *The Journal of membrane biology* 2017, 250 (1), 1. [PubMed: 27383230]
- (268). Shirakashi R; Kostner CM; Muller KJ; Kurschner M; Zimmermann U; Sukhorukov VL Intracellular delivery of trehalose into mammalian cells by electroporation. *J Membrane Biol* 2002, 189 (1), 45. [PubMed: 12202951]
- (269). Chang LQ; Hu JM; Chen F; Chen Z; Shi JF; Yang ZG; Li YW; Lee LJ Nanoscale bio-platforms for living cell interrogation: current status and future perspectives. *Nanoscale* 2016, 8 (6), 3181. [PubMed: 26745513]
- (270). So HM; Won K; Kim YH; Kim BK; Ryu BH; Na PS; Kim H; Lee JO Single-walled carbon nanotube biosensors using aptamers as molecular recognition elements. *J Am Chem Soc* 2005, 127 (34), 11906. [PubMed: 16117506]
- (271). Heller DA; Baik S; Eurell TE; Strano MS Single-walled carbon nanotube spectroscopy in live cells: Towards long-term labels and optical sensors. *Adv Mater* 2005, 17 (23), 2793.
- (272). Fakhri N; Wessel AD; Willms C; Pasquali M; Klopfenstein DR; MacKintosh FC; Schmidt CF High-resolution mapping of intracellular fluctuations using carbon nanotubes. *Science* 2014, 344 (6187), 1031. [PubMed: 24876498]

- (273). Derfus AM; Chan WCW; Bhatia SN Intracellular delivery of quantum dots for live cell labeling and organelle tracking. *Adv Mater* 2004, 16 (12), 961.
- (274). Michalet X; Pinaud FF; Bentolila LA; Tsay JM; Doose S; Li JJ; Sundaresan G; Wu AM; Gambhir SS; Weiss S Quantum dots for live cells, in vivo imaging, and diagnostics. *Science* 2005, 307 (5709), 538. [PubMed: 15681376]
- (275). Chinen AB; Guan CM; Ferrer JR; Barnaby SN; Merkel TJ; Mirkin CA Nanoparticle Probes for the Detection of Cancer Biomarkers, Cells, and Tissues by Fluorescence. *Chem Rev* 2015, 115 (19), 10530. [PubMed: 26313138]
- (276). Schulz A; McDonagh C Intracellular sensing and cell diagnostics using fluorescent silica nanoparticles. *Soft Matter* 2012, 8 (9), 2579.
- (277). Liu JW; Cao ZH; Lu Y Functional Nucleic Acid Sensors. *Chem Rev* 2009, 109 (5), 1948. [PubMed: 19301873]
- (278). Lee SE; Liu GL; Kim F; Lee LP Remote Optical Switch for Localized and Selective Control of Gene Interference. *Nano Lett* 2009, 9 (2), 562. [PubMed: 19128006]
- (279). Breger J; Delehanty JB; Medintz IL Continuing progress toward controlled intracellular delivery of semiconductor quantum dots. *Wiley interdisciplinary reviews. Nanomedicine and nanobiotechnology* 2014.
- (280). Hong GS; Diao SO; Antaris AL; Dai HJ Carbon Nanomaterials for Biological Imaging and Nanomedicinal Therapy. *Chem Rev* 2015, 115 (19), 10816. [PubMed: 25997028]
- (281). Ajayan PM Nanotubes from carbon. *Chem Rev* 1999, 99 (7), 1787. [PubMed: 11849010]
- (282). Zhang YB; Petibone D; Xu Y; Mahmood M; Karmakar A; Casciano D; Ali S; Biris AS Toxicity and efficacy of carbon nanotubes and graphene: the utility of carbon-based nanoparticles in nanomedicine. *Drug Metab Rev* 2014, 46 (2), 232. [PubMed: 24506522]
- (283). Holt BD; Shawky JH; Dahl KN; Davidson LA; Islam MF Distribution of single wall carbon nanotubes in the *Xenopus laevis* embryo after microinjection. *J Appl Toxicol* 2016, 36 (4), 568. [PubMed: 26510384]
- (284). Medintz IL; Uyeda HT; Goldman ER; Mattoussi H Quantum dot bioconjugates for imaging, labelling and sensing. *Nat Mater* 2005, 4 (6), 435. [PubMed: 15928695]
- (285). Courty S; Luccardini C; Bellaiche Y; Cappello G; Dahan M Tracking individual kinesin motors in living cells using single quantum-dot imaging. *Nano Lett* 2006, 6 (7), 1491. [PubMed: 16834436]
- (286). Liu BR; Huang YW; Chiang HJ; Lee HJ Cell-Penetrating Peptide-Functionalized Quantum Dots for Intracellular Delivery. *J Nanosci Nanotechnol* 2010, 10 (12), 7897.
- (287). Lee J; Sharei A; Sim WY; Adamo A; Langer R; Jensen KF; Bawendi MG Nonendocytic Delivery of Functional Engineered Nanoparticles into the Cytoplasm of Live Cells Using a Novel, High-Throughput Microfluidic Device. *Nano Lett* 2012, 12 (12), 6322. [PubMed: 23145796]
- (288). Xu JM; Teslaa T; Wu TH; Chiou PY; Teitell MA; Weiss S Nanoblade Delivery and Incorporation of Quantum Dot Conjugates into Tubulin Networks in Live Cells. *Nano Lett* 2012, 12 (11), 5669. [PubMed: 23094784]
- (289). Xiong RH; Joris F; De Cock I; Demeester J; De Smedt SC; Skirtach AG; Braeckmans K Efficient delivery of quantum dots in live cells by gold nanoparticle mediated photoporation. *Colloidal Nanoparticles for Biomedical Applications X* 2015, 9338.
- (290). Medepalli K; Alphenaar BW; Keynton RS; Sethu P A new technique for reversible permeabilization of live cells for intracellular delivery of quantum dots. *Nanotechnology* 2013, 24 (20).
- (291). Sun C; Cao ZN; Wu M; Lu C Intracellular Tracking of Single Native Molecules with Electroporation-Delivered Quantum Dots. *Anal Chem* 2014, 86 (22), 11403. [PubMed: 25341054]
- (292). Ma Y; Wang M; Li W; Zhang Z; Zhang X; Tan T; Zhang X-E; Cui Z Live cell imaging of single genomic loci with quantum dot-labeled TALEs. *Nat Commun* 2017, 8, 15318. [PubMed: 28480886]

- (293). Biju V; Itoh T; Ishikawa M Delivering quantum dots to cells: bioconjugated quantum dots for targeted and nonspecific extracellular and intracellular imaging. *Chemical Society reviews* 2010, 39 (8), 3031. [PubMed: 20508886]
- (294). Delehanty JB; Mattoussi H; Medintz IL Delivering quantum dots into cells: strategies, progress and remaining issues. *Anal Bioanal Chem* 2009, 393 (4), 1091. [PubMed: 18836855]
- (295). Baffou G; Rigneault H; Marguet D; Jullien L A critique of methods for temperature imaging in single cells. *Nat Methods* 2014, 11 (9), 899. [PubMed: 25166869]
- (296). Kucsko G; Maurer PC; Yao NY; Kubo M; Noh HJ; Lo PK; Park H; Lukin MD Nanometre-scale thermometry in a living cell. *Nature* 2013, 500 (7460), 54. [PubMed: 23903748]
- (297). Okabe K; Inada N; Gota C; Harada Y; Funatsu T; Uchiyama S Intracellular temperature mapping with a fluorescent polymeric thermometer and fluorescence lifetime imaging microscopy. *Nat Commun* 2012, 3.
- (298). Barber MA A technic for the inoculation of bacteria and other substances into living cells. *J Infect Dis* 1911, 8 (3), 348.
- (299). Korzh V; Strahle U Marshall Barber and the century of microinjection: from cloning of bacteria to cloning of everything. *Differentiation* 2002, 70 (6), 221. [PubMed: 12190984]
- (300). Briggs R; King TJ Transplantation of Living Nuclei from Blastula Cells into Enucleated Frogs Eggs. *P Natl Acad Sci USA* 1952, 38 (5), 455.
- (301). Fischberg M; Gurdon JB; Elsdale TR Nuclear Transplantation in *Xenopus Laevis*. *Nature* 1958, 181 (4606), 424.
- (302). Gurdon JB Adult Frogs Derived from Nuclei of Single Somatic Cells. *Dev Biol* 1962, 4 (2), 256. [PubMed: 13903027]
- (303). Wilmut I; Schnieke AE; McWhir J; Kind AJ; Campbell KHS Viable offspring derived from fetal and adult mammalian cells. *Nature* 1997, 385 (6619), 810. [PubMed: 9039911]
- (304). Craven L; Tuppen HA; Greggains GD; Harbottle SJ; Murphy JL; Cree LM; Murdoch AP; Chinnery PF; Taylor RW; Lightowlers RNet al. Pronuclear transfer in human embryos to prevent transmission of mitochondrial DNA disease. *Nature* 2010, 465 (7294), 82. [PubMed: 20393463]
- (305). Hiramoto Y Microinjection of Live Spermatozoa into Sea Urchin Eggs. *Exp Cell Res* 1962, 27 (3), 416. [PubMed: 13954730]
- (306). Palermo G; Joris H; Devroey P; Van Steirteghem AC Pregnancies after intracytoplasmic injection of single spermatozoon into an oocyte. *Lancet* 1992, 340 (8810), 17. [PubMed: 1351601]
- (307). Diacumakos EG Methods for micromanipulation of human somatic cells in culture. *Methods Cell Biol* 1973, 7, 287. [PubMed: 4781110]
- (308). Co DO; Borowski AH; Leung JD; van der Kaa J; Hengst S; Platenburg GJ; Pieper FR; Perez CF; Jirik FR; Drayer JI Generation of transgenic mice and germline transmission of a mammalian artificial chromosome introduced into embryos by pronuclear microinjection. *Chromosome Res* 2000, 8 (3), 183. [PubMed: 10841045]
- (309). Monteith DP; Leung JD; Borowski AH; Co DO; Praznovszky T; Jirik FR; Hadlaczy G; Perez CF Pronuclear microinjection of purified artificial chromosomes for generation of transgenic mice: pick-and-inject technique. *Methods Mol Biol* 2004, 240, 227. [PubMed: 14970413]
- (310). Knowles JK An improved microinjection technique in *Paramecium aurelia*. Transfer of mitochondria conferring erythromycin-resistance. *Exp Cell Res* 1974, 88 (1), 79. [PubMed: 4422201]
- (311). King MP; Attardi G Injection of Mitochondria into Human-Cells Leads to a Rapid Replacement of the Endogenous Mitochondrial-DNA. *Cell* 1988, 52 (6), 811. [PubMed: 3349520]
- (312). Pinkert CA; Irwin MH; Johnson LW; Moffatt RJ Mitochondria transfer into mouse ova by microinjection. *Transgenic research* 1997, 6 (6), 379. [PubMed: 9423287]
- (313). Wu TH; Teslaa T; Kalim S; French CT; Moghadam S; Wall R; Miller JF; Witte ON; Teitell MA; Chiou PY Photothermal Nanoblade for Large Cargo Delivery into Mammalian Cells. *Anal Chem* 2011, 83 (4), 1321. [PubMed: 21247066]
- (314). Wu YC; Wu TH; Clemens DL; Lee BY; Wen XM; Horwitz MA; Teitell MA; Chiou PY Massively parallel delivery of large cargo into mammalian cells with light pulses. *Nat Methods* 2015, 12 (5), 439. [PubMed: 25849636]

- (315). Wu TH; Sagullo E; Case D; Zheng X; Li YJ; Hong JS; TeSlaa T; Patananan AN; McCaffery JM; Niazi Ket al. Mitochondrial Transfer by Photothermal Nanoblade Restores Metabolite Profile in Mammalian Cells. *Cell Metab* 2016, 23 (5), 921. [PubMed: 27166949]
- (316). King MP; Attardi G Human-Cells Lacking Mtdna - Repopulation with Exogenous Mitochondria by Complementation. *Science* 1989, 246 (4929), 500. [PubMed: 2814477]
- (317). Moraes CT; Dey R; Barrientos A Transmitochondrial technology in animal cells. *Methods in Cell Biology*, Vol 65 2001, 65, 397. [PubMed: 11381606]
- (318). Fournier REK; Ruddle FH Microcell-Mediated Transfer of Murine Chromosomes into Mouse, Chinese-Hamster, and Human Somatic-Cells. *P Natl Acad Sci USA* 1977, 74 (1), 319.
- (319). Tomizuka K; Yoshida H; Uejima H; Kugoh H; Sato K; Ohguma A; Hayasaka M; Hanaoka K; Oshimura M; Ishida I Functional expression and germline transmission of a human chromosome fragment in chimaeric mice. *Nat Genet* 1997, 16 (2), 133. [PubMed: 9171824]
- (320). Kazuki Y; Hoshiya H; Takiguchi M; Abe S; Iida Y; Osaki M; Katoh M; Hiratsuka M; Shirayoshi Y; Hiramatsu Ket al. Refined human artificial chromosome vectors for gene therapy and animal transgenesis. *Gene Ther* 2011, 18 (4), 384. [PubMed: 21085194]
- (321). Tedesco FS; Hoshiya H; D'Antona G; Gerli MFM; Messina G; Antonini S; Tonlorenzi R; Benedetti S; Berghella L; Torrente Yet al. Stem Cell-Mediated Transfer of a Human Artificial Chromosome Ameliorates Muscular Dystrophy. *Sci Transl Med* 2011, 3 (96).
- (322). Tseng Y; Kole TP; Wirtz D Micromechanical mapping of live cells by multiple-particle-tracking microrheology. *Biophys J* 2002, 83 (6), 3162. [PubMed: 12496086]
- (323). Ehrenberg M; McGrath JL Binding between particles and proteins in extracts: implications for microrheology and toxicity. *Acta Biomater* 2005, 1 (3), 305. [PubMed: 16701809]
- (324). Wirtz D Particle-Tracking Microrheology of Living Cells: Principles and Applications. *Annual Review of Biophysics* 2009, 38, 301.
- (325). Thompson MS; Wirtz D Sensing Cytoskeletal Mechanics by Ballistic Intracellular Nanorheology (BIN) Coupled with Cell Transfection. *Method Cell Biol* 2008, 89, 467.
- (326). Li YX; Vanapalli SA; Duits MHG Dynamics of ballistically injected latex particles in living human endothelial cells. *Biorheology* 2009, 46 (4), 309. [PubMed: 19721192]
- (327). Wu PH; Hale CM; Chen WC; Lee JSH; Tseng Y; Wirtz D High-throughput ballistic injection nanorheology to measure cell mechanics. *Nature protocols* 2012, 7 (1), 155. [PubMed: 22222790]
- (328). Guo M; Ehrlicher AJ; Jensen MH; Renz M; Moore JR; Goldman RD; Lippincott-Schwartz J; Mackintosh FC; Weitz DA Probing the stochastic, motor-driven properties of the cytoplasm using force spectrum microscopy. *Cell* 2014, 158 (4), 822. [PubMed: 25126787]
- (329). Gomez-Martinez R; Hernandez-Pinto AM; Duch M; Vazquez P; Zinoviev K; de la Rosa EJ; Esteve J; Suarez T; Plaza JA Silicon chips detect intracellular pressure changes in living cells. *Nature nanotechnology* 2013, 8 (7), 517.
- (330). Novo S; Barrios L; Santalo J; Gomez-Martinez R; Duch M; Esteve J; Plaza JA; Nogues C; Ibanez E A novel embryo identification system by direct tagging of mouse embryos using silicon-based barcodes. *Hum Reprod* 2011, 26 (1), 96. [PubMed: 21088013]
- (331). Meacham JM; Durvasula K; Degertekin FL; Fedorov AG Physical Methods for Intracellular Delivery: Practical Aspects from Laboratory Use to Industrial-Scale Processing. *Jala-J Lab Autom* 2014, 19 (1), 1.
- (332). Mellott AJ; Forrest ML; Detamore MS Physical Non-Viral Gene Delivery Methods for Tissue Engineering. *Ann Biomed Eng* 2013, 41 (3), 446. [PubMed: 23099792]
- (333). Lakshmanan S; Gupta GK; Avci P; Chandran R; Sadasivam M; Jorge AE; Hamblin MR Physical energy for drug delivery; poration, concentration and activation. *Adv Drug Deliv Rev* 2013.
- (334). Villemejeane J; Mir LM Physical methods of nucleic acid transfer: general concepts and applications. *Brit J Pharmacol* 2009, 157 (2), 207. [PubMed: 19154421]
- (335). Mehier-Humbert S; Guy RH Physical methods for gene transfer: Improving the kinetics of gene delivery into cells. *Adv Drug Deliver Rev* 2005, 57 (5), 733.
- (336). Sahay G; Alakhova DY; Kabanov AV Endocytosis of nanomedicines. *Journal of Controlled Release* 2010, 145 (3), 182. [PubMed: 20226220]

- (337). Luo D; Saltzman WM Synthetic DNA delivery systems. *Nat Biotechnol* 2000, 18 (1), 33. [PubMed: 10625387]
- (338). Schaffer DV; Fidelman NA; Dan N; Lauffenburger DA Vector unpacking as a potential barrier for receptor-mediated polyplex gene delivery. *Biotechnol Bioeng* 2000, 67 (5), 598. [PubMed: 10649234]
- (339). Lv HT; Zhang SB; Wang B; Cui SH; Yan J Toxicity of cationic lipids and cationic polymers in gene delivery. *Journal of Controlled Release* 2006, 114 (1), 100. [PubMed: 16831482]
- (340). Goff SP; Berg P Construction of hybrid viruses containing SV40 and lambda phage DNA segments and their propagation in cultured monkey cells. *Cell* 1976, 9 (4 PT 2), 695. [PubMed: 189942]
- (341). Williams DA; Lemischka IR; Nathan DG; Mulligan RC Introduction of new genetic material into pluripotent haematopoietic stem cells of the mouse. *Nature* 1984, 310 (5977), 476. [PubMed: 6087158]
- (342). Cepko CL; Roberts BE; Mulligan RC Construction and Applications of a Highly Transmissible Murine Retrovirus Shuttle Vector. *Cell* 1984, 37 (3), 1053. [PubMed: 6331674]
- (343). Mingozi F; High KA Therapeutic in vivo gene transfer for genetic disease using AAV: progress and challenges. *Nat Rev Genet* 2011, 12 (5), 341. [PubMed: 21499295]
- (344). Kay MA State-of-the-art gene-based therapies: the road ahead. *Nat Rev Genet* 2011, 12 (5), 316. [PubMed: 21468099]
- (345). Waehler R; Russell SJ; Curiel DT Engineering targeted viral vectors for gene therapy. *Nat Rev Genet* 2007, 8 (8), 573. [PubMed: 17607305]
- (346). van der Loo JC; Wright JF Progress and challenges in viral vector manufacturing. *Hum Mol Genet* 2015.
- (347). Jafari M; Soltani M; Naahidi S; Karunaratne DN; Chen P Nonviral Approach for Targeted Nucleic Acid Delivery. *Curr Med Chem* 2012, 19 (2), 197. [PubMed: 22320298]
- (348). Mitragotri S; Burke PA; Langer R Overcoming the challenges in administering biopharmaceuticals: formulation and delivery strategies. *Nat Rev Drug Discov* 2014, 13 (9), 655. [PubMed: 25103255]
- (349). Iversen TG; Skotland T; Sandvig K Endocytosis and intracellular transport of nanoparticles: Present knowledge and need for future studies. *Nano Today* 2011, 6 (2), 176.
- (350). Duncan R; Richardson SCW Endocytosis and Intracellular Trafficking as Gateways for Nanomedicine Delivery: Opportunities and Challenges. *Mol Pharmaceut* 2012, 9 (9), 2380.
- (351). Stewart MP; Lorenz A; Dahlman J; Sahay G Challenges in carrier-mediated intracellular delivery: moving beyond endosomal barriers. *Wiley Interdisciplinary Reviews: Nanomedicine and Nanobiotechnology* 2015, n/a.
- (352). Sahay G; Querbes W; Alabi C; Eltoukhy A; Sarkar S; Zurenko C; Karagiannis E; Love K; Chen DL; Zoncu R et al. Efficiency of siRNA delivery by lipid nanoparticles is limited by endocytic recycling. *Nat Biotechnol* 2013, 31 (7), 653. [PubMed: 23792629]
- (353). Gilleron J; Querbes W; Zeigerer A; Borodovsky A; Marsico G; Schubert U; Manygoats K; Seifert S; Andree C; Stoter M et al. Image-based analysis of lipid nanoparticle-mediated siRNA delivery, intracellular trafficking and endosomal escape. *Nat Biotechnol* 2013, 31 (7), 638. [PubMed: 23792630]
- (354). Wittrup A; Ai A; Liu X; Hamar P; Trifonova R; Charisse K; Manoharan M; Kirchhausen T; Lieberman J Visualizing lipid-formulated siRNA release from endosomes and target gene knockdown. *Nat Biotechnol* 2015, 33 (8), 870. [PubMed: 26192320]
- (355). Felgner PL Particulate systems and polymers for in vitro and in vivo delivery of polynucleotides. *Adv Drug Deliver Rev* 1990, 5 (3), 163.
- (356). Rehman ZU; Hoekstra D; Zuhorn IS Mechanism of Polyplex- and Lipoplex-Mediated Delivery of Nucleic Acids: Real-Time Visualization of Transient Membrane Destabilization without Endosomal Lysis. *ACS Nano* 2013, 7 (5), 3767. [PubMed: 23597090]
- (357). Helenius A; Doxsey S; Mellman I Viruses as Tools in Drug Delivery. *Annals of the New York Academy of Sciences* 1987, 507, 1.
- (358). Daemen T; de Mare A; Bungener L; de Jonge J; Huckriede A; Wilschut J Virosomes for antigen and DNA delivery. *Adv Drug Deliver Rev* 2005, 57 (3), 451.

- (359). Montecalvo A; Larregina AT; Shufesky WJ; Stolz DB; Sullivan MLG; Karlsson JM; Baty CJ; Gibson GA; Erdos G; Wang Z et al. Mechanism of transfer of functional microRNAs between mouse dendritic cells via exosomes. *Blood* 2012, 119 (3), 756. [PubMed: 22031862]
- (360). El Andaloussi S; Maeger I; Breakefield XO; Wood MJA Extracellular vesicles: biology and emerging therapeutic opportunities. *Nat Rev Drug Discov* 2013, 12 (5), 348.
- (361). Feramisco J; Perona R; Lacal JC In *Microinjection*; Lacal J; Feramisco J; Perona R, Eds.; Birkhäuser Basel, 1999.
- (362). McAllister DV; Wang PM; Davis SP; Park JH; Canatella PJ; Allen MG; Prausnitz MR Microfabricated needles for transdermal delivery of macromolecules and nanoparticles: fabrication methods and transport studies. *Proc Natl Acad Sci U S A* 2003, 100 (24), 13755. [PubMed: 14623977]
- (363). McKnight TE; Melechko AV; Griffin GD; Guillorn MA; Merkulov VI; Serna F; Hensley DK; Doktycz MJ; Lowndes DH; Simpson ML Intracellular integration of synthetic nanostructures with viable cells for controlled biochemical manipulation. *Nanotechnology* 2003, 14 (5), 551.
- (364). Klein TM; Wolf ED; Wu R; Sanford JC High-Velocity Microprojectiles for Delivering Nucleic-Acids into Living Cells. *Nature* 1987, 327 (6117), 70.
- (365). Stephens DJ; Pepperkok R The many ways to cross the plasma membrane. *P Natl Acad Sci USA* 2001, 98 (8), 4295.
- (366). Hapala I Breaking the barrier: Methods for reversible permeabilization of cellular membranes. *Crit Rev Biotechnol* 1997, 17 (2), 105. [PubMed: 9192473]
- (367). Schulz I Permeabilizing Cells - Some Methods and Applications for the Study of Intracellular Processes. *Method Enzymol* 1990, 192, 280.
- (368). Cooper ST; McNeil PL Membrane Repair: Mechanisms and Pathophysiology. *Physiol Rev* 2015, 95 (4), 1205. [PubMed: 26336031]
- (369). Bischofberger M; Iacovache I; van der Goot FG Pathogenic Pore-Forming Proteins: Function and Host Response. *Cell Host Microbe* 2012, 12 (3), 266. [PubMed: 22980324]
- (370). Shinoda W Permeability across lipid membranes. *Biochimica et biophysica acta* 2016.
- (371). Holthuis JC; Menon AK Lipid landscapes and pipelines in membrane homeostasis. *Nature* 2014, 510 (7503), 48. [PubMed: 24899304]
- (372). van Meer G; Voelker DR; Feigenson GW Membrane lipids: where they are and how they behave. *Nat Rev Mol Cell Bio* 2008, 9 (2), 112. [PubMed: 18216768]
- (373). Simons K; Sampaio JL Membrane Organization and Lipid Rafts. *Csh Perspect Biol* 2011, 3 (10).
- (374). Lingwood D; Simons K Lipid Rafts As a Membrane-Organizing Principle. *Science* 2010, 327 (5961), 46. [PubMed: 20044567]
- (375). Parton RG; Simons K The multiple faces of caveolae. *Nat Rev Mol Cell Bio* 2007, 8 (3), 185. [PubMed: 17318224]
- (376). Tweten RK; Hotze EM; Wade KR The Unique Molecular Choreography of Giant Pore Formation by the Cholesterol-Dependent Cytolysins of Gram-Positive Bacteria. *Annu Rev Microbiol* 2015, 69, 323. [PubMed: 26488276]
- (377). Gogelein H; Huby A Interaction of Saponin and Digitonin with Black Lipid-Membranes and Lipid Monolayers. *Biochimica et biophysica acta* 1984, 773 (1), 32. [PubMed: 6733096]
- (378). Pfaff RT; Liu J; Gao D; Peter AT; Li TK; Critser JK Water and DMSO membrane permeability characteristics of in-vivo- and in-vitro-derived and cultured murine oocytes and embryos. *Mol Hum Reprod* 1998, 4 (1), 51. [PubMed: 9510011]
- (379). Gurtovenko AA; Anwar J; Vattulainen I Defect-Mediated Trafficking across Cell Membranes: Insights from in Silico Modeling. *Chem Rev* 2010, 110 (10), 6077. [PubMed: 20690701]
- (380). King LS; Kozono D; Agre P From structure to disease: The evolving tale of aquaporin biology. *Nat Rev Mol Cell Bio* 2004, 5 (9), 687. [PubMed: 15340377]
- (381). Dobson PD; Patel Y; Kell DB 'Metabolite-likeness' as a criterion in the design and selection of pharmaceutical drug libraries. *Drug Discov Today* 2009, 14 (1-2), 31. [PubMed: 19049901]

- (382). Reitsma S; Slaaf DW; Vink H; van Zandvoort MAMJ; Egbrink MGAO The endothelial glycocalyx: composition, functions, and visualization. *Pflugers Archiv-European Journal of Physiology* 2007, 454 (3), 345. [PubMed: 17256154]
- (383). Clark AG; Wartlick O; Salbreux G; Paluch EK Stresses at the Cell Surface during Animal Cell Morphogenesis. *Curr Biol* 2014, 24 (10), R484. [PubMed: 24845681]
- (384). Groulx N; Boudreault F; Orlov SN; Grygorczyk R Membrane reserves and hypotonic cell swelling. *J Membrane Biol* 2006, 214 (1–2), 43. [PubMed: 17598067]
- (385). Sinha B; Koster D; Ruez R; Gonnord P; Bastiani M; Abankwa D; Stan RV; Butler-Browne G; Védie B; Johannes Let al. Cells Respond to Mechanical Stress by Rapid Disassembly of Caveolae. *Cell* 2011, 144 (3), 402. [PubMed: 21295700]
- (386). Aalipour A; Xu AM; Leal-Ortiz S; Garner CC; Melosh NA Plasma Membrane and Actin Cytoskeleton as Synergistic Barriers to Nanowire Cell Penetration. *Langmuir* 2014, 30 (41), 12362. [PubMed: 25244597]
- (387). Xu AM; Aalipour A; Leal-Ortiz S; Mekhdjian AH; Xie X; Dunn AR; Garner CC; Melosh NA Quantification of nanowire penetration into living cells. *Nat Commun* 2014, 5.
- (388). Weaver JC; Chizmadzhev YA Theory of electroporation: A review. *Bioelectroch Bioener* 1996, 41 (2), 135.
- (389). Neu JC; Krassowska W Asymptotic model of electroporation. *Physical Review E* 1999, 59 (3), 3471.
- (390). Evans E; Heinrich V; Ludwig F; Rawicz W Dynamic tension spectroscopy and strength of biomembranes. *Biophys J* 2003, 85 (4), 2342. [PubMed: 14507698]
- (391). Karatekin E; Sandre O; Guitouni H; Borghi N; Puech PH; Brochard-Wyart F Cascades of transient pores in giant vesicles: Line tension and transport. *Biophys J* 2003, 84 (3), 1734. [PubMed: 12609875]
- (392). McNeil PL; Steinhardt RA Plasma membrane disruption: Repair, prevention, adaptation. *Annual Review of Cell and Developmental Biology* 2003, 19, 697.
- (393). Bloom M; Evans E; Mouritsen OG Physical-Properties of the Fluid Lipid-Bilayer Component of Cell-Membranes - a Perspective. *Q Rev Biophys* 1991, 24 (3), 293. [PubMed: 1749824]
- (394). Last NB; Schlamadinger DE; Miranker AD A common landscape for membrane-active peptides. *Protein Sci* 2013, 22 (7), 870. [PubMed: 23649542]
- (395). Bennett WFD; Tieleman DP The Importance of Membrane Defects-Lessons from Simulations. *Accounts Chem Res* 2014, 47 (8), 2244.
- (396). Wang TY; Libardo MD; Angeles-Boza AM; Pellois JP Membrane oxidation in cell delivery and cell killing applications. *ACS Chem Biol* 2017.
- (397). Riske KA; Sudbrack TP; Archilha NL; Uchoa AF; Schroder AP; Marques CM; Baptista MS; Itri R Giant Vesicles under Oxidative Stress Induced by a Membrane-Anchored Photosensitizer. *Biophys J* 2009, 97 (5), 1362. [PubMed: 19720024]
- (398). Makky A; Tanaka M Impact of Lipid Oxidization on Biophysical Properties of Model Cell Membranes. *J Phys Chem B* 2015, 119 (18), 5857. [PubMed: 25870900]
- (399). Boonnoy P; Jarerattanachai V; Karttunen M; Wong-ekkabut J Bilayer Deformation, Pores, and Micellation Induced by Oxidized Lipids. *J Phys Chem Lett* 2015, 6 (24), 4884. [PubMed: 26673194]
- (400). Peraro MD; van der Goot FG Pore-forming toxins: ancient, but never really out of fashion. *Nat Rev Micro* 2015, advance online publication.
- (401). Sun DL; Forsman J; Woodward CE Current Understanding of the Mechanisms by which Membrane-Active Peptides Permeate and Disrupt Model Lipid Membranes. *Curr Top Med Chem* 2016, 16 (2), 170.
- (402). Heerklotz H Interactions of surfactants with lipid membranes. *Q Rev Biophys* 2008, 41 (3–4), 205. [PubMed: 19079805]
- (403). Lichtenberg D; Ahyayauch H; Goni FM The Mechanism of Detergent Solubilization of Lipid Bilayers. *Biophys J* 2013, 105 (2), 289. [PubMed: 23870250]
- (404). Steinhardt RA; Bi GQ; Alderton JM Cell-Membrane Resealing by a Vesicular Mechanism Similar to Neurotransmitter Release. *Science* 1994, 263 (5145), 390. [PubMed: 7904084]

- (405). McNeil PL; Kirchhausen T An emergency response team for membrane repair. *Nat Rev Mol Cell Bio* 2005, 6 (6), 499. [PubMed: 15928713]
- (406). Jimenez AJ; Perez F Plasma membrane repair: the adaptable cell life-insurance. *Curr Opin Cell Biol* 2017, 47, 99. [PubMed: 28511145]
- (407). Demonbreun AR; McNally EM In *Current Topics in Membranes*; Academic Press, 2016.
- (408). Moe A; Golding AE; Bement WM Cell healing: Calcium, repair and regeneration. *Semin Cell Dev Biol* 2015.
- (409). Lauritzen SP; Boye TL; Nylandsted J Annexins are instrumental for efficient plasma membrane repair in cancer cells. *Semin Cell Dev Biol* 2015.
- (410). Jimenez AJ; Perez F Physico-chemical and biological considerations for membrane wound evolution and repair in animal cells. *Semin Cell Dev Biol* 2015.
- (411). Cheng X; Zhang X; Yu L; Xu H Calcium signaling in membrane repair. *Semin Cell Dev Biol* 2015.
- (412). Boucher E; Mandato CA Plasma membrane and cytoskeleton dynamics during single-cell wound healing. *Biochimica et biophysica acta* 2015.
- (413). Babychuk EB; Draeger A Defying death: cellular survival strategies following plasmalemmal injury by bacterial toxins. *Semin Cell Dev Biol* 2015.
- (414). Andrews NW; Corrotte M; Castro-Gomes T Above the fray: Surface remodeling by secreted lysosomal enzymes leads to endocytosis-mediated plasma membrane repair. *Semin Cell Dev Biol* 2015.
- (415). Jimenez AJ; Maiuri P; Lafaurie-Janvore J; Divoux S; Piel M; Perez F ESCRT Machinery Is Required for Plasma Membrane Repair. *Science* 2014.
- (416). Andrews NW; Almeida PE; Corrotte M Damage control: cellular mechanisms of plasma membrane repair. *Trends Cell Biol* 2014.
- (417). Draeger A; Schoenauer R; Atanassoff AP; Wolfmeier H; Babychuk EB Dealing with damage: Plasma membrane repair mechanisms. *Biochimie* 2014.
- (418). Bhakdi S; Weller U; Walev I; Martin E; Jonas D; Palmer M A Guide to the Use of Pore-Forming Toxins for Controlled Permeabilization of Cell-Membranes. *Med Microbiol Immun* 1993, 182 (4), 167.
- (419). Weaver JC Electroporation of biological membranes from multicellular to nano scales. *Dielectrics and Electrical Insulation, IEEE Transactions on* 2003, 10 (5), 754.
- (420). Yasuda S; Townsend D; Michele DE; Favre EG; Day SM; Metzger JM Dystrophic heart failure blocked by membrane sealant poloxamer. *Nature* 2005, 436 (7053), 1025. [PubMed: 16025101]
- (421). Agarwal J; Walsh A; Lee RC Multimodal strategies for resuscitating injured cells. *Ann Ny Acad Sci* 2005, 1066, 295. [PubMed: 16533933]
- (422). Sengupta A; Dwivedi N; Kelly SC; Tucci L; Thadhani NN; Prausnitz MR Poloxamer surfactant preserves cell viability during photoacoustic delivery of molecules into cells. *Biotechnol Bioeng* 2014.
- (423). Serbest G; Horwitz J; Barbee K The effect of Poloxamer-188 on neuronal cell recovery from mechanical injury. *J Neurotraum* 2005, 22 (1), 119.
- (424). Hartikka J; Sukhu I; Buchner C; Hazard D; Bozoukova V; Margalith M; Nishioka WK; Wheeler CJ; Manthorpe M; Sawdey M Electroporation-facilitated delivery of plasmid DNA in skeletal muscle: Plasmid dependence of muscle damage and effect of poloxamer 188. *Mol Ther* 2001, 4 (5), 407. [PubMed: 11708877]
- (425). Bittner G; Spaeth C; Poon A; Burgess Z; McGill C Repair of traumatic plasmalemmal damage to neurons and other eukaryotic cells. *Neural Regeneration Research* 2016, 11 (7), 1033. [PubMed: 27630671]
- (426). Howard AC; McNeil AK; McNeil PL Promotion of plasma membrane repair by vitamin E. *Nat Commun* 2011, 2.
- (427). Labazi M; McNeil AK; Kurtz T; Lee TC; Pegg RB; Friedmann J; Conrad M; McNeil PL The Antioxidant Requirement for Plasma Membrane Repair in Skeletal Muscle. *Free radical biology & medicine* 2015.

- (428). Duan X; Chan KT; Lee KK; Mak AF Oxidative Stress and Plasma Membrane Repair in Single Myoblasts After Femtosecond Laser Photoporation. *Ann Biomed Eng* 2015.
- (429). Golzio M; Mora MP; Raynaud C; Delteil C; Teissie J; Rols MP Control by osmotic pressure of voltage-induced permeabilization and gene transfer in mammalian cells. *Biophys J* 1998, 74 (6), 3015. [PubMed: 9635756]
- (430). Ferret E; Evrard C; Foucal A; Gervais P Volume changes of isolated human K562 leukemia cells induced by electric field pulses. *Biotechnol Bioeng* 2000, 67 (5), 520. [PubMed: 10649227]
- (431). Shirakashi R; Sukhorukov VL; Tanasawa I; Zimmermann U Measurement of the permeability and resealing time constant of the electroporated mammalian cell membranes. *Int J Heat Mass Tran* 2004, 47 (21), 4517.
- (432). Pavlin M; Kanduser M; Rebersek M; Pucihar G; Hart FX; Magjarevic R; Miklavcic D Effect of cell electroporation on the conductivity of a cell suspension. *Biophys J* 2005, 88 (6), 4378. [PubMed: 15792975]
- (433). Wang HY; Lu C High-throughput and real-time study of single cell electroporation using microfluidics: Effects of medium osmolarity. *Biotechnol Bioeng* 2006, 95 (6), 1116. [PubMed: 16817188]
- (434). Usaj M; Trontelj K; Hudej R; Kanduser M; Miklavcic D Cell size dynamics and viability of cells exposed to hypotonic treatment and electroporation for electrofusion optimization. *Radiol Oncol* 2009, 43 (2), 108.
- (435). Nesin OM; Pakhomova ON; Xiao S; Pakhomov AG Manipulation of cell volume and membrane pore comparison following single cell permeabilization with 60-and 600-ns electric pulses. *Bba-Biomembranes* 2011, 1808 (3), 792. [PubMed: 21182825]
- (436). Pakhomov AG; Xiao S; Pakhomova ON; Semenov I; Kuipers MA; Ibey BL Disassembly of actin structures by nanosecond pulsed electric field is a downstream effect of cell swelling. *Bioelectrochemistry* 2014, 100, 88. [PubMed: 24507565]
- (437). Romeo S; Wu YH; Levine ZA; Gundersen MA; Vernier PT Water influx and cell swelling after nanosecond electroporeabilization. *Biochimica et biophysica acta* 2013, 1828 (8), 1715. [PubMed: 23500618]
- (438). Sozer EB; Wu YH; Romeo S; Vernier PT Nanometer-Scale Permeabilization and Osmotic Swelling Induced by 5-ns Pulsed Electric Fields. *The Journal of membrane biology* 2017, 250 (1), 21. [PubMed: 27435216]
- (439). Anderson SE; Bau HH Electrical detection of cellular penetration during microinjection with carbon nanopipettes. *Nanotechnology* 2014, 25 (24).
- (440). Beier HT; Tolstykh GP; Musick JD; Thomas RJ; Ibey BL Plasma membrane nanoporation as a possible mechanism behind infrared excitation of cells. *J Neural Eng* 2014, 11 (6).
- (441). Davis AA; Farrar MJ; Nishimura N; Jin MM; Schaffer CB Optoporation and Genetic Manipulation of Cells Using Femtosecond Laser†Pulses. *Biophys J* 2013, 105 (4), 862. [PubMed: 23972838]
- (442). Antkowiak M; Torres-Mapa ML; Dholakia K; Gunn-Moore FJ Quantitative phase study of the dynamic cellular response in femtosecond laser photoporation. *Biomedical optics express* 2010, 1 (2), 414. [PubMed: 21258476]
- (443). Baumgart J; Bintig W; Ngezahayo A; Willenbrock S; Murua Escobar H; Ertmer W; Lubatschowski H; Heisterkamp A Quantified femtosecond laser based opto-perforation of living GFSHR-17 and MTH53 a cells. *Optics express* 2008, 16 (5), 3021. [PubMed: 18542388]
- (444). Stevenson D; Agate B; Tsampoula X; Fischer P; Brown CTA; Sibbett W; Riches A; Gunn-Moore F; Dholakia K Femtosecond optical transfection of cells: viability and efficiency. *Optics express* 2006, 14 (16), 7125. [PubMed: 19529083]
- (445). Kohli V; Acker JP; Elezzabi AY Reversible permeabilization using high-intensity femtosecond laser pulses: Applications to biopreservation. *Biotechnol Bioeng* 2005, 92 (7), 889. [PubMed: 16189821]
- (446). Krasieva TB; Chapman CF; LaMorte VJ; Venugopalan V; Berns MW; Tromberg BJ Cell permeabilization and molecular transport by laser microirradiation. *P Soc Photo-Opt Ins* 1998, 3260, 38.

- (447). Li ZG; Liu AQ; Klaseboer E; Zhang JB; Ohl CD Single cell membrane poration by bubble-induced microjets in a microfluidic chip. *Lab on a chip* 2013, 13 (6), 1144. [PubMed: 23364762]
- (448). Miyake K; McNeil PL Vesicle accumulation and exocytosis at sites of plasma membrane disruption. *J Cell Biol* 1995, 131 (6), 1737. [PubMed: 8557741]
- (449). Wang HY; Lu C Electroporation of mammalian cells in a microfluidic channel with geometric variation. *Anal Chem* 2006, 78 (14), 5158. [PubMed: 16841942]
- (450). Hui SW; Li LH In vitro and ex vivo gene delivery to cells by electroporation. *Methods Mol Med* 2000, 37, 157. [PubMed: 21445734]
- (451). Hoffmann EK; Lambert IH; Pedersen SF Physiology of Cell Volume Regulation in Vertebrates. *Physiol Rev* 2009, 89 (1), 193. [PubMed: 19126758]
- (452). Fink SL; Cookson BT Apoptosis, pyroptosis, and necrosis: mechanistic description of dead and dying eukaryotic cells. *Infect Immun* 2005, 73 (4), 1907. [PubMed: 15784530]
- (453). Fulda S; Gorman AM; Hori O; Samali A Cellular stress responses: cell survival and cell death. *Int J Cell Biol* 2010, 2010, 214074. [PubMed: 20182529]
- (454). Abidor IG; Li LH; Hui SW Studies of Cell Pellets .2. Osmotic Properties, Electroporation, and Related Phenomena - Membrane Interactions. *Biophys J* 1994, 67 (1), 427. [PubMed: 7522598]
- (455). Gonzalez MR; Bischofberger M; Freche B; Ho S; Parton RG; van der Goot FG Pore-forming toxins induce multiple cellular responses promoting survival. *Cellular Microbiology* 2011, 13 (7), 1026. [PubMed: 21518219]
- (456). Kosowski H; Matthias R; Schild L; Halangk W Electropulsing of Acinar-Cells Isolated from Rat Pancreas - Dependence of Reversible Membrane Perforation on Cellular-Energy State. *Bioelectroch Bioener* 1995, 38 (2), 377.
- (457). Walev I; Bhakdi SC; Hofmann F; Djonder N; Valeva A; Aktories K; Bhakdi S Delivery of proteins into living cells by reversible membrane permeabilization with streptolysin-O. *P Natl Acad Sci USA* 2001, 98 (6), 3185.
- (458). Wald T; Petry-Podgorska I; Fiser R; Matousek T; Dedina J; Osicka R; Sebo P; Masin J Quantification of potassium levels in cells treated with Bordetella adenylate cyclase toxin. *Anal Biochem* 2014, 450, 57. [PubMed: 24412166]
- (459). Orrenius S; McConkey DJ; Bellomo G; Nicotera P Role of Ca²⁺ in toxic cell killing. *Trends Pharmacol Sci* 1989, 10 (7), 281. [PubMed: 2672472]
- (460). Babiyuchuk EB; Monastyrskaya K; Potez S; Draeger A Intracellular Ca²⁺ operates a switch between repair and lysis of streptolysin O-perforated cells. *Cell Death Differ* 2009, 16 (8), 1126. [PubMed: 19325569]
- (461). Wolfmeier H; Schoenauer R; Atanassoff AP; Neill DR; Kadioglu A; Draeger A; Babiyuchuk EB Ca-dependent repair of pneumolysin pores: A new paradigm for host cellular defense against bacterial pore-forming toxins. *Biochimica et biophysica acta* 2014.
- (462). Blangero C; Rols MP; Teissie J Cytoskeletal Reorganization during Electric-Field-Induced Fusion of Chinese-Hamster Ovary Cells Grown in Monolayers. *Biochimica et biophysica acta* 1989, 981 (2), 295. [PubMed: 2567186]
- (463). Harkin DG; Hay ED Effects of electroporation on the tubulin cytoskeleton and directed migration of corneal fibroblasts cultured within collagen matrices. *Cell Motility and the Cytoskeleton* 1996, 35 (4), 345. [PubMed: 8956005]
- (464). Kanthou C; Kranjc S; Sersa G; Tozer G; Zupanic A; Cemazar M The endothelial cytoskeleton as a target of electroporation-based therapies. *Mol Cancer Ther* 2006, 5 (12), 3145. [PubMed: 17172418]
- (465). Thompson GL; Roth CC; Dalzell DR; Kuipers M; Ibey BL Calcium influx affects intracellular transport and membrane repair following nanosecond pulsed electric field exposure. *J Biomed Opt* 2014, 19 (5).
- (466). Keith C; Dipaola M; Maxfield FR; Shelanski ML Microinjection of Ca⁺⁺-Calmodulin Causes a Localized Depolymerization of Microtubules. *J Cell Biol* 1983, 97 (6), 1918. [PubMed: 6358237]
- (467). Togo T Disruption of the plasma membrane stimulates rearrangement of microtubules and lipid traffic toward the wound site. *J Cell Sci* 2006, 119 (13), 2780. [PubMed: 16772335]

- (468). Kano F; Nakatsu D; Noguchi Y; Yamamoto A; Murata M A Resealed-Cell System for Analyzing Pathogenic Intracellular Events: Perturbation of Endocytic Pathways under Diabetic Conditions. *Plos One* 2012, 7 (8).
- (469). Saklayen N; Kalies S; Madrid M; Nuzzo V; Huber M; Shen W; Sinanan-Singh J; Heinemann D; Heisterkamp A; Mazur E Analysis of poration-induced changes in cells from laser-activated plasmonic substrates. *Biomedical optics express* 2017, 8 (10), 4756. [PubMed: 29082100]
- (470). Bischof LJ; Kao CY; Los FCO; Gonzalez MR; Shen ZX; Briggs SP; van der Goot FG; Aroian RV Activation of the Unfolded Protein Response Is Required for Defenses against Bacterial Pore-Forming Toxin In Vivo. *Plos Pathog* 2008, 4 (10).
- (471). Pillich H; Loose M; Zimmer KP; Chakraborty T Activation of the unfolded protein response by *Listeria monocytogenes*. *Cell Microbiol* 2012, 14 (6), 949. [PubMed: 22321539]
- (472). Stassen M; Muller C; Richter C; Neudorfl C; Hultner L; Bhakdi S; Walev I; Schmitt E The streptococcal exotoxin streptolysin O activates mast cells to produce tumor necrosis factor alpha by p38 mitogen-activated protein kinase- and protein kinase C-dependent pathways. *Infection and Immunity* 2003, 71 (11), 6171. [PubMed: 14573633]
- (473). Cassidy SK; Hagar JA; Kanneganti TD; Franchi L; Nunez G; O'Riordan MX Membrane damage during *Listeria monocytogenes* infection triggers a caspase-7 dependent cytoprotective response. *Plos Pathog* 2012, 8 (7), e1002628. [PubMed: 22807671]
- (474). Tang P; Rosenshine I; Cossart P; Finlay BB Listeriolysin O activates mitogen-activated protein kinase in eucaryotic cells. *Infection and Immunity* 1996, 64 (6), 2359. [PubMed: 8675352]
- (475). Kao CY; Los FCO; Huffman DL; Wachi S; Kloft N; Husmann M; Karabrahimi V; Schwartz JL; Bellier A; Ha Cet al. Global Functional Analyses of Cellular Responses to Pore-Forming Toxins. *Plos Pathog* 2011, 7 (3).
- (476). Porta H; Cancino-Rodezno A; Soberon M; Bravo A Role of MAPK p38 in the cellular responses to pore-forming toxins. *Peptides* 2011, 32 (3), 601. [PubMed: 20599578]
- (477). Cabezas S; Ho S; Ros U; Lanio ME; Alvarez C; van der Goot FG Damage of eukaryotic cells by the pore-forming toxin sticholysin II: Consequences of the potassium efflux. *Biochimica et biophysica acta* 2017, 1859 (5), 982. [PubMed: 28173991]
- (478). Kloft N; Busch T; Neukirch C; Weis S; Boukhallouk F; Bobkiewicz W; Cibis I; Bhakdi S; Husmann M Pore-forming toxins activate MAPK p38 by causing loss of cellular potassium. *Biochem Bioph Res Co* 2009, 385 (4), 503.
- (479). Nagahama M; Shibutani M; Seike S; Yonezaki M; Takagishi T; Oda M; Kobayashi K; Sakurai J The p38 MAPK and JNK Pathways Protect Host Cells against *Clostridium perfringens* Beta-Toxin. *Infection and Immunity* 2013, 81 (10), 3703. [PubMed: 23876806]
- (480). Grembowicz KP; Sprague D; McNeil PL Temporary disruption of the plasma membrane is required for c-fos expression in response to mechanical stress. *Mol Biol Cell* 1999, 10 (4), 1247. [PubMed: 10198070]
- (481). Kayal S; Lilienbaum A; Poyart C; Memet S; Israel A; Berche P Listeriolysin O-dependent activation of endothelial cells during infection with *Listeria monocytogenes*: activation of NF-kappa B and upregulation of adhesion molecules and chemokines. *Molecular Microbiology* 1999, 31 (6), 1709. [PubMed: 10209744]
- (482). Togo T; Alderton JM; Bi GQ; Steinhardt RA The mechanism of facilitated cell membrane resealing. *J Cell Sci* 1999, 112 (5), 719. [PubMed: 9973606]
- (483). Togo T; Alderton JM; Steinhardt RA Long-term potentiation of exocytosis and cell membrane repair in fibroblasts. *Mol Biol Cell* 2003, 14 (1), 93. [PubMed: 12529429]
- (484). Togo T Long-term potentiation of wound-induced exocytosis and plasma membrane repair is dependant on cAMP-response element-mediated transcription via a protein kinase C- and p38 MAPK-dependent pathway. *J Biol Chem* 2004, 279 (43), 44996. [PubMed: 15317814]
- (485). Tolstykh GP; Beier HT; Roth CC; Thompson GL; Payne JA; Kuipers MA; Ibey BL Activation of intracellular phosphoinositide signaling after a single 600 nanosecond electric pulse. *Bioelectrochemistry* 2013, 94, 23. [PubMed: 23747521]
- (486). Morotomi-Yano K; Akiyama H; Yano K Nanosecond pulsed electric fields activate MAPK pathways in human cells. *Arch Biochem Biophys* 2011, 515 (1-2), 99. [PubMed: 21933660]

- (487). Roth CC; Glickman RD; Tolstykh GP; Estlack LE; Moen EK; Echchgadda I; Beier HT; Barnes RA Jr.; Ibey BL Evaluation of the Genetic Response of U937 and Jurkat Cells to 10-Nanosecond Electrical Pulses (nsEP). *Plos One* 2016, 11 (5), e0154555. [PubMed: 27135944]
- (488). Ullery JC; Tarango M; Roth CC; Ibey BL Activation of autophagy in response to nanosecond pulsed electric field exposure. *Biochem Bioph Res Co* 2015, 458 (2), 411.
- (489). Pinero J; LopezBaena M; Ortiz T; Cortes F Apoptotic and necrotic cell death are both induced by electroporation in HL60 human promyeloid leukaemia cells. *Apoptosis* 1997, 2 (3), 330. [PubMed: 14646546]
- (490). Li LH; Sen A; Murphy SP; Jahreis GP; Fuji H; Hui SW Apoptosis induced by DNA uptake limits transfection efficiency. *Exp Cell Res* 1999, 253 (2), 541. [PubMed: 10585278]
- (491). Sukharev SI; Klenchin VA; Serov SM; Chernomordik LV; Chizmadzhev YA Electroporation and Electrophoretic DNA Transfer into Cells - the Effect of DNA Interaction with Electropores. *Biophys J* 1992, 63 (5), 1320. [PubMed: 1282374]
- (492). Rols MP; Teissie J Electroporation of mammalian cells to macromolecules: Control by pulse duration. *Biophys J* 1998, 75 (3), 1415. [PubMed: 9726943]
- (493). Rols MP; Teissie J Electroporation of Mammalian-Cells - Quantitative-Analysis of the Phenomenon. *Biophys J* 1990, 58 (5), 1089. [PubMed: 2291935]
- (494). Rols MP; Teissie J Modulation of Electrically Induced Permeabilization and Fusion of Chinese Hamster Ovary Cells by Osmotic-Pressure. *Biochemistry* 1990, 29 (19), 4561. [PubMed: 2372540]
- (495). Kwee S; Nielsen HV; Celis JE Electroporation of Human Cultured-Cells Grown in Monolayers - Incorporation of Monoclonal-Antibodies. *Bioelectroch Bioener* 1990, 23 (1), 65.
- (496). Blangero C; Teissie J Ionic Modulation of Electrically Induced Fusion of Mammalian-Cells. *J Membrane Biol* 1985, 86 (3), 247. [PubMed: 4046011]
- (497). Johnson JA; Gray MO; Karliner JS; Chen CH; MochlyRosen D An improved permeabilization protocol for the introduction of peptides into cardiac myocytes - Application to protein kinase C research. *Circ Res* 1996, 79 (6), 1086. [PubMed: 8943947]
- (498). Bru T; Clarke C; McGrew MJ; Sang HM; Wilmut I; Blow JJ Rapid induction of pluripotency genes after exposure of human somatic cells to mouse ES cell extracts. *Exp Cell Res* 2008, 314 (14), 2634. [PubMed: 18571647]
- (499). Miller MR; Castellot JJ Jr.; Pardee AB A permeable animal cell preparation for studying macromolecular synthesis. DNA synthesis and the role of deoxyribonucleotides in S phase initiation. *Biochemistry* 1978, 17 (6), 1073. [PubMed: 629946]
- (500). Baker PF; Knight DE High-Voltage Techniques for Gaining Access to the Interior of Cells - Application to the Study of Exocytosis and Membrane Turnover. *Method Enzymol* 1983, 98, 28.
- (501). Mcneil PL; Taylor DL Aequorin Entrapment in Mammalian-Cells. *Cell Calcium* 1985, 6 (1-2), 83. [PubMed: 4016895]
- (502). Knight DE; Scrutton MC Gaining Access to the Cytosol - the Technique and Some Applications of Electroporation. *Biochem J* 1986, 234 (3), 497. [PubMed: 3521588]
- (503). Fechheimer M; Boylan JF; Parker S; Siskin JE; Patel GL; Zimmer SG Transfection of Mammalian-Cells with Plasmid DNA by Scrape Loading and Sonication Loading. *P Natl Acad Sci USA* 1987, 84 (23), 8463.
- (504). Michel MR; Elgizoli M; Koblet H; Kempf C Diffusion Loading Conditions Determine Recovery of Protein-Synthesis in Electroporated P3x63ag8 Cells. *Experientia* 1988, 44 (3), 199. [PubMed: 2450774]
- (505). van den Hoff MJB; Moonman AFM; Lamers WH Electroporation in Intracellular Buffer Increases Cell-Survival. *Nucleic Acids Res* 1992, 20 (11), 2902. [PubMed: 1614888]
- (506). van den Hoff MJ; Christoffels VM; Labruyere WT; Moorman AF; Lamers WH Electrotransfection with "intracellular" buffer. *Methods Mol Biol* 1995, 48, 185. [PubMed: 8528391]
- (507). Baron S; Poast J; Rizzo D; McFarland E; Kieff E Electroporation of antibodies, DNA, and other macromolecules into cells: a highly efficient method. *J Immunol Methods* 2000, 242 (1-2), 115. [PubMed: 10986394]

- (508). Riemen G; Lorbach E; Helfrich J; Siebenkotten G; Muller-Hartmann H; Rothmann-Cosic K; Thiel C; Weigel M; Wessendorf H; Brosterbus H; Google Patents, 2005.
- (509). Chicaybam L; Sodre AL; Curzio BA; Bonamino MH An Efficient Low Cost Method for Gene Transfer to T Lymphocytes. *Plos One* 2013, 8 (3).
- (510). Parreno J; Delve E; Andrejevic K; Paez-Parent S; Wu PH; Kandel R Efficient, Low-Cost Nucleofection of Passaged Chondrocytes. *Cartilage* 2016, 7 (1), 82. [PubMed: 26958320]
- (511). Chicaybam L; Barcelos C; Peixoto B; Carneiro M; Limia CG; Redondo P; Lira C; Paraguassu-Braga F; Vasconcelos ZF; Barros Let al. An Efficient Electroporation Protocol for the Genetic Modification of Mammalian Cells. *Front Bioeng Biotechnol* 2016, 4, 99. [PubMed: 28168187]
- (512). Kang J; Ramu S; Lee S; Aguilar B; Ganesan SK; Yoo J; Kalra VK; Koh CJ; Hong YK Phosphate-buffered saline-based nucleofection of primary endothelial cells. *Anal Biochem* 2009, 386 (2), 251. [PubMed: 19150324]
- (513). Patel N; Kalra VK Placenta Growth Factor-induced Early Growth Response 1 (Egr-1) Regulates Hypoxia-inducible Factor-1 alpha (HIF-1 alpha) in Endothelial Cells. *J Biol Chem* 2010, 285 (27), 20570. [PubMed: 20448047]
- (514). Potter H Transfection by electroporation. *Curr Protoc Mol Biol* 2003, Chapter 9, Unit 9 3.
- (515). Potter H; Heller R Transfection by electroporation. *Current protocols in cell biology / editorial board, Juan S. Bonifacino ... [et al.]* 2011, Chapter 20, Unit20 5.
- (516). Kim JA; Cho KC; Shin MS; Lee WG; Jung NC; Chung CI; Chang JK A novel electroporation method using a capillary and wire-type electrode. *Biosensors & bioelectronics* 2008, 23 (9), 1353. [PubMed: 18242073]
- (517). Brees C; Franssen M A cost-effective approach to microporate mammalian cells with the Neon Transfection System. *Anal Biochem* 2014, 466, 49. [PubMed: 25172131]
- (518). Wilgenhof S; Corthals J; Van Nuffel AMT; Benteyn D; Heirman C; Bonehill A; Thielemans K; Neyns B Long-term clinical outcome of melanoma patients treated with messenger RNA-electroporated dendritic cell therapy following complete resection of metastases. *Cancer Immunol Immun* 2015, 64 (3), 381.
- (519). Soneru AP; Beckett MA; Weichselbaum RR; Lee RC Mg Atp and Antioxidants Augment the Radioprotective Effect of Surfactant Copolymers. *Health Phys* 2011, 101 (6), 731. [PubMed: 22048491]
- (520). Volpe SL Magnesium in disease prevention and overall health. *Adv Nutr* 2013, 4 (3), 378S. [PubMed: 23674807]
- (521). Schoenauer R; Atanassoff AP; Wolfmeier H; Pelegrin P; Babiychuk EB; Draeger A P2X7 receptors mediate resistance to toxin-induced cell lysis. *Bba-Mol Cell Res* 2014, 1843 (5), 915.
- (522). Rols MP; Delteil C; Golzio M; Teissie J Control by ATP and ADP of voltage-induced mammalian-cell-membrane permeabilization, gene transfer and resulting expression. *Eur J Biochem* 1998, 254 (2), 382. [PubMed: 9660195]
- (523). Draeger A; Babiychuk EB Ceramide in plasma membrane repair. *Handbook of experimental pharmacology* 2013, (216), 341. [PubMed: 23563665]
- (524). Potez S; Luginbul M; Monastyrskaya K; Hostettler A; Draeger A; Babiychuk EB Tailored Protection against Plasmalemmal Injury by Annexins with Different Ca²⁺ Sensitivities. *J Biol Chem* 2011, 286 (20), 17982. [PubMed: 21454475]
- (525). Draeger A; Monastyrskaya K; Babiychuk EB Plasma membrane repair and cellular damage control: The annexin survival kit. *Biochem Pharmacol* 2011, 81 (6), 703. [PubMed: 21219882]
- (526). Cai C; Lin P; Zhu H; Ko JK; Hwang M; Tan T; Pan Z; Korichneva I; Ma J Zinc Binding to MG53 Facilitates Repair of Injury to Cell Membrane. *J Biol Chem* 2015.
- (527). Li H; Duann P; Lin PH; Zhao L; Fan Z; Tan T; Zhou X; Sun M; Fu M; Orange Met al. Modulation of wound healing and scar formation by MG53-mediated cell membrane repair. *J Biol Chem* 2015.
- (528). Kim SC; Kellett T; Wang S; Nishi M; Nagre N; Zhou B; Flodby P; Shilo K; Ghadiali SN; Takeshima Het al. Modulation of TRIM72 Alters the Repair Capacity of Lung Epithelial Cells. *Annals of the American Thoracic Society* 2015, 12 Suppl 1, S72.

- (529). Jia Y; Chen K; Lin P; Lieber G; Nishi M; Yan R; Wang Z; Yao Y; Li Y; Whitson BA et al. Treatment of acute lung injury by targeting MG53-mediated cell membrane repair. *Nat Commun* 2014, 5, 4387. [PubMed: 25034454]
- (530). Bouter A; Gounou C; Berat R; Tan S; Gallois B; Granier T; d'Estaintot BL; Poschl E; Brachvogel B; Brisson AR Annexin-A5 assembled into two-dimensional arrays promotes cell membrane repair. *Nat Commun* 2011, 2.
- (531). Miller H; Castro-Gomes T; Corrotte M; Tam C; Mangel TK; Andrews NW; Song W Lipid raft-dependent plasma membrane repair interferes with the activation of B lymphocytes. *J Cell Biol* 2015, 211 (6), 1193. [PubMed: 26694840]
- (532). Friedrich U; Stachowicz N; Simm A; Fuhr G; Lucas K; Zimmermann U High efficiency electrotransfection with aluminum electrodes using microsecond controlled pulses. *Bioelectroch Bioener* 1998, 47 (1), 103.
- (533). Kanduser M; Sentjurs M; Miklavcic D The temperature effect during pulse application on cell membrane fluidity and permeabilization. *Bioelectrochemistry* 2008, 74 (1), 52. [PubMed: 18502189]
- (534). Corrotte M; Castro-Gomes T; Koushik AB; Andrews NW Approaches for plasma membrane wounding and assessment of lysosome-mediated repair responses. *Methods Cell Biol* 2015, 126, 139. [PubMed: 25665445]
- (535). Babychuk EB; Monastyrskaya K; Potez S; Draeger A Blebbing confers resistance against cell lysis. *Cell Death Differ* 2011, 18 (1), 80. [PubMed: 20596076]
- (536). Carmeille R; Degrelle SA; Plawinski L; Bouvet F; Gounou C; Evain-Brion D; Brisson AR; Bouter A Annexin-A5 promotes membrane resealing in human trophoblasts. *Biochimica et biophysica acta* 2015.
- (537). Weaver JC; Smith KC; Esser AT; Son RS; Gowrishankar TR A brief overview of electroporation pulse strength-duration space: A region where additional intracellular effects are expected. *Bioelectrochemistry* 2012, 87, 236. [PubMed: 22475953]
- (538). Beckers CJM; Keller DS; Balch WE Semi-Intact Cells Permeable to Macromolecules - Use in Reconstitution of Protein-Transport from the Endoplasmic-Reticulum to the Golgi-Complex. *Cell* 1987, 50 (4), 523. [PubMed: 3038335]
- (539). Donaldson JG; Lippincottschwartz J; Klausner RD Guanine-Nucleotides Modulate the Effects of Brefeldin-a in Semipermeable Cells - Regulation of the Association of a 110-Kd Peripheral Membrane-Protein with the Golgi-Apparatus. *J Cell Biol* 1991, 112 (4), 579. [PubMed: 1993732]
- (540). Simons K; Virta H Perforated Mdk Cells Support Intracellular-Transport. *Embo J* 1987, 6 (8), 2241. [PubMed: 3665874]
- (541). Burgess GM; Mckinney JS; Fabiato A; Leslie BA; Putney JW Calcium Pools in Saponin-Permeabilized Guinea-Pig Hepatocytes. *J Biol Chem* 1983, 258 (24), 5336.
- (542). Holz RW; Senter RA Plasma-Membrane and Chromaffin Granule Characteristics in Digitonin-Treated Chromaffin Cells. *J Neurochem* 1985, 45 (5), 1548. [PubMed: 3876408]
- (543). Wassler M; Jonasson I; Persson R; Fries E Differential Permeabilization of Membranes by Saponin Treatment of Isolated Rat Hepatocytes - Release of Secretory Proteins. *Biochem J* 1987, 247 (2), 407. [PubMed: 3426543]
- (544). Mick GJ; Bonn T; Steinberg J; McCormick K Preservation of Intermediary Metabolism in Saponin-Permeabilized Rat Adipocytes. *J Biol Chem* 1988, 263 (22), 10667. [PubMed: 3392034]
- (545). Mooney RA Use of Digitonin-Permeabilized Adipocytes for Camp Studies. *Method Enzymol* 1988, 159, 193.
- (546). Miller SG; Moore HPH Reconstitution of Constitutive Secretion Using Semi-Intact Cells - Regulation by Gtp but Not Calcium. *J Cell Biol* 1991, 112 (1), 39. [PubMed: 1986006]
- (547). Plutner H; Davidson HW; Saraste J; Balch WE Morphological Analysis of Protein-Transport from the Er to Golgi Membranes in Digitonin-Permeabilized Cells - Role of the P58 Containing Compartment. *J Cell Biol* 1992, 119 (5), 1097. [PubMed: 1447290]
- (548). Wilson R; Allen AJ; Oliver J; Brookman JL; High S; Bulleid NJ The Translocation, Folding, Assembly and Redox-Dependent Degradation of Secretory and Membrane-Proteins in Semi-Permeabilized Mammalian-Cells. *Biochem J* 1995, 307, 679. [PubMed: 7741697]

- (549). Negrutskii BS; Stapulionis R; Deutscher MP Supramolecular Organization of the Mammalian Translation System. *P Natl Acad Sci USA* 1994, 91 (3), 964.
- (550). Adam SA; Marr RS; Gerace L Nuclear-Protein Import in Permeabilized Mammalian-Cells Requires Soluble Cytoplasmic Factors. *J Cell Biol* 1990, 111 (3), 807. [PubMed: 2391365]
- (551). Hagstrom JE; Ludtke JJ; Bassik MC; Sebestyen MG; Adam SA; Wolff JA Nuclear import of DNA in digitonin-permeabilized cells. *J Cell Sci* 1997, 110, 2323. [PubMed: 9378781]
- (552). Kuznetsov AV; Veksler V; Gellerich FN; Saks V; Margreiter R; Kunz WS Analysis of mitochondrial function in situ in permeabilized muscle fibers, tissues and cells. *Nature protocols* 2008, 3 (6), 965. [PubMed: 18536644]
- (553). Kite GL Studies on the permeability of the internal cytoplasm of animal and plant cells. *American Journal of Physiology* 1915, 37 (2), 282.
- (554). Chambers R New apparatus and methods for the dissection and injection of living cells. *Anatomical Record* 1922, 24 (1), 1.
- (555). Hildebrand EM Micrurgy and the Plant Cell. *Bot Rev* 1960, 26 (3), 277.
- (556). Chambers R; Chambers EL Explorations into the Nature of the Living Cell. *Academic Medicine* 1961, 36 (8).
- (557). Wilson JF Micrurgical Techniques for Neurospora. *Am J Bot* 1961, 48 (1), 46.
- (558). Jeon KW; Danielli JF Micrurgical studies with large free-living amebas. *Int Rev Cytol* 1971, 30, 49. [PubMed: 4944678]
- (559). Terreros DA; Grantham JJ Barber, Marshall and the Origins of Micropipet Methods. *American Journal of Physiology* 1982, 242 (3), F293. [PubMed: 7039350]
- (560). Llinas R; Nicholson C; Blinks JR Calcium Transient in Presynaptic Terminal of Squid Giant Synapse -Detection with Aequorin. *Science* 1972, 176 (4039), 1127. [PubMed: 4338461]
- (561). Maller JL; Kemp BE; Krebs EG In vivo phosphorylation of a synthetic peptide substrate of cyclic AMP-dependent protein kinase. *Proc Natl Acad Sci U S A* 1978, 75 (1), 248. [PubMed: 203933]
- (562). Burrige K; Feramisco JR Microinjection and localization of a 130K protein in living fibroblasts: a relationship to actin and fibronectin. *Cell* 1980, 19 (3), 587. [PubMed: 6988083]
- (563). Stacey DW; Allfrey VG Microinjection Studies of Duck Globin Messenger-Rna Translation in Human and Avian Cells. *Cell* 1976, 9 (4), 725. [PubMed: 1035136]
- (564). Graessmann M; Graessmann A; Hoffmann E; Niebel J; Pilaski K The biological activity of different forms of Polyoma Virus DNA and viral DNA fragments. *Mol Biol Rep* 1973, 1 (4), 233. [PubMed: 24197572]
- (565). Gordon JW; Scangos GA; Plotkin DJ; Barbosa JA; Ruddle FH Genetic transformation of mouse embryos by microinjection of purified DNA. *Proc Natl Acad Sci U S A* 1980, 77 (12), 7380. [PubMed: 6261253]
- (566). Wormington WM Stable Repression of Ribosomal-Protein L1 Synthesis in Xenopus Oocytes by Microinjection of Antisense Rna. *P Natl Acad Sci USA* 1986, 83 (22), 8639.
- (567). Zhang YY; Ballas CB; Rao MP Towards Ultrahigh Throughput Microinjection: MEMS-based Massively-parallelized Mechanoporation. *Ieee Eng Med Bio* 2012, 594.
- (568). Knoblauch M; Hibberd JM; Gray JC; van Bel AJE A galinstan expansion femtosyringe for microinjection of eukaryotic organelles and prokaryotes. *Nat Biotechnol* 1999, 17 (9), 906. [PubMed: 10471935]
- (569). Laforge FO; Carpino J; Rotenberg SA; Mirkin MV Electrochemical attosyringe. *P Natl Acad Sci USA* 2007, 104 (29), 11895.
- (570). Singhal R; Orynbayeva Z; Sundaram RVK; Niu JJ; Bhattacharyya S; Vitol EA; Schrlau MG; Papazoglou ES; Friedman G; Gogotsi Y Multifunctional carbon-nanotube cellular endoscopes. *Nature nanotechnology* 2011, 6 (1), 57.
- (571). Simonis M; Hubner W; Wilking A; Huser T; Hennig S Survival rate of eukaryotic cells following electrophoretic nanoinjection. *Sci Rep* 2017, 7, 41277. [PubMed: 28120926]
- (572). Guillaume-Gentil O; Potthoff E; Ossola D; Franz CM; Zambelli T; Vorholt JA Force-controlled manipulation of single cells: from AFM to FluidFM. *Trends Biotechnol* 2014, 32 (7), 381. [PubMed: 24856959]

- (573). Meister A; Gabi M; Behr P; Studer P; Voros J; Niedermann P; Bitterli J; Polesel-Maris J; Liley M; Heinzlmann H et al. FluidFM: Combining Atomic Force Microscopy and Nanofluidics in a Universal Liquid Delivery System for Single Cell Applications and Beyond. *Nano Lett* 2009, 9 (6), 2501. [PubMed: 19453133]
- (574). Guillaume-Gentil O; Grindberg RV; Kooger R; Dorwling-Carter L; Martinez V; Ossola D; Pilhofer M; Zambelli T; Vorholt JA Tunable Single-Cell Extraction for Molecular Analyses. *Cell* 2016, 166 (2), 506. [PubMed: 27419874]
- (575). Guillaume-Gentil O; Rey T; Kiefer P; Ibanez AJ; Steinhoff R; Bronnimann R; Dorwling-Carter L; Zambelli T; Zenobi R; Vorholt JA Single-Cell Mass Spectrometry of Metabolites Extracted from Live Cells by Fluidic Force Microscopy. *Anal Chem* 2017, 89 (9), 5017. [PubMed: 28363018]
- (576). Guillaume-Gentil O; Potthoff E; Ossola D; Dorig P; Zambelli T; Vorholt JA Force-Controlled Fluidic Injection into Single Cell Nuclei. *Small* 2013, 9 (11), 1904. [PubMed: 23166090]
- (577). Seger RA; Actis P; Penfold C; Maalouf M; Vilozny B; Pourmand N Voltage controlled nano-injection system for single-cell surgery. *Nanoscale* 2012, 4 (19), 5843. [PubMed: 22899383]
- (578). Pepperkok R; Schneider C; Philipson L; Ansoerge W Single Cell Assay with an Automated Capillary Microinjection System. *Exp Cell Res* 1988, 178 (2), 369. [PubMed: 2458952]
- (579). Ansoerge W; Pepperkok R Performance of an Automated-System for Capillary Microinjection into Living Cells. *J Biochem Bioph Meth* 1988, 16 (4), 283.
- (580). Wang W; Liu X; Gelinas D; Ciruna B; Sun Y A fully automated robotic system for microinjection of zebrafish embryos. *Plos One* 2007, 2 (9), e862. [PubMed: 17848993]
- (581). Wang WH; Sun Y; Zhang M; Anderson R; Langille L; Chan W A system for high-speed microinjection of adherent cells. *Review of Scientific Instruments* 2008, 79 (10).
- (582). Adamo A; Jensen KF Microfluidic based single cell microinjection. *Lab on a chip* 2008, 8 (8), 1258. [PubMed: 18651065]
- (583). Adamo A; Roushdy O; Dokov R; Sharei A; Jensen KF Microfluidic jet injection for delivering macromolecules into cells. *J Micromech Microeng* 2013, 23 (3).
- (584). Klein TM; Fitzpatrick-McElligott S Particle bombardment: a universal approach for gene transfer to cells and tissues. *Curr Opin Biotechnol* 1993, 4 (5), 583. [PubMed: 7764210]
- (585). Sanford JC; Smith FD; Russell JA Optimizing the Biolistic Process for Different Biological Applications. *Method Enzymol* 1993, 217, 483.
- (586). Williams RS; Johnston SA; Riedy M; Devit MJ; Mcelligott SG; Sanford JC Introduction of Foreign Genes into Tissues of Living Mice by DNA-Coated Microprojectiles. *P Natl Acad Sci USA* 1991, 88 (7), 2726.
- (587). Yang NS; Burkholder J; Roberts B; Martinell B; McCabe D In vivo and in vitro gene transfer to mammalian somatic cells by particle bombardment. *Proc Natl Acad Sci U S A* 1990, 87 (24), 9568. [PubMed: 2175906]
- (588). Zelenin AV; Titomirov AV; Kolesnikov VA Genetic transformation of mouse cultured cells with the help of high-velocity mechanical DNA injection. *FEBS Lett* 1989, 244 (1), 65. [PubMed: 2924911]
- (589). Russell JA; Roy MK; Sanford JC Physical Trauma and Tungsten Toxicity Reduce the Efficiency of Biolistic Transformation. *Plant Physiol* 1992, 98 (3), 1050. [PubMed: 16668726]
- (590). Fitzpatrick-McElligott S Gene-Transfer to Tumor-Infiltrating Lymphocytes and Other Mammalian Somatic-Cells by Microprojectile Bombardment. *Bio-Technol* 1992, 10 (9), 1036.
- (591). Burkholder JK; Decker J; Yang NS Rapid transgene expression in lymphocyte and macrophage primary cultures after particle bombardment-mediated gene transfer. *J Immunol Methods* 1993, 165 (2), 149. [PubMed: 8228267]
- (592). Woffendin C; Yang ZY; Udaykumar; Xu L; Yang NS; Sheehy MJ; Nabel GJ Nonviral and Viral Delivery of a Human-Immunodeficiency-Virus Protective Gene into Primary Human T-Cells. *P Natl Acad Sci USA* 1994, 91 (24), 11581.
- (593). Verma S; Woffendin C; Bahner I; Ranga U; Xu L; Yang ZY; King SR; Kohn DB; Nabel GJ Gene transfer into human umbilical cord blood-derived CD34(+) cells by particle-mediated gene transfer. *Gene Ther* 1998, 5 (5), 692. [PubMed: 9797875]

- (594). Ye ZQ; Qiu P; Burkholder JK; Turner J; Culp J; Roberts T; Shahidi NT; Yang NS Cytokine transgene expression and promoter usage in primary CD34(+) cells using particle-mediated gene delivery. *Hum Gene Ther* 1998, 9 (15), 2197. [PubMed: 9794204]
- (595). Mahvi DM; Burkholder JK; Turner J; Culp J; Malter JS; Sondel PM; Yang NS Particle-mediated gene transfer of granulocyte-macrophage colony-stimulating factor cDNA to tumor cells: Implications for a clinically relevant tumor vaccine. *Hum Gene Ther* 1996, 7 (13), 1535. [PubMed: 8864754]
- (596). Uchida M; Li XW; Mertens P; Alpar HO Transfection by particle bombardment: Delivery of plasmid DNA into mammalian cells using gene gun. *Bba-Gen Subjects* 2009, 1790 (8), 754.
- (597). Zhang SB; Gu J; Yang NS; Kao CH; Gardner TA; Eble JN; Cheng L Relative promoter strengths in four human prostate cancer cell lines evaluated by particle bombardment-mediated gene transfer. *Prostate* 2002, 51 (4), 286. [PubMed: 11987157]
- (598). O'Brien JA; Lummis SCR Biolistic transfection of neuronal cultures using a hand-held gene gun. *Nature protocols* 2006, 1 (2), 977. [PubMed: 17406333]
- (599). Antolik C; De Deyne PG; Bloch RJ Biolistic transfection of cultured myotubes. *Sci STKE* 2003, 2003 (192), PL11. [PubMed: 12881614]
- (600). Heiser WC Gene-Transfer into Mammalian-Cells by Particle Bombardment. *Anal Biochem* 1994, 217 (2), 185. [PubMed: 8203746]
- (601). Johnston SA; Tang DC Gene Gun Transfection of Animal-Cells and Genetic Immunization. *Methods in Cell Biology*, Vol 43 1994, 43, 353. [PubMed: 7823871]
- (602). Thompson TA; Gould MN; Burkholder JK; Yang NS Transient Promoter Activity in Primary Rat Mammary Epithelial-Cells Evaluated Using Particle Bombardment Gene-Transfer. *In Vitro Cell Dev-An* 1993, 29 (2), 165.
- (603). Bridgman PC; Brown ME; Balan I Biolistic Transfection. *Neurons: Methods and Applications for the Cell Biologist* 2003, 71, 353.
- (604). O'Brien JA; Lummis SC Diolistic labeling of neuronal cultures and intact tissue using a hand-held gene gun. *Nature protocols* 2006, 1 (3), 1517. [PubMed: 17406443]
- (605). Klimaschewski L; Nindl W; Pimpl M; Waltinger P; Pfaller K Biolistic transfection and morphological analysis of cultured sympathetic neurons. *J Neurosci Meth* 2002, 113 (1), 63.
- (606). Usachev YM; Khammanivong A; Campbell C; Thayer SA Particle-mediated gene transfer to rat neurons in primary culture. *Pflugers Archiv-European Journal of Physiology* 2000, 439 (6), 730. [PubMed: 10784347]
- (607). McAllister AK Biolistic transfection of neurons. *Sci STKE* 2000, 2000 (51), p11.
- (608). Wellmann H; Kaltschmidt B; Kaltschmidt C Optimized protocol for biolistic transfection of brain slices and dissociated cultured neurons with a hand-held gene gun. *J Neurosci Meth* 1999, 92 (1-2), 55.
- (609). Biewenga JE; Destree OHJ; Schrama LH Plasmid-mediated gene transfer in neurons using the biolistics technique. *J Neurosci Meth* 1997, 71 (1), 67.
- (610). Lin MTS; Pulkkinen L; Uitto J; Yoon K The gene gun: current applications in cutaneous gene therapy. *Int J Dermatol* 2000, 39 (3), 161. [PubMed: 10759952]
- (611). Fuller DH; Loudon P; Schmaljohn C Preclinical and clinical progress of particle-mediated DNA vaccines for infectious diseases. *Methods* 2006, 40 (1), 86. [PubMed: 16997717]
- (612). Lin CC; Yen MC; Lin CM; Huang SS; Yang HJ; Chow NH; Lai MD Delivery of noncarrier naked DNA vaccine into the skin by supersonic flow induces a polarized T helper type 1 immune response to cancer. *J Gene Med* 2008, 10 (6), 679. [PubMed: 18324638]
- (613). Fynan EF; Webster RG; Fuller DH; Haynes JR; Santoro JC; Robinson HL DNA Vaccines - Protective Immunizations by Parenteral, Mucosal, and Gene-Gun Inoculations. *P Natl Acad Sci USA* 1993, 90 (24), 11478.
- (614). Raju PA; McSloy N; Truong NK; Kendall MAF Assessment of epidermal cell viability by near infrared multi-photon microscopy following ballistic delivery of gold micro-particles. *Vaccine* 2006, 24 (21), 4644. [PubMed: 16168530]
- (615). Yang NS; Sun WH; McCabe D Developing particle-mediated gene-transfer technology for research into gene therapy of cancer. *Mol Med Today* 1996, 2 (11), 476. [PubMed: 8947913]

- (616). Benediktsson AM; Schachtele SJ; Green SH; Dailey ME Ballistic labeling and dynamic imaging of astrocytes in organotypic hippocampal slice cultures. *J Neurosci Methods* 2005, 141 (1), 41. [PubMed: 15585287]
- (617). Kettunen P; Demas J; Lohmann C; Kasthuri N; Gong YD; Wong ROL; Gan WB Imaging calcium dynamics in the nervous system by means of ballistic delivery of indicators. *J Neurosci Meth* 2002, 119 (1), 37.
- (618). Gan WB; Grutzendler J; Wong WT; Wong ROL; Lichtman JW Multicolor "DiOlistic" labeling of the nervous system using lipophilic dye combinations. *Neuron* 2000, 27 (2), 219. [PubMed: 10985343]
- (619). Grutzendler J; Tsai J; Gan WB Rapid labeling of neuronal populations by ballistic delivery of fluorescent dyes. *Methods* 2003, 30 (1), 79. [PubMed: 12695105]
- (620). Davis RE; Parra A; LoVerde PT; Ribeiro E; Glorioso G; Hodgson S Transient expression of DNA and RNA in parasitic helminths by using particle bombardment. *P Natl Acad Sci USA* 1999, 96 (15), 8687.
- (621). Sohn RL; Murray MT; Schwarz K; Nyitray J; Purray P; Franko AP; Palmer KC; Diebel LN; Dulchavsky SA In-vivo particle mediated delivery of mRNA to mammalian tissues: ballistic and biologic effects. *Wound Repair Regen* 2001, 9 (4), 287. [PubMed: 11679137]
- (622). Schwarz KW; Murray MT; Sylora R; Sohn RL; Dulchavsky SA Augmentation of wound healing with translation initiation factor eIF4E mRNA. *J Surg Res* 2002, 103 (2), 175. [PubMed: 11922732]
- (623). Svarovsky S; Borovkov A; Sykes K Cationic gold microparticles for biolistic delivery of nucleic acids. *Biotechniques* 2008, 45 (5), 535. [PubMed: 19007338]
- (624). Belyantseva IA Helios Gene Gun-mediated transfection of the inner ear sensory epithelium. *Methods Mol Biol* 2009, 493, 103. [PubMed: 18839344]
- (625). Nishizawa K; Bremerich M; Ayade H; Schmidt CF; Ariga T; Mizuno D Feedback-tracking microrheology in living cells. *Science Advances* 2017, 3 (9).
- (626). Wu J; Du HW; Liao XW; Zhao Y; Li LG; Yang LY An improved particle bombardment for the generation of transgenic plants by direct immobilization of releasable Tn5 transposases onto gold particles. *Plant Mol Biol* 2011, 77 (1–2), 117. [PubMed: 21643845]
- (627). Martin-Ortigosa S; Valenstein JS; Lin VSY; Trewyn BG; Wang K Gold Functionalized Mesoporous Silica Nanoparticle Mediated Protein and DNA Codelivery to Plant Cells Via the Biolistic Method. *Adv Funct Mater* 2012, 22 (17), 3576.
- (628). Martin-Ortigosa S; Wang K Proteolistics: a biolistic method for intracellular delivery of proteins. *Transgenic research* 2014.
- (629). Liang Z; Chen KL; Li TD; Zhang Y; Wang YP; Zhao Q; Liu JX; Zhang HW; Liu CM; Ran YD et al. Efficient DNA-free genome editing of bread wheat using CRISPR/Cas9 ribonucleoprotein complexes. *Nat Commun* 2017, 8.
- (630). Zhang DW; Das DB; Rielly CD Potential of microneedle-assisted micro-particle delivery by gene guns: a review. *Drug Deliv* 2014, 21 (8), 571. [PubMed: 24313864]
- (631). O'Brien JA; Lummis SCR Nano-biolistics: a method of biolistic transfection of cells and tissues using a gene gun with novel nanometer-sized projectiles. *Bmc Biotechnol* 2011, 11.
- (632). Roizenblatt R; Weiland JD; Carcieri S; Qiu G; Behrend M; Humayun MS; Chow RH Nanobiolistic delivery of indicators to the living mouse retina. *J Neurosci Methods* 2006, 153 (1), 154. [PubMed: 16290199]
- (633). Cai D; Mataraza JM; Qin ZH; Huang ZP; Huang JY; Chiles TC; Carnahan D; Kempa K; Ren ZF Highly efficient molecular delivery into mammalian cells using carbon nanotube spearing. *Nat Methods* 2005, 2 (6), 449. [PubMed: 15908924]
- (634). McKnight TE; Melechko AV; Hensley DK; Mann DGJ; Griffin GD; Simpson ML Tracking gene expression after DNA delivery using spatially indexed nanofiber Arrays. *Nano Lett* 2004, 4 (7), 1213.
- (635). Mann DGJ; McKnight TE; McPherson JT; Hoyt PR; Melechko AV; Simpson ML; Saylor GS Inducible RNA interference-mediated gene silencing using nanostructured gene delivery arrays. *ACS Nano* 2008, 2 (1), 69. [PubMed: 19206549]

- (636). Kim W; Ng JK; Kunitake ME; Conklin BR; Yang PD Interfacing silicon nanowires with mammalian cells. *J Am Chem Soc* 2007, 129 (23), 7228. [PubMed: 17516647]
- (637). Shalek AK; Gaubblomme JT; Wang LL; Yosef N; Chevrier N; Andersen MS; Robinson JT; Pochet N; Neuberg D; Gertner RSet al. Nanowire-Mediated Delivery Enables Functional Interrogation of Primary Immune Cells: Application to the Analysis of Chronic Lymphocytic Leukemia. *Nano Lett* 2012, 12 (12), 6498. [PubMed: 23190424]
- (638). Choi M; Lee SH; Kim WB; Gujrati V; Kim D; Lee J; Kim J-I; Kim H; Saw PE; Jon S Intracellular Delivery of Bioactive Cargos to Hard-to-Transfect Cells Using Carbon Nanosyringe Arrays under an Applied Centrifugal g-Force. *Advanced Healthcare Materials* 2015, n/a.
- (639). Nair BG; Hagiwara K; Ueda M; Yu HH; Tseng HR; Ito Y High Density of Aligned Nanowire Treated with Polydopamine for Efficient Gene Silencing by siRNA According to Cell Membrane Perturbation. *ACS Appl Mater Interfaces* 2016.
- (640). Matsumoto D; Rao Sathuluri R; Kato Y; Silberberg YR; Kawamura R; Iwata F; Kobayashi T; Nakamura C Oscillating high-aspect-ratio monolithic silicon nanoneedle array enables efficient delivery of functional bio-macromolecules into living cells. *Sci Rep* 2015, 5, 15325. [PubMed: 26471006]
- (641). Kawamura R; Shimizu K; Matsumoto Y; Yamagishi A; Silberberg YR; Iijima M; Kuroda S; Fukazawa K; Ishihara K; Nakamura C High efficiency penetration of antibody-immobilized nanoneedle thorough plasma membrane for in situ detection of cytoskeletal proteins in living cells. *J Nanobiotechnol* 2016, 14.
- (642). Kim KH; Kim J; Choi JS; Bae S; Kwon D; Park I; Kim DH; Seo TS Rapid, High-Throughput, and Direct Molecular Beacon Delivery to Human Cancer Cells Using a Nanowire-Incorporated and Pneumatic Pressure-Driven Microdevice. *Small* 2015.
- (643). Park S; Kim YS; Kim WB; Jon S Carbon Nanosyringe Array as a Platform for Intracellular Delivery. *Nano Lett* 2009, 9 (4), 1325. [PubMed: 19254005]
- (644). Chan MS; Lo PK Nanoneedle-Assisted Delivery of Site-Selective Peptide-Functionalized DNA Nanocages for Targeting Mitochondria and Nuclei. *Small* 2014, 10 (7), 1255. [PubMed: 24323905]
- (645). Yosef N; Shalek AK; Gaubblomme JT; Jin HL; Lee YJ; Awasthi A; Wu C; Karwacz K; Xiao S; Jorgolli Met al. Dynamic regulatory network controlling T(H)17 cell differentiation. *Nature* 2013, 496 (7446), 461. [PubMed: 23467089]
- (646). Elnathan R; Delalat B; Brodoceanu D; Alhmod H; Harding FJ; Buehler K; Nelson A; Isa L; Kraus T; Voelcker NH Maximizing Transfection Efficiency of Vertically Aligned Silicon Nanowire Arrays. *Adv Funct Mater* 2015, 25 (46), 7215.
- (647). Mumm F; Beckwith KM; Bonde S; Martinez KL; Sikorski P A Transparent Nanowire-Based Cell Impalement Device Suitable for Detailed Cell-Nanowire Interaction Studies. *Small* 2013, 9 (2), 263. [PubMed: 23034997]
- (648). Hanson L; Lin ZC; Xie C; Cui Y; Cui BX Characterization of the Cell-Nanopillar Interface by Transmission Electron Microscopy. *Nano Lett* 2012, 12 (11), 5815. [PubMed: 23030066]
- (649). Berthing T; Bonde S; Rostgaard KR; Madsen MH; Sorensen CB; Nygard J; Martinez KL Cell membrane conformation at vertical nanowire array interface revealed by fluorescence imaging. *Nanotechnology* 2012, 23 (41).
- (650). Xie X; Xu AM; Angle MR; Tayebi N; Verma P; Melosh NA Mechanical Model of Vertical Nanowire Cell Penetration. *Nano Lett* 2013, 13 (12), 6002. [PubMed: 24237230]
- (651). Bae S; Park S; Kim J; Choi JS; Kim KH; Kwon D; Jin E; Park I; Kim DH; Seo TS Exogenous Gene Integration for Microalgal Cell Transformation Using a Nanowire-Incorporated Microdevice. *ACS Appl Mater Interfaces* 2015.
- (652). Lee D; Lee D; Won Y; Hong H; Kim Y; Song H; Pyun JC; Cho YS; Ryu W; Moon J Insertion of Vertically Aligned Nanowires into Living Cells by Inkjet Printing of Cells. *Small* 2016.
- (653). Xie X; Aalipour A; Gupta SV; Melosh NA Determining the Time Window for Dynamic Nanowire Cell Penetration Processes. *Acs Nano* 2015.
- (654). Wang Y; Yang Y; Yan L; Kwok SY; Li W; Wang ZG; Zhu XY; Zhu GY; Zhang WJ; Chen XFet al. Poking cells for efficient vector-free intracellular delivery. *Nat Commun* 2014, 5.

- (655). Vakarelski IU; Brown SC; Higashitani K; Moudgil BM Penetration of living cell membranes with fortified carbon nanotube tips. *Langmuir* 2007, 23 (22), 10893. [PubMed: 17894512]
- (656). Obataya I; Nakamura C; Han S; Nakamura N; Miyake J Nanoscale operation of a living cell using an atomic force microscope with a nanoneedle. *Nano Lett* 2005, 5 (1), 27. [PubMed: 15792407]
- (657). Obataya F; Nakamura C; Han SW; Nakamura N; Miyake J Mechanical sensing of the penetration of various nanoneedles into a living cell using atomic force microscopy. *Biosensors & bioelectronics* 2005, 20 (8), 1652. [PubMed: 15626623]
- (658). Han SW; Nakamura C; Obataya I; Nakamura N; Miyake J Gene expression using an ultrathin needle enabling accurate displacement and low invasiveness. *Biochem Bioph Res Co* 2005, 332 (3), 633.
- (659). Angle MR; Wang A; Thomas A; Schaefer AT; Melosh NA Penetration of Cell Membranes and Synthetic Lipid Bilayers by Nanoprobes. *Biophys J* 2014, 107 (9), 2091. [PubMed: 25418094]
- (660). Prinz CN Interactions between semiconductor nanowires and living cells. *J Phys-Condens Mat* 2015, 27 (23).
- (661). Persson H; Kobler C; Molhave K; Samuelson L; Tegenfeldt JO; Oredsson S; Prinz CN Fibroblasts Cultured on Nanowires Exhibit Low Motility, Impaired Cell Division, and DNA Damage. *Small* 2013, 9 (23), 4006. [PubMed: 23813871]
- (662). Persson H; Li Z; Tegenfeldt JO; Oredsson S; Prinz CN From immobilized cells to motile cells on a bed-of-nails: effects of vertical nanowire array density on cell behaviour. *Sci Rep-Uk* 2015, 5.
- (663). Bonde S; Berthing T; Madsen MH; Andersen TK; Buch-Manson N; Guo L; Li XM; Badique F; Anselme K; Nygard Jet al. Tuning InAs Nanowire Density for HEK293 Cell Viability, Adhesion, and Morphology: Perspectives for Nanowire-Based Biosensors. *ACS Appl Mater Inter* 2013, 5 (21), 10510.
- (664). VanDersarl JJ; Xu AM; Melosh NA Nanostraws for Direct Fluidic Intracellular Access. *Nano Lett* 2012, 12 (8), 3881. [PubMed: 22166016]
- (665). Peer E; Artzy-Schnirman A; Gepstein L; Sivan U Hollow Nanoneedle Array and Its Utilization for Repeated Administration of Biomolecules to the Same Cells. *ACS Nano* 2012, 6 (6), 4940. [PubMed: 22632128]
- (666). Xie X; Xu AM; Leal-Ortiz S; Cao YH; Garner CC; Melosh NA Nanostraw-Electroporation System for Highly Efficient Intracellular Delivery and Transfection. *ACS Nano* 2013, 7 (5), 4351. [PubMed: 23597131]
- (667). Xu AM; Kim SA; Wang DS; Aalipour A; Melosh NA Temporally resolved direct delivery of second messengers into cells using nanostraws. *Lab on a chip* 2016, 16 (13), 2434. [PubMed: 27292263]
- (668). Xu AM; Wang DS; Shieh P; Cao YH; Melosh NA Direct Intracellular Delivery of Cell-Impermeable Probes of Protein Glycosylation by Using Nanostraws. *Chembiochem* 2017, 18 (7), 623. [PubMed: 28130882]
- (669). Cao Y; Hjort M; Chen H; Birey F; Leal-Ortiz SA; Han CM; Santiago JG; Pasca SP; Wu JC; Melosh NA Nondestructive nanostraw intracellular sampling for longitudinal cell monitoring. *Proc Natl Acad Sci U S A* 2017.
- (670). Durney AR; Frenette LC; Hodvedt EC; Krauss TD; Mukaibo H Fabrication of Tapered Microtube Arrays and Their Application as a Microalgal Injection Platform. *ACS Appl Mater Inter* 2016, 8 (50), 34198.
- (671). Golshadi M; Wright LK; Dickerson IM; Schrlau MG High-Efficiency Gene Transfection of Cells through Carbon Nanotube Arrays. *Small* 2016, 12 (22), 3014. [PubMed: 27059518]
- (672). Chen X; Kis A; Zettl A; Bertozzi CR A cell nanoinjector based on carbon nanotubes. *P Natl Acad Sci USA* 2007, 104 (20), 8218.
- (673). Han SW; Nakamura C; Obataya I; Nakamura N; Miyake J A molecular delivery system by using AFM and nanoneedle. *Biosensors & bioelectronics* 2005, 20 (10), 2120. [PubMed: 15741084]
- (674). Cuerrier CM; Lebel R; Grandbois M Single cell transfection using plasmid decorated AFM probes. *Biochem Bioph Res Co* 2007, 355 (3), 632.

- (675). Aten QT; Jensen BD; Tamowski S; Wilson AM; Howell LL; Burnett SH Nanoinjection: pronuclear DNA delivery using a charged lance. *Transgenic research* 2012, 21 (6), 1279. [PubMed: 22415347]
- (676). Yoo SM; Kang M; Kang T; Kim DM; Lee SY; Kim B Electrotriggered, Spatioselective, Quantitative Gene Delivery into a Single Cell Nucleus by Au Nanowire Nanoinjector. *Nano Lett* 2013, 13 (6), 2431. [PubMed: 23638772]
- (677). Park K; Kim KC; Lee H; Sung Y; Kang M; Lee YM; Ahn JY; Lim JM; Kang T; Kim B et al. Suppressing mosaicism by Au nanowire injector-driven direct delivery of plasmids into mouse embryos. *Biomaterials* 2017, 138, 169. [PubMed: 28578294]
- (678). Hara C; Tateyama K; Akamatsu N; Imabayashi H; Karaki K; Nomura N; Okano H; Miyawaki A A practical device for pinpoint delivery of molecules into multiple neurons in culture. *Brain Cell Biol* 2006, 35 (4–6), 229. [PubMed: 18392728]
- (679). Yamamoto F; Furusawa M A simple microinjection technique not employing a micromanipulator. *Exp Cell Res* 1978, 117 (2), 441. [PubMed: 720420]
- (680). Yamamoto F; Furusawa M; Takamatsu K; Miura N; Uchida T Intracellular introduction of a fixed quantity of substances by pricking cells using a modified microscope. *Exp Cell Res* 1981, 135 (2), 341. [PubMed: 7308295]
- (681). Yamamoto F; Furusawa M; Furusawa I; Obinata M The ‘pricking’ method. A new efficient technique for mechanically introducing foreign DNA into the nuclei of culture cells. *Exp Cell Res* 1982, 142 (1), 79. [PubMed: 6958471]
- (682). Kudo A; Yamamoto F; Furusawa M; Kuroiwa A; Natori S; Obinata M Structure of Thymidine Kinase Gene Introduced into Mouse Ltk-Cells by a New Injection Method. *Gene* 1982, 19 (1), 11. [PubMed: 6292043]
- (683). Teichert GH; Burnett S; Jensen BD A microneedle array able to inject tens of thousands of cells simultaneously. *J Micromech Microeng* 2013, 23 (9).
- (684). Lee K; Lingampalli N; Pisano AP; Murthy N; So H Physical Delivery of Macromolecules using High-Aspect Ratio Nanostructured Materials. *ACS Appl Mater Inter* 2015.
- (685). Kwak M; Han L; Chen JJ; Fan R Interfacing Inorganic Nanowire Arrays and Living Cells for Cellular Function Analysis. *Small* 2015.
- (686). Sharma P; Cho HA; Lee JW; Ham WS; Park BC; Cho NH; Kim YK Efficient intracellular delivery of biomacromolecules employing clusters of zinc oxide nanowires. *Nanoscale* 2017.
- (687). Pan J; Yuan Y; Wang H; Liu F; Xiong X; Chen H; Yuan L Efficient Transfection by Using PDMAEMA Modified SiNWAs as a Platform for Ca²⁺-Dependent Gene Delivery. *ACS Appl Mater Inter* 2016.
- (688). Nateri AS; Tzavelas C; Bildirici L; Rickwood D Transfection of human peripheral blood mononuclear cells using immunoporation. *J Immunol* 2005, 26 (3), 169.
- (689). Tzavelas C; Bildirici L; Rickwood D Factors that affect the efficiency of cell transfection by immunoporation. *Anal Biochem* 2004, 328 (2), 219. [PubMed: 15113700]
- (690). Tzavelas C; Bildirici L; Rickwood D Production of stably transfected cell lines using immunoporation. *Biotechniques* 2004, 37 (2), 276. [PubMed: 15335220]
- (691). Bildirici L; Tzavelas C; Rickwood D Immunoporation of adherent cells in situ. *Mol Biol Cell* 2004, 15, 446A.
- (692). Bildirici L; Rickwood D Comparisons of different types of antibody-coated beads for cell transfection using immunoporation. *Mol Biol Cell* 2004, 15, 446A.
- (693). Bildirici L; Smith P; Tzavelas C; Horefti E; Rickwood D *Biotechniques* - Transfection of cells by immunoporation. *Nature* 2000, 405 (6784), 298. [PubMed: 10830950]
- (694). Rickwood D; Bildirici L; Smith P; Tromberg H Immunoporation: A novel method for transfecting cells selectively and at high efficiency. *Mol Biol Cell* 1999, 10, 271A. [PubMed: 9950676]
- (695). Manders EMM; Kimura H; Cook PR Direct imaging of DNA in living cells reveals the dynamics of chromosome formation. *J Cell Biol* 1999, 144 (5), 813. [PubMed: 10085283]
- (696). Cox D; Berg JS; Cammer M; Chingwundoh JO; Dale BM; Cheney RE; Greenberg S Myosin X is a downstream effector of PI(3)K during phagocytosis. *Nat Cell Biol* 2002, 4 (7), 469. [PubMed: 12055636]

- (697). Santic M; Molmeret M; Barker JR; Klose KE; Dekanic A; Doric M; Abu Kwaik Y A Francisella tularensis pathogenicity island protein essential for bacterial proliferation within the host cell cytosol. Cellular Microbiology 2007, 9 (10), 2391. [PubMed: 17517064]
- (698). Besteiro S; Michelin A; Poncet J; Dubremetz JF; Lebrun M Export of a Toxoplasma gondii Rhopty Neck Protein Complex at the Host Cell Membrane to Form the Moving Junction during Invasion. Plos Pathog 2009, 5 (2).
- (699). Rosqvist R; Forsberg A; Wolfwatz H Intracellular Targeting of the Yersinia Yope Cytotoxin in Mammalian-Cells Induces Actin Microfilament Disruption. Infection and Immunity 1991, 59 (12), 4562. [PubMed: 1937815]
- (700). Gilmore AP; Romer LH Inhibition of focal adhesion kinase (FAK) signaling in focal adhesions decreases cell motility and proliferation. Mol Biol Cell 1996, 7 (8), 1209. [PubMed: 8856665]
- (701). Memedula S; Belmont AS Sequential recruitment of HAT and SWI/SNF components to condensed chromatin by VP16. Curr Biol 2003, 13 (3), 241. [PubMed: 12573221]
- (702). Rai AK; Rai A; Ramaiya AJ; Jha R; Mallik R Molecular Adaptations Allow Dynein to Generate Large Collective Forces inside Cells. Cell 2013, 152 (1–2), 172. [PubMed: 23332753]
- (703). Becker T; Volchuk A; Rothman JE Differential use of endoplasmic reticulum membrane for phagocytosis in J774 macrophages. P Natl Acad Sci USA 2005, 102 (11), 4022.
- (704). Morisaki T; Lyon K; DeLuca KF; DeLuca JG; English BP; Zhang ZJ; Lavis LD; Grimm JB; Viswanathan S; Looger L et al. Real-time quantification of single RNA translation dynamics in living cells. Science 2016, 352 (6292), 1425. [PubMed: 27313040]
- (705). Molenaar C; Wiesmeijer K; Verwoerd NP; Khazen S; Eils R; Tanke HJ; Dirks RW Visualizing telomere dynamics in living mammalian cells using PNA probes. Embo J 2003, 22 (24), 6631. [PubMed: 14657034]
- (706). Jones SA; Shim SH; He J; Zhuang XW Fast, three-dimensional super-resolution imaging of live cells. Nat Methods 2011, 8 (6), 499. [PubMed: 21552254]
- (707). Cheng JP; Fernando KAS; Veca LM; Sun YP; Lamond AI; Lam YW; Cheng SH Reversible Accumulation of PEGylated Single-Walled Carbon Nanotubes in the Mammalian Nucleus. ACS Nano 2008, 2 (10), 2085. [PubMed: 19206455]
- (708). Emerson NT; Hsia CH; Rafalska-Metcalf IU; Yang H Mechanodelivery of nanoparticles to the cytoplasm of living cells. Nanoscale 2014, 6 (9), 4538. [PubMed: 24664211]
- (709). Frankel AD; Pabo CO Cellular uptake of the tat protein from human immunodeficiency virus. Cell 1988, 55 (6), 1189. [PubMed: 2849510]
- (710). Gentz R; Chen CH; Rosen CA Bioassay for Trans-Activation Using Purified Human Immunodeficiency Virus Tat-Encoded Protein - Trans-Activation Requires Messenger-Rna Synthesis. P Natl Acad Sci USA 1989, 86 (3), 821.
- (711). Malcolm KC; Elliott CM; Exton JH Evidence for Rho-mediated agonist stimulation of phospholipase D in Rat1 fibroblasts - Effects of Clostridium botulinum C3 exoenzyme. J Biol Chem 1996, 271 (22), 13135. [PubMed: 8662844]
- (712). Flinn HM; Ridley AJ Rho stimulates tyrosine phosphorylation of focal adhesion kinase, p130 and paxillin. J Cell Sci 1996, 109, 1133. [PubMed: 8743960]
- (713). Ubezio P; Civoli F Flow Cytometric Detection of Hydrogen-Peroxide Production Induced by Doxorubicin in Cancer-Cells. Free Radical Bio Med 1994, 16 (4), 509. [PubMed: 8005536]
- (714). Cusato K; Bosco A; Rozental R; Guimaraes CA; Reese BE; Linden R; Spray DC Gap junctions mediate bystander cell death in developing retina. Journal of Neuroscience 2003, 23 (16), 6413. [PubMed: 12878681]
- (715). Kamijo K; Ohara N; Abe M; Uchimura T; Hosoya H; Lee JS; Miki T Dissecting the role of Rho-mediated signaling in contractile ring Formation. Mol Biol Cell 2006, 17 (1), 43. [PubMed: 16236794]
- (716). Bernat RL; Borisy GG; Rothfield NF; Earnshaw WC Injection of Anticentromere Antibodies in Interphase Disrupts Events Required for Chromosome Movement at Mitosis. J Cell Biol 1990, 111 (4), 1519. [PubMed: 2211824]
- (717). Hollenbeck PJ; Swanson JA Radial Extension of Macrophage Tubular Lysosomes Supported by Kinesin. Nature 1990, 346 (6287), 864. [PubMed: 1697403]

- (718). Araki N; Hatae T; Yamada T; Hirohashi S Actinin-4 is preferentially involved in circular ruffling and macropinocytosis in mouse macrophages: analysis by fluorescence ratio imaging. *J Cell Sci* 2000, 113 (18), 3329. [PubMed: 10954430]
- (719). Adler V; Pincus MR; Polotskaya A; Montano X; Friedman FK; Ronai Z Activation of c-Jun-NH2-kinase by UV irradiation is dependent on p21(ras). *J Biol Chem* 1996, 271 (38), 23304. [PubMed: 8798530]
- (720). Riedl J; Crevenna AH; Kessenbrock K; Yu JH; Neukirchen D; Bista M; Bradke F; Jenne D; Holak TA; Werb Z et al. Lifeact: a versatile marker to visualize F-actin. *Nat Methods* 2008, 5 (7), 605. [PubMed: 18536722]
- (721). Partridge M; Vincent A; Matthews P; Puma J; Stein D; Summerton J A simple method for delivering morpholino antisense oligos into the cytoplasm of cells. *Antisense Nucleic A* 1996, 6 (3), 169.
- (722). Altan N; Chen Y; Schindler M; Simon SM Tamoxifen inhibits acidification in cells independent of the estrogen receptor. *P Natl Acad Sci USA* 1999, 96 (8), 4432.
- (723). O'Riordan M; Yi CH; Gonzales R; Lee KD; Portnoy DA Innate recognition of bacteria by a macrophage cytosolic surveillance pathway. *P Natl Acad Sci USA* 2002, 99 (21), 13861.
- (724). Steinberg TH; Newman AS; Swanson JA; Silverstein SC Macrophages Possess Probenecid-Inhibitable Organic Anion Transporters That Remove Fluorescent Dyes from the Cytoplasmic Matrix. *J Cell Biol* 1987, 105 (6), 2695. [PubMed: 3693397]
- (725). Cheng BX; Zhao SJ; Luo J; Sprague E; Bonewald LF; Jiang JX Expression of functional gap junctions and regulation by fluid flow in osteocyte-like MLO-Y4 cells. *J Bone Miner Res* 2001, 16 (2), 249. [PubMed: 11204425]
- (726). Wu MM; Grabe M; Adams S; Tsien RY; Moore HPH; Machen TE Mechanisms of pH regulation in the regulated secretory pathway. *J Biol Chem* 2001, 276 (35), 33027. [PubMed: 11402049]
- (727). Swanson JA; Mcneil PL Nuclear Reassembly Excludes Large Macromolecules. *Science* 1987, 238 (4826), 548. [PubMed: 2443981]
- (728). Legenzov EA; Dirda NDA; Hagen BM; Kao JPY Synthesis and Characterization of 8-O-Carboxymethylpyranine (CM-Pyranine) as a Bright, Violet-Emitting, Fluid-Phase Fluorescent Marker in Cell Biology. *Plos One* 2015, 10 (7).
- (729). Schermelleh L; Solovei I; Zink D; Cremer T Two-color fluorescence labeling of early and mid-to-late replicating chromatin in living cells. *Chromosome Res* 2001, 9 (1), 77. [PubMed: 11272795]
- (730). Lin YC; Ho CH; Grinnell F Fibroblasts contracting collagen matrices form transient plasma membrane passages through which the cells take up fluorescein isothiocyanate-dextran and Ca2+. *Mol Biol Cell* 1997, 8 (1), 59. [PubMed: 9017595]
- (731). Grinnell F Fibroblast-collagen-matrix contraction: growth-factor signalling and mechanical loading. *Trends Cell Biol* 2000, 10 (9), 362. [PubMed: 10932093]
- (732). Pellegrin P; Fernandez A; Lamb NJC; Bennes R Macromolecular uptake is a spontaneous event during mitosis in cultured fibroblasts: Implications for vector-dependent plasmid transfection. *Mol Biol Cell* 2002, 13 (2), 570. [PubMed: 11854413]
- (733). Sit KH; Bay BH; Wong KP Distinctive Uptake of Neutral Red by Mitotic Cancer-Cells. *Biotech Histochem* 1992, 67 (4), 196. [PubMed: 1504181]
- (734). Sit KH Cell rounding with "rip off" detachment. *Histol Histopathol* 1996, 11 (1), 215. [PubMed: 8720465]
- (735). Lemons R; Forster S; Thoene J Protein Microinjection by Protease Permeabilization of Fibroblasts. *Anal Biochem* 1988, 172 (1), 219. [PubMed: 2847580]
- (736). Brugmans M; Cassiman JJ; Vanleuven F; Vandenberghe H Quantitative Assessment of the Amount and the Activity of Trypsin Associated with Trypsinized Cells. *Cell Biol Int Rep* 1979, 3 (3), 257. [PubMed: 445582]
- (737). Borowski P; Oehlmann K; Heiland M; Laufs R Nonstructural protein 3 of hepatitis C virus blocks the distribution of the free catalytic subunit of cyclic AMP-dependent protein kinase. *J Virol* 1997, 71 (4), 2838. [PubMed: 9060639]

- (738). Borowski P; zur Wiesch JS; Resch K; Feucht H; Laufs R; Schmitz H Protein kinase C recognizes the protein kinase A-binding motif of nonstructural protein 3 of hepatitis C virus. *J Biol Chem* 1999, 274 (43), 30722. [PubMed: 10521461]
- (739). Stewart MP, TU Dresden, 2012.
- (740). Sautter C; Waldner H; Neuhaus G; Galli A; Neuhaus G; Potrykus I Micro-Targeting - High-Efficiency Gene-Transfer Using a Novel-Approach for the Acceleration of Micro-Projectiles. *Bio-Technol* 1991, 9 (11), 1080.
- (741). Williams AR; Bao S; Miller DL Filtration: A simple, reliable technique for transfection and macromolecular loading of cells in suspension. *Biotechnol Bioeng* 1999, 65 (3), 341. [PubMed: 10486133]
- (742). Sharei A; Cho N; Mao S; Jackson E; Pocevičiute R; Adamo A; Zoldan J; Langer R; Jensen KF Cell Squeezing as a Robust, Microfluidic Intracellular Delivery Platform. *J Vis Exp* 2013, (81), e50980. [PubMed: 24300077]
- (743). Sharei A; Pocevičiute R; Jackson EL; Cho N; Mao S; Hartoularos GC; Jang DY; Jhunjhunwala S; Eyerman A; Schoettle Tet al. Plasma membrane recovery kinetics of a microfluidic intracellular delivery platform. *Integr Biol (Camb)* 2014.
- (744). Sharei A; Trifonova R; Jhunjhunwala S; Hartoularos GC; Eyerman AT; Lytton-Jean A; Angin M; Sharma S; Pocevičiute R; Mao Set al. Ex Vivo Cytosolic Delivery of Functional Macromolecules to Immune Cells. *Plos One* 2015, 10 (4).
- (745). Szeto GL; Van Egeren D; Worku H; Sharei A; Alejandro B; Park C; Frew K; Brefo M; Mao S; Heimann Met al. Microfluidic squeezing for intracellular antigen loading in polyclonal B-cells as cellular vaccines. *Sci Rep-Uk* 2015, 5.
- (746). Griesbeck M; Ziegler S; Laffont S; Smith N; Chauveau L; Tomezsko P; Sharei A; Kourjian G; Porichis F; Hart Met al. Sex Differences in Plasmacytoid Dendritic Cell Levels of IRF5 Drive Higher IFN-alpha Production in Women. *J Immunol* 2015, 195 (11), 5327. [PubMed: 26519527]
- (747). Tu C; Santo L; Mishima Y; Raje N; Smilansky Z; Zoldan J Monitoring protein synthesis in single live cancer cells. *Integr Biol (Camb)* 2016, 8 (5), 645. [PubMed: 26956582]
- (748). Saung MT; Sharei A; Adalsteinsson VA; Cho N; Kamath T; Ruiz C; Kirkpatrick J; Patel N; Mino-Kenudson M; Thayer SP et al. A Size-Selective Intracellular Delivery Platform. *Small* 2016, 12 (42), 5873. [PubMed: 27594517]
- (749). Ding X; Stewart MP; Sharei A; Weaver JC; Langer RS; Jensen KF High-throughput nuclear delivery and rapid expression of DNA via mechanical and electrical cell-membrane disruption. *Nature Biomedical Engineering* 2017, 1, 0039.
- (750). Liu Z; Han X; Zhou Q; Chen R; Fruge S; Jo MC; Ma Y; Li Z; Yokoi K; Qin L Integrated Microfluidic System for Gene Silencing and Cell Migration. *Advanced Biosystems* 2017, 1700054. [PubMed: 28890929]
- (751). Raab M; Gentili M; de Belly H; Thiam HR; Vargas P; Jimenez AJ; Lautenschlaeger F; Voituriez R; Lennon-Dumenil AM; Manel Net al. ESCRT III repairs nuclear envelope ruptures during cell migration to limit DNA damage and cell death. *Science* 2016, 352 (6283), 359. [PubMed: 27013426]
- (752). Denais CM; Gilbert RM; Isermann P; McGregor AL; te Lindert M; Weigelin B; Davidson PM; Friedl P; Wolf K; Lammerding J Nuclear envelope rupture and repair during cancer cell migration. *Science* 2016, 352 (6283), 353. [PubMed: 27013428]
- (753). Olmos Y; Hodgson L; Mantell J; Verkade P; Carlton JG ESCRT-III controls nuclear envelope reformation. *Nature* 2015, 522 (7555), 236. [PubMed: 26040713]
- (754). Han X; Liu ZB; Jo MC; Zhang K; Li Y; Zeng ZH; Li N; Zu YL; Qin LD CRISPR-Cas9 delivery to hard-to-transfect cells via membrane deformation. *Science Advances* 2015, 1 (7).
- (755). Ma Y; Han X; Bustamante OQ; de Castro RB; Zhang K; Zhang PC; Li Y; Liu ZB; Liu XW; Ferrari Met al. Highly efficient genome editing of human hematopoietic stem cells via a nano-silicon-blade delivery approach. *Integr Biol-Uk* 2017, 9 (6), 548.
- (756). Versaavel M; Riaz M; Grevesse T; Gabriele S Cell confinement: putting the squeeze on the nucleus. *Soft Matter* 2013, 9 (29), 6665.
- (757). Rowat AC; Jaalouk DE; Zwerger M; Ung WL; Eydelnant IA; Olins DE; Olins AL; Herrmann H; Weitz DA; Lammerding J Nuclear Envelope Composition Determines the Ability of

- Neutrophil-type Cells to Passage through Micron-scale Constrictions. *J Biol Chem* 2013, 288 (12), 8610. [PubMed: 23355469]
- (758). Harada T; Swift J; Irianto J; Shin JW; Spinler KR; Athirasala A; Diegmiller R; Dingal PCDP; Ivanovska IL; Discher DE Nuclear lamin stiffness is a barrier to 3D migration, but softness can limit survival. *J Cell Biol* 2014, 204 (5), 669. [PubMed: 24567359]
- (759). Mayr M; Hu YH; Hainaut P; Xu QB Mechanical stress-induced DNA damage and rac-p38MAPK signal pathways mediate p53-dependent apoptosis in vascular smooth muscle cells. *Faseb J* 2002, 16 (9), 1423. [PubMed: 12205035]
- (760). Wood DK; Weingeist DM; Bhatia SN; Engelward BP Single cell trapping and DNA damage analysis using microwell arrays. *P Natl Acad Sci USA* 2010, 107 (22), 10008.
- (761). Matsumoto D; Yamagishi A; Saito M; Sathuluri RR; Silberberg YR; Iwata F; Kobayashi T; Nakamura C Mechanoporation of living cells for delivery of macromolecules using nanoneedle array. *J Biosci Bioeng* 2016, 122 (6), 748. [PubMed: 27316458]
- (762). Yan L; Zhang J; Lee CS; Chen X Micro- and Nanotechnologies for Intracellular Delivery. *Small* 2014.
- (763). Hanasaki I; Walther JH; Kawano S; Koumoutsakos P Coarse-grained molecular dynamics simulations of shear-induced instabilities of lipid bilayer membranes in water. *Physical Review E* 2010, 82 (5).
- (764). Yuan F; Yang C; Zhong P Cell membrane deformation and bioeffects produced by tandem bubble-induced jetting flow. *Proc Natl Acad Sci U S A* 2015, 112 (51), E7039. [PubMed: 26663913]
- (765). Waldman AS; Waldman BC Stable transfection of mammalian cells by syringe-mediated mechanical loading of DNA. *Anal Biochem* 1998, 258 (2), 216. [PubMed: 9570832]
- (766). Ghosh C; Iversen PL Intracellular delivery strategies for antisense phosphorodiamidate morpholino oligomers. *Antisense Nucleic A* 2000, 10 (4), 263.
- (767). Laudanna C; Campbell JJ; Butcher EC Role of Rho in chemoattractant-activated leukocyte adhesion through integrins. *Science* 1996, 271 (5251), 981. [PubMed: 8584934]
- (768). Meyer CJ; Alenghat FJ; Rim P; Fong JHJ; Fabry B; Ingber DE Mechanical control of cyclic AMP signalling and gene transcription through integrins. *Nat Cell Biol* 2000, 2 (9), 666. [PubMed: 10980709]
- (769). Hollenbeck PJ Products of Endocytosis and Autophagy Are Retrieved from Axons by Regulated Retrograde Organelle Transport. *J Cell Biol* 1993, 121 (2), 305. [PubMed: 7682217]
- (770). Tachibana K; Sato T; Davirro N; Morimoto C Direct Association of Pp125(Fak) with Paxillin, the Focal Adhesion-Targeting Mechanism of Pp125(Fak). *J Exp Med* 1995, 182 (4), 1089. [PubMed: 7561682]
- (771). VanNhiu GT; Krukonis ES; Reszka AA; Horwitz AF; Isberg RR Mutations in the cytoplasmic domain of the integrin beta(1) chain indicate a role for endocytosis factors in bacterial internalization. *J Biol Chem* 1996, 271 (13), 7665. [PubMed: 8631804]
- (772). Sydor AM; Su AL; Wang FS; Xu A; Jay DG Talin and vinculin play distinct roles in filopodial motility in the neuronal growth cone. *J Cell Biol* 1996, 134 (5), 1197. [PubMed: 8794861]
- (773). De Vos K; Goossens V; Boone E; Vercammen D; Vancompernelle K; Vandenaabeele P; Haegeman G; Fiers W; Grooten J The 55-kDa tumor necrosis factor receptor induces clustering of mitochondria through its membrane-proximal region. *J Biol Chem* 1998, 273 (16), 9673. [PubMed: 9545301]
- (774). Kaiser DA; Vinson VK; Murphy DB; Pollard TD Profilin is predominantly associated with monomeric actin in *Acanthamoeba*. *J Cell Sci* 1999, 112 (21), 3779. [PubMed: 10523513]
- (775). Adams JC; Schwartz MA Stimulation of fascin spikes by thrombospondin-1 is mediated by the GTPases Rac and Cdc42. *J Cell Biol* 2000, 150 (4), 807. [PubMed: 10953005]
- (776). Tzima E; Del Pozo MA; Kiosses WB; Mohamed SA; Li S; Chien S; Schwartz MA Activation of Rac1 by shear stress in endothelial cells mediates both cytoskeletal reorganization and effects on gene expression. *Embo J* 2002, 21 (24), 6791. [PubMed: 12486000]
- (777). Katsumi A; Milanini J; Kiosses WB; del Pozo MA; Kaunas R; Chien S; Hahn KM; Schwartz MA Effects of cell tension on the small GTPase Rac. *J Cell Biol* 2002, 158 (1), 153. [PubMed: 12105187]

- (778). Shoeman RL; Huttermann C; Hartig R; Traub P Amino-terminal polypeptides of vimentin are responsible for the changes in nuclear architecture associated with human immunodeficiency virus type 1 protease activity in tissue culture cells. *Mol Biol Cell* 2001, 12 (1), 143. [PubMed: 11160829]
- (779). Phillips RM; Six DA; Dennis EA; Ghosh P In vivo phospholipase activity of the *Pseudomonas aeruginosa* cytotoxin ExoU and protection of mammalian cells with phospholipase A(2) inhibitors. *J Biol Chem* 2003, 278 (42), 41326. [PubMed: 12915403]
- (780). Xu L; Shen XH; Bryan A; Banga S; Swanson MS; Luo ZQ Inhibition of Host Vacuolar H⁺-ATPase Activity by a *Legionella pneumophila* Effector. *Plos Pathog* 2010, 6 (3).
- (781). Copeland AM; Newcomb WW; Brown JC Herpes simplex virus replication: roles of viral proteins and nucleoporins in capsid-nucleus attachment. *J Virol* 2009, 83 (4), 1660. [PubMed: 19073727]
- (782). McNeil PL In *Current Protocols in Cell Biology*; John Wiley & Sons, Inc, 2001.
- (783). Hallow DM; Seeger RA; Kamaev PP; Prado GR; LaPlaca MC; Prausnitz MR Shear-induced intracellular loading of cells with molecules by controlled microfluidics. *Biotechnol Bioeng* 2008, 99 (4), 846. [PubMed: 17879304]
- (784). LaPlaca MC; Lee VMY; Thibault LE An in vitro model of traumatic neuronal injury: Loading rate-dependent changes in acute cytosolic calcium and lactate dehydrogenase release. *J Neurotraum* 1997, 14 (6), 355.
- (785). Blackman BR; Barbee KA; Thibault LE In vitro cell shearing device to investigate the dynamic response of cells in a controlled hydrodynamic environment. *Ann Biomed Eng* 2000, 28 (4), 363. [PubMed: 10870893]
- (786). Kilinc D; Gallo G; Barbee KA Mechanically-induced membrane poration causes axonal beading and localized cytoskeletal damage. *Experimental neurology* 2008, 212 (2), 422. [PubMed: 18572167]
- (787). Chouinard-Pelletier G; Leduc M; Guay D; Coulombe S; Leask RL; Jones EAV Use of inert gas jets to measure the forces required for mechanical gene transfection. *Biomed Eng Online* 2012, 11. [PubMed: 22394477]
- (788). Cooper S; Jonak P; Chouinard-Pelletier G; Coulombe S; Jones E; Leask RL Permeabilization of Adhered Cells Using an Inert Gas Jet 2013, (79), e50612.
- (789). Fechheimer M; Denny C; Murphy RF; Taylor DL Measurement of Cytoplasmic Ph in *Dictyostelium Discoideum* by Using a New Method for Introducing Macromolecules into Living Cells. *European Journal of Cell Biology* 1986, 40 (2), 242. [PubMed: 3709548]
- (790). Fechheimer M; Taylor DL Introduction of Exogenous Molecules into the Cytoplasm of *Dictyostelium-Discoideum* Amebas by Controlled Sonication. *Methods in Cell Biology* 1987, 28, 179. [PubMed: 3298991]
- (791). Furukawa R; Wampler JE; Fechheimer M Measurement of the Cytoplasmic Ph of *Dictyostelium-Discoideum* Using a Low Light Level Microspectrofluorometer. *J Cell Biol* 1988, 107 (6), 2541. [PubMed: 2849608]
- (792). Wyber JA; Andrews J; DEmanuele A The use of sonication for the efficient delivery of plasmid DNA into cells. *Pharm Res-Dordr* 1997, 14 (6), 750.
- (793). Bao SP; Thrall BD; Miller DL Transfection of a reporter plasmid into cultured cells by sonoporation in vitro. *Ultrasound Med Biol* 1997, 23 (6), 953. [PubMed: 9300999]
- (794). Kim HJ; Greenleaf JF; Kinnick RR; Bronk JT; Bolander ME Ultrasound-mediated transfection of mammalian cells. *Hum Gene Ther* 1996, 7 (11), 1339. [PubMed: 8818721]
- (795). Miller DL; Pislaru SV; Greenleaf JE Sonoporation: mechanical DNA delivery by ultrasonic cavitation. *Somatic cell and molecular genetics* 2002, 27 (1-6), 115. [PubMed: 12774945]
- (796). Kennedy JE; ter Haar GR; Cranston D High intensity focused ultrasound: surgery of the future? *Brit J Radiol* 2003, 76 (909), 590. [PubMed: 14500272]
- (797). Hill CR; terHaar GR Review article: High intensity focused ultrasound-potential for cancer treatment. *Brit J Radiol* 1995, 68 (816), 1296. [PubMed: 8777589]
- (798). Mitragotri S Innovation - Healing sound: the use of ultrasound in drug delivery and other therapeutic applications. *Nat Rev Drug Discov* 2005, 4 (3), 255. [PubMed: 15738980]

- (799). Miller MW; Miller DL; Brayman AA A review of in vitro bioeffects of inertial ultrasonic cavitation from a mechanistic perspective. *Ultrasound Med Biol* 1996, 22 (9), 1131. [PubMed: 9123638]
- (800). Greenleaf WJ; Bolander ME; Sarkar G; Goldring MB; Greenleaf JF Enhancement of ultrasonically induced cell transfection with artificial cavitation nuclei. 1997 *Ieee Ultrasonics Symposium Proceedings, Vols 1 & 2* 1997, 1365.
- (801). Greenleaf WJ; Bolander ME; Sarkar G; Goldring MB; Greenleaf JF Artificial cavitation nuclei significantly enhance acoustically induced cell transfection. *Ultrasound Med Biol* 1998, 24 (4), 587. [PubMed: 9651968]
- (802). Oberli MA; Schoellhammer CM; Langer R; Blankschtein D Ultrasound-enhanced transdermal delivery: recent advances and future challenges. *Therapeutic delivery* 2014, 5 (7), 843. [PubMed: 25287389]
- (803). Lentacker I; De Cock I; Deckers R; De Smedt SC; Moonen CT Understanding ultrasound induced sonoporation: Definitions and underlying mechanisms. *Adv Drug Deliv Rev* 2014, 72C, 49.
- (804). Kooiman K; Vos HJ; Versluis M; de Jong N Acoustic behavior of microbubbles and implications for drug delivery. *Adv Drug Deliv Rev* 2014, 72C, 28.
- (805). Fan Z; Kumon RE; Deng CX Mechanisms of microbubble-facilitated sonoporation for drug and gene delivery. *Therapeutic delivery* 2014, 5 (4), 467. [PubMed: 24856171]
- (806). Sutton JT; Haworth KJ; Pyne-Geithman G; Holland BK Ultrasound-mediated drug delivery for cardiovascular disease. *Expert Opin Drug Del* 2013, 10 (5), 573.
- (807). Liu Y; Yan J; Prausnitz MR Can Ultrasound Enable Efficient Intracellular Uptake of Molecules? A Retrospective Literature Review and Analysis. *Ultrasound Med Biol* 2012, 38 (5), 876. [PubMed: 22425381]
- (808). van Wamel A; Kooiman K; Hartevelde M; Emmer M; ten Cate FJ; Versluis M; de Jong N Vibrating microbubbles poking individual cells: Drug transfer into cells via sonoporation. *Journal of Controlled Release* 2006, 112 (2), 149. [PubMed: 16556469]
- (809). Delalande A; Kotopoulis S; Postema M; Midoux P; Pichon C Sonoporation: Mechanistic insights and ongoing challenges for gene transfer. *Gene* 2013, 525 (2), 191. [PubMed: 23566843]
- (810). Guo XS; Cai CL; Xu GY; Yang YY; Tu J; Huang PT; Zhang D Interaction between cavitation microbubble and cell: A simulation of sonoporation using boundary element method (BEM). *Ultrason Sonochem* 2017, 39, 863. [PubMed: 28733016]
- (811). Marmottant P; Hilgenfeldt S Controlled vesicle deformation and lysis by single oscillating bubbles. *Nature* 2003, 423 (6936), 153. [PubMed: 12736680]
- (812). Forbes MM; Steinberg RL; O'Brien WD Examination of Inertial Cavitation of Optison in Producing Sonoporation of Chinese Hamster Ovary Cells. *Ultrasound Med Biol* 2008, 34 (12), 2009. [PubMed: 18692296]
- (813). Schlicher RK; Radhakrishna H; Tolentino TP; Apkarian RP; Zarnitsyn V; Prausnitz MR Mechanism of intracellular delivery by acoustic cavitation. *Ultrasound Med Biol* 2006, 32 (6), 915. [PubMed: 16785013]
- (814). Zarnitsyn V; Rostad CA; Prausnitz MR Modeling Transmembrane Transport through Cell Membrane Wounds Created by Acoustic Cavitation. *Biophys J* 2008, 95 (9), 4124. [PubMed: 18676653]
- (815). Kudo N; Okada K; Yamamoto K Sonoporation by Single-Shot Pulsed Ultrasound with Microbubbles Adjacent to Cells. *Biophys J* 2009, 96 (12), 4866. [PubMed: 19527645]
- (816). Huber PE; Pfisterer P In vitro and in vivo transfection of plasmid DNA in the Dunning prostate tumor R3327-AT1 is enhanced by focused ultrasound. *Gene Ther* 2000, 7 (17), 1516. [PubMed: 11001372]
- (817). Frenkel PA; Chen SY; Thai T; Shohet RV; Grayburn PA DNA-loaded albumin microbubbles enhance ultrasound-mediated transfection in vitro. *Ultrasound Med Biol* 2002, 28 (6), 817. [PubMed: 12113794]
- (818). Zarnitsyn VG; Prausnitz MR Physical parameters influencing optimization of ultrasound-mediated DNA transfection. *Ultrasound Med Biol* 2004, 30 (4), 527. [PubMed: 15121255]

- (819). Meijering BDM; Henning RH; Van Gilst WH; Gavrilovic I; Van Wamel A; Deelman LE Optimization of ultrasound and microbubbles targeted gene delivery to cultured primary endothelial cells. *J Drug Target* 2007, 15 (10), 664. [PubMed: 18041634]
- (820). Zarnitsyn VG; Meacham JM; Varady MJ; Hao CH; Degertekin FL; Fedorov AG Electrosonic ejector microarray for drug and gene delivery. *Biomed Microdevices* 2008, 10 (2), 299. [PubMed: 17994280]
- (821). Fan Z; Chen D; Deng CX Improving ultrasound gene transfection efficiency by controlling ultrasound excitation of microbubbles. *Journal of controlled release : official journal of the Controlled Release Society* 2013, 170 (3), 401. [PubMed: 23770009]
- (822). Liu Y; Yan J; Santangelo PJ; Prausnitz MR DNA uptake, intracellular trafficking and gene transfection after ultrasound exposure. *Journal of controlled release : official journal of the Controlled Release Society* 2016.
- (823). Miura S; Tachibana K; Okamoto T; Saku K In vitro transfer of antisense oligodeoxynucleotides into coronary endothelial cells by ultrasound. *Biochem Bioph Res Co* 2002, 298 (4), 587.
- (824). Kinoshita M; Hynynen K A novel method for the intracellular delivery of siRNA using microbubble-enhanced focused ultrasound. *Biochem Bioph Res Co* 2005, 335 (2), 393.
- (825). Vandenbroucke RE; Lentacker I; Demeester J; De Smedt SC; Sanders NN Ultrasound assisted siRNA delivery using PEG-siPlex loaded microbubbles. *Journal of Controlled Release* 2008, 126 (3), 265. [PubMed: 18237813]
- (826). De Temmerman ML; Dewitte H; Vandenbroucke RE; Lucas B; Libert C; Demeester J; De Smedt SC; Lentacker I; Rejman J mRNA-Lipoplex loaded microbubble contrast agents for ultrasound-assisted transfection of dendritic cells. *Biomaterials* 2011, 32 (34), 9128. [PubMed: 21868088]
- (827). Saito K; Miyake K; McNeil PL; Kato K; Yago K; Sugai N Plasma membrane disruption underlies injury of the corneal endothelium by ultrasound. *Exp Eye Res* 1999, 68 (4), 431. [PubMed: 10192800]
- (828). Guzman HR; Nguyen DX; McNamara AJ; Prausnitz MR Equilibrium loading of cells with macromolecules by ultrasound: Effects of molecular size and acoustic energy. *J Pharm Sci-US* 2002, 91 (7), 1693.
- (829). Armstrong JK; Wenby RB; Meiselman HJ; Fisher TC The hydrodynamic radii of macromolecules and their effect on red blood cell aggregation. *Biophys J* 2004, 87 (6), 4259. [PubMed: 15361408]
- (830). Karshafian R; Bevan PD; Burns PN; Karshafian R; Samac S; Banerjee M; Bevan PD Ultrasound-induced uptake of different size markers in mammalian cells. *Ultrason* 2005, 13.
- (831). Mehier-Humbert S; Bettinger T; Yan F; Guy RH Plasma membrane poration induced by ultrasound exposure: Implication for drug delivery. *Journal of Controlled Release* 2005, 104 (1), 213. [PubMed: 15866347]
- (832). Meijering BDM; Juffermans LJM; van Wamel A; Henning RH; Zuhorn IS; Emmer M; Versteilen AMG; Paulus WJ; van Gilst WH; Kooiman Ket al. Ultrasound and Microbubble-Targeted Delivery of Macromolecules Is Regulated by Induction of Endocytosis and Pore Formation. *Circ Res* 2009, 104 (5), 679. [PubMed: 19168443]
- (833). Karshafian R; Bevan PD; Williams R; Samac S; Burns PN Sonoporation by Ultrasound-Activated Microbubble Contrast Agents: Effect of Acoustic Exposure Parameters on Cell Membrane Permeability and Cell Viability. *Ultrasound Med Biol* 2009, 35 (5), 847. [PubMed: 19110370]
- (834). Karshafian R; Samac S; Bevan PD; Burns PN Microbubble mediated sonoporation of cells in suspension: Clonogenic viability and influence of molecular size on uptake. *Ultrasonics* 2010, 50 (7), 691. [PubMed: 20153497]
- (835). Carugo D; Ankrett DN; Glynn-Jones P; Capretto L; Boltryk RJ; Zhang XL; Townsend PA; Hill M Contrast agent-free sonoporation: The use of an ultrasonic standing wave microfluidic system for the delivery of pharmaceutical agents. *Biomicrofluidics* 2011, 5 (4).
- (836). Yoon S; Kim MG; Chiu CT; Hwang JY; Kim HH; Wang Y; Shung KK Direct and sustained intracellular delivery of exogenous molecules using acoustic-transfection with high frequency ultrasound. *Sci Rep-Uk* 2016, 6, 20477.

- (837). Furukawa R; Wampler JE; Fechheimer M Cytoplasmic Ph of Dictyostelium-Discoideum Amebae during Early Development - Identification of 2 Cell Subpopulations before the Aggregation Stage. *J Cell Biol* 1990, 110 (6), 1947. [PubMed: 2161854]
- (838). Keyhani K; Guzman HR; Parsons A; Lewis TN; Prausnitz MR Intracellular drug delivery using low-frequency ultrasound: Quantification of molecular uptake and cell viability. *Pharm Res-Dordr* 2001, 18 (11), 1514.
- (839). Guzman HR; Nguyen DX; Khan S; Prausnitz MR Ultrasound-mediated disruption of cell membranes. II. Heterogeneous effects on cells. *J Acoust Soc Am* 2001, 110 (1), 597. [PubMed: 11508985]
- (840). Hallow DM; Mahajan AD; McCutchen TE; Prausnitz MR Measurement and correlation of acoustic cavitation with cellular bioeffects. *Ultrasound Med Biol* 2006, 32 (7), 1111. [PubMed: 16829325]
- (841). Hutcheson JD; Schlicher RK; Hicks HK; Prausnitz MR Saving Cells from Ultrasound-Induced Apoptosis: Quantification of Cell Death and Uptake Following Sonication and Effects of Targeted Calcium Chelation. *Ultrasound Med Biol* 2010, 36 (6), 1008. [PubMed: 20447754]
- (842). Schlicher RK; Hutcheson JD; Radhakrishna H; Apkarian RP; Prausnitz MR Changes in Cell Morphology Due to Plasma Membrane Wounding by Acoustic Cavitation. *Ultrasound Med Biol* 2010, 36 (4), 677. [PubMed: 20350691]
- (843). Fan ZZ; Liu HY; Mayer M; Deng CX Spatiotemporally controlled single cell sonoporation. *P Natl Acad Sci USA* 2012, 109 (41), 16486.
- (844). Dixon AJ; Dhanaliwala AH; Chen JL; Hossack JA Enhanced Intracellular Delivery of a Model Drug Using Microbubbles Produced by a Microfluidic Device. *Ultrasound Med Biol* 2013, 39 (7), 1267. [PubMed: 23643062]
- (845). Helfield B; Chen XC; Watkins SC; Villanueva FS Biophysical insight into mechanisms of sonoporation. *P Natl Acad Sci USA* 2016, 113 (36), 9983.
- (846). Tachibana K; Uchida T; Tamura K; Eguchi H; Yamashita N; Ogawa K Enhanced cytotoxic effect of Ara-C by low intensity ultrasound to HL-60 cells. *Cancer Lett* 2000, 149 (1-2), 189. [PubMed: 10737723]
- (847). Tachibana K; Uchida T; Ogawa K; Yamashita N; Tamura K Induction of cell-membrane porosity by ultrasound. *Lancet* 1999, 353 (9162), 1409.
- (848). Tachibana K; Uchida T; Hisano S; Morioka E Eliminating adult T-cell leukaemia cells with ultrasound. *Lancet* 1997, 349 (9048), 325.
- (849). Paliwal S; Sundaram J; Mitragotri S Induction of cancer-specific cytotoxicity towards human prostate and skin cells using quercetin and ultrasound. *Brit J Cancer* 2005, 92 (3), 499. [PubMed: 15685239]
- (850). Escoffre JM; Piron J; Novell A; Bouakaz A Doxorubicin Delivery into Tumor Cells with Ultrasound and Microbubbles. *Mol Pharmaceut* 2011, 8 (3), 799.
- (851). Joersbo M; Brunstedt J Inoculation of Sugar-Beet Protoplasts with Beet Necrotic Yellow Vein Virus-Particles by Mild Sonication. *J Virol Methods* 1990, 29 (1), 63. [PubMed: 2211957]
- (852). Furukawa R; Butz S; Fleischmann E; Fechheimer M The Dictyostelium-Discoideum 30,000 Dalton Protein Contributes to Phagocytosis. *Protoplasma* 1992, 169 (1-2), 18.
- (853). van Wamel A; Bouakaz A; Bernard B; ten Cate F; de Jong N Radionuclide tumour therapy with ultrasound contrast microbubbles. *Ultrasonics* 2004, 42 (1-9), 903. [PubMed: 15047404]
- (854). Li YS; Davidson E; Reid CN; McHale AP Optimising ultrasound-mediated gene transfer (sonoporation) in vitro and prolonged expression of a transgene in vivo: Potential applications for gene therapy of cancer. *Cancer Lett* 2009, 273 (1), 62. [PubMed: 18829156]
- (855). Tlaxca JL; Anderson CR; Klibanov AL; Lowrey B; Hossack JA; Alexander JS; Lawrence MB; Rychak JJ Analysis of in Vitro Transfection by Sonoporation Using Cationic and Neutral Microbubbles. *Ultrasound Med Biol* 2010, 36 (11), 1907. [PubMed: 20800945]
- (856). Juffermans LJM; Dijkmans PA; Musters RJP; Visser CA; Kamp O Transient permeabilization of cell membranes by ultrasound-exposed microbubbles is related to formation of hydrogen peroxide. *Am J Physiol-Heart C* 2006, 291 (4), H1595.
- (857). Hutchins DA Ultrasonic Generation by Pulsed Lasers. *Phys Acoustics* 1988, 18, 21.

- (858). Lokhandwalla M; Sturtevant B Mechanical haemolysis in shock wave lithotripsy (SWL): I. Analysis of cell deformation due to SWL flow-fields. *Phys Med Biol* 2001, 46 (2), 413. [PubMed: 11229723]
- (859). Lokhandwalla M; McAteer JA; Williams JC; Sturtevant B Mechanical haemolysis in shock wave lithotripsy (SWL): II. In vitro cell lysis due to shear. *Phys Med Biol* 2001, 46 (4), 1245. [PubMed: 11324963]
- (860). Gambihler S; Delius M; Ellwart JW Permeabilization of the Plasma-Membrane of L1210 Mouse Leukemia-Cells Using Lithotripter Shock-Waves. *J Membrane Biol* 1994, 141 (3), 267. [PubMed: 7528805]
- (861). Gambihler S; Delius M; Brendel W Biological Effects of Shock-Waves - Cell Disruption, Viability, and Proliferation of L1210-Cells Exposed to Shock-Waves In vitro. *Ultrasound Med Biol* 1990, 16 (6), 587. [PubMed: 2238267]
- (862). Kodama T; Doukas AG; Hamblin MR Shock wave-mediated molecular delivery into cells. *Bba-Mol Cell Res* 2002, 1542 (1-3), 186.
- (863). Kodama T; Hamblin MR; Doukas AG Cytoplasmic molecular delivery with shock waves: Importance of impulse. *Biophys J* 2000, 79 (4), 1821. [PubMed: 11023888]
- (864). Kodama T; Doukas AG; Hamblin MR Delivery of ribosome-inactivating protein toxin into cancer cells with shock waves. *Cancer Lett* 2003, 189 (1), 69. [PubMed: 12445679]
- (865). Brummer F; Brenner J; Brauner T; Hulser DF Effect of shock waves on suspended and immobilized L1210 cells. *Ultrasound Med Biol* 1989, 15 (3), 229. [PubMed: 2741251]
- (866). Sonden A; Svensson B; Roman N; Brismar B; Palmblad J; Kjellstrom BT Mechanisms of shock wave induced endothelial cell injury. *Laser Surg Med* 2002, 31 (4), 233.
- (867). Soughayer JS; Krasieva T; Jacobson SC; Ramsey JM; Tromberg BJ; Allbritton NL Characterization of cellular optoporation with distance. *Anal Chem* 2000, 72 (6), 1342. [PubMed: 10740880]
- (868). Mulholland SE; Lee S; McAuliffe DJ; Doukas AG Cell loading with laser-generated stress waves: The role of the stress gradient. *Pharm Res-Dordr* 1999, 16 (4), 514.
- (869). Lee S; Anderson T; Zhang H; Flotte TJ; Doukas AG Alteration of cell membrane by stress waves in vitro. *Ultrasound Med Biol* 1996, 22 (9), 1285. [PubMed: 9123654]
- (870). Doukas AG; Flotte TJ Physical characteristics and biological effects of laser-induced stress waves. *Ultrasound Med Biol* 1996, 22 (2), 151. [PubMed: 8735525]
- (871). Doukas AG; McAuliffe DJ; Lee S; Venugopalan V; Flotte TJ Physical Factors Involved in Stress-Wave-Induced Cell Injury - the Effect of Stress Gradient. *Ultrasound Med Biol* 1995, 21 (7), 961. [PubMed: 7491750]
- (872). Doukas AG; McAuliffe DJ; Flotte TJ Biological Effects of Laser-Induced Shock-Waves - Structural and Functional Cell-Damage In Vitro. *Ultrasound Med Biol* 1993, 19 (2), 137. [PubMed: 8516960]
- (873). Ohl CD; Arora M; Ikink R; de Jong N; Versluis M; Delius M; Lohse D Sonoporation from jetting cavitation bubbles. *Biophys J* 2006, 91 (11), 4285. [PubMed: 16950843]
- (874). Boulais E; Lachaine R; Hatef A; Meunier M Plasmonics for pulsed-laser cell nanosurgery: Fundamentals and applications. *J Photoch Photobio C* 2013, 17, 26.
- (875). Xiong RH; Samal SK; Demeester J; Skirtach AG; De Smedt SC; Braeckmans K Laser-assisted photoporation: fundamentals, technological advances and applications. *Adv Phys-X* 2016, 1 (4), 596.
- (876). Fan Q; Hu W; Ohta AT Efficient single-cell poration by microsecond laser pulses. *Lab on a chip* 2015.
- (877). Le Gac S; Zwaan E; van den Berg A; Ohl CD Sonoporation of suspension cells with a single cavitation bubble in a microfluidic confinement. *Lab on a chip* 2007, 7 (12), 1666. [PubMed: 18030385]
- (878). Quinto-Su PA; Suzuki M; Ohl CD Fast temperature measurement following single laser-induced cavitation inside a microfluidic gap. *Sci Rep-Uk* 2014, 4.
- (879). Pitsillides CM; Joe EK; Wei XB; Anderson RR; Lin CP Selective cell targeting with light-absorbing microparticles and nanoparticles. *Biophys J* 2003, 84 (6), 4023. [PubMed: 12770906]

- (880). Lukianova-Hleb EY; Samaniego AP; Wen JG; Metelitsa LS; Chang CC; Lapotko DO Selective gene transfection of individual cells in vitro with plasmonic nanobubbles. *Journal of Controlled Release* 2011, 152 (2), 286. [PubMed: 21315120]
- (881). Lukianova-Hleb EY; Wagner DS; Brenner MK; Lapotko DO Cell-specific transmembrane injection of molecular cargo with gold nanoparticle-generated transient plasmonic nanobubbles. *Biomaterials* 2012, 33 (21), 5441. [PubMed: 22521612]
- (882). Chakravarty P; Qian W; El-Sayed MA; Prausnitz MR Delivery of molecules into cells using carbon nanoparticles activated by femtosecond laser pulses. *Nature nanotechnology* 2010, 5 (8), 607.
- (883). Sengupta A; Gray MD; Kelly SC; Holguin SY; Thadhani NN; Prausnitz MR Energy Transfer Mechanisms during Molecular Delivery to Cells by Laser-Activated Carbon Nanoparticles. *Biophys J* 2017, 112 (6), 1258. [PubMed: 28355552]
- (884). Sengupta A; Mezenцев R; McDonald JF; Prausnitz MR Delivery of siRNA to ovarian cancer cells using laser-activated carbon nanoparticles. *Nanomedicine-Uk* 2015, 10 (11), 1775.
- (885). Sengupta A; Kelly SC; Dwivedi N; Thadhani N; Prausnitz MR Efficient Intracellular Delivery of Molecules with High Cell Viability Using Nanosecond-Pulsed Laser-Activated Carbon Nanoparticles. *Acs Nano* 2014.
- (886). Xiong RH; Raemdonck K; Peynshaert K; Lentacker I; De Cock I; Demeester J; De Smedt SC; Skirtach AG; Braeckmans K Comparison of Gold Nanoparticle Mediated Photoporation: Vapor Nanobubbles Outperform Direct Heating for Delivering Macromolecules in Live Cells. *Acs Nano* 2014, 8 (6), 6288. [PubMed: 24870061]
- (887). Wayteck L; Xiong R; Braeckmans K; De Smedt SC; Raemdonck K Comparing photoporation and nucleofection for delivery of small interfering RNA to cytotoxic T cells. *Journal of controlled release : official journal of the Controlled Release Society* 2017.
- (888). Boulais E; Lachaine R; Meunier M Plasma Mediated off-Resonance Plasmonic Enhanced Ultrafast Laser-Induced Nanocavitation. *Nano Lett* 2012, 12 (9), 4763. [PubMed: 22845691]
- (889). St-Louis Lalonde B; Boulais E; Lebrun JJ; Meunier M Visible and near infrared resonance plasmonic enhanced nanosecond laser optoporation of cancer cells. *Biomedical optics express* 2013, 4 (4), 490. [PubMed: 23577284]
- (890). Fan QH; Hu WQ; Ohta AT Laser-induced microbubble poration of localized single cells. *Lab on a chip* 2014, 14 (9), 1572. [PubMed: 24632785]
- (891). Courvoisier S; Saklayen N; Huber M; Chen J; Diebold ED; Bonacina L; Wolf JP; Mazur E Plasmonic Tipless Pyramid Arrays for Cell Poration. *Nano Lett* 2015, 15 (7), 4461. [PubMed: 26079771]
- (892). Saklayen N; Huber M; Madrid M; Nuzzo V; Vulis DI; Shen W; Nelson J; McClelland AA; Heisterkamp A; Mazur E Intracellular Delivery Using Nanosecond-Laser Excitation of Large-Area Plasmonic Substrates. *Acs Nano* 2017.
- (893). Chen J; Saklayen N; Courvoisier S; Shen ZH; Lu J; Ni XW; Mazur E Dynamics of transient microbubbles generated by fs-laser irradiation of plasmonic micropylamids. *Appl Phys Lett* 2017, 110 (15).
- (894). Yamane D; Wu YC; Wu TH; Toshiyoshi H; Teitell MA; Chiou PY Electrical Impedance Monitoring of Photothermal Porated Mammalian Cells. *Jala-J Lab Autom* 2014, 19 (1), 50.
- (895). Chakrabarti R; Pfeiffer NE; Wylie DE; Schuster SM Incorporation of Monoclonal-Antibodies into Cells by Osmotic Permeabilization - Effect on Cellular-Metabolism. *J Biol Chem* 1989, 264 (14), 8214. [PubMed: 2566602]
- (896). Hoffman JF Active Transport of Sodium by Ghosts of Human Red Blood Cells. *J Gen Physiol* 1962, 45 (5), 837. [PubMed: 13908117]
- (897). Dodge JT; Hanahan DJ; Mitchell C Preparation and Chemical Characteristics of Hemoglobin-Free Ghosts of Human Erythrocytes. *Arch Biochem Biophys* 1963, 100 (1), 119. [PubMed: 14028302]
- (898). Baker RF Entry of Ferritin into Human Red Cells during Hypotonic Haemolysis. *Nature* 1967, 215 (5099), 424. [PubMed: 6058309]

- (899). Bodemann H; Passow H Factors controlling the resealing of the membrane of human erythrocyte ghosts after hypotonic hemolysis. *The Journal of membrane biology* 1972, 8 (1), 1. [PubMed: 4628383]
- (900). Schwoch G; Passow H Preparation and Properties of Human Erythrocyte-Ghosts. *Molecular and Cellular Biochemistry* 1973, 2 (2), 197. [PubMed: 4272551]
- (901). Rechsteiner MC In *Techniques in Somatic Cell Genetics*; Shay JW, Ed.; Springer US: Boston, MA, 1982.
- (902). Seeman P Transient holes in the erythrocyte membrane during hypotonic hemolysis and stable holes in the membrane after lysis by saponin and lysolecithin. *J Cell Biol* 1967, 32 (1), 55. [PubMed: 10976201]
- (903). Seeman P; Cheng D; Iles GH Structure of Membrane Holes in Osmotic and Saponin Hemolysis. *J Cell Biol* 1973, 56 (2), 519. [PubMed: 4566525]
- (904). Lieber MR; Steck TL A Description of the Holes in Human-Erythrocyte Membrane Ghosts. *J Biol Chem* 1982, 257 (19), 1651. [PubMed: 7056734]
- (905). Ihler GM; Glew RH; Schnure FW Enzyme Loading of Erythrocytes. *P Natl Acad Sci USA* 1973, 70 (9), 2663.
- (906). Dale GL; Villacorte DG; Beutler E High-Yield Entrapment of Proteins into Erythrocytes. *Biochem Med Metab B* 1977, 18 (2), 220.
- (907). Ihler GM Erythrocyte Carriers. *Pharmacol Therapeut* 1983, 20 (2), 151.
- (908). Hamidi M; Tajerzadeh H Carrier erythrocytes: An overview. *Drug Deliv* 2003, 10 (1), 9. [PubMed: 12554359]
- (909). Millan CG; Marinero MLS; Castaneda AZ; Lanao JM Drug, enzyme and peptide delivery using erythrocytes as carriers. *Journal of Controlled Release* 2004, 95 (1), 27. [PubMed: 15013230]
- (910). Shi JH; Kundrat L; Pishesha N; Bilate A; Theile C; Maruyama T; Dougan SK; Ploegh HL; Lodish HF Engineered red blood cells as carriers for systemic delivery of a wide array of functional probes. *P Natl Acad Sci USA* 2014, 111 (28), 10131.
- (911). Furusawa M; Yamaizumi M; Nishimura T; Uchida T; Okada Y Chapter 5 Use of Erythrocyte Ghosts for Injection of Substances into Animal Cells by Cell Fusion. *Methods in Cell Biology* 1976, 14, 73. [PubMed: 187901]
- (912). Kaltoft K; Celis JE Ghost-mediated transfer of human hypoxanthine-guanine phosphoribosyl transferase into deficient Chinese hamster ovary cells by means of polyethylene glycol-induced fusion. *Exp Cell Res* 1978, 115 (2), 423. [PubMed: 689099]
- (913). Klabusay M; Skopalik J; Erceg S; Hrdlicka A Aequorin as Intracellular Ca²⁺ Indicator Incorporated in Follicular Lymphoma Cells by Hypoosmotic Shock Treatment. *Folia Biol (Praha)* 2015, 61 (4), 134. [PubMed: 26441202]
- (914). Koberna K; Stanek D; Malinsky J; Eltsov M; Pliss A; Ctrnacta V; Cermanova S; Raska I Nuclear organization studied with the help of a hypotonic shift: its use permits hydrophilic molecules to enter into living cells. *Chromosoma* 1999, 108 (5), 325. [PubMed: 10525969]
- (915). Malinsky J; Koberna K; Stanek D; Masata M; Votruba I; Raska I The supply of exogenous deoxyribonucleotides accelerates the speed of the replication fork in early S-phase. *J Cell Sci* 2001, 114 (4), 747. [PubMed: 11171380]
- (916). Ahmad K; Henikoff S Centromeres are specialized replication domains in heterochromatin. *J Cell Biol* 2001, 153 (1), 101. [PubMed: 11285277]
- (917). Koberna K; Ligasova A; Malinsky J; Pliss A; Siegel AJ; Cvackova Z; Fidlerova H; Masata M; Fialova M; Raska I et al. Electron microscopy of DNA replication in 3-D: Evidence for similar-sized replication foci throughout S-phase. *J Cell Biochem* 2005, 94 (1), 126. [PubMed: 15523671]
- (918). Panning MM; Gilbert DM Spatio-temporal organization of DNA replication in murine embryonic stem, primary, and immortalized cells. *J Cell Biochem* 2005, 95 (1), 74. [PubMed: 15723284]
- (919). Takebayashi S; Tamura T; Matsuoka C; Okano M Major and essential role for the DNA methylation mark in mouse embryogenesis and stable association of DNMT1 with newly replicated regions. *Mol Cell Biol* 2007, 27 (23), 8243. [PubMed: 17893328]

- (920). Sharif J; Muto M; Takebayashi SI; Suetake I; Iwamatsu A; Endo TA; Shinga J; Mizutani-Koseki Y; Toyoda T; Okamura K et al. The SRA protein Np95 mediates epigenetic inheritance by recruiting Dnmt1 to methylated DNA. *Nature* 2007, 450 (7171), 908. [PubMed: 17994007]
- (921). Hori M; Satou K; Harashima H; Kamiya H Suppression of mutagenesis by 8-hydroxy-2'-deoxyguanosine 5'-triphosphate (7,8-dihydro-8-oxo-2'-deoxyguanosine 5'-triphosphate) by human MTH1, MTH2, and NUDT5. *Free Radical Bio Med* 2010, 48 (9), 1197. [PubMed: 20144704]
- (922). Yamazaki S; Ishii A; Kanoh Y; Oda M; Nishito Y; Masai H Rif1 regulates the replication timing domains on the human genome. *Embo J* 2012, 31 (18), 3667. [PubMed: 22850674]
- (923). Alabert C; Bukowski-Wills JC; Lee SB; Kustatscher G; Nakamura K; Alves FD; Menard P; Mejlvang J; Rappsilber J; Groth A Nascent chromatin capture proteomics determines chromatin dynamics during DNA replication and identifies unknown fork components. *Nat Cell Biol* 2014, 16 (3), 281. [PubMed: 24561620]
- (924). Pliss A; Koberna K; Vecerova J; Malinsky J; Masata M; Fialova M; Raska I; Berezney R Spatio-temporal dynamics at rDNA foci: Global switching between DNA replication and transcription. *J Cell Biochem* 2005, 94 (3), 554. [PubMed: 15543556]
- (925). Bhattacharya D; Mazumder A; Miriam SA; Shivashankar GV EGFP-tagged core and linker histones diffuse via distinct mechanisms within living cells. *Biophys J* 2006, 91 (6), 2326. [PubMed: 16815908]
- (926). Mazumder A; Shivashankar GV Gold-nanoparticle-assisted laser perturbation of chromatin assembly reveals unusual aspects of nuclear architecture within living cells. *Biophys J* 2007, 93 (6), 2209. [PubMed: 17496030]
- (927). Mills CL; Pereira MMC; Dormer RL; Mcpherson MA An Antibody against a Cfr-Derived Synthetic Peptide, Incorporated into Living Submandibular Cells, Inhibits Beta-Adrenergic Stimulation of Mucin Secretion. *Biochem Bioph Res Co* 1992, 188 (3), 1146.
- (928). Mills CL; Dormer RL; Mcpherson MA Introduction of Bapta into Intact Rat Submandibular Acini Inhibits Mucin Secretion in Response to Cholinergic and Beta-Adrenergic Agonists. *Febs Letters* 1991, 289 (2), 141. [PubMed: 1915837]
- (929). Bradbury NA; Dormer RL; Mcpherson MA Introduction of Cyclic-Amp Phosphodiesterase into Rat Submandibular Acini Prevents Isoproterenol-Stimulated Cyclic-Amp Rise without Affecting Mucin Secretion. *Biochem Bioph Res Co* 1989, 161 (2), 661.
- (930). Di Gregorio E; Ferrauto G; Gianolio E; Aime S Gd loading by hypotonic swelling: an efficient and safe route for cellular labeling. *Contrast Media Mol I* 2013, 8 (6), 475.
- (931). Yang Y; Yang F; Gong YJ; Chen JL; Goldfarb D; Su XC A Reactive, Rigid GdIII Labeling Tag for In-Cell EPR Distance Measurements in Proteins. *Angew Chem Int Ed Engl* 2017, 56 (11), 2914. [PubMed: 28145030]
- (932). Markov DE; Boeve H; Gleich B; Borgert J; Antonelli A; Sfara C; Magnani M Human erythrocytes as nanoparticle carriers for magnetic particle imaging. *Phys Med Biol* 2010, 55 (21), 6461. [PubMed: 20959685]
- (933). Martorana A; Bellapadrona G; Feintuch A; Di Gregorio E; Aime S; Goldfarb D Probing Protein Conformation in Cells by EPR Distance Measurements using Gd3+ Spin Labeling. *J Am Chem Soc* 2014, 136 (38), 13458. [PubMed: 25163412]
- (934). Ferrauto G; Castelli DD; Di Gregorio E; Langereis S; Burdinski D; Grull H; Terreno E; Aime S Lanthanide-Loaded Erythrocytes As Highly Sensitive Chemical Exchange Saturation Transfer MRI Contrast Agents. *J Am Chem Soc* 2014, 136 (2), 638. [PubMed: 24359116]
- (935). Ferrauto G; Di Gregorio E; Dastru W; Lanzardo S; Aime S Gd-loaded-RBCs for the assessment of tumor vascular volume by contrast-enhanced-MRI. *Biomaterials* 2015, 58, 82. [PubMed: 25941785]
- (936). Di Gregorio E; Ferrauto G; Gianolio E; Lanzardo S; Carrera C; Fedeli F; Aime S An MRI Method To Map Tumor Hypoxia Using Red Blood Cells Loaded with a pO(2)-Responsive Gd-Agent. *ACS Nano* 2015, 9 (8), 8239. [PubMed: 26234938]
- (937). Widdicombe JH; Azizi F; Kang T; Pittet JF Transient permeabilization of airway epithelium by mucosal water. *J Appl Physiol* 1996, 81 (1), 491. [PubMed: 8828701]

- (938). Sawa T; Miyazaki H; Pittet JF; Widdicombe JH; Gropper MA; Hashimoto S; Conrad DJ; Folkesson HG; Debs R; Forsayeth JRet al. Intraluminal water increases expression of plasmid DNA in rat lung. *Hum Gene Ther* 1996, 7 (8), 933. [PubMed: 8727507]
- (939). Lemoine JL; Farley R; Huang L Mechanism of efficient transfection of the nasal airway epithelium by hypotonic shock. *Gene Ther* 2005, 12 (16), 1275. [PubMed: 15889135]
- (940). Rudolph C; Schillinger U; Ortiz A; Plank C; Golas MM; Sander B; Stark H; Rosenecker J Aerosolized nanogram quantities of plasmid DNA mediate highly efficient gene delivery to mouse airway epithelium. *Mol Ther* 2005, 12 (3), 493. [PubMed: 16099412]
- (941). Zhang GF; Budker V; Wolff JA High levels of foreign gene expression in hepatocytes after tail vein injections of naked plasmid DNA. *Hum Gene Ther* 1999, 10 (10), 1735. [PubMed: 10428218]
- (942). Liu F; Song YK; Liu D Hydrodynamics-based transfection in animals by systemic administration of plasmid DNA. *Gene Ther* 1999, 6 (7), 1258. [PubMed: 10455434]
- (943). Zhang G; Gao X; Song YK; Vollmer R; Stolz DB; Gasiorowski JZ; Dean DA; Liu D Hydroporation as the mechanism of hydrodynamic delivery. *Gene Ther* 2004, 11 (8), 675. [PubMed: 14724673]
- (944). Chang JH; Sigal LJ; Lerro A; Taylor J Replication of the human hepatitis delta virus genome is initiated in mouse hepatocytes following intravenous injection of naked DNA or RNA sequences. *J Virol* 2001, 75 (7), 3469. [PubMed: 11238873]
- (945). McCaffrey AP; Meuse L; Pham TTT; Conklin DS; Hannon GJ; Kay MA Gene expression - RNA interference in adult mice. *Nature* 2002, 418 (6893), 38. [PubMed: 12097900]
- (946). Magin-Lachmann C; Kotzamanis G; D' Aiuto L; Cooke H; Huxley C; Wagner E In vitro and in vivo delivery of intact BAC DNA - comparison of different methods. *J Gene Med* 2004, 6 (2), 195. [PubMed: 14978773]
- (947). Kobayashi N; Nishikawa M; Hirata K; Takakura Y Hydrodynamics-based procedure involves transient hyperpermeability in the hepatic cellular membrane: implication of a nonspecific process in efficient intracellular gene delivery. *J Gene Med* 2004, 6 (5), 584. [PubMed: 15133769]
- (948). Al-Dosari MS; Knapp JE; Liu DX Hydrodynamic Delivery. *Adv Genet* 2005, 54, 65. [PubMed: 16096008]
- (949). Herweijer H; Wolff JA Gene therapy progress and prospects: Hydrodynamic gene delivery. *Gene Ther* 2007, 14 (2), 99. [PubMed: 17167496]
- (950). Bonamassa B; Hai L; Liu DX Hydrodynamic Gene Delivery and Its Applications in Pharmaceutical Research. *Pharm Res-Dordr* 2011, 28 (4), 694.
- (951). Yin H; Xue W; Chen S; Bogorad RL; Benedetti E; Grompe M; Koteliensky V; Sharp PA; Jacks T; Anderson DG Genome editing with Cas9 in adult mice corrects a disease mutation and phenotype. *Nat Biotechnol* 2014, 32 (6), 551. [PubMed: 24681508]
- (952). Xue W; Chen SD; Yin H; Tammela T; Papagiannakopoulos T; Joshi NS; Cai WX; Yang GL; Bronson R; Crowley DGet al. CRISPR-mediated direct mutation of cancer genes in the mouse liver. *Nature* 2014, 514 (7522), 380. [PubMed: 25119044]
- (953). Zhen S; Hua L; Liu YH; Gao LC; Fu J; Wan DY; Dong LH; Song HF; Gao X Harnessing the clustered regularly interspaced short palindromic repeat (CRISPR)/CRISPR-associated Cas9 system to disrupt the hepatitis B virus. *Gene Ther* 2015, 22 (5), 404. [PubMed: 25652100]
- (954). Sakurai T; Kamiyoshi A; Kawate H; Mori C; Watanabe S; Tanaka M; Uetake R; Sato M; Shindo T A non-inheritable maternal Cas9-based multiple-gene editing system in mice. *Sci Rep-Uk* 2016, 6.
- (955). Wolff JA; Budker V The Mechanism of Naked DNA Uptake and Expression. *Adv Genet* 2005, 54, 3. [PubMed: 16096005]
- (956). Budker V; Budker T; Zhang GF; Subbotin V; Loomis A; Wolff JA Hypothesis: naked plasmid DNA is taken up by cells in vivo by a receptor-mediated process. *J Gene Med* 2000, 2 (2), 76. [PubMed: 10809141]
- (957). Gao X; Kim KS; Liu DX Nonviral gene delivery: What we know and what is next. *Aaps J* 2007, 9 (1), E92. [PubMed: 17408239]

- (958). Suda T; Liu D Hydrodynamic gene delivery: Its principles and applications. *Mol Ther* 2007, 15 (12), 2063. [PubMed: 17912237]
- (959). Mann MJ; Gibbons GH; Hutchinson H; Poston RS; Hoyt EG; Robbins RC; Dzau VJ Pressure-mediated oligonucleotide transfection of rat and human cardiovascular tissues. *P Natl Acad Sci USA* 1999, 96 (11), 6411.
- (960). Andersen ND; Chopra A; Monahan TS; Malek JY; Jain M; Pradhan L; Ferran C; LoGerfo FW Endothelial cells are susceptible to rapid siRNA transfection and gene silencing ex vivo. *J Vasc Surg* 2010, 52 (6), 1608. [PubMed: 20801607]
- (961). von der Leyen HE; Braun-Dullaeus R; Mann MJ; Zhang LN; Niebauer J; Dzau VJ A pressure-mediated nonviral method for efficient arterial gene and oligonucleotide transfer. *Hum Gene Ther* 1999, 10 (14), 2355. [PubMed: 10515455]
- (962). Mann MJ; Whittemore AD; Donaldson MC; Belkin M; Conte MS; Polak JF; Orav EJ; Ehsan A; Dell'Acqua G; Dzau VJ Ex-vivo gene therapy of human vascular bypass grafts with E2F decoy: the PREVENT single-centre, randomised, controlled trial. *Lancet* 1999, 354 (9189), 1493. [PubMed: 10551494]
- (963). Miniati DN; Hoyt EG; Feeley BT; Poston RS; Robbins RC Ex vivo antisense oligonucleotides to proliferating cell nuclear antigen and Cdc2 kinase inhibit graft coronary artery disease. *Circulation* 2000, 102 (19), 237.
- (964). Feeley BT; Miniati DN; Park AK; Hoyt EG; Robbins RC Nuclear factor-kappaB transcription factor decoy treatment inhibits graft coronary artery disease after cardiac transplantation in rodents. *Transplantation* 2000, 70 (11), 1560. [PubMed: 11152216]
- (965). Miyake T; Aoki M; Shiraya S; Tanemoto K; Ogihara T; Kaneda Y; Morishita R Inhibitory effects of NFkappaB decoy oligodeoxynucleotides on neointimal hyperplasia in a rabbit vein graft model. *J Mol Cell Cardiol* 2006, 41 (3), 431. [PubMed: 16762361]
- (966). Suzuki M; Ishizaka N; Tsukamoto K; Minami K; Taguchi J; Nagai R; Ohno M Pressurization facilitates adenovirus-mediated gene transfer into vein graft. *Febs Letters* 2000, 470 (3), 370. [PubMed: 10745099]
- (967). Vecchione C; Aretini A; Marino G; Bettarini U; Poulet R; Maffei A; Sbroglio M; Pastore L; Gentile MT; Notte A et al. Selective Rac-1 inhibition protects from diabetes-induced vascular injury. *Circ Res* 2006, 98 (2), 218. [PubMed: 16357302]
- (968). Ander S; MacLennan M; Bentil S; Leavitt B; Chesler M Pressure-induced vector transport in human saphenous vein. *Ann Biomed Eng* 2005, 33 (2), 202. [PubMed: 15771273]
- (969). Park RD; Sullivan PC; Storrie B Hypertonic Sucrose Inhibition of Endocytic Transport Suggests Multiple Early Endocytic Compartments. *J. Cell. Physiol* 1988, 135 (3), 443. [PubMed: 3397386]
- (970). Durante M; Grossi GF; Napolitano M; Gialanella G Repair of potentially lethal damage by introduction of T4 DNA ligase in eucaryotic cells. *International journal of radiation biology* 1991, 59 (4), 963. [PubMed: 1674280]
- (971). Chin DT; Kuehl L; Rechsteiner M Conjugation of Ubiquitin to Denatured Hemoglobin Is Proportional to the Rate of Hemoglobin Degradation in Hela-Cells. *P Natl Acad Sci-Biol* 1982, 79 (19), 5857.
- (972). Hough R; Rechsteiner M Effects of Temperature on the Degradation of Proteins in Rabbit Reticulocyte Lysates and after Injection into Hela-Cells. *P Natl Acad Sci-Biol* 1984, 81 (1), 90.
- (973). Schmid DS; Tite JP; Ruddle NH DNA Fragmentation - Manifestation of Target-Cell Destruction Mediated by Cytotoxic T-Cell Lines, Lymphotoxin-Secreting Helper T-Cell Clones, and Cell-Free Lymphotoxin-Containing Supernatant. *P Natl Acad Sci USA* 1986, 83 (6), 1881.
- (974). Rubin EJ; Gill DM; Boquet P; Popoff MR Functional Modification of a 21-Kilodalton G-Protein When Adp-Ribosylated by Exoenzyme-C3 of Clostridium-Botulinum. *Mol Cell Biol* 1988, 8 (1), 418. [PubMed: 3122025]
- (975). Winegar RA; Preston RJ The Induction of Chromosome-Aberrations by Restriction Endonucleases That Produce Blunt-End or Cohesive-End Double-Strand Breaks. *Mutat Res* 1988, 197 (1), 141. [PubMed: 2827018]
- (976). Cornwell TL; Lincoln TM Regulation of Intracellular Ca-2+ Levels in Cultured Vascular Smooth-Muscle Cells - Reduction of Ca-2+ by Atriopeptin and 8-Bromo-Cyclic Gmp Is

- Mediated by Cyclic Gmp-Dependent Protein-Kinase. *J Biol Chem* 1989, 264 (2), 1146. [PubMed: 2536016]
- (977). Rock KL; Gamble S; Rothstein L Presentation of Exogenous Antigen with Class-I Major Histocompatibility Complex-Molecules. *Science* 1990, 249 (4971), 918. [PubMed: 2392683]
- (978). Rock KL; Rothstein LE; Gamble SR; Benacerraf B Reassociation with Beta-2-Microglobulin Is Necessary for Kb Class-I Major Histocompatibility Complex Binding of Exogenous Peptides. *P Natl Acad Sci USA* 1990, 87 (19), 7517.
- (979). Bowen JC; Nair SK; Reddy R; Rouse BT Cholera-Toxin Acts as a Potent Adjuvant for the Induction of Cytotoxic T-Lymphocyte Responses with Nonreplicating Antigens. *Immunology* 1994, 81 (3), 338. [PubMed: 8206507]
- (980). Williams MS; Henkart PA Apoptotic Cell-Death Induced by Intracellular Proteolysis. *J Immunol* 1994, 153 (9), 4247. [PubMed: 7930626]
- (981). Zeng Q; Lagunoff D; Masaracchia R; Goeckeler Z; Cote G; Wysolmerski R Endothelial cell retraction is induced by PAK2 monophosphorylation of myosin II. *J Cell Sci* 2000, 113 (3), 471. [PubMed: 10639334]
- (982). Geluk A; van Meijgaarden KE; Franken KLMC; Drijfhout JW; D'Souza S; Necker A; Huygen K; Ottenhoff THM Identification of major epitopes of *Mycobacterium tuberculosis* AG85B that are recognized by HLA-A*0201-restricted CD8(+) T cells in HLA-transgenic mice and humans. *J Immunol* 2000, 165 (11), 6463. [PubMed: 11086086]
- (983). Calautti E; Grossi M; Mammucari C; Aoyama Y; Pirro M; Ono Y; Li J; Dotto GP Fyn tyrosine kinase is a downstream mediator of Rho/PRK2 function in keratinocyte cell-cell adhesion. *J Cell Biol* 2002, 156 (1), 137. [PubMed: 11777936]
- (984). Gonciarz-Swiatek M; Rechsteiner M Proteasomes and antigen presentation: evidence that a KEKE motif does not promote presentation of the class I epitope SIINFEKL. *Mol Immunol* 2006, 43 (12), 1993. [PubMed: 16423396]
- (985). Shii K; Roth RA Inhibition of Insulin Degradation by Hepatoma-Cells after Microinjection of Monoclonal-Antibodies to a Specific Cytosolic Protease. *P Natl Acad Sci USA* 1986, 83 (12), 4147.
- (986). Morgan DO; Roth RA Acute Insulin Action Requires Insulin-Receptor Kinase-Activity - Introduction of an Inhibitory Monoclonal-Antibody into Mammalian-Cells Blocks the Rapid Effects of Insulin. *P Natl Acad Sci USA* 1987, 84 (1), 41.
- (987). Ahmad F; Li PM; Meyerovitch J; Goldstein BJ Osmotic Loading of Neutralizing Antibodies Demonstrates a Role for Protein-Tyrosine-Phosphatase 1b in Negative Regulation of the Insulin Action Pathway. *J Biol Chem* 1995, 270 (35), 20503. [PubMed: 7544790]
- (988). Agazie YM; Burkholder GD; Lee JS Triplex DNA in the nucleus: Direct binding of triplex-specific antibodies and their effect on transcription, replication and cell growth. *Biochem J* 1996, 316, 461. [PubMed: 8687388]
- (989). Mather S; Dora KA; Sandow SL; Winter P; Garland CJ Rapid endothelial cell-selective loading of connexin 40 antibody blocks endothelium-derived hyperpolarizing factor dilation in rat small mesenteric arteries. *Circ Res* 2005, 97 (4), 399. [PubMed: 16037574]
- (990). Lee G; Delohery TM; Ronai Z; Brandtrauf PW; Pincus MR; Murphy RB; Weinstein IB A Comparison of Techniques for Introducing Macromolecules into Living Cells. *Cytometry* 1993, 14 (3), 265. [PubMed: 7682492]
- (991). Hughey JJ; Wikswo JP; Seale KT Intra-microfluidic pinocytic loading of human T cells. 2007 *Ieee/Nih Life Science Systems and Applications Workshop 2007*, 132.
- (992). Kawashima I; Tsai V; Southwood S; Takesako K; Sette A; Celis E Identification of HLA-A3-restricted cytotoxic T lymphocyte epitopes from carcinoembryonic antigen and HER-2/neu by primary in vitro immunization with peptide-pulsed dendritic cells. *Cancer Res* 1999, 59 (2), 431. [PubMed: 9927058]
- (993). Matura T; Kai M; Fujii Y; Ito H; Yamada K Hydrogen peroxide-induced apoptosis in HL-60 cells requires caspase-3 activation. *Free Radical Res* 1999, 30 (1), 73. [PubMed: 10193575]
- (994). Li H; Sims CE; Kaluzova M; Stanbridge EJ; Allbritton NL A quantitative single-cell assay for protein kinase B reveals important insights into the biochemical behavior of an intracellular substrate peptide. *Biochemistry* 2004, 43 (6), 1599. [PubMed: 14769036]

- (995). Tjoa B; Boynton A; Kenny G; Ragde H; Misrock SL; Murphy G Presentation of prostate tumor antigens by dendritic cells stimulates T-cell proliferation and cytotoxicity. *Prostate* 1996, 28 (1), 65. [PubMed: 8545283]
- (996). Prehm P Hyaluronate Is Synthesized at Plasma-Membranes. *Biochem J* 1984, 220 (2), 597. [PubMed: 6743290]
- (997). Schulz T; Schumacher U; Prehm P Hyaluronan export by the ABC transporter MRP5 and its modulation by intracellular cGMP. *J Biol Chem* 2007, 282 (29), 20999. [PubMed: 17540771]
- (998). Puhlev I; Guo N; Brown DR; Levine F Desiccation tolerance in human cells. *Cryobiology* 2001, 42 (3), 207. [PubMed: 11578120]
- (999). Jones RA; Smail A; Wilson MR Detecting mitochondrial permeability transition by confocal imaging of intact cells pinocytically loaded with calcein. *Eur J Biochem* 2002, 269 (16), 3990. [PubMed: 12180975]
- (1000). Brecht M; Mayer U; Schlosser E; Prehm P Increased Hyaluronate Synthesis Is Required for Fibroblast Detachment and Mitosis. *Biochem J* 1986, 239 (2), 445. [PubMed: 3101667]
- (1001). Summerton J Morpholino antisense oligomers: the case for an RNase H-independent structural type. *Bba-Gene Struct Expr* 1999, 1489 (1), 141.
- (1002). Tewari MK; Sinnathamby G; Rajagopal D; Eisenlohr LC A cytosolic pathway for MHC class II-restricted antigen processing that is proteasome and TAP dependent. *Nat Immunol* 2005, 6 (3), 287. [PubMed: 15711549]
- (1003). Nelson SR; Ali MY; Trybus KM; Warsaw DM Random walk of processive, quantum dot-labeled myosin Va molecules within the actin cortex of COS-7 cells. *Biophys J* 2009, 97 (2), 509. [PubMed: 19619465]
- (1004). Pierobon P; Achouri S; Courty S; Dunn AR; Spudich JA; Dahan M; Cappello G Velocity, Processivity, and Individual Steps of Single Myosin V Molecules in Live Cells. *Biophys J* 2009, 96 (10), 4268. [PubMed: 19450497]
- (1005). Gruber J; Boese G; Tuschl T; Osborn M; Weber K RNA interference by osmotic lysis of pinosomes: liposome-independent transfection of siRNAs into mammalian cells. *Biotechniques* 2004, 37 (1), 96. [PubMed: 15283206]
- (1006). Aoki M; Ishii T; Kanaoka M; Kimura T RNA interference in immune cells by use of osmotic delivery of siRNA. *Biochem Bioph Res Co* 2006, 341 (2), 326.
- (1007). Rechsteiner M Osmotic Lysis of Pinosomes. *Method Enzymol* 1987, 149, 42.
- (1008). Neumann E; Rosenhec K Permeability Changes Induced by Electric Impulses in Vesicular Membranes. *J Membrane Biol* 1972, 10 (3–4), 279. [PubMed: 4667921]
- (1009). Kinosita K; Tsong TY Formation and Resealing of Pores of Controlled Sizes in Human Erythrocyte-Membrane. *Nature* 1977, 268 (5619), 438. [PubMed: 895849]
- (1010). Gehl J Electroporation: theory and methods, perspectives for drug delivery, gene therapy and research. *Acta Physiol Scand* 2003, 177 (4), 437. [PubMed: 12648161]
- (1011). Kandušer M; Miklavcic D In *Electrotechnologies for Extraction from Food Plants and Biomaterials*; Springer New York, 2008.
- (1012). Yarmush ML; Golberg A; Sersa G; Kotnik T; Miklavcic D *Electroporation-Based Technologies for Medicine: Principles, Applications, and Challenges. Annual Review of Biomedical Engineering, Vol 16* 2014, 16, 295.
- (1013). Weaver JC Electroporation theory. Concepts and mechanisms. *Methods Mol Biol* 1995, 55, 3. [PubMed: 8528421]
- (1014). Smith KC; Son RS; Gowrishankar TR; Weaver JC Emergence of a large pore subpopulation during electroporating pulses. *Bioelectrochemistry* 2014, 100, 3. [PubMed: 24290730]
- (1015). Sukhorukov VL; Mussauer H; Zimmermann U The effect of electrical deformation forces on the electroporeabilization of erythrocyte membranes in low-and high-conductivity media. *J Membrane Biol* 1998, 163 (3), 235. [PubMed: 9625780]
- (1016). Akinlaja J; Sachs F The breakdown of cell membranes by electrical and mechanical stress. *Biophys J* 1998, 74 (2), A374.

- (1017). Barrau C; Teissie J; Gabriel B Osmotically induced membrane tension facilitates the triggering of living cell electropermeabilization. *Bioelectrochemistry* 2004, 63 (1–2), 327. [PubMed: 15110297]
- (1018). Tieleman DP; Leontiadou H; Mark AE; Marrink SJ Simulation of pore formation in lipid bilayers by mechanical stress and electric fields. *J Am Chem Soc* 2003, 125 (21), 6382. [PubMed: 12785774]
- (1019). Gurtovenko AA; Lyulina AS Electroporation of Asymmetric Phospholipid Membranes. *J Phys Chem B* 2014, 118 (33), 9909. [PubMed: 24986456]
- (1020). Gabriel B; Teissie J Time courses of mammalian cell electropermeabilization observed by millisecond imaging of membrane property changes during the pulse. *Biophys J* 1999, 76 (4), 2158. [PubMed: 10096909]
- (1021). Rols MP Electropermeabilization, a physical method for the delivery of therapeutic molecules into cells. *Bba-Biomembranes* 2006, 1758 (3), 423. [PubMed: 16483538]
- (1022). Sengel JT; Wallace MI Imaging the dynamics of individual electropores. *Proc Natl Acad Sci U S A* 2016.
- (1023). Teissie J; Golzio M; Rols MP Mechanisms of cell membrane electropermeabilization: A minireview of our present (lack of ?) knowledge. *Bba-Gen Subjects* 2005, 1724 (3), 270.
- (1024). Tsong TY Electroporation of Cell-Membranes. *Biophys J* 1991, 60 (2), 297. [PubMed: 1912274]
- (1025). Teissie J; Eynard N; Gabriel B; Rols MP Electropermeabilization of cell membranes. *Adv Drug Deliver Rev* 1999, 35 (1), 3.
- (1026). Gissel H; Lee RC; Gehl J Electroporation and Cellular Physiology. *Clinical Aspects of Electroporation* 2011, 9.
- (1027). Schoenbach KH; Beebe SJ; Buescher ES Intracellular effect of ultrashort electrical pulses. *Bioelectromagnetics* 2001, 22 (6), 440. [PubMed: 11536285]
- (1028). Beebe SJ; Fox PM; Rec LJ; Willis LK; Schoenbach KH Nanosecond, high-intensity pulsed electric fields induce apoptosis in human cells. *Faseb J* 2003, 17 (9), 1493. [PubMed: 12824299]
- (1029). Nuccitelli R; Pliquett U; Chen XH; Ford W; Swanson RJ; Beebe SJ; Kolb JF; Schoenbach KH Nanosecond pulsed electric fields cause melanomas to self-destruct. *Biochem Bioph Res Co* 2006, 343 (2), 351.
- (1030). Bartoletti DC; Harrison GI; Weaver JC The number of molecules taken up by electroporated cells: quantitative determination. *FEBS Lett* 1989, 256 (1–2), 4. [PubMed: 2478392]
- (1031). Dinchuk JE; Kelley KA; Callahan GN Flow Cytometric Analysis of Transport Activity in Lymphocytes Electroporated with a Fluorescent Organic Anion Dye. *J Immunol Methods* 1992, 155 (2), 257. [PubMed: 1431154]
- (1032). Neumann E; Toensing K; Kakorin S; Budde P; Frey J Mechanism of electroporative dye uptake by mouse B cells. *Biophys J* 1998, 74 (1), 98. [PubMed: 9449314]
- (1033). He HQ; Chang DC; Lee YK Using a micro electroporation chip to determine the optimal physical parameters in the uptake of biomolecules in HeLa cells. *Bioelectrochemistry* 2007, 70 (2), 363. [PubMed: 16820330]
- (1034). Jones PM; Salmon DMW; Howell SL Protein-Phosphorylation in Electrically Permeabilized Islets of Langerhans - Effects of Ca-2+, Cyclic-Amp, a Phorbol Ester and Noradrenaline. *Biochem J* 1988, 254 (2), 397. [PubMed: 2845950]
- (1035). Engstrom PE; Persson BRR; Salford LG Studies of in vivo electropermeabilization by gamma camera measurements of Tc-99m-DTPA. *Bba-Gen Subjects* 1999, 1473 (2–3), 321.
- (1036). Kinoshita K Jr.; Tsong TY Survival of sucrose-loaded erythrocytes in the circulation. *Nature* 1978, 272 (5650), 258. [PubMed: 628451]
- (1037). Gordon PB; Tolleshaug H; Seglen PO Autophagic Sequestration of [C-14]Sucrose Introduced into Isolated Rat Hepatocytes by Electrical and Non-Electrical Methods. *Exp Cell Res* 1985, 160 (2), 449. [PubMed: 4043252]
- (1038). Saulis G; Venslauskas MS; Naktinis J Kinetics of Pore Resealing in Cell-Membranes after Electroporation. *Bioelectroch Bioener* 1991, 26 (1), 1.

- (1039). Melvik JE; Pettersen EO; Gordon PB; Seglen PO Increase in Cis-Dichlorodiammineplatinum(II) Cytotoxicity Upon Reversible Electroporation of the Plasma-Membrane in Cultured Human Nhik-3025 Cells. *Eur J Cancer Clin On* 1986, 22 (12), 1523.
- (1040). Gehl J; Skovsgaard T; Mir LM Enhancement of cytotoxicity by electroporation: an improved method for screening drugs. *Anti-Cancer Drug* 1998, 9 (4), 319.
- (1041). Pavlin M; Leben V; Miklavcic D Electroporation in dense cell suspension--theoretical and experimental analysis of ion diffusion and cell permeabilization. *Biochimica et biophysica acta* 2007, 1770 (1), 12. [PubMed: 16935427]
- (1042). Bowman AM; Nesin OM; Pakhomova ON; Pakhomov AG Analysis of Plasma Membrane Integrity by Fluorescent Detection of Tl+ Uptake. *J Membrane Biol* 2010, 236 (1), 15. [PubMed: 20623351]
- (1043). Chen AK; Behlke MA; Tsourkas A Sub-cellular trafficking and functionality of 2'-O-methyl and 2'-O-methyl-phosphorothioate molecular beacons. *Nucleic Acids Res* 2009, 37 (22).
- (1044). Chen AK; Davydenko O; Behlke MA; Tsourkas A Ratiometric bimolecular beacons for the sensitive detection of RNA in single living cells. *Nucleic Acids Res* 2010, 38 (14).
- (1045). Graziadei L; Burfeind P; Barsagi D Introduction of Unlabeled Proteins into Living Cells by Electroporation and Isolation of Viable Protein-Loaded Cells Using Dextran Fluorescein Isothiocyanate as a Marker for Protein-Uptake. *Anal Biochem* 1991, 194 (1), 198. [PubMed: 1714252]
- (1046). Wilson AK; Horwitz J; Delanerolle P Evaluation of the Electroporation Method for Introducing Proteins into Living Cells. *American Journal of Physiology* 1991, 260 (2), C355. [PubMed: 1996616]
- (1047). Dagher SF; Conrad SE; Werner EA; Patterson RJ Phenotypic Conversion of Tk-Deficient Cells Following Electroporation of Functional Tk Enzyme. *Exp Cell Res* 1992, 198 (1), 36. [PubMed: 1727056]
- (1048). Li Y; Ke Y; Gottlieb PD; Kapp JA Delivery of Exogenous Antigen into the Major Histocompatibility Complex Class-I and Class-II Pathways by Electroporation. *J Leukocyte Biol* 1994, 56 (5), 616. [PubMed: 7525819]
- (1049). Prausnitz MR; Milano CD; Gimm JA; Langer R; Weaver JC Quantitative Study of Molecular-Transport Due to Electroporation - Uptake of Bovine Serum-Albumin by Erythrocyte-Ghosts. *Biophys J* 1994, 66 (5), 1522. [PubMed: 8061201]
- (1050). Morgan W; Day J In *Animal Cell Electroporation and Electrofusion Protocols*; Nickoloff J, Ed.; Humana Press, 1995; Vol. 48.
- (1051). Sontag RL; Mihai C; Orr G; Savchenko A; Skarina T; Cui H; Cort JR; Adkins JN; Brown RN Electroporation of Functional Bacterial Effectors into Mammalian Cells. *J Vis Exp* 2015, (95).
- (1052). Berglund DL; Starkey JR Isolation of Viable Tumor-Cells Following Introduction of Labeled Antibody to an Intracellular Oncogene Product Using Electroporation. *J Immunol Methods* 1989, 125 (1-2), 79. [PubMed: 2691578]
- (1053). Lukas J; Bartek J; Strauss M Efficient Transfer of Antibodies into Mammalian-Cells by Electroporation. *J Immunol Methods* 1994, 170 (2), 255. [PubMed: 8158003]
- (1054). Campbell P; McCluskey J; Yeo J; Toh B-H In *Animal Cell Electroporation and Electrofusion Protocols*; Nickoloff J, Ed.; Humana Press, 1995; Vol. 48.
- (1055). Verspohl EJ; Kaiserling-Buddemeier I; Wienecke A Introducing specific antibodies into electroporated cells is a valuable tool for eliminating specific cell functions. *Cell Biochem Funct* 1997, 15 (2), 127. [PubMed: 9253165]
- (1056). Rui M; Chen YY; Zhang YM; Ma DL Transfer of anti-TFAR19 monoclonal antibody into HeLa cells by in situ electroporation can inhibit the apoptosis. *Life Sciences* 2002, 71 (15), 1771. [PubMed: 12151055]
- (1057). Hou P; Chen S; Wang S; Yu X; Chen Y; Jiang M; Zhuang K; Ho W; Hou W; Huang J et al. Genome editing of CXCR4 by CRISPR/cas9 confers cells resistant to HIV-1 infection. *Sci Rep* 2015, 5, 15577. [PubMed: 26481100]

- (1058). Spiller DG; Giles RV; Grzybowski J; Tidd DM; Clark RE Improving the intracellular delivery and molecular efficacy of antisense oligonucleotides in chronic myeloid leukemia cells: A comparison of streptolysin-O permeabilization, electroporation, and lipophilic conjugation. *Blood* 1998, 91 (12), 4738. [PubMed: 9616172]
- (1059). Walters DK; Jelinek DF The effectiveness of double-stranded short inhibitory RNAs (siRNAs) may depend on the method of transfection. *Antisense Nucleic A* 2002, 12 (6), 411.
- (1060). Calegari F; Haubensak W; Yang D; Huttner WB; Buchholz F Tissue-specific RNA interference in postimplantation mouse embryos with endoribonuclease-prepared short interfering RNA. *P Natl Acad Sci USA* 2002, 99 (22), 14236.
- (1061). Pekarik V; Bourikas D; Miglino N; Joset P; Preiswerk S; Stoeckli ET Screening for gene function in chicken embryo using RNAi and electroporation. *Nat Biotechnol* 2003, 21 (1), 93. [PubMed: 12496763]
- (1062). Gresch O; Engel FB; Nestic D; Tran TT; England HM; Hickman ES; Korner I; Gan L; Chen S; Castro-Obregon S et al. New non-viral method for gene transfer into primary cells. *Methods* 2004, 33 (2), 151. [PubMed: 15121170]
- (1063). Prechtel AT; Turza NM; Theodoridis AA; Kummer M; Steinkasserer A Small interfering RNA (siRNA) delivery into monocyte-derived dendritic cells by electroporation. *J Immunol Methods* 2006, 311 (1–2), 139. [PubMed: 16556448]
- (1064). Saeboe-Larssen S; Fossberg E; Gaudernack G mRNA-based electrotransfection of human dendritic cells and induction of cytotoxic T lymphocyte responses against the telomerase catalytic subunit (hTERT). *J Immunol Methods* 2002, 259 (1–2), 191. [PubMed: 11730854]
- (1065). Takahashi M; Narita M; Ayres F; Satoh N; Abe T; Yanao T; Furukawa T; Toba K; Hirohashi T; Aizawa Y Cytoplasmic expression of EGFP in dendritic cells transfected with in vitro transcribed mRNA or cellular total RNA extracted from EGFP expressing leukemia cells. *Med Oncol* 2003, 20 (4), 335. [PubMed: 14716029]
- (1066). Chu G; Hayakawa H; Berg P Electroporation for the efficient transfection of mammalian cells with DNA. *Nucleic Acids Res* 1987, 15 (3), 1311. [PubMed: 3029703]
- (1067). Klenchin VA; Sukharev SI; Serov SM; Chernomordik LV; Chizmadzhev Yu A Electrically induced DNA uptake by cells is a fast process involving DNA electrophoresis. *Biophys J* 1991, 60 (4), 804. [PubMed: 1660315]
- (1068). Katrukha EA; Mikhaylova M; van Brakel HX; Henegouwen PMVE; Akhmanova A; Hoogenraad CC; Kapitein LC Probing cytoskeletal modulation of passive and active intracellular dynamics using nanobody-functionalized quantum dots. *Nat Commun* 2017, 8.
- (1069). Lambert H; Pankov R; Gauthier J; Hancock R Electroporation-Mediated Uptake of Proteins into Mammalian-Cells. *Biochem Cell Biol* 1990, 68 (4), 729. [PubMed: 2222997]
- (1070). Gabriel B; Teissie J Direct observation in the millisecond time range of fluorescent molecule asymmetrical interaction with the electropermeabilized cell membrane. *Biophys J* 1997, 73 (5), 2630. [PubMed: 9370457]
- (1071). Pucihar G; Kotnik T; Miklavcic D; Teissie J Kinetics of transmembrane transport of small molecules into electropermeabilized cells. *Biophys J* 2008, 95 (6), 2837. [PubMed: 18539632]
- (1072). Escoffre JM; Portet T; Favard C; Teissie J; Dean DS; Rols MP Electromediated formation of DNA complexes with cell membranes and its consequences for gene delivery. *Biochimica et biophysica acta* 2011, 1808 (6), 1538. [PubMed: 21035428]
- (1073). Parsegian A Energy of an Ion Crossing a Low Dielectric Membrane - Solutions to 4 Relevant Electrostatic Problems. *Nature* 1969, 221 (5183), 844. [PubMed: 5765058]
- (1074). Venslauskas MS; Satkauskas S; Rodaite-Riseviciene R Efficiency of the delivery of small charged molecules into cells in vitro. *Bioelectrochemistry* 2010, 79 (1), 130. [PubMed: 19897424]
- (1075). Pakhomov AG; Shevin R; White JA; Kolb JF; Pakhomova ON; Joshi RP; Schoenbach KH Membrane permeabilization and cell damage by ultrashort electric field shocks. *Arch Biochem Biophys* 2007, 465 (1), 109. [PubMed: 17555703]
- (1076). Glogauer M; Mcculloch CAG Introduction of Large Molecules into Viable Fibroblasts by Electroporation - Optimization of Loading and Identification of Labeled Cellular Compartments. *Exp Cell Res* 1992, 200 (2), 227. [PubMed: 1374035]

- (1077). Zaharoff DA; Henshaw JW; Mossop B; Yuan F Mechanistic analysis of electroporation-induced cellular uptake of macromolecules. *Experimental Biology and Medicine* 2008, 233 (1), 94. [PubMed: 18156311]
- (1078). Sadik MM; Yu M; Zheng MD; Zahn JD; Shan JW; Shreiber DI; Lin H Scaling Relationship and Optimization of Double-Pulse Electroporation. *Biophys J* 2014, 106 (4), 801. [PubMed: 24559983]
- (1079). Demiryurek Y; Nickaen M; Zheng MD; Yu M; Zahn JD; Shreiber DI; Lin H; Shan JW Transport, resealing, and re-poration dynamics of two-pulse electroporation-mediated molecular delivery. *Bba-Biomembranes* 2015, 1848 (8), 1706. [PubMed: 25911207]
- (1080). Liang H; Purucker WJ; Stenger DA; Kubiniec RT; Hui SW Uptake of Fluorescence-Labeled Dextran by 10t-½ Fibroblasts Following Permeation by Rectangular and Exponential-Decay Electric-Field Pulses. *Biotechniques* 1988, 6 (6), 550. [PubMed: 2483506]
- (1081). Dimitrov DS; Sowers AE Membrane Electroporation - Fast Molecular-Exchange by Electroosmosis. *Biochimica et biophysica acta* 1990, 1022 (3), 381. [PubMed: 1690573]
- (1082). Prausnitz MR; Corbett JD; Gimm JA; Golan DE; Langer R; Weaver JC Millisecond Measurement of Transport during and after an Electroporation Pulse. *Biophys J* 1995, 68 (5), 1864. [PubMed: 7612828]
- (1083). Prausnitz MR A practical assessment of transdermal drug delivery by skin electroporation. *Adv Drug Deliver Rev* 1999, 35 (1), 61.
- (1084). Rols MP; Femenia P; Teissie J Long-Lived Macropinocytosis Takes Place in Electroporabilized Mammalian-Cells. *Biochem Bioph Res Co* 1995, 208 (1), 26.
- (1085). Escoffre JM; Portet T; Wasungu L; Teissie J; Dean D; Rols MP What is (still not) known of the mechanism by which electroporation mediates gene transfer and expression in cells and tissues. *Molecular biotechnology* 2009, 41 (3), 286. [PubMed: 19016008]
- (1086). Rosazza C; Meglic SH; Zumbusch A; Rols MP; Miklavcic D Gene Electrotransfer: A Mechanistic Perspective. *Curr Gene Ther* 2016, 16 (2), 98. [PubMed: 27029943]
- (1087). Lambricht L; Lopes A; Kos S; Sersa G; Preat V; Vandermeulen G Clinical potential of electroporation for gene therapy and DNA vaccine delivery. *Expert Opin Drug Del* 2016, 13 (2), 295.
- (1088). Potter H; Weir L; Leder P Enhancer-Dependent Expression of Human Kappa-Immunoglobulin Genes Introduced into Mouse Pre-B Lymphocytes by Electroporation. *P Natl Acad Sci-Biol* 1984, 81 (22), 7161.
- (1089). Wolf H; Rols MP; Boldt E; Neumann E; Teissie J Control by Pulse Parameters of Electric Field-Mediated Gene-Transfer in Mammalian-Cells. *Biophys J* 1994, 66 (2), 524. [PubMed: 8161705]
- (1090). Spassova M; Tsoneva I; Petrov AG; Petkova JI; Neumann E Dip Patch-Clamp Currents Suggest Electrodiffusive Transport of the Polyelectrolyte DNA through Lipid Bilayers. *Biophys Chem* 1994, 52 (3), 267. [PubMed: 7999976]
- (1091). Golzio M; Teissie J; Rols MP Direct visualization at the single-cell level of electrically mediated gene delivery. *P Natl Acad Sci USA* 2002, 99 (3), 1292.
- (1092). Rosazza C; Deschout H; Buntz A; Braeckmans K; Rols MP; Zumbusch A Endocytosis and Endosomal Trafficking of DNA After Gene Electrotransfer In Vitro. *Mol Ther Nucleic Acids* 2016, 5, e286. [PubMed: 26859199]
- (1093). Rosazza C; Buntz A; Riess T; Woll D; Zumbusch A; Rols MP Intracellular Tracking of Single-plasmid DNA Particles After Delivery by Electroporation. *Mol Ther* 2013, 21 (12), 2217. [PubMed: 23941812]
- (1094). Brunner S; Furtbauer E; Sauer T; Kursa M; Wagner E Overcoming the nuclear barrier: Cell cycle independent nonviral gene transfer with linear polyethylenimine or electroporation. *Mol Ther* 2002, 5 (1), 80. [PubMed: 11786049]
- (1095). Badding MA; Lapek JD; Friedman AE; Dean DA Proteomic and Functional Analyses of Protein-DNA Complexes During Gene Transfer. *Mol Ther* 2013, 21 (4), 775. [PubMed: 23164933]

- (1096). Paganin-Gioanni A; Bellard E; Escoffre JM; Rols MP; Teissie J; Golzio M Direct visualization at the single-cell level of siRNA electrotransfer into cancer cells. *P Natl Acad Sci USA* 2011, 108 (26), 10443.
- (1097). Pliquett U; Gift EA; Weaver JC Determination of the electric field and anomalous heating caused by exponential pulses with aluminum electrodes in electroporation experiments. *Bioelectroch Bioener* 1996, 39 (1), 39.
- (1098). Canatella PJ; Karr JF; Petros JA; Prausnitz MR Quantitative study of electroporation-mediated molecular uptake and cell viability. *Biophys J* 2001, 80 (2), 755. [PubMed: 11159443]
- (1099). Sukhorukov VL; Reuss R; Zimmermann D; Held C; Muller KJ; Kiesel M; Gessner P; Steinbach A; Schenk WA; Bamberg E et al. Surviving high-intensity field pulses: strategies for improving robustness and performance of electrotransfection and electrofusion. *The Journal of membrane biology* 2005, 206 (3), 187. [PubMed: 16456714]
- (1100). Jordan ET; Collins M; Terefe J; Ugozzoli L; Rubio T Optimizing electroporation conditions in primary and other difficult-to-transfect cells. *Journal of biomolecular techniques : JBT* 2008, 19 (5), 328. [PubMed: 19183796]
- (1101). Kanduser M; Miklavcic D; Pavlin M Mechanisms involved in gene electrotransfer using high- and low-voltage pulses - An in vitro study. *Bioelectrochemistry* 2009, 74 (2), 265. [PubMed: 18930698]
- (1102). Heller R; Jaroszeski M; Atkin A; Moradpour D; Gilbert R; Wands J; Nicolau C In vivo gene electroinjection and expression in rat liver. *Febs Letters* 1996, 389 (3), 225. [PubMed: 8766704]
- (1103). Mir LM; Bureau MF; Gehl J; Rangara R; Rouy D; Caillaud JM; Delaere P; Branellec D; Schwartz B; Scherman D High-efficiency gene transfer into skeletal muscle mediated by electric pulses. *P Natl Acad Sci USA* 1999, 96 (8), 4262.
- (1104). Andreason GL; Evans GA Optimization of Electroporation for Transfection of Mammalian-Cell Lines. *Anal Biochem* 1989, 180 (2), 269. [PubMed: 2817356]
- (1105). Yockell-Lelievre J; Riendeau V; Gagnon SN; Garenc C; Audette M Efficient Transfection of Endothelial Cells by a Double-Pulse Electroporation Method. *DNA Cell Biol* 2009, 28 (11), 561. [PubMed: 19630533]
- (1106). Stroth T; Erben U; Kuhl AA; Zeitz M; Siegmund B Combined Pulse Electroporation - A Novel Strategy for Highly Efficient Transfection of Human and Mouse Cells. *Plos One* 2010, 5 (3).
- (1107). Hamm A; Krott N; Breibach I; Blindt R; Bosserhoff AK Efficient transfection method for primary cells. *Tissue Eng* 2002, 8 (2), 235. [PubMed: 12031113]
- (1108). Zeitelhofer M; Vessey JP; Xie YL; Tubing F; Thomas S; Kiebler M; Dahm R High-efficiency transfection of mammalian neurons via nucleofection. *Nature protocols* 2007, 2 (7), 1692. [PubMed: 17641634]
- (1109). Muller-Hartmann H; Riemen G; Rothmann-Cosic K; Thiel C; Altrogge L; Weigel M; Christine R; Lorbach E; Helfrich J; Wessendorf H; Google Patents, 2004.
- (1110). Martinet W; Schrijvers DM; Kockx MM Nucleofection as an efficient nonviral transfection method for human monocytic cells. *Biotechnol Lett* 2003, 25 (13), 1025. [PubMed: 12889809]
- (1111). Dauty E; Verkman AS Actin cytoskeleton as the principal determinant of size-dependent DNA mobility in cytoplasm. *J Biol Chem* 2005, 280 (9), 7823. [PubMed: 15632160]
- (1112). Lukacs GL; Haggie P; Seksek O; Lechardeur D; Freedman N; Verkman AS Size-dependent DNA mobility in cytoplasm and nucleus. *J Biol Chem* 2000, 275 (3), 1625. [PubMed: 10636854]
- (1113). Luby-Phelps K Cytoarchitecture and physical properties of cytoplasm: Volume, viscosity, diffusion, intracellular surface area. *Int Rev Cytol* 2000, 192, 189. [PubMed: 10553280]
- (1114). Aluigi M; Fogli M; Curti A; Isidori A; Gruppioni E; Chiodoni C; Colombo MP; Versura P; D'Errico-Grigioni A; Ferri E et al. Nucleofection is an efficient nonviral transfection technique for human bone marrow-derived mesenchymal stem cells. *Stem Cells* 2006, 24 (2), 454. [PubMed: 16099993]
- (1115). Aslan H; Zilberman Y; Arbeli V; Sheyn D; Matan Y; Liebergall M; Li JZ; Helm GA; Gazit D; Gazit Z Nucleofection-based ex vivo nonviral gene delivery to human stem cells as a platform for tissue regeneration. *Tissue Eng* 2006, 12 (4), 877. [PubMed: 16674300]

- (1116). Lenz P; Bacot SM; Frazier-Jessen MR; Feldman GM Nucleoporation of dendritic cells: efficient, gene transfer by electroporation into human monocyte-derived dendritic cells. *Febs Letters* 2003, 538 (1–3), 149. [PubMed: 12633869]
- (1117). Landi A; Babiuk LA; Littel-van den Hurk SV High transfection efficiency, gene expression, and viability of monocyte-derived human dendritic cells after nonviral gene transfer. *J Leukocyte Biol* 2007, 82 (4), 849. [PubMed: 17626798]
- (1118). Schakowski F; Buttgerit P; Mazur M; Marten A; Schottker B; Gorschluter M; Schmidt-Wolf IG Novel non-viral method for transfection of primary leukemia cells and cell lines. *Genet Vaccines Ther* 2004, 2 (1), 1. [PubMed: 14715084]
- (1119). Van Bockstaele F; Pede V; Naessens E; Van Coppennolle S; Van Tendeloo V; Verhasselt B; Philippe J Efficient gene transfer in CLL by mRNA electroporation. *Leukemia* 2008, 22 (2), 323. [PubMed: 17972950]
- (1120). Trompeter HI; Weinhold S; Thiel C; Wernet P; Uhrberg M Rapid and highly efficient gene transfer into natural killer cells by nucleofection. *J Immunol Methods* 2003, 274 (1–2), 245. [PubMed: 12609550]
- (1121). Maasho K; Marusina A; Reynolds NM; Coligan JE; Borrego F Efficient gene transfer into the human natural killer cell line, NKL, using the Amaxa nucleofection system (TM). *J Immunol Methods* 2004, 284 (1–2), 133. [PubMed: 14736423]
- (1122). Lai W; Chang CH; Farber DL Gene transfection and expression in resting and activated murine CD4 T cell subsets. *J Immunol Methods* 2003, 282 (1–2), 93. [PubMed: 14604544]
- (1123). Goffinet C; Keppler OT Efficient nonviral gene delivery into primary lymphocytes from rats and mice. *Faseb J* 2006, 20 (1), 500. [PubMed: 16401643]
- (1124). Lakshminpathy U; Pelacho B; Sudo K; Linehan JL; Coucouvanis E; Kaufman DS; Verfaillie CM Efficient transfection of embryonic and adult stem cells. *Stem Cells* 2004, 22 (4), 531. [PubMed: 15277699]
- (1125). Siemen H; Nix M; Endl E; Koch P; Itskovitz-Eldor J; Brustle O Nucleofection of human embryonic stem cells. *Stem Cells Dev* 2005, 14 (4), 378. [PubMed: 16137226]
- (1126). Leclere PG; Panjwani A; Docherty R; Berry M; Pizzey J; Tonge DA Effective gene delivery to adult neurons by a modified form of electroporation. *J Neurosci Meth* 2005, 142 (1), 137.
- (1127). Bischof JC; Padanilam J; Holmes WH; Ezzell RM; Lee RC; Tompkins RG; Yarmush ML; Toner M Dynamics of Cell-Membrane Permeability Changes at Supraphysiological Temperatures. *Biophys J* 1995, 68 (6), 2608. [PubMed: 7647264]
- (1128). Loomishusselbee JW; Cullen PJ; Irvine RF; Dawson AP Electroporation Can Cause Artifacts Due to Solubilization of Cations from the Electrode Plates - Aluminum Ions Enhance Conversion of Inositol 1,3,4,5-Tetrakisphosphate into Inositol 1,4,5-Trisphosphate in Electroporated L1210 Cells. *Biochem J* 1991, 277, 883. [PubMed: 1872818]
- (1129). Stapulionis R Electric pulse-induced precipitation of biological macromolecules in electroporation. *Bioelectroch Bioener* 1999, 48 (1), 249.
- (1130). Tomov T; Tsoneva I Are the stainless steel electrodes inert? *Bioelectrochemistry* 2000, 51 (2), 207. [PubMed: 10910171]
- (1131). Kotnik T; Miklavcic D; Mir LM Cell membrane electroporation by symmetrical bipolar rectangular pulses - Part II. Reduced electrolytic contamination. *Bioelectrochemistry* 2001, 54 (1), 91. [PubMed: 11506979]
- (1132). Rodaite-Riseviciene R; Saule R; Snitka V; Saulis G Release of Iron Ions from the Stainless Steel Anode Occurring During High-Voltage Pulses and Its Consequences for Cell Electroporation Technology. *Ieee T Plasma Sci* 2014, 42 (1), 249.
- (1133). Chafai DE; Mehle A; Tilmatine A; Maouche B; Miklagic D Assessment of the electrochemical effects of pulsed electric fields in a biological cell suspension. *Bioelectrochemistry* 2015, 106, 249. [PubMed: 26315352]
- (1134). Saulis G; Lape R; Praneviciute R; Mickevicius D Changes of the solution pH due to exposure by high-voltage electric pulses. *Bioelectrochemistry* 2005, 67 (1), 101. [PubMed: 15967404]
- (1135). Turjanski P; Olaiz N; Maglietti F; Michinski S; Suarez C; Molina FV; Marshall G The Role of pH Fronts in Reversible Electroporation. *Plos One* 2011, 6 (4).

- (1136). Li Y; Wu M; Zhao D; Wei Z; Zhong W; Wang X; Liang Z; Li Z Electroporation on microchips: the harmful effects of pH changes and scaling down. *Sci Rep* 2015, 5, 17817. [PubMed: 26658168]
- (1137). Saulis G; Rodaite-Riseviciene R; Snitka V Increase of the roughness of the stainless-steel anode surface due to the exposure to high-voltage electric pulses as revealed by atomic force microscopy. *Bioelectrochemistry* 2007, 70 (2), 519. [PubMed: 17289442]
- (1138). Pataro G; Falcone M; Donsi G; Ferrari G Metal release from stainless steel electrodes of a PEF treatment chamber: Effects of electrical parameters and food composition. *Innov Food Sci Emerg* 2014, 21, 58.
- (1139). Pucihar G; Kotnik T; Valic B; Miklavcic D Numerical determination of transmembrane voltage induced on irregularly shaped cells. *Ann Biomed Eng* 2006, 34 (4), 642. [PubMed: 16547608]
- (1140). Swezey RR; Epel D Stable, Resealable Pores Formed in Sea-Urchin Eggs by Electric-Discharge (Electroporation) Permit Substrate Loading for Assay of Enzymes *In Vivo*. *Cell Regul* 1989, 1 (1), 65. [PubMed: 2519619]
- (1141). Benov LC; Antonov PA; Ribarov SR Oxidative Damage of the Membrane-Lipids after Electroporation. *Gen Physiol Biophys* 1994, 13 (2), 85. [PubMed: 7806071]
- (1142). Maccarrone M; Rosato N; Agro AF Electroporation Enhances Cell-Membrane Peroxidation and Luminescence. *Biochem Bioph Res Co* 1995, 206 (1), 238.
- (1143). Maccarrone M; Bladergroen MR; Rosato N; Agro AF Role of Lipid-Peroxidation in Electroporation-Induced Cell-Permeability. *Biochem Bioph Res Co* 1995, 209 (2), 417.
- (1144). Gabriel B; Teissie J Generation of Reactive-Oxygen Species Induced by Electropermeabilization of Chinese-Hamster Ovary Cells and Their Consequence on Cell Viability. *Eur J Biochem* 1994, 223 (1), 25. [PubMed: 8033899]
- (1145). Bonnafous P; Vernhes MC; Teissie J; Gabriel B The generation of reactive-oxygen species associated with long-lasting pulse-induced electropermeabilisation of mammalian cells is based on a non-destructive alteration of the plasma membrane. *Bba-Biomembranes* 1999, 1461 (1), 123. [PubMed: 10556494]
- (1146). Vatteroni L; Piras A; Simi S; Mariani L; Moretti A; Citti L; Mariani T; Rainaldi G Analysis of Electroporation-Induced Genetic Damages in V79/Ap4 Chinese-Hamster Cells. *Mutat Res* 1993, 291 (3), 163. [PubMed: 7685057]
- (1147). Meaking WS; Edgerton J; Wharton CW; Meldrum RA Electroporation-induced damage in mammalian cell DNA. *Bba-Gene Struct Expr* 1995, 1264 (3), 357.
- (1148). Zhou Y; Berry CK; Storer PA; Raphael RM Peroxidation of polyunsaturated phosphatidylcholine lipids during electroformation. *Biomaterials* 2007, 28 (6), 1298. [PubMed: 17107709]
- (1149). Vernier PT; Levine ZA; Wu YH; Joubert V; Ziegler MJ; Mir LM; Tieleman DP Electroporating Fields Target Oxidatively Damaged Areas in the Cell Membrane. *Plos One* 2009, 4 (11).
- (1150). Chen W; Lee RC Altered Ion-Channel Conductance and Ionic Selectivity Induced by Large Imposed Membrane-Potential Pulse. *Biophys J* 1994, 67 (2), 603. [PubMed: 7948676]
- (1151). Chen W; Han Y; Chen Y; Astumian D Electric field - induced functional reductions in the K⁺ channels mainly resulted from supramembrane potential-mediated electroconformational changes. *Biophys J* 1998, 75 (1), 196. [PubMed: 9649379]
- (1152). Chen W; Zhang ZS; Lee RC Supramembrane potential-induced electroconformational changes in sodium channel proteins: A potential mechanism involved in electric injury. *Burns* 2006, 32 (1), 52. [PubMed: 16384650]
- (1153). Chen W; Han Y; Chen Y; Lee RC Supramembrane potential induced electroconformational changes of the voltage-gated Na channels is a possible mechanism in electrical injury. *Electricity and Magnetism in Biology and Medicine* 1999, 837.
- (1154). Lee RC Cell injury by electric forces. *Ann Ny Acad Sci* 2005, 1066, 85. [PubMed: 16533920]
- (1155). Chen W Electroconformational denaturation of membrane proteins. *Ann Ny Acad Sci* 2005, 1066, 92. [PubMed: 16533921]
- (1156). Huang FR; Fang ZH; Mast J; Chen W Comparison of membrane electroporation and protein denature in response to pulsed electric field with different durations. *Bioelectromagnetics* 2013, 34 (4), 253. [PubMed: 23322376]

- (1157). Nesin V; Bowman AM; Xiao S; Pakhomov AG Cell permeabilization and inhibition of voltage-gated Ca²⁺ and Na⁺ channel currents by nanosecond pulsed electric field. *Bioelectromagnetics* 2012, 33 (5), 394. [PubMed: 22213081]
- (1158). Beebe SJ Considering effects of nanosecond pulsed electric fields on proteins. *Bioelectrochemistry* 2015, 103, 52. [PubMed: 25218277]
- (1159). Nuccitelli R; Lui KY; Kreis M; Athos B; Nuccitelli P Nanosecond pulsed electric field stimulation of reactive oxygen species in human pancreatic cancer cells is Ca²⁺-dependent. *Biochem Biophys Res Commun* 2013, 435 (4), 580.
- (1160). Pakhomova ON; Khorokhorina VA; Bowman AM; Rodaite-Riseviciene R; Saulis G; Xiao S; Pakhomov AG Oxidative effects of nanosecond pulsed electric field exposure in cells and cell-free media. *Arch Biochem Biophys* 2012, 527 (1), 55. [PubMed: 22910297]
- (1161). Golberg A; Yarmush ML Nonthermal Irreversible Electroporation: Fundamentals, Applications, and Challenges. *Ieee T Bio-Med Eng* 2013, 60 (3), 707.
- (1162). Schwarz S; Haest CWM; Deuticke B Extensive electroporation abolishes experimentally induced shape transformations of erythrocytes: a consequence of phospholipid symmetrization. *Bba-Biomembranes* 1999, 1421 (2), 361. [PubMed: 10518706]
- (1163). Vernier PT; Sun YH; Marcu L; Craft CM; Gundersen MA Nanoelectropulse-induced phosphatidylserine translocation. *Biophys J* 2004, 86 (6), 4040. [PubMed: 15189899]
- (1164). Vernier PT; Ziegler MJ; Sun YH; Chang WV; Gundersen MA; Tieleman DP Nanopore formation and phosphatidylserine externalization in a phospholipid bilayer at high transmembrane potential. *J Am Chem Soc* 2006, 128 (19), 6288. [PubMed: 16683772]
- (1165). Vincelette RL; Roth CC; McConnell MP; Payne JA; Beier HT; Ibey BL Thresholds for Phosphatidylserine Externalization in Chinese Hamster Ovarian Cells following Exposure to Nanosecond Pulsed Electrical Fields (nsPEF). *Plos One* 2013, 8 (4).
- (1166). Escoffre JM; Bellard E; Faurie C; Sebai SC; Golzio M; Teissie J; Rols MP Membrane disorder and phospholipid scrambling in electroporated and viable cells. *Bba-Biomembranes* 2014, 1838 (7), 1701. [PubMed: 24583083]
- (1167). Kooijmans SAA; Stremersch S; Braeckmans K; de Smedt SC; Hendrix A; Wood MJA; Schiffelers RM; Raemdonck K; Vader P Electroporation -induced siRNA precipitation obscures the efficiency of siRNA loading into extracellular vesicles. *Journal of Controlled Release* 2013, 172 (1), 229. [PubMed: 23994516]
- (1168). Fox MB; Esveld DC; Valero A; Luttge R; Mastwijk HC; Bartels PV; van den Berg A; Boom RM Electroporation of cells in microfluidic devices: a review. *Anal Bioanal Chem* 2006, 385 (3), 474. [PubMed: 16534574]
- (1169). Wang MY; Orwar O; Olofsson J; Weber SG Single-cell electroporation. *Anal Bioanal Chem* 2010, 397 (8), 3235. [PubMed: 20496058]
- (1170). Movahed S; Li DQ Microfluidics cell electroporation. *Microfluid Nanofluid* 2011, 10 (4), 703.
- (1171). Geng T; Lu C Microfluidic electroporation for cellular analysis and delivery. *Lab on a chip* 2013.
- (1172). Wang S; Lee LJ Micro-/nanofluidics based cell electroporation. *Biomicrofluidics* 2013, 7 (1), 11301. [PubMed: 23405056]
- (1173). Yang ZG; Chang LQ; Chiang CL; Lee LJ Micro-/Nano - Electroporation for Active Gene Delivery. *Curr Pharm Design* 2015, 21 (42), 6081.
- (1174). Huang Y; Rubinsky B Micro-Electroporation: Improving the Efficiency and Understanding of Electrical Permeabilization of Cells. *Biomed Microdevices* 1999, 2 (2), 145.
- (1175). Huang Y; Rubinsky B Flow-through micro-electroporation chip for high efficiency single-cell genetic manipulation. *Sensor Actuat a-Phys* 2003, 104 (3), 205.
- (1176). Seemann R; Brinkmann M; Pfohl T; Herminghaus S Droplet based microfluidics. *Rep Prog Phys* 2012, 75 (1), 016601. [PubMed: 22790308]
- (1177). Zhan YH; Wang J; Bao N; Lu C Electroporation of Cells in Microfluidic Droplets. *Anal Chem* 2009, 81 (5), 2027. [PubMed: 19199389]
- (1178). Geng T; Zhan YH; Wang HY; Witting SR; Cornetta KG; Lu C Flow-through electroporation based on constant voltage for large-volume transfection of cells. *Journal of Controlled Release* 2010, 144 (1), 91. [PubMed: 20117155]

- (1179). Zhu T; Luo CX; Huang JY; Xiong CY; Ouyang Q; Fang J Electroporation based on hydrodynamic focusing of microfluidics with low DC voltage. *Biomed Microdevices* 2010, 12 (1), 35. [PubMed: 19757070]
- (1180). Wang J; Zhan YH; Ugaz VM; Lu C Vortex -assisted DNA delivery. *Lab on a chip* 2010, 10 (16), 2057. [PubMed: 20563345]
- (1181). Yun H; Hur SC Sequential multi-molecule delivery using vortex-assisted electroporation. *Lab on a chip* 2013, 13 (14), 2764. [PubMed: 23727978]
- (1182). Zheng MD; Shan JW; Lin H; Shreiber DI; Zahn JD Hydrodynamically controlled cell rotation in an electroporation microchip to circumferentially deliver molecules into single cells. *Microfluid Nanofluid* 2016, 20 (1).
- (1183). Ouyang M; Hill W; Lee JH; Hur SC Microscale Symmetrical Electroporator Array as a Versatile Molecular Delivery System. *Sci Rep* 2017, 7, 44757. [PubMed: 28317836]
- (1184). Boukany PE; Morss A; Liao WC; Henslee B; Jung HC; Zhang XL; Yu B; Wang XM; Wu Y; Li Let al. Nanochannel electroporation delivers precise amounts of biomolecules into living cells. *Nature nanotechnology* 2011, 6 (11), 747.
- (1185). Chang LQ; Bertani P; Gallego-Perez D; Yang ZG; Chen F; Chiang CL; Malkoc V; Kuang TR; Gao KL; Lee LJet al. 3D nanochannel electroporation for high-throughput cell transfection with high uniformity and dosage control. *Nanoscale* 2016, 8 (1), 243. [PubMed: 26309218]
- (1186). Kurosawa O; Oana H; Matsuka S; Noma A; Kotera H; Washizu M Electroporation through a micro-fabricated orifice and its application to the measurement of cell response to external stimuli. *Meas Sci Technol* 2006, 17 (12), 3127.
- (1187). Seo J; Ionescu-Zanetti C; Diamond J; Lal R; Lee LP Integrated multiple patch-clamp array chip via lateral cell trapping junctions. *Appl Phys Lett* 2004, 84 (11), 1973.
- (1188). Khine M; Lau A; Ionescu-Zanetti C; Seo J; Lee LP A single cell electroporation chip. *Lab on a chip* 2005, 5 (1), 38. [PubMed: 15616738]
- (1189). Khine M; Ionescu-Zanetti C; Blatz A; Wang LP; Lee LP Single-cell electroporation arrays with real-time monitoring and feedback control. *Lab on a chip* 2007, 7 (4), 457. [PubMed: 17389961]
- (1190). Ionescu-Zanetti C; Blatz A; Khine M Electrophoresis-assisted single-cell electroporation for efficient intracellular delivery. *Biomed Microdevices* 2008, 10 (1), 113. [PubMed: 17828458]
- (1191). Valero A; Post JN; van Nieuwkasteele JW; ter Braak PM; Kruijer W; van den Berg A Gene transfer and protein dynamics in stem cells using single cell electroporation in a microfluidic device. *Lab on a chip* 2008, 8 (1), 62. [PubMed: 18094762]
- (1192). Kang WM; Yavari F; Minary-Jolandan M; Giraldo-Vela JP; Safi A; McNaughton RL; Parpoil V; Espinosa HD Nanofountain Probe Electroporation (NFP-E) of Single Cells. *Nano Lett* 2013, 13 (6), 2448. [PubMed: 23650871]
- (1193). Giraldo-Vela JP; Kang W; McNaughton RL; Zhang XM; Wile BM; Tsourkas A; Bao G; Espinosa HD Single-Cell Detection of mRNA Expression Using Nanofountain-Probe Electroporated Molecular Beacons. *Small* 2015, 11 (20), 2386. [PubMed: 25641752]
- (1194). Charoo NA; Rahman Z; Repka MA; Murthy SN Electroporation: an avenue for transdermal drug delivery. *Curr Drug Deliv* 2010, 7 (2), 125. [PubMed: 20158490]
- (1195). Sardesai NY; Weiner DB Electroporation delivery of DNA vaccines: prospects for success. *Curr Opin Immunol* 2011, 23 (3), 421. [PubMed: 21530212]
- (1196). Mali B; Jarm T; Snoj M; Sersa G; Miklavcic D Antitumor effectiveness of electrochemotherapy: A systematic review and meta-analysis. *Ejso-Eur J Surg Onc* 2013, 39 (1), 4.
- (1197). Jiang CL; Davalos RV; Bischof JC A Review of Basic to Clinical Studies of Irreversible Electroporation Therapy. *Ieee T Bio-Med Eng* 2015, 62 (1), 4.
- (1198). Calvet CY; Mir LM The promising alliance of anti-cancer electrochemotherapy with immunotherapy. *Cancer Metastasis Rev* 2016.
- (1199). Kotnik T; Frey W; Sack M; Meglic SH; Peterka M; Miklavcic D Electroporation-based applications in biotechnology. *Trends Biotechnol* 2015, 33 (8), 480. [PubMed: 26116227]
- (1200). Orłowski S; Mir LM Cell Electroporabilization - a New Tool for Biochemical and Pharmacological Studies. *Biochimica et biophysica acta* 1993, 1154 (1), 51. [PubMed: 8507646]

- (1201). Pham PL; Kamen A; Durocher Y Large -scale Transfection of mammalian cells for the fast production of recombinant protein. *Molecular biotechnology* 2006, 34 (2), 225. [PubMed: 17172668]
- (1202). Wurm FM Production of recombinant protein therapeutics in cultivated mammalian cells. *Nat Biotechnol* 2004, 22 (11), 1393. [PubMed: 15529164]
- (1203). Baldi L; Hacker DL; Adam M; Wurm FM Recombinant protein production by large-scale transient gene expression in mammalian cells: state of the art and future perspectives. *Biotechnol Lett* 2007, 29 (5), 677. [PubMed: 17235486]
- (1204). Merten OW; Charrier S; Laroudie N; Fauchille S; Dugue C; Jenny C; Audit M; Zanta-Boussif MA; Chautard H; Radrizzani Met al. Large-Scale Manufacture and Characterization of a Lentiviral Vector Produced for Clinical Ex Vivo Gene Therapy Application. *Hum Gene Ther* 2011, 22 (3), 343. [PubMed: 21043787]
- (1205). Lock M; Alvira M; Vandenberghe LH; Samanta A; Toelen J; Debyser Z; Wilson JM Rapid, Simple, and Versatile Manufacturing of Recombinant Adeno-Associated Viral Vectors at Scale. *Hum Gene Ther* 2010, 21 (10), 1259. [PubMed: 20497038]
- (1206). Zeltins A Construction and Characterization of Virus-Like Particles: A Review. *Molecular biotechnology* 2013, 53 (1), 92. [PubMed: 23001867]
- (1207). Li LH; Shivakumar R; Feller S; Allen C; Weiss JM; Dzekunov S; Singh V; Holaday J; Fratantoni J; Liu LN Highly Efficient, Large Volume Flow Electroporation. *Technol Cancer Res T* 2002, 1 (5), 341.
- (1208). Witting SR; Li LH; Jasti A; Allen C; Cornetta K; Brady J; Shivakumar R; Peshwa MV Efficient Large Volume Lentiviral Vector Production Using Flow Electroporation. *Hum Gene Ther* 2012, 23 (2), 243. [PubMed: 21933028]
- (1209). Zhao DY; Huang D; Li Y; Wu MX; Zhong WF; Cheng Q; Wang XX; Wu YD; Zhou X; Wei ZWet al. A Flow-Through Cell Electroporation Device for Rapidly and Efficiently Transfecting Massive Amounts of Cells in vitro and ex vivo. *Sci Rep-Uk* 2016, 6 .
- (1210). Selmeczi D; Hansen TS; Met O; Svane IM; Larsen NB Efficient large volume electroporation of dendritic cells through micrometer scale manipulation of flow in a disposable polymer chip. *Biomed Microdevices* 2011, 13 (2), 383. [PubMed: 21207149]
- (1211). Sather BD; Romano Ibarra GS; Sommer K; Curinga G; Hale M; Khan IF; Singh S; Song Y; Gwiazda K; Sahni Jet al. Efficient modification of CCR5 in primary human hematopoietic cells using a megaTAL nuclease and AAV donor template. *Sci Transl Med* 2015, 7 (307), 307ra156.
- (1212). Dullaers M; Breckpot K; Van Meirvenne S; Bonehill A; Tuybaerts S; Michiels A; Straetman L; Heirman C; De Greef C; Van Der Bruggen Pet al. Side-by-side comparison of lentivirally transduced and mRNA-electroporated dendritic cells: Implications for cancer immunotherapy protocols. *Mol Ther* 2004, 10 (4), 768. [PubMed: 15451461]
- (1213). Dalby B; Cates S; Harris A; Ohki EC; Tilkins ML; Price PJ; Ciccarone VC Advanced transfection with Lipofectamine 2000 reagent: primary neurons, siRNA, and high-throughput applications. *Methods* 2004, 33 (2), 95. [PubMed: 15121163]
- (1214). Coughlin CM; Vance BA; Grupp SA; Vonderheide RH RNA-transfected CD40-activated B cells induce functional T-cell responses against viral and tumor antigen targets: implications for pediatric immunotherapy. *Blood* 2004, 103 (6), 2046. [PubMed: 14630810]
- (1215). Schaft N; Dorrie J; Muller I; Beck V; Baumann S; Schunder T; Kampgen E; Schuler G A new way to generate cytolytic tumor-specific T cells: electroporation of RNA coding for a T cell receptor into T lymphocytes. *Cancer Immunol Immun* 2006, 55 (9), 1132.
- (1216). Kunii N; Zhao YB; Jiang SG; Liu XJ; Scholler J; Balagopalan L; Samelson LE; Milone MC; June CH Enhanced Function of Redirected Human T Cells Expressing Linker for Activation of T Cells That Is Resistant to Ubiquitylation. *Hum Gene Ther* 2013, 24 (1), 27. [PubMed: 22998346]
- (1217). Riet T; Holzinger A; Dorrie J; Schaft N; Schuler G; Abken H Nonviral RNA transfection to transiently modify T cells with chimeric antigen receptors for adoptive therapy. *Methods Mol Biol* 2013, 969, 187. [PubMed: 23296935]
- (1218). Krug C; Wiesinger M; Abken H; Schuler-Thurner B; Schuler G; Dorrie J; Schaft N A GMP-compliant protocol to expand and transfect cancer patient T cells with mRNA encoding a tumor-specific chimeric antigen receptor. *Cancer Immunol Immun* 2014, 63 (10), 999.

- (1219). Wang J; DeClercq JJ; Hayward SB; Li PW; Shivak DA; Gregory PD; Lee G; Holmes MC Highly efficient homology -driven genome editing in human T cells by combining zinc-finger nuclease mRNA and AAV6 donor delivery. *Nucleic Acids Res* 2015.
- (1220). Grunebach F; Muller MR; Nencioni A; Brossart P Delivery of tumor-derived RNA for the induction of cytotoxic T-lymphocytes. *Gene Ther* 2003, 10 (5), 367. [PubMed: 12601391]
- (1221). Van Nuffel AMT; Corthals J; Neyns B; Heirman C; Thielemans K; Bonehill A Immunotherapy of Cancer with Dendritic Cells Loaded with Tumor Antigens and Activated Through mRNA Electroporation. *Rna Therapeutics: Function, Design, and Delivery* 2010, 629, 403.
- (1222). Van den Bosch GA; Ponsaerts P; Nijs G; Lenjou M; Vanham G; Van Bockstaele DR; Berneman ZN; Van Tendeloo VFI Ex vivo induction of viral antigen-specific CD8(+) T cell responses using mRNA-electroporated CD40-activated B cells. *Clin Exp Immunol* 2005, 139 (3), 458. [PubMed: 15730391]
- (1223). Lee J; Dollins CM; Boczkowski D; Sullenger BA; Nair S Activated B cells modified by electroporation of multiple mRNAs encoding immune stimulatory molecules are comparable to mature dendritic cells in inducing in vitro antigen-specific T -cell responses. *Immunology* 2008, 125 (2), 229. [PubMed: 18393968]
- (1224). Li LH; Biagi E; Allen C; Shivakumar R; Weiss JM; Feller S; Yvon E; Fratantoni JC; Liu LN Rapid and efficient nonviral gene delivery of CD154 to primary chronic lymphocytic leukemia cells. *Cancer Gene Ther* 2006, 13 (2), 215. [PubMed: 16082377]
- (1225). Li L; Liu LN; Feller S; Allen C; Shivakumar R; Fratantoni J; Wolfrain LA; Fujisaki H; Campana D; Chopas Net al. Expression of chimeric antigen receptors in natural killer cells with a regulatory-compliant non-viral method. *Cancer Gene Ther* 2010, 17 (3), 147. [PubMed: 19745843]
- (1226). Shimasaki N; Fujisaki H; Cho D; Masselli M; Lockey T; Eldridge P; Leung W; Campana D A clinically adaptable method to enhance the cytotoxicity of natural killer cells against B -cell malignancies. *Cytotherapy* 2012, 14 (7), 830. [PubMed: 22458956]
- (1227). Bilal MY; Vacaflares A; Houtman JCD Optimization of methods for the genetic modification of human T cells. *Immunol Cell Biol* 2015, 93 (10), 896. [PubMed: 26027856]
- (1228). Zhang M; Ma Z; Selliah N; Weiss G; Genin A; Finkel TH; Cron RQ The impact of Nucleofection (R) on the activation state of primary human CD4 T cells. *J Immunol Methods* 2014, 408, 123. [PubMed: 24910411]
- (1229). Anderson BR; Kariko K; Weissman D Nucleofection induces transient eIF2alpha phosphorylation by GCN2 and PERK. *Gene Ther* 2013, 20 (2), 136. [PubMed: 22301437]
- (1230). Wilgenhof S; Van Nuffel AMT; Benteyn D; Corthals J; Aerts C; Heirman C; Van Riet I; Bonehill A; Thielemans K; Neyns B A phase IB study on intravenous synthetic mRNA electroporated dendritic cell immunotherapy in pretreated advanced melanoma patients. *Ann Oncol* 2013, 24 (10), 2686. [PubMed: 23904461]
- (1231). Gill S; June CH Going viral: chimeric antigen receptor T-cell therapy for hematological malignancies. *Immunol Rev* 2015, 263 (1), 68. [PubMed: 25510272]
- (1232). Yewdell JW; Bennink JR; Hosaka Y Cells process exogenous proteins for recognition by cytotoxic T lymphocytes. *Science* 1988, 239 (4840), 637. [PubMed: 3257585]
- (1233). Tacke PJ; de Vries IJM; Torensma R; Figdor C Dendritic-cell immunotherapy: from ex vivo loading to in vivo targeting. *Nat Rev Immunol* 2007, 7 (10), 790. [PubMed: 17853902]
- (1234). Mitchell DA; Nair SK RNA-transfected dendritic cells in cancer immunotherapy. *Journal of Clinical Investigation* 2000, 106 (9), 1065. [PubMed: 11067858]
- (1235). Van Tendeloo VFI; Snoeck HW; Lardon F; Vanham GLEE; Nijs G; Lenjou M; Hendriks L; Van Broeckhoven C; Moulijn A; Rodrigus Iet al. Nonviral transfection of distinct types of human dendritic cells: high-efficiency gene transfer by electroporation into hematopoietic progenitor-but not monocyte-derived dendritic cells. *Gene Ther* 1998, 5 (5), 700. [PubMed: 9797876]
- (1236). Ponsaerts P; Van Tendeloo VFI; Berneman ZN Cancer immunotherapy using RNA-loaded dendritic cells. *Clin Exp Immunol* 2003, 134 (3), 378. [PubMed: 14632740]
- (1237). Li S Electroporation gene therapy: new developments in vivo and in vitro. *Curr Gene Ther* 2004, 4 (3), 309. [PubMed: 15384944]

- (1238). Wilgenhof S; Van Nuffel AMT; Corthals J; Heirman C; Tuyaeerts S; Bentejn D; De Coninck A; Van Riet I; Verfaillie G; Vandelooy Jet al. Therapeutic Vaccination With an Autologous mRNA Electroporated Dendritic Cell Vaccine in Patients With Advanced Melanoma. *J Immunother* 2011, 34 (5), 448. [PubMed: 21577140]
- (1239). Kalos M; June CH Adoptive T Cell Transfer for Cancer Immunotherapy in the Era of Synthetic Biology. *Immunity* 2013, 39 (1), 49. [PubMed: 23890063]
- (1240). Morvan MG; Lanier LL NK cells and cancer: you can teach innate cells new tricks. *Nature Reviews Cancer* 2016, 16 (1), 7. [PubMed: 26694935]
- (1241). Mitchell DA; Karikari I; Cui XY; Xie WH; Schmittling R; Sampson JH Selective modification of antigen-specific T cells by RNA electroporation. *Hum Gene Ther* 2008, 19 (5), 511. [PubMed: 18471037]
- (1242). Yoon SH; Lee JM; Cho HI; Kim EK; Kim HS; Park MY; Kim TG Adoptive immunotherapy using human peripheral blood lymphocytes transferred with RNA encoding Her-2/neu-specific chimeric immune receptor in ovarian cancer xenograft model. *Cancer Gene Ther* 2009, 16 (6), 489. [PubMed: 19096447]
- (1243). Maus MV; Haas AR; Beatty GL; Albelda SM; Levine BL; Liu XJ; Zhao YB; Kalos M; June CH T Cells Expressing Chimeric Antigen Receptors Can Cause Anaphylaxis in Humans. *Cancer Immunol Res* 2013, 1 (1), 26.
- (1244). Imai C; Iwamoto S; Campana D Genetic modification of primary natural killer cells overcomes inhibitory signals and induces specific killing of leukemic cells. *Blood* 2005, 106 (1), 376. [PubMed: 15755898]
- (1245). Tebas P; Stein D; Tang WW; Frank I; Wang SQ; Lee G; Spratt SK; Surosky RT; Giedlin MA; Nichol Get al. Gene Editing of CCR5 in Autologous CD4 T Cells of Persons Infected with HIV. *New Engl J Med* 2014, 370 (10), 901. [PubMed: 24597865]
- (1246). Biffi A; Montini E; Lorioli L; Cesani M; Fumagalli F; Plati T; Baldoli C; Martino S; Calabria A; Canale Set al. Lentiviral Hematopoietic Stem Cell Gene Therapy Benefits Metachromatic Leukodystrophy. *Science* 2013, 341 (6148), 864.
- (1247). Aiuti A; Biasco L; Scaramuzza S; Ferrua F; Cicalese MP; Baricordi C; Dionisio F; Calabria A; Giannelli S; Castiello MC et al. Lentiviral Hematopoietic Stem Cell Gene Therapy in Patients with Wiskott-Aldrich Syndrome. *Science* 2013, 341 (6148), 865.
- (1248). Lombardo A; Naldini L Genome Editing: A Tool For Research and Therapy: Targeted genome editing hits the clinic. *Nat Med* 2014, 20 (10), 1101. [PubMed: 25295939]
- (1249). Kanehisa MI; Tsong TY Cluster Model of Lipid Phase-Transitions with Application to Passive Permeation of Molecules and Structure Relaxations in Lipid Bilayers. *J Am Chem Soc* 1978, 100 (2), 424.
- (1250). Heimburg T In *Thermal Biophysics of Membranes*; Wiley-VCH Verlag GmbH & Co KGaA, 2007.
- (1251). Jacobson K; Papahadjopoulos D Phase-Transitions and Phase Separations in Phospholipid Membranes Induced by Changes in Temperature, Ph, and Concentration of Bivalent-Cations. *Biochemistry* 1975, 14 (1), 152. [PubMed: 234017]
- (1252). Mandel M; Higa A Calcium-Dependent Bacteriophage DNA Infection. *J Mol Biol* 1970, 53 (1), 159. [PubMed: 4922220]
- (1253). Hanahan D Studies on Transformation of Escherichia-Coli with Plasmids. *J Mol Biol* 1983, 166 (4), 557. [PubMed: 6345791]
- (1254). Vandie IM; Bergmans HEN; Hoekstra WPM Transformation in Escherichia-Coli - Studies on the Role of the Heat-Shock in Induction of Competence. *J Gen Microbiol* 1983, 129 (Mar), 663. [PubMed: 6348205]
- (1255). Panja S; Aich P; Jana B; Basu T How does plasmid DNA penetrate cell membranes in artificial transformation process of Escherichia coli? *Mol Membr Biol* 2008, 25 (5), 411. [PubMed: 18651316]
- (1256). Tripp VT; Maza JC; Young DD Development of rapid microwave-mediated and low-temperature bacterial transformations. *J Chem Biol* 2013, 6 (3), 135. [PubMed: 24432129]
- (1257). Li S; Anderson LM; Yang JM; Lin L; Yang H DNA transformation via local heat shock. *Appl Phys Lett* 2007, 91 (1).

- (1258). Nichols RA; Wu WCS; Haycock JW; Greengard P Introduction of Impermeant Molecules into Synaptosomes Using Freeze Thaw Permeabilization. *J Neurochem* 1989, 52 (2), 521. [PubMed: 2536075]
- (1259). Nath AR; Chen RHC; Stanley EF Cryoloading: introducing large molecules into live synaptosomes. *Front Cell Neurosci* 2014, 8.
- (1260). Yi PN; Chang CS; Tallen M; Bayer W; Ball S Hyperthermia-Induced Intracellular Ionic Level Changes in Tumor-Cells. *Radiat Res* 1983, 93 (3), 534. [PubMed: 6304803]
- (1261). Ivanov IT; Todorova R; Zlatanov I Spectrofluorometric and microcalorimetric study of the thermal poration relevant to the mechanism of thermohaemolysis. *Int J Hyperther* 1999, 15 (1), 29.
- (1262). Ivanov IT Investigation of surface and shape changes accompanying the membrane alteration responsible for the heat-induced lysis of human erythrocytes. *Colloid Surface B* 1999, 13 (6), 311.
- (1263). Merchant FA; Holmes WH; Capelli-Schellpfeffer M; Lee RC; Toner M Poloxamer 188 enhances functional recovery of lethally heat-shocked fibroblasts. *J Surg Res* 1998, 74 (2), 131. [PubMed: 9587351]
- (1264). Terakawa M; Ogura M; Sato S; Wakisaka H; Ashida H; Uenoyama M; Masaki Y; Obara M Gene transfer into mammalian cells by use of a nanosecond pulsed laser-induced stress wave. *Opt Lett* 2004, 29 (11), 1227. [PubMed: 15209255]
- (1265). Xu T; Rohozinski J; Zhao WX; Moorefield EC; Atala A; Yoo JJ Inkjet-Mediated Gene Transfection into Living Cells Combined with Targeted Delivery. *Tissue Eng Pt A* 2009, 15 (1), 95.
- (1266). Cui X; Dean D; Ruggeri ZM; Boland T Cell damage evaluation of thermal inkjet printed Chinese hamster ovary cells. *Biotechnol Bioeng* 2010, 106 (6), 963. [PubMed: 20589673]
- (1267). Cui XF; Boland T Human microvasculature fabrication using thermal inkjet printing technology. *Biomaterials* 2009, 30 (31), 6221. [PubMed: 19695697]
- (1268). Stevenson DJ; Gunn-Moore FJ; Campbell P; Dholakia K Single cell optical transfection. *Journal of the Royal Society Interface* 2010, 7 (47), 863.
- (1269). Yao CP; Zhang ZX; Rahmzadeh R; Huettmann G Laser-based gene transfection and gene therapy. *Ieee T Nanobiosci* 2008, 7 (2), 111.
- (1270). Vogel A; Linz N; Freidank S; Paltauf G Femtosecond-laser-induced nanocavitation in water: Implications for optical breakdown threshold and cell surgery. *Physical Review Letters* 2008, 100 (3).
- (1271). Umebayashi Y; Miyamoto Y; Wakita M; Kobayashi A; Nishisaka T Elevation of plasma membrane permeability on laser irradiation of extracellular latex particles. *Journal of biochemistry* 2003, 134 (2), 219. [PubMed: 12966070]
- (1272). Yao CP; Rahmzadeh R; Endl E; Zhang ZX; Gerdes J; Huttman G Elevation of plasma membrane permeability by laser irradiation of selectively bound nanoparticles. *J Biomed Opt* 2005, 10 (6).
- (1273). Yao CP; Qu XC; Zhang ZX; Huttman G; Rahmzadeh R Influence of laser parameters on nanoparticle-induced membrane permeabilization. *J Biomed Opt* 2009, 14 (5).
- (1274). Tong L; Zhao Y; Huff TB; Hansen MN; Wei A; Cheng JX Gold nanorods mediate tumor cell death by compromising membrane integrity. *Adv Mater* 2007, 19 (20), 3136. [PubMed: 19020672]
- (1275). Gu L; Koymen AR; Mohanty SK Crystalline magnetic carbon nanoparticle assisted photothermal delivery into cells using CW near-infrared laser beam. *Sci Rep-Uk* 2014, 4.
- (1276). Lyu ZL; Zhou F; Liu Q; Xue H; Yu Q; Chen H A Universal Platform for Macromolecular Delivery into Cells Using Gold Nanoparticle Layers via the Photoporation Effect. *Adv Funct Mater* 2016, 26 (32), 5787.
- (1277). Palumbo G; Caruso M; Crescenzi E; Tecce MF; Roberti G; Colasanti A Targeted gene transfer in eucaryotic cells by dye-assisted laser optoporation. *J Photoch Photobio B* 1996, 36 (1), 41.
- (1278). Vogel A; Noack J; Huttman G; Paltauf G Mechanisms of femtosecond laser nanosurgery of cells and tissues. *Appl Phys B-Lasers O* 2005, 81 (8), 1015.

- (1279). Paterson L; Agate B; Comrie M; Ferguson R; Lake TK; Morris JE; Carruthers AE; Brown CTA; Sibbett W; Bryant PE et al. Photoporation and cell transfection using a violet diode laser. *Optics express* 2005, 13 (2), 595. [PubMed: 19488389]
- (1280). Rhodes K; Clark I; Zatcoff M; Eustaquio T; Hoyte KL; Koller MR Cellular laserfection. *Laser Manipulation of Cells and Tissues* 2007, 82, 309.
- (1281). Tsukakoshi M; Kurata S; Nomiya Y; Ikawa Y; Kasuya T A Novel Method of DNA Transfection by Laser Microbeam Cell Surgery. *Appl Phys B-Photo* 1984, 35 (3), 135.
- (1282). Kurata S; Tsukakoshi M; Kasuya T; Ikawa Y The Laser Method for Efficient Introduction of Foreign DNA into Cultured-Cells. *Exp Cell Res* 1986, 162 (2), 372. [PubMed: 3943549]
- (1283). Tao W; Wilkinson J; Stanbridge EJ; Berns MW Direct Gene-Transfer into Human Cultured-Cells Facilitated by Laser Micropuncture of the Cell-Membrane. *P Natl Acad Sci USA* 1987, 84 (12), 4180.
- (1284). Tirlapur UK; Konig K Targeted transfection by femtosecond laser. *Nature* 2002, 418 (6895), 290. [PubMed: 12124612]
- (1285). Guo YD; Liang H; Berns MW Laser-Mediated Gene-Transfer in Rice. *Physiol Plantarum* 1995, 93 (1), 19.
- (1286). Shirahata Y; Ohkohchi N; Itagak H; Satomi S New technique for gene transfection using laser irradiation. *J Invest Med* 2001, 49 (2), 184.
- (1287). Schneckenburger H; Hendinger A; Sailer R; Strauss WS; Schmitt M Laser-assisted optoporation of single cells. *J Biomed Opt* 2002, 7 (3), 410. [PubMed: 12175291]
- (1288). Mohanty SK; Sharma M; Gupta PK Laser-assisted microinjection into targeted animal cells. *Biotechnol Lett* 2003, 25 (11), 895. [PubMed: 12889802]
- (1289). Sagi S; Knoll T; Trojan L; Schaaf A; Alken P; Michel MS Gene delivery into prostate cancer cells by holmium laser application. *Prostate Cancer P D* 2003, 6 (2), 127.
- (1290). Clark IB; Hanania EG; Stevens J; Gallina M; Fieck A; Brandes R; Palsson BO; Koller MR Optoinjection for efficient targeted delivery of a broad range of compounds and macromolecules into diverse cell types. *J Biomed Opt* 2006, 11 (1).
- (1291). Tsampoula X; Garcés-Chavez V; Comrie M; Stevenson DJ; Agate B; Brown CTA; Gunn-Moore F; Dholakia K Femtosecond cellular transfection using a nondiffracting light beam. *Appl Phys Lett* 2007, 91 (5).
- (1292). He H; Kong SK; Lee RK; Suen YK; Chan KT Targeted photoporation and transfection in human HepG2 cells by a fiber femtosecond laser at 1554 nm. *Opt Lett* 2008, 33 (24), 2961. [PubMed: 19079506]
- (1293). Schinkel H; Jacobs P; Schillberg S; Wehner M Infrared picosecond laser for perforation of single plant cells. *Biotechnol Bioeng* 2008, 99 (1), 244. [PubMed: 17614330]
- (1294). Tsampoula X; Taguchi K; Cizmar T; Garcés-Chavez V; Ma N; Mohanty S; Mohanty K; Gunn-Moore F; Dholakia K Fibre based cellular transfection. *Optics express* 2008, 16 (21), 17007. [PubMed: 18852810]
- (1295). Uchugonova A; Konig K; Bueckle R; Isemann A; Tempea G Targeted transfection of stem cells with sub -20 femtosecond laser pulses. *Optics express* 2008, 16 (13), 9357. [PubMed: 18575499]
- (1296). Hosokawa Y; Iguchi S; Yasukuni R; Hiraki Y; Shukunami C; Masuhara H Gene delivery process in a single animal cell after femtosecond laser microinjection. *Appl Surf Sci* 2009, 255 (24), 9880.
- (1297). Antkowiak M; Torres-Mapa ML; Gunn-Moore F; Dholakia K Application of dynamic diffractive optics for enhanced femtosecond laser based cell transfection. *J Biophotonics* 2010, 3 (10-11), 696. [PubMed: 20583035]
- (1298). Mthunzi P; Dholakia K; Gunn -Moore F Phototransfection of mammalian cells using femtosecond laser pulses: optimization and applicability to stem cell differentiation. *J Biomed Opt* 2010, 15 (4).
- (1299). Torres-Mapa ML; Angus L; Ploschner M; Dholakia K; Gunn-Moore FJ Transient transfection of mammalian cells using a violet diode laser. *J Biomed Opt* 2010, 15 (4).

- (1300). Hosokawa Y; Ochi H; Iino T; Hiraoka A; Tanaka M Photoporation of Biomolecules into Single Cells in Living Vertebrate Embryos Induced by a Femtosecond Laser Amplifier. *Plos One* 2011, 6 (11).
- (1301). Soman P; Zhang WD; Umeda A; Zhang ZJ; Chen C Femtosecond Laser-Assisted Optoporation for Drug and Gene Delivery into Single Mammalian Cells. *J Biomed Nanotechnol* 2011, 7 (3), 334. [PubMed: 21830473]
- (1302). Antkowiak M; Torres-Mapa ML; Witts EC; Miles GB; Dholakia K; Gunn-Moore FJ Fast targeted gene transfection and optogenetic modification of single neurons using femtosecond laser irradiation. *Sci Rep- Uk* 2013, 3.
- (1303). Breunig HG; Uchugonova A; Batista A; Konig K High-Throughput Continuous Flow Femtosecond Laser-Assisted Cell Optoporation and Transfection. *Microscopy Research and Technique* 2014, 77 (12), 974. [PubMed: 25123087]
- (1304). Breunig HG; Uchugonova A; Batista A; Konig K Software -aided automatic laser optoporation and transfection of cells. *Sci Rep-Uk* 2015, 5.
- (1305). Uchugonova A; Breunig HG; Batista A; Konig K Optical reprogramming of human cells in an ultrashort femtosecond laser microfluidic transfection platform. *J Biophotonics* 2015.
- (1306). Dhakal K; Black B; Mohanty S Introduction of impermeable actin-staining molecules to mammalian cells by optoporation. *Sci Rep-Uk* 2014, 4.
- (1307). Stracke F; Rieman I; Konig K Optical nanoinjection of macromolecules into vital cells. *J Photoch Photobio B* 2005, 81 (3), 136.
- (1308). Torres-Mapa ML; Antkowiak M; Cizmarova H; Ferrier DEK; Dholakia K; Gunn -Moore FJ Integrated holographic system for all-optical manipulation of developing embryos. *Biomedical optics express* 2011, 2 (6), 1564. [PubMed: 21698019]
- (1309). Peng C; Palazzo RE; Wilke I Laser intensity dependence of femtosecond near-infrared optoinjection. *Physical Review E* 2007, 75 (4).
- (1310). Lei M; Xu HP; Yang H; Yao BL Femtosecond laser- assisted microinjection into living neurons. *J Neurosci Meth* 2008, 174 (2), 215.
- (1311). Marchington RF; Arita Y; Tsampoula X; Gunn-Moore FJ; Dholakia K Optical injection of mammalian cells using a microfluidic platform. *Biomedical optics express* 2010, 1 (2), 527. [PubMed: 21258487]
- (1312). Rendall HA; Marchington RF; Praveen BB; Bergmann G; Arita Y; Heisterkamp A; Gunn-Moore FJ; Dholakia K High -throughput optical injection of mammalian cells using a Bessel light beam. *Lab on a chip* 2012, 12 (22), 4816. [PubMed: 23007197]
- (1313). Rudhall AP; Antkowiak M; Tsampoula X; Mazilu M; Metzger NK; Gunn-Moore F; Dholakia K Exploring the ultrashort pulse laser parameter space for membrane permeabilisation in mammalian cells. *Sci Rep-Uk* 2012, 2.
- (1314). Foldes-Papp Z; Konig K; Studier H; Buckle R; Breunig HG; Uchugonova A; Kostner GM Trafficking of Mature miRNA-122 into the Nucleus of Live Liver Cells. *Curr Pharm Biotechno* 2009, 10 (6), 569.
- (1315). Roth CC; Barnes RA; Ibey BL; Glickman RD; Beier HT Short Infrared (IR) Laser Pulses Can Induce Nanoporation. *Clinical and Translational Neurophotonics; Neural Imaging and Sensing; and Optogenetics and Optical Manipulation* 2016, 9690.
- (1316). McDougall C; Stevenson DJ; Brown CTA; Gunn-Moore F; Dholakia K Targeted optical injection of gold nanoparticles into single mammalian cells. *J Biophotonics* 2009, 2 (12), 736. [PubMed: 19603388]
- (1317). Umanzor-Alvarez J; Wade EC; Gifford A; Nontapot K; Cruz-Reese A; Gotoh T; Sible JC; Khodaparast G Near-infrared laser delivery of nanoparticles to developing embryos: A study of efficacy and viability. *Biotechnology Journal* 2011, 6 (5), 519. [PubMed: 21381199]
- (1318). Waleed M; Hwang SU; Kim JD; Shabbir I; Shin SM; Lee YG Single-cell optoporation and transfection using femtosecond laser and optical tweezers. *Biomedical optics express* 2013, 4 (9), 1533. [PubMed: 24049675]
- (1319). Karande P; Jain A; Ergun K; Kispersky V; Mitragotri S Design principles of chemical penetration enhancers for transdermal drug delivery. *P Natl Acad Sci USA* 2005, 102 (13), 4688.

- (1320). Faizal A; Geelen D Saponins and their role in biological processes in plants. *Phytochem Rev* 2013, 12 (4), 877.
- (1321). Yu ZW; Quinn PJ The modulation of membrane structure and stability by dimethyl sulphoxide (Review). *Mol Membr Biol* 1998, 15 (2), 59. [PubMed: 9724923]
- (1322). Anchordoguy TJ; Carpenter JF; Crowe JH; Crowe LM Temperature-Dependent Perturbation of Phospholipid-Bilayers by Dimethylsulfoxide. *Biochimica et biophysica acta* 1992, 1104 (1), 117. [PubMed: 1550838]
- (1323). Gurtovenko AA; Anwar J Modulating the structure and properties of cell membranes: The molecular mechanism of action of dimethyl sulfoxide. *J Phys Chem B* 2007, 111 (35), 10453. [PubMed: 17661513]
- (1324). Hughes ZE; Mancera RL Molecular dynamics simulations of mixed DOPC-beta-sitosterol bilayers and their interactions with DMSO. *Soft Matter* 2013, 9 (10), 2920.
- (1325). Gurtovenko AA; Anwar J Interaction of Ethanol with Biological Membranes: The Formation of Non-bilayer Structures within the Membrane Interior and their Significance. *J Phys Chem B* 2009, 113 (7), 1983. [PubMed: 19199697]
- (1326). Holte LL; Gawrisch K Determining ethanol distribution in phospholipid multilayers with MAS-NOESY spectra. *Biochemistry* 1997, 36 (15), 4669. [PubMed: 9109678]
- (1327). Feller SE; Brown CA; Nizza DT; Gawrisch K Nuclear overhauser enhancement spectroscopy cross-relaxation rates and ethanol distribution across membranes. *Biophys J* 2002, 82 (3), 1396. [PubMed: 11867455]
- (1328). Ly HV; Longo ML The influence of short-chain alcohols on interfacial tension, mechanical properties, area/molecule, and permeability of fluid lipid bilayers. *Biophys J* 2004, 87 (2), 1013. [PubMed: 15298907]
- (1329). Dickey AN; Faller R How alcohol chain-length and concentration modulate hydrogen bond formation in a lipid bilayer. *Biophys J* 2007, 92 (7), 2366. [PubMed: 17218462]
- (1330). O'Dea S; Annibaldi V; Gallagher L; Mulholland J; Molloy EL; Breen CJ; Gilbert JL; Martin DS; Maguire M; Curry FR Vector-free intracellular delivery by reversible permeabilization. *Plos One* 2017, 12 (3), e0174779. [PubMed: 28358921]
- (1331). Jamur MC; Oliver C Permeabilization of Cell Membranes. *Immunocytochemical Methods and Protocols, Third Edition* 2010, 588, 63.
- (1332). Fernandez ML; Reigada R Effects of Dimethyl Sulfoxide on Lipid Membrane Electroporation. *J Phys Chem B* 2014, 118 (31), 9306. [PubMed: 25035931]
- (1333). Helenius A; Simons K Solubilization of Membranes by Detergents. *Biochimica et biophysica acta* 1975, 415 (1), 29. [PubMed: 1091302]
- (1334). Linke D Detergents: An Overview. *Guide to Protein Purification, Second Edition* 2009, 463, 603.
- (1335). Lichtenberg D; Ahyayauch H; Alonso A; Goni FM Detergent solubilization of lipid bilayers: a balance of driving forces. *Trends Biochem.Sci* 2013, 38 (2), 85. [PubMed: 23290685]
- (1336). Lorent JH; Quetin-Leclercq J; Mingeot-Leclercq MP The amphiphilic nature of saponins and their effects on artificial and biological membranes and potential consequences for red blood and cancer cells. *Org Biomol Chem* 2014, 12 (44), 8803. [PubMed: 25295776]
- (1337). Nazari M; Kurdi M; Heerklotz H Classifying Surfactants with Respect to Their Effect on Lipid Membrane Order. *Biophys J* 2012, 102 (3), 498. [PubMed: 22325272]
- (1338). Vaidyanathan S; Orr BG; Holl MMB Detergent Induction of HEK 293A Cell Membrane Permeability Measured under Quiescent and Superfusion Conditions Using Whole Cell Patch Clamp. *J Phys Chem B* 2014, 118 (8), 2112. [PubMed: 24548291]
- (1339). Koley D; Bard AJ Triton X-100 concentration effects on membrane permeability of a single HeLa cell by scanning electrochemical microscopy (SECM). *P Natl Acad Sci USA* 2010, 107 (39), 16783.
- (1340). Francis G; Kerem Z; Makkar HPS; Becker K The biological action of saponins in animal systems: a review. *Brit J Nutr* 2002, 88 (6), 587. [PubMed: 12493081]
- (1341). Papadopoulou K; Melton RE; Leggett M; Daniels MJ; Osbourn AE Compromised disease resistance in saponin-deficient plants. *P Natl Acad Sci USA* 1999, 96 (22), 12923.

- (1342). Podolak I; Galanty A; Sobolewska D Saponins as cytotoxic agents: a review. *Phytochem Rev* 2010, 9 (3), 425. [PubMed: 20835386]
- (1343). Sun HX; Xie Y; Ye YP Advances in saponin-based adjuvants. *Vaccine* 2009, 27 (12), 1787. [PubMed: 19208455]
- (1344). Fuchs H; Bachran D; Panjideh H; Schellmann N; Weng A; Melzig MF; Sutherland M; Bachran C Saponins as Tool for Improved Targeted Tumor Therapies. *Curr Drug Targets* 2009, 10 (2), 140. [PubMed: 19199910]
- (1345). Bangham AD; Glauert AM; Horne RW; Dingle JT; Lucy JA Action of Saponin on Biological Cell Membranes. *Nature* 1962, 196 (4858), 952. [PubMed: 13966357]
- (1346). Lepers A; Cacan R; Verbert A Permeabilized Cells as a Way of Gaining Access to Intracellular Organelles - an Approach to Glycosylation Reactions. *Biochimie* 1990, 72 (1), 1. [PubMed: 2160287]
- (1347). Keeney S; Linn S A Critical-Review of Permeabilized Cell Systems for Studying Mammalian DNA-Repair. *Mutat Res* 1990, 236 (2 -3), 239. [PubMed: 2119002]
- (1348). Elias PM; Friend DS; Goerke J Membrane Sterol Heterogeneity - Freeze-Fracture Detection with Saponins and Filipin. *J Histochem Cytochem* 1979, 27 (9), 1247. [PubMed: 479568]
- (1349). Frenkel N; Makky A; Sudji IR; Wink M; Tanaka M Mechanistic Investigation of Interactions between Steroidal Saponin Digitonin and Cell Membrane Models. *J Phys Chem B* 2014, 118 (50), 14632. [PubMed: 25412206]
- (1350). Gilbert-Oriol R; Mergel K; Thakur M; von Mallinckrodt B; Melzig MF; Fuchs H; Weng A Real-time analysis of membrane permeabilizing effects of oleanane saponins. *Biorgan Med Chem* 2013, 21 (8), 2387.
- (1351). Lorent J; Lins L; Domenech O; Quetin-Leclercq J; Brasseur R; Mingeot-Leclercq MP Domain Formation and Permeabilization Induced by the Saponin alpha-Hederin and Its Aglycone Hederagenin in a Cholesterol-Containing Bilayer. *Langmuir* 2014, 30 (16), 4556. [PubMed: 24690040]
- (1352). Lorent J; Le Duff CS; Quetin-Leclercq J; Mingeot-Leclercq MP Induction of Highly Curved Structures in Relation to Membrane Permeabilization and Budding by the Triterpenoid Saponins, alpha- and delta-Hederin. *J Biol Chem* 2013, 288 (20), 14000. [PubMed: 23530040]
- (1353). Li XX; Davis B; Haridas V; Gutterman JU; Colombini M Proapoptotic triterpene electrophiles (Avicins) form channels in membranes: Cholesterol dependence. *Biophys J* 2005, 88 (4), 2577. [PubMed: 15653745]
- (1354). Wakasugi H; Kimura T; Haase W; Kribben A; Kaufmann R; Schulz I Calcium-Uptake into Acini from Rat Pancreas - Evidence for Intracellular Atp-Dependent Calcium Sequestration. *J Membrane Biol* 1982, 65 (3), 205. [PubMed: 6801263]
- (1355). Dunn LA; Holz RW Catecholamine Secretion from Digitonin -Treated Adrenal-Medullary Chromaffin Cells. *J Biol Chem* 1983, 258 (8), 4989. [PubMed: 6833287]
- (1356). Authi KS; Evenden BJ; Crawford N Metabolic and Functional Consequences of Introducing Inositol 1,4,5-Trisphosphate into Saponin-Permeabilized Human-Platelets. *Biochem J* 1986, 233 (3), 707. [PubMed: 2939827]
- (1357). Weigel PH; Ray DA; Oka JA Quantitation of Intracellular Membrane-Bound Enzymes and Receptors in Digitonin-Permeabilized Cells. *Anal Biochem* 1983, 133 (2), 437. [PubMed: 6314844]
- (1358). Miyamoto K; Yamashita T; Tsukiyama T; Kitamura N; Minami N; Yamada M; Imai H Reversible Membrane Permeabilization of Mammalian Cells Treated with Digitonin and Its Use for Inducing Nuclear Reprogramming by Xenopus Egg Extracts. *Cloning Stem Cells* 2008, 10 (4), 535. [PubMed: 19049416]
- (1359). Lukyanenko V Permeabilization of cell membrane for delivery of nano -objects to cellular sub-domains. *Methods Mol Biol* 2013, 991, 57. [PubMed: 23546659]
- (1360). Jacob MC; Favre M; Bensa JC Membrane Cell Permeabilization with Saponin and Multiparametric Analysis by Flow-Cytometry. *Cytometry* 1991, 12 (6), 550. [PubMed: 1764979]
- (1361). Sander B; Andersson J; Andersson U Assessment of Cytokines by Immunofluorescence and the Paraformaldehyde-Saponin Procedure. *Immunol Rev* 1991, 119, 65. [PubMed: 2045123]

- (1362). Jung T; Schauer U; Heusser C; Neumann C; Rieger C Detection of Intracellular Cytokines by Flow-Cytometry. *J Immunol Methods* 1993, 159 (1–2), 197. [PubMed: 8445253]
- (1363). Pala P; Hussell T; Openshaw PJM Flow cytometric measurement of intracellular cytokines. *J Immunol Methods* 2000, 243 (1–2), 107. [PubMed: 10986410]
- (1364). Miller MR; Castellot JJ; Pardee AB General-Method for Permeabilizing Monolayer and Suspension Cultured Animal-Cells. *Exp Cell Res* 1979, 120 (2), 421. [PubMed: 436970]
- (1365). Balinska M; Samsonoff WA; Galivan J Reversibly permeable hepatoma cells in culture. *Biochimica et biophysica acta* 1982, 721 (3), 253. [PubMed: 7171628]
- (1366). Nomura S; Kamiya T; Oishi M A procedure to introduce protein molecules into living mammalian cells. *Exp Cell Res* 1986, 163 (2), 434. [PubMed: 2420621]
- (1367). Siwko ME; de Vries AH; Mark AE; Kozubek A; Marrink SJ Disturb or Stabilize? A Molecular Dynamics Study of the Effects of Resorcinolic Lipids on Phospholipid Bilayers. *Biophys J* 2009, 96 (8), 3140. [PubMed: 19383459]
- (1368). Esteban-Martin S; Risselada HJ; Salgado J; Marrink SJ Stability of Asymmetric Lipid Bilayers Assessed by Molecular Dynamics Simulations. *J Am Chem Soc* 2009, 131 (42), 15194. [PubMed: 19795891]
- (1369). Kilinc D; Peyrin JM; Soubeyre V; Magnifico S; Saias L; Viovy JL; Brugg B Wallerian-Like Degeneration of Central Neurons After Synchronized and Geometrically Registered Mass Axotomy in a Three-Compartmental Microfluidic Chip. *Neurotox Res* 2011, 19 (1), 149. [PubMed: 20162389]
- (1370). Lee CY; Romanova EV; Sweedler JV Laminar stream of detergents for subcellular neurite damage in a microfluidic device: a simple tool for the study of neuroregeneration. *J Neural Eng* 2013, 10 (3).
- (1371). Oftedal L; Myhren L; Jokela J; Gausdal G; Sivonen K; Doskeland SO; Herfindal L The lipopeptide toxins anabaenolysin A and B target biological membranes in a cholesterol - dependent manner. *Bba-Biomembranes* 2012, 1818 (12), 3000. [PubMed: 22842546]
- (1372). Zasloff M Antimicrobial peptides of multicellular organisms. *Nature* 2002, 415 (6870), 389. [PubMed: 11807545]
- (1373). Brogden KA Antimicrobial peptides: Pore formers or metabolic inhibitors in bacteria? *Nature Reviews Microbiology* 2005, 3 (3), 238. [PubMed: 15703760]
- (1374). Zhao XW; Wu HY; Lu HR; Li GD; Huang QS LAMP: A Database Linking Antimicrobial Peptides. *Plos One* 2013, 8 (6).
- (1375). Waghugh FH; Gopi L; Barai RS; Ramteke P; Nizami B; Idicula -Thomas S CAMP: Collection of sequences and structures of antimicrobial peptides. *Nucleic Acids Res* 2014, 42 (D1), D1154. [PubMed: 24265220]
- (1376). Bahar AA; Ren D Antimicrobial peptides. *Pharmaceuticals (Basel)* 2013, 6 (12), 1543. [PubMed: 24287494]
- (1377). Wimley WC Describing the Mechanism of Antimicrobial Peptide Action with the Interfacial Activity Model. *Acs Chemical Biology* 2010, 5 (10), 905. [PubMed: 20698568]
- (1378). Huang HW Action of antimicrobial peptides: Two-state model. *Biochemistry* 2000, 39 (29), 8347. [PubMed: 10913240]
- (1379). Raghuraman H; Chattopadhyay A Melittin: A membrane-active peptide with diverse functions. *Bioscience reports* 2007, 27 (4 –5), 189. [PubMed: 17139559]
- (1380). Ladokhin AS; Selsted ME; White SH Sizing membrane pores in lipid vesicles by leakage of co-encapsulated markers: Pore formation by melittin. *Biophys J* 1997, 72 (4), 1762. [PubMed: 9083680]
- (1381). Lee MT; Hung WC; Chen FY; Huang HW Mechanism and kinetics of pore formation in membranes by water-soluble amphipathic peptides. *P Natl Acad Sci USA* 2008, 105 (13), 5087.
- (1382). Lee MT; Sun TL; Hung WC; Huang HW Process of inducing pores in membranes by melittin. *P Natl Acad Sci USA* 2013, 110 (35), 14243.
- (1383). Tamba Y; Yamazaki M Magainin 2-Induced Pore Formation in the Lipid Membranes Depends on Its Concentration in the Membrane Interface. *J Phys Chem B* 2009, 113 (14), 4846. [PubMed: 19267489]

- (1384). Tamba Y; Ariyama H; Levadny V; Yamazaki M Kinetic Pathway of Antimicrobial Peptide Magainin 2-Induced Pore Formation in Lipid Membranes. *J Phys Chem B* 2010, 114 (37), 12018. [PubMed: 20799752]
- (1385). Gregory SM; Pokorny A; Almeida PFF Magainin 2 Revisited: A Test of the Quantitative Model for the All-or-None Permeabilization of Phospholipid Vesicles. *Biophys J* 2009, 96 (1), 116. [PubMed: 19134472]
- (1386). Lee CC; Sun Y; Qian S; Huang HW Transmembrane Pores Formed by Human Antimicrobial Peptide LL-37. *Biophys J* 2011, 100 (7), 1688. [PubMed: 21463582]
- (1387). Patel H; Huynh Q; Barlehner D; Heerklotz H Additive and synergistic membrane permeabilization by antimicrobial (lipo)peptides and detergents. *Biophys J* 2014, 106 (10), 2115. [PubMed: 24853740]
- (1388). Rakowska PD; Jiang HB; Ray S; Pyne A; Lamarre B; Carr M; Judge PJ; Ravi J; Gerling UIM; Koksche B et al. Nanoscale imaging reveals laterally expanding antimicrobial pores in lipid bilayers. *P Natl Acad Sci USA* 2013, 110 (22), 8918.
- (1389). Sengupta D; Leontiadou H; Mark AE; Marrink SJ Toroidal pores formed by antimicrobial peptides show significant disorder. *Bba-Biomembranes* 2008, 1778 (10), 2308. [PubMed: 18602889]
- (1390). Binder H; Lindblom G Charge-dependent translocation of the Trojan peptide penetratin across lipid membranes. *Biophys J* 2003, 85 (2), 982. [PubMed: 12885645]
- (1391). Miteva M; Andersson M; Karshikoff A; Otting G Molecular electroporation: a unifying concept for the description of membrane pore formation by antibacterial peptides, exemplified with NK-lysin. *Febs Letters* 1999, 462 (1–2), 155. [PubMed: 10580110]
- (1392). Gurtovenko AA; Vattulainen I Pore formation coupled to ion transport through lipid membranes as induced by transmembrane ionic charge imbalance: Atomistic molecular dynamics study. *J Am Chem Soc* 2005, 127 (50), 17570. [PubMed: 16351063]
- (1393). Leontiadou H; Mark AE; Marrink SJ Antimicrobial peptides in action. *J Am Chem Soc* 2006, 128 (37), 12156. [PubMed: 16967965]
- (1394). Jean-Francois F; Elezgaray J; Berson P; Vacher P; Dufourc EJ Pore Formation Induced by an Antimicrobial Peptide: Electrostatic Effects. *Biophys J* 2008, 95 (12), 5748. [PubMed: 18820233]
- (1395). Herce HD; Garcia AE Molecular dynamics simulations suggest a mechanism for translocation of the HIV-1 TAT peptide across lipid membranes. *P Natl Acad Sci USA* 2007, 104 (52), 20805.
- (1396). Last NB; Miranker AD Common mechanism unites membrane poration by amyloid and antimicrobial peptides. *P Natl Acad Sci USA* 2013, 110 (16), 6382.
- (1397). Lee MT; Chen FY; Huang HW Energetics of pore formation induced by membrane active peptides. *Biochemistry* 2004, 43 (12), 3590. [PubMed: 15035629]
- (1398). Gregory SM; Cavanaugh A; Journigan V; Pokorny A; Almeida PFF A quantitative model for the all-or-none permeabilization of phospholipid vesicles by the antimicrobial peptide cecropin A. *Biophys J* 2008, 94 (5), 1667. [PubMed: 17921201]
- (1399). Wang YK; Ulmschneider JP; Zhao SD How Reliable are Molecular Dynamics Simulations of Membrane Active Antimicrobial Peptides. *Biophys J* 2015, 108 (2), 78a.
- (1400). Henriques ST; Melo MN; Castanho MARB Cell-penetrating peptides and antimicrobial peptides: how different are they? *Biochem J* 2006, 399, 1. [PubMed: 16956326]
- (1401). Plank C; Zauner W; Wagner E Application of membrane-active peptides for drug and gene delivery across cellular membranes. *Adv Drug Deliver Rev* 1998, 34 (1), 21.
- (1402). Ferrer-Miralles N; Vazquez E; Villaverde A Membrane-active peptides for non-viral gene therapy: making the safest easier. *Trends Biotechnol* 2008, 26 (5), 267. [PubMed: 18358551]
- (1403). Czajkowsky DM; Hotze EM; Shao ZF; Tweten RK Vertical collapse of a cytolysin prepore moves its transmembrane beta-hairpins to the membrane. *Embo J* 2004, 23 (16), 3206. [PubMed: 15297878]
- (1404). Hodel AW; Leung C; Dudkina NV; Saibil HR; Hoogenboom BW Atomic force microscopy of membrane pore formation by cholesterol dependent cytolysins. *Curr Opin Struct Biol* 2016, 39, 8. [PubMed: 27062575]

- (1405). Ahnerthilger G; Mach W; Fohr KJ; Gratzl M Poration by Alpha-Toxin and Streptolysin-O - an Approach to Analyze Intracellular Processes. *Methods in Cell Biology* 1989, 31, 63. [PubMed: 2779453]
- (1406). Wendland M; Subramani S Cytosol-Dependent Peroxisomal Protein Import in a Permeabilized Cell System. *J Cell Biol* 1993, 120 (3), 675. [PubMed: 8425896]
- (1407). Barry ELR; Gesek FA; Friedman PA Introduction of Antisense Oligonucleotides into Cells by Permeabilization with Streptolysin-O. *Biotechniques* 1993, 15 (6), 1016. [PubMed: 8292333]
- (1408). Harvey AN; Costa ND; Savage JRK Electroporation and Streptolysin-O - a Comparison of Poration Techniques. *Mutat Res* 1994, 315 (1), 17. [PubMed: 7517006]
- (1409). Fawcett JM; Harrison SM; Orchard CH A method for reversible permeabilization of isolated rat ventricular myocytes. *Exp Physiol* 1998, 83 (3), 293. [PubMed: 9639340]
- (1410). Ogino S; Kubo S; Umemoto R; Huang SX; Nishida N; Shimada I Observation of NMR Signals from Proteins Introduced into Living Mammalian Cells by Reversible Membrane Permeabilization Using a Pore-Forming Toxin, Streptolysin O. *J Am Chem Soc* 2009, 131 (31), 10834. [PubMed: 19603816]
- (1411). Ma X; Zhou P; Wong SW; Warner M; Chaulagain C; Comenzo RL siRNA targeting the kappa light chain constant region: preclinical testing of an approach to nonfibrillar and fibrillar light chain deposition diseases. *Gene Ther* 2016, 23 (10), 727. [PubMed: 27383253]
- (1412). Spiller DG; Tidd DM Nuclear Delivery of Antisense Oligodeoxynucleotides through Reversible Permeabilization of Human Leukemia-Cells with Streptolysin-O. *Antisense Res Dev* 1995, 5 (1), 13. [PubMed: 7613071]
- (1413). Broughton CM; Spiller DG; Pender N; Komorovskaya M; Grzybowski J; Giles RV; Tidd DM; Clark RE Preclinical studies of streptolysin-O in enhancing antisense oligonucleotide uptake in harvests from chronic myeloid leukaemia patients. *Leukemia* 1997, 11 (9), 1435. [PubMed: 9305594]
- (1414). Giles RV; Grzybowski J; Spiller DG; Tidd DM Enhanced antisense effects resulting from an improved streptolysin-O protocol for oligodeoxynucleotide delivery into human leukaemia cells. *Nucleos Nucleot* 1997, 16 (7-9), 1155.
- (1415). Giles RV; Spiller DG; Clark RE; Tidd DM C-MYC antisense morpholino oligonucleotide analogue induces mis-splicing of mRNA in living cells. *Blood* 1998, 92 (10), 244b.
- (1416). Giles RV; Spiller DG; Grzybowski J; Clark RE; Tidd DM Selecting optimal oligonucleotide composition for maximal antisense effect following streptolysin O-mediated delivery into human leukaemia cells. *Nucleic Acids Res* 1998, 26 (7), 1567. [PubMed: 9512525]
- (1417). Clark RE; Grzybowski J; Broughton CM; Pender NT; Spiller DG; Brammer CG; Giles RV; Tidd DM Clinical use of streptolysin-O to facilitate antisense oligodeoxyribonucleotide delivery for purging autografts in chronic myeloid leukaemia. *Bone Marrow Transplant* 1999, 23 (12), 1303. [PubMed: 10414920]
- (1418). Giles RV; Spiller DG; Clark RE; Tidd DM Antisense morpholino oligonucleotide analog induces missplicing of c-myc mRNA. *Antisense Nucleic A* 1999, 9 (2), 213.
- (1419). Giles RV; Spiller DG; Tidd DM Chimeric oligodeoxynucleotide analogs: Chemical synthesis, purification, and molecular and cellular biology protocols. *Antisense Technology, Pt A* 2000, 313, 95.
- (1420). Lin YP; Ma WL; Benchimol S Pidd, a new death-domain -containing protein, is induced by p53 and promotes apoptosis. *Nat Genet* 2000, 26 (1), 122. [PubMed: 10973264]
- (1421). Faria M; Spiller DG; Dubertret C; Nelson JS; White MRH; Scherman D; Helene C; Giovannangeli C Phosphoramidate oligonucleotides as potent antisense molecules in cells and in vivo. *Nat Biotechnol* 2001, 19 (1), 40. [PubMed: 11135550]
- (1422). Wu JR; Berland KM Comparing the intracellular mobility of fluorescent proteins following in vitro expression or cell loading with streptolysin-O. *J Biomed Opt* 2008, 13 (3).
- (1423). Nagahama M; Ohkubo A; Oda M; Kobayashi K; Amimoto K; Miyamoto K; Sakurai J *Clostridium perfringens* TpeL Glycosylates the Rac and Ras Subfamily Proteins. *Infection and Immunity* 2011, 79 (2), 905. [PubMed: 21098103]
- (1424). Teng KW; Ishitsuka Y; Ren P; Youn YA; Deng X; Ge PH; Belmont AS; Selvin PR Labeling proteins inside living cells using external fluorophores for microscopy. *Elife* 2016, 5.

- (1425). Fu HM; Ding J; Flutter B; Gao B Investigation of endogenous antigen processing by delivery of an intact protein into cells. *J Immunol Methods* 2008, 335 (1–2), 90. [PubMed: 18406420]
- (1426). Bekei B; Rose HM; Herzig M; Selenko P In-cell NMR in mammalian cells: part 2. *Methods Mol Biol* 2012, 895, 55. [PubMed: 22760312]
- (1427). Hakelien AM; Landsverk HB; Robl JM; Skalhegg BS; Collas P Reprogramming fibroblasts to express T-cell functions using cell extracts. *Nat Biotechnol* 2002, 20 (5), 460. [PubMed: 11981558]
- (1428). Hakelien AM; Gaustad KG; Collas P Transient alteration of cell fate using a nuclear and cytoplasmic extract of an insulinoma cell line. *Biochem Bioph Res Co* 2004, 316 (3), 834.
- (1429). Taranger CK; Noer A; Sorensen AL; Hakelien AM; Boquest AC; Collas P Induction of dedifferentiation, genomewide transcriptional programming, and epigenetic reprogramming by extracts of carcinoma and embryonic stem cells. *Mol Biol Cell* 2005, 16 (12), 5719. [PubMed: 16195347]
- (1430). Håkelién A-M; Gaustad KG; Collas P In Nuclear Reprogramming: Methods and Protocols ; Pells S, Ed.; Humana Press: Totowa, NJ, 2006.
- (1431). Neri T; Monti M; Rebuzzini P; Merico V; Garagna S; Redi CA; Zuccott M Mouse fibroblasts are reprogrammed to Oct -4 and Rex -1 gene expression and alkaline phosphatase activity by embryonic stem cell extracts. *Cloning Stem Cells* 2007, 9 (3), 394. [PubMed: 17907950]
- (1432). Miyamoto K; Furusawa T; Ohnuki M; Goel S; Tokunaga T; Minami N; Yamada M; Ohsumi K; Imai H Reprogramming events of mammalian somatic cells induced by *Xenopus laevis* egg extracts. *Mol Reprod Dev* 2007, 74 (10), 1268. [PubMed: 17474094]
- (1433). Bui HT; Wakayama S; Kishigami S; Kim JH; Van Thuan N; Wakayama T The cytoplasm of mouse germinal vesicle stage oocytes can enhance somatic cell nuclear reprogramming. *Development* 2008, 135 (23), 3935. [PubMed: 18997114]
- (1434). Singhal N; Graumann J; Wu GM; Arauzo-Bravo MJ; Han DW; Greber B; Gentile L; Mann M; Scholer HR Chromatin-Remodeling Components of the BAF Complex Facilitate Reprogramming. *Cell* 2010, 141 (6), 943. [PubMed: 20550931]
- (1435). Zhan WJ; Liu ZP; Liu Y; Ke QC; Ding YY; Lu XY; Wang ZC Modulation of rabbit corneal epithelial cells fate using embryonic stem cell extract. *Mol Vis* 2010, 16(128–29), 1154. [PubMed: 20664691]
- (1436). Cho HJ; Lee CS; Kwon YW; Paek JS; Lee SH; Hur J; Lee EJ; Roh TY; Chu IS; Leem SH et al. Induction of pluripotent stem cells from adult somatic cells by protein -based reprogramming without genetic manipulation. *Blood* 2010, 116 (3), 386. [PubMed: 20439621]
- (1437). Han JN; Sachdev PS; Sidhu KS A Combined Epigenetic and Non-Genetic Approach for Reprogramming Human Somatic Cells. *Plos One* 2010, 5 (8).
- (1438). Ganier O; Brocquet S; Peiffer I; Brochard V; Arnaud P; Puy A; Jouneau A; Feil R; Renard JP; Mechali M Synergic reprogramming of mammalian cells by combined exposure to mitotic *Xenopus* egg extracts and transcription factors. *P Natl Acad Sci USA* 2011, 108 (42), 17331.
- (1439). Ostrup O; Hyttel P; Klaerke DA; Collas P Remodeling of ribosomal genes in somatic cells by *Xenopus* egg extract. *Biochem Bioph Res Co* 2011, 412 (3), 487.
- (1440). Bui HT; Kwon DN; Kang MH; Oh MH; Park MR; Park WJ; Paik SS; Thuan NV; Kim JH Epigenetic reprogramming in somatic cells induced by extract from germinal vesicle stage pig oocytes. *Development* 2012, 139 (23), 4330. [PubMed: 23132243]
- (1441). Rathbone AJ; Liddell S; Campbell KHS Proteomic Analysis of Early Reprogramming Events in Murine Somatic Cells Incubated with *Xenopus laevis* Oocyte Extracts Demonstrates Network Associations with Induced Pluripotency Markers. *Cell Reprogram* 2013, 15 (4), 269. [PubMed: 23768116]
- (1442). Xiong XR; Lan DL; Li J; Zi XD; Ma L; Wang Y Cellular Extract Facilitates Nuclear Reprogramming by Altering DNA Methylation and Pluripotency Gene Expression. *Cell Reprogram* 2014, 16 (3), 215. [PubMed: 24738992]
- (1443). Faruqi AF; Egholm M; Glazer PM Peptide nucleic acid-targeted mutagenesis of a chromosomal gene in mouse cells. *P Natl Acad Sci USA* 1998, 95 (4), 1398.
- (1444). Boutimah-Hamoudi F; Leforestier E; Senamaud-Beaufort C; Nielsen PE; Giovannangeli C; Saison -Behmoaras TE Cellular antisense activity of peptide nucleic acid (PNAs) targeted to

- HIV-1 polypurine tract (PPT) containing RNA. *Nucleic Acids Res* 2007, 35 (12), 3907. [PubMed: 17537815]
- (1445). Kummer S; Knoll A; Socher E; Bethge L; Herrmann A; Seitz O Fluorescence Imaging of Influenza H1N1 mRNA in Living Infected Cells Using Single-Chromophore FIT-PNA. *Angew Chem Int Edit* 2011, 50 (8), 1931.
- (1446). Paillasson S; vandeCorput M; Dirks RW; Tanke HJ; RobertNicoud M; Ronot X In situ hybridization in living cells: Detection of RNA molecules. *Exp Cell Res* 1997, 231 (1), 226. [PubMed: 9056430]
- (1447). Santangelo PJ; Nix B; Tsourkas A; Bao G Dual FRET molecular beacons for mRNA detection in living cells. *Nucleic Acids Res* 2004, 32 (6), e57. [PubMed: 15084672]
- (1448). Santangelo PJ; Nitin N; Bao G Direct visualization of mRNA colocalization with mitochondria in living cells using molecular beacons. *J Biomed Opt* 2005, 10 (4).
- (1449). Santangelo P; Nitin N; LaConte L; Woolums A; Bao G Live-cell characterization and analysis of a clinical isolate of bovine respiratory syncytial virus, using molecular beacons. *J Virol* 2006, 80 (2), 682. [PubMed: 16378971]
- (1450). Abe H; Kool ET Flow cytometric detection of specific RNAs in native human cells with quenched autoligating FRET probes. *P Natl Acad Sci USA* 2006, 103 (2), 263.
- (1451). Santangelo PJ; Bao G Dynamics of filamentous viral RNPs prior to egress. *Nucleic Acids Res* 2007, 35 (11), 3602. [PubMed: 17485480]
- (1452). Rhee WJ; Santangelo PJ; Jo HJ; Bao G Target accessibility and signal specificity in live-cell detection of BMP-4 mRNA using molecular beacons. *Nucleic Acids Res* 2008, 36 (5).
- (1453). Arian D; Clo E; Gothelf KV; Mokhir A A Nucleic Acid Dependent Chemical Photocatalysis in Live Human Cells. *Chem-Eur J* 2010, 16 (1), 288. [PubMed: 19894234]
- (1454). Schatter B; Walev I; Klein J Mitogenic effects of phospholipase D and phosphatidic acid in transiently permeabilized astrocytes: effects of ethanol. *J Neurochem* 2003, 87 (1), 95. [PubMed: 12969256]
- (1455). Furukawa K; Abe H; Hibino K; Sako Y; Tsuneda S; Ito Y Reduction-Triggered Fluorescent Amplification Probe for the Detection of Endogenous RNAs in Living Human Cells. *Bioconjugate Chem* 2009, 20 (5), 1026.
- (1456). Lifland AW; Zurla C; Santangelo PJ Single Molecule Sensitive Multivalent Polyethylene Glycol Probes for RNA Imaging. *Bioconjugate Chem* 2010, 21 (3), 483.
- (1457). Liang Y; Zhang ZP; Wei HP; Hu QX; Deng JY; Guo DY; Cui ZQ; Zhang XE Aptamer beacons for visualization of endogenous protein HIV-1 reverse transcriptase in living cells. *Biosensors & bioelectronics* 2011, 28 (1), 270. [PubMed: 21824761]
- (1458). Rajapakse HE; Miller LW Time-Resolved Luminescence Resonance Energy Transfer Imaging of Protein-Protein Interactions in Living Cells. *Methods in Enzymology, Vol 505: Imaging and Spectroscopic Analysis of Living Cells* 2012, 505, 329.
- (1459). Levy R; Shaheen U; Cesbron Y; See V Gold nanoparticles delivery in mammalian live cells: a critical review. *Nano Rev* 2010, 1.
- (1460). Provoda CJ; Lee KD Bacterial pore-forming hemolysins and their use in the cytosolic delivery of macromolecules. *Adv Drug Deliver Rev* 2000, 41 (2), 209.
- (1461). Provoda CJ; Stier EM; Lee KD Tumor cell killing enabled by listeriolysin O -liposome-mediated delivery of the protein toxin gelonin. *J Biol Chem* 2003, 278 (37), 35102. [PubMed: 12832408]
- (1462). Thiery J; Lieberman J Perforin: a key pore-forming protein for immune control of viruses and cancer. *Sub-cellular biochemistry* 2014, 80, 197. [PubMed: 24798013]
- (1463). Thiery J; Keefe D; Boulant S; Boucrot E; Walch M; Martinvalet D; Goping IS; Bleackley RC; Kirchhausen T; Lieberman J Perforin pores in the endosomal membrane trigger the release of endocytosed granzyme B into the cytosol of target cells. *Nat Immunol* 2011, 12 (8), 770. [PubMed: 21685908]
- (1464). Luisoni S; Suomalainen M; Boucke K; Tanner LB; Wenk MR; Guan XL; Grzybek M; Coskun U; Greber UF Co-option of Membrane Wounding Enables Virus Penetration into Cells. *Cell Host Microbe* 2015, 18 (1), 75. [PubMed: 26159720]

- (1465). Rabideau AE; Liao XL; Akcay G; Pentelute BL Translocation of Non-Canonical Polypeptides into Cells Using Protective Antigen. *Sci Rep-Uk* 2015, 5 .
- (1466). Dingjan I; Verboogen DR; Paardekoooper LM; Revelo NH; Sittig SP; Visser LJ; Mollard GF; Henriet SS; Figdor CG; Ter Beest Met al. Lipid peroxidation causes endosomal antigen release for cross-presentation. *Sci Rep* 2016, 6, 22064. [PubMed: 26907999]
- (1467). Jurkiewicz P; Olzynska A; Cwiklik L; Conte E; Jungwirth P; Megli FM; Hof M Biophysics of lipid bilayers containing oxidatively modified phospholipids: Insights from fluorescence and EPR experiments and from MD simulations. *Bba-Biomembranes* 2012, 1818 (10), 2388. [PubMed: 22634274]
- (1468). Itri R; Junqueira HC; Mertins O; Baptista MS Membrane changes under oxidative stress: the impact of oxidized lipids. *Biophysical Reviews* 2014, 6 (1), 47. [PubMed: 28509959]
- (1469). Schomaker M; Heinemann D; Kalies S; Willenbrock S; Wagner S; Nolte I; Ripken T; Escobar HM; Meyer H; Heisterkamp A Characterization of nanoparticle mediated laser transfection by femtosecond laser pulses for applications in molecular medicine. *J Nanobiotechnol* 2015, 13.
- (1470). Gomperts BD Involvement of Guanine Nucleotide-Binding Protein in the Gating of Ca-2+ by Receptors. *Nature* 1983, 306 (5938), 64. [PubMed: 6195532]
- (1471). Gomperts BD; Fernandez JM Techniques for Membrane Permeabilization. *Trends Biochem.Sci* 1985, 10 (11), 414.
- (1472). Steinberg TH; Newman AS; Swanson JA; Silverstein SC Atp4- P ermeabilizes the Plasma-Membrane of Mouse Macrophages to Fluorescent Dyes. *J Biol Chem* 1987, 262 (18), 8884. [PubMed: 3597398]
- (1473). Elliott GD; Liu XH; Cusick JL; Menze M; Vincent J; Witt T; Hand S; Toner M Trehalose uptake through P2X(7) purinergic channels provides dehydration protection. *Cryobiology* 2006, 52 (1), 114. [PubMed: 16338230]
- (1474). Reuss R; Ludwig J; Shirakashi R; Ehrhart F; Zimmermann H; Schneider S; Weber MM; Zimmermann U; Schneider H; Sukhorukov VL Intracellular delivery of carbohydrates into mammalian cells through swelling-activated pathways. *J Membrane Biol* 2004, 200 (2), 67. [PubMed: 15520905]
- (1475). Sukhorukov VL; Imes D; Woellhaf MW; Andronic J; Kiesel M; Shirakashi R; Zimmermann U; Zimmermann H Pore size of swelling-activated channels for organic osmolytes in Jurkat lymphocytes, probed by differential polymer exclusion. *Bba-Biomembranes* 2009, 1788 (9), 1841. [PubMed: 19560440]
- (1476). Andronic J; Shirakashi R; Pickel SU; Westerling KM; Klein T; Holm T; Sauer M; Sukhorukov VL Hypotonic Activation of the Myo-Inositol Transporter SLC5A3 in HEK293 Cells Probed by Cell Volumetry, Confocal and Super-Resolution Microscopy. *Plos One* 2015, 10 (3).
- (1477). Russo MJ; Bayley H; Toner M Reversible permeabilization of plasma membranes with an engineered switchable pore. *Nat Biotechnol* 1997, 15 (3), 278. [PubMed: 9062930]
- (1478). Bayley H; Jayasinghe L Functional engineered channels and pores - (Review). *Mol Membr Biol* 2004, 21 (4), 209. [PubMed: 15371010]
- (1479). Bonardi F; Nouwen N; Feringa BL; Driessen AJM Protein conducting channels-mechanisms, structures and applications. *Mol Biosyst* 2012, 8 (3), 709. [PubMed: 22258412]
- (1480). Kocer A; Walko M; Meijberg W; Feringa BL A light-actuated nanovalve derived from a channel protein. *Science* 2005, 309 (5735), 755. [PubMed: 16051792]
- (1481). Boyden ES; Zhang F; Bamberg E; Nagel G; Deisseroth K Millisecond-timescale, genetically targeted optical control of neural activity. *Nat Neurosci* 2005, 8 (9), 1263. [PubMed: 16116447]
- (1482). Doerner JF; Febvay S; Clapham DE Controlled delivery of bioactive molecules into live cells using the bacterial mechanosensitive channel MscL. *Nat Commun* 2012, 3.
- (1483). Langecker M; Arnaut V; Martin TG; List J; Renner S; Mayer M; Dietz H; Simmel FC Synthetic Lipid Membrane Channels Formed by Designed DNA Nanostructures. *Science* 2012, 338 (6109), 932. [PubMed: 23161995]
- (1484). Geng J; Kim K; Zhang J; Escalada A; Tunuguntla R; Comolli LR; Allen FI; Shnyrova AV; Cho KR; Munoz Det al. Stochastic transport through carbon nanotubes in lipid bilayers and live cell membranes. *Nature* 2014, 514 (7524), 612. [PubMed: 25355362]

- (1485). Garcia-Lopez V; Chen F; Nilewski LG; Duret G; Aliyan A; Kolomeisky AB; Robinson JT; Wang G; Pal R; Tour JM Molecular machines open cell membranes. *Nature* 2017, 548 (7669), 567. [PubMed: 28858304]
- (1486). Evans E; Heinrich V; Rawicz W Using dynamic tension Spectroscopy to explore destabilization of membranes by antimicrobial peptides. *Biophys J* 2004, 86 (1), 330a.
- (1487). Jaenisch R; Mintz B Simian Virus 40 DNA Sequences in DNA of Healthy Adult Mice Derived from Preimplantation Blastocysts Injected with Viral DNA. *P Natl Acad Sci USA* 1974, 71 (4), 1250.
- (1488). Kreis TE; Geiger B; Schmid E; Jorcano JL; Franke WW De novo synthesis and specific assembly of keratin filaments in nonepithelial cells after microinjection of mRNA for epidermal keratin. *Cell* 1983, 32 (4), 1125. [PubMed: 6188536]
- (1489). Kreis TE; Birchmeier W Microinjection of fluorescently labeled proteins into living cells with emphasis on cytoskeletal proteins. *Int Rev Cytol* 1982, 75, 209. [PubMed: 6809685]
- (1490). Klymkowsky MW Intermediate filaments in 3T3 cells collapse after intracellular injection of a monoclonal anti-intermediate filament antibody. *Nature* 1981, 291 (5812), 249. [PubMed: 6785655]
- (1491). Wehland J; Osborn M; Weber K Phalloidin-induced actin polymerization in the cytoplasm of cultured cells interferes with cell locomotion and growth. *Proc Natl Acad Sci U S A* 1977, 74 (12), 5613. [PubMed: 341163]
- (1492). Paine PL; Moore LC; Horowitz SB Nuclear-Envelope Permeability. *Nature* 1975, 254 (5496), 109. [PubMed: 1117994]
- (1493). Eroglu A; Toner M; Toth TL Beneficial effect of microinjected trehalose on the cryosurvival of human oocytes. *Fertil Steril* 2002, 77 (1), 152. [PubMed: 11779606]
- (1494). Dubertret B; Skourides P; Norris DJ; Noireaux V; Brivanlou AH; Libchaber A In vivo imaging of quantum dots encapsulated in phospholipid micelles. *Science* 2002, 298 (5599), 1759. [PubMed: 12459582]
- (1495). Rieger S; Kulkarni RP; Darcy D; Fraser SE; Koster RW Quantum dots are powerful multipurpose vital labeling agents in zebrafish embryos. *Dev Dyn* 2005, 234 (3), 670. [PubMed: 16110511]
- (1496). Koike S; Jahn R Probing and manipulating intracellular membrane traffic by microinjection of artificial vesicles. *Proceedings of the National Academy of Sciences* 2017.
- (1497). Adams RJ; Bray D Rapid transport of foreign particles microinjected into crab axons 1983, 303, 718.
- (1498). Beckerle MC Microinjected fluorescent polystyrene beads exhibit saltatory motion in tissue culture cells. *J Cell Biol* 1984, 98 (6), 2126. [PubMed: 6373791]
- (1499). Zhang Y; Liang Z; Zong Y; Wang YP; Liu JX; Chen KL; Qiu JL; Gao CX Efficient and transgene-free genome editing in wheat through transient expression of CRISPR/Cas9 DNA or RNA. *Nat Commun* 2016, 7.
- (1500). O'Brien JA; Lummis SCR Diolistics: incorporating fluorescent dyes into biological samples using a gene gun. *Trends Biotechnol* 2007, 25 (11), 530. [PubMed: 17945370]
- (1501). Webster A; Coupland P; Houghton FD; Leese HJ; Aylott JW The delivery of PEBBLE nanosensors to measure the intracellular environment. *Biochem Soc T* 2007, 35, 538.
- (1502). Sessions JW; Skousen CS; Price KD; Hanks BW; Hope S; Alder JK; Jensen BD CRISPR-Cas9 directed knock-out of a constitutively expressed gene using lance array nano-injection. *Springerplus* 2016, 5.
- (1503). Stein DA; Skilling DE; Iversen PL; Smith AW Inhibition of vesivirus infections in mammalian tissue culture with antisense morpholino oligomers. *Antisense Nucleic A* 2001, 11 (5), 317.
- (1504). Amantana A; London CA; Iversen PL; Devi GR X-linked inhibitor of apoptosis protein inhibition induces apoptosis and enhances chemotherapy sensitivity in human prostate cancer cells. *Mol Cancer Ther* 2004, 3 (6), 699. [PubMed: 15210856]
- (1505). Neuman BW; Stein DA; Kroeker AD; Paulino AD; Moulton HM; Iversen PL; Buchmeier MJ Antisense morpholino-oligomers directed against the 5' end of the genome inhibit coronavirus proliferation and growth. *J Virol* 2004, 78 (11), 5891. [PubMed: 15140987]

- (1506). Seksek O; Biwersi J; Verkman AS Translational diffusion of macromolecule-sized solutes in cytoplasm and nucleus. *J Cell Biol* 1997, 138 (1), 131. [PubMed: 9214387]
- (1507). Dirks RW; Molenaar C; Tanke HJ Methods for visualizing RNA processing and transport pathways in living cells. *Histochem Cell Biol* 2001, 115 (1), 3. [PubMed: 11219605]
- (1508). Kollmannsperger A; Sharei A; Raulf A; Heilemann M; Langer R; Jensen KF; Wieneke R; Tampe R Live-cell protein labelling with nanometre precision by cell squeezing. *Nat Commun* 2016, 7.
- (1509). Li J; Wang B; Juba BM; Vazquez M; Kortum SW; Pierce BS; Pacheco M; Roberts L; Strohbach JW; Jones LH et al. Microfluidic-enabled intracellular delivery of membrane impermeable inhibitors to study target engagement in human primary cells. *ACS Chemical Biology* 2017.
- (1510). Geddes DM; Cargill RS; LaPlaca MC Mechanical stretch to neurons results in a strain rate and magnitude-dependent increase in plasma membrane permeability. *J Neurotraum* 2003, 20 (10), 1039.
- (1511). Zhang Z; Wang Y; Zhang H; Tang Z; Liu W; Lu Y; Wang Z; Yang H; Pang W; Zhang H et al. Hypersonic Poration: A New Versatile Cell Poration Method to Enhance Cellular Uptake Using a Piezoelectric Nano-Electromechanical Device. *Small* 2017.
- (1512). Terakawa M; Sato S; Ashida H; Aizawa K; Uenoyama M; Masaki Y; Obara M In vitro gene transfer to mammalian cells by the use of laser-induced stress waves: effects of stress wave parameters, ambient temperature, and cell type. *J Biomed Opt* 2006, 11 (1).
- (1513). Magana-Ortiz D; Coconi-Linares N; Ortiz-Vazquez E; Fernandez F; Loske AM; Gomez-Lim MA A novel and highly efficient method for genetic transformation of fungi employing shock waves. *Fungal Genet Biol* 2013, 56, 9. [PubMed: 23583899]
- (1514). Loske AM; Fernandez F; Magana-Ortiz D; Coconi-Linares N; Ortiz-Vazquez E; Gomez-Lim MA Tandem shock waves to enhance genetic transformation of *Aspergillus niger*. *Ultrasonics* 2014, 54 (6), 1656. [PubMed: 24680880]
- (1515). Tschöep K; Hartmann G; Jox R; Thompson S; Eigler A; Krug A; Erhardt S; Adams G; Endres S; Delius M Shock waves: a novel method for cytoplasmic delivery of antisense oligonucleotides. *J Mol Med-Jmm* 2001, 79 (5–6), 306.
- (1516). Frairia R; Catalano MG; Fortunati N; Fazzari A; Raineri M; Berta L High energy shock waves (HESW) enhance paclitaxel cytotoxicity in MCF-7 cells. *Breast Cancer Res Tr* 2003, 81 (1), 11.
- (1517). Arita Y; Ploschner M; Antkowiak M; Gunn-Moore F; Dholakia K Laser-induced breakdown of an optically trapped gold nanoparticle for single cell transfection. *Opt Lett* 2013, 38 (17), 3402. [PubMed: 23988969]
- (1518). Hellman AN; Rau KR; Yoon HH; Venugopalan V Biophysical response to pulsed laser microbeam-induced cell lysis and molecular delivery. *J Biophotonics* 2008, 1 (1), 24. [PubMed: 19343632]
- (1519). Compton JL; Hellman AN; Venugopalan V Hydrodynamic Determinants of Cell Necrosis and Molecular Delivery Produced by Pulsed Laser Microbeam Irradiation of Adherent Cells. *Biophys J* 2013, 105 (9), 2221. [PubMed: 24209868]
- (1520). Chakravarty P; Lane CD; Orlando TM; Prausnitz MR Parameters affecting intracellular delivery of molecules using laser-activated carbon nanoparticles. *Nanomedicine: Nanotechnology, Biology and Medicine* 2016.
- (1521). Xiong R; Drullion C; Verstraelen P; Demeester J; Skirtach AG; Abbadie C; De Vos WH; De Smedt SC; Braeckmans K Fast spatial-selective delivery into live cells. *Journal of Controlled Release* 2017.
- (1522). Dijkink R; Le Gac S; Nijhuis E; van den Berg A; Vermes I; Poot A; Ohl CD Controlled cavitation-cell interaction: trans-membrane transport and viability studies. *Phys Med Biol* 2008, 53 (2), 375. [PubMed: 18184993]
- (1523). Li M; Lohmuller T; Feldmann J Optical Injection of Gold Nanoparticles into Living Cells. *Nano Lett* 2015, 15 (1), 770. [PubMed: 25496343]
- (1524). Pedrini MRD; Dupont S; Camara AD; Beney L; Gervais P Osmoporation: a simple way to internalize hydrophilic molecules into yeast. *Appl Microbiol Biot* 2014, 98 (3), 1271.

- (1525). Gan BS; Krump E; Shrode LD; Grinstein S Loading pyranine via purinergic receptors or hypotonic stress for measurement of cytosolic pH by imaging. *Am J Physiol-Cell Ph* 1998, 275 (4), C1158.
- (1526). Grunenfelder J; Miniati DN; Murata S; Falk V; Hoyt EG; Robbins RC Up-regulation of bcl-2 through hyperbaric pressure transfection of TGF-beta 1 ameliorates ischemia-reperfusion injury in rat cardiac allografts. *J Heart Lung Transpl* 2002, 21 (2), 244.
- (1527). Bartlett DW; Davis ME Insights into the kinetics of siRNA-mediated gene silencing from live-cell and live-animal bioluminescent imaging. *Nucleic Acids Res* 2006, 34 (1), 322. [PubMed: 16410612]
- (1528). Lin SR; Yang HC; Kuo YT; Liu CJ; Yang TY; Sung KC; Lin YY; Wang HY; Wang CC; Shen YC et al. The CRISPR/Cas9 System Facilitates Clearance of the Intrahepatic HBV Templates In Vivo. *Mol Ther-Nucl Acids* 2014, 3.
- (1529). McCaffrey AP; Meuse L; Karimi M; Contag CH; Kay MA A potent and specific morpholino antisense inhibitor of hepatitis C translation in mice. *Hepatology* 2003, 38 (2), 503. [PubMed: 12883495]
- (1530). Kobayashi N; Kuramoto T; Yamaoka K; Hashida M; Takakura Y Hepatic uptake and gene expression mechanisms following intravenous administration of plasmid DNA by conventional and hydrodynamics-based procedures. *J Pharmacol Exp Ther* 2001, 297 (3), 853. [PubMed: 11356904]
- (1531). Pons T; Lequeux N; Mahler B; Sasnouski S; Fragola A; Dubertret B Synthesis of Near-Infrared-Emitting, Water-Soluble CdTeSe/CdZnS Core/Shell Quantum Dots. *Chem Mater* 2009, 21 (8), 1418.
- (1532). Wei ZW; Zhao DY; Li XM; Wu MX; Wang W; Huang H; Wang XX; Du Q; Liang ZC; Li ZH A Laminar Flow Electroporation System for Efficient DNA and siRNA Delivery. *Anal Chem* 2011, 83 (15), 5881. [PubMed: 21678996]
- (1533). Owczarczak AB; Shuford SO; Wood ST; Deitch S; Dean D Creating transient cell membrane pores using a standard inkjet printer. *J Vis Exp* 2012, (61).
- (1534). Heinemann D; Schomaker M; Kalies S; Schieck M; Carlson R; Escobar HM; Ripken T; Meyer H; Heisterkamp A Gold Nanoparticle Mediated Laser Transfection for Efficient siRNA Mediated Gene Knock Down. *Plos One* 2013, 8 (3).
- (1535). Bhattacharyya K; Mehta S; Viator J Optically absorbing nanoparticle mediated cell membrane permeabilization. *Opt Lett* 2012, 37 (21), 4474. [PubMed: 23114334]
- (1536). Bukhari M; Deng H; Jones N; Towne Z; Woodworth CD; Samways DSK Selective permeabilization of cervical cancer cells to an ionic DNA-binding cytotoxin by activation of P2Y receptors. *Febs Letters* 2015, 589 (13), 1498. [PubMed: 25937122]
- (1537). Bukhari M; Burm H; Samways DSK Ion channel-mediated uptake of cationic vital dyes into live cells: a potential source of error when assessing cell viability. *Cell Biol Toxicol* 2016, 32 (5), 363. [PubMed: 27423453]

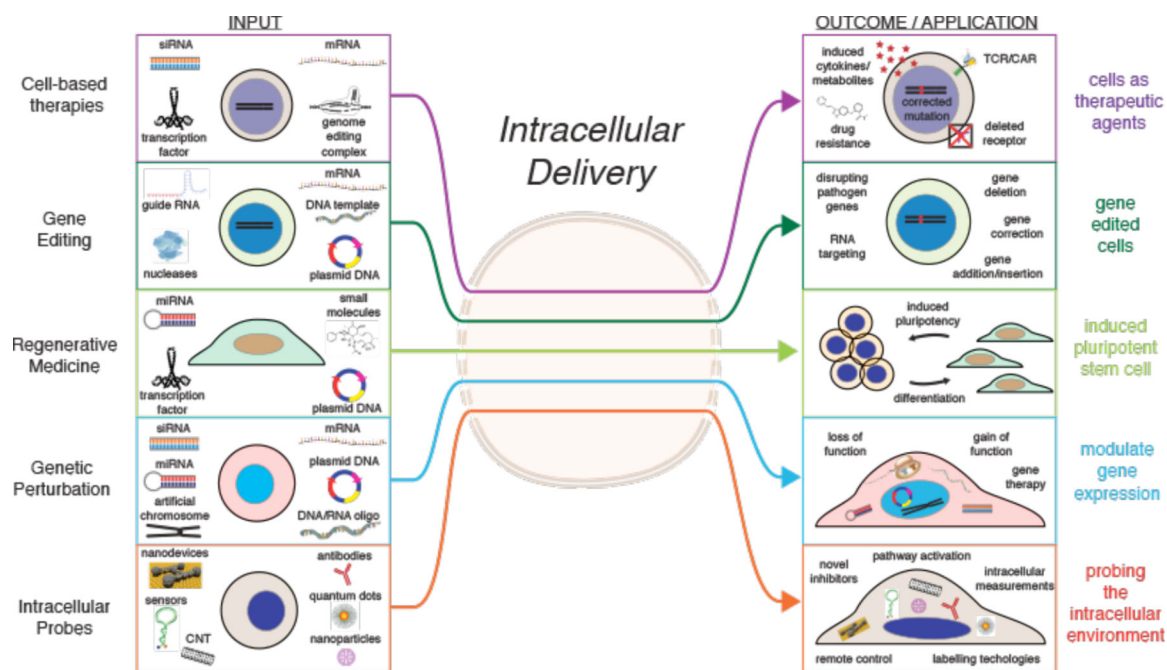


Figure 1.

Example motivations for intracellular delivery. Cells and example cargo are shown on the left. Through intracellular delivery these molecules and materials are able to confer the outcome or application depicted on the right. The horizontal tiers are not mutually exclusive and substantial overlap exists the different groups. Abbreviations: TCR = T cell receptor. CAR = chimeric antigen receptor. CNT = carbon nanotube.

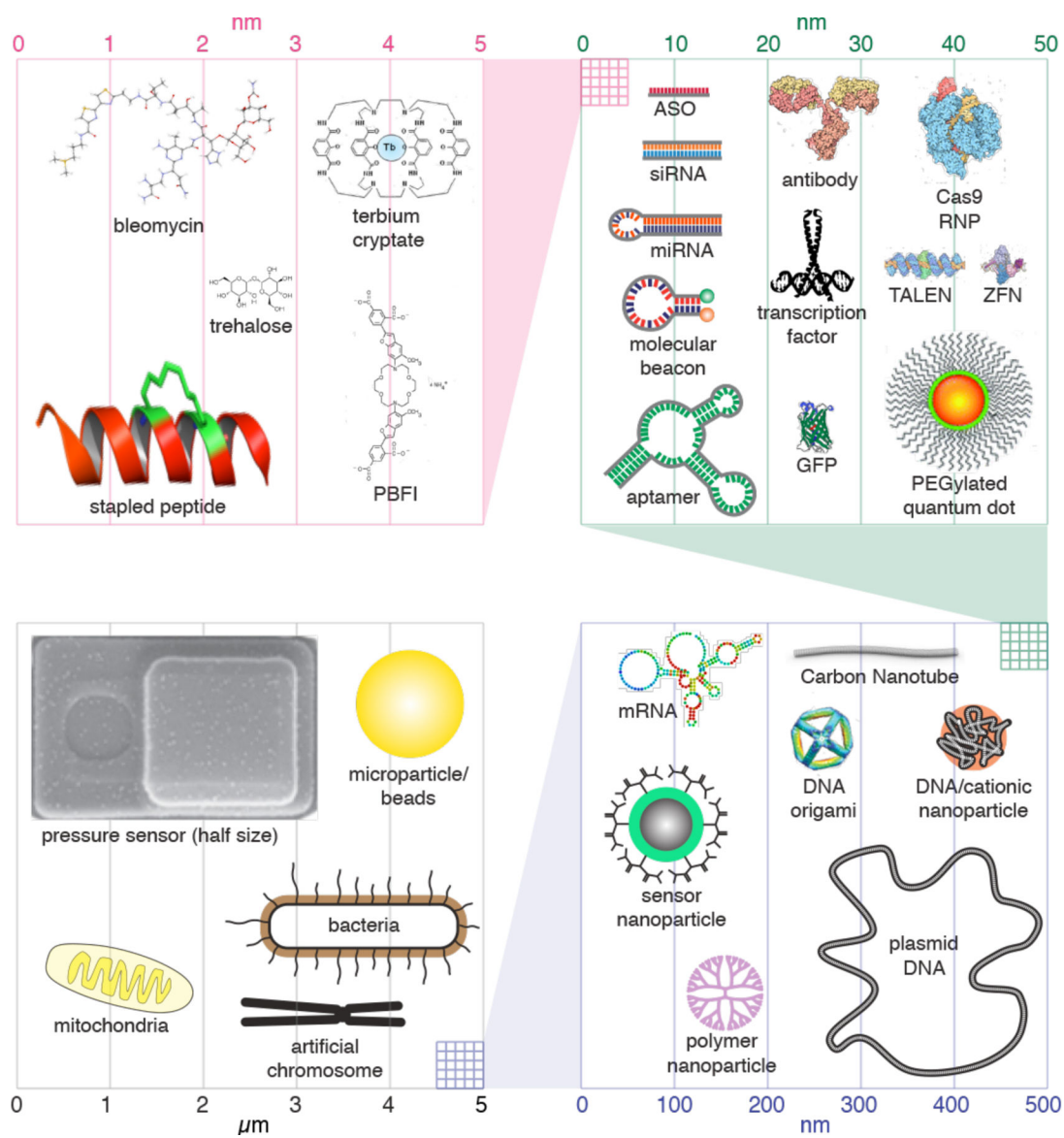


Figure 2.

Size scale of cargoes of interest for intracellular delivery. The top left quadrant represents 5 nm. The top right quadrant represents 50 nm, including a pink box showing the scale of the 5 nm quadrant. The bottom right quadrant represents 500 nm, including a green box showing the scale of the 50 nm quadrant. The bottom left quadrant represents 5 μm , including a blue box showing the scale of the 500 nm quadrant. The properties of each of the cargoes and their applications are discussed throughout chapter 2. PBF1 is a potassium indicator. ASO: antisense oligonucleotide. siRNA: small interfering RNA. miRNA: micro RNA. GFP: green fluorescent protein. RNP: ribonucleoproteins. TALEN: Transcription activator-like effector nuclease. ZFN: zinc finger nuclease. The pressure sensor is actually 6 μm long but here scaled to half size for presentation purposes.

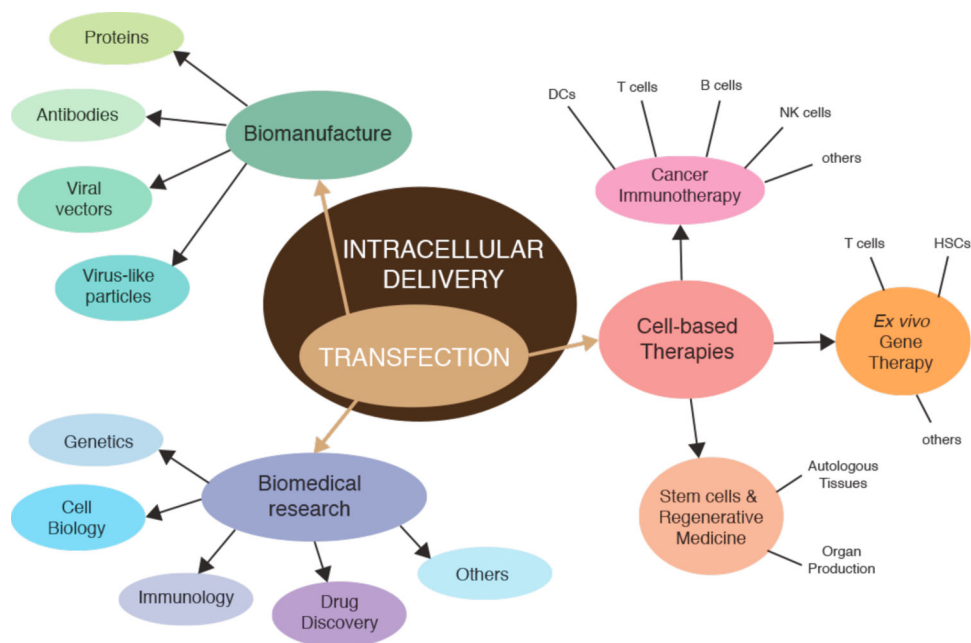


Figure 3. Concept map displaying the main applications areas of transfection. In terms of market share and research, medical, and industrial activity, transfection is the largest sub-component of intracellular delivery.

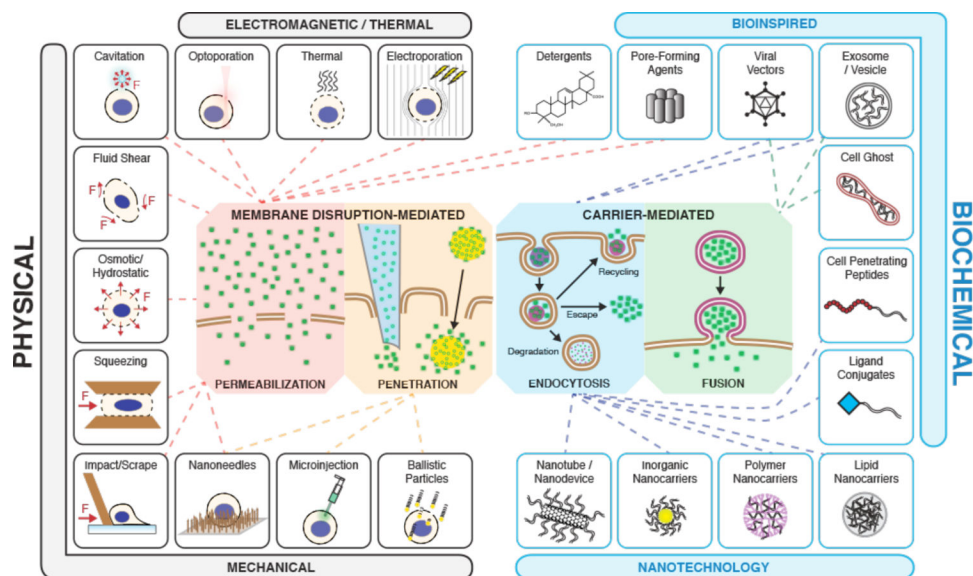


Figure 4.

A map of intracellular delivery methods and their mechanisms. Current intracellular delivery methods are shown sorted within the four indicated mechanisms: permeabilization, penetration, endocytosis, and fusion. Methods that overlap on more than one mechanism may promote intracellular delivery via multiple mechanisms depending on the context. For example, most viral vectors are believed to go through endocytosis but some fuse directly with the plasma membrane.

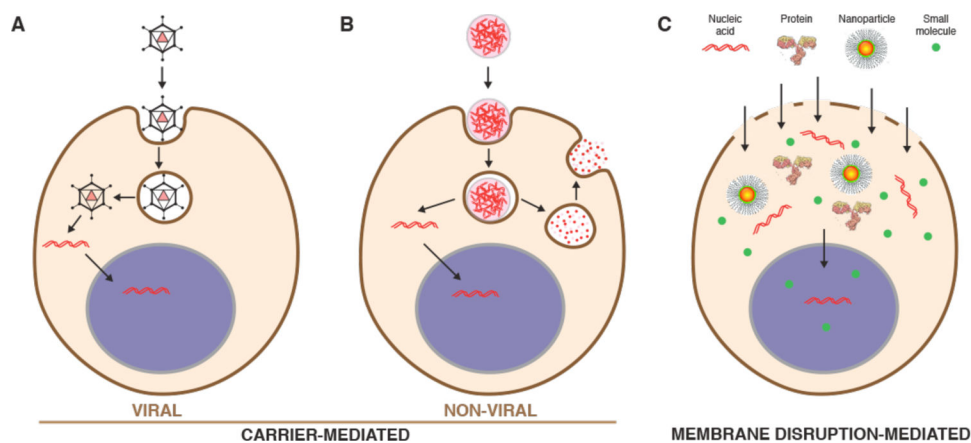


Figure 5. Cargo delivery trajectories for the main intracellular delivery categories. (A) Viral vectors only deliver nucleic acids but do so very efficiently (endocytosis example). (B) Most non-viral carriers are optimized for nucleic acid delivery although some adaptations can carry other materials. Non-viral carriers are endocytosed into the cell with small amounts of nucleic acid breaking out into the cytoplasm while the majority are degraded in lysosomes or recycled back out to the extracellular space. (C) Membrane disruption is able to deliver any cargo that can be dispersed in solution provided it is small enough to fit through transient openings in the plasma membrane. Nucleus is depicted in purple.

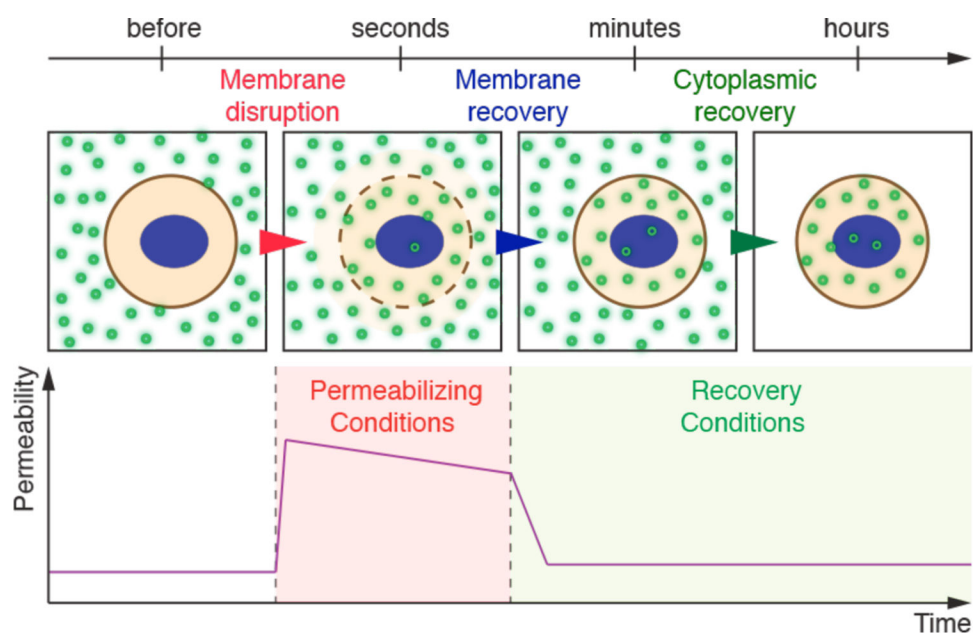


Figure 6. Key events associated with permeabilized-based intracellular delivery. Acute membrane disruption triggers an increase in permeability to the cargo of interest (green). Cargo then begins to diffuse into the cell according to its concentration gradient while some cytoplasmic materials are lost (orange). Within seconds of membrane disruption, the cell responds with membrane active repair processes that can take tens of seconds up to minutes to complete. Once membrane integrity is restored, the cell engages metabolic and transport processes to restore cytoplasmic composition. It may take hours for the cell to fully return to the pre-perturbation state.

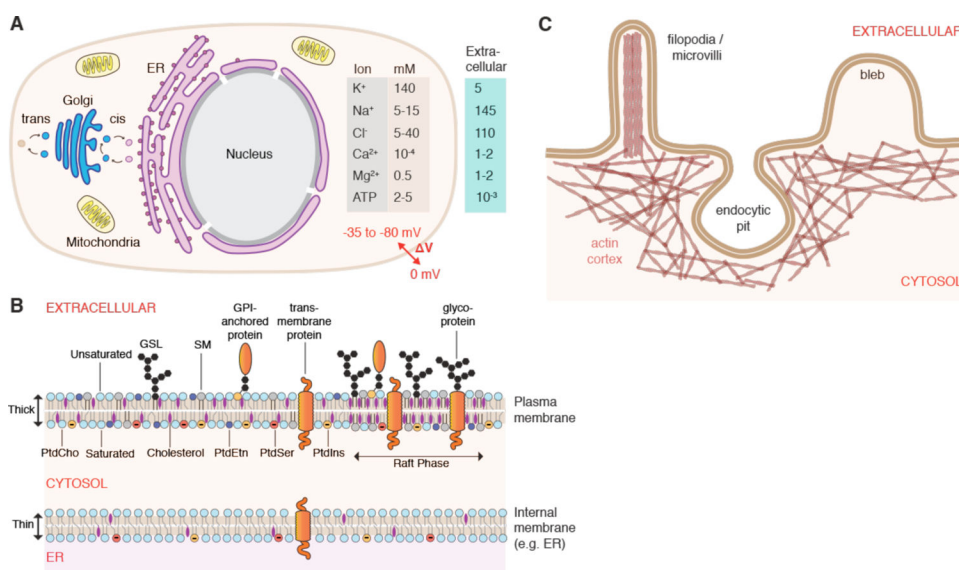
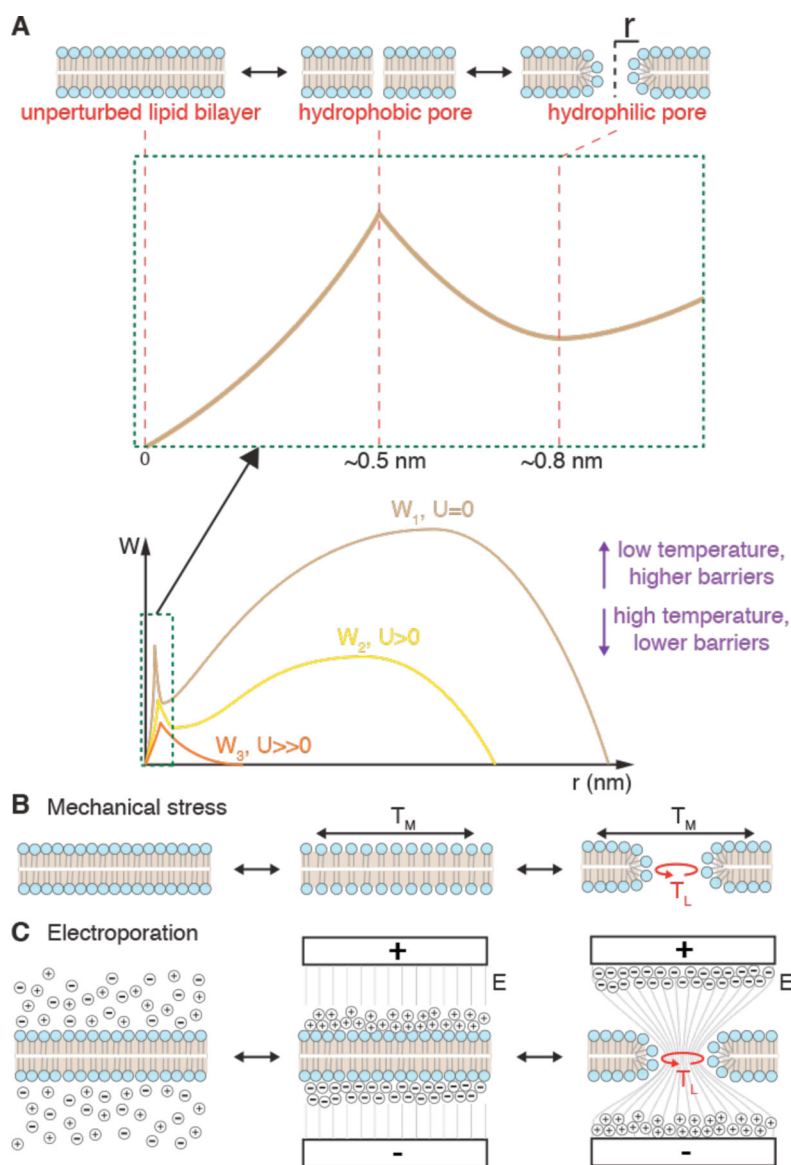


Figure 7. Structure and properties of the cell interior and surface. (A) Overview of typical animal cell structure with basic organelles, intra- and extracellular ion concentrations, and negative membrane potential (ΔV). ER: endoplasmic reticulum. (B) Features of the plasma membrane including lipid asymmetry across bilayer leaflets and lateral segregation into domains, such as raft phases. Abbreviations are phosphatidylcholine (PtdCho), phosphatidylethanolamine (PtdEtn), phosphatidylserine (PtdSer), and phosphatidylinositol (PtdIns), sphingomyelin (SM), glycosphingolipids (GSL). Carbohydrate residues depicted in black, cholesterol in purple. Note the highly regulated heterogeneous distribution of molecules between different types of membranes and leaflets. As a result, the ER membrane is thinner and sparser than plasma membrane, with more unsaturated lipid tails. (C) Plasma membrane reservoirs and their relationship with the underlying actin cortex. Actin rods support filopodia and microvilli. Blebs are typically devoid of actin until they are pulled back in. The actin cytoskeleton accommodates formation and stabilization of endocytic pits.

**Figure 8.**

Theory of mechanical and electrical disruption of lipid bilayers according to energy landscape of defect formation. (A) Energy landscape according to hydrophilic pore theory. Energy is required to open up hydrophobic defects with radius ~ 0.5 nm. Further growth to a hydrophilic, toroidal pore with lipid head groups facing inward is associated with a local energy minimum at pore radius ~ 0.8 nm. W_1 represents the energy landscape at rest with no external mechanical or electrical input, W_2 (yellow) represents an intermediate mechanical or electrical stress, while W_3 (orange) indicates the effect of a large mechanical or electrical potential. Low temperature is synonymous with increased barrier heights while high temperature favors membrane destabilization. (B) Illustration of pore formation due to mechanical stress where the membrane is first stretched before pore formation. The applied in plane tension (T_M) and the line tension (T_L) within a lipid pore are diametrically opposed. (C) Illustration of pore formation due to application of electrical potential normal to

membrane where E is the electric field strength and T_L = line tension within a hydrophilic pore. Hydrophilic pores are conducting, thus leading to relaxation of charge buildup and a reduction of entropy in the system.

Author Manuscript

Author Manuscript

Author Manuscript

Author Manuscript

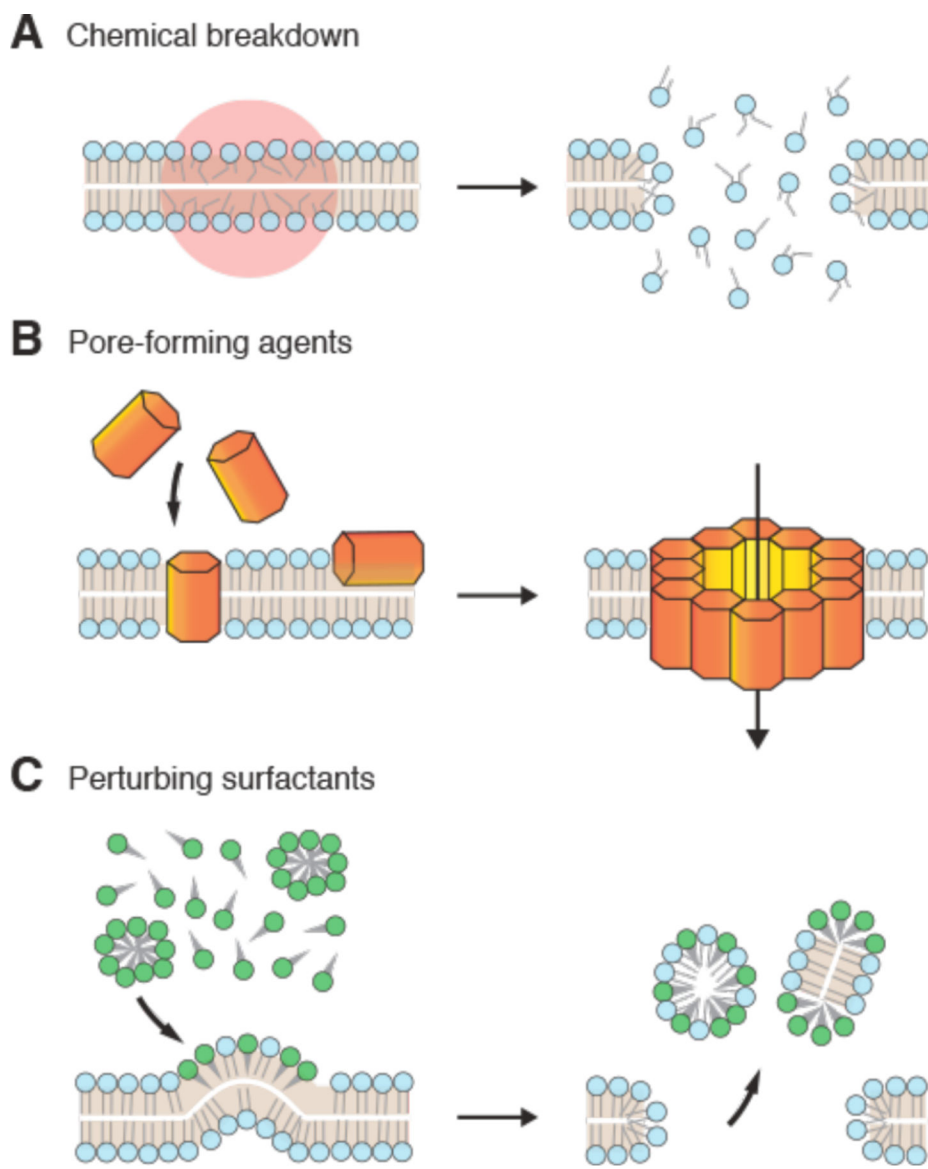


Figure 9. Chemical approaches for generating disruptions in lipid bilayers. (A) Chemical breakdown within a local region (red circle) can lead to disintegration of membrane integrity via breaking of bonds or distortion caused by unsaturation of lipid tails. (B) Pore-forming agents can interact with a membrane to assemble an oligomeric pore. (C) Perturbing surfactants (such as detergents) can embed into the bilayer and induce curvatures that distort the membrane and lead to loss of bilayer structure and pore formation.

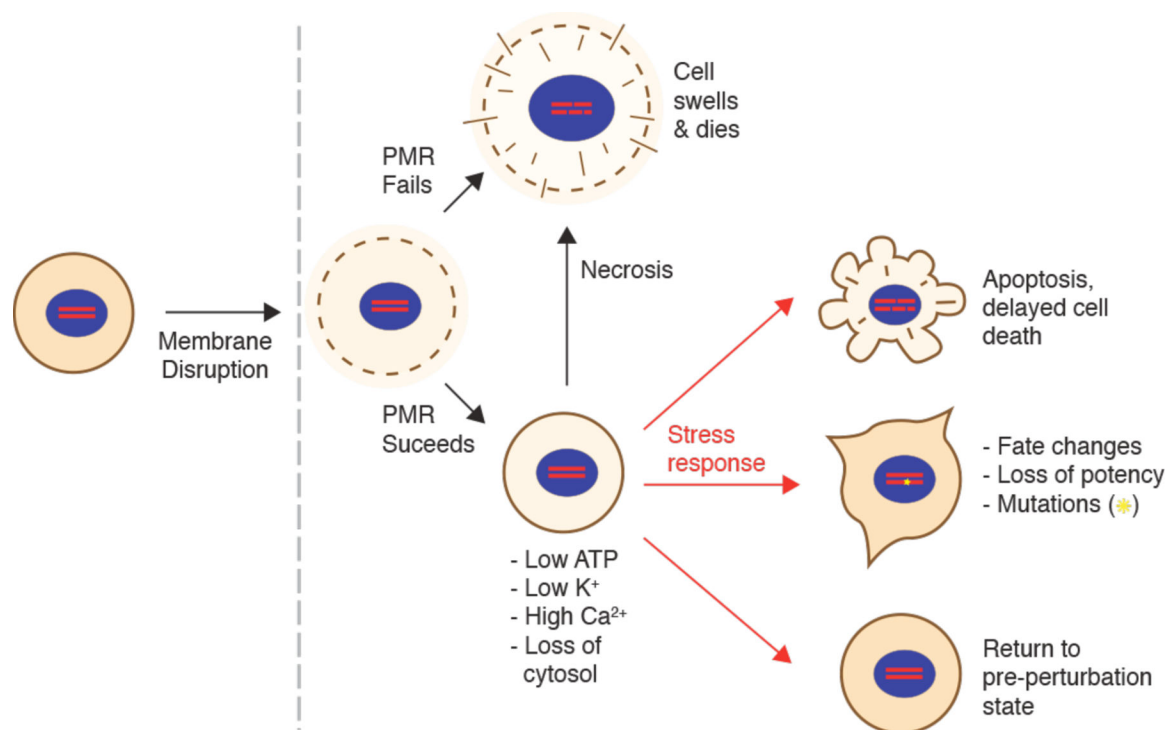


Figure 10.

Cell response to membrane disruption. First, plasma membrane repair (PMR) engages within seconds to minutes to rescue the cell. If PMR fails the cell depolarizes, swells, and dies. Shown are the altered cytoplasmic contents that eventuate if membrane disruption is conducted in a physiological buffer. If PMR is successful, the cell is left in a perturbed state with loss of cytosol. Stress response guides the cell to return to the pre-perturbation homeostatic state or into apoptosis. In some cases trauma or off-target damage involved with disruption recovery cycle may cause mutations, fate changes, or loss of cell potency.

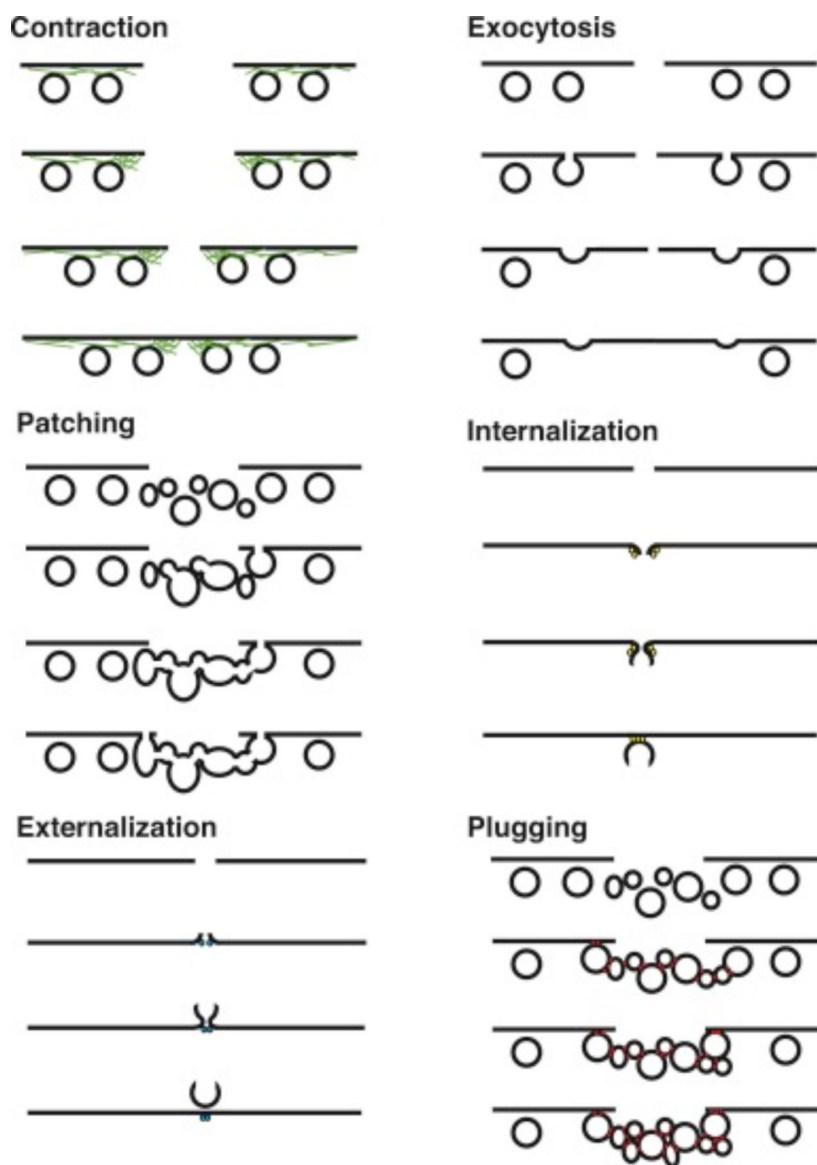


Figure 11.

Proposed mechanisms of membrane resealing. In each case, the black line with gap represents the plasma membrane with a wound-induced hole and healing progresses from top to bottom. Black circles represent vesicles in the cell. Green lines in “Contraction” represent cortical cytoskeleton; yellow dots in “Internalization” represent machinery powering endocytic invagination and pinching; blue dots in “Externalization” represent ESCRT machinery powering scission; red dots in “Plugging” represent proteins crosslinking membranous compartments. Figure taken from Moe et al.⁴⁰⁸.

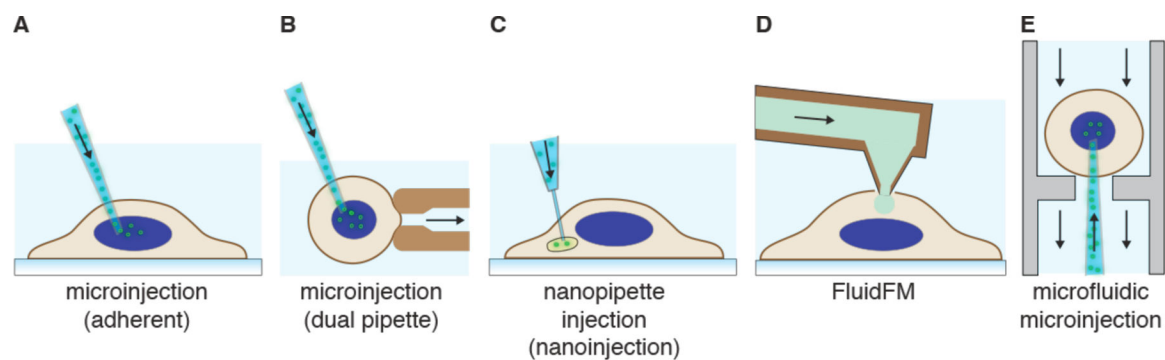


Figure 12.

Intracellular delivery via microinjection. (A) Depiction of an adherent cell being microinjected with a glass micropipette. (B) Microinjection of a suspended cell that is held in place by a secondary holding pipette. (C) Nanopipette injection (nanoinjection) where the penetrating aperture consists of a nanotube. In this illustration an intracellular organelle is being injected. (D) Use of a hollow AFM cantilever to inject cells (FluidFM) (E) Microfluidic microinjection where a cell is pushed onto a sharp micropipette via flow. Pressure is then generated in the micropipette to deliver into the cell. Reversing the flow of the main microfluidic channel can be used to eject the cell.

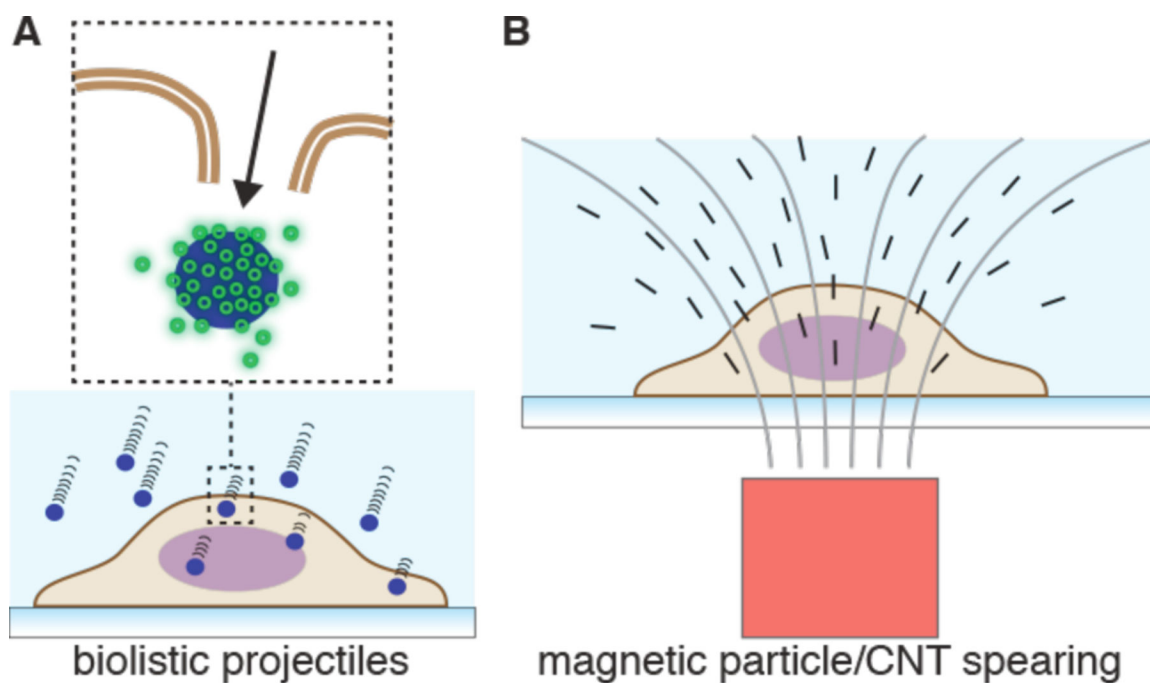


Figure 13.

Intracellular delivery via penetrating projectiles. (A) Biolistic projectiles consisting of metal beads are propelled towards a cell with enough force to burst through the plasma membrane. The metal beads are coated with cargo, which then releases inside the cell. Inset shows an example of a single cargo-covered bead disrupting the plasma membrane. (B) A magnetic field is used to attract magnetically functionalized particles (such as CNTs) through the plasma membrane into the target cell for delivery of attached cargo.

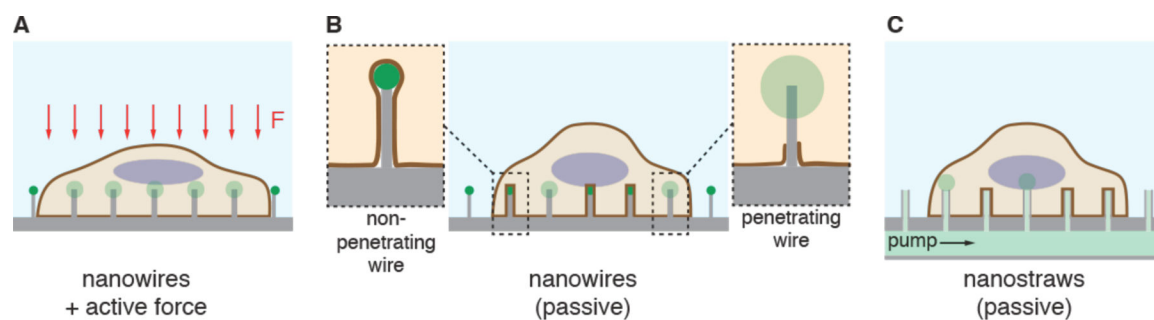


Figure 14.

Intracellular delivery via penetrating nanowires/nanoneedles and nanostraws. (A) Cell pushed onto an array of nanowires with active force (F), such as centrifugation. The number of penetrating nanowires increases given the same needles as in B. (B) Passive settling and adhesion of a cell onto an array of nanoneedles coated with cargo molecules at the tip (green). In this case some nanowires may penetrate through the plasma membrane into the cytosol to release their contents inside the cell (green cloud). (C) Hollow nanowires (nanostraws) used for intracellular delivery by pumping cargo from a reservoir connected to the nanostraws.

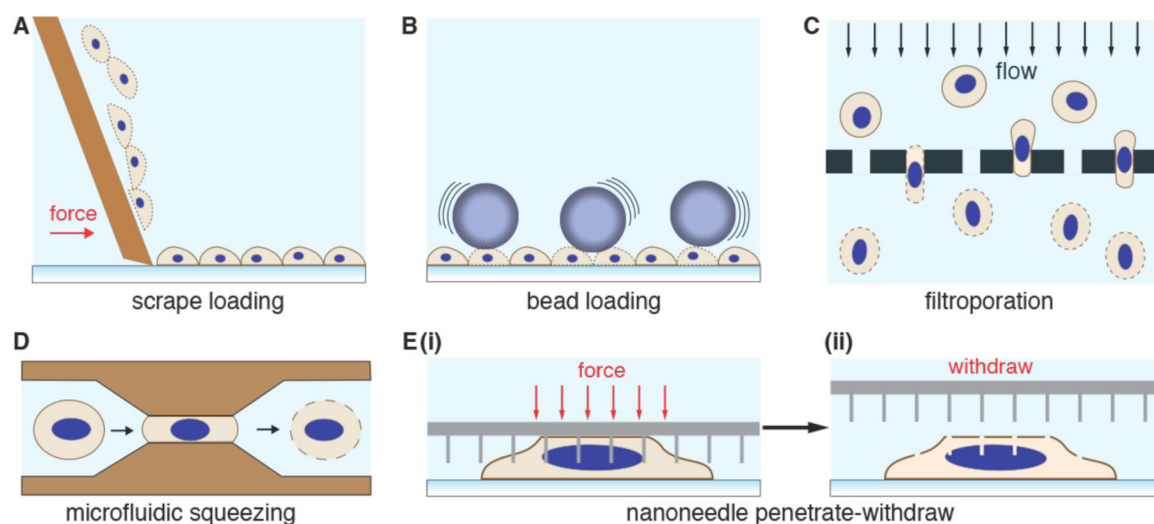


Figure 15.

Mechanical membrane permeabilization by direct contact. (A) Scrape loading, where a rubber spatula or similar scraping object can be used to simultaneously dislodge cells and permeabilize them. (B) Bead loading, wherein micron-scale beads can be rolled across a cell monolayer for controlled cell injury via collisions. (C) Filtroperation, where a solution of cells is passed through holes in filter membranes, such as a track-etched polycarbonate filter. (D) Microfluidic cell squeezing, where cells membranes are disrupted by rapid deformation that occurs with passage through microfabricated constrictions. (E) Permeabilization with nanoneedle arrays. (i) The array is first centrifuged or otherwise pressed against cells adhered to a rigid substrate. (ii) The array is then removed to enable cargo influx through membrane disruptions in the target cells.

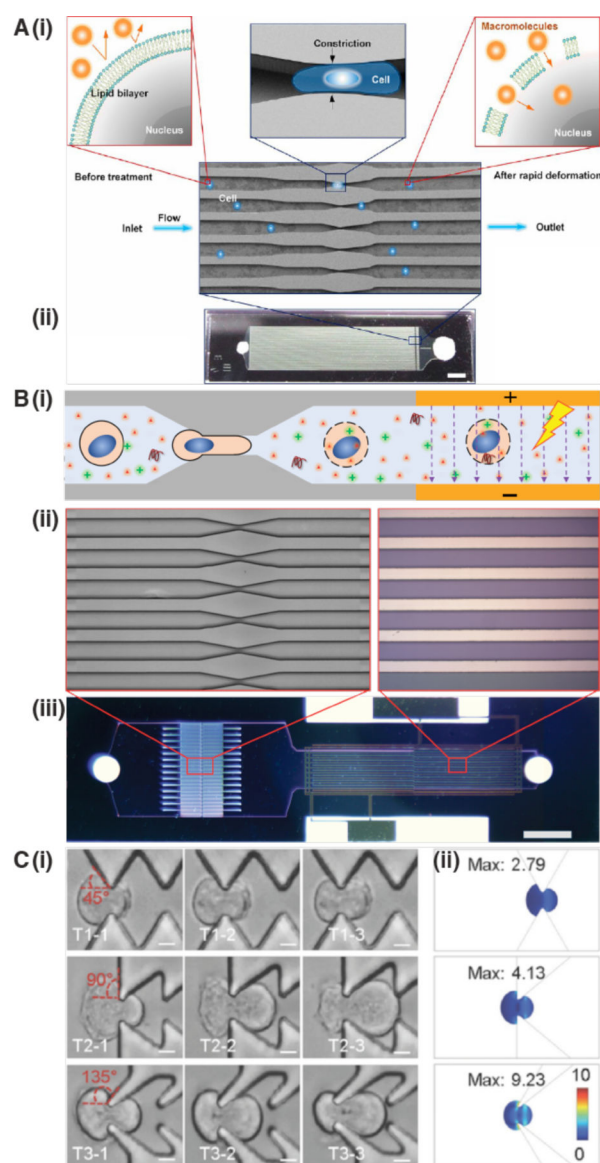


Figure 16.

Different variations of cell squeezing for membrane permeabilization. (A) The original microfluidic platform for cell squeezing¹⁸⁴. (i) The deformation the cell experiences upon passage through the constriction transiently permeabilizes the plasma membrane, allowing influx of cargo molecules into the cytosol. (ii) microfluidic chip, consisting of a silicon parallel microchannels produced by deep reactive ion-etching and sealed from the top with glass. Inlets and outlets are also visible. (B) Similar to cell squeezing in panel A but with addition of a downstream electric field. The electric field enhances delivery of large nucleic acids, such as plasmid DNA, into the cell by electrophoretic forces. In this case the device was optimized for delivery of plasmids into the cell nucleus at high throughput⁷⁴⁹. Panel (i) shows the delivery concept. Panel (ii) shows the architecture of the constriction and electrode zones. Panel (iii) shows a view of the whole chip. (C) Cell squeezing with different constriction geometries in PDMS device. (i) Comparison of 45° pyramidal pattern, 90° saw

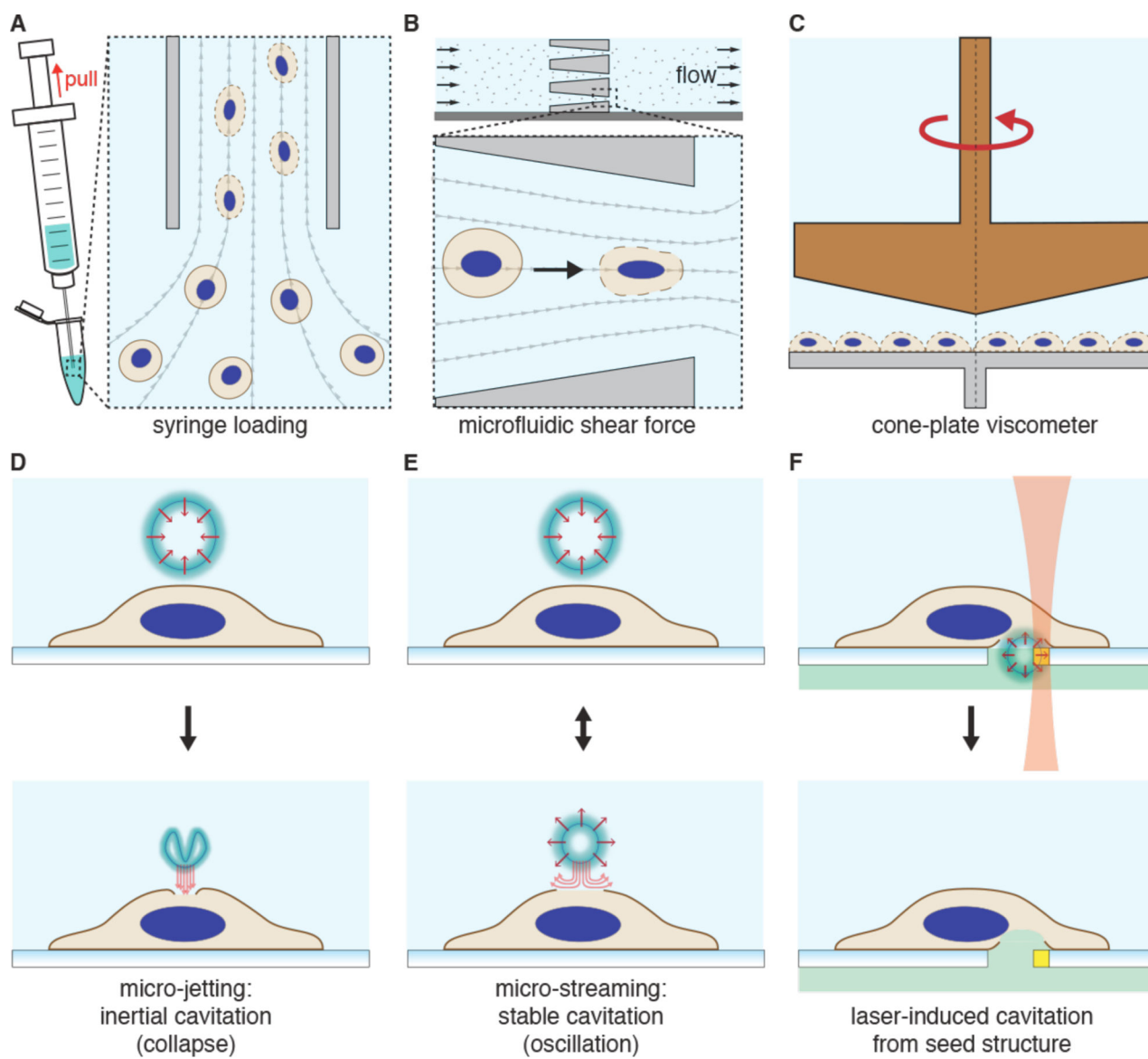
tooth pattern, and 135° reverse wishbone pattern of repeated constrictions. (ii) COMSOL modeling indicates the stress ($\text{N}\cdot\text{m}^{-2}$) that the cell membrane undergoes upon passage through the different types of constrictions. Experiments and modeling showed the reverse wishbone pattern as the most effective for membrane disruption in this platform⁷⁵⁰.

Author Manuscript

Author Manuscript

Author Manuscript

Author Manuscript

**Figure 17.**

Mechanical membrane permeabilization by fluid shear forces. (A) Syringe loading, where a cell solution is repeatedly aspirated and ejected through the terminal aperture of a syringe needle. Shear forces at the nozzle promote membrane disruption. The inset illustrates cell deformation associated with shear forces. (B) Microfluidic shear-based permeabilization. Similar to syringe loading but exploiting the increase of shear forces associated with flow through narrowing microfluidic channels. The inset illustrates cell deformation upon flow through a single constriction. (C) Cone-plate viscometer. Generation of permeabilizing shear forces via rotation of a viscometer plate above a monolayer of cells. (D) Generation of local shear forces via collapse of a cavitation bubble. (E) Generation of local shear forces via oscillation of cavitation bubble. (F) Induction of cavitation bubbles on the basal side of cells through arrayed seed structures that absorb laser energy. The cavitation bubble can produce a

large hole in the plasma membrane that allows influx from a separate fluid reservoir underneath the cells.

Author Manuscript

Author Manuscript

Author Manuscript

Author Manuscript

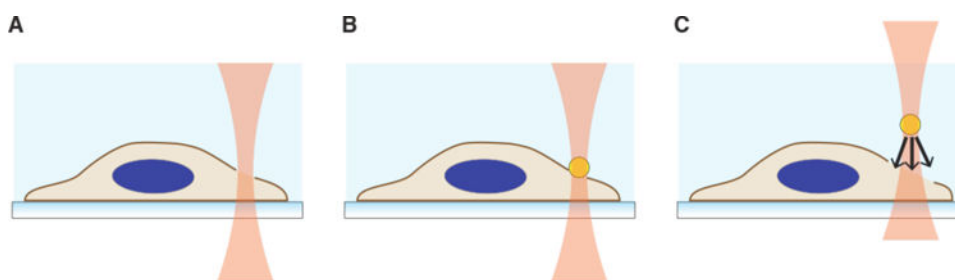


Figure 18.

Modes of laser-induced membrane disruption. (A) Laser optoporation occurs when incident energy is absorbed by the plasma membrane, directly disrupting it. Optoporation is covered in section 6.4. (B) Laser absorption by an absorbing agent in contact with the cell (such as a particle or interface), which then generates secondary effects (heat, fluid shear, chemical breakdown) to disrupt the plasma membrane. (C) Laser absorption by an absorbing agent distant from the plasma membrane. In these cases fluid shear from cavitation and/or shock waves is the most likely cause of membrane disruption.

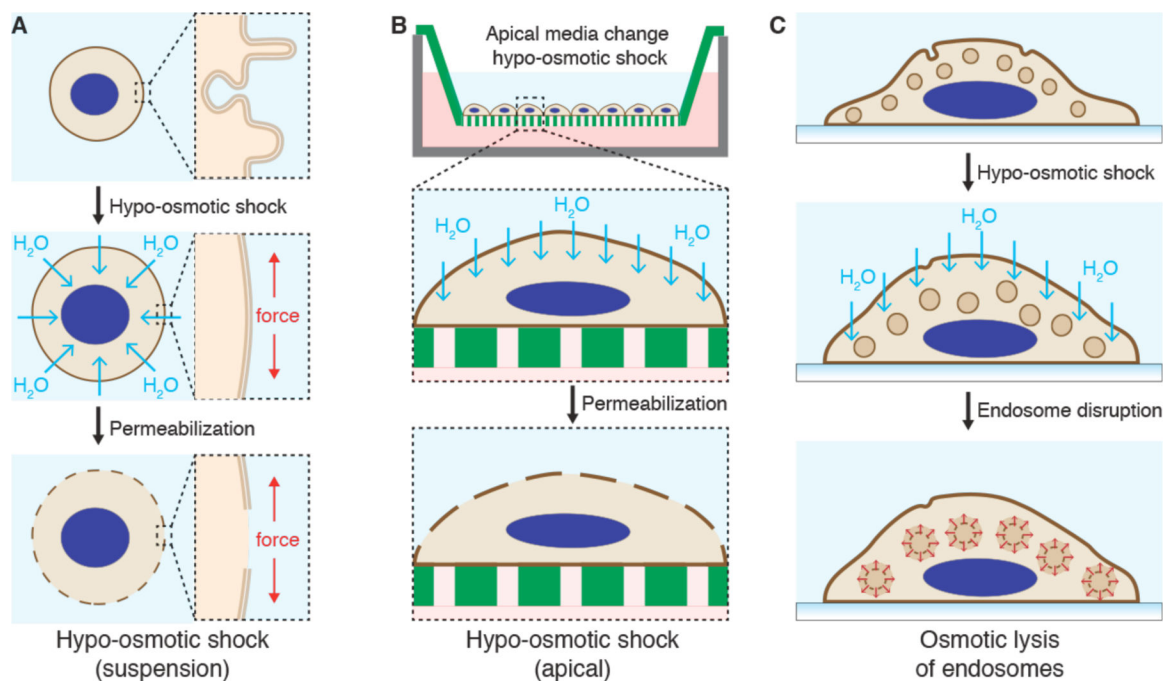


Figure 19.

Mechanical membrane disruption via osmotic pressure changes. (A) Cells in suspension subject to hypotonic shock will first swell, which unravels membrane reservoirs. If the membrane strain is sufficient in response to the swelling force, permeabilization will occur. The inset shows microscale conformation of the plasma membrane. (B) Cells in an adherent monolayer cultured on a porous substrate can be subject to a perturbing osmotic gradient via hypotonic shock at their apical surface. Swelling and subsequent permeabilization occur similarly as in panel A but the permeabilization is localized to the apical side of the cell. (C) In a scenario where endosomes are pre-loaded with osmolytes and cargo to be delivered, a hypotonic shock can be used to cause lysis of endosomes.

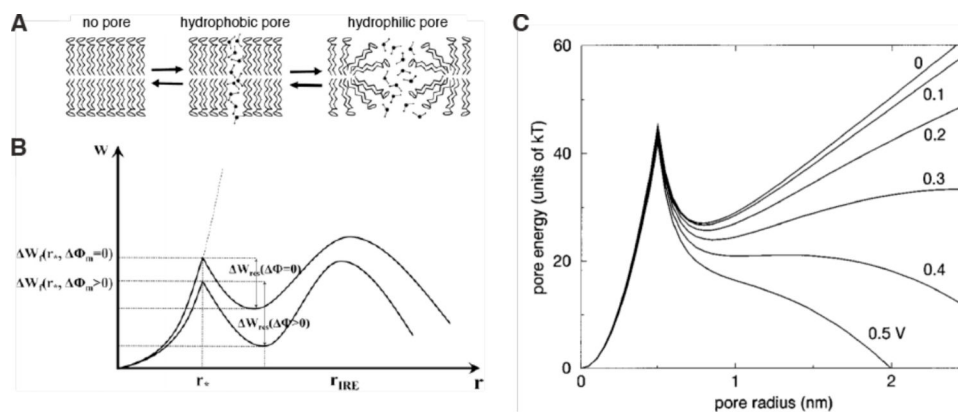


Figure 20.

Theory of pore formation in membranes by electric fields. (A) Schematic of pore formation showing the transition from a hydrophobic pore to a hydrophilic (conducting) pore. (B) Graphs of relationship between free energy of pores W and pore radius r for $\Phi_m = 0$ (upper curve) and at $\Phi_m > 0$ (lower curve). r_* is the critical radius corresponding to the transition from hydrophobic to hydrophilic pore. W_f corresponds to the height of the energy barrier for pore formation while W_{res} relates to the energy barrier height for pore resealing. r_{ire} is the pore radius corresponding to state of irreversible electroporation. Φ_m is the electrical potential difference across the membrane. Panel A and B reproduced from reference 239²³⁹. (C) Calculations of the effect of applied voltage on the energy landscape of pore formation with transmembrane potentials ranging from 0 to 0.5 V. Panel C reproduced from reference 389³⁸⁹.

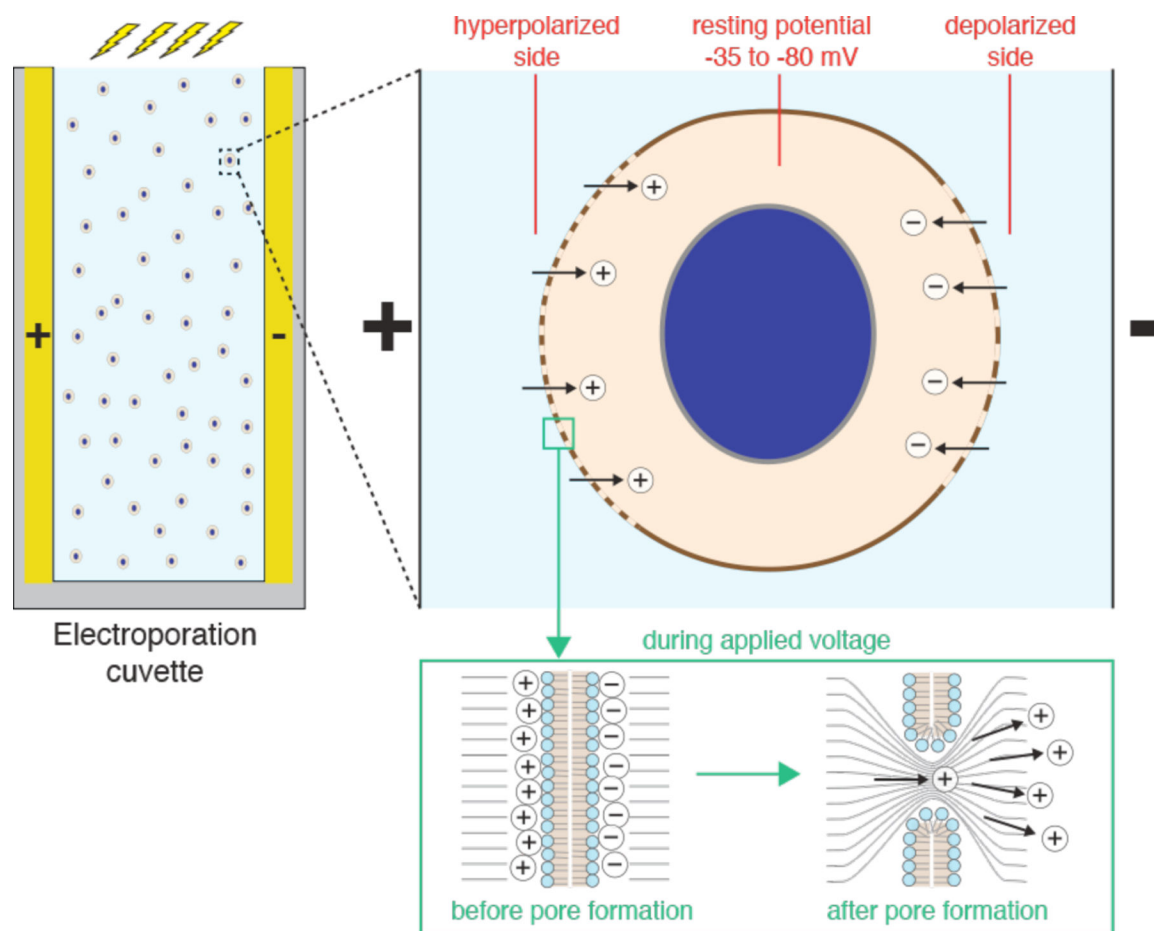


Figure 21.

A conventional parallel plate cuvette configuration for electroporation of suspended cells (left). Zoom-in (right) shows the approximate distribution of pores over the cell surface as a function of orientation and polarization under applied electric field. The surface area of poration and number of pores is greater on the hyperpolarized side compared to the depolarized side. Further zoom-in (bottom) illustrates the capacitor-like function of the lipid bilayer before poration and the flow of positive charge once a conducting pore is formed (opposite movement of negatively charged objects not shown). Electric field lines are displayed in grey.

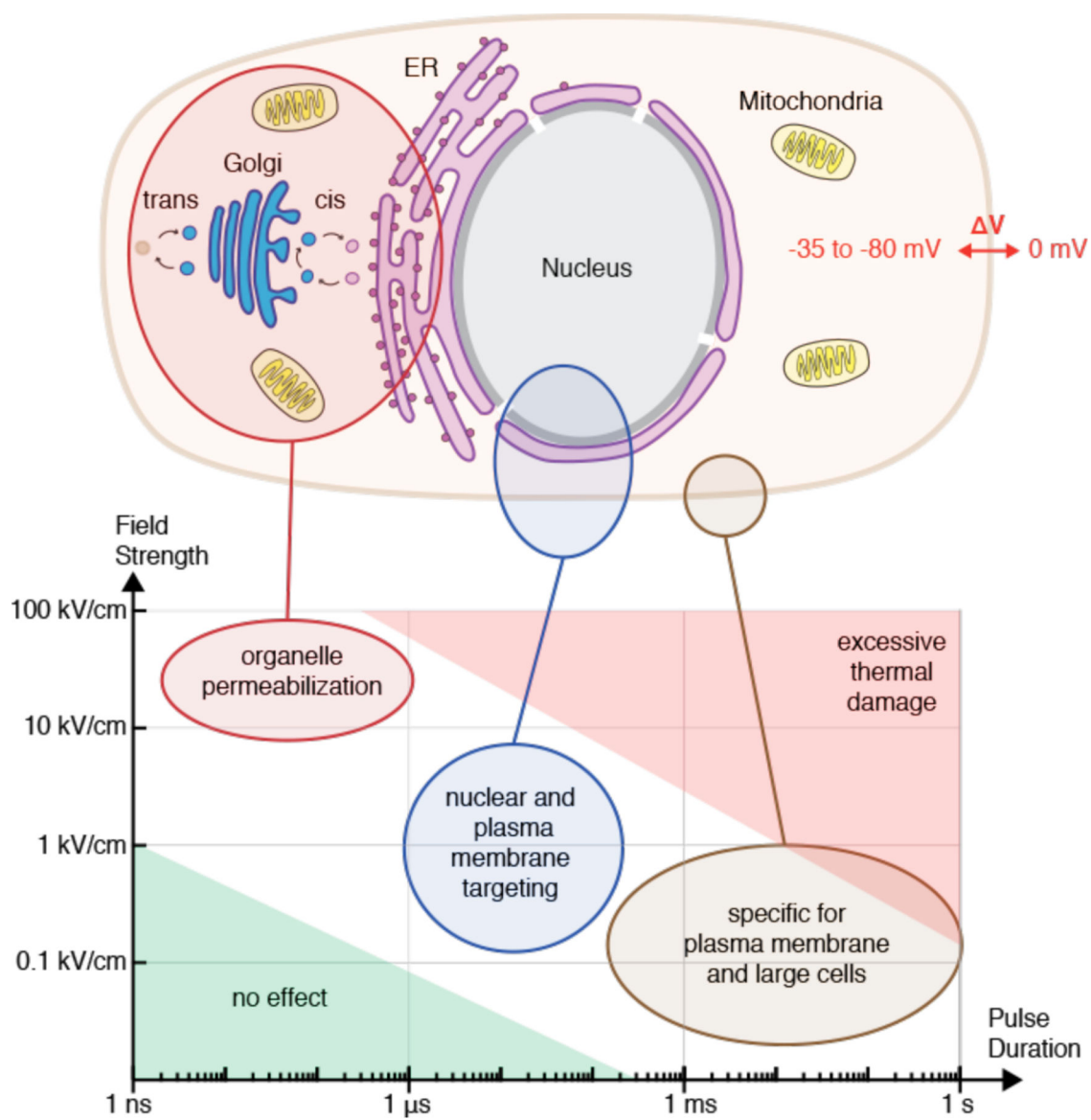


Figure 22. Relationship between the pulse strength-duration parameter space and subcellular targeting. High intensity short pulses are biased toward perturbing small membrane bound bodies like organelles while milder, longer pulses are more specific for the plasma membrane and larger cells. At large field strengths and longer durations thermal damage due to heating becomes an issue, being also dependent on buffer conductivity.

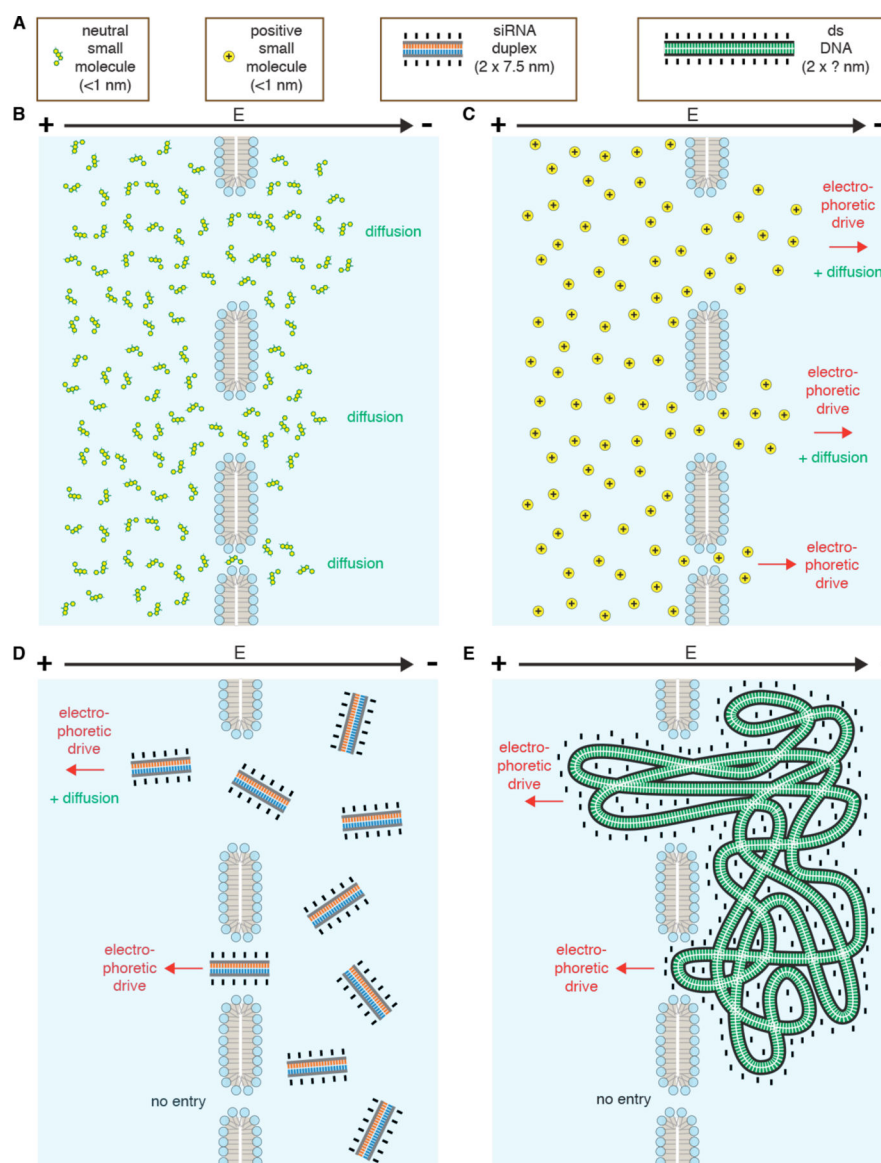


Figure 23. Relationship between size and charge of cargo molecule and mechanisms of entry through a given pore size for electroporation. (A) Depiction of approximate size and charge properties of molecules illustrated in scenarios from panels B to E. The depictions are based on knowledge from the literature and explained in the text.

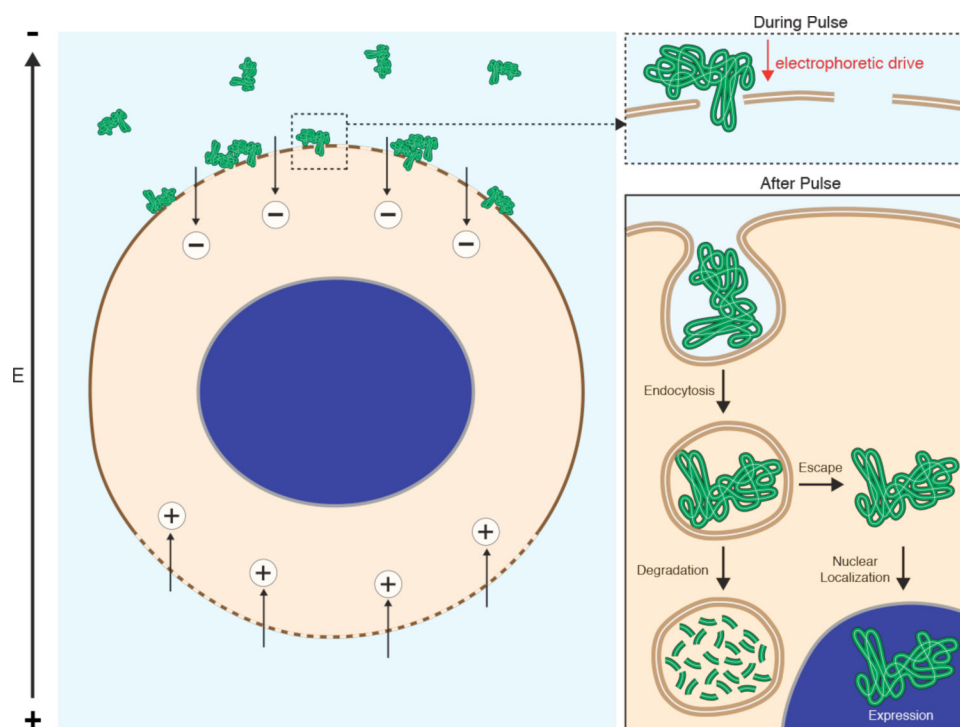


Figure 24.

Model for endocytosis of electroporation-induced DNA aggregates at the cell surface.

During the electric field pulse, negatively charged plasmid DNA is propelled into the side of the cell facing the negative electrode. Due to conformational flexibility some parts of the DNA may be threaded through pores in the cell membrane. Aggregates are then endocytosed, from which they either escape and find their way to the nucleus for the purpose of expression or are degraded by lysosomes.

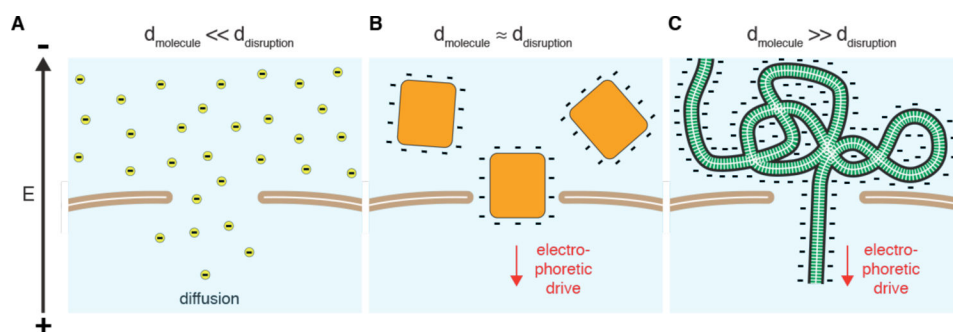


Figure 25. Schematic of the mechanisms of influx in relation to disruption size, molecule size, molecule charge, and conformational flexibility. For charged objects approaching the disruption size or larger, electrophoretic forces are crucial for delivery. (A) Shown is the case for a molecule much smaller the size of the membrane disruption. Regardless of charge, delivery is mostly via diffusion. (B) Shown is the case for a negatively charged molecule of similar size to the membrane disruption. Delivery requires an electrophoretic driving force. (C) Shown is the case for a flexible molecule (here a DNA plasmid) that is much larger than the membrane disruption. Electrophoretic force can thread part of the molecule into the cell.

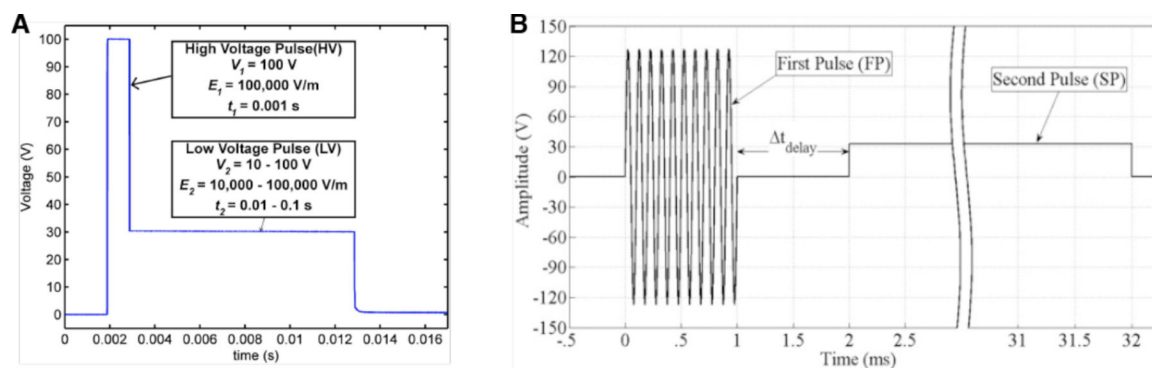


Figure 26.

Examples of dual-pulse electroporation protocols from the literature. (A) The first pulse has a field strength of 1 kV cm^{-1} and duration of 1 ms . The second pulse 0.3 kV cm^{-1} in strength and 10 ms in duration. Figure taken from reference 1078¹⁰⁷⁸. (B) Schematic of a pulse sequence consisting of AC first followed by a pre-programmed delay then a second DC pulse. In this case, the first pulse is 1 ms and the second one is 30 ms . Figure taken from reference 1079¹⁰⁷⁹.

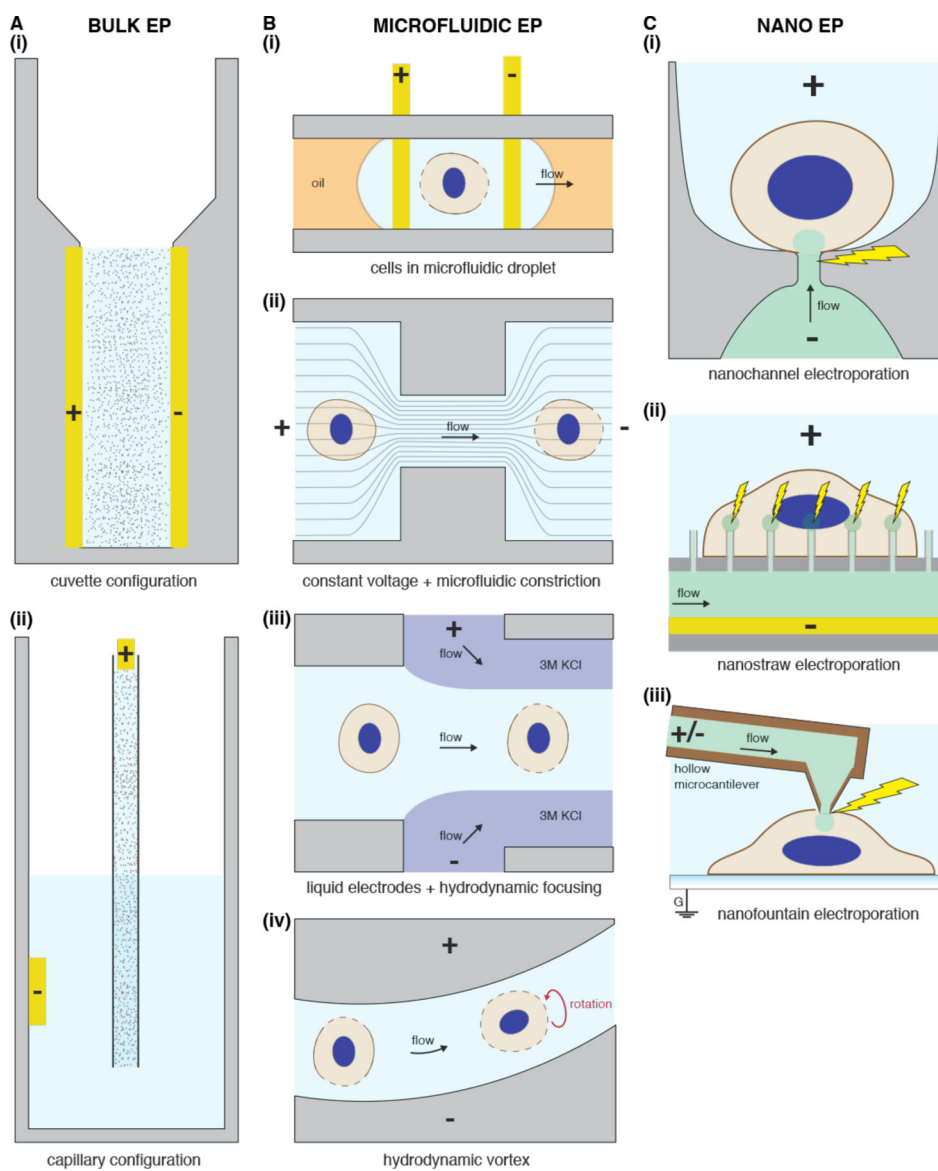
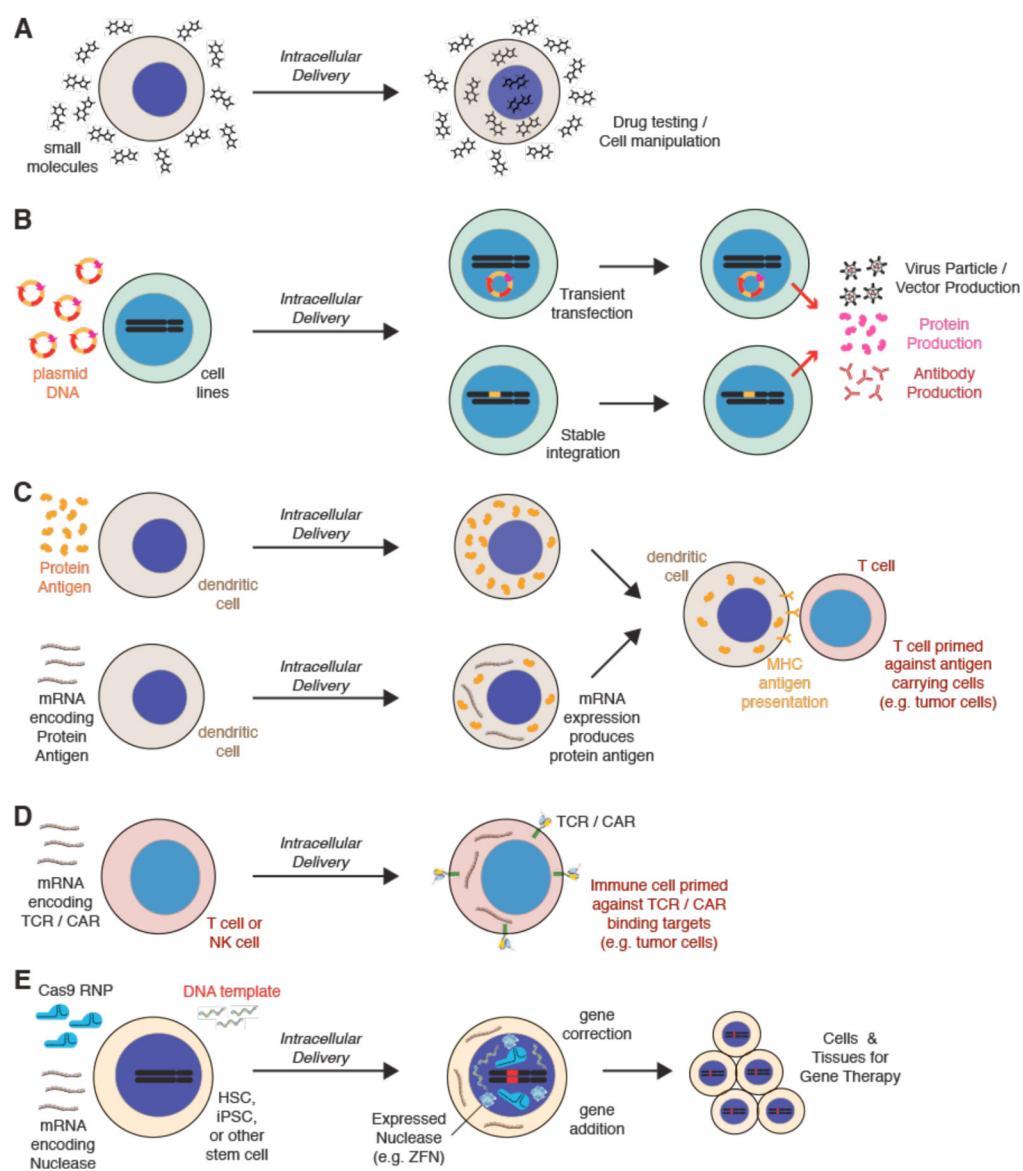


Figure 27. Electroporation (EP) configurations. (A) Bulk (conventional) electroporation in parallel plate cuvette (i) and capillary (ii) geometries. (B) Microscale electroporation examples showing electroporation in droplets (i), the use of channel architecture to manipulate voltage pulses (ii), hydrodynamic focusing to generate liquid electrodes (iii), and hydrodynamic vortices to rotate cells through electric fields (iv). (C) Nanoscale electroporation with examples of nanochannel electroporation, where cells are pressed against nanoscale apertures (i); nanostraw electroporation, in which the electric field is concentrated onto the end of a nanostraw (ii); and nanofountain electroporation, which exploits a hollow AFM tip for addressing individual cells (iii).

**Figure 28.**

In vitro and *ex vivo* applications of intracellular delivery achieved with electroporation. (A) Delivery of impermeable drugs to the intracellular space for drug testing and/or cell manipulation. (B) Transfection with plasmid DNA encoding proteins, antibodies, and viral components for biomanufacturing purposes. (C) Loading of protein antigens or mRNA encoding such into dendritic cells. Presentation of antigen fragments through MHC pathways is able to prime T cells against cells carrying the antigens and may be useful for cancer immunotherapy. (D) Transfection of cytotoxic immune cells with mRNA encoding TCRs and/or CARs can be used to direct immune cells against specific cell targets, such as cancer cells. TCR = T cell receptor. CAR = chimeric antigen receptor. (E) Genome-editing molecules can be delivered into stem cells for purposes of adding, deleting, or correcting genes. Modified stem cells can then be expanded for potential deployment in cell- and tissue-

based gene therapy. Red signifies areas of the genome that have been edited. ZFN = zinc finger nuclease.

Author Manuscript

Author Manuscript

Author Manuscript

Author Manuscript

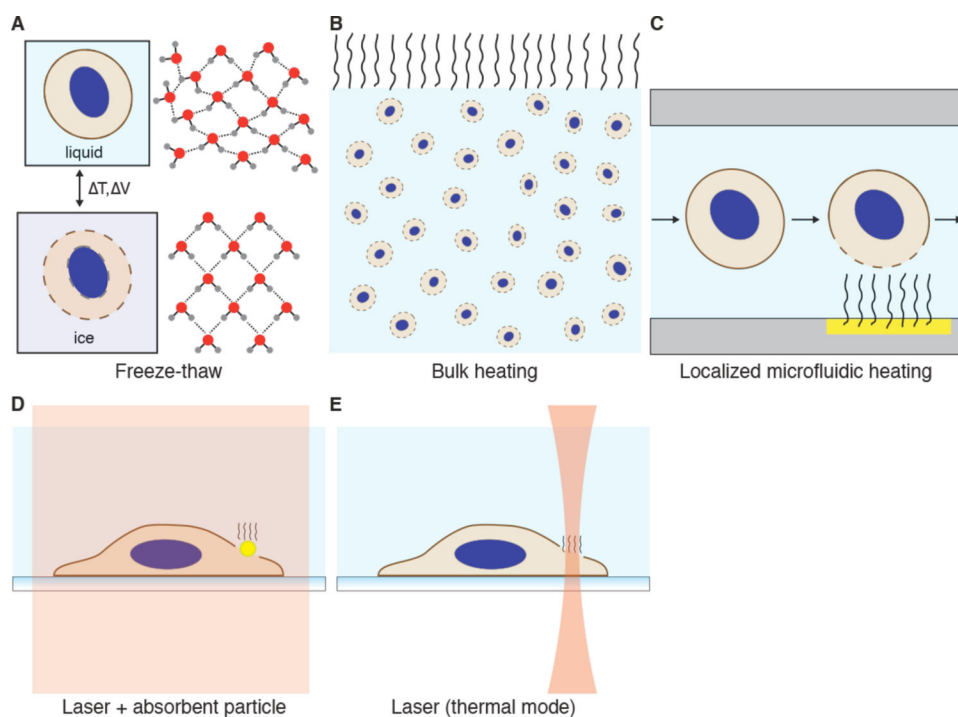


Figure 29.

Thermal membrane disruption. (A) Membrane disruption by freeze-thaw cycles. Formation of ice crystals leads to volume expansion due to the changes in hydrogen bonding arrangement. Volume expansions are thought to be related to cracking of membranes during ice crystal formation. (B) Heating of cells above 42 °C increases the chances of spontaneous defect formation in membranes. (C) Microfluidic geometries may be used to confine the heating locally to a part of the cell, such as is possibly the case for thermal inkjet printing. (D) Absorbent nanoparticles may be used to locally convert laser power into local heating for membrane perturbation. (E) A focused laser can generate local heating at the membrane with selection of appropriate parameters.

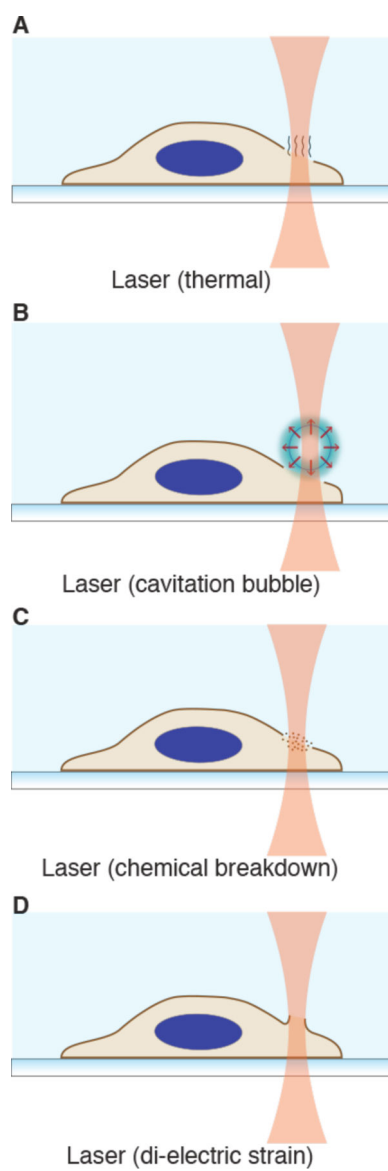


Figure 30 | Optoporation strategies for membrane disruption. Focused laser can inflict (A) thermal (B) cavitation (C) chemical breakdown, or (D) mechanical effects against lipid bilayers.

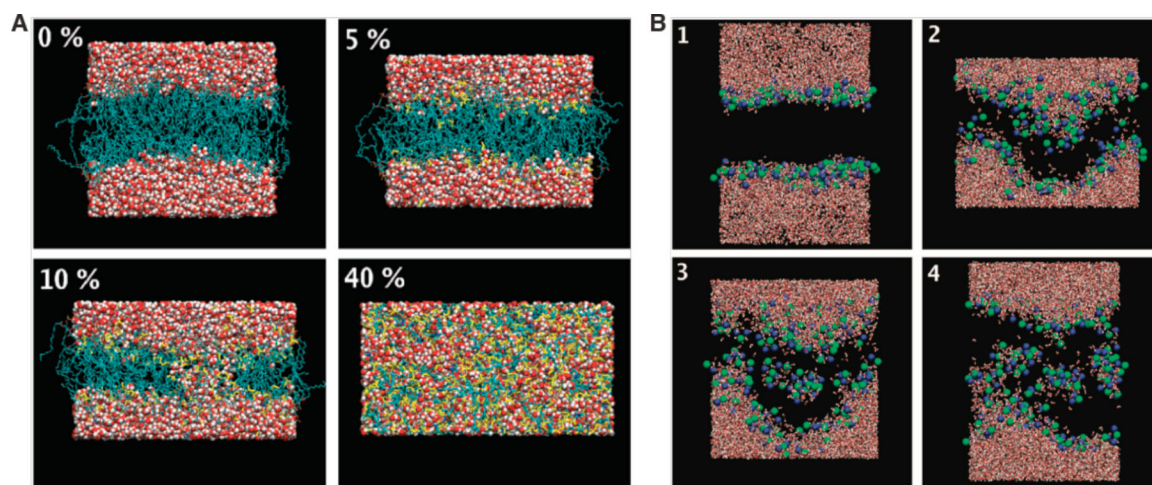


Figure 31.

Simulations of membrane bilayer perturbation with DMSO and Ethanol. (A) Presented are side views of the final structures for the bilayer systems containing 0, 5, 10, and 40 mol% of DMSO. Lipids are shown in cyan, water in red, and DMSO in yellow. Taken from reference 1323¹³²³. (B) Formation of non-bilayer structures within the membrane interior with 15 mol % of ethanol: (1) 3100 ps; (2) 13,180 ps; (3) 19,920 ps; (4) 30,000 ps. Shown are water molecules (red and white) and phosphorus (green) and nitrogen (blue) atoms of lipid head groups. The rest of the lipid atoms as well as ethanol molecules are not shown. Taken from reference 1325¹³²⁵.

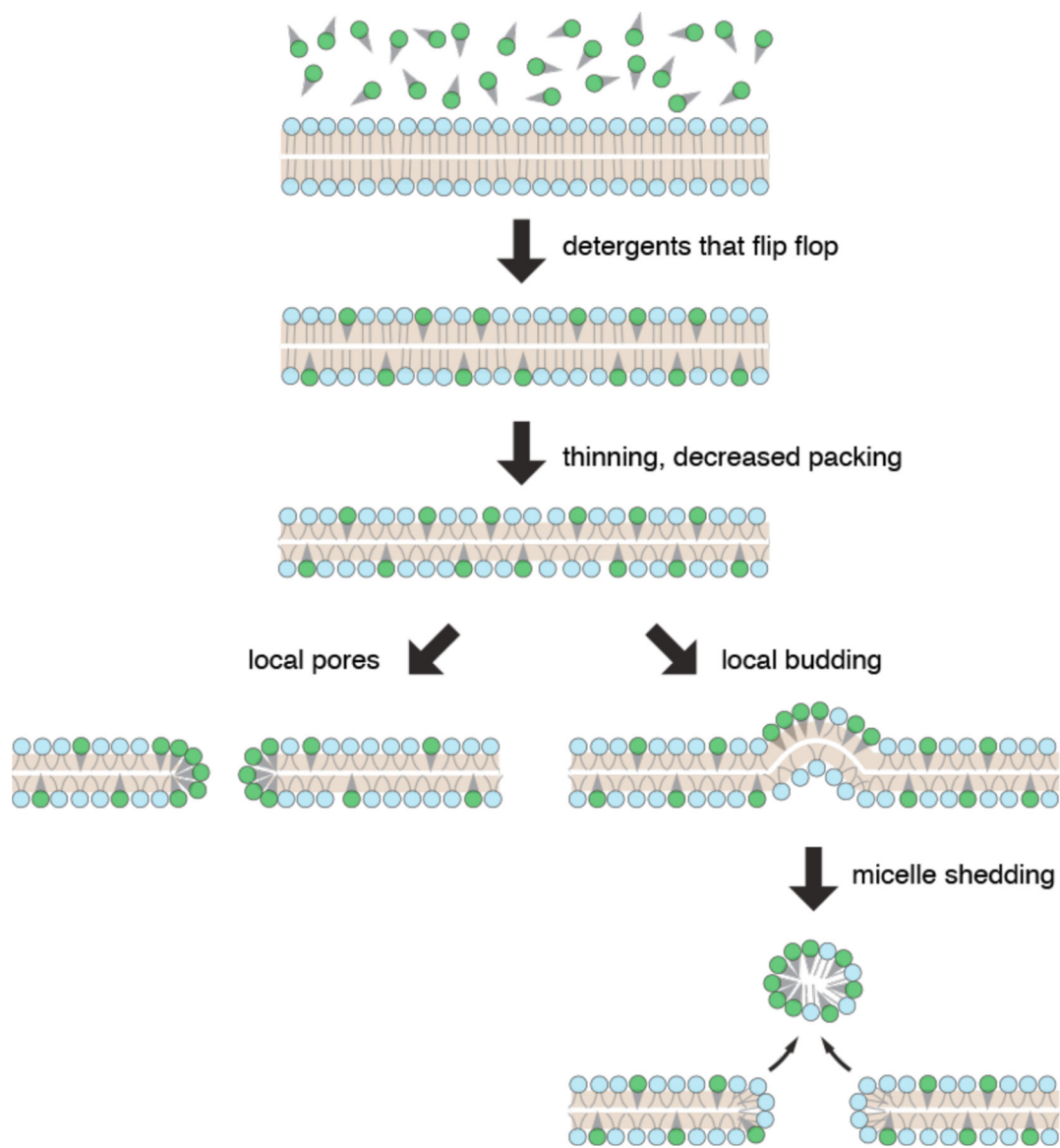


Figure 32. Proposed mechanisms of membrane permeabilization by detergents that flip flop. Integration of detergent monomers perturbs membrane integrity while stochastic local enrichment of detergents leads to formation of pores.

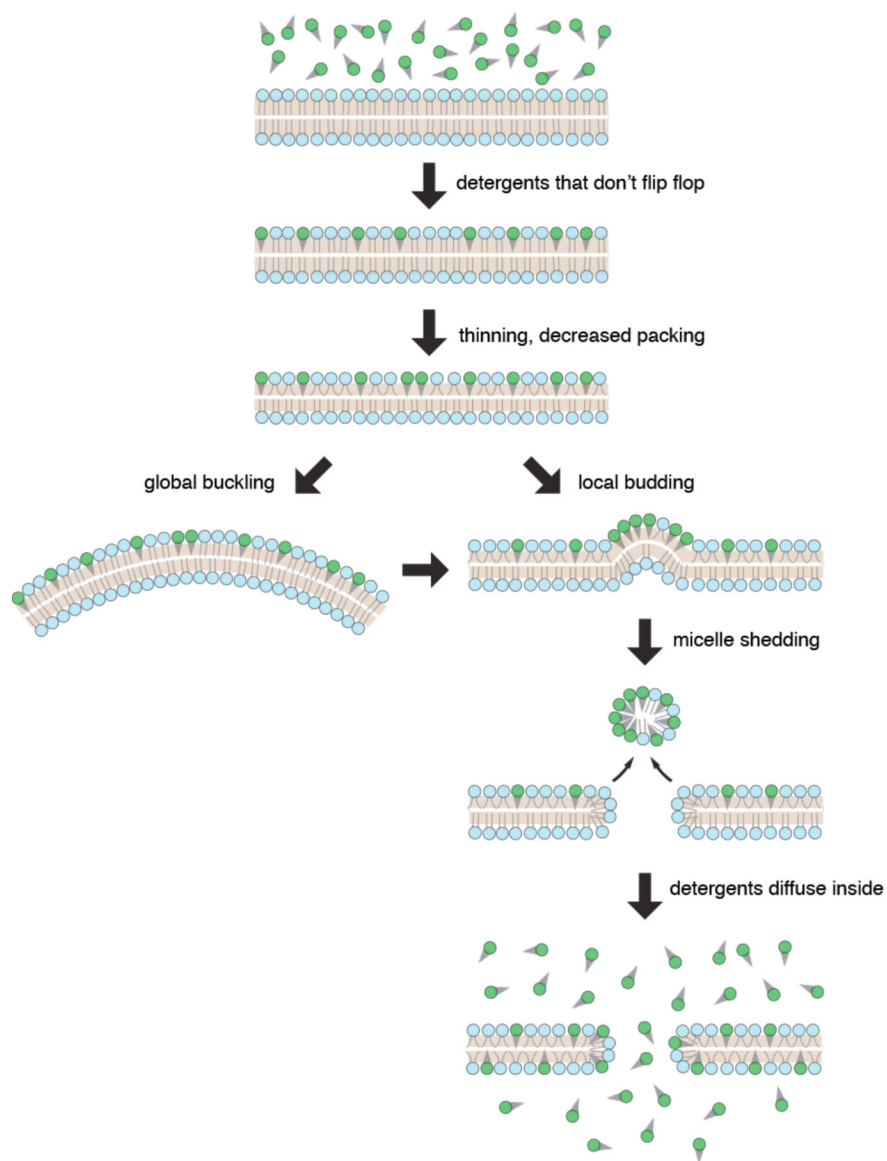


Figure 33. Proposed mechanisms of membrane permeabilization by detergents that do not flip flop. Once detergent monomers gain access to the interior side of the membrane, they can distribute to both leaflets and perturb the membrane by mechanisms similar to detergents that flip flop (see figure 32).

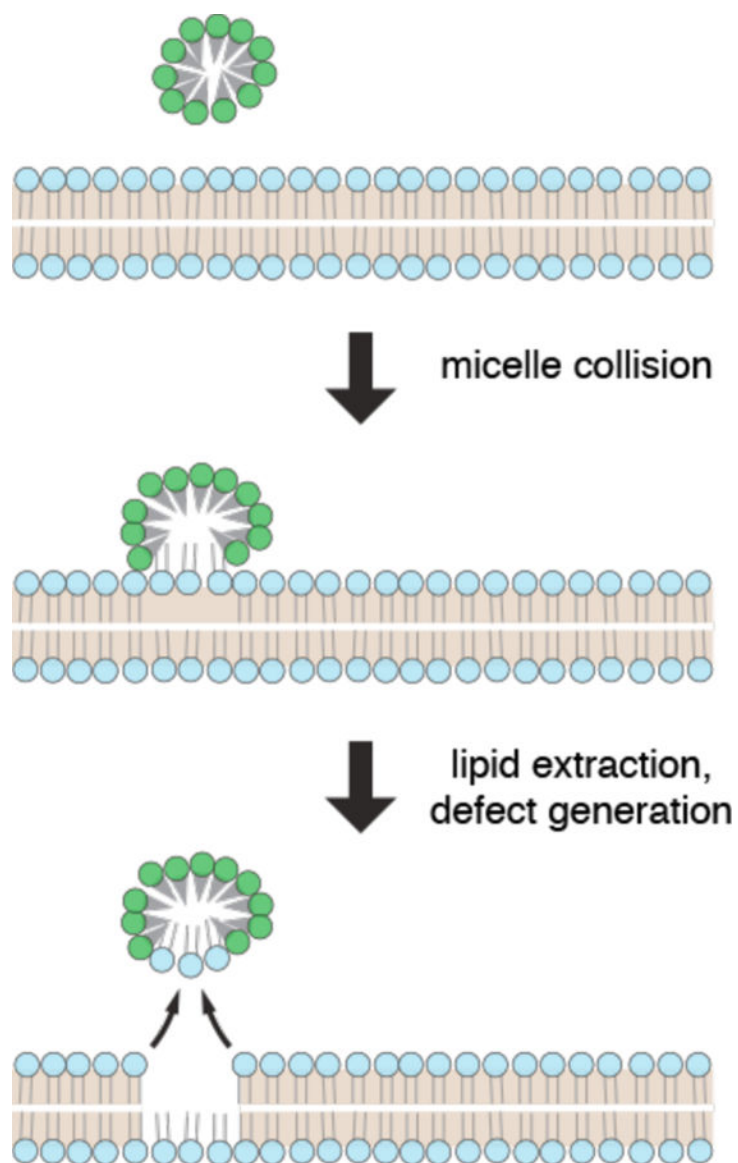


Figure 34. Proposed mechanisms of membrane permeabilization by detergent micelle collisions. Micelles colliding with the membrane can create defects by sequestering lipid molecules from the bilayer.

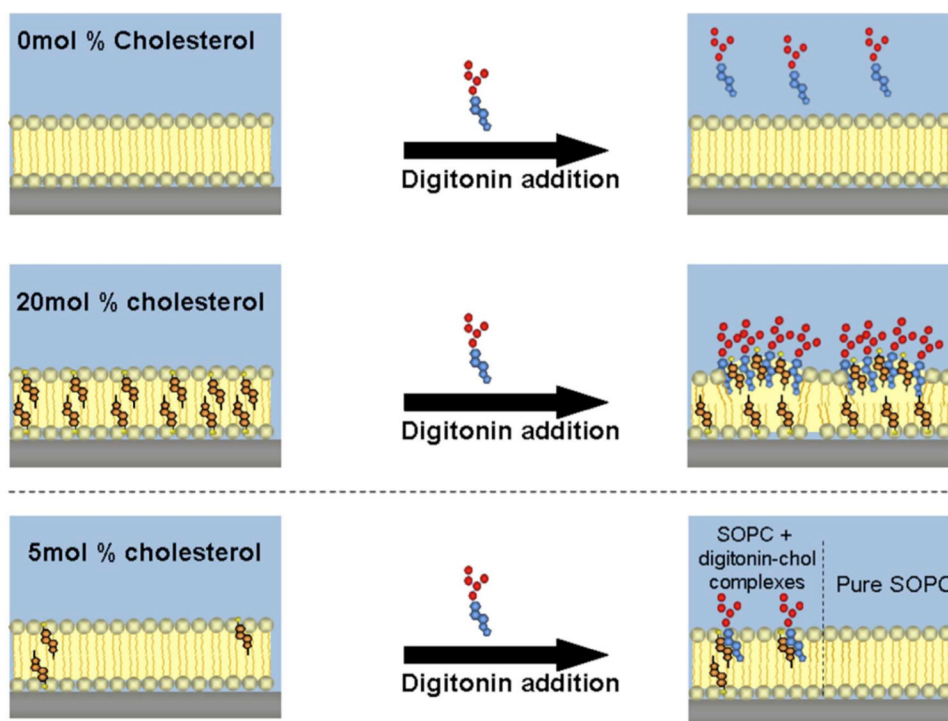


Figure 35. Interactions of digitonin with phospholipid membranes containing varying amounts of cholesterol. Taken from reference 1349¹³⁴⁹.

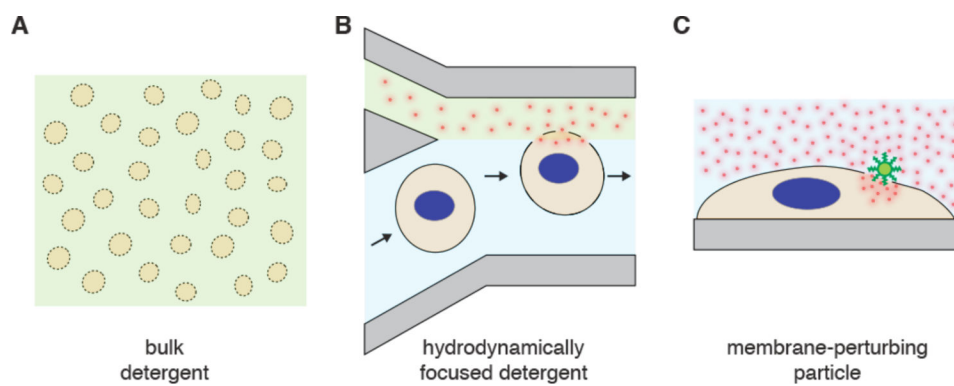


Figure 36. Schematic of exposure to membrane-perturbing detergent and/or surfactants by (A) bulk mixing, (B) microfluidic hydrodynamic focusing, and (C) localization to a nanoscale particle.

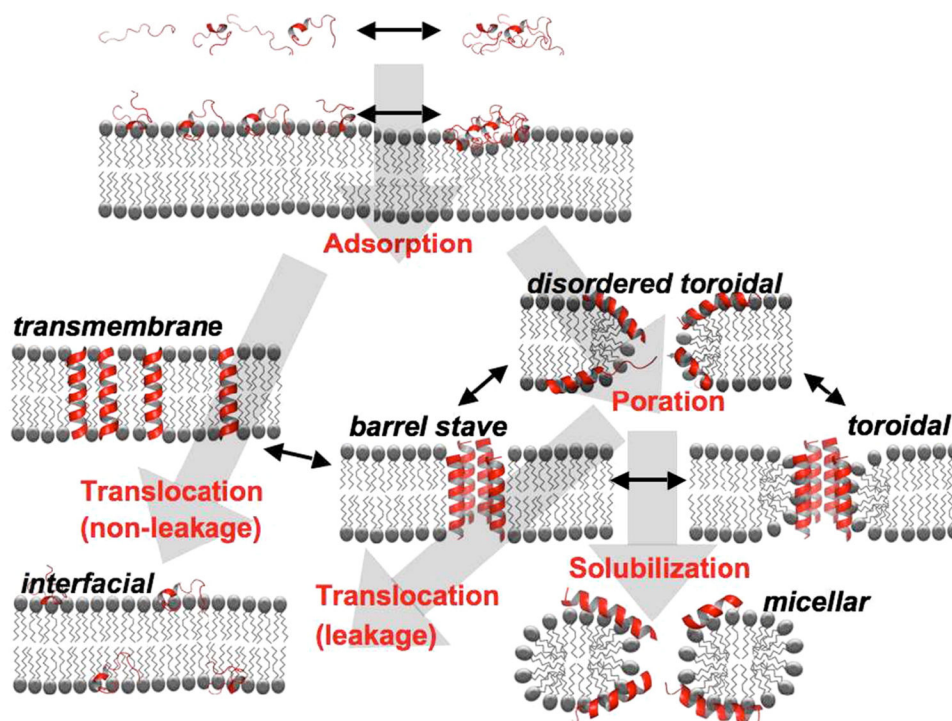


Figure 37.

Schematic overview of the possible interaction pathways of an antimicrobial peptide with a lipid bilayer. Possible thermodynamic states (either stable or metastable) are indicated by black labels, the major kinetic pathways connecting them by gray arrows and red labels. Short black arrows represent additional inter-conversion pathways. Outside the target membrane, peptide monomers and small aggregates exist in equilibrium. At the target membrane, the peptides bind to the interface (Adsorption). At the interface an equilibrium may exist between monomeric and polymeric aggregation states. For a symmetric bilayer, the asymmetric membrane bound state is not thermodynamically stable. Eventually the peptides will distribute equally between the two monolayer leaflets. This can occur via two alternative translocation pathways. In the non-leaky variant the peptides are able to cross the bilayer without the formation of a pore. In some cases, the intermediate transmembrane state is thermodynamically stable (e.g. hydrophobic peptides which adopt a transmembrane orientation). The key feature of many antimicrobial peptides is that they permeabilize the membrane following a leaky translocation pathway. Above a certain peptide–lipid ratio, the peptides insert into the bilayer to form a porated lamellar phase (Poration). A variety of different pore structures may be formed, including the barrel-stave, the toroidal and the disordered toroidal state. These separate states should be interpreted as extreme cases with mixed varieties of these models, and conversion between alternative states is likely to occur. The porated states can be stable themselves, but they can also be transient structures in the translocation pathway. In that case, once enough peptides are adsorbed at the opposing monolayer leaflet, the pores seal. On the other hand, increased accumulation of certain peptides may lead to a detergent-like disintegration of the membrane resulting in formation of non-lamellar, e.g. micellar, systems (solubilization pathway). Note that the secondary structure of the peptides could vary along the various pathways. The helical or random

configurations drawn here are merely illustrative of these processes and should not be taken literally. Figure legend and image taken from reference 1389¹³⁸⁹.

Author Manuscript

Author Manuscript

Author Manuscript

Author Manuscript

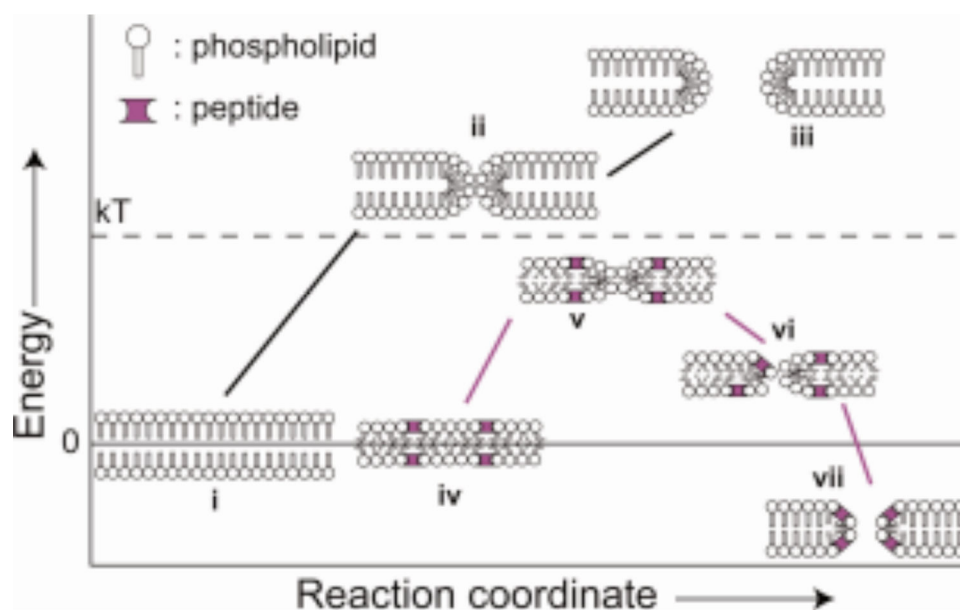


Figure 38.

Schematic of the effect of peptide binding on lipid bilayer integrity. (i) The reference state for energy change is an intact phospholipid bilayer. (ii) Spontaneous fluctuations result in the sampling of membrane defects. These are energetically unfavorable and therefore sampled infrequently. (iii) Widening of the defect to permit leakage results in a further energetic penalty. (iv) In the presence of surface-bound protein (magenta), membrane tension is induced. (v) Protein binding increases the frequency of defect formation. (vi) Surface tension is released by pore formation¹³⁹⁷ and stabilized by peptide binding resulting in equilibrium poration (vii). Note, many forms of defect, such as chaotic pores¹³⁹⁸, can be accommodated by this model, and defect characteristics may differ between alternate peptides or the same peptide under alternate conditions. Figure legend and image taken from reference 1396¹³⁹⁶.

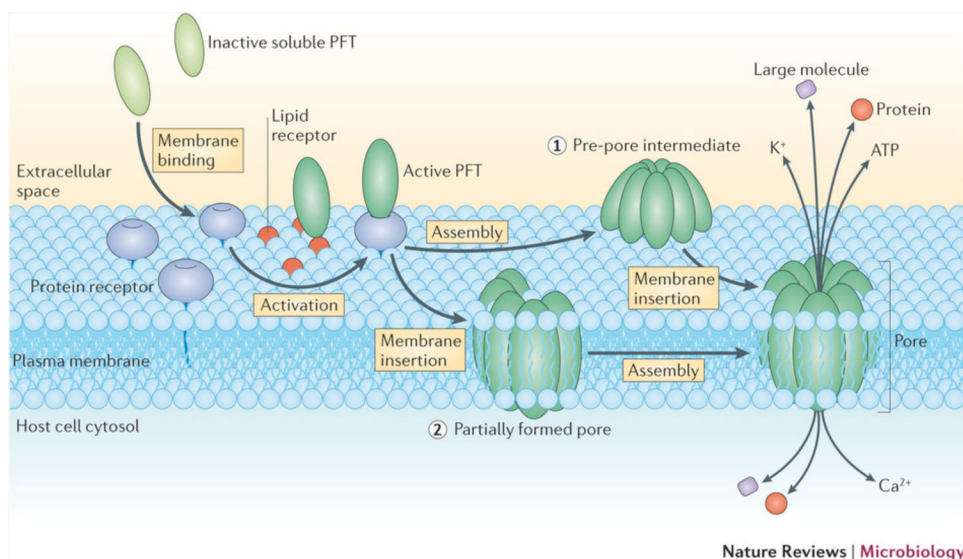


Figure 39.

Schematic representation of the pore formation pathway of pore-forming toxins (PFTs). Soluble PFTs are recruited to the host membrane by protein receptors and/or specific interactions with lipids (for example, sphingomyelin for actinoporins or sterols for cholesterol-dependent cytolysins (CDCs)). Upon membrane binding, the toxins concentrate and start the oligomerization process, which usually follows one of two pathways. In the pathway followed by most β -PFTs, oligomerization occurs at the membrane surface, producing an intermediate structure known as a pre-pore (mechanism 1), which eventually undergoes conformational rearrangements that lead to concerted membrane insertion. In the pathway followed by most α -PFTs, PFT insertion into the membrane occurs concomitantly with a sequential oligomerization mechanism, which can lead to the formation of either a partially formed, but active, pore (mechanism 2), or the formation of complete pores. Although classified as β -PFTs, CDCs also share some of the features of this second pathway, as they can also form intermediate structures (known as ‘arcs’, named after their shape) during pore formation. In both α -PFT and β -PFT pathways, the final result is the formation of a transmembrane pore with different architecture, stoichiometry, size and conduction features, which promote the influx or efflux of ions, small molecules and proteins through the host membrane, and trigger various secondary responses involved in the repair of the host membrane. Note that, although the host membrane shown here is the eukaryotic plasma membrane, some PFTs are antibacterial and form pores in the inner membranes of Gram-negative bacteria or the cell membranes of gram-positive bacteria. Figure legend and image taken from reference 400⁴⁰⁰.

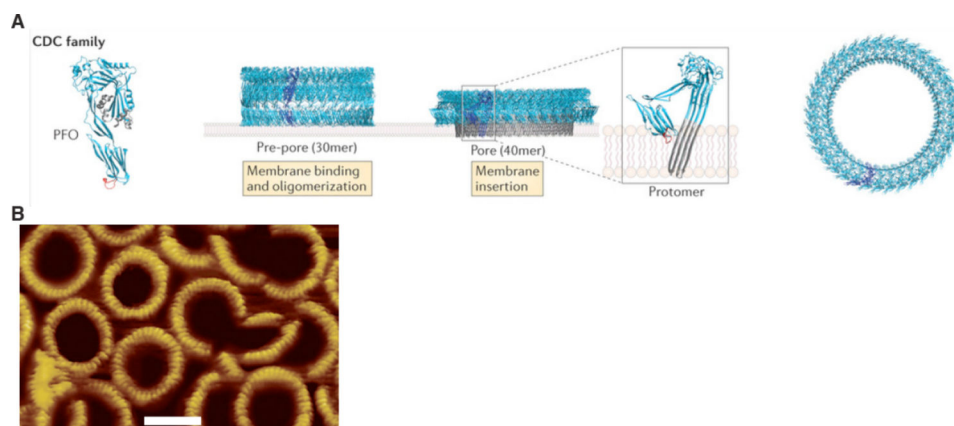


Figure 40. The structure of pores created by CDC pore-forming toxins. (A) CDC family members, such as Perfringolysin O (PFO), oligomerize to form large pre-pores, which, after an extended conformational change, form a membrane-inserted β -barrel. Figure taken from reference 400⁴⁰⁰. (B) AFM images of the PFO pore complexes in supported lipid bilayers that contain cholesterol. Scale bar 25 nm. Figure taken from reference 1403¹⁴⁰³.

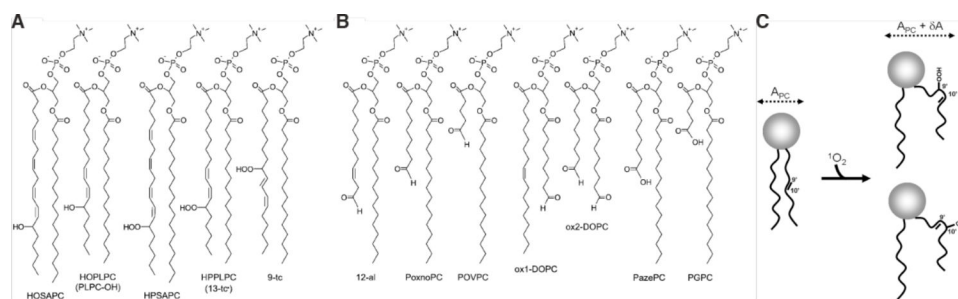


Figure 41.

Chemical structures of oxidized phosphatidylcholines and their effects on bilayer packing. (A) Hydroxy- (HOSAPC and HOPLPC) and hydroperoxy- (HPSAPC, HPPLPC, and 9-tc) phosphatidylcholines. Different *cis/trans* isomers are possible. 13-tc refers to *trans*-11, *cis*-9 isomer of HPPLPC. (B) Truncated (cleaved chain) phosphatidylcholines with aldehyde (12-al, PONPC, POVPC, ox1-DOPC, and ox2-DOPC) and carboxylic (PAzPC and PGPC), functional groups. For further details see reference 1467¹⁴⁶⁷. (C) Example of conformation changes that lipid molecules undergo due to peroxidation. In this case singlet oxygen adds the more hydrophilic group-OOH at either 9 or 10 position, which migrates to the bilayer surface. This imposes a kink to the acyl chain, with an accompanying increase in area δA per lipid. Figure taken from reference 397³⁹⁷.

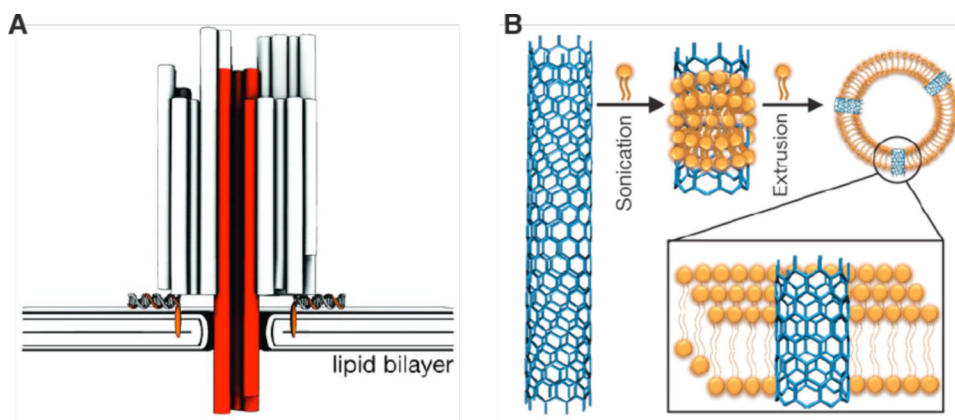


Figure 42. Synthetic nanodevices for use as membrane-embedded valves or channels. (A) DNA origami nanostructures assembled to form a membrane channel. Figure taken from reference 1483¹⁴⁸³. (B) Carbon nanotubes embedded within lipid bilayers for molecular transport. Figure taken from reference 1484¹⁴⁸⁴.

Table 1.

Characteristics of common cargo molecules of interest for intracellular delivery.

Cargo	Typical size (units)	Approx. Mass (Da)	Dimensions in solution (nm)	Charge at neutral pH
Nucleic acids				
plasmid DNA	2 – 10 kilo-basepairs DNA (double stranded)	~650 Da per base pair	Hundreds of nm –depends on supercoiling	–1 per base
mRNA	0.5 – 10 kilo-bases RNA (single stranded)	~320 Da per base	Tens to hundreds of nm	–1 per base
siRNA / miRNA	21–23 basepair duplex	13–15 kDa	2 wide × 7.5 nm long	–1 per base
ASO	13–25 bases (single stranded)	4 – 8 kDa	Length of 4 – 8 nm if linear	–1 per base
Peptides	< 40 amino acids	~110 Da per amino acid	~0.2 – 3 nm	Varies according to amino acid composition
Proteins	20 to 1000's of amino acids	~110 Da per amino acid	~2 – 25 nm	Varies according to amino acid composition
Cas9 RNP	~1400 amino acids, ~100 base RNA	~188 kDa (~158 kDa protein, ~30 kDa RNA)	~12–15 nm	~–80 (+22 protein, –100 RNA)
Small molecules	N/A	< 900 Da	< 1 nm	Variable. Often neutral to promote permeability

Table 2.

Disruption buffers used in papers compiled in this review. Note that some papers use multiple buffers so percentages may not add to 100%. Not specified is likely to be room cell media or Na-rich buffer by default.

MODE OF MEMBRANE DISRUPTION:	Cell media	Na-rich “physiological” buffer	K-rich “intracellular” buffer	Buffered sugar solution	Not specified / other
ALL	37% (n=110)	34% (n=101)	9% (n=27)	17% (n=52)	12% (n=35)
Electroporation	28% (n=47)	31% (n=52)	7% (n=12)	25% (n=42)	17% (n=28)
Physical (non-electroporation)	58% (n=49)	32% (n=27)	7% (n=6)	5% (n=4)	7% (n=6)
Biochemical	28% (n=13)	43% (n=20)	22% (n=10)	15% (n=7)	0% (n=0)

Table 3.

Disruption temperatures used in papers compiled in this review. Note that some papers use multiple temperatures so percentages may not add to 100%. RT denotes room temperature and varies considerably between publications. Not specified is probably room temperature by default.

MODE OF MEMBRANE DISRUPTION:	37 °C	RT (~18 – 25 °C)	< 4 °C	Not Specified
ALL	22% (n=65)	46% (n=139)	16% (n=47)	16% (n=49)
Electroporation	9% (n=15)	67% (n=112)	11% (n=19)	13% (n=22)
Physical (non-electroporation)	34% (n=30)	25% (n=22)	12% (n=11)	27% (n=24)
Biochemical	43% (n=20)	13% (n=6)	38% (n=18)	6% (n=3)

Author Manuscript

Author Manuscript

Author Manuscript

Author Manuscript

Cargo delivery mechanism versus scale of throughput for nano- and micro-mechanical membrane disruption techniques. For injection mechanisms, the nano or micro-mechanical element is hollow, thus allowing injection of cargo. Dissociation-based delivery works by enabling cargo to detach from the penetrating element once inside the cell. For permeabilization, the cargo is in the extracellular solution and flows into the cell by diffusion upon withdrawal of the penetrating element. References for each example are included.

Table 4.

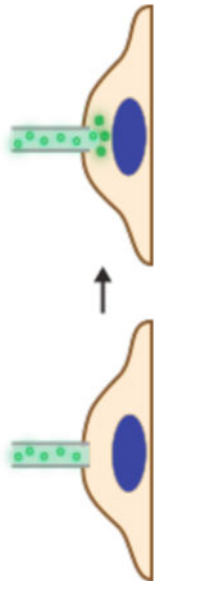
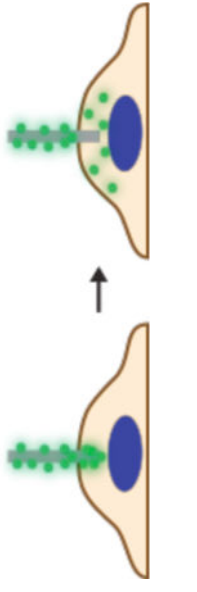
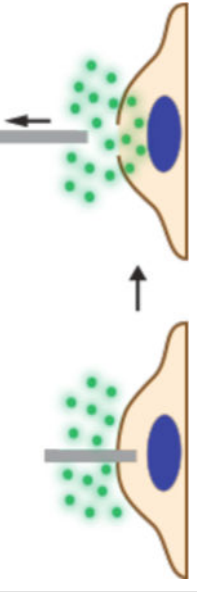
	Injection	Dissociation	Permeabilization
Single cell	 Microinjection ²⁹⁸ Nanoinjection ⁵⁶⁸⁻⁵⁷¹ FluidFM ⁵⁷³	 AFM-controlled CNT tip ⁶⁷² AFM-controlled nanoneedle ^{656-658,673,674} Micromanipulator-controlled metal nanowire ⁶⁷⁵⁻⁶⁷⁷	 CellBee ⁶⁷⁸ Cell Pricking ⁶⁷⁹⁻⁶⁸²
Parallelized Systems	Nanostraws ^{387,664-666}	Nanowire arrays ^{185,363,634}	Cell Poking ⁶⁵⁴ Microneedle array ⁶⁸³

Table 5.

Summary of membrane disruption approaches covered in this review. Several are widely used for intracellular delivery while others have barely been attempted.

Modality	Methods	Membrane Disruption Mechanisms	Disruption / Pore Distribution	Disruption / Pore Size	Throughput / Scalability	Suspension / Adherent
DIRECT PENETRATION						
Mechanical	Microinjection	Mechanical forces at contact zone. Membranes only tolerate 2–3% lateral strain ³⁹³ . Can be strain rate dependent ^{390,1486}	At contact zone	Depends on size of injection tip, usually 0.3 – 1 μ m	Low, could be improved via automation	Mostly adherent, suspension cells require second holding pipette
	Penetrating Projectiles (Biolistics)			Depends on size of projectile, usually micron-size	Potentially high	Primarily adherent, some reports on suspension cells
	Nanowires & Nanostraws			Depends on size of nanoneedle tip: reported range 50 – 1000 nm	Potentially high	Mostly adherent, suspension cells must be forced onto the array
PERMEABILIZATION						
Mechanical (Solid Contact)	Cell Scraping	Mechanical forces transmitted by contact/cell deformation. Membranes only tolerate 2–3% lateral strain ³⁹³ . Can be strain rate dependent ^{390,1486}	Variable: Presumably at contact zone otherwise at weak points/defects due to global membrane strain	Variable: probably depending on force, strain rate, size of contact zone, direction of strain	High	Adherent
	Bead Loading				High	Adherent
	Scratch Loading				Low/Medium	Adherent
	Microfluidic Cell Squeezing				High	Suspension
	Nanowires for Transient Permeabilization				Potentially high	Adherent
	Sudden Cell Shape Changes and Protease Treatments	Possibly tearing forces at adhesion sites	Unknown	Unknown	Potentially high	Adherent
Mechanical (Fluid Shear)	Syringe Loading / Microfluidic Channel	Fluid shear	Unknown	Unknown	Potentially high	Suspension only
	Sonoporation / Shockwaves	Stale Cavitation (Microstreaming), Inertial Cavitation (Jetting), other Acoustic Effects	Presumably a single hole per cavitation bubble	From nanometers to several micron depending on cavitation intensity and stand-off distance	High	Both
	Laser-controlled Cavitation				High	Both
Mechanical (Pressure)	Hypo-osmotic shock	Mechanical forces transmitted by osmotic/hydrostatic pressure. Membranes only tolerate 2–3% lateral strain ³⁹³ . Can be strain rate dependent ^{390,1486}	Presumably at weak points or nucleating at membrane defects	Variable: depending on membrane reservoirs, attachment / reinforcement of membrane, and magnitude / rate of pressure	High	Both
	Hydrostatic pressure				High	Both

Modality	Methods	Membrane Disruption Mechanisms	Disruption / Pore Distribution	Disruption / Pore Size	Throughput / Scalability	Suspension / Adherent
	Osmotic rupture of endosomes			Limited by endosome	High	Both
Electroporation	Conventional Electroporation	Probability of defect formation for given pulse-strength duration at a given temperature	At cell poles. More permeabilization expected on hyperpolarized side	Nucleate as small defects then grow as a function of voltage and duration	High	Primarily Suspension, but Adherent also possible
	Micro-electroporation		Depends on geometry		Potentially high	Primarily Suspension
	Nano-electroporation		Usually single hole at aperture		Currently Medium / Low	Both, depending on system
Thermal	Freeze-thaw	Expansive mechanical strain due to ice crystal formation	Location of ice crystals	Presumably variable	High	Both
	Rapid temperature transitions	Defect formation due to phase transitions	Probably near lipid domain boundaries and protein clusters	Presumably small defects	High	Both
	Supraphysiological heating	Dissociation of bilayer structure leading to defect formation	Site of maximal heat	Presumably small defects	High	Both
	Laser absorption at membrane or particle/structure	Absorption causes high local temperature to trigger membrane disruption	Laser focal point or location of absorbent structure	Presumably variable depending on local temperature effects	High	Both
Optoporation	Lasers variables: - Continuous wave or pulsed - Wavelength - Frequency - Power / Intensity	Can be a mix of: - Chemical (low energy plasma) - Mechanical (cavitation, shock waves, thermoelastic stress) - Thermal (Heat in focal region)	Maximal in focal region. Usually one hole	Depending on parameters and mechanisms. Nanometers to several micron	Low to high - limited by laser focusing approach	Primarily Adherent, but suspension also possible
Biochemical	Organic solvents and penetration enhancers	Perturb bilayer structure by burying their hydrophobic residues into the membrane	Indiscriminate in bulk, otherwise depends on local concentration	Presumably small defects then disintegration of the whole bilayer at high concentration	High	Both
	Detergents / surfactants – generic	Insert into bilayer and distort the structure, leading to defects, pore formation, and micellization	Indiscriminate in bulk, otherwise depends on local concentration	Presumably small defects then disintegration of the whole bilayer at high concentration	High	Both
	Detergents – saponin family	Extracts of cholesterol out of the bilayer core to form a surface complex, induces curvature and defect/pore formation	Cholesterol rich sites. Indiscriminate in bulk, otherwise depends on local concentration	From nanometers to micron	High	Both

Modality	Methods	Membrane Disruption Mechanisms	Disruption / Pore Distribution	Disruption / Pore Size	Throughput / Scalability	Suspension / Adherent
	Pore-forming toxins – CDC family	Insertion and oligermization into pore structure in cholesterol-rich membranes	Cholesterol rich sites. Indiscriminate in bulk, otherwise depends on local concentration	20 – 50 nm	High	Both
	Membrane-active peptides	Adopt active conformation upon membrane binding. Concentration dependent aggregation / insertion	Depend on membrane composition. Indiscriminate in bulk, otherwise depends on local concentration	Presumably small defects, but large holes have been suggested	High	Both
	Chemical destabilization	Lipid peroxidation leads to structural interference / distortion of membranes to form pores and defects	Depends on source of oxidation. If local, can be confined.	Presumably small defects, but large holes are conceivable	High	Both
Gated Channels and Valves	Endogenous or engineered membrane transporters and channels	Appropriate stimuli (e.g. mechanical, chemical, optical) can gate opening and closing activity	Depends on location of the membrane transporters / channels	Limited by size of the channel. Usually only amenable for transport of small molecules < 1 kDa	High	Both
	Synthetic nanodevices	Insertion of constructs into host membrane. Gating may be engineered	Presumably depends on location of insertion and lateral diffusion throughout membrane	Limited by size of the engineered central channel	Potentially High	Both

Table 6.

Cargo loaded versus membrane disruption approach. Techniques marked with red text represent accessible methods that are either commercially available or trivial to perform with common lab equipment.

MODALITY	METHOD	CARGO						Large Cargo: Bacteria, Organelles, Beads etc.	
		Nucleic Acids and their Analogues		Peptides / Proteins / Antibodies / RNPs etc.	Generic Macromolecules (e.g. Dextrans)	Small Molecule Drugs / Probes / Dyes / Sugars / Ions etc.	qDots / CNTs / Synthetic Nanomaterials etc.		
		vector DNA	mRNA						Oligos
DIRECT PENETRATION									
Mechanical	Micro-injection	pDNA ^{70-72, 565} , Viral DNA ^{70,564,1487}	mRNA ^{109,1488}	Antisense Oligonucleotides ^{81,566} , siRNA ⁸⁵	Proteins ^{162-166, 562,148} , Antibodies ¹⁴⁹⁰ , Peptides ^{561, 1491} , Cas9 protein / RNP ²²⁴	Dextrans ¹⁴⁹²	Dyes ⁵⁵³ , Mercury ²⁹⁸ , Trehalose ¹⁴⁹³	qDots ^{273,1494,1495} , MW-CNTs ²⁹⁴ , SW-CNTs ²⁸³	Bacteria ²⁹⁸ , Nuclear transplant ³⁰⁰⁻³⁰² , Chromosome transplant ³⁰⁷ , Sperm / IVP ^{305,306} , Mito-chondria ³¹⁰ , Artificial vesicles ¹⁴⁹⁶ , Beads ^{1497,1498} , Silicon barcode ³³⁰
		pDNA ^{364,600}	Cas9 mRNA ¹⁴⁹⁹ , mRNA ⁶²⁰⁻⁶²²	siRNA ^{623,624}	Proteins ⁶²⁶⁻⁶²⁸ , Cas9 protein / RNP ⁶²⁹		Dyes ^{618,1500} , Indicators ⁶¹⁷	PEBBLE nano-sensors ¹⁵⁰¹	Beads ^{325,327} , Latex particles ³²⁶
		pDNA ^{185,363, 634,643,677,1502}		siRNA ^{185,638,639}	Proteins ^{185,638} , Peptides ¹⁸⁵ , Cre Recombinase ⁶⁴⁰ , Antibodies ⁶⁴¹		Drugs ¹⁸⁵ , Molecular Beacons ⁶⁴²	qDots ⁶⁴³ , DNA Nano-cages ⁶⁴⁴	
		pDNA ^{664,666, 671}			Proteins ⁶⁷¹	Dextrans ^{665, 671}	Dyes ^{664,666} , Co ²⁺ ions ³⁸⁷ , Ca ²⁺ ions ⁶⁶⁷ , Small molecule probes ⁶⁶⁸	qDots ⁶⁷⁰	
PERMEABILIZATION									
Mechanical (Solid Contact)	Cell Scraping	pDNA ⁵⁰³		Antisense Morpholinos ^{721,1503-1505}	Proteins ^{176,501, 709-715} , Antibodies ⁷¹⁶⁻⁷¹⁸ , Peptides ^{719,720}	Dextrans ^{176, 722} , Lipopolysaccharide ⁷²³	Dyes ⁷²⁴⁻⁷²⁶		

MODALITY	METHOD	CARGO						Large Cargo: Bacteria, Organelles, Beads etc.	
		Nucleic Acids and their Analogues			Peptides / Proteins / Antibodies / RNFs etc.	Generic Macromolecules (e.g. Dextrans)	Small Molecule Drugs / Probes / Dyes / Sugars / Ions etc.		qDots / CNTs / Synthetic Nanomaterials etc.
		vector DNA	mRNA	Oligos					
Mechanical (Fluid Shear)	Bead Loading	pDNA ⁶⁹³			Proteins ⁶⁹⁹⁻⁷⁰¹ , Fab Fragments ^{703,704} , Antibodies ⁶⁹⁶⁻⁶⁹⁸ , Peptides ⁷⁰²	Dextrans ^{171,699,1506}	Nucleotides ^{695,919} , RNA probes ¹⁵⁰⁷ , PNA ⁷⁰⁵ , SNAP-reactive dyes ⁷⁰⁶	qDots ⁷⁰⁸ , SW-CNTs ⁷⁰⁷	
	Scratch Loading					Dextrans ⁷²⁷	Dyes ⁷²⁸	qDots ⁷⁰⁸	
	Microfluidic Cell Squeezing / Constriction Mediated Disruption	pDNA ^{227,741,749,754,755}	mRNA ^{184,749}	siRNA ^{184,227} , tRNA ⁷⁴⁷	Proteins ^{184,744,745,749,1508} , Cas9 RNFs ^{227,755}	Dextrans ^{184,227,741,744,750}	Dyes ^{184,741,755} , Tags ¹⁵⁰⁸ , Drugs ¹⁵⁰⁹	qDots ²⁸⁷ , CNTs ¹⁸⁴	
	Nanowire Permeabilization	Lipid-pDNA complexes ⁶⁵⁴ , pDNA ⁷⁶¹			Antibodies ⁶⁵⁴	Dextrans ⁷⁶¹	Dyes ^{678,883}	qDots ⁶⁵⁴	~200 nm polystyrene beads ⁶⁵⁴
	Sudden Cell Shape Changes / Protease Treatment			Oligonucleotides ⁷³²	Proteins ^{732,735,737,738} , Peptides ⁷³²	Dextrans ^{730,732,1510}	Dyes ⁷³³		
	Syringe Loading / Microfluidic / Bulk Fluid Shear	pDNA ^{765,787}		Antisense morpholinos ⁷⁶⁶	Proteins ^{770,774,776-780,783} , Antibodies ^{771-773,775,781}	Dextrans ^{178,769,783,785,787}	Dyes ⁷⁸⁶ , Nucleotides ^{767,768}		
	Sono-poration	pDNA ^{503,792,793,795,801,816-822,1511}	mRNA ⁸²⁶	siRNA ^{824,825} , Antisense oligonucleotides ⁸²³ , ssDNA ¹⁵¹¹	Proteins ^{790,828} , Antibodies ⁸⁵² , Peptides ⁸⁵³	Dextrans ^{503,789,790,812-814,827,828,830-836}	Dyes ^{764,808,813,814,820,828,835,837-845,869} , Drugs ^{835,846-850}	25-75 nm nanoparticle ^{es} ⁸³¹	Viral particles ⁸⁵¹
	Shock Wave-Mediated Permeabilization	pDNA ^{1264,1512-1514}		Antisense oligonucleotides ¹⁵¹⁵	Proteins ⁸⁶⁴ , Peptides ⁸⁶⁷	Dextrans ^{860,862,863}	Dyes ^{862,866,868,869,872} , Drugs ¹⁵¹⁶		
	Laser-Induced Cavitation	pDNA ^{313,876,880,882,1517}	mRNA ³¹³	siRNA ^{884,886,887}	Proteins ^{314,882} , Antibodies ¹²⁷²	Dextrans ^{876,881,885,887,890,892,1518-1521}	Dyes ^{447,843,877,881,882,885,889,891,892,1520,1522}	qDots ^{288,289,1521} , Gold nanoparticles ¹⁵²³	Bacteria ^{313,314} , Mitochondria ³¹⁵ , ~200 nm polystyrene beads ³¹³

MODALITY	METHOD	CARGO				Large Cargo: Bacteria, Organelles, Beads etc.		
		Nucleic Acids and their Analogues		Peptides / Proteins / Antibodies / RNPs etc.	Generic Macromolecules (e.g. Dextrans)		Small Molecule Drugs / Probes / Dyes / Sugars / Ions etc.	qDots / CNTs / Synthetic Nanomaterials etc.
		vector DNA	mRNA					
Mechanical (Pressure)	Hypo-Osmotic Shock	pDNA ⁹³⁸ 944,947,952,953, 961,966,967,1526-1528 Bacterial artificial chromo-somes (BACs) ⁹⁴⁶	mRNA ⁹⁴⁷	ssODN ^{951,952} , gRNA ⁹⁵⁴ , siRNA ^{944,945} , 960,1527 Antisense morpholinos ¹⁵²⁹ , Antisense oligonucleotides ^{959,961-965}	Dextrans ⁹²⁵ , 937,1524	Dyes ^{914,1525} , Lanthanide ions/complexes ⁹³⁰⁻⁹³⁵ , Nucleotides ⁹¹⁴⁻⁹²³ , Nucleosides ⁹¹⁴ , BAPTA ⁹²⁸	qDots ²⁹⁰ , ~5 nm gold nanoparticle es ⁹²⁶	
	Hydrostatic Pressure			Proteins ^{943,1530} , Antibodies ¹⁵³⁰	Dyes ^{943,947}		~100 nm Polystyrene microspheres ⁹⁶⁸	
Electroporation	Osmotic Rupture of Endosomes			Proteins ^{174,175} , 970-984 Antibodies ⁹⁷⁶ , 985-989 Peptides ⁹⁹²⁻⁹⁹⁴ , Cell lysate ⁹⁹⁵	Dextran ¹⁷⁴ , 989-991, Hyaluronan ^{996,997}	Trehalose ⁹⁹⁸ , Lanthanide imaging probes ^{260,261} , Dyes ^{989,999} , UDP-glucuronic acid ¹⁰⁰⁰	qDots ¹⁵³¹ , Protein-conjugated qDots ^{285,1003,1004}	Virus particles ¹⁰⁰²
	Conventional Electroporation	pDNA ^{53,1066} , 1067	mRNA ^{25,54,56} , 124,126-128, 221,518,1064, 1065,1211,1214, 1219,1223,1225,1226, 1238,1241,1242	Antisense oligonucleotides ¹⁰⁵⁸ , siRNA ^{104,1059-1063}	Dextrans ⁵⁰⁴ , 1030,1080,1207	Dyes ^{180,1030-1033} , Radio-tracers ¹⁰³⁵ , SNAP-reactive dyes ⁷⁰⁶ , Sugars ^{268,430,1036,1037} , Metabolites ^{1034,1038} , Drugs ^{254,255,1039,1040} , Ions ^{1041,1042} , Molecular Beacons ^{1043,1044}	qDots ^{273,291,292,1068} , 20nm gold nanoparticles ¹⁰⁶⁹	
Thermal	Microelectroporation	pDNA ^{1175,1177} , 1178,1180,1181, 1183,1532		siRNA ^{1183,1532} , miRNA ¹¹⁸³	Dextrans ¹¹⁸²	Dyes ^{449,1175,1179-1183}		
	Nanoelectroporation	pDNA ^{566,1184} , 1185		siRNA ¹¹⁸⁴ , Oligonucleotides ¹¹⁸⁴	Dextrans ¹¹⁹² , 1193	Dyes ^{666,1184} , Molecular Beacons ^{1184,1193}	qDots ¹¹⁸⁴	
	Cooling-Heating Cycle					Trehalose ^{262,264,998}		
Supraphysiological Heating		pDNA ^{1265,1266}		Proteins ¹⁵³³		Dyes ¹¹²⁷		

MODALITY	METHOD	CARGO						Large Cargo: Bacteria, Organelles, Beads etc.	
		Nucleic Acids and their Analogues			Peptides / Proteins / Antibodies / RNFs etc.	Generic Macromolecules (e.g. Dextrans)	Small Molecule Drugs / Probes / Dyes / Sugars / Ions etc.		qDots / CNTs / Synthetic Nanomaterials etc.
		vector DNA	mRNA	Oligos					
Optoporation	Laser Absorption Converted to Heat	pDNA ^{1275,1276}		siRNA ¹⁵³⁴	Antibodies ¹²⁷³	Dextrans ^{1272,1276}	Dyes ^{1271,1272,1274-1276,1535}		
	Laser Optoporation	pDNA ^{441,443,444,1277,1279-1305}	mRNA ^{121,1300}	siRNA ^{1280,1290,1299} , Antisense morpholinos ¹³⁰⁰	Peptides ^{446,1306} , Proteins ^{1280,1290}	Dextrans ^{1280,1290,1296,1300,1307,1308}	Dyes ^{121,440-444,446,1280,1287,1288,1290,1292,1293,1295,1301,1304,1308-1313} , Sucrose ⁴⁴⁵ , Molecular Beacons ¹³¹⁴ , Ions ^{1280,1290,1315}	Semiconductor nanocrystals ^{1280,1290} , Gold nanoparticles ¹³¹⁶ , qDots ¹³¹⁷	~1 μm, Polystyrene beads ¹³¹⁸
Biochemical	Organic Solvents & Penetration Enhancers	pDNA ¹³³⁰	mRNA ¹³³⁰		Proteins ¹³³⁰				
	Detergents & Surfactant: Generic				Proteins ¹³⁶⁶ , Antibodies ^{179,1366}		Nucleosides ¹³⁶⁵ , Dyes ¹³⁶⁵ , Nutrients & Metabolites ¹³⁶⁶ , Ferro-cyanide ¹³³⁹		
	Detergent: Saponin Family				Proteins ⁴⁹⁷ , Peptides ⁴⁹⁷ , Antibodies ¹³⁶⁰ , Cytoplasmic extracts ¹³⁵⁸	Dextrans ¹³⁵⁸	Inositol ¹³⁵⁶	~20 nm nanoparticles ¹³⁵⁹ , qDots ²⁹⁰	
	Pore-Forming Toxins: CDC Family			siRNA ^{107,108,1411} , Antisense oligonucleotides ^{1058,1407,1412-1421}	Proteins ^{182,196,457,1408} , Peptides ^{1409,1422-1424} , Peptides ^{1410,1425,1426} , Cytoplasmic extracts ^{468,498,1427-1442}	Dextrans ¹⁴⁰⁹	PNA probes ¹⁴⁴³⁻¹⁴⁴⁵ , Molecular Beacons ^{1043,1446-1452} , Photosensitizers ¹⁴⁵³ , Phosphatidic acid ¹⁴⁵⁴ , Rb ⁺ ions ¹⁸² , ATP ¹⁸² , Various RNA probes ¹⁴⁵⁵⁻¹⁴⁵⁷ , Lanthanum probes ^{261,1458}	Gold nanoparticles ¹⁴⁵⁹	
	Membrane-Active Peptides								

MODALITY	METHOD	CARGO							
		Nucleic Acids and their Analogues			Peptides / Proteins / Antibodies / RNPs etc.	Generic Macromole cules (e.g. Dextrans)	Small Molecule Drugs / Probes / Dyes / Sugars / Ions etc.	qDots / CNTs / Synthetic Nanomater ials etc.	Large Cargo: Bacteria, Organelles, Beads etc.
		vector DNA	mRNA	Oligos					
Gated Channels & Valves	Lipid Peroxidation Membrane Transporters & Channels			siRNA ¹⁴⁶⁹	Proteins ¹⁴⁸² , Peptides ¹⁴⁸²		Dyes ^{1470,1472, 1480,1485,1536, 1537} , Ions ¹⁴⁸¹ , Trehalose ²⁶⁶		